University of Southampton

PROCESSES OF SLOPE DEGRADATION IN THE BARTON CLAY CLIFFS OF CHRISTCHURCH BAY

Volume 1

UNIVERSITY OF SOUTHAMPTON

ABSTRACT

FACULTY OF ENGINEERING

CIVIL ENGINEERING

Master of Philosophy

PROCESSES OF SLOPE DEGRADATION IN THE BARTON CLAY CLIFFS OF CHRISTCHURCH BAY

by Brian John Coles

Research into the processes of slope degradation has primarily concentrated on the factors which influence the dominant processes on a degrading slope, Bromhead (1979), Hutchinson (1967), Brunsden and Jones (1976) and the mechanics of individual processes of slope degradation, Hutchinson (1970), De Freitas and Watters (1974) and Hutchinson and Bhandari (1971). No published research has quantified the rates of movement, the depths to shear surfaces and the volumes of material transported by each process in a degrading coastal clay slope.

A detailed two year field study, involving regular surveying and monitoring, into the nature and pattern of degradational processes present in an actively eroding stretch of the Barton Clay cliffs have been carried out. Seven processes contributing to the slope degradation have been identified.

An area of 25,520m^2 has been monitored by 154 survey pegs, 11 inclinometers, 24 slip indicates, 10 spalling rods and 8 piezometers. Subsurface investigations and field observations located 11 active shear surfaces.

Surface investigation identified three phases of annual movement consisting of a summer, a surge and a winter period.

Between July 1981 and July 1983, a total of 9.598m^3 of soil debris was removed from the study area, which represented 12% of the total colluvial volume in July 1981.

Stability analyses have shown that the Influence line approach Hutchinson (1977, 1984) is a good method to quantify the effect of a cliff top slump block on the stability of the degrading slope.

PREFACE

This thesis details part of a study into the degradation of a coastal slope in Christchurch Bay, England. The complete study, funded by the Science and Engineering Research Council (S.E.R.C), consists of two parts.

(i) A study of mass movement processes in a degrading cliff slope.

(ii) A water balance study in a degrading cliff slope.

Part (i) is the subject investigated in this thesis. Part (ii) has been studied by Dr R I Thomson in the Department of Civil Engineering, University of Southampton and is reported in Thomson (1987).

ACKNOWLEDGEMENTS

This research project has been performed with the help of many people. I am grateful to the Science and Engineering Research Council who awarded the research assitantship for this study. I would like to thank Dr Max Barton who has provided continual help and encouragement with the research, this thesis and my career in Geotechnics. My appreciation is also given to Mr Andrew Brookes with whom I shared the cold, mud and much enjoyment to collect the field data. I would like to acknowledge the assistance of Dr Bob Thomson, Mr Tom Pickett and Mr Brian Mould for both field and laboratory support. For the typing I am indebted to Mrs G Cooper for her prompt and speedy work.

Finally I would like to thank all my friends and colleagues who made my time at University so pleasant.

VOLUME 1

CONTENTS

ABSTRACT

PREFACE

ACKNOWLEDGEMENTS

CONTENTS

CHAPTER 1: AN INTRODUCTION TO SLOPE DEGRADATIONAL STUDIES

1.0 Introduction

1.1 The behaviour of slopes

1.2 Engineering geomorphology

1.2.1 The engineering geomorphology of slopes
1.2.2 Nomenclature of slope degradation
1.2.3 Slope evolution
1.2.4 The mechanics of degradation processes
1.2.4.1 Slides
1.2.4.2 Flows
1.2.4.3 Falls
1.2.5 Detailed site studies

1.3 The aims of the research project

CHAPTER 2: THE STUDY AREA

2.0 Introduction

2.0.1 Location
2.0.2 Topography
2.0.3 Coastal environment
2.0.3.1 The evolution of Christchurch Bay
2.0.3.2 Marine contours
2.0.3.3 Wave climate
2.0.3.4 Tides

2.1 The geology of the study area

2.1.1 Barton Clay
2.1.1.1 Stratigraphy
2.1.1.2 Depositional history
2.1.1.3 Composition of the Barton Clay
2.1.2 Plateau Gravel
2.1.3 Brickearth

2.2 The area of detailed study

2.2.1 Selection of the study area
2.2.2 Topography
2.2.3 Hydrogeology
2.2.4 Vegetation

2.3 Slope degradational processes

2.3.1 Bench slides
2.3.2 Mudslides
2.3.3 Mudruns
2.3.4 Debris slides
2.3.5 Cliff top failure-slumping
2.3.6 Spalling
2.3.7 Stream erosion
2.3.8 Human disturbance

2.4 The geomorphology of the whole undefended Barton Clay coastline

2.4.1 The topography and slope degradational processes
2.4.2 The area covered by each slope degradational process
2.4.3 Comparison between the study area and the total undefended undercliff

2.5 Conclusions

CHAPTER 3: THE FIELD RESEARCH

3.0 The field research

3.0.1 The data collected

3.1 The ground survey network

3.1.1 Previous surface movement monitoring
3.1.2 Survey method used at Highcliffe
3.1.2.1 The choice of method
3.1.2.2 Instrumentation
3.1.2.3 Stations
3.1.2.4 Survey method
3.1.2.5 The cliff top grid
3.1.2.6 Undercliff survey pegs

3.2 The subsurface investigation

3.2.1 Inclinometers
3.2.1.1 Installation
3.2.1.2 Monitoring
3.2.1.3 Tube applications
3.2.2 Slip indicatiors
3.2.2.1 Installations
3.2.2.2 Monitoring
3.2.2.3 Slip indicator performance
3.2.3 Surveying of exposures

3.3 The ground water regime

3.3.1 The preliminary ground water study
3.3.1.1 Installation
3.3.1.2 Monitoring
3.3.1.3 Piezometer performance

3.4 Monitoring of scarp slopes

3.4.1 Pin performance

3.5 Cliff top slumping

3.5.1 Field measurements

3.6 Field work limitations

CHAPTER 4: THE RESULTS OF THE FIELD RESEARCH

4.0 The field research

4.1 Landslide movements

4.2 Bedding plane shear surfaces

4.2.1 Shear plane locations
4.2.2 Surface movements
4.2.3 Benchslide movements

4.3 Mudslides

4.3.1 Shear plane location
4.3.2 Surface movements
4.3.3 Mudslide movements

4.4 Debris slides

4.4.1 Shear planes
4.4.2 Surface movements
4.4.3 Debris slide movement

4.5 Amphitheatre slide

4.5.1 Shear planes
4.5.2 Surface movements

4.6 The detection of shear planes in a degrading area

4.6.1 Shear planes in a degrading cliff

CHAPTER 5: MULTI-LAYERED LANDSLIDES

5.0 Introduction

5.0.1 Formation
5.0.2 Detection
5.0.3 Significance

5.1 Description of surface movements

5.1.1 Debris slide 1
5.1.2 Debris slide 2
5.1.2.1 Movements on debris slide 2
5.1.2.2 Movements on the ampitheatre floor
5.1.3 Other areas of multi-layered landslides

5.2 The analysis and presentation of surface movement with two or more components

5.2.1 Highcliffe data
5.2.2 Algebraic substraction

5.3 Theoretical surface movements on a two layered landslide

5.3.1 Translation of the surface layer
5.3.2 Surface movements on a pure rotational failure
5.3.3 Two layer movement
5.3.4 Debris slide 1 - Simulation
5.3.4.1 First Summer - simulation (S1)
5.3.4.2 First Winter - simulation (W1/1)
5.3.4.3 Significance

5.4 Conclusions

CHAPTER 6: THE COLLUVIAL BUDGET

6.0 Introduction

6.1 The budgetary study area

6.2 The budgetary system

6.3 A detailed description of the movement of landslide debris in the study area

6.3.1 Cliff Top to F Bench
6.3.2 F Bench to D Bench
6.3.3 D Bench to A3 Bench
6.3.4 A3/Mudslide B to Beach

6.4 Application of the budgetary analysis to the understanding and prediction of undercliff changes

6.4.1 Historic rates of movement
6.4.2 Rates of slide activity
6.4.3 Supply and discharge

6.5 Budgetary records

6.5.1 Fairy Dell, Dorset
6.5.2 Hadleigh, Essex
6.5.3 Dee Estuary, Lancashire

6.6 Factors affecting the colluvial budget

6.6.1 Geology
6.6.2 Topography
6.6.3 Climate

6.7 Conclusions

CHAPTER 7: THE APPLICATION OF THE FIELD RESULTS TO AN UNDERSTANDING OF THE STABILITY OF THE UNDERCLIFF

7.0 Introduction

7.1 Back analysis

7.1.1 Topography
7.1.2 Shear surfaces
7.1.3 Pore water pressures
7.1.4 Landslide debris density

7.2 The method of analysis

7.2.1 Back analysis
7.2.2 Spatial variation in pore water pressures

7.3 Stability analysis

7.3.1 Slump progression and the influence line technique
7.3.2 Stability zones
7.3.3 Influence lines on the D Bench
7.3.4 Conclusions

CHAPTER 8: DISCUSSIONS

8.0 Introduction

8.1 Surface movements

8.1.1 Toe erosion
8.1.2 Rainfall
8.1.3 Pattern of movement
8.1.4 Surges - their origin

8.2 Amphitheatre failure

8.3 Summary

CHAPTER 9: CONCLUSIONS

9.0 Methods of field study

9.1 Methods of desk study

9.2 Pattern of movement

9.2.1 Shear surfaces
9.2.2 Surface movements
9.2.3 Multi-layered landslides

9.3 Geomorphological processes

9.4 Debris budget

9.5 Stability calculations

9.6 The relation between the study area and the whole outcrop of Barton Clay

9.7 Summary.

VOLUME 2

TABLES

FIGURES

REFERENCES

APPENDICES

APPENDIX A: THE SURVEY METHOD AND ERRORS

A.0 Introduction

A.1 The survey method

A.2 The calculation of the theodolite position

A.2.1 Symbols
A.2.2 Equations

A.3 The calculation of the survey peg position

A.4 The survey errors

A.4.1 The cliff top stations
A.4.2 The errors in the position of the survey pegs

APPENDIX B: THE AERIAL PHOTOGRAPHIC COVERAGE AND THE CONTOURED MAPS OF THE BARTON CLAY CLIFFS

B.0 Areial photographic coverage

B.1 The contour maps

B.1.1 Preparation of the maps
B.1.2 Contour map information

APPENDIX C: BACK ANALYSIS AND STABILITY ANALYSIS PROGRAMS

APPENDIX D: THE F BEDDING PLANE SHEAR SURFACE

D.0 Introduction

D.1 Sampling site

D.2 Visual identification

D.3 Engineering properties

D.4 Mineralogy

D.5 Chemistry

D.6 Structure

D.7 Preliminary conclusions

APPENDIX E: THE DETAILS OF THE CROSS SECTIONS USED IN THE BACK ANALYSIS AND STABILITY ANALYSIS

APPENDIX F: THE FIELD INVESTIGATION

F.0 Introduction

F.1 Subsurface results

F.2 Inclinometer results

- F.2.1 Individual tube results
- F.2.1.1 I1
- F.2.1.2 I2
- F.2.1.3 I3
- F.2.1.4 I4
- F.2.1.5 I5
- F.2.1.6 I6
- F.2.1.7 I7
- F.2.1.8 I8
- F.2.1.9 I9
- F.2.1.10 I10
- F.2.1.11 I11

F.3 Slip indicator results

- F.3.1 Failure depths
- F.3.1.1 F Bench
- F.3.1.2 D Bench
- F.3.1.3 Amphitheatre
- F.3.1.4 Debris slide 3

F.4 Auger detection of shear surfaces

- F.4.1 Piezometer installation
- F.4.2 Debris slide 4
- F.4.3 Mudslide A

F.5 Surveyed shear surfaces

F.6 The application of the ground survey to surface movements

- F.6.1 The data collection
- F.6.2 The data calculations
- F.6.3 Division of the movement cycle
- F.6.3.2 The movement characteristics of the geomorphological processes
- F.6.4 Movement data notation

F.7 The overall pattern of surface movement

- F.7.1 First summer (S1)
- F.7.2 First winter, part one (W1/1)
- F.7.3 First surge (SG1)
- F.7.4 First winter, part two (W1/2)
- F.7.5 Second summer (S2 and SP2)
- F.7.6 Second surge (SG2 and SGP2)
- F.7.7 Second winter (W2 and SP2)
- F.7.8 Third summer (S3 and SP3)

F.8 The movement characteristics of the geomorphological processes

F.8.1 Benches
F.8.1.1 F Bench
F.8.1.2 D Bench
F.8.1.3 A3 Bench
F.8.1.4 Bench slide characteristics
F.8.2 Mudslides
F.8.2.1 Mudslide A
F.8.2.2 Mudslide B
F.8.2.3 Mudslide characteristics
F.8.3 Debris slides
F.8.3.1 Debris slide 1
F.8.3.2 Debris slide 2
F.8.3.3 Debris slide 3
F.8.3.4 Debris slide 4
F.8.3.5 Debris slide 5
F.8.3.6 Debris slide characteristics

F.9 General conclusions

CHAPTER 1: AN INTRODUCTION TO SLOPE DEGRADATIONAL STUDIES

CHAPTER 1: AN INTRODUCTION TO SLOPE DEGRADATIONAL STUDIES

1.0 Introduction

The area selected for study is one of the remaining coastal outcrops of argillaceous material in Southern England which has not been protected by coastal defence works. It is located on the coast of Christchurch Bay, 9km to the west of the Isle of Wight, Fig. 1-1. The coast line is comprised of Tertiary strata and the study area is located in an exposure of overconsolidated marine clay called Barton Clay. The action of marine erosion at the toe of the coastal slope has maintained an unstable slope profile which has proved suitable for field research into processes of slope degradation.

1.1 The behaviour of slopes

An understanding of the behaviour of slopes is of fundamental importance to Civil Engineering. Their performance during and after construction or in their natural state has widespread effects on people, structures and communications. In spite of many decades of detailed study, slope failures are still common.

In addition to the well publicized failures which have caused substantial loss of life e.g. Abervan, South Wales (144 dead) and Vaiont, Italy (2018 dead), there have been large numbers of slope failures which have caused severe disruption and have been expensive to repair. These have occurred in a wide variety of circumstances i.e. coastal landslips at Folkestone Warren, Kent which severely damaged the Folkestone to Dover railway (Hutchinson (1969) and Hutchinson, Bromhead and Lupini (1980)), failures in a man-made excavation e.g. Bradwell, Essex (Skempton and LaRochelle, 1965) and mudslide surges which discharge onto roads e.g. Antrim, N. Ireland (Hutchinson, Prior and

Stephens, 1974). Research is frequently undertaken to discover the cause and the knowledge gained should lessen the probability of similar accidents in the future.

The task of a Geotechnical Engineer in the field of slope studies can be summarised as follows:-

1. To assess the effects on a natural slope of a change in the stress conditions from the natural equilibrium state.

2. To design man-made slopes which are stable both during and after construction.

3. To recognize an area already affected by landslide activity and design accordingly.

1.2 Engineering geomorphology

The application of the study of earth surface processes (Geomorphology) to enhance the design of engineering works is called Engineering Geomorphology. It is a discipline which includes the study of fluvial, glacial and coastal processes and the evaluation of slopes.

1.2.1 The engineering geomorphology of slopes

The study of surface processes on slopes has taken place in a variety of environments and geological settings. However, research has concentrated on coastal sites where the action of marine erosion at the toe of the slope has maintained an unstable slope profile e.g. Hutchinson (1967, 1969, 1970, 1973, 1980 and 1983), Hutchinson and Bhandari (1971), Hutchinson and Gostelow (1976), Bromhead (1978 and 1979), Brunsden (1973), Brunsden and Jones (1976), Chandler (1972) and Prior (1977). Due to the

concentration of research work on coastal sites the discussion below reflects this trend.

Slope research can be divided into three categories:-

1. The evolution of the slope.

2. The mechanics of the processes which cause slope degradation.

3. The detailed study of individual sites.

Before these categories are discussed it is necessary to consider the nomenclature used to describe the various forms of slope degradation.

1.2.2 Nomenclature in slope degradation

The classification of the various types of failures on slopes has been generally based on three published systems i.e. Hutchinson (1968a), Skempton and Hutchinson (1960) and Varnes (1958, 1978). Of these three systems the earliest was published by Varnes (1958), this system being modified by a revision in Varnes (1978). The revised system is presented in an illustrative tabular form and differentiates between types of movement, types of material (before failure) and rates of movement. These three major subdivisions are shown in Table 1-1.

Hutchinson (1968a) introduced a classification system mainly based on the mechanism of movement and the morphology of the movement process. This system defined three broad categories of mass movement into which more specific forms of slope failures were divided. The three main categories were:-

a. Creep
b. Frozen Ground Phenomena
c. Landslides

Skempton and Hutchinson (1969) produce a classification system specifically for landslides on clay slopes. The identification and categorization of a slope failure was based on the shape of the moving mass in a down slope section at the time of failure. It is therefore dependant on knowledge of both the position and shape of the shear surface used by the slide. The basic type of landslides identified were divided into seven categories as follows:-

1. Falls
2. Rotational slides
3. Compound slides
4. Translational slides
5. Flows
6. Multiple landslides
7. Complex landslides

The three classification systems briefly described above have been used by many authors and is a common frame of reference to describe the type of mass movement which has occurred on a slope. Each system has approached the classification in a different manner; Varnes (1978) has produced a very descriptive/illustrative system which due to its generality does not provide a detailed definition in all areas. Five types of flows in 'earth' are described but landslides in 'earth' have only two categories either an earth slump or an earth block slide. In contrast the systems of Hutchinson (1968a) and Skempton and Hutchinson (1969) are both based on more definitive approach. Hutchinson (1968a) adopted mechanism and morphology which resulted in a definition of six varieties of slide movements. Skempton and Hutchinson (1969) gave greatest weight to the shape of the moving mass at failure

and expanded the types of slide failure to thirteen.

It is the greater variety of types of slide failure defined by Skempton and Hutchinson (1969) which has resulted in a greater usage of their classification system. Examples of adoption of this system are to be found in Prior and Stephens (1971), Muir Wood (1971), Sauer (1983) and Steward and Cripps (1983). In particular it is in the area of complex and multiple landslides where authors directly quote the nomenclature of Skempton and Hutchinson (1969), e.g. Sauer (1983), who describes a landslide in Saskatchewan, Canada as a 'retrogressive translation' failure. The system of Varnes (1978) has however not been ignored and Pack, Keaton, Jeppson and Anderson (1984) quoted the term 'earthflow' to describe the Thistle landslide in Utah, U.S.A.

In this thesis the labelling of the processes of slope degradation will be with reference to the system of Skempton and Hutchinson (1969) and each process will be described in detail to illustrate specific features.

1.2.3 Slope evolution

The evolution or development of a slope is determined by a variety of factors which can be grouped under two main headings:

(i) Characteristics of the slope
- Composition
- Location
- Geometry

(ii) Characteristics of surface processes
- Type
- Intensity

Publications which have discussed slope evolution have used variability in the composition of the slope, Bromhead (1979), location of the slope, Hutchinson (1983) and intensity of erosion at the base of the slope, Hutchinson (1967, 1973) and Hutchinson and Gostelow (1976) to discuss the various types of mass movements which occur. All the authors above have discussed either a coastal slope actively degrading or an abandoned coastal cliff.

Hutchinson (1967) and Hutchinson and Gostelow (1976) considered the development of coastal slopes in London Clay where erosion at the base or 'toe' of the slope had ceased. Hutchinson (1967) examined a large number of unstable coastal cliffs in London Clay and concluded that once abandoned the slopes degrade by a series of shallow and stepped rotational slips until the angle of ultimate stability against landsliding is reached. Hutchinson and Gostelow (1976) produced a detailed account of an abandoned cliff in London Clay at Hadleigh, Essex. The account included the development of the cliff since its abandonment and an analysis of the present day slope stability.

Hutchinson (1973) expanded his consideration of abandoned slopes by discussing which major degradational process would be present on a slope for different rates of erosion at the base. He concluded that the processes of mass movement would change from the shallow landslides of free degradation, where there is zero toe erosion, to extensive mudsliding, where erosion is in balance with weathering, and finally, to deep seated failure when toe erosion is more aggressive than weathering and rapid over-steepening occurs. With uniform lithology, within London Clay exposure, actual rates of cliff top erosion were quoted which should allow the prediction of the dominant form of degradation on a London Clay slope.

Hutchinson (1983) described another circumstance where

varying the balance between toe erosion and weathering of a slope would determine the major type of mass movement present. A variety of sites were detailed where a stiff-fissured clay overlies a more resistant stratum. The contact between the strata has a gentle ($\frac{1}{2}°$ - 2°) component of coastal dip. Five field examples were studied which indicate that a zone of mudsliding exists where the base of the clay lies within the tidal range and slope weathering is in balance with toe erosion. Up-dip of this zone the cliff slope is characterised by small slips and mudslides. Here a form of free degradation exists where there is no direct erosion of the base of the slope although debris is free to fall onto the beach and be removed. The slope is in the early stages of free degradation before the establishment of an accumulation zone at it's base. If the underlying competent strata can resist the marine erosion entirely then the clay slope would degrade until it reaches its angle of ultimate stability against landsliding. Down dip, marine erosion of the in-situ clay causes over-steepening of the cliff slope and major deep seated landslides occur. Here erosion of the base of the slope exceeds the supply of weathered material and in-situ clay is removed from the toe of the slope.

The common theme of Hutchinson (1967, 1973 and 1983) and Hutchinson and Gostelow (1976) is the balance between the supply of weathered material to the base of the slope and the removal of the material by marine erosion. The balance is shown to change both with varying rates of marine erosion and the location of the clay slope with respect to the zone of marine erosion and this balance determines the dominant agent of mass movement on the slope.

Bromhead (1979) attributed the dominance of the mudslide process on coastal slopes to sites where the material which forms the crest of the slope is similar in nature to

the rest of the slope. Deep seated rotational landslides occur where the crest is composed of a stronger or better drained material than the rest of the slope. The significance of the crest material and to a lesser extent the groundwater hydrology is based on whether a slope can maintain a 'mudslide barrier' which prevent erosion of in-situ material and hence over-steepening. In fact Bromhead (1979) has approached the balance equation from another angle and identified the composition of the slope crest as governing the supply of weathered material to the 'mudslide barrier' and again it is the balance between this supply and the rate of marine erosion which governs the dominant agent of mass movement.

To summarise both Hutchinson (1967, 1973 and 1983), Hutchinson and Gostelow (1976) and Bromhead (1979) have identified that the determinant of the main type of mass movement on coastal slopes is a balance between the rate of weathering within the slope and the rate of erosion at the slope base. The balance is affected by the composition of the slope, the location of the slope and the intensity of marine erosion.

1.2.4 The mechanics of degradational processes

In section 1.2.2 the generally accepted nomenclatures for types of mass movement are given. Within all three classification systems there are three fundamental types of movement.

(i) Slides
(ii) Flows
(iii) Falls

These will be discussed separately although there are areas of overlap.

1.2.4.1 Slides

Within the generic term slide there are several distinct types. They are all characterised by the movement of one body of material with respect to another along a clearly defined plane commonly called a 'shear plane'. It is beyond the scope of this thesis to detail the many advances in the study of slide phenomenon on slopes. Several publications summarize the state-of-the-art within both the areas of field research and stability analysis i.e. Bromhead (1987) and Chowdhury (1975). One of the fields however, that is worth detailing is the study of mudslides. Mudslides are common on degrading clay slope and have been researched in this thesis. They have been and still are often classed as 'mudflows' due to the common acceptance of the term. The study of mudslides is an example of the development of an idea from field observations, to a specifically designed piece of field research and finally to an accepted theory on the mechanism of mudslide movement.

The characteristics and the mechanics of movement of mudslides have been the subject of several publications i.e. Hutchinson (1970), Hutchinson and Bhandari (1971), Prior and Stephens (1971) and Hutchinson, Prior and Stephens (1974). Work has concentrated on the following aspects:-

(a) The characteristics of mudslides and their patterns of movement.
(b) The mechanics of movement.

Until Hutchinson (1970), the type of mass movement characterised by the movement of soil or rock fragments in a soft debris matrix had been generally labelled as either a debris flow or a mudflow: Johnson and Raha (1970). Detailed study of the mudslide at Beltinge, North Kent by Hutchinson (1970) has shown the presence of discrete

boundary lateral and basal shear surfaces which distinguish slide phenomena from flows. Hence the term mudslide has been adopted by several authors e.g. Bromhead (1979), Brunsden and Jones (1976) and Sidle and Swanston (1982). It should be noted that despite the identification of many mudflows as sliding mechanisms the term mudflow has persisted in use as a classification base on morphology of the movements as opposed strictly to its mechanism of movement e.g. Prior and Stephens (1972) and Barton (1973).

The pattern of movement of mudslides has been researched by Hutchinson (1970), Prior and Stephens (1971) and Hutchinson, Prior and Stephens (1974). Hutchinson (1970) recorded movements both on the surface and with depth, by installing inclinometer access tubes. The data recorded shows that the distribution of displacements on a vertical profile is nearly constant with depth. Surface movements indicated both slip at the lateral boundary and movement due to internal deformation.

Hutchinson (1970), Prior and Stephens (1971) and Hutchinson, Prior and Stephens (1974) also published records of surface displacements with time. All the publications concluded that the variation in the rates of movement, especially the high rates of acceleration, as witnessed by Hutchinson, Prior and Stephens (1974), were related to climatic conditions. In addition, Hutchinson (1970) proposed that pore water pressures were generated within the mudslide when rapid loading occurred from an upslope area and this would generate both rapid rates of movement and the movement of mudslides over slopes below the ultimate angle of stability as predicted by Skempton and Delory (1957).

Field evidence of the generation of pore water pressures by rapid loading of a mudslide by debris was published by Hutchinson and Bhandari (1971). Electrical piezometers

were installed into a mudslide on the Isle of Sheppey and after a period of rapid loading pore water pressures were observed greater than the 'normal' hydrostatic head. These readings, confirmed the theory of 'undrained loading' and established a mechanism for mudslide movement.

The above research into the characteristics of mudslides, their pattern of movement and the mechanics of movement have provided a good basis for an understanding of the process of mudsliding. The conclusion, by Hutchinson (1970), that high pore water pressures are generated by the rapid loading of a mudslide by debris and its confirmation by field work, Hutchinson and Bhandari (1971) has produced the now established theory of 'undrained loading'. This has been often quoted to explain the sliding movement of mudslide debris e.g. Chandler (1972) and Bromhead (1979).

1.2.4.2 Flows

The term flow has been frequently used in the classification of the processes of mass movement on degrading clay slopes e.g. mudflows and debris flows. These two processes have derived their names more from their morphology i.e. shape and form, than the mechanics of movement. As described in section 1.2.4.1 the process commonly termed a mudflow has been proven by Hutchinson (1970) to be a sliding form of mass movement and the term mudslide is now in common usage.

An alternative theory to the sliding process for mudslides has been discussed by Vallejo (1980). It should be noted that the basic assumption of Vallejo's that 'Mudflows consisting of a matrix of hard clay fragments or rocks with mud can be regarded as a mass of concentrated grains in a flowing medium' is flawed in that no evidence is

presented to confirm that the mudslide matrix is a flowing medium.

The calculations which follow used Bagnold's theoretical method of grain flow, Bagnold (1954, 1956), to explain the movement of the reported mudflows on low angle slopes. The lowest slope angles for mudflow mobilisation calculated by Vallejo (1980) compare well with those obtained in the field and published by Hutchinson (1970), Hutchinson and Bhandari (1971), Prior (1977) and Chandler (1972). The method of analysing mudflow modilization by grain flow theory was therefore put forward as an alternative to the theory of 'undrained loading', Hutchinson and Bhandari (1971) and also as an explanation of excess pore pressures observed by Chandler (1972) and McRoberts and Morgenstern (1974).

Whilst true flow movements are probably, in part, the result of mechanics similar to the grain flow phenomena detailed by Vallejo (1980), Vallejo omits to differentiate between material transported in a slide and a flow and fails to acknowledge field evidence of sliding, published by Hutchinson (1970). In addition, the cases described by Chandler (1972) and McRoberts and Morgenstern (1974) are both in areas of periglacial activity. Both of these accounts of mass movements include an explanation of the role of thawing ice within a mudflow and are examples of periglacial solifluction and therefore bear little direct comparison with the temperate mudflows of Hutchinson (1970). Vallejo's (1980) mechanics of mudflow movement therefore remain unproven and have not replaced the new established mechanics of sliding and 'undrained loading' in temperate mudslides.

True flow movement can occur where high moisture contents have caused the breakdown of the soil structure. The broken down soil is transported in suspension by water and only comes to rest when the soil particles fall out of

suspension due to a drop in fluid velocity. This process of transportation of material by a medium such as ice, snow, water or air has been termed mass transport by Hutchinson (1968).

This section has considered the mechanics of flow both from the standpoint of 'grain flow' being an alternative to sliding on low angled slopes in mudslides and that true flows are a form of mass transport and mass movement. It should be noted that in terms of slope degradation on coastal clay cliffs, as described by Hutchinson (1968b, 1970, 1973 and 1983) and Bromhead (1978 and 1979), the mechanism of flowing does not play a significant role.

1.2.4.3 Falls

The complete detachment of a discrete piece of material from a slope and its movement, by gravity, downslope is the third fundamental mechanism of mass movement in a slope. The isolation of the falling mass may have occurred due to either physical or chemical weathering within either an in-situ slope or a slope comprised of landslide debris. A description of falls within clay slopes is given by Skempton and Hutchinson (1969).

Particular types of falls are described by DeFreitas and Watters (1973) and Barton, Coles and Tiller (1983). DeFreitas and Watters (1973) detailed a specific kind of falling failure where the centre of gravity of a unit of rock or soil overhangs a pivot point within the unit. A block of material will then 'topple' forward and fall downslope. Barton, Coles and Tiller (1983) describe a mode of falling where material becomes detached, by weathering, from an in-situ face and falls onto an area of landslide debris below. This process is called spalling although it is synonymous with the falls of Skempton and Hutchinson (1969).

The mechanism of a fall is self-evident, in that, once detached from a slope the block will fall under gravity until it comes to rest on the ground below, probably after tumbling further downslope after impact. The reason for the detachment of the block is often not as clear. The elements which retain material within a slope are normally a combination of those listed below:-

(i) Physical
- Inter-particle friction
- Cohesion
- Negative pore water pressure
- Plant roots

(ii) Chemical
- Cementation

The overcoming of these elements will cause gravitational force to move the material to a more 'stable' location further downslope.

Skempton and Hutchinson (1969) noted that falls on clay slopes are generally insignificant and rarely described in the literature.

1.2.5 Detailed site studies

There have been many detailed investigations of individual sites of slope degradation and Table 1.2 lists 23 published examples. The studies vary in their location, their geology, their aims and the methods of investigation.

Two studies of potential significance to this research project detail methods of evaluating the volume of material transported by individual processes.

Rapp (1960) published a detailed account of both the

nature of processes acting within a degrading area and a table of the volumes of material transported by each process. Unfortunately the study was located in a mountainous region of Northern Lappland and any comparison with coastal clay slopes is very limited. Brunsden and Jones (1972), Brunsden (1973), Brunsden (1974) and Brunsden and Jones (1976) produced a series of publications on the coastal landslide complex at Fairy Dell, Dorset. They detail both historical and contemporary accounts of the development of this degrading coastline. In addition Brunsden (1973) presents the concept of a budgetary system, based on Fairy Dell, to describe the various components of slope degradation and this is put forward as a framework into which quantities of material could be added. Unfortunately, whilst details were given of a method to measure the volume of material contained within a mudflow system, no details of quantities were published.

Due to the variety of geology, topography and types of slope degradation it is difficult to identify a pattern in the site studies. The research studies eminate from both Geomorphologists and Engineers and this can lead to a different approach to a similar project. This difference in approach is well illustrated by two publications on two different coastal landslide complexes. An extensive account of mass movements at Folkestone Warren, Kent and Fairy Dell, Dorset were published by Hutchinson (1969) and Brunsden (1974) respectively. The former study includes details on the mechanism of the landsliding, correlation of the incidence of landslides and seasonal variations in piezometer levels and extensive slope stability analysis on a variety of cross sections throughout the complex. Brunsden (1974) presents several geomorphological maps to illustrate the evolution of the slope, selective data on small scale mass movements and changes in slope profiles with time. The 'Engineering' approach of Hutchinson (1969) is concerned with the mechanics of the mass

movement, the relationship between slope geometry and the state of stress within the slope profile and this knowledge may result in the ability to predict or even prevent further movement within the slope. The 'Geomorphologist' details the past, present and future form of the slope and describes the processes of degradation but there is no recourse to their mechanics.

The emergence of Engineering Geomorphology does indicate a need to quantify mass movement characteristics. It also requires constructive ideas on containing degradational processes where they disrupt engineering works. This approach was exemplified by Jones, Brunsden and Goudie (1983) when discussing the Engineering Geomorphology of roads in relation to route location through mountainous areas.

1.3 The aims of the research project

This thesis presents a detailed field study of a small representative length (270m) of degrading cliff slope. The aims of the study can be summarised as follows:-

1. To study the geomorphological processes which are responsible for the degradation of the slope.

2. To establish both the relative and absolute quantities of colluvium transported by each geomorphological process in a two year period.

3. To assess how the change of colluvial volume contained within the undercliff affects the stability of the slope.

4. To compare the study area with other sites described in the technical literature.

The fulfilment of these aims was based on the collection of field data. A considerable desk study had then to be undertaken to organise and use the data collected. The field study involved frequent site visits over a two year period. The methods, results and conclusions of this thesis are described in nine chapters.

The area studied is described with respect to the coastal environment, the geological setting, the topography and the geomorphology at the beginning of the field study in October 1980. The techniques and problems of obtaining details of the degradational activities are discussed.

CHAPTER 2: THE STUDY AREA

CHAPTER 2: THE STUDY AREA

2.0 Introduction

This chapter describes the topography, geology, geomorphology and marine conditions of both the area studied and the adjacent coastline.

In this thesis the location of any major coastal feature is described by a single easting value. The quoted easting, which defines a north-south grid line, is traced to where it bisects the coastline. This is considered to be a permissible method of location because a large proportion of the coast lies approximately east-west.

2.0.1 Location

The study area is located on a coastal exposure of the Barton Clay in Christchurch Bay, Hampshire. The exposure forms the sea frontage for two towns: Highcliffe and Barton-on-Sea (Fig. 2-1). Barton Clay is present along 4.8km of the coast and forms 31% of the length of the Christchurch Bay coast.

The lowest beds in the Barton Clay formation are found 1.2km east of Mudeford, at Cliff End, National Grid Reference (N.G.R.) 419625E. The dip, 3/4° ENE (Barton, 1973) results in the clay dipping completely out of sight at N.G.R. 424425E, 4.8km to the east, (Fig. 2-1a).

Within the Barton Clay coastal exposure a central section, 1.4km long, is undefended. Defences for the two flanking areas were built between 1962 and 1974. The undefended section is bounded in the west by a valley locally known as Chewton Bunny and in the east by the Barton-on-Sea strongpoint. The whole of the undefended section is actively degrading.

2.0.2 Topography

Around the coastline of Christchurch Bay the topography of the cliffs reflect the Tertiary beds from which they are composed. At Hengistbury Head the Bracklesham Beds lie on a deposit of resistant ironstone and the headland reaches a local coastal maximum elevation of 36m above Ordnance Datum (A.O.D.). Further east, at Mudeford, the Upper Bracklesham Beds form a 5m high, 80° cliff face. This is immediately followed by the Barton Clay and Barton Sand exposures which are characterised by gentler coastal slopes of 10° to 20°. Between Barton-on-Sea and Becton Bunny the lower Headon Beds form steeper 60° slopes, 25m high. To the east, at Milford-on-Sea, the cliffs are only 15m high. The coastline from Milford to Hurst Spit is entirely formed of shingle which rises to a maximum elevation of 5m A.O.D.

A detailed study of Christchurch Bay shows that 37% of the length of the coast has been protected by coastal defence works while natural coastal topography forms 63%. In the 4.8km Barton Clay exposure, 1.4km is unprotected.

Barton (1973) described the coast between Cliff End, Mudeford and Barton-on-Sea as a sequence of benches and scarps. He associated each bench with a bedding plane shear surface. The regime is illustrated in Fig. 2-2. The stratigraphic horizons which act as shear surfaces are active over the whole Barton Clay exposure. Barton (1973) identified 7 bedding plane shear surfaces, four of which were described as 'prominent'. Preliminary investigations into these preferred failure surfaces are discussed in Appendix D.

The Barton Clay exposure between Cliff End, Mudeford and Chewton Bunny can be divided into three sections (see Fig. 2-2a). The first is from Cliff End to N.G.R. 420530E; here the cliff slope is stable. A sandy beach exists above the

high water mark and wooded vegetation rests on a uniform slope at 140 and 15m in height. In the next section, N.G.R. 420530E to 421100E, the slope actively degrades although in 1966 a permeable wooden revetment was built from N.G.R. 420530E to Chewton Bunny. Mass movement is slow and the build up of debris masks the bench scarp topography. The higher slopes of the undercliff are heavily vegetated with shrubs and bushes from collapsed gardens. From N.G.R. 421100E to Chewton Bunny the coastal slope has been regraded. Vegetation is sparse and the newly formed terraces have been seeded. There is little evidence of degradation since the conclusion of the capital works in 1974.

The small river valley known as Chewton Bunny was extensively altered during the construction of the defensive works. The former surface stream is now piped the last 180m to the sea. Both sides of the valley have been reprofiled to a 25° slope.

To the east of Chewton Bunny the natural profile of the undercliff contains 3 bench/scarp systems (see Fig. 2-2b). The A3 bench is the lowest in elevation. It can be recognized to the east of the regraded valley slope of Chewton Bunny at a surface bench height of 10m A.O.D. The 3/4° ENE dip of the beds lowers the bench eastwards until at N.G.R. 422288E the bench disappears into the beach. The associated scarp has a maximum height of 4m at N.G.R. 421850E. The A3 bench is present over a length of 438m.

Above the A3, the D bench is also recognizable to the east of Chewton Bunny. It is 9m above the A3 bench at its western limit but does not develop as a constant feature until N.G.R. 422220E when the top of the bench is at 18m A.O.D. The D scarp has a maximum height of 8m and dips eastwards until N.G.R. 423080E when it merges with the beach: 1200m to the east of its initial exposure. The F bench does not become recognizable until N.G.R. 422210E at

26m A.O.D. and does not become a permanent feature until N.G.R. 422510E at 23.5m A.O.D. It is masked at N.G.R. 423120E, surface elevation 16m A.O.D., due to the start of the Barton-on-Sea defence works.

From Barton-on-Sea east the cliff profile is man-made and runs for 1.65km. The cliff height is constant at 32m A.O.D. until east of the defence works where it falls to beach level at Becton Bunny. Detailed information of the Barton-on-Sea coastal defence works is given in Chapter 7.

2.0.3 Coastal environment

The coastline of Christchurch Bay forms a 'crenulate' shaped bay. The curvature of the shoreline is greatest in the lee of the updrift headland, Hengistbury Head, and decreases uniformly in the direction of the downdrift headland; Hurst Spit.

The updrift headland is composed of the Bracklesham Beds overlying an ironstone deposit. Resistance of the ironstone to marine erosion has left a seaward extension of the headland called Christchurch ledge. This underwater ridge varies in width between 400m and 1200m and extends for a distance of 6km in a south easterly direction. The upper surface of the ledge shelves from an average depth of -2.5m A.O.D. at the coast to -12.5m A.O.D. at its seaward extremity.

From the headland 2km N.E. around the coast is the entrance to Christchurch harbour, the only harbour in the bay. The entrance to the harbour is formed from a sand and shingle spit which runs parallel to the adjacent coastline. The harbour entrance is locally known as the 'run' and its periodic change in position has been documented by Burton (1931). The rest of the bay is marked only by two small river valleys incised into the

coastline; Chewton Bunny and Becton Bunny, 4.75km and 8.25km east of Hengistbury Head respectively.

The downdrift headland is formed by Hurst Spit. The spit is mainly composed of Pleistocene gravel derived from the eroding coastline to the west. Shingle is carried eastwards by the longshore drift and deposited along the promontory. Little of the material enters the west Solent as the net tidal flow is south westerly.

2.0.3.1 The evolution of Christchurch Bay

The majority of published work on crenulate bay formation has been produced by Silvester (1960, 1972, 1974 and 1976). Whilst a detailed account on the theory of crenulate bay formation is outside the scope of this thesis, the discussion concerning the idealised bay formation and the formation of Christchurch Bay, as outlined by Wright (1981), is worth noting.

Wright (1981) compared the planimetric bay shape of six bays on the Dorset and Hampshire coasts with relationships established by Silvester (1972). Comparison of the conditions inherent in the formation of the idealised bay with those specific to the formation of Poole and Christchurch Bay differed from the idealised shape. These are summarised in Table 2-1. Wright (1981) suggested that the plan shape of Christchurch Bay exhibits two features which explained its recent evolutionary history:-

1. A straight section of shoreline between Hengistbury Head and the logarithmically curved bay.
2. The lack of rigid downdrift headland.

He speculated that these features indicated a parallel retreat, in plan, for the shoreline of Christchurch Bay in

a north north easterly direction. Furthermore, the bay was stable in shape but not in position. The conditions for this evolutionary trend were extended to include two types of headland behaviour.

(a) The updrift headland is subject to significant recession and the position of the downdrift limit of the bay is not rigidly controlled by a downdrift headland,

or

(b) Both the updrift and downdrift headlands are subject to significant and equal rates of recession.

The former case is found in Christchurch Bay where Hengistbury Head is subject to cliff recession and Hurst Spit has receded at an approximate rate of 4.3m/y between 1969 and 1980 (R. Nicholls, pers. comm.). These factors help explain the continual cliffline recession found around substantial sections of the bay.

In the longer term the continual recession of Hengistbury Head, if left undefended, could result in Poole and Christchurch Bay merging to form a single crenulate bay. The three hundred metre wide neck of land separating Christchurch Harbour and Poole Bay, when breached, would isolate Hengistbury Head into an island and Christchurch Bay would loose its rigid updrift headland.

2.0.3.2 Marine contours

Over the whole of Christchurch Bay the sea bed shelves southwards to reach a maximum depth of 22m below chart datum, 8.4km south east of Hengistbury Head. The mean depth of the bay is 7m below chart datum (Henderson and Webber, 1979).

Two areas of shallows exist. To the west Christchurch

ledge and to the east the Shingles. The ledge marks an abrupt drop in bed level to the southwest where the general bed level of Poole Bay is 19m to 20m below chart datum. North east of the ledge the bed slopes gently seawards from an average depth of 2m or less adjacent at the landward end of the ledge to a general level of 14m to 15m below chart datum adjacent at its seaward limit.

The Shingles is a deposit derived from Pleistocene gravels. It runs from a position 1km SW of Hurst Castle for another 5.6km in the same direction. It is shallower than Christchurch ledge and small areas dry out at low tidal conditions.

2.0.3.3 Wave climate

Waves are the principal agent for shaping the coastline, both by erosion and littoral drift. In Christchurch Bay the maximum fetch is 110km, south to Cherbourg. The largest waves, however, originate in the Atlantic and travel up the English Channel. The greatest wave heights are associated with south-westerly generated storms. The storms produce short period waves of less than 8s and wave lengths between 70m and 85m (Henderson and Webber, 1977).

Refraction of the waves can concentrate the wave energy onto certain points along the coastline. Henderson and Webber (1979) have indicated by numerical analysis that when south-westerly waves with a 9 second period are present the highest concentrations of wave energy occur at Hengistbury Head and the coastline at Barton-on-Sea, (Fig. 2-1).

These concentrations of wave energy directly contribute to the continual recession of the updrift headland, Hengistbury Head, and therefore maintain conditions which result in parallel retreat of the coastline in

Christchurch Bay (Wright, 1981). In addition, the focusing of wave energy on the coastline at Barton-on-Sea, enhances the degradation of a section of the bay where a relatively weak strata, the Barton Clay, is exposed.

2.0.3.4 Tides

The range of tides in Christchurch Bay is small; 2m at spring tides and 1m at neap tides. Storm surges can increase tidal levels by 1 metre. They are generated by conditions in both the North Sea and the N. Atlantic (e.g. 14 October 1976), Henderson and Webber (1977). This latter type of storm surge is associated with the large wind generated waves. The combined effect of a surge and large waves can be very damaging to the toe of the cliff. Large quantities of landslide material and in-situ material are removed from the beach. This process helps to maintain the unstable cliff profile.

2.1 The geology of the study area

The Barton Clay and the Barton Sand are part of the lower Tertiary deposits which form the coastline of Christchurch Bay. The sequence, exposed around Christchurch Bay from east to west, is

Headon Beds
Barton Beds - Barton Sand
- Barton Clay
Bracklesham Beds

Recent work by Melville and Freshney (1982) has combined the lower Headon Beds and Barton Beds into one formation: the Barton Formation. This formation is divided into four members: Hordle, Becton, Naish and Highcliffe. They correspond to the Lower Headon, Upper Barton, Middle

Barton and Lower Barton beds respectively. The lower and middle Barton Beds contain the Barton Clay and the Upper Barton Beds the Barton Sand.

2.1.1 Barton Clay

2.1.1.1 Stratigraphy

The oldest formation in the Barton series is exposed 1.2km east of Mudeford at Cliff End. Here the Barton Clay overlies a sand bed which has been given several names; the Highcliffe sands, Gardner, Keeping and Monckton (1888) and Gilkes (1968): the Mudeford Sands, Barton (1973) and the Upper Bracklesham Beds, Burton (1925, 1929, 1933), Curry (1958, 1965), Chatwin (1960), Melville and Freshney (1982). It is the latter name which is most applicable as the sand bed does represent the upper layer of the Bracklesham Beds. The top of the Bracklesham series is marked by a pebble bed 1.8m thick.

The exact position of the junction between the Bracklesham Beds and the Barton Beds has been defined differently by several authors. Early works by Gardner, Keeping and Monckton (1888) and Burton (1925, 1929, 1933) positioned the base of the Barton Beds 3m above the pebble bed on an ironstone band. This added 3m of green sandy clay to the Bracklesham series. Curry (1958) regarded the pebble bed as the natural marker bed between the Bracklesham series and the Barton Beds. This basal horizon has been quoted subsequently by Barton (1973), Hooker (1975) and Melville and Freshney (1982).

Gardner, Keeping and Monckton (1888) divided the Barton Beds into 3 zones. The Barton Clay was divided into the two lower zones and the Barton sand occupied all the upper division. Burton (1929) proposed a more detailed zonal classification for the Barton beds based on the relative abundance of byrozoan remains. Fourteen horizons, a total

of 18 zones, were listed. They were labelled A to L inclusive: horizons A1, A2, A3 and B forming the lower division. Horizons C, D, E and F the middle division and horizons G, H, I, J, K and L the upper division. Curry (1958) relisted these zones with some minor revision to the zonal thicknesses. Barton (1973) published a type section for the Barton Clay based on lithological features in preference to the palaeontological features used by Burton (1929). The thickness of each zone was revised using results from boreholes and levelling work. The type section divides the Barton Clay into eleven zones the same number as listed by Burton (1929) although Burton (1933) revised this to nine zones. Melville and Freshney (1982) returned to the Burton (1929) classification and zonal depths.

The total depth of the Barton members is listed in Table 2-2. The thickness of the clay formation is quoted as 32.5m to 35.3m by all the authors except Barton (1973). His revised depth of 46.4m resulted from the inclusion of the pebble bed (1.8m), substantial increases in the thickness of zones A2, C and D and the addition of a new clay zone labelled F2. Figure 2-3 illustrates the three published sections.

Survey work carried out by the author has substantiated part of the type section given by Barton (1973). The Barton Clay exposure in the study area ranges from A3 to F1 inclusive: the author has noted an inclusive thickness between these two beds of 23.5m. Barton (1973) indicates an inclusive thickness of 23.4m. The Barton Sand, not reviewed by Barton (1973), has a range of published depths between 27.4m and 29.3m.

2.1.1.2 Depositional history

The Barton Clay was deposited 50 million years B.P. during the fifth of seven cycles of sedimentation which took

place during the Eocene and Oligocene. These cycles deposited strata in four synclinal structures: the London Basin, the Hampshire Basin, the Paris Basin and the Belgium Basin. The sequence of deposition is given in Table 2-3.

The end of the fourth cycle was marked by the expansion of the sea filling the sedimentary basins. The lower Barton Beds were deposited in a marine environment. The sea became brackish during the deposition of the higher beds. The upper Barton Sands were sedimented in shallowing water which became a freshwater lake when the lower Headon Beds were sedimented.

The Barton Beds are not extensively exposed. Only the Hampshire coast and the Isle of Wight contain major exposures. The type section at Barton-on-Sea, Hampshire, has an estimated depth between 61.5m and 64.6m. The Isle of Wight deposits at Alum Bay are much thicker: 103m. The Barton Beds are not found in the London Basin or the Paris Basin.

2.1.1.2 Composition of the Barton Clay

Barton (1973) divided the Barton Clay into 11 zones. Each division indicated a change in lithology. Figure 2-4 illustrates the Barton Clay type section produced by Barton (1973). The particle size distribution for each zone from Kilbourn (1971) and Ho (1982) are given in Table 2-4.

The change in composition through the section does not show any trend, Fig. 2-5. There are sand rich zones A0, A3 and lower D. There are clay rich layers F1 and F2. Glauconite is present in the A0, A2, C and D zones. Within the section there are three layers of septarian nodules, a band of concretionary limestone and a bed of marly clay.

The mineralogy of the clay fraction was researched by Gilkes (1968) and Ho (1982). Gilkes (1968) produced estimates of mean clay mineral content for eight zones and Ho (1982) for two. These are listed in Table 2-5. The clay mineralogy throughout the Barton Clay section is very similar. Illite, Montmorillonite, Kaolinite and Chlorite are found in all the zones. Any change in material properties between the Barton Clay zones is therefore probably due to the different proportions of clay to silt to sand rather than the constituent clay minerals.

2.1.2 Plateau Gravel

The Barton Clay coastal outcrop is entirely covered with Plateau Gravel. The Plateau Gravel has a range of depths across the study area of 1.4m to 7m. It is free draining and often has a vertical or overhung slope.

It is not certain why the Plateau Gravel faces stand steeper than φ', which was reported as 50° by Bailey (1983). Negative pore water pressures are probably not generated due to the 'very high' permeability of the Plateau Gravel, reported by Barton and Thomson (1984), and the drying effect of the onshore winds. An element of cohesion may exist within the Plateau Gravel mass due to the presence of iron cement, Thomson (1987), although the characteristic iron staining associated with this type of chemical cementation is very localised on the exposed Plateau Gravel cliff top scarp.

Analyses by Keen (1980) of gravel collected from 9 sites in Southern Hampshire, which included both the Highcliffe and Barton-on-Sea exposures, has shown that 78% to 95% of the stones are flints. Quartz stones represent between 0.8% to 12.7% of the gravel and Greensand chert 0.8% to 3.8%. The flint stones were classified as subangular and the quartz as well-rounded. The bedding of the gravels,

Keen (1980), indicates a current orientation between 220°N and 340°N. This suggests an easterly flow of the current which deposited the gravels.

The origins of the gravel have been subject to much discussion. Theories advocating a marine origin (Corington 1870; Everard 1954), a fluvio-glacial origin (Kellaway 1971; Kellaway, Redding, Shepard-Thorn and Destombes 1975) and a fluvial origin have been proposed. The latest evidence discussed in Keen (1980) suggests the fluvial origin as the most plausible. It accounts for the bedding of the gravels, the constituents of the gravel and the pockets of Brickearth found in close association with many of the Plateau Gravel exposures.

The Plateau Gravel in the Highcliffe region is thought to represent the oldest of the gravel deposits accreted by the Solent river.

2.1.3 Brickearth

The Brickearth present above the Plateau Gravel is thought to be a flood plain loam (White, 1917 and Fisher 1971, 1975). Grain size analysis of fourteen samples (Keen, 1980) has shown the mean percentage grain size fraction for fine sand is 50%, for silts is 30% and clays 20%. At Highcliffe the presence of Brickearth is patchy. In the area of detailed study, defined in section 2.2, no Brickearth is present.

2.2 The area of detailed study

The undefended section of the Barton Clay coast contains seven active slope degradational processes (Barton and Coles, 1984). The distribution of these processes over the complete 1.4km of exposed cliff line is discussed in

section 2.4 and illustrated in Fig. 2-6. Initial field observations indicated that the detailed field studies would have to be restricted to a small section of the undercliff. The topography of the undercliff and the large number of individual geomorphological units present would prevent a comprehensive site investigation over the complete undefended exposure.

The applicability of a small area to the whole actively degrading undercliff is considered in section 2.4. The percentage area of coastal strip covered by each slope degradational process in the study area is compared to the geomorphology of the complete undefended section in September 1975 and November 1980.

2.2.1 Selection of the study area

The criteria for the selection of the study area were twofold:-

(1) To allow both the individual and the collective study of the geomorphological processes the area had to contain all the processes active on the undercliff.
(2) The area selected should ideally contain all three benches present in the undefended section of the coastline.

Two areas were selected for study. The first was used to monitor surface movements and for the study of the slope degradational processes. The area is bounded by N.G.R. lines 422080E to 422350E and 093100N to 093220N, (Fig. 2-7).

The criteria for choosing this 270m length of undercliff was based on the practical limit of data collection. The centre section of the study area contained two mudslides, described in section 2.3.2, and a large degrading cliff

top failure, section 2.3.5. In both the easterly and westerly directions lay areas of relatively flat undercliff. At both extremes of the study area, 422080E to the west and 422350E to the east, spurs of the in-situ Barton Clay extended into the study area. The western spur coincides with the outer edge of a debris slide, section 2.3.3, which had created an upstanding western rim. The eastern spur coincides with an area of periglacial activity, identified by Barton (1984). The spurs can be identified on the contour map, Fig. 2-7, at the extremes of the study area. These spurs effectively limit the visibility of the undercliff beyond and form a physical barrier to surveying the undercliff within an exceptable length of time i.e. a day, see section 3.1.2.1.

The second area is contained within the boundaries of the first. This smaller area, 200m long, is bounded by N.G.R. lines 422100E to 422300E and 093100N to 093220N, (Fig. 2-7). This area was used for the calculation of the colluvial budget in Chapter 7. The use of a second, smaller area for the volumetric calculations was required by the distribution of field data from the surface and sub-surface investigation.

In total 70m of undercliff were excluded from the eastern and western extremes where field data was sparse.

2.2.2 Topography

A map of the ground contours is shown in Fig. 2-7.

The three bench/scarp regimes are in three different stages of development. The F bench emerges on the western edge of the study area N.G.R. 422110E. It widens east to an identifiable maximum of 10m at N.G.R. 422210E. The

average bench width is 7.8m. Further east, the bench is ill-defined due to an anticlinal disturbance thought to be a valley bulge structure, Barton (1984). The associated in-situ F scarp is only exposed over 30m and has a maximum height of 2m. The exposure does, however, contain the F preferred bedding plane shear surface.

The D bench is prominent throughout the whole study area. It has a maximum width of 55m at N.G.R. 422245E, an average width of 46.4m and a maximum in-situ scarp height of 6m at N.G.R. 422222E.

The A3 bench is very near the level of the beach within the study area. There is no associated scarp present. The maximum bench width is 27m at N.G.R. 422080E; the average bench width is 15.6m.

In November 1980 the benches covered 67% of the surface area of the study region. Whilst all three have been formed by the activation of a preferred bedding plane shear surface the different levels at which they occur give them different characteristics. The F bench emerges at 26.5m A.O.D. and is only 2m to 10m wide. The landslide debris, from which it is formed, varies in thickness from 1.4m to 2.5m. The bench has a surface slope between 6° and 40° and is covered in partly degraded slump blocks and material derived from the Plateau Gravel. The in-situ F scarp is poorly exposed. Substantial areas of debris on the rear of the D bench mask the F shear plane. It is only exposed between N.G.R. 422180E to 422185E where an active debris slide on the rear of the D bench has removed the debris.

In contrast to the F bench, the D bench is wider, has a thicker layer of debris, is flatter and has a high prominent in-situ scarp slope throughout its length. The bench varies in width between 35m and 55m. The depth of rubble above the D shear plane is between 1.5m and 12.6m.

The surface slopes range between 1° and 12°. Debris on the D bench is well mixed and the surface covering of Plateau Gravel prominent on the F bench, is now intermixed into the clay. The in-situ D scarp provides the largest area of exposed in-situ clay in the study area, 830m^2. When landslide debris is moving across the bench the D shear plane is visible as a continuous line along the scarp.

The A3 bench is not as extensive as the D. Before it dips into the bench it is continuous with a width range of 7m to 22m. The depth of debris ranges from 1.2m to 3.5m: the surface slope from 2.6° to 21.8°. The debris is composed of clay scree from the in-situ D scarp, blocks of in-situ clay and bench rubble fallen from the D bench above. Plateau Gravel, whilst present, is well mixed into the clay debris. At the western extreme of the study area the low level of the A3 shear plane, at 2.55m A.O.D. is only 1.55m clear of the beach and the clearance decreases eastwards. The in-situ scarp is usually covered by debris which has moved across the A3 bench and has been pushed onto the sand. It covers the A3 scarp and A3 shear plane. It is only after heavy marine erosion that the scarp and the shear plane are both exposed, Fig. 2-8.

Imposed on the bench scarp regime of the study area are features which have resulted from the degradation processes. At the bottom of the clay top scarp gravel forms scree slopes away from the free standing face. They rest at a maximum angle of 40° and to a maximum height of 1.5m. Further downslope the scarp between the F and D benches is covered in landslide debris. These debris slopes rest between 13° and 30°: they occupy 17% of the study area.

In addition to degraded material, the undercliff also contains compound type landslides in various stages of degradation. Small failures, which have used the F shear

plane as a basal failure surface are numerous on the F bench. The largest slump block is 8.65m long and has a maximum width of 2.6m.

The D bench contains the remains of a very large slump. It failed between March 1977 and April 1978. Measurements from aerial photographs taken on the 6th April 1978 indicate that the slump was 42m long and 13m wide. This has degraded to form the rim of a large semi-circular depression known as the 'amphitheatre'. The degraded back tilted slump block has formed a ridge between N.G.R. 422160E, 093160N and 422210E, 093160N. The ridge marks the edge of the back scarp to the amphitheatre. This occupies 6.5% of the study area. It is characterised by a back scarp 7m higher than the floor of the depression. The ridge extends fully round to the west but does not enclose the eastern rim. The back scarp runs down into the floor of the amphitheatre by a 26° debris slope. The western rim is a steeper debris slope of 34° and in parts has a scarp face 4m high. Across the floor to the east the edge is marked by a mudslide channel together with a clump of vegetation situated on an old slump block. The amphitheatre floor coincides with the level of the eastern edge at 16m A.O.D.

Inside the amphitheatre the western and eastern boundaries are occupied by mudslide A and mudslide B respectively. Mudslide A has a surface pond and a surface slope increasing from 11° to 30° in a seawards direction. Mudslide B is larger, inclined to a maximum slope of 56° and has cut a channel into the in-situ material. The lower section of mudslide B is in the A3 bench. The debris moves across the A3 bedding plane shear surface at shallow surface angles of 8° to 11°. The amphitheatre is wholly in the D bench; its seaward boundary is the edge of the D scarp.

Slump blocks, totally within the debris, occur along the

edge of the D scarp. They use the D shear plane as a basal failure surface. These slumps can reach a maximum recorded size of 35m long by 5m wide.

The other major alteration to the regular bench scarp regime is an area of low cliff top elevation and periglacially disturbed material between N.G.R. 422260E and 422300E. The cliff top drops to 28.5m A.O.D. giving a difference in elevation of 3m compared to surrounding cliff top levels. This feature obscures the development of the F bench/scarp system until N.G.R. 422550E, 250m to the east of the study area. The structure and possible origin of this periglacial feature is discussed by Barton (1984).

2.2.3 Hydrogeology

The hydrogeology of the study area is complex. The movement of ground water is governed by three criteria. A comprehensive study of the hydrogeology in the study area has been carried out by Thomson (1987).

(1) The topography

Ground movements within the undercliff produces a continually changing topography. As a consequence preferred paths of ground water flow are subject to frequent alteration.

(2) The material through which the water flows

The variety of materials has produced a large range of permeabilities. Plateau Gravel provides a well drained stratum, the slip debris can provide a large range of permeabilities and the in-situ clay is poorly drained.

(3) The source of ground water

There are three main sources of ground water. Firstly, the main source is the Plateau Gravel

overlying the Barton Clay. Recent work by Thomson (1987) has shown that the water table falls rapidly towards the cliff face suggesting good drainage from the gravels to the undercliff. Secondly, there is ground water flow through the in-situ Barton Clay, Barton and Thomson (1984). Thirdly, water can enter the undercliff from direct rainfall. Since October 1982 meteorological data has been available from a weather station established in the Naish Farm holiday estate. It is located at N.G.R. 422720E. Data was collected weekly and has been being correlated with the ground water conditions in the cliff top and on the undercliff. The data analysis and correlation was performed by Dr. R.I. Thomson.

In the study area surface water is present in ponds. The surface area and depth of each pond varies with the seasons. There are six sites occupied by ponds in the study area. None are permanent and all six dried out in August 1981. The amount of ground surface covered by the ponds in November 1980 was 690m^2 (1% of the total area).

Only two surface streams are present. One flows over the saturated surface of mudslide A and the second to the east of the amphitheatre. Their rate of flow is seasonal but only small values have been recorded. In the drier months these streams cease to flow.

In addition to a ground water table the degradational processes have caused the build up of perched water tables. These are only temporary features due to the continual disruption caused by landsliding.

2.2.4 Vegetation

Despite continual material movements the study area has vegetational cover on the D bench and on the larger slump

blocks. This totals 12,540m²; 50% of the study area. The vegetation is mainly grass and only three areas have deeply rooting plants. All three vegetational clumps have originated from the cliff top. Their position within the undercliff results from the movement of the slump blocks after failure.

The presence of vegetation is discussed by Zaruba and Mencl (1969) who stated that vegetational growth has two functions: "the drying out of the surface and their consolidation by a network of roots". Within the study area the 50% of the ground surface which is vegetated will result in some drying out of the ground surface. However the absence of vegetation from the remaining 50% and the presence of mainly grasses, with shallow root systems, would imply that the effect of drying out on the water balance within the undercliff would be minimal. In addition the shallow roots would only 'tie together' a thin layer of debris and not penetrate the active shear surfaces which were generally in excess of 1m below ground surface.

2.3 Slope degradational processes

The study area contains all the major slope degradational processes which contribute to the movement of material within the undercliff. They are illustrated in Fig. 2-9 and examples are pictured in Fig. 2-10 to 2-16. The processes are not unique to the Barton Clay.

2.3.1 Bench slides (Fig. 2-10)

The movement of landslide debris across a preferred bedding plane shear surface is defined as bench sliding. The bounding shear surface is compound in shape (Skempton and Hutchinson, 1969); the horizontal part of the surface

conforms to a preferred bedding plane within the Barton Clay. The steeply sloping back surface is linked to the bedding plane section by a tight radius of curvature.

Movement across the bench transports material to a scarp face. The bench rubble is either pushed over the scarp by active bench sliding or is included in a separate rotational edge failure. The latter failure mechanism causes both greatly accelerated rates of movement at the front of the bench and a proliferation of tension cracks.

The three benches present in the study area covered 68% of the plan area in November 1980 and 61% in July 1982. They contain over 90% of the colluvium. Whilst the benches appear as uniform geomorphological units they do not have uniform rates of surface movement.

The term bench slide is used here to specifically describe the movement of colluvium over the preferred bedding plane shear surfaces. It should not be confused with lobate mudslides (Hutchinson, 1970) or debris sliding (Varnes, 1978). The mudslides present in the study area and those described by Hutchinson (1970), Hutchinson and Bhandari (1971) and Hutchinson, Prior and Stephens (1974) do not regularly use a bedding plane as a basal shear surface. They cut through various stratigraphic levels of in-situ material. Mudslide B presents an excellent example of this structure. Figure 2-16 illustrates the notch worn into the in-situ D scarp. This is the feeder zone. It has a maximum surface slope of 56°; the basal surface of the feeder zone cuts through the lower levels of zone D and the complete depth of zone, C, B and A3.

Another distinction between bench slides and mudslides is the moisture content of the debris. The debris within mudslides is wet and soft when it is most active.

Table 2-6 lists some typical moisture contents of

Highcliffe benches, Highcliffe mudslides and mudslides in the literature. The range of moisture contents recorded for mudslides is distinctly higher than for any of the three benches.

Debris slides are also present in the study area. They are distinguished from the bench slide because they are only active on steep slopes between 25° and 40°, are rarely more than 2m thick and never use a bedding plane as a basal shear surface.

The use of a bedding plane as a shear surface is illustrated in sections through the Miramar landslide (Bromhead, 1978), Folkestone Warren (Hutchinson, 1969), Fairy Dell (Brunsden and Jones, 1976) and Blackgang, Isle of Wight (Hutchinson, Chandler and Bromhead, 1981). However, apart from Fairy Dell the other three cases reflect a change from an incompetent to a competent sub-stratum. Only Fig. 13 (Brunsden and Jones, 1976) infers a shear surface consistent with the bedding but still within the Green Ammonite Beds. At Highcliffe only one of the seven of the bedding plane shear surfaces listed by Barton (1973) occurs at a junction between two stratagraphic horizons. The remaining six occur within a particular zone. Table 2-7 lists the positions within the Barton Clay. Appendix D presents the results from a preliminary investigation into the occurrence of these layers of weakness.

The stepped profile which is prominent in any Highcliffe cross section conforms to a series of successive slips, Skempton and Hutchinson (1969). However, the shear surfaces are all compound in shape and are not rotational as illustrated by Skempton and Hutchinson (1969), Fig. 2. A similar series of compound slides is illustrated in the Fairy Dell complex, Brunsden and Jones (1976).

2.3.2 Mudslides (Fig. 2-11)

Two mudslides are present in the study area. They are both lobate, have feeder zones in the D bench and discrete bounding shear surfaces which have no direct relation to the stratigraphy. In both form and material characteristics they can be identified with the mudslides described at Beltinge, (Hutchinson, 1970), Isle of Sheppey (Hutchinson and Bhandari, 1971), on the Antrim coast (Prior, Stephens and Archer, 1968, Prior and Stephens, 1971, Prior and Stephens, 1972 and Hutchinson, Prior and Stephens, 1974).

Mudslide A is contained entirely within the D bench. The basal shear surface slopes seawards parallel to the ground surface of the mudslide. The depth of the mudslide material is constant: five cross sections taken in January 1981 gave a range of maximum depth between 1.0 and 1.2m. Only at the seaward edge of the bench does the basal surface reach the in-situ clay.

Mudslide A is only comprised of one element and is not a two element mudslide of the Beltinge and Antrim type. It is similar to a feeder zone and has a surface slope between 11° and 30°. Mudslide debris is transported to the edge of the D bench and falls onto the A3 bench, 4 metres below. No link exists between the mudslide and the A3 bench. Material newly fallen onto the A3 bench coalesces with the bench rubble and is transported by benchsliding.

Figure 2-17 illustrates the plan shape of mudslide A. It has a maximum width of 20m and a maximum length of 48m.

Whilst mudslide B is the same geomorphological process as mudslide A it is physically different. It is a two zone mudslide with a feeder zone and an accumulation zone similar to the elements of the Beltinge mudslide described

by Hutchinson (1970). The feeder zone is enclosed in a gully cut through the D scarp and has a maximum slope of 56°. Seawards, the mudslide flattens into the accumulation zone and has a surface slope between 8° and 11°. The accumulation zone is located within the A3 bench and is bounded by distinct lateral shear surfaces. These lateral boundaries can easily be identified especially in the winter when the accumulation zone has been recorded as moving five times faster than the surrounding A3 bench.

A plan and cross section of mudslide B are given in Fig. 2-18 and 2-19. The mudslide has an overall length of 38m and a maximum width of 12m.

The location of the mudslides within the study area is thought by the author to be a result of ground water concentration. Although no signs of ground water issuing from the cliff top immediately above the positions of the mudslides were noted, the location of the mudslides at either extremity of a deep seated compound failure indicates the possible influence of the slumped block. This phenomenon has been noted by Hutchinson (1968b) and Bromhead (1979). Ground water is believed to pond behind the back tilted block of a rotational failure and then flow to either end where the ground water concentration reduces the strength of the landslide debris sufficiently to form a mudslide.

2.3.3 Mudruns (Fig. 2-11a)

A form of transportation process linked to the mudslide is the movement of fluidised mud which occurs after periods of heavy rain. The mud provides a superficial layer, 20mm to 30mm thick, which can cover a small proportion of the steepest slope of a mudslide. Material is carried downslope in suspension: the moisture content of a mudrun measured in April 1983 was 61%.

Kilbourn (1971) published an extensive list of index properties for the Barton Clay. The possible source of the particles, in the mudrun tested, ranges from zone C to zone F where the range of liquid limits is from 45% to 82%. The solid constituents of the mudrun have therefore exceeded their liquid limit and turned into a liquid state.

The process described as a mudrun, is a true mudflow which Varnes (1978) describes at 'the wet end of the scale of mudflows, which are the soupy end member of the family of predominantly fine-grained earth flows'. Zäruba and Mencl (1969) describe an earth flow as originating as follows, 'Heavy rainfall may trigger the movement of the loose mass which, in the form of a narrow flow, travels towards the foot of the slope forming there a loaf-shaped bulge'.

An example of a mudrun is seen in Fig. 2-11a. It occupied the upper 15m of mudslide B and can be seen to have stopped by the author's feet: this position coincides with an abrupt change in slope angle.

In the study area mudruns have only been noted on mudslide B. The total amount of colluvium moved by this process is negligible.

2.3.4 Debris slides (DS) (Fig. 2-12

On some steep slopes loose accumulations of debris form units of moving material. They are identified as debris slide and are characterised by the non-coherent nature of their movement. Within the Skempton and Hutchinson (1969) classification, debris slides would be included in the general group of slides in colluvium. Examples are described by Sidle and Swanston (1982). There were five debris slides present in the study area at the end of the field investigations in July 1983; three became active

during the field study. They exist on slopes between 25° and 40°.

A debris slide is composed of both scree and colluvium. Figure 2-6 indicates the position of the five debris slides. Two DS1 and DS4, are composed primarily of bench rubble from the F bench. DS2 and DS5 are composed of rubble from the degrading back scarp of the amphitheatre. DS3, the largest debris slide, is composed of material direct from the cliff top scarp where the local rate of recession was 6m in 21 months, between November 1980 and July 1982.

The debris forms a thin layer, rarely more than 2m thick, which terminates downslope in an identifiable over-turned toe or snout. During movement the accumulated debris can undergo internal rearrangements and occasionally the underlying straited shear surface is exposed, Fig. 2-20. At Highcliffe all the slides terminate where the scarp slopes flatten out onto the D bench (DS1, DS3 and DS4) or onto the amphitheatre floor (DS2 and DS5).

The prime distinction between the debris slides and mudslides observed in the study area is the cohesionless nature of the material contained with the debris slides and highlighted in Fig. 2-20. This contrasts with the material contained within MSA and MSB which was identified as similar to the 'plug' form highlighted by Hutchinson (1968b) in the Beltinge Cliff, N. Kent.

Close study of bench areas near scarp slopes has allowed the identification of relic debris slide toes. The overturned relic snouts are vegetated in contrast to the bare snouts of active slides. Fresh slides can override these relic forms and produce an area with two or more dormant shear surfaces stacked one upon another (Fig. 2-12a).

Debris slides have been commonly identified elsewhere. Varnes (1978) distinguished between the debris slide, flow and avalanche. The slide "breaks up into smaller and smaller parts as it advances towards the foot, and the movement is usually slow". Slow is defined as a movement rate between approximately 4mm and 40mm a day. Debris slide DS1 has exhibited a range of summer movement from 3 to 11mm a day and a winter range from 21mm to 49mm a day.

2.3.5 Cliff top failure - Slumping (Fig. 2-13)

The first time failure of an in-situ scarp slope, along a compound type shear surface has been a cliff top slump by Barton, Coles and Tiller (1983). The scarp failure displaces colluvium at its toe.

The bounding shear surface comprises of a near vertical back surface which drops to a level near the basal surface of the slump. The linking surface has a tight radius of curvature and joins to a preferred bedding plane shear surface which acts as the basal failure zone. The bedding plane shear surface chosen is the preferred bedding plane shear surface (Barton, 1984).

The cliff top slump is the major form of cliff top recession along the study area coastline.

Slump blocks of various sizes and states of disruption can be identified throughout the width of the study area. They usually remain back tilted after the initial failure. The amphitheatre back scarp is formed from the leading edge of a cliff top slump.

Individually the slumps are similar to the single 'retrogressive' slides illustrated by Hutchinson (1969) at Folkestone Warren. Although at Highcliffe they usually degraded too rapidly to form a true "multiple

retrogressive" zone illustrated by Skempton and Hutchinson (1969). The Highcliffe slumps would fall into the category of earth slumps, Varnes (1978). Rib and Liang (1978), Chapter 3, list four slump characteristics, all present within the study area.

(1) Tension cracks near the head of the slump.
(2) Back rotation.
(3) A zone of compression where material is compressed by the load above and there are no open cracks.
(4) Long transverse ridges beyond the foot of the slumps separated by tension cracks.

Slumps have additionally been described by Bromhead (1978), Brunsden (1974) and Brunsden and Jones (1976). The degraded relicts of cliff top slumps in the Dorset Cliffs are called landslide blocks by Brunsden and Jones (1976) who describe there evolution through the coastal slope.

Statistical data on the size and location of cliff top slumps along the Barton Clay outcrop is given by Barton, Coles and Tiller (1983).

2.3.6 Spalling (Fig. 2-14)

All the scarp slopes are subject to weathering processes. These processes cause material to fall or topple from a scarp face and produce a build up of scree or talus.

At Highcliffe the weathering processes are mainly:

(i) Changes in moisture content with accompanied shrinkage and swelling.
(ii) Changes in temperature.
(iii) The physical effect of rain wash.
(iv) Wind erosion, especially at the cliff top where

wind speed can be very high.

The rate of scarp recession caused by spalling has been monitored both in the clay and the gravel scarps. Higher peak localised rates have been observed where fresh slumping and the accompanying stress relief has occurred.

The build up of scree at the base of a scarp face will protect the bottom of the face from the weathering processes. Therefore a scarp slope degrading purely by spalling may slowly flatten.

In the study area the movement of colluvium does not allow such an accumulation and no appreciable flattening of the cliff slope occurs.

Brunsden and Jones (1976) suggested that the recession of the scarp at Fairy Dell, Dorset by weathering processes was of considerable importance. Measured spalling rates gave an average spalling rate of 0.15m/yr compared to an overall range of cliff top retreat from 0.34m/yr to 1.4m/yr. At Highcliffe data collected between 21 May 1981 and 13 July 1983 has produced an annual spalling rate for the plateau gravel of 0.12m/yr compared to a cliff top recession rate, over approximately the same period, of 0.6m/yr.

2.3.7 Stream erosion (Fig. 2-15)

The erosion and transport of materials by running water has a negligible effect within the study area. No permanent streams cross the undercliff and only during very heavy rainfall does water flow down clay scarps and move argillaceous debris.

2.3.8 Human disturbance

The whole of the undefended section of the undercliff is subject to disturbance by human activity. People walk the area both in the cause of scientific research and the pursuit of personal pleasure. The extent of the disruption is impossible to quantify. However, the two activities which probably cause the largest disturbance are:-

(1) The trafficking of loose debris slopes. This causes the movement of material downslope.
(2) The excavation of in-situ material for engineering and palaeontological purposes.

Whilst these activities can appear to contribute significantly to the overall degradation of the undercliff the amount of material affected is negligible compared to the total volume of colluvium within the undercliff. This was estimated to be 80,150m^3 (Barton and Coles, 1984) within the 25,870m^2 study area.

2.4 The geomorphology of the whole undefended Barton Clay coastline

In section 2.2 details are given of the study area. This portion of the undercliff represents 22% of the surface area of the whole undefended section. Before describing the research techniques and results it is important to discuss how representative the study area is with respect to the remaining 78% of the undefended coastline.

2.4.1 The topography and slope degradational processes

The basic topography of the whole undercliff is governed by the outcrop of the bench and scarp regimes described in

section 2.0.2. The remaining topographical features and geomorphological features are imposed on this basic form. The study area should therefore contain approximately the same proportions of characteristic features.

Seven slope degradational processes have been identified in the study area. Field observations across the remaining undercliff have shown that there are no other significant slope degradational processes.

2.4.2 The areas covered by each slope degradational process

The surface area covered by the main geomorphological features are listed in Table 2-8. The table was compiled by two methods.

(1) Total undefended undercliff

Vertical stereoscopic photographs were studied to divide the undercliff into individual geomorphological units. These were drawn on base maps, at 1:2500 scale, provided by the contour maps dated 5th September 1975 and 26th November 1980.

(2) Study area

Field observations of the study area enabled the areas covered by each geomorphological unit to be drawn onto base maps. Two maps were drawn: the first for the 26 November 1980 and the second for July 1982.

2.4.3 Comparison between the study area and the total undefended undercliff

Table 2-8 allows 5 points to be made concerning the areas covered by the different geomorphological processes.

(1) The study area covers 22% of the undefended undercliff.

(2) The proportion of area covered by bench slides is similar for the total undercliff and the study area. On the 26th November 1980 67% of the study area was covered by a summation of the individual areas covered by the A3, D and F benches. At the same time 68% of the total undefended Barton Clay coast was covered by bench slides.

(3) Field study of debris slides in the study area has identified an average coverage of 20% in November 1980 and July 1982. This greatly exceeds the average 3% identified in the complete undercliff from photographs for September 1975 and November 1980. If, however, the areas covered by scarp slopes and debris slopes are combined the percentage coverage is similar for both the study area and the total undefended cliffline. This anomaly is caused by the difficulty in distinguishing between scarp slopes and debris slides on the aerial photographs. The vast vertical exaggeration seen through a mirror stereoscope masks the distinguishing features of debris slides and scarp slopes.

(4) The area covered by both surface water (ponds) and mudslides is small. Neither exceed 3% and similar proportions are present in the study area and the complete undefended section.

(5) The proportion of area occupied by individual benches reflect the position of the study area along the undercliff. The detailed area has a low proportion of the F bench, a slightly elevated proportion of the D bench and a larger percentage of the A3 bench than the overall undefended undercliff.

The study area therefore contains each geomorphological process in the same proportions as the rest of the undefended undercliff. It can therefore be considered to be representation of the undefended coastline.

2.5 Conclusions

The coastline of Christchurch Bay has been formed primarily by the action of wave erosion. The geology of the strata around the bay has promoted conditions where parallel retreat of the coastline would occur if the coast was left undefended from marine attack. A 1.4km section of the Barton Clay near Highcliffe has been left with no sea defence works and erosion of the exposed strata is taking place. The weathering of the coast slope is being caused by a variety of degradational processes. Within the 1.4km length of coast actively eroding a 270m long section has been chosen for study. The study area contains all the geomorphological processes responsible for the degradation of the slope.

Early work by Barton (1979) and Barton and Coles (1984) has identified seven preferred bedding plane shear surfaces within the whole exposure of the Barton Clay and three within the study area. The presence of these surfaces dictate the topography of the coastal slope and their regularity makes the site suitable for the calculation of the volumes of debris occupying the study area. Together with research into the other processes on the slope this will enable a volumetric budget to be calculated for degrading slope.

CHAPTER 3: THE FIELD RESEARCH

CHAPTER 3: THE FIELD RESEARCH

3.0 The field research

To enable the aims of the research project, outlined in Section 1.3 to be fulfilled a considerable quantity of field data has been collected. The field research has adopted both traditional methods of studying degrading slopes and devised new techniques of investigation.

Central to the study of the degrading slope was a comprehensive survey network to monitor the surface movements of all the active processes on the slope. This was supported by investigations into both the water level regime within the undercliff and the depth of active shear planes.

3.0.1 The data collected

The collection of field data was required to understand the mechanism of the slope degradational processes and to estimate the volume of landslide debris which entered, traversed and left the study area. These latter three aspects were studied as follows:-

(1) Input
Material enters the undercliff from the weathering of in-situ material. Four processes, spalling, toppling, cliff top slumping and deep seated compound failures account for all this input. All four forms of degradation were monitored over the complete study period.

(2) Undercliff Activity
The movement of colluvium across the undercliff was monitored by a comprehensive network of surface survey pegs. Regular ground surveys were carried out to evaluate surface movements. The positions of

active shear surfaces were found by the installation of inclinometers, slip indicators and the survey of exposures.

(3) Output

The movement of material out of the study area and onto the beach was estimated by the ground surveys, the sub-surface investigation and the study of contoured aerial photographs.

3.1 The ground survey network

3.1.1 Previous surface movement monitoring

The study of surface movements in landslide areas can determine both the extent of the activity and the rate of movement of a degrading slope. Where landslide activity is suspected the rate of change of surface movement can in some circumstances give a warning of catastrophic failure (Saito, 1965).

Table 3-1. summarises some field investigations where surface movements have been recorded.

3.1.2 Survey method used at Highcliffe

3.1.2.1 The choice of the method

The list of survey methods given in Table 3-1. shows two distinct approaches to the measurement of surface movements. Penman and Charles (1974) and Burland, Longworth and Moore (1978) used theodolites and precise levelling techniques to produce a surface network accurate to ±1mm. These methods were developed and used in projects where both the location and resources allowed the application of expensive techniques. In contrast Prior, Stephens and Archer (1968) and Hutchinson (1970) used

tapes and dumpy levels which are simpler, quicker, less expensive and more suited to 'rough' locations. Naturally these latter techniques yield less accurate results, quoted as ±15mm by Hutchinson (1970).

The choice of survey technique used at Highcliffe was governed by the following five constraints.

(1) The site

The survey technique had to allow the measurement of surface movements over 32,400m². The only stable ground was the cliff top. The site was exposed and accessible to the general public and therefore continuous monitoring equipment could not be left unattended.

(2) The range of movements.

This was anticipated to be from zero for an in-situ exposure, to a maximum of 250mm/day on a mudslide. This is comparable to the mudslide movements recorded by Hutchinson (1970).

(3) Required accuracy.

The results of the ground survey work were used to calculate the volumes of material which moved across the undercliff by each geomorphological process. The calculation of both the areas covered by these processes and the depths to which they were active cannot be measured to a high order of accuracy. The surface movement did not, therefore, need to be very precise. A standard error of 15mm was chosen as a target figure: this is comparable with the work carried out by Hutchinson (1970).

(4) Available equipment.

An Electronic Distance Measurement (E.D.M.) apparatus and a 10 second theodolite were made available. Over seventy survey pegs were manufactured to allow a comprehensive ground coverage.

(5) Time

A ground survey had to be completed in one day and by

not more than two operators.

Within these constraints three survey techniques were considered.

a/. The theodolite - E.D.M. station could be set up over a series of permanent cliff edge stations on the stable cliff top. This would provide firm ground for the tripod to be erected and would lessen the number of instrument readings. Sightings would be taken directly onto the undercliff pegs.

There are two disadvantages. Firstly, the cliff edge is often subject to an onshore wind. During the winter months this would frequently make the cliff top stations unusable. Secondly, there are blind spots on the undercliff irrespective of the cliff top position adopted.

b/. The theodolite - E.D.M. station could be set up over each survey peg in turn and sightings taken back to the permanent cliff top stations. This would probably provide the most accurate method of peg location. Each survey marker being individually triangulated.

Again there are two disadvantages. Firstly, over 50% of the survey pegs are located on sites with either an inclination greater than 20° or comprised of very loose debris. Stable instrument erection would be impossible. Secondly, the time taken for seventy individual instrument set-ups would be prohibitive.

c/. The theodolite - E.D.M. station could be erected on the undercliff on a site which is firm, level and enables all the survey pegs to be seen. The instrument would be located relation to the cliff top by sightings to the cliff top stations and then each survey peg could be located with a single sighting. The wind on the undercliff is much less than that at the cliff top. The

complete survey is possible in a single day.

There are two disadvantages. Firstly, there is always a risk of movement on a landslide complex even on a flat and firm site. Secondly, the need to position the instrument relative to the cliff top grid and then locate the survey pegs relative to the instrument must result in the accumulation of survey errors.

These survey errors were believed to be within the target of required accuracy (± 15mm) and on balance it was decided to use this method, because of its advantage in speed, as the only practical solution.

3.1.2.2 Instrumentation

To allow the measurement of horizontal angles, vertical angles and distances from the same instrument a combination of Wild T1-A theodolite and Kern DM102 electro-optical distance meter was used. The theodolite can be directly read to 20 seconds and estimated to 10 seconds. It is fitted with a telescope adaptor to receive the distance meter. Distances are measured to a telescopic hand held rod fitted with a cube reflector and target. The Kern DM102 has a range of 1000 metres with a single reflector and an accuracy of ±(5mm + 5ppm) mean standard error.

3.1.2.3 Stations

(i) Permanent cliff top stations

During the first period of surveying the cliff top grid contained five permanent stations, A1, B1, C1, G1 and H1. After two notable cliff top slumps on the 16 February 1982 and the 18 March 1982 an additional five stations were

added to enable the survey grid to be preserved if any of the original stations failed. In November 1982 two extra stations were constructed to allow a better estimate of the accuracy of the survey technique.

Each station was constructed from a 600mm length of 12mm diameter reinforcement bar. This was driven into the Plateau Gravel and concrete was poured around the bar to form a 200mm x 200mm x 100mm deep base. The top of the bar had to be below ground surface to prevent damage occurring to the grass cutting equipment of the holiday estate. To locate the tapered point of the prism pole the reinforcement bars were machined to allow a positive fit.

(ii) Field survey pegs

The majority of the survey pegs used in the field were manufactured from tubular steel. Initially wooden pegs with a 50mm square section and a length of 300mm had been installed. They were painted to enable easy location and identification. Unfortunately the ease of location meant an unacceptable loss due to vandalism. In addition the chain man found difficulty in locating the prism pole on the wooden peg when it had become inclined.

To eliminate these problems in June 1981 steel pegs were installed. They were constructed from 500mm long scaffold poles with a 100mm outside diameter. The peg was driven 450mm into the undercliff. To each pole a 20mm diameter nut was welded at one end and the pole was numbered with weld flux. The nut allows positive location of the tapered prism pole: the weld flux number did not erode and its numerical value could be found by tactile means if visual identification proved difficult. Weathered steel, whilst not exactly the same colour as the landslide debris, proved inconspicuous and, even if located, the long poles were difficult to remove. Relocation of pegs by the survey team had to become a matter of accurate

field description instead of visual identification.

3.1.2.4 Survey method

The survey pegs were located on a three dimensional network based on the permanent cliff top grid.

The instrument was set up on the undercliff where both the cliff top stations and the survey pegs to be located could be seen. One site was normally sufficient for all the routine observations. At the beginning of the survey readings of inclined distance, vertical circle and horizontal circle were taken to all visible cliff top stations. Each undercliff survey peg was then observed in the same manner. During a survey, with a normal duration of five hours, sitings were taken to a temporary reference station on the cliff top to check the instruments stability. This check was performed after every ten survey peg locations. At the end of the survey the cliff top positions were reobserved.

3.1.2.5 The cliff top grid

A full explanation of the calculation of co-ordinates for the survey pegs is given in Appendix A.

The basis of the cliff top grid, in metres, is the allocation of site C1 with the arbitrary co-ordinates 500X, 100Y, 50Z and the selection of the line between C1 and B1 as the Y axis. Station B1 therefore has a Y co-ordinate of 100. The choice of an arbitrary set of grid co-ordinates, as opposed to the ordnance survey system, was required due to the difficulty of accurately measuring the O.S. co-ordinates of the permanent stations. The transfer of the co-ordinates from the nearest precisely located point at Barton-on-Sea, 4km to the east,

was thought too time consuming. Accurate location of the permanent stations by the Nesbitt method of resection (Admiralty, 1970) was impossible due to the poor location of resection points. Only those on the southerly side were visible and the large break between the Isle of Wight and Hengistbury Head restricted the choice of resection triangles Fig. 3-1.

The allocation of arbitrary co-ordinates caused no restriction in the usefulness of the survey work as the movements recorded only needed to be relative to a fixed datum, not to a national reference grid.

To establish the permanence of the cliff top station triangulation surveys were carried out during the study period. Survey stations were established inland, beyond the influence of the cliff instability. The triangulation co-ordinates for the two cliff top stations which form the basis of the undercliff network are given in Appendix A. The maximum variation in any co-ordinate was 6mm. The accuracy of the triangulation was 1st to 2nd order for the unadjusted horizontal distance and 2nd to 3rd order for the unadjusted horizontal angles (Bannister and Raymond, 1975).

3.1.2.6 Undercliff survey pegs

The survey pegs within the undercliff were positioned to provide information on the movements of the geomorphological processes present. The distribution of the survey pegs was not on a regular grid.

This system allowed areas with a uniformity of movement, such as the D bench, to be thinly covered. Areas with a wide range of rates of movement could have a denser coverage. Over the two year study period 151 peg positions were used. Twenty five pegs survived the

complete two year cycle. At any one time a maximum of 70 pegs were in use.

3.2 The subsurface investigation

To enable the calculation of a degradational budget the position of the shear planes within the landslide complex is needed. The research project used three methods to locate these failure surfaces.

(1) Inclinometers
(2) Slip indicators
(3) Survey of exposures

Due to the inaccessibility of the undercliff to powered vehicles the installation of all instrumentation was carried out by hand. Ten out of eleven inclinometers and fourteen of the slip indicators were installed into hand augered boreholes. The restrictions of hand augering were found to be two-fold.

(i) The maximum depth of any borehole was limited to 5.5m. This could only be achieved under 'ideal' ground conditions. Where the debris was loose or very wet, collapse of the borehole was common at depths greater than 3 metres.

(ii) It was impossible to hand auger through gravel lenses.

These limitations meant that the preferred bedding plane shear surfaces could only be pierced on the A3 bench and in the frontal area of the amphitheatre. The minimum depth of the debris elsewhere on the D bench was 6 metres and the F bench was covered in gravel debris.

3.2.1 Inclinometers

An inclinometer allows the measurement of horizontal ground movements. A shear surface is the junction between two layers of soil or rock which are moving at different rates. If an inclinometer tube is placed across this junction the different rates of ground movement at different depths causes distortion of the tube and allows the location of the failure zone.

The early development of the inclinometer has been described by Ward (1948), Wilson (1959) and Bromwell, Ryan and Toth (1971). The deficiencies of these early models were highlighted by Green (1973). Two models, a SINCO Wilson 200B Series Slope Indicator and a Soil Instruments Mk 1 Inclinometer, were performance tested on a calibration frame. He concluded that whilst the accuracy was acceptable for most engineering purposes there was a lack of robustness and subsequent reliability.

Hutchinson (1970) described in detail the design and performance of an inclinometer manufactured to negotiate tight bends in flexible inclinometer tubing. Both the instrument and tubing were developed to measure the velocity profile in mudslides where, due to the low shear strength of the soil, a conventional tube would be too stiff to accurately represent the subsurface movements. Hutchinson noted that in this particular design inclinometer accuracy, quoted at ±20', was sacrificed to achieve an ability to negotiate bends in the tube down to a radius of 1m. In contrast the inclinometer used in this research project, a Soil Instruments Mark III, was marketed as being accurate to ±2' although it could only negotiate a tube curvature of 3m radius.

The improved field performance of modern instruments was illustrated by Maugeri, Costa and Ranadazzo (1981) who achieved a standard error of 0.7mm over a 25m hole using

an Italian manufactured instrument. Barton and Coles (1983a) recorded a standard error of 0.1mm over 1m, ±0.34', using a Soil Instrument Mark III Inclinometer over a three year period.

3.2.1.1 Installation

During the study period ten inclinometer tubes were installed in the undercliff and one in the cliff top. The ten tubes in the landslide areas were installed in hand augered boreholes. One inclinometer was inserted in a 9 metre borehole drilled by a powered borehole rig.

A typical undercliff inclinometer installation took a complete working day. When a suitable drilling site had been selected (an area with an absence of gravel) the team started to auger a hole using a 6" auger bucket. Drilling was continued until progress became very difficult. A 4" bucket was then used until no more progress was physically possible. The physical limit was reached when no increase in depth could be achieved. The inclinometer tubing installed was standard plastic access tube as supplied by Soil Instruments Ltd. It was not considered necessary to use a more flexible tubing as the bench rubble was comprised of Plateau Gravel and Barton Clay, a stiff clay in various stages of degradation. The bench rubble proved very difficult to penetrate by hand augering and the borehole walls were generally very stable. This is in contrast to the condition of the 'soft mudflow', described by Hutchinson (1970), where the flexible plastic tube with helical wire reinforcement used was capable of following a wide range of velocity distributions.

The tubing was assembled from 1.5m lengths, chosen for ease of transport, and a length, 0.5m longer than the total hole depth, was lowered to the bottom of the borehole. The tube was rotated into position to ensure

that the keys were aligned parallel and perpendicular to the direction of anticipated movement. The inclinometer tube was then filled with clean water collected from an undercliff pond. The annulus between the borehole and the tubing was backfilled with small pieces of dry clay which was frequently tamped into place. This type of backfill was considered suitable as the dry clay would become wet from the ground water and swell to totally fill the annulus around the tube but not restrict the deformation of the tube due to ground movements.

The installation was completed by sawing off any protruding tubing, camouflaging with any adjacent sods and fitting a locking cap.

3.2.1.2 Monitoring

The first profile of the inclinometer tube was repeated to ensure a reliable initial datum. A tube was profiled at weekly intervals until a suitable monitoring interval was decided. The monitoring instrument used was a Soil Instruments Mark III inclinometer. The inclination of the tube was read every 0.5 metres; the top of the inclinometer tube was used as the datum level.

3.2.1.3 Tube applications

Table 3-2. lists the performance of all eleven tubes installed and their results are fully discussed in Chapter 4. These results do however highlight the two possible ways in which inclinometers can be used in a slope.

(i) To locate a basal shear plane.

This is the 'normal' mode of operation where the inclinometer tube is installed to a depth greater than the assumed shear plane location. With movement across the

shear plane the inclinometer tubing distorts into a characteristic sinuous shape as reported by Mitchell and Eden (1972) and Barton and Coles (1983a). The actual location of the shear plane can then be estimated from the deformed tube profile.

(ii) To study the distribution of displacements with depth

The ability to measure the inclination of the tubing at any depth enables the tube to be profiled and indicate the distribution of movement with depth. Whilst this process is no different from the usage described above in (i) if the tube is not anchored in a stationary strata then providing the tube is not too stiff it will deform with movement of the soil profile and the displacement with depth can be measured.

An application of inclinometer tubing for this precise purpose is described in Hutchinson (1970) where the specially designed flexible tubing was installed in a mudflow. The resultant measurement enabled the surface displacement to be related to those throughout the vertical profile of the mudflow.

3.2.2 Slip indicators

The slip indicator is a length of semi-rigid tube which is installed to a depth in excess of a presumed failure plane. Activity along the failure plane is detected by either:

(1) A bamboo cane; this is inserted along the whole length of the tube. It is broken when the landslide activates.

(2) Regular probing with steel rods which indicates a change in the depth to which they can penetrate.

(3) The lifting of a weight on a length of twine until it meets an obstruction and the lowering of a weight until it can fall no further.

The slip indicator method was described by Toms and Bartlett (1962). It was a technique used to discover the depth of slipping on a failed embankment or cutting. They described a 'convenient' method where a borehole, sunk to obtain samples, had liners inserted down the hole. The liners were 3" to 4" diameter asbestos cement tubes which had their joints wrapped in hessian. The annular ring outside the liner was filled with sand and slipping revealed by distortion of the liners at the failure plane. A plummet lowered from the surface detected the depth of failure.

Another method used by the Western region of British Rail describes the insertion of polythene tubing vertically into a slope by means of a mandrel tube. This is subsequently removed and deformation of the tubing investigated by the lowering of a short steel rod on a cord or the pulling up of a mandrel originally lowered to the bottom of the tube. The method was applied to five embankment failures and gave realistic shapes for the failure surfaces.

The third method of failure plane identification used the direction of surface movements to indicate the depth and shape of the slip surface.

The method adopted in this field study used a flexible plastic tube. A lead weight was lowered from the top of the tube and another lifted from the bottom of the tube to locate any zone of distortion.

3.2.2.1 Installation

Twenty-one slip indicators were placed in the study area. The first seven were installed using a petrol driven vibrating jack hammer and the remaining fourteen by hand augering.

a/. Vibrating Jack Hammer

One metre lengths of galvanised gas pipe, 1" internal diameter, were driven vertically into the ground by a vibrating jack hammer. Each tube was threaded at each end to allow the lengths to be coupled together. The driving of the tubes stopped when either the desired depth was reached or the driving force could not exceed the soil resistance. A flexible rubber tube 17mm outside diameter, 12mm inside diameter, was pushed down the inside of the gas barrel to the full depth of the driven tube. The steel pipe was then jacked out of the ground using a hydraulic jacking system. This left the flexible pipe still standing in the full depth of the driven hole. The gap between the flexible tube and the side wall of the hole was small and was not backfilled.

A twenty two gram lead weight was lowered to the bottom of the tube on a length of non-stretch twine and left in position.

The initial installations were troubled by the ingress of ground water which caused difficulty in defining the bottom of the tube. The bottom of the slip indicator tube was subsequently sealed and filled with clean water to prevent problems with buoyancy.

b/. Hand Auger Installation

Auger installation required a 40mm diameter hole to be drilled to a depth at least one metre greater than the

presumed failure plane. A semi-rigid PVC pipe, external diameter 22mm, wall thickness 2mm, was lowered vertically down the hole. The bottom of the tube was sealed and when in place the whole of the slip indicator tube filled with clean water. The small gap between the tube and the hole did not need to be backfilled. A twenty two gram lead weight on non-stretch twine was left resting at the bottom of the hole.

It should be noted that a semi-rigid tube is needed for the auger installation to stop the tube fouling the side walls of the augered hole whilst it is being lowered.

3.2.2.2 Monitoring

The slip indicator tubes were checked on a weekly basis. A tube failure was indicated by the difficulty in lifting the permanent weight: it was rechecked by the lowering of a weight from the surface. The length of twine extracted and the length of twine lowered indicated the limits of the failure zone.

3.2.2.3 Slip indicator performance

Out of the twenty one installations ten indicators failed and their failure depth measured. One tube was vandalised and seven out of the nine located on debris slide 3 were covered by the movement of the debris slide material before a failure depth could be recorded. All three tubes on the A3 bench were covered in colluvium from the D bench before any indication of tube distortion was registered. The performance of all the slip indicators is listed in Table 3-3. and Chapter 4 discusses the results.

Although less than 50% of the slip indicators installed registered failures, compared to 63% of inclinometers, it

is the former which is most suited to the location of shear surfaces within the study area. They provide a cheap and rapid method of detecting failure surfaces. A minimum of four could be installed in one day compared to one inclinometer installation. Results were not adversly affected by an instant failure and the indicators were less liable to irreversible damage by vandalism. The vibrating jack hammer allowed installation through any material and to depths not possible by the hand augering methods needed for inclinometer installation.

3.2.3 Surveying of exposures

The bench/scarp regime, discussed in Chapter 2 and first described by Barton (1973), can result in the exposure of a bedding plane shear surface at the seaward edge of a bench area. This is illustrated in Fig. 2-8 and Fig. 2-10. These surface exposures have allowed their position and level to be surveyed. All three bedding plane shear surfaces within the study area have been located by this method. The distribution is discussed in Chapter 4.

3.3 The ground water regime

Study of the ground water regime was required both to help in the understanding of the movement of material within the undercliff and to enable realistic slope stability calculations to be carried out. The study of the ground water regime was initially undertaken as part of this research project and the author installed and monitored seven piezometers between October 1980 and April 1981. It was, however, soon realized that there was an opportunity for the study of a complete hydrological system within a degrading slope and a research project was begun in September 1981. The results and conclusions of the study are presented in Thomson (1987). This project not only

monitored ground water levels within the undercliff but also the water levels behind the degrading slope, the soil moisture content of the debris, the local meterological conditions and the permeability of the constituent materials.

The main conclusions of the hydrological study carried out by Thomson (1987) were as follows:-

i) The Plateau Gravel/Barton Clay interface contains channels and ridges aligned in a NE-SW direction.

ii) Water is present in the Plateau Gravel at all times.

iii) The Plateau Gravel is recharged due to rainfall and the main discharge occurs due to lateral flow. Lateral flow was generally found to be perpendicular to the cliff face.

iv) Permeability within the Barton Clay varies spatially due to stress relief, vertical variations in fissuring and lithology.

v) Ground water flow within the Barton Clay is downward and towards the undercliff and the Barton Clay domain is recharged from the Plateau Gravel. The Barton Clay is not however a very significant source of seepage to the undercliff.

vi) Ground water flow within the colluvium is mainly via gravel seams and tension cracks.

vii) The general direction of ground water flow within the colluvium is downward and seaward. The majority of the flow at the base of the colluvium will be along the impermeable shear surface separating the colluvium from the Barton Clay.

viii) Meterological variations cause large fluctuations in ground water levels at the F bedding plane shear surface and the failure of slumps utilizing this surface has occurred when levels were high.

ix) The existence of ground water level fluctuation at the D preferred bedding plane shear surface is less certain and fluctuations due to meterological conditions are minimal. Failure of the cliff top slumps utilizing the D bedding plane shear surface are thought to be a result of a reduction in lateral support from colluvium on the undercliff.

x) The movement of colluvium within the undercliff is highly variable and due to landslide activity the ground water flow regime is complex. Ground water levels which cause movements vary with time due to the changing geometry of the degrading slope.

These conclusions draw obvious relationships between meterological conditions, the levels of ground water within both the in-situ materials (Barton Clay and Plateau Gravels) and the landslide colluvium. The movement of water within the undercliff is described as complex due to the changing geometry of the slope, the variety of routes of water flow and the wide range in permeabilities found within the colluvium.

3.3.2 The preliminary ground water study

Prior to the commencement of the work by Dr. R.I. Thomson in 1981 a preliminary study of the ground water regime was carried out and it is detailed below.

3.3.2.1 Installation

An initial group of four piezometers were installed along a line of section through the centre of the study area. Fig. 3-2 shows the position of P1, P2, P3 and P4. All the piezometers were Cambridge drive-in type supplied by Soil Instruments Ltd. The piezometers had a ceramic tip which was connected by mild steel tubing to the surface. The tube was driven into the ground in one metre lengths. The bottom section incorporated the tip. The tip was shielded from the soil through which it was driven by a metal sheath. When the tip was at the desired depth a rod was placed inside the piezometer tubing. This enabled the sheath to be tapped clear of the ceramic porous tip and allow the piezometer to equilibrate.

The three other piezometers installed were based on the drive-in concept. Semi-rigid PVC tubing, external diameter 22mm was plugged at one end. At the same end four millimetre diameter holes were drilled all around the tube for a length of 100 millimetres. The perforated end was filled with pea gravel to act as a coarse filter. A metal sheath was placed over the perforated section. The piezometers were three metres long. All three were 'pushed', as opposed to driven, vertically into the soft matrix of mudslide A until the resistance to penetration suddenly increased. The sheath was tapped off using metal rods.

3.3.2.2 Monitoring

The level of ground water in the piezometer was measured using a water level meter supplied by Soil Instruments Ltd.

After installation each piezometer was dipped as frequently as possible. The piezometers which survived

until the establishment of the water balance study, Thomson (1987), were incorporated in the weekly field monitoring programme. The position of the piezometers were recorded in the surface movement survey to enable the absolute ground water levels of each site to be calculated.

3.3.2.3 Piezometer performance

The piezometer positions are shown in Fig. 3-2.

The maximum depth to which any of the tubes were installed did not exceed 3 metres. The piezometers were introduced to monitor the ground water table which was estimated not to drop below 3 metres from the ground surface. In addition, shallow installation lessened the probability of the tube being sheared by a subsurface movement. None of the piezometers were dry during their operation. All seven were lost after a maximum operating life of 18 months. P1 and TP1 moved seaward and ceased to operate when they were included in the local failure of the edge of the D bench. TP2 and TP3 were vandalised. P2, P3 and P4 were covered in debris.

The performance of the piezometers described above is not recorded in this thesis due to their initial infrequency of monitoring. Their results are however included in the results published by Thomson (1986a, 1986b, 1986c).

Selected data from the work by Thomson has been used in the slope stability analysis in Chapter 7 and full acknowledgement is given to their use.

3.4 Monitoring of scarp slopes

Weathering of in-situ scarp slopes adds fresh soil debris

to the undercliff. The weathering causes spalling and toppling: these processes are defined in Section 2.3.6. Exposed faces of both Plateau Gravel and Barton Clay are present over the whole of the undefended section of the Barton Clay coastal exposure. In the study area 490m² of Plateau Gravel is exposed at the cliff top. In-situ Barton Clay is exposed in the D scarp and in isolated exposures of the F scarp. They combine to have a total exposure of 920m². These are other clay scarps but these are associated with the landslide debris and their weathering does not contribute fresh material to the undercliff.

The rate of scarp weathering is an essential component in the calculation of the volume of material in the undercliff budget. On both the gravel and clay scarps a method was needed to estimate the amount of recession. Schumm (1956) documented a method to measure the erosion of badland slopes at Perth Ambay, New Jersy, U.S.A. Wooden dowels, one quarter inch in diameter and one and a half feet long, were driven into the slopes until they were flush with the surface. The amount of dowel exposed was subsequently measured to indicate the rate of slope erosion. A similar method was used by Brunsden (1973); steel bars 7mm in diameter and 600mm long were driven into a weathering sandstone scarp. These 'erosion' pins were measured to estimate the ground loss from the scarp.

At Highcliffe, erosion pins were driven into both the Plateau Gravel cliff top scarp and the Barton Clay exposure on the D scarp. At each site five one metre long steel reinforcing bars were driven into the scarp perpendicular to the face. They formed a square of one metre sides as shown in Fig. 3-3. The length of an exposed bar was measured using a 300mm square piece of perspex with a hole, drilled in the centre, the same diameter as the bar. The square was pushed over the pin until it lay on the scarp face. The distance from the

free end of the bar to the spalling square was noted.

The spalling square was developed to eliminate any errors from very local failure of the scarp. This was thought a particular problem in the gravel face where the detachment of an individual cobble could give a locally high recession rate, if the length of exposed pin from tip to entry into the face was measured directly. The protrusion of isolated cobbles was also considered a potential problem but this did not occur. The square proved a success and the accuracy was established, at times when spalling was negligible, to be ±5mm.

3.4.1 Pin performance

The installation of the steel pins must have caused disturbance within the scarp. However, there was no obvious pits or hollows developed near to the bar locations and it appears that the recession recorded in this way is typical of the recession occurring over the whole scarp during the period of measurement.

The clay erosion pins were monitored from 21 May 1981 to 4 November 1981 (270 days). Monitoring over the winter months was not possible because of the increased rate of movement on the D bench. The increased rate pushed material over the D scarp, Fig. 3-4. This rapidly bent the steel bars to make them inoperative. In addition there was a rapid build up of scree at the bottom of the slope which engulfed the lower and central pins making them inaccessible for both monitoring and to weathering. The spalling record is therefore short but it does indicate a sudden increase as winter approaches Fig. 3-5. Clay scarp recession data for the budget was supplemented by measurements from the contour maps.

The gravel erosion pins were monitored from 21 May 1981 to

13 July 1983 (783 days). No large build up of scree occurred at the bottom of the scarp but the lower pins were bent. Only the exposures of the upper three bars have been averaged to produce Fig. 3-6.

3.5 Cliff top slumping

The study of cliff top slumping, section 2.3.5, was not solely confined to the area of detailed study. An extended area was used because during the three years of the research project only one notable cliff top failure occurred in the study area. It was located between N.G.R. 422197.35 E and 422206.1 E, had a maximum length of 8.65m and maximum breadth of 2.6m. Recession elsewhere in the study area, which has accounted for a cliff top area loss of 340m^2 between July 1981 and July 1983, had occurred by small local falls. These failures did not activate the F bedding plane shear surface.

3.5.1 Field measurements

Two kilometres of coastal cliff from National Grid lines N.G.R. 421800 E to 423800 E were studied in association with Mr. G. Tiller. The research undertaken was a statistical survey of 42 slumps measured over the winters of 1980/81 and 1981/82. The slumps were measured at the cliff top in terms of maximum breadth, which was usually measured normal to the cliff edge, and the length measured parallel to the cliff edge. The majority of the slumps were recent. They were discernible by a small vertical displacement from the cliff top. Two slumps at the extreme east, where recession has been slowed by engineering works, were much older. Only those slumps of which the dimensions could be unequivocally measured were included. Slumps often break up into several blocks after falling through a large vertical displacement and this

prevents the accurate measurement of dimensions.

For each slump the maximum breadth (b) and the length (ℓ) was recorded to the nearest 0.1m. The b/ℓ ratio, a measurement of the slump shape, and the cliff top plan area was calculated. The area was estimated by applying a formula given by Bronshtein and Semendyayev (1973) where the area (A) is given by

$$A = b\left[6\ell + 8\left(\left(\tfrac{1}{2}\ell\right)^2 + b^2\right)^{\frac{1}{2}}\right]/15$$

This is normally used to calculate the area of a circular segment where (ℓ) is the chord length and (b) the maximum distance between the chord and perimeter.

A slump (No. 20) was carefully surveyed to find the extent of the error from this approximation. The true area was 14.15m^2, the formula area 15.85m^2: an over-estimate of 12%. This is considered acceptable since it saved a great deal of field work time.

The position of the slumps along the cliff top were also recorded. The results of the statistical survey are given in Barton, Coles and Tiller (1983).

The data collected within the study area is used in Chapter 6 to evaluate the volume of slope debris input into the undercliff.

3.6 Field work limitations

The earlier discussion of field work methods used in the study area have been accompanied by comment on the problems presented by each technique used. It is worth summarizing these problems common to all the techniques and the solutions used at Highcliffe.

(1) A degrading area

Any instrumentation in a continually moving area has a limited working life. The instruments used should be easy to install and considered disposable. Lengthy installation is costly in time as well as equipment if the end result is a negligible amount of field data.

At Highcliffe extensive use as made of PVC slip indicators, scaffold pole survey pegs and 'push-in' PVC piezometers.

(2) Vandalism

Even if an instrument is considered disposable loss by vandalism is not desirable. Care must be taken not only to fortify the installation but also to place the instrument away from well trodden paths. Colouration must be subdued. This is in direct contrast to the requirements of a construction site where easy observation can prolong an instrument's life. Therefore the deliberate bright colours used by some manufacturers have to be painted over. This often has the effect of making location difficult. An accurate note is needed of conspicuous field features to allow easy rediscovery.

During the preliminary year of field work brightly painted wooden survey pegs were placed in the undercliff. Loss by vandalism exceeded 50%. The steel replacements suffered only a 5% loss in two years.

(3) Reference Datum

A feature of a landslide area is the lack of stable ground to act as a reference datum. At Highcliffe the only stable areas are the cliff top and the in-situ clay beneath the landslide debris. This restricted both the type of ground survey technique which could be used and,

due to the lack of access for powered augering equipment, did not allow anchorage of inclinometer tubes into the underlying in-situ clay.

CHAPTER 4: THE RESULTS OF THE FIELD RESEARCH

CHAPTER 4: THE RESULTS OF THE FIELD RESEARCH

4.0 The field research

The methods of field research described in Chapter 3 were used between October 1980 and July 1983, to gather a large volume of data on the degradation of the study area. The bulk of the results from this investigatory work is given in Appendix F and the basic surface movement data is published in Coles (1983). This chapter briefly summaries the field data recorded and discusses various aspects of the results.

4.1 Landslide movements

The movement of colluvium can occur by sliding, by suspension of soil particles in soil/water mix and subsequent fluid motion. The last two mechanisms are not thought to play a significant part in the degradation of the coastal slopes being studied. The only mechanism which transports a significant volume of material is sliding.

The term landslide has been defined in the following ways:

(1) "the failure of a mass of soil located beneath a slope is called a slide. It involves a downward and outward movement of the entire mass of soil that participates in the failure."

Ter zaghi and Peck (1948)

(2) "Landslides are relatively rapid movements involving failure. In further contrast to mantle and mass creep movements, where there is generally a continuous gradation between the stationary and the moving material the movement in landslides takes place characteristically on one or more discrete

surfaces which define sharply the moving mass."

Hutchinson (1968a)

(3) "The generic term landslide embraces these down-slope movements of soil or rock masses which occurs primarily as a result of shear failure at the boundaries of the moving mass."

Skempton and Hutchinson (1969)

The latter two definitions identify the presence of a confining shear surface. The surface is the junction between two soil masses moving at different rates. Knowledge of its position, shape, formation and post failure properties are fundamental to the design of engineering works in any area where landslides are likely to occur.

The main methods of shear surface detection are summarised in Table 4-1. They are split between geophysical investigations, the installation of instrumentation and visual identification of a surface either after excavation or from a surface exposure. Each method has advantages and a complete investigation of either a natural slope, a site for possible construction or a post failure examination usually requires the use of several techniques.

An assessment of the amount of movement on a shear surface is often measured by a comprehensive network of surface pegs. It is assumed that the velocity profile throughout the depth of the sliding mass is uniform and movement on the surface of the slide is the same as on the shear plane.

Actual data on the velocity profile can be obtained by the installations of inclinometers.

4.2 Bedding plane shear surfaces

The presence of bedding plane shear surfaces in the study area has been established by Barton (1973) and preliminary data on movement patterns has been published by Barton and Coles (1984). The field work has investigated all three bedding plane surfaces present in the study area and gathered data on surface movements over a two year period.

4.2.1 Shear plane locations

The depths of the bedding plane shear surfaces were investigated by inclinometers, slip indicators, auger detection and visual identification. Their locations and depths are given in Fig. 4-1.

The F bedding plane shear surface was located at nine different positions along a 130m length of the undercliff. The located depths vary between 25.74m A.O.D. and 22.3m A. O.D. These extremes were detected 110m apart and imply a dip of at least 2° in the bedding which is larger than the ¾° ENE presented by Barton (1973). This variation to the previously published bedding plane dip was also noted in respect to the D bedding plane shear surface although not the A3 shear plane. Possible reasons for variations in the bedding are fully discussed in section 4.6.

No inclinometers were installed in the F bench due to the frequent pockets of plateau gravel and the velocity profile for this bench was therefore not measured.

Inclinometers were installed in both the A3 and D benches. The tubing installed is described in Chapter 3 and the stiff nature of the bench rubble, which proved difficult to penetrate with a hand auger, was considered a suitable medium to accept standard inclinometer tubing. This is in contrast to the specially flexible tubing chosen by

Hutchinson (1970) to measure velocity profiles in the much softer mudslide debris.

The D bedding plane shear surface was detected in nine locations, seven of these were within the amphitheatre feature where the depth of colluvium covering the basal shear surface was less, by up to 4m, compared to the surrounding bench. The range of detected elevations is large, between 7.6m A.O.D. and 9.6m A.O.D., these variations are discussed in section 4.6. The velocity profile with depth is best illustrated by studying the inclinometer profiles recorded in Figs. F-1, F-3 and F-8 for I2, I5 and I10 respectively. All three profiles show a fairly uniform velocity profile and in particular I2, which penetrated the D preferred bedding plane shear surface, indicates uniform movement from the bedding plane shear surface to the ground surface over an 84 day period with a seaward displacement of 2.28m. I10, which was located 45m to the east of the amphitheatre, indicated a seaward movement of 0.22m during an 82 day period over its complete 4.5m depth.

The A3 preferred bedding plane shear surface was detected in six locations, the range of levels was between 1.5 A.O.D. and 2.6m A.O.D. These levels align with a dip angle of $\frac{3}{4}°$ ENE. The only inclinometer in the A3 bench, I3, failed 5 days after installation but remained accessible for another 171 days during which the tube translated 6.5m seaward across the A3 bench and illustrated the translational nature of the bench sliding across the A3 shear surface. The tube was finally recovered on the beach, 264 days after installation, and had slid 10.08m seawards. Figures F-11 and F-12 illustrate its recovered shape.

4.2.2 Surface movements

Full details of surface movements on the benches are given in Appendix F. This section is a summary of the results. Only the F and D benches were surveyed throughout the 734 day study period as the A3 bench could not be traversed all the year round.

On the F bench 3 survey pegs, No. 150, 154 and 155, were monitored all through the study period and 2 additional records have been produced by combining two peg records No. 151/224 and 152/225. These pegs cover a 110m length of the undercliff and their displacement with time is shown in Fig. F-25. The maximum recorded movement was 3.2m for 152/225 which was located, centrally behind the amphitheatre, on the F bench. In contrast peg no. 155 was effectively stationary during the whole study period. Chapter 8 discusses the relationship between rainfall data and the changes in the rates of movement for the movement data recorded on benches, mudslides and debris slides.

The D bench, due to its size, was monitored by far more pegs than the F bench. Thirteen pegs remained serviceable for the complete study period and Fig. F-26 illustrates 5 examples of displacement with time. The range of recorded movement is between 2.19m and 8.51m for the total study period. This wide range is caused by various internal deformations within the sliding colluvium. The largest movements occurred at the seaward extreme of the bench. Failure of the seaward edge of the bench resulted in pegs being included in compound slides with movement rates far in excess of the D bench sliding. The more representative D bench sliding rate was monitored by pegs 161, 162, 164 and 165; these four survey markers covered a 85m central portion of the D bench and their recorded seaward movements were within the range 2.19m to 2.45m.

Movement records on the A3 bench were restricted to the

three pegs illustrated in Fig. F-27. The maximum length of monitoring was 264 days during which inclinometer I3 slid 10.08m seawards. Pegs 216 and 217 were monitored for only 62 and 154 days respectively and translated 0.59m and 3.96m.

4.2.3 Benchslide movements

The data collected concerning the subsurface and surface indicates that benchsliding is a translational slide across a bedding plane shear surface. The velocity profile indicated by the inclinometers shows a uniformity throughout the depth. The velocity characteristics of the three benches present in the study area show differences in magnitude. These differences show that the benches are not continuous masses of landslide debris and are subject to internal lateral deformation.

The areas of highest movement rates occur close to the seaward edge of the bench where the free-standing face either topples forward onto the bench below or is incorporated in a slide failure with a compound shear plane.

Study of the displacement with time graphs illustrated in Figures F-25 to F-27 for the three benches, annual patterns of movement that can be sub-divided into three phases. These are called summer, surge and winter periods. They are characterised by common rates of movement amongst sets of pegs on the same geomorphological unit. These are discussed in detail in Appendix F and the reasons behind their occurrence is given in Chapter 8.

4.3 Mudslides

The field investigation of the movements and shear surface

location within the two mudslides in the study area were restricted fundamentally to mudslide A due to the extremely treacherous nature of mudslide B.

4.3.1 Shear plane location

Figure F-14 illustrates both a plan and the position of five cross-sections taken of mudslide A. The basal shear surface undulates and the maximum depth of the channel is 1.2m. The basal surface does not utilize a bedding plane shear surface until very close to the edge of the seaward scarp where it becomes coincident with the D bench bedding plane shear surface.

The shape of mudslide channels has not been widely investigated excellent work however has been presented with down-slope sections by Hutchinson (1970), Hutchinson and Bhandari (1971), Hutchinson, Prior and Stephens (1974) and Chandler (1972). The depth of the mudslides described varies between 1.5m for periglacial mudslides (Chandler, 1972) and 5m for the Beltinge mudslide (Hutchinson, 1970).

Due to the variety in both locality and geology it is unlikely that all mudslide channels will conform to a common shape and depth. The 5m depth of the Beltinge mudslide and the large size of the individual units which make up that mudslide complex, 60m x 25m for Slide II, reflect the volume of material being supplied to the mudslide from the degrading of a 30m cliff. Mudslide A by comparison was only 15m long x 5m wide and fed from surrounding degrading debris blocks. Mudslide B, with material sourced from D bench sliding was approximately 25m x 10m wide.

Mudslide depths can also be transient and the overriding of an existing surface has been noted by Hutchinson and

Bhandari (1971) and Hutchinson, Prior and Stephens (1974). The overriding of a mudslide by fresh material rapidly increases the thickness of debris overlying the basal shear plane.

4.3.2 Surface movements

The surface movements of mudslides A and B are presented in Figs. F-28 and F-29 respectively. Mudslide A has already been described in section 2.3.2 as a single element mudslide. It is difficult to classify the mudslide using the terminology used by Hutchinson (1970) to represent elements of a mudslide. In one respect it can be considered to be a feeder zone which is supplying debris to an accumulation zone which is indistinguishable from the A3 bench. Alternatively the mudslide has a down-slope profile which gently increases from 11° to 30° having already accumulated debris from the disrupted bench rubble. The movement record illustrates one single peg and two combinations which were studied for all, pegs 168 and 30/214, or the majority, peg 220/267, of the study period. In addition to these long term records Figs. F-17 to F-24 illustrate shorter term displacements for eight seasons which are defined in Appendix F. Records for mudslide A are therefore examples of medium and long term patterns of movement for a mudslide feeder zone in the Barton Clay. The maximum displacement recorded during the whole study period was 22.17m for peg no. 30/214 this being the largest displacement record for the whole undercliff.

Mudslide B has been identified as consisting of both feeder and accumulation zones, see Fig. 2-11. The surface movement record presented in Fig. F-29 illustrates a 26 day period in Spring 1982 when activity within the mudslide was observed to be high. The markers were located in the accumulation zone. The record of the

surface movements for mudslide B can be regarded as an example of high rates of movement, although not the maximum possible, for an accumulation zone in Barton Clay.

Table 4-2 presents the rates of surface movement recorded on mudslide A and B with values published by Hutchinson (1970), Prior and Stephens (1970) and Hutchinson, Prior and Stephens (1974) for other mudslides. Direct comparison can only be made where movement records are equal or exceed one years duration, to remove any seasonal effects. The only example of these long term records in Table 4-2 is provided by Hutchinson (1970) where the near 5 year displacement data for Beltinge gives similar overall rates of movement to the 2 year study period conducted on mudslide A.

The remaining data provides examples of the range of movements recorded for temperate mudslides in the U.K. The highest rates of movement were all produced in Antrim, N. Ireland where continuous monitoring equipment enabled surges in mudslide movements to be identified and the movement rates recorded. The very short term periods of elevated rates of movement are believed, by the author, to exist in most mudslides. Their identification can only be carried out in areas where monitoring equipment can be left unattended. If this were possible at any mudslide location the apparently exceptionally high values recorded at Antrim could well be matched by similar rates from other mudslides.

The comparisons of movement rates between feeder and accumulation zones are not conclusive. Hutchinson, Prior and Stephens (1974) describe movements within a feeder/accumulation system where relatively steady movement of the upslope feeder zone loaded the accumulation zone, which finally failed in a 'catastrophic' fashion and produced very high short term failure rates of 8m/min. However where movement rates

cannot be monitored continuously it is difficult to distinguish surges and the overall rates monitored in the feeder and accumulation zones will reflect the geometry of the mudslide channel. Where continuity of sliding is maintained narrow mudslide channels will exhibit high velocities and where the mudslide channel becomes more open e.g. at a change from a feeder zone to an accumulation zone, then mudslide velocities will decrease.

4.3.3 Mudslide movements

The study of mudslide movement characteristics in Christchurch Bay has been restricted to two 'small' mudslide features. Due to the accessibility to the public, instrumentation has been limited and the only long term data recorded has been the surface movements of mudslide A. Full comparison with other temperate mudslides in the U.K. is restricted due to the lack of data on the vertical velocity profile within the mudslides and no measurements of the pore water conditions within the mudslide.

4.4 Debris slides

Five debris slides were active within the study area two of which having been formed during the study period. All five were monitored to obtain surface movement data but only DS1, DS3 and DS4 were subject to a sub-surface investigation. Debris slides covered 23% of the surface area of the study area in November 1980, this was second in area coverage only to the benches.

Previous to this study debris slides had not been recognised as a process of slope degradation in this undercliff (as described in Barton, 1973). The movement of loose, non-coherent debris over a definite shear

surface has been recorded in steep terrain (Varnes, 1958 and 1978) but they had not been recorded as such in the overconsolidated clay cliffs of the U.K.

4.4.1 Shear planes

The subsurface investigation detected the basal shear surface in three of the five debris slides active in the study area. The depth of colluvium overlying these surfaces varied from near zero, see Fig. 2-20, to a maximum depth between 2.84m and 3.24m in debris slide 4. Shear surfaces were detected by inclinometer, I8 and I9, by slip indicators in debris slide 3 and by auger detection in debris slide 4. The active nature of the debris slides caused failure in the instrumentation within a few days and the longest period between installation and failure was 6 days for the two slip indicators in debris slide 3.

The depths recorded for the basal shear planes of the debris slides show that none have utilized a bedding plane shear surface. Within the study area all the debris slides have been observed to rest on either in-situ scarp slopes (DS1, DS3 and DS4) or vertically displaced scarp slopes which are part of a failure block (DS2 and DS5). The scarp slope forms the rear portion of the debris slide shear surface and is extended further downslope by a surface formed within the bench. Cross sections through debris slides 3 and 4 are shown in Fig. 4-2 and these illustrate the two part nature of the debris slide slopes. The rearmost sections of the slides have angles of 26° and 25° for DS3 and DS4 respectively and gentler seaward slopes of between 0° and 3°. Published details of debris slides by Sidle and Swanston (1981) give slope angles for silty sandy gravel slopes in Alaska of 14 to 43° with a range of debris thickness of 0.08m to 0.53m.

4.4.2 Surface movements

The surface movement records of the five debris slides has produced a variety of displacement/time graphs: these are illustrated in Fig. F-30 to F-34. Detailed discussion on each debris slide is given in Appendix F and this section summaries the data collected.

Debris slides 1 and 2 were identifiable at the beginning of the study period. Records for both were collected from 8 July 1981 but their total displacements for the whole study period are significantly different. DS1 registered a maximum displacement of 8.56m for peg no. 159 compared to 16.4m for peg no. 187 on DS2. The cause of this disparity is due to the location of the debris slides within the study area. Debris slide 1 rests on the F scarp and its downslope extreme is on the D bench. Debris slide 2 is contained with the scarp slope of the amphitheatre and its toe rests on the amphitheatre floor. The larger velocities recorded on DS2 were caused by both fresh material loading the top of the debris slide, supplied by the degradation of the scarp edge, and the sliding movements within the amphitheatre unloading the toe section of the slide. Debris slide 1 did not receive appreciable volumes of debris from the F bench to trigger any increase in the movement of the slide.

Debris slide 3 became active in January 1982 after local recession of the cliff top immediately upslope and peg no. 244 registered 11.83m of seaward movement in 61 days. This short term 'sprint' was followed by a period of quiescence which lasted until the end of the study period and was characterised by a recorded of 1.46m in 415 days.

Debris slide 4 formed in March 1982 after a cliff top slump pushed debris across the bench and onto the scree slope resting on the F scarp. Figure F-33 illustrates the total recorded movement on DS4 of 7.95m for peg no. 252

between 9 March 1982 and 12 July 1983. Debris slide 5 formed in mid-November 1982 due to continuing degradation of the amphitheatre scarp and movements of the amphitheatre floor. The displacement records of peg no. 184 and 192 show a marked increase in displacement after 18 November 1982. Peg no. 193 slid 22.11m in the complete study period of which 17.20m occurred in the last 224 days of the 734 day study period.

No published records of surface movements on debris slides have been encountered. The only reference to debris slide movement was published by Sidle and Swanston (1982) who described the failure of a debris slide which moved 22m downslope in a 3 day period. Varnes (1978) classifies debris slides as exhibiting surface movement rates between 0.06m/y and 0.3m/min. These wide bounds enclose the study area data although it also includes all the movement data in the undercliff.

4.4.3 Debris slide movement

The movement of debris slides has shown a large variety in rates which can be related to the stage of evolution of the debris slide. In particular both DS3 and DS5 illustrating proportionately high rates of movement immediately after their formation. DS3 maintained an average daily rate of 194mm over 61 days after its activation although this dropped to 4mm per day for the remaining 415 days of the study after the cessation of cliff top failure which caused its formation.

From this data and field observations of the broken nature of the slide material where the shear surface was in places exposed, see Figure 2-20, the prime factor in the movement of debris slides was the supply of fresh debris. Pore water pressures at the basal shear surface must be small and the activation of the slide continued by the

loading of the rear section of the debris slide slope.

4.5 Amphitheatre slide

The amphitheatre feature, described in section 2.2.2, was found to have surface movements different in magnitude to those of the surrounding D bench. The general effect of these characteristics are considered in section 5.0.3.

4.5.1 Shear planes

Within the amphitheatre area nine shear plane depths were registered. Four of these can be associated with the D bedding plane shear surface but the remaining five detections occurred at levels above this. The range of detailed levels was between 11.1m and 12.7m A.O.D. and covered the majority of the amphitheatre floor. The origin of this elevated surface is discussed in section 5.0.1.

4.5.2 Surface movements

Two pegs were monitored during the complete study period, no. 33 and 197, and the surface movements within the amphitheatre were found to exceed those of the D bench. The average value of D bench movements immediately to the rear of the amphitheatre was approximately 2.4m compared to individual values of 14.3m and 8.9m for pegs no. 33 and 197 respectively. The cause of these elevated displacement values is discussed in Chapter 5.

4.6 The detection of shear planes in a degrading area

The recorded elevations of the bedding plane shear

surfaces were not always encountered at the elevations predicted by the assumed constant dip of the bedding ($\frac{3}{4}°$ NNE). The three possible reasons for this are as follows:-

(i) The accuracy of the determination of a shear plane depth

The accuracy of the shear plane depth detection will vary according to the method used for its location. In Fig. 4-3 the range or zone within which the shear plane is located is given. The thickness of the zone is not the same for each method of detection and the logic behind each adopted range is as follows. Within the study area the failure of inclinometer tubes was not preceded by a period when a characteristic pre-failure stage was recorded although this feature has been noted by Mitchell and Eden (1972) and Barton and Coles (1984). It has therefore been assumed that failure occurs relatively suddenly and tube distortions are reduced from those noted during slower rates of failure. The failure zone presented extended over 1m and is calculated as extending 1m below the furthest point below which the inclinometer torpedo could not fall. This compares with the 2m zone observed by Barton and Coles (1984) over a 1098 day period and two 4m zones noted by Mitchell and Eden (1973) which was defined over 60 days and 1065 days.

The slip indicators results are also presented with a 1m failure zone. This is based on a central reading ±0.5m; the central reading is the mean depth from the two weighted plumb lines installed in each slip indicator tube. An alternative method would be to place the limits of the shear surface between the upper and lower plumb bob readings. This method was not adopted as frequently the range exceeded 2m due to difficulty in raising the lower weight.

The failure zone for shear plane detection by hand augering is estimated as ±0.2m of the registered depth. This is purely an estimation of the location and is adopted to include the indistinct transition from colluvium to in-situ material. The visual identification and the subsequent conventional levelling technique is quoted to the nearest 0.1m.

(ii) Variations in the level of the bedding plane

Within the bedding of the Barton Clay some undulation of the bedding planes have been noted. This was particularly noted to the west of the study area on the A3 bedding plane shear surface.

(iii) The displacement of a preferred bedding plane shear due to degradation of the slope, particularly due to sliding on the underlying bedding plane shear surface.

The vertical displacement of bedding features will occur on the undercliff due to the disruptive nature of the degrading undercliff. A clear example of this disruption was detected in the eastern section of the F Bench. A slip indicator and a visual identification gave levels of 21.8m to 22.8m A.O.D. and 23.0m A.O.D. respectively on a shear plane. These levels are approximately 1.5m to 2m below the predicted level for the shear plane given the adoption of the definitive level shown in Fig. 4-3. Close inspection of the exposed shear surface confirmed that it was approximately 0.1m above the concretionary limestone band specified by Barton (1973) as the position of the F preferred bedding plane shear surface. This section of the F bench had therefore been subject to a vertical displacement. In addition the raised level of the most seaward of the shear plane levels over the other implies a degree of back tilting. The angle of back tilt is in the

range 0.6° to 3.8°, dependant on the exact level of the rearward shear plane and the failure mechanism corresponds to the mechanism of cliff top failure outlined in Barton, Coles and Tiller (1983) and commonly noted elsewhere, it should be noted that the failure block did not utilize the F bedding plane shear surface as its basal surface but used a deeper shear plane, this is most likely to have been the D surface.

Figure 4-4 presents a comparison of the detected depths of shear planes compared with the predicted depths from a known level and dip angle/direction. The level for each of the three bedding plane shear surfaces were chosen by visual inspection and all are underlined in Figure 4-3. Most of the actual recorded depths are close to or within the range adopted for a particular detection technique.

4.6.1 Shear planes in a degrading cliff

The study of the shear planes within this degrading slope has given a unique opportunity to relate the geology of the strata to the profusion of shear planes contained within an actively degrading coastal undercliff. Other detailed studies of degrading slopes have included Hutchinson and Gostelow (1976) and Brunsden and Jones (1976). Hutchinson and Gostelow (1976) presented a comprehensive account of an abandoned cliff at Hadleigh, Essex where a series of shallow landslides were detected along a 280m down slope section of the cliff. The cross sections presented do not relate the geology with failure surfaces although in several areas borehole and trial pit information has allowed some correlation. It should however be noted that the stratigraphy of the London Clay is far less distinct than the Barton Clay and the correlation between shear plane location and geological structure is very difficult.

Brunsden and Jones (1976) described the form and evolution of the Fairy Dell landslide complex in Dorset and presented both geomorphological maps and geological sections to depict the degradation of the slope. The study did not use instrumentation to locate the shear planes present within the undercliff and the position of the shear planes are extrapolated from surface features.

This study does correlate field results with a known geological structure and a complex degrading slope. It is important to highlight the following:-

i) Debris slides have been recognised as a process of slope degradation. They do not use bedding plane shear surfaces as basal shear planes.

ii) Rates of surface movement and depths to shear planes have been recorded for the three sliding processes active on the undercliff.

iii) The highest rates of movement have been recorded within the mudslides. This surface movement data is used in Chapter 6 to generate the rate of debris movement volume through the degrading study area.

CHAPTER 5: MULTI-LAYERED LANDSLIDES

CHAPTER 5: MULTI-LAYERED LANDSLIDES

5.0 Introduction

The definitions of a landslide presented in Chapter 4 all refer to the existence of a basal shear surface. The illustrative classifications of mass and slope movements presented by Hutchinson (1968a), Skempton and Hutchinson (1969, Figure 1 and 2) and Varnes (1978, Figure 21.) show a single basal shear surface. The existence of more than one active basal shear surface in a vertical section has been discovered in seven areas at Naish Farm, Table 5-1.

The concept of multi-layered landslides has been described by Ter-Stepanian and Goldstein (1969). They classed landslides as simple or complex slopes. The simple unit was used to illustrate the movement of surface points down a slope. Eleven theoretical cases were described; each case varied in the direction of the dip of the slope and the position of the seat of sliding. The movement of the surface points were graphically presented. In one of the eleven cases two levels of simultaneous sliding was considered. Ter-Stepanian and Ter-Stepanian (1971) described an example of a multi-layered landslide in Sochi, on the Caucasian coast of the Black Sea. This landslide had three layers; the lower element was a rotational failure with a basal shear surface approximately 60m below the ground surface, an intermediate shear surface 23m below the ground and the surface layer was an earth flow with an average depth of 8m.

The areas of multiple failure surfaces detected at Highcliffe are both simple and complex types.

5.0.1 Formation

The formation of a multi-layered landslide, where two or

more shear planes are active, can most easily occur in a degrading slope. In an area where a slope failure has occurred any degradational sliding process which is located above the basal shear plane of the main slide forms a multi-layer landslide. In the study area multi-layered slides are formed by the five debris slides, amphitheatre floor and mudslide A. Six out of the seven identified multi-layered landslides have two basal shear surfaces and one area has three.

The only site not associated with either a debris slide or a mudslide is within the amphitheatre depression. Subsurface investigations, detailed in Chapter 4, indicated an active shear surface 3m above the D preferred bedding plane shear surface. Whilst debris slide and mudslide formation is well documented (Barton and Coles (1984), Hutchinson (1970) and Varnes (1978)) the origins of the amphitheatre surface is less clear. The topography of the amphitheatre, in November 1980, is illustrated in Figure 2-7. The rear scarp, which defines the landward boundary, rises from an average floor level of 16.5m A.O.D. to the rim of the back scarp at 21m A.O.D. The scarp had an average slope of 27°.

Inspection of aerial photographs collected for this research project had enabled the evolution of the amphitheatre feature to be followed.

The cliff top failure which forms the rear of the amphitheatre occurred between 18 March 1977 and 6 April 1978 and is fully discussed in Chapter 8. The initial failure block was 41 metres long and had a maximum width of 13 metres. The down-slope disruption, which is evident 30 metres from the cliff top, indicates that the slump used the D bedding plane shear surface and subsequently incorporated a substantial portion of the F bench. By 6 April 1978 the slump block was starting to degrade.

On 15 September 1979 the block was less well defined. The rear edge had moved seawards approximately eight metres from the April 1978 position and lay 14.6m from the cliff edge. The advancement of the slump block caused the widening of a breach in a ridge of old slump blocks which lined the seaward edge of the D bench. The breach contained a mudslide channel which had been identifiable since 24 April 1975. Immediately behind the breach an area of colluvium formed a distinct patch of unvegetated soil which became the amphitheatre floor.

The next aerial photograph, on 13 March 1980, shows the amphitheatre to have formed. The unvegetated floor occupies the breach near the D scarp edge. The floor is depressed in relation to the undercliff on the western side. On the A3 bench a large volume of colluvium is evident. Two mudslides, A and B, are identifiable and their activity partially explains the change of elevation of the amphitheatre floor.

The latest aerial coverage in November 1980 shows the amphitheatre fully developed. Both western and northern limits of the floor are defined by an upstanding rim. The cliff top slump block is tilted back. The floor area contains several prominent pressure ridges.

The evolution of the amphitheatre and the formation of the elevated shear surfaces is illustrated in Figure 5-1. Visual evidence that the rates of movement of the amphitheatre floor were in excess of the surrounding bench can be found in the amount of colluvium deposited on the A3 bench. Whilst mudslides A and B were active in the same area subsequent data from the survey of surface movements does confirm slow to moderate rates of movement for the amphitheatre floor. A significant characteristic of the mudslides is that material does not move laterally into the mudslide channels. Therefore the depression of the central amphitheatre floor between the mudslides is

not due to mudslide activity but is due to the accelerated movement of the amphitheatre floor. The progressive section, drawn in Figure 5-1, shows the possible movement of the F bench, which was incorporated within the initial failure, downslope and the subsequent utilization of the F bedding plane shear surface within the amphitheatre floor. Whilst this concept of amphitheatre evolution is difficult to substantiate, augering experience from the installation of both inclinometers and slip indicators indicated a distinct change in material stiffness well above the level of the in-situ clay of the D zone. The evolution outlined above would result in a zone of F_1 Barton Clay immediately below the upper amphitheatre shear surface.

Additional evidence of the origin of the amphitheatre shear plane is provided by relative levels of the slump block and the shear surface. The difference in level between the cliff top and F bedding plane shear surface before failure was approximately 5.5m. At present the shear surface is at 12.5m A.O.D. and the average level of the slump block at 19.5m A.O.D. The upper amphitheatre shear surface is probably a displaced section of the F preferred bedding plane shear plane.

The study area therefore contains two types of multi-layered landslide. The first type has resulted from the formation of a shear surface within material already incorporated in a deep seated failure. The second has been formed by the movement of an existing shear surface already contained in a failed block, before failure, to a position overlying another existing shear surface.

5.0.2 Detection

In an actively degrading slope the presence of debris slides and mudslides provides visual evidence of the

possibility of layered landslides. In an area where once active processes have become dormant the detection of more than one shear surface in a vertical section may be difficult.

At Highcliffe the presence of widely exposed preferred bedding plane shear surfaces gives strong visual evidence of the position of active shear surfaces within the cliff section. However, where the D bench is overlain by an active debris slide it is impossible to physically detect movement on the lower surface.

The difficulty in locating two superimposed shear surfaces is centred on the difference in movement rates between the two layers of colluvium. Figure 5-2 illustrates an idealized section through a two layered landslide. Six cases are drawn which indicate all the possible combinations of relative rates of movement and the effect on an inclinometer or slip indicator tube. The tube is assumed to have been installed vertically.

If the tube is an inclinometer both shear planes will only be detected if the difference in velocity between any two layers is small enough to allow the accommodation of both movements without blocking the access for the measurement torpedo.

A slip indicator is normally used only to detect the position of one shear surface. In a multi-layered slide it would detect the junction between the two layers with the greatest velocity difference. If a multi-layered landslide was not anticipated the slip indicator would then be abandoned. Where a multi-layered regime is suspected a series of slip-indicators could be installed to various depths to identify different levels of shear surface activity. However, a second shear plane could only be detected if it was above a surface with the greater velocity difference.

The amphitheatre floor was the only area where two active shear surfaces were physically detected. Three inclinometers and one slip indicator registered failure at approximately 12.5m A.O.D. One slip indicator failed on the D bedding plane shear surface at 9.29m A.O.D.

The possibility of a multi-layered landslide area can be investigated by a comprehensive network of surface movement points. A sudden increase in surface velocities in a confined area which had previously only registered rates similar to the surrounds may indicate the activation of an extra shear surface. At Highcliffe the surface movements recorded during the first summer period for the amphitheatre floor was very similar to the surrounding D bench. Average seaward movements of 60mm and 70mm were recorded, during the first summer, for the central D bench and the amphitheatre floor respectively. Consequently the mechanism of movement in the two areas was thought to be the same. Observations for the period W1/2 indicated that the amphitheatre floor had accelerated to an average total seaward movement of 2,490mm compared to 340mm for the D bench. This implied an alteration to the mechanism of sliding; sub-surface investigation subsequently confirmed the presence of two shear surfaces.

5.0.3 Significance

The presence of any shear surface whether active or dormant is fundamental to the understanding of the movements and the stability conditions of a slope. If two or more shear surfaces are present but only one shear surface is anticipated and only one failure plane positively located then an engineering project could be put at risk.

In this research project a full awareness of both the number and position of all shear surfaces, whether they

were single or layered, was required for three reasons.

(1) To interpret the pattern of surface velocities for each geomorphological process.
(2) To enable the application of the appropriate velocity component to calculate the rate of colluvium transfer by any geomorphological process.
(3) To enable the calculation of the volume of colluvium contained within each geomorphological process.

5.1 Description of surface movements

Any point on the surface of a two or three layered slide moves as a result of the combination of the displacement vectors of each level. In the study area it has been possible to measure sufficient displacement vectors to allow the calculation of all the component vectors of the debris slides, mudslide A and the amphitheatre floor.

In this section an account will be given of a two layered landslide area and a three layered landslide area. The velocity components for the seven sites within the study area are summarized in Table 5-2.

5.1.1 Debris slide 1

Debris slide 1 is positioned on the rear portion of the D bench. The section, Figure 5-3, through the centre of the slide illustrates two active shear planes. Inclinometer I9 indicated a failure surface 1.82m below ground level. It has not been possible to detect the lower curved surface which links the D bedding plane shear surface to the exposed in-situ clay of the F scarp.

The observed movements for DS1 and the central region of the bench have been monitored by seven pegs. The movement

characteristics of the debris slide are divided into three areas corresponding to the upper, middle and lower elements of the slope. The upper element was represented by three different pegs to allow a movement pattern over the complete study period to be compiled. The slope angle varied between 20° and 35° and had a maximum width of 5 metres in a downslope direction. Both the middle and lower slope elements were monitored by one peg. Peg 159 was located in the middle area; this portion of the slope varied in angle between 15° and 27°. Further downslope peg 157 was located on the gentler slopes of the lower section where angles were between 10° and 15°.

To allow comparison with the movements of the D bench two pegs in the central region have been used: pegs 161 and 162. The separation of the velocity components is carried out only for the seaward direction (Y). Table 5-2 lists the observed displacements of DS1 and the D bench. If the observed movement of the debris slide is a combination of the actual debris slide displacement and the D bench displacement then the difference between the two observed rates is the true debris slide component e.g.

Observed debris slide movement	=	a + b
Observed D bench movement	=	a
Actual debris slide component	=	b

The cumulative displacements are plotted in Figure 5-4. The characteristics of the isolated debris slide movement differs from the observed characteristics as follows:-

(1) The total movement for the debris slide is less than the observed movement of pegs located within the slide. The lower, middle and upper sections indicated 56%, 71% and 72% of the total observed movement.

Therefore the activity of the slide, in particular the lower section is only just in excess of the D bench.

(2) The observed rates, debris slide plus bench movements, of movement for DS1 never, of necessity, fell below the velocity recorded by the D bench. The true debris slide velocity ranged from moderate to extremely slow. In three separate periods the actual debris slide moved slower than the bench. The three periods were 8 July 1981 to 22 September 1981, 23 March 1982 to 1 June 1982 and 4 January 1983 to 12 July 1983.

The last period registered only 10mm Y of seaward advance for the upper region of DS1 and 160mm Y for the D bench, peg 162.

The separation of the velocity components therefore indicates the seasonal variation of rate of movement of the debris slide and their larger range. The maximum observed range from DS1 was 5mm Yd to 143mm Yd.

(3) The overall pattern of debris slide movement is very similar to the D bench.

The separated patterns do indicate the proportion of movement along each shear surface during the surge movements. The first surge period, between 11 November and 24 November 1981, indicated that 52% to 56% of the movement occurred on the D bedding plane shear surface. The second surge period, 6 October 1982 to 2 November 1982, indicated a wider range of 48% to 64% for the D bench component: This depended on which debris slide area is being considered.

This can be contrasted with the movements associated with the March 1982 slump. Between 9 and 18 March 1982 the observed seaward movements for DS1 were 430mm Y, 540mm Y and 1300mm Y for the lower, middle and upper slope elements. The division of the movements between the actual debris slide movements and the D bench sliding results in the following percentage split:-

Element	Debris Slide	D Bench
Upper	95%	5%
Middle	80%	20%
Lower	86%	14%

Therefore the effect of the slump on the debris slide was to accelerate the movement along the shallow basal surface of the debris slide. In contrast the surge movements, whilst accelerating the observed debris slide, were primarily movements along the D preferred bedding plane shear surface.

5.1.2 Debris slide 2

Figure 5-5 illustrates a section through the centre of the amphitheatre. Three shear surfaces are indicated as being active.

To represent the seaward velocity component of each individual process the following algebraic summation of components is assumed:

Observed movement on DS2	= a + b + c
Observed movement on Amphitheatre Floor	= a + b
Observed movement on D bench	= a
Movement along amphitheatre shear surface	= b
Movement along basal plane of debris slide	= c

The study period for this multi-layered slide, was limited to 482 days because of the development of debris slide 5 during the second winter. This debris slide caused acceleration of the pegs monitoring the amphitheatre floor. It is not known exactly how the arrangement of shear surfaces altered during the winter 1982-1983.

Figure 5-6 illustrates the cumulative seaward velocity of

both the observed movements and the component movements for the three layered landslide. The movement of the central D bench and the amphitheatre is indicated by the eastern most peg in each case. Debris slide 2 is represented by two peg records which cover both the western and eastern portions. Unlike DS1 this debris slide is not divided into slope elements as insufficient movement data was available to allow further sub-division. Pegs 186 and 187 moved from the steep upper slope regions to the lower gentler areas in the study period.

5.1.2.1 Movements on Debris slide 2

The movement of colluvium across the shallow basal shear surface of debris slide 2 was significantly different than the observed velocities. Pegs 186/230 and 187 registered field movement totals of 11,060mm Y and 13,470mm Y: the actual debris slide component was 4,990mm Y and 7,400mm Y, 45% and 55% of the total respectively.

Debris slide 2 registered two periods of zero movement. They both coincided with stationary periods recorded for Debris slide 1. The initial dormant period was 8 July 1981 to 22 September 1981: the actual movements of debris slide 2 was comprised only of the D bench component. The second period was from 23 March 1982 to 6 October 1982.

The pattern of the debris slide movement was unlike either the D bench or amphitheatre floor. Both the DS2 pegs exhibited a large seaward movement between 9 December 1981 and 27 January 1982 of 3390mm Y and 3970mm Y for pegs 186 and 187 respectively. A feature not noted on the D bench. Movements in the debris slide were either in the slow to moderate category or extremely slow to dormant (Varnes, 1978). Both the central D bench and the amphitheatre floor had periods of more gradual slow movements with rates of 4mm Yd and 6mm Yd respectively.

The debris sliding component was generally the substantial component of any observed debris slide movement, however the contribution to SG1 and SG2 was relatively low at an average percentage contribution of 14% and 18% respectively.

5.1.2.2 Movements on the amphitheatre floor

The middle layer of this three layered landslide moved along a basal shear surface at 12.5m A.O.D. The seaward component of the amphitheatre slide moved on average 3870mm Y. This compares with the observed movement of peg 33 which equalled 6070mm Y over the same two year period: the component equalled 64% of the total.

Only one period of zero movement was recorded, this was over the first summer period S1 and extended between 8 July 1981 and 22 September 1981. During the second summer the amphitheatre maintained a rate in excess of the D bench, 2mm Yd compared to 1mm Yd.

The section through the centre of the amphitheatre, Fig. 5-5 indicates that in addition to the amphitheatre floor being the middle layer in a three layer landslide it is also the top layer in a two layer landslide immediately downslope of the debris slide. The percentage contribution of the amphitheatre seaward velocity component to both the two and three layer complexes is summarised in Table 5-3.

The amphitheatre slide was more active than the central D bench: the total average seaward displacement was 3870mm Y and 2200mm Y respectively.

5.1.3 Other areas of multi-layered landslides

The tabulation of the seaward velocity components for the

remaining five areas of multi-layered failure is shown in Table 5-2.

Debris slides 4 and 5, which both formed in 1982 and are therefore relatively recent, have high percentages of debris slide component. These are 84% and 95% respectively. In contrast debris slide 3, which formed in November 1981, but lost its supply of fresh debris after March 1982, had a debris slide component of 42%.

Mudslide A moved 22,050mm Y in 734 days. The large majority of this total 89%, occurred due to movement along the mudslide basal shear plane.

When active both mudslide A and the debris slides dominate the movement characteristic of their bench area. They can account for a maximum of 95% of the seaward movement recorded.

5.2 The analysis and presentation of surface movements with two or more components

The surface movements of a landslide are vector quantities. They can be analysed graphically or algebraically. Where the displacement is a result of movement along only one shear surface graphical presentation of the results is adequate to describe the movements within the slide. If the observed movement is the resultant of two or more active shear surfaces then the constituent vectors are best calculated algebraically.

The conventional method used to display either displacement vectors or velocity vectors is to overlay them on a topographical or geomorphological background. this technique does give a good pictorial representation of movements within an area although it is restrictive in two aspects.

(1) Only movements in two dimensions can be individually presented.

(2) Where displacement vectors are transferred directly on to a background map two different scales are normally required for the movement and the topography. The displacement vectors do not therefore identify the start and finish position of a survey point.

Examples of the superposition of movement vectors on to topographical/geomorphological maps are given in Merriam (1960), Fukuoko (1953) and Hutchinson (1970). All these studies have considered single layer slides. The construction of geometric shapes to represent the observed movement and its constituent elements in a multi-layered slide is confusing on a background map.

Another method of visual presentation is the construction of a graph. The axes are normally labelled distance against time. Distance is presented as either a cumulative figure Hutchinson (1970) and Barton and Coles (1984) or an amount of displacement over a certain time period Prior et al.(1968). Analytically the presentation of data on a graph is superior to pictorial representation because it allows the considerations of the change in movement rates with time. However, only a limited amount of data points can be displayed.

The presentation of vectors purely in a graphical form without any background map does allow the subtraction of displacement or velocity vectors to obtain the movement of a superimposed process. This technique was used by Ter-Stepanian and Goldstein (1969). They described a method where for a given surface point on a sliding solid mass the velocity vector for a particular time period is separated into the three velocity components Vx, Vy and Vz. Each surface position was then represented by one point on each of two graphs. One construction defines the

horizontal plane Vx and Vy. The second plot a vertical plane Vxy and Vz. If the resultant velocity vectors of a two layer landslide and one of the constituents are known then the plot graphical represents the unknown component. A simplification of the Ter-Stepanian and Goldstein (1969) illustration is given in Figure 5-7. This method of vector subtraction could have been performed algebraically.

The advantages of the Ter-Stepanian and Goldstein technique, in addition to the vector subtraction, is that a single mass can be described by several positions on a section line. The distribution of points on the velocity component graph can also indicate the nature of the slide. The examples quoted differentiate between planar and rotational depth creep, a retreating or advancing slide, and an earth flow. It also indicates the position of the seat of sliding.

However, where either three or more layers are on the same slope or a high degree of accuracy is required, algebraic subtraction is to be preferred.

5.2.1 Highcliffe data

To further illustrate the technique used by Ter-Stepanian and Goldstein (1969) an example of multi-layered movements recorded at Highcliffe will be presented in the same manner.

The initial analysis of displacement in Debris slide 1 simply considered the seaward direction of movement (+ Y). Figure 5-4. illustrates the cumulative seaward displacement with time. Subtraction of the central D bench records from the observed debris slide data gives the movement of the colluvium over the shallow basal shear surface of the debris slide, Table 5-4.

The data presented in Figures 5-8, 5-9, 5-10 and 5-11 differ from the Ter-Stepanian and Goldstein figures by replacing velocity vector components with displacement vector components. This change does not alter the interpretation of the resultant plot. The actual points plotted represent the displacements observed during each of the seven subdivisions of the total 734 day study period. Unlike the theoretical case considered by Ter-Stepanian and Goldstein (1969) the movement of an actual process is an average of the observed points. No construction is presented on any of the figures but it is illustrated algebraically in section 5.2.2.

The points plotted in Figures 5-8 and 5-9. are the displacements in the horizontal plane and vertical plane respectively for the three summer periods. Figure 5-8. emphasises the extremely low rates of movement for the debris slide component where the ranges of movement for the D bench and debris slide for S1 and S3 virtually overlap. The larger separation during S2 was caused by the extended affect the March 1982 slump. Figure 5-9 illustrates a very similar trend to that described for Fig. 5-8 although differences in the change of elevation (Z) were slightly greater than either the X or Y direction.

The winter and surge periods are presented on Figures 5-10 and 5-11. In contrast to the summer data the activity of the debris slide shear plane has produced a far larger separation of the observed debris slide and D bench points. Figure 5-10 emphasises both the predominant seaward direction of the movement and the relatively large percentage of surge movement which occurred along the D preferred bedding plane shear surface. Only areas W1/1 and W2 are close; the position of W1/2 again emphasises the effect of the March 1982 slump. Figure 5-11 also reflects these trends; the range of changes in elevation for the W1/2 period is large. The greatest change in

elevation was recorded on survey peg 223: at - 3860mm Z on the rear of the slide.

Study of the pattern of distribution of the points indicate four features.

(1) The movement of the D bench is a slow seaward displacement. Whether the movement is rotational or translational is not clear. Cross sections drawn through the bench indicate that the shear surface underlying the D bench must begin to curve upwards to joint the F scarp seen exposed further to the west.

(2) The movement of the debris slide in summer indicates a slow seaward displacement. This is more rotational than would be expected for the shallow translational movement of a debris slide. The movement of the surface of the debris slide in summer is due to bench sliding. The component produced by movement along the basal surface of the debris slide is small.

(3) The movement of the D bench during the winter represents an increase in movement velocity but no change in the direction of the displacement across the bench.

(4) Winter movements on the debris slide have displayed a large variety of rates. The observed movements are produced by a combination of translational sliding on the debris slide basal shear surface and movement on the D preferred bedding plane shear surface.

5.2.2 Algebraic subtraction

An example of the production of displacement components for Debris Slide 1 during the first summer is given below. The average observed movement for DS1 is calculated for three pegs 152, 157 and 159.

Peg No.	Displacement (metres) during first summer (S1)		
	x	y	z
152	-0.01	0.03	0
157	-0.01	0.05	-0.05
159	0.01	0.07	-0.03
Total	-0.01	0.15	-0.08

Average observed movement for debris slide 1.

$$a_x = -0.01m$$
$$a_y = 0.05m$$
$$a_z = -0.03m$$

The average observed movement for the central D bench is calculated from pegs 161, 162 and 163.

Peg No.	Displacement (metres) during first summer (S1)		
	x	y	z
161	0	0.05	-0.03
162	-0.01	0.05	0
163	-0.02	0.04	-0.01
Total	-0.03	0.14	-0.04

Average observed movement for the central D bench.

$$b_x = -0.01m$$
$$b_y = 0.05m$$
$$b_z = -0.01m$$

The actual average movements of the debris slide is equal to the following:-

$$c_x = a_x - b_x$$
$$c_y = a_y - b_y$$
$$c_z = a_z - b_z$$

$$\epsilon_x = 0$$
$$\epsilon_y = 0$$
$$\epsilon_z = -0.02m$$

Displacement of the debris slide was zero in the horizontal plane and -20mm in the vertical plane.

Table 5-4 details the displacement vector components for the complete study period.

5.3 Theoretical surface movements on a two layered landslide

The surface movements of a two layer landslide is determined by the slope geometry, extent of movement of each layer and the initial position of the surface point.

Figure 5-12 illustrates a theoretical landslide which is composed of a rotational slide with a circular slip surface overlain by a translational slide. The slope is drawn in three failure positions corresponding to pure translation of the surface, pure rotation of the deeper circular failure and a combination of the two. Three vectors are drawn to represent the three types of failure.

5.3.1 Translation of the surface layer

For a shear surface displacement M on a surface inclined at $\theta°$ the change in position for point P is

$$\Delta Yp = M \cos \theta$$
$$\Delta Zp = M \sin \theta$$

5.3.2 Surface movements on a pure rotational failure (See Figure 5-13)

The movements of a point P on the landslide surface can be calculated as follows:

Let H = Height of Slope
R = Radius of Slip Circle
t = Thickness of Translational Slide
θ = Angle of Slope
φ = Angle of rotation of circular slip
Yo, Zo = Co-ordinates of the bottom of the inclined slope
Ya, Za = Co-ordinates of the downslope extreme of the circular slip circle
Ys, Zs = Co-ordinates of the centre of the slip circle
Yp, Zp = Co-ordinates of the surface point
ΔY = Change in Y ordinate after a rotation of $\theta°$ of the circular slip
ΔZ = Change in Z ordinate after a rotation of $\theta°$ of the circular slip
SP = Height of P above slope base

$$Ya = Yo - t \sin\theta$$

$$Za = Zo - t \cos\theta$$

$$\alpha = 90° - \theta - \cos^{-1}\left(\frac{H}{2R\sin\theta}\right)$$

$$Ys = Ya - R \sin\alpha$$

$$Zs = Za + R \cos\alpha$$

$$Zp = Zo + SP$$

$$Yp = Yo - (Zp/\tan\theta)$$

$$r = \sqrt{(Yp - Ys)^2 + (Zs - Zp)^2}$$

$$\beta = \tan^{-1}\left(\frac{Yp - Ys}{Zs - Zp}\right)$$

$$\varphi_1 = 180 + \beta$$

$$\varphi_2 = \varphi_1 + \varphi$$

$$Y = r\ (\text{Sin}\ \varphi_1 - \text{Sin}\ \varphi_2)$$
$$Z = r\ (\text{Cos}\ \varphi_2 - \text{Cos}\ \varphi_1)$$

The displacement of the point describes a circle with radius r, centred at the co-ordinates Ys and Zs.

5.3.3 Two layer movement

Where displacement occurs both along the translational slide and the rotational slide then the total movement along the surface of the slide is an addition of the two displacement vectors.

Figure 5-12. illustrates the two component displacement vectors for the translation and rotation. In the field these processes would occur simultaneously. In the theoretical case the two slide movements can be considered as acting one after the other. The displacement vectors are commutative.

5.3.4 Debris slide 1 - Simulation

To simulate the velocities observed on DS1, Figure 5-3. shows a section through the centre of the debris slide. To allow theoretical modelling of the movements the section was represented by two idealised slides. DS1 is replaced by a translational slide and the D bench under DS1 by a circular slip surface.

The construction of the slip circle used on the cross section was based on observations of the F scarp exposure just below the F preferred bedding plane shear surface and the level of the D shear surface. Data from the graphical construction and field surveying provided the following information:

H = 10.3m
R = 15.5m
t = 1.4m
θ = 21.5°

YO = 134.6m
ZO = 14.2m

5.3.4.1 First summer - Simulation (S1)

Survey data, Figure 5-4. and Table 5-4, have shown that during the first 76 days of the study period movement of the debris slide was only caused by displacement along the D bedding plane shear surface.

For five points on the slide surface the change in position for both the Y and Z dimension were calculated. These changes are plotted on Figures 5-14 together with the measured summer movements for the debris slide. Two angles of slip circle rotation were chosen, $\varphi = 0.5°$ and $\varphi = 1.0°$. The three observed movements are positioned between the two theoretical sets of displacement but do not indicate the same decrease in elevation. All these survey pegs were located in the lower third of the slide.

5.3.4.2 First winter - Simulation (W1/1)

The first winter period caused movement to begin along the basal shear surface of DS1. To simulate the displacement on the slide during this period an estimation of both the rotation of the circular slip and the amount of translation along the debris slide was needed. Figure 5-4 can be used to estimate the seaward translation of the debris slide. For all three areas of the slide this was 0.28m Y.

Figure 5.15. illustrates the displacement vectors composed Y and Z for W1/1 and for theoretical slip circle rotations of 2° and 3°. The same three survey pegs as used above

were again plotted for W1/1. Pegs 157 and 159 are close to the theoretical movement on the lower slope. Peg 158 with a large value of Y indicates a translation in excess of that recorded elsewhere.

5.3.4.3 Significance

The comparison of actual recorded movements with those generated from modelling indicates that the concept of superimposed slides is valid.

5.4 Conclusions

This chapter has identified the presence of multi-layered landslide in the study area. Seven areas have been identified which have been shown to contain more than one shear surface in a vertical plane.

The origins of a multi-layered slide can be divided into two categories. Firstly where processes of slope degradation i.e. a mudslide or debris slide develop on a block of soil which has been displaced on an independent failure plane. Secondly where an existing shear plane or potential shear plane is included in a failure block and this plane is then activated by the change in position of the failed block. Examples of both categories are described and identified in the study area.

It is emphasised that the detection of more than one shear plane in a vertical section is difficult. Firstly, multi-layered slides are not generally anticipated and an investigation may approach a slope study with the expectation of there being only a single shear plane. Secondly, instrumentation through a multi-layered slide may only detect one shear plane before it is either destroyed or abandoned. The resultant remedial design for

the slope could be incorrect for the whole slope.

The above situation should be avoided if the slope is subject to a thorough desk study with aerial photographic coverage and a detailed study of the geomorphology. This should identify the origin of the instability and highlight the various forms of slope degradation present.

Where multi-layered landslides are known to exist the representation of surface movement is difficult. It is considered best to restrict the superposition of velocity vectors onto background maps to single layer slides only. The graphical presentation of two layer slides can be performed on graphs. If three or more layers are present algebraic methods are needed to calculate the individual slide components.

CHAPTER 6: THE COLLUVIAL BUDGET

CHAPTER 6: THE COLLUVIAL BUDGET

6.0 Introduction

Brunsden (1973) suggested that the concept of systems analysis could be applied to slopes. By careful field measurement the study of slope degradational processes can be applied to the transfer of debris in a mass movement system. The system is arranged to model the transfer of material and water downslope. This approach was applied to a landslide complex at Stonebarrow Hill, Dorset which is also described in Brunsden and Jones (1972), Brunsden (1974) and Brunsden and Jones (1976). Although it should be noted that they did not have sufficient measurements to draw up the budget quantitatively.

The budgetary approach simply considers the volume of material and water which enters and exits the slope and therefore allows the calculation of any change in the volume of material and water stored in the slope. Brunsden (1973) applied the budget approach to a mudflow system and defined the methods of study and the inputs into the mudflow system. However no actual quantitative results were published.

The production of a budget for a landslide system demonstrates how the evolution of the slope is subject to various forms of slope degradation. The gain or loss in volume of a particular element of the budgetary system and the identification of the process causing the change indicates the rate of change, the significance of a particular process and potentially the overall evolutionary pattern of the slope. The changing geometry of a slope will indicate areas of potential instability.

The objective of the study with respect to the colluvial budget were as follows:-

1. To provide a basis for a quantitative and detailed examination of an actively degrading landslide complex.

2. To determine the relative contributions of the various components degradational processes to the overall movement of material.

3. To find whether this systems approach to landslide studies yields fresh insight into the general understanding of mass movements.

This Chapter specifically describes the budget of the study area with respect to landslide debris. The problem of determining the movement of free water across the undercliff was discussed by Thomson (1987) who showed that surface run-off in particular was very difficult to evaluate and was best found from solution of the other factors making up the overall water balance. Where water is bound with the landslide debris it is included in the budgetary study. The data from the two year field study is used to calculate the change in volume of all the elements in the system.

6.1 The budgetary study area

Unlike the study area defined in Chapter 2 the calculation of the colluvial budget was restricted to a 200m length of coastline. This strip of coastal slope lies within the 270m section considered in Chapters 2 to 5. It is bounded by N.G.R. 422100E and 422300E see Fig. 2-7. The reduction in the width of the study area was required to utilise the limited coverage of the undercliff offered by the contoured aerial photographs and the field data. The relationship between the study area and the complete undefended coastline is discussed in Chapter 2.

The budgetary zone differs from the full study area in the extent of bench coverage either side of the amphitheatre. The north/south limit of the area remained the cliff top and the beach.

6.2 The budgetary system

To move from the cliff top to the beach the colluvium has to be transported through a series of geomorphological units. Similar systems have been described by Brunsden (1973) for the Upper Lias cliffs of Dorset and by Pitts (1983) for cliffs composed of glacial deposits in the Dee Estuary. An initial description of the budgetary system for the Naish Farm frontage was given by Barton and Coles (1984).

To enable the calculation of the volumes of colluvium which move between the slope elements the study area is divided into five sections:

(1) Cliff Top
(2) F Bench
(3) D Bench
(4) A3 Bench
(5) Beach

The movement of material between these sections is illustrated in Fig. 6-1. This flow chart can be compared to the debris 'cascade' presented by Brunsden (1973), Fig. 6. The Stonebarrow Hill complex is a four element undercliff.

a. Cliff Top
b. Landslide store
c. Mudflow store
d. Beach

Movement between each element is divided into input from the primary material store and debris throughput. All possible sources are considered including basal and lateral inclusion of both the landslide and mudslide processes.

The Naish Farm flow chart presents a simpler system. Only those elements of the transportation system which could be evaluated in terms of volumes moved are included. This requires the omission of all basal and lateral inclusions. In the case of the benches there is no basal inclusion and no lateral inclusion.

In debris slides and mudslides any lateral inclusion can only effect the route taken by the debris and does not change the total volume. Basal inclusion must alter the shape or the elevation of the failure surface. No evidence of this has been noted.

The processes illustrated in Figure 2-9 can be divided into two types:

(1) Actively Degrading Process
- spalling
- slumping

(2) Transporting Process
- bench slides
- mudslides
- debris slides

The actively degrading processes occur on the in-situ scarp faces of the cliff top, D scarp, F scarp and A3 scarp.

The primary transportation mode is bench sliding, this occurs across each bench and finally deposits debris onto the beach. Only Debris Slide 3 transport debris directly

from one bench to another. The other debris slides are contained within the D bench. Mudslide A transports debris from the D bench onto the A3 bench. Mudslide B, fed by the D bench, provides a channel cutting across the A3 bench and deposits debris onto the beach at a faster rate than the A3 bench sliding.

6.3 A detailed description of the movement of landslide debris in the study area

Whilst the account of the Stonebarrow Hill landslide complex gives a comprehensive picture of the debris cascade no attempt was made to produce a quantitative colluvial budget. The intensive field work performed during the two year study period at Highcliffe has enabled such a budget to be compiled for the restricted study area.

The data available was a combination of field work observations and data from the contour maps. The following sections give an account of the methods used to calculate the colluvial budget presented in Table 6-1 and Table 6-2.

6.3.1 Cliff Top to F Bench (Table 6-3)

The total recession of the cliff top scarp is caused by spalling and slumping of both the gravel and clay face. The contour maps, dated 26 November 1980 and July 1982 showed a total land loss of 230m^2 across the budgetary study area. The recession for the first year, July 1981 to July 1982, was estimated as 141m^2. The second year was precisely monitored using the July 1982 contour map and a July 1983 cliff top survey. Ninety square meters were lost. Total recession volumes were calculated using the total area of cliff lost multiplied by the average height

of the exposed cliff top scarp. Since the budget calculations are in volume terms the change from in-situ material to landslide debris is accompanied by bulking. Where recession of the Plateau Gravel, Barton Clay and the inclusion of fresh slumps are considered a bulking factor is incorporated. No in-situ densities were measured at Naish Farm in the Plateau Gravel and Barton Clay and a bulking factor of 1.3 was used after Hutchinson (1970).

The only component of the recession which could be measured directly was the spalling rate of the gravel face. Frequent monitoring of three reinforcement bars enabled recession to be calculated for the total gravel exposure. Only one slump block was large enough to be reliably measured.

The results from the field study are given in Table 6-3 and the following observations made.

(1) During the two year study period 13% of the material which fell onto the F bench resulted from spalling of the exposed Plateau Gravel face. Twenty seven per cent was derived from a single slump and the remaining 60% originated from small failures of the cliff top scarp.

(2) The spalling of the Plateau Gravel plays a minor role in the overall retreat of the cliff top.

Very few direct measurements have been taken on the weathering rate of in-situ cliff faces. Only Schumm (1956) and Brunsden (1973) have described the use of erosion pins for this work. Schumm monitored sixteen slope profiles in the Badlands of New Jersey, U.S.A. Brunsden described the use of steel erosion pins in a sandstone scarp. Monitoring, initiated in 1968, was reported by Brunsden and Jones (1976) to have shown an annual recession rate of 0.15m in a clay slope. This is comparable with the rate recorded at Naish Farm of 0.11m

per year.

(3) A large volume of material can be detached from the cliff top scarp by a single slump failure. The only measured slump in the study period was 8.65m long. The slump block enclosed 27% of the total volume of cliff debris derived from cliff edge recession over the two year period.

Study of the aerial photographic coverage in 23 April 1978 allows the measurement of the size of a large slump block. The segmental area, calculated from the formula for the area of a circular segment (Bronshtein and Semendyayeu, 1973) is 349m^2. The slump is thought to have used the D preferred bedding plane shear surface as its basal surface. If the cliff top was 30.5m A.O.D. and the shear surface 9.5m A.O.D., the volume of the slump was approximately 7,330m^3. This represents 9% of the total volume of colluvium contained in the whole study area in July 1981.

(4) The long term balance between cliff top slumping and the smaller scale spalls is difficult to assess. The forty two slumps reported in 1.73km of cliff line, Barton, Coles and Tiller (1983), and the slow rate of gravel spalling indicates that generally recession due to cliff top slumps is significant.

6.3.2 F Bench to D Bench (Table 6-4)

The two transportation modes used to move debris from the F bench to the D bench were F bench sliding and debris slide 3.

The benchslide was active only in a central, 110m wide section. The active area was divided into three sub-sections for the first year and into two sub-sections

for the second. In any one sub-section the seaward velocities were similar and the average movement is multiplied by the frontal area of the bench to give an estimate of volumetric movement. The frontal area is illustrated in Figure 6-2. It is an area which can be considered to have been displaced seawards by the average displacement. The multiplication of frontal area by seaward movement per year results in a yearly figure for the volume of colluvium which has been displaced onto the D bench.

During the first year of study, July 1981 to July 1982, debris slide 3 became active and transported 280m^3 of colluvium onto the D bench. This volume was estimated by considering the average depth of the slide from SPI13, SPI14 and I8 multiplied by the width of the slide. The width was taken at the section where the inclined portion, which lay on the F scarp, met the flatter section, which lay on the D bench proper. The average movements were calculated using the seaward velocities recorded for the debris slide minus the component of movement for the D bench.

After July 1982 the debris slide coalesced into the D bench and did not actively transport colluvium during July 1982 to July 1983.

Table 6-4 contains the detailed results from the field work and these have lead to the following conclusions.

(1) The transfer of colluvium from the F bench to the D bench did not exceed the total volume of material gained from recession of the cliff top scarp. The F bench was the only geomorphological unit to increase in colluvial volume.

(2) The volume of material lost from the F bench was virtually constant over the two years; 140m^3 and 101m^3.

(3) Debris slide 3 moved 54% of the total volume gained by the D bench.

(4) The low volume of colluvium transported by the F bench sliding is supplemented by the formation of debris slides and cliff top slumps. F bench sliding in this section of the undercliff cannot supply enough debris to maintain the volume of colluvium in the D bench. The F bench is shallow and has an average depth of 2.5m. During the study period only 110m of the bench activity transported material to the D bench. The confinement of bench sliding to the central portion of the F bench can be related to the spatial distribution of the cliff top recession during the study period. Figure 6-3 shows the recession of the cliff top between November 1980 and July 1983. Areas of recession are one to the extreme west, where a 35m length of cliff top has receded up to a maximum of 4.7m, this concentrated cliff top degradation lead to the formation of debris slide 3. In the central region the second area, 70m in length, is directly behind the area of bench sliding on the F bench noted in the budget calculations. The activity of the F bench in this region is therefore stimulated by a fresh supply of material from the cliff top.

The reason for , during any one period of time, cliff top recession being concentrated at any one particular section of cliff top is probably a combination of the following effects:-

i) The cliff face intercepts the flow of water along the Plateau Gravel/Barton Clay interface. This interface has been reported by Thomson (1987) to consist of a series of troughs and ridges running in a south westerly direction. Thomson illustrates, reproduced in Fig. 6-4, that both concentrations of cliff top recession correspond to the outlet of a trough at the cliff face. The higher volumes of water flow would

cause increased seepage forces in the area and possibly weaken the Plateau Gravel mass locally.

ii) The localised concentration of water flow from the troughs would cause locally increased movement rates in the undercliff due to 'wetting' of debris and the generation of higher pore water pressures. Increased movement of the undercliff and in particular the F bench could decrease the toe loading on the potential failures due to cliff top slumping. The cliff top slump failure in February 1982 may by an example of this mechanism.

iii) The Plateau Gravel in any area may be locally 'weaker' due to the conditions during its sedimentation. This could have affected the degree of cementation between particles or the particle size distribution which would determine the bulk permeability of the Plateau Gravel mass.

iv) Areas of the undercliff at Naish Farm have been subject to building works associated with the holiday estate. Underground services have been installed which could result in very localised weakening of the cliff face when recession reaches a service trench.

6.3.3 D Bench to A3 Bench (Table 6-5)

The movement of material from the D bench and the D scarp onto the A3 bench was divided between five processes. All five were active during the full two year study period.

The bench was divided into three regions; one either side of the amphitheatre and the amphitheatre itself. The amphitheatre was divided into a section occupied by mudslide A and the remaining area. The same procedure for the calculation of frontal areas and the average seaward

movement was used as described in section 6.3.2.

The amphitheatre frontage was divided into two levels of sliding.

(1) The uppermost slide utilizing the elevated shear surface discussed in Chapter 4. It contained debris bounded by the shear surface at 12.5m A.O.D. and the ground surface. Velocities for this slide were obtained from survey pegs within the amphitheatre.

(2) The lower slide; this was sandwiched between the D preferred bedding plane shear surface and the elevated shear surface. Bench slide velocities were derived from survey pegs behind the amphitheatre complex.

Mudslide A was monitored by a chronological sequence of survey pegs during the two year study period. The total component of seaward movement exceeded the maximum possible distance travelled by a single peg. An estimate of the average depth of mudslide A was derived from the penetration tests described in Chapter 4.

Recession of the D scarp, by spalling and slumping of the exposed clay, was evaluated from the contour maps. The first yearly record was derived from the modification of the recession from November 1980 to July 1982 by consideration of the spalling rate of the gravel face. The second study year was not concluded with a contour map. It was not possible to obtain a direct measurement of the scarp recession rate. The rate was approximated by a comparison with the July 1982 to July 1983 gravel recession rates. Whilst this was not ideal the predicted recession 148m^3 compared to 252m^3 for 1981-1982 reflected the general decrease in volume movements during 1982-1983.

Table 6-5 details the results of the field study and the results have been summarised as follows:

(1) Between July 1981 and July 1983 the D bench lost 7,923m^3 of colluvium, 10% of the total colluvium volume for the whole 200m study area in July 1981.

(2) Seventy two percent of the colluvium was transported by bench sliding. Mudslide A moved 2%, the amphitheatre slide 11% and D scarp recession 15%.

(3) The loss of 7,923m^3 of debris from the study area is equal to an average drop in elevation of 0.75m over the total plan area of the D bench.

All the survey pegs on the D bench dropped in elevation as they moved towards the A3 bench. The change in elevation ranged between 0.59m and 2.68m.

(4) The amphitheatre slide declined in volume output from July 81/July 82 to July 82/July 83. The frontal area decreased by 47% although this was partly offset by a 35% increase in seaward velocities.

(5) The in-situ scarp receded 1 metre per year over the whole 200m study width. Direct measurement of the spalling rate of a clay face was carried out between 21 May 1981 and 4 November 1981. The erosion pins recorded 0.22m of recession; an extrapolated yearly rate would only equal 0.48m. The recorded clay spalling record did however show a rapid increase in recession rate after mid September and a six monthly division of rates into summer and winter would indicate a more realistic yearly rate of 0.7m.

A comparable figure for the recession of a clay cliff slope is given by Hutchinson (1970) for the scarp in London Clay above the Beltinge mudslides. The recession rate of 0.44m per year, measured over a 4½ year period, occurred with no suggestion of slumping activity.

6.3.4 A3/Mudslide B to Beach (Table 6-6)

Colluvium was transported from the A3/mudslide B area to the beach by translational movement across the A3 bedding plane shear surface. The larger rates of movement recorded for mudslide B has produced a distinctive channel through which greater volumes of debris move than the equivalent width of A3 bench.

Due to adverse field conditions found on the A3 bench rates of seaward movement were restricted to a 264 day period. This period was between 12 March 1981 and 1 December 1981. For the first 365 day period the seaward movement was scaled in direct proportion. Since the movement recorded did not include a full winter period it can be considered as a minimum yearly rate.

The second year was scaled in proportion to the actual volume of debris feed to the A3 bench. Since the mechanism of undrained loading is considered to be one of the causes of sliding it is thought to be a good guide to the activity of the A3 bench.

The seaward movements of mudslide B were calculated by combining the movements recorded for the A3 bench and individual short term records for mudslide B. The survey data was restricted to July 1981 to July 1982. The second yearly figure was proportioned according to the direct debris feed recorded onto mudslide B.

The field results are given in Table 6-6 and they are summarised as follows:

(1) The volume of colluvium transported by sliding across the A3 preferred bedding plane shear surface is greater than any other process.

(2) The A3 bench has an average depth of 1.89m. The

frontal area was less than the D bench, 374m² compared to 404m² in the two study years respectively. The overall loss of 2,015m³ from the A3 bench was caused by large seaward movements estimated at 13.87m and 10.98m for the two years.

(3) Mudslide B transported 7.7% of the colluvium which moved from the D bench to the A3 bench.

(4) The A3 in-situ scarp is exposed only after wave erosion has removed the colluvium which covers the scarp. Whilst the scarp-line must retreat it proved impossible to assess the rate. The actual volume of material eroded from the retreating A3 scarp would be small due to the low level of exposure.

6.4 Applications of budgetary analysis to the understanding and predicting of undercliff changes

In this section the detailed volume changes outlined in section 6.3 are used to:-

(1) Back analyse the rate of movement in the undercliff since 1947.

(2) Predict the capability of particular types of slide to sustain various rates of movement.

6.4.1 Historical rates of movement

Hutchinson (1970) compared the rate of cliff top retreat predicted by mudflow discharge against the actual rate of cliff recession measured in the field. It was assumed that the discharge from the mudflow at Beltingle, N. Kent was approximately equal to the volume of material supplied to the undercliff by recession of the cliff top. In the

comparison the measured cliff recession was approximately 10% less than the figure calculated from the mudflow discharge.

This method of predicting cliff top recession has been used in the Naish Farm study area. Table 6-7 details the debris loss from the study area, the average cliff height, the equivalent rates of cliff top recession and the actual rates of cliff retreat. The overestimation of recession rate, by an average of 30%, indicates reduction in the volume of landslide debris in the undercliff. This is confirmed by the budget summary in Table 6-2.

The errors in predicting rates of debris supply from debris loss are primarily due to changes in the total volume of colluvium contained in the undercliff. If the undercliff maintained a constant volume the volume of debris input into the slope would equal output. Any change in the rate of debris supply would be immediately reflected in an increase in debris discharge. A time lag is caused by the movement of the landslide debris across the undercliff. In a wide undercliff the time required for debris to physically cross from the entry to the exit could be large.

At Highcliffe, where the undercliff is approximately 100m wide, debris which moved at the average D bench slide rate, between July 1981 and July 1983, of 1.98m/Y would take approximately 25 years to cross the 50m wide central D bench. However, the time lag between an increase in debris supply and debris discharge would be far less. The increase in load caused by the debris input would decrease slope stability, increase the rate of debris movement and volume discharge. The length of the time lag will partly depend on the size of the increase in debris input. The large cliff top slump which failed during February 1982 was observed to cause a virtually instantaneous increase in slide activity in the area adjacent to the failure. A

smaller failure observed during March 1982 increased local slide velocities but did not produce any increase in movements beyond 20 metres downslope.

The prediction of undercliff movement between 1947 and 1983 is based on the known rates of debris supply from cliff recession. This is in contrast to the prediction of rates of debris supply from debris discharge. The calculation of undercliff movement results in an average rate of seaward displacement for the whole D bench in the study area. The calculations are based on the following assumptions:-

(1) The undercliff maintains a constant debris volume.

(2) All landslide debris moves through the D bench.

(3) Debris is supplied to the D bench only by recession of the in-situ cliff top above the 'D' plane.

(4) The volume of debris supplied to the D bench is equal to V_S, where V_S is equal to:-

$$V_S = H \times R \times L$$

V_S = Volume of debris supplied to the D bench per year (m^3/Y)
R = Cliff top recession rate (m/Y)
L = Length of undercliff in the study area (m)
H = Height of cliff face above the D preferred bedding plane shear surface (m)

(5) The volume of debris discharged onto the A3 bench or mudslide B is equal to V_D, where V_D is equal to:-

$$V_D = D \times L \times RB$$

V_D = Volume of debris discharged per year (m^3/Y)
D = Average depth of the D bench (m)
L = Length of undercliff in the study area (m)
RB = Average rate of movement in the D bench (m/Y)

Table 6-8 lists the resultant average rate of movement for the D bench. The only directly comparable movement data is also detailed in Table 6-8.

The data for the period July 1982 to July 1983 is averaged according to a weighting scheme based on the cross sectional area represented by each displacement. The average is 1.81m/Y. The rate predicted from the cliff top recession, for the same period, is 1.3m/Y. The underestimate is due to an overall reduction in the volume of debris contained in the undercliff. The rate of movement to transport the volume of debris supplied from cliff top recession across the undercliff is exceeded in the field data. Therefore more debris is being discharged from the bench than supplied to it. This is confirmed in Table 6-2.

In Table 6-8 the maximum predicted displacement rate occurred between May 1976 and April 1978. This period corresponds with the initial failure of the amphitheatre cliff top slump. The calculated rate of displacement for the D bench was 8.0m per year (22m per day). The range of movement rates recorded for the D bench during the total study period was 0 to 68mm per day.

The calculated average rate of movement for the D bench over the last 36 years has been 3.42m/Y or 9.4mm per day. This is substantially larger than 1.05m/Y or 2.8mm per day recorded between July 1981 and July 1983 for the central D bench.

The relatively low rate of D bench movement recorded between July 1981 and July 1983 compared to the rate

calculated for the period between January 1947 and July 1983 implies that the study period contained reduced bench activity. This is partly due to the lack of a large scale deep seated failure in the small study area over the short study period. Due to the absence of a large failure the volume of material moved by a large slump cannot be estimated.

6.4.2 Rates of slide activity

The method used in section 6.4.1 to calculate the average rate of D bench sliding from historical rates of cliff retreat can be expanded to include the A3 bench and mudslide B. The rate of cliff top retreat determines the volume of debris supplied to the D bench and the D bench, in turn, supplies the A3 bench and Mudslide B.

Determination of the slide velocities was based on the transportation of material by the D bench, the A3 bench and mudslide B of the same volume of debris as produced by the cliff top recession. The calculations are based on the undercliff retaining the same volume throughout the transfer of material i.e. there is no change in the volume of debris stored on the slope.

Table 6-9 details the velocity of the D bench, A3 bench and mudslide B for rates of cliff top recession between 0 and 3 metres per year. The rates for both mudslide B and the A3 bench include the additional debris input from the recession of the in-situ D scarp. The velocities for mudslide B and the A3 bench are approximately 10 and 4 times greater than for the D bench with a cliff top recession rate of 3 metres per year. The relatively shallow depth of the mudslide (3.36m) and the A3 bench (1.77m) necessitate higher velocities. In mudslide B, the width of the corrie occupying the head of the mudslide was used to calculate the volume of debris input into the

feeder zone. Downslope the mudslide narrows from the 10m width of the corrie to a 7m width. The displacement rates calculated are for the 7m wide section of the mudslide.

The slide velocities recorded during the study period are summarized in Table 6-10 and plotted on Figure 6-5. The actual and calculated values for the D bench velocity are close: 2.14m/y and 2.06m/y for the first year and 1.82m/y and 1.34m/y for the second. The velocities recorded for the A3 bench and mudslide B were respectively more and less than those predicted.

The response of each slide process to a changing rate of cliff top recession will depend on their distance from the cliff top. The D bench is nearest to the input of landslide debris from the cliff top. An increase in the cliff edge failure rate will result in extra material moving onto the rear of the bench. The mechanism of undrained loading (Hutchinson and Bhandari, 1971) could increase pore water pressures and enhance movement.

Mudslide B and the A3 bench are both fed from the D bench. Their response to cliff top failures will be governed by the time taken for debris to move across the D bench. The time lag, however, will not be large because the acceleration of the D bench will immediately feed the A3 bench and mudslide B.

The same technique of slide velocity prediction can be applied to the mudslide complex at Beltinge, N. Kent. Hutchinson (1970) gave the average observed rate of cliff edge retreat between September 1961 and December 1966 as 0.39m/y. The shallow slides from the sides and rear of the mudslide corrie were estimated to contribute 70% of the debris supply material to the mudslide. The receding cliff edge had a height of 30.5m above the mudslide basal shear surface.

Table 6-11 summarizes the total debris supply and the predicted mudslide movement rate for different rates of cliff top recession. To calculate the velocity of mudslide II at Beltinge Figure 2 of Hutchinson (1970) was used to obtain the maximum corrie width (56 metres). This width supplied debris to a section of the accumulation zone of mudslide II with a stated cross sectional area of $70m^2$ (Hutchinson, 1970). The velocity of debris movement required to transport the supply volume through a cross sectional area of $70m^2$ was increased by a factor of 1/0.9 to simulate the actual surface velocities recorded. Hutchinson (1970) suggested that the surface velocities recorded at Beltinge had to be reduced by 0.9 to indicate the average rate of subsurface movement. The actual mudslide velocities recorded were across the same cross section.

The figure predicted by the author's method and the observed value of mudslide velocity at Beltinge were 15.09m/y and 18.67m/y, respectively. This covers the period between September 1961 and December 1966.

The greater value for the actual displacement rate indicates an overall reduction in the volume of debris contained within the mudslide channel.

The difference between a predicted and actual rate of slide movement may indicate:-

(i) A wide undercliff. This would produce a time lag between any change in the rate of cliff top recession and the rate of slide displacement.

(ii) A change in the overall shape of the undercliff. This will require the movement of landslide debris.

(iii) Another source of landslide debris. All the previous predicted rates of movement use the recession of

the cliff top as the only source of debris input. Where the actual slide velocities recorded were greater than those predicted, by known debris sources, material could be input from either the basal or lateral shear surfaces.

6.4.3 Supply and discharge

The budgetary system detailed in section 6.3 is a two year 'view' of the evolution of the degrading undercliff. It has shown that the rate of debris loss is far larger than the supply and consequently the volume of debris enclosed in the degrading undercliff is decreasing.

The short fall in supply of newly degraded debris does indicate that either an increased rate of spalling must occur during the longer term evolution of the slope or more numerous or larger cliff top slumps need to occur to supplement the observed debris supply. Visual evidence on the undercliff does indicate that a variety of different slump sizes do occur and the knowledge that the single slump measured during the study period proved 27% of the total debris input into the study area illustrates the significance of this process.

6.5 Budgetary records

Detailed studies of degrading slopes which have resulted in the publication of a budgetary system and/or the calculation of the volumes of degrading material within the slope have been found in Rapp (1960), Brunsden (1973), Brunsden (1974), Brunsden and Jones (1976), Hutchinson and Gostelow (1976) and Pitts (1983).

Rapp (1960) published a comprehensive description of an area of high mountain relief in Scandinavia. The area studied covered 15km^2 and the research was between 1952

and 1960. The results were used to calculate the mass of material incorporated incorporated in eleven geomorphological processes. Whilst this study has produced a volume budget for a degrading area the geology, topography and weathering environment are very different from those present in Christchurch Bay and therefore excludes any comparison.

All the remaining sites are located on the English coast and whilst their geological structure is not identical to the study area the forms of slope degradation were similar to those present at Highcliffe.

6.5.1 Fairy Dell, Dorset

The undercliff which forms the southern extreme of Stonebarrow Hill is an actively degrading slope. It is a large amphitheatre feature 1,400m long, with a maximum width of 350m and is 85m high. The coast is formed by lower cretaceous beds. Brunsden has described the geological setting, the topographical form, the geomorphology and the evolution of the landslide complex.

Brunsden (1973) outlined the application of systems theory to the study of mass movement in this area. A framework to describe the debris 'cascade' at Fairy Dell was presented as a flow diagram. The application of the systems theory to the undercliff formed the basis of a field program. This was briefly described in 1973 and further reported in 1974. Details of small scale mass movements from the free face, changes in slope geometry, slope erosion and maps of erosion and accumulation zones were presented. The record of small scale mass movements from the free face (Brunsden 1976, Table II) was the only presentation of debris volumes. A small portion of the undercliff 100m wide was mapped from September 1966 to September 1969. Measurements of the width, depth and

length of fresh failures were taken with a steel tape. Annual volumes of 188m^3, 97m^3 and 224m^3 were recorded. These volumes are comparable with the small scale failures at Highcliffe, 72m^3 and 93m^3 for the two study years.

The measurement of six cliff slope profiles to establish the rate an form of slope recession was performed using erosion pins and an Abney level. Only one 'total pin ground loss' was published, 21.6cms in five years. This was recorded on a gault clay face. The annual rate of 4.3cms is substantially lower than both the gravel and clay annual spalling rate recorded at Highcliffe which were 11cms and 314cms respectively. No further records of rates or volumes of debris movement were presented.

Whilst the study of Fairy Dell included details of geological setting, landslide slope evolution, slope erosion and systems analysis of the debris cascade no budget calculations were produced.

6.5.2 Hadleigh, Essex

Hutchinson and Gostelow (1976) considered the evolution of an abandoned cliff in London clay at Hadleigh, Essex. Degradation of the slope was divided into four main stages dating back over 10,000 years B.P. Knowledge of the position and volumes of the landslide units within the slope enabled the earlier position of the cliff profile to be reconstructed.

The abandoned nature of the slope precluded the present 'active' slope degradation processes although the rear degrading portion of the coastal slope was still subject to landslipping.

6.5.3 Dee Estuary, Lancashire

Pitts (1983) published geomorphological observations on the south eastern shore of the Dee Estuary. The unstable cliffs are formed of glacial deposits. To aid the design of coastal protection works the slope budget was discussed. Pitt (1983) identified and illustrated after Brunsden (1974):-

(i) the exact route which material took when moving downslope.
(ii) where the material originated from.
(iii) where the material was stored on the slope.

Figure 7.5 illustrates the cliff section presented in Pitt (1983, Figure 7). A three layered section of sand, upper Boulder Clay and Bedded series is shown. The section has marked similarities with the bench profile found at Naish Farm. The junction between the sand and Upper Boulder clay and the Upper Boulder clay and bedded series is shown to act as a bedding plane shear surface. The undercliff is divided into four subsystems:

(1) The landslide
(2) The toe slope
(3) The back scar
(4) The beach

Material input is shown from the sand backscar and the basal shear surfaces of the rotational slides and compound slides. The landslide storage section contains the degrading rotational slides which transport debris onto the inclined toe slope area. Mudslides and mudflows occur in this section and deposit colluvium onto the beach subsystem.

Six geomorphological processes are identified; wind erosion, ground water seepage, rotational slips, creep,

mudslides and mudflows. The development of the coastline in terms of these processes is described. No measurement of the volumes involved in the slope budget is presented.

6.6 Factors affecting the colluvial budget

The brief outline of the known published studies of slope degradation where budgetary systems have been considered or the volume of any element of the degrading slope have been calculated indicate that this study of slope degradation is unique in its consideration of both aspects. This position does not however prevent a discussion on the factors which effect the processes on a slope.

The total number of degradational processes which occur on a landslide is limited. They can be divided into 5 groups.

(i) Slides
(ii) Flows
(iii) Water erosion, suspension and solution
(iv) Wind erosion
(v) Falls

Table 6-12 presents the combination of geology, climate and topography which favours the activity of each category of process.

6.6.1 Geology

Fairy Dell, Hadleigh, Dee Estuary and Christchurch Bay are characterised by the 'regular' bedding of argillaceous sediments. Even the glacial deposits of the Dee Estuary display enough bedding structure to determine the most active form of degradation. All four areas contain slides

which utilize bedding plane shear surfaces. Whilst quantative data on Fairy Dell and the Dee Estuary has not been published, the Naish Farm study has shown that sliding processes transport virtually 100% of the landslip debris. These areas are not susceptible to chemical weathering by running water or to support any significant volume of surface water charged with sediment.

6.6.2 Topography

The topography of an area is the product of climatic and weathering processes on a geological structure. Any link between topography and geomorphology is linked with these two fundamental conditions. There are conditions in the study area which demonstrate how changes in topography can affect the geomorphic development of an area.

(1) In any of the sea cliffs marine erosion can cause an oversteepening of the cliff slope. Oversteepening can cause the mechanism of slope failure to change from shallow to deep seated slides.

(2) In regions where there are exposures of in-situ material weathering processes can degrade the free standing face. The type of material and severity of the weathering will determine the rate of recession but the volume produced is partially dependent on the topography.

(3) The steepness of a slope can determine the severity of erosion by surface water. Steep slopes produce high run-off velocities and the capability of transporting degraded material by bed loading as well as in suspension and solution.

6.6.3 Climate

The climatic conditions in any area will affect the colluvial budget. The seasonal variation in one area will change the balance within a year. The conditions which affect geomorphic processes the most are rainfall, temperature and winds.

(a) Rainfall

Three of the five basic groups of degradational processes are dependent on the amount of groundwater in an area. Slides are normally promoted by high pore water pressures, flows by saturation of an area and the activity of surface water by its availability. In the Highcliffe area the balance of geomorphical activity will change as the amount of rainfall increases. From a relatively 'dry' background state an increase in the groundwater levels will initially promote the movement of bench slides, debris slides and mudslides. If rainfall continues mudruns form on the surface of the mudslides and bench slides. With heavy rain falling onto a saturated area, surface stream flow will occur. Streams charged with sediment are discharged onto the benches where the sediment is dropped. Therefore for a limited period the budgetary balance of the area will change from that quantified in this thesis for a complete year.

(b) Temperature

The range of temperatures experienced has a direct effect on the weathering of exposed faces. Freeze/thaw processes will only occur where the air temperature is depressed long enough to allow the solidification of pore water and is elevated long enough to allow the water to thaw. Whilst the weathering of exposed faces will continue all year there is a distinct increase in rates during winter conditions. This is illustrated in Figure 3-6 where the

rate of Plateau Gravel retreat increased from 5mm in 83 days to 115mm in 174 days during the study year 1981-82. This increase may be due to the presence of freeze/thaw conditions in the colder months and an increase in seasonal rainfall.

The other study areas do not provide variation in process rates during the year.

(c) Wind

Where wind erosion occurs, it is reported on the Dee Estuary, the direction and wind speed will determine the volume of material removed from the degrading slope.

6.7 Conclusions

6.7.1 Detailed summary

(1) Between May 1976 and July 1983 the 200m wide study area has decreased in debris volume by 50,280m^3.

(2) During the two year study period only the F bench gained in colluvial volume, an addition of 192m^3. Both the D bench and the A3 bench lost debris, a decrease in volume of 7,401m^3 and 2,015m^3 respectively.

(3) The prediction of slide movement velocities using the volume of debris supplied to each process gave reasonable agreement with recorded rates with a maximum difference of 38% in the A3 bench. the slide processes considered were the D bench, the A3 bench, mudslide B at Naish Farm and a mudslide at Beltinge, N. Kent.

(4) Prediction of historical rates of movement from known rates of cliff top recession indicated a peak yearly displacement of 8m between May 1976 and April 1978 for the

D bench.

(5) The dominant form of geomorphological process in any one area is dependent on the geology, topography and climate present. Within the structure the seasonal variation in climate can result in a seasonal variation in the activity of the geomorphic processes within a yearly cycle.

(6) The study of a degrading slope to determine the volume of material moved by the 'active' degradational processes present will indicate both the inter-relationship between the processes and the relative contribution of all those processes present.

The degradation of the coastal slope at Naish Farm is seen as a complex relationship between five slope degradational processes. The geological structure of the Barton Clay has determined that the dominant form of degradation within the study area is sliding along compound plane shear surfaces as their basal portion. The budgetary calculations have indicated that the supply of newly degraded material onto the slope is significantly less than that being discharged onto the beach. These changes in both the supply/discharge balance and its affect on the distribution of landslide debris within an area can indicate the stability trend of the slope. The effect on the study area is analysed in Chapter 7 but an appreciation of the change of debris distribution in any degrading slope is significant where a warning of failure is required. In any area where degradational processes are active the redistribution of debris can change the factor of safety for either the whole or part of the slope.

Where an area is being considered for stabilisation a full understanding of both the processes present and their inter-relation is required to prevent a remedial measure

either intensifying an active process or being made ineffective by the continued presence of a degradational process. A degrading slope is a complex and varied system of moving debris, changing topography and varying hydrological conditions (Thomson, 1987) and a full understanding is required if any treatment to enhance the stability of the cliff or enable the area to be utilized for communications e.g. roads or railways or structures is considered.

6.7.2 General Conclusions

The objectives given in section 6.0 have lead to the following conclusions:-

(1) It is possible to produce a detailed budgetary analysis of the colluvium within the degrading slope. This is best achieved by dividing the slope into subsystems. The input, storage and output for each element can then be calculated and the individual parts summated to indicate the status of the complete slope.

(2) The budgetary analysis has shown the bench sliding transports the large majority of the material within the degrading slope. Mudsliding and debris sliding contribute relatively little.

During the period of detailed study the study area has decreased in the volume of degraded material held in the slope.

(3) The overall loss of degraded material between July 1981 and July 1983 indicates a potential decrease in stability within the study area. Colluvium on the undercliff can act as a 'toe weighting' and provide a resisting force to further 'first time failures' of the cliff slope.

CHAPTER 7: THE APPLICATION OF THE FIELD RESULTS TO AN UNDERSTANDING OF THE STABILITY OF THE UNDERCLIFF

CHAPTER 7: THE APPLICATION OF THE FIELD RESULTS TO AN UNDERSTANDING OF THE STABILITY OF THE UNDERCLIFF

7.0 Introduction

The main aims of the field study have been to investigate three aspects of slope failure.

(1) The processes which cause the degradation of the undercliff.
(2) The changes in debris volume and slope topography due to the degradational processes.
(3) The pattern of debris movement within the degrading undercliff including the relative contribution of the various processes.

In this chapter these results are discussed with respect to the stability of the coastal slope.

In the first section (7.1 and 7.2) three cross sections through the D bench are back analysed. The results are compared to residual shear strengths published elsewhere for Barton Clay. Other publications are discussed which detail back analysis techniques and errors.

The second section (7.3) considers the stability of one of the cross sections after a change in slope profile. Stability analyses were performed using the shear strength values indicated in section 7.2. The effect on bench stability of the down slope progression of a cliff top slump is presented.

7.1 Back analysis

The back analysis of a slope failure can be used to evaluate the shear strength parameters along the shear

surface. The analysis ideally represents the precise moment when the failure occurred and the factor of safety was equal to one.

The peg movements recorded in the vicinity of three cross sections indicate continuous movement, at varying rates, throughout the two year study period. These records allow two assumptions:

(i) The factor of safety along each cross section is equal to one.
(ii) The landslide debris at the shear surface is in a state of residual shear strength.

Three cross sections were chosen for analysis. Their positioning was governed by the available groundwater information. Each cross section is confined to the D bench. This feature is treated as an individual slope unit as the stability is not directly influenced by the F or A3 benches.

The position of the three cross sections within the study area is shown in Figure 7-1. Cross section 1 is west of the amphitheatre. It cuts through the largest pond in the undercliff. Cross section 2 is centrally placed and includes the amphitheatre. Cross section 3 is in the eastern portion of the study area.

7.1.1 Topography

The ground contours for all three cross sections were measured from the November 1980 contour map, Figure 7-1.

The vertical elevations were plotted to the nearest 0.5m and the horizontal distances to the nearest 0.1m.

7.1.2 Shear surfaces

The shape of the shear surfaces were drawn from direct field observations. The elevation of the horizontal section of the shear plane, corresponding to the D bedding plane shear surface, was calculated from survey data. This horizontal surface extends landward until it is intercepted by the steeply angled rear surface. The angle of the rear surface was assumed to be equal to the free standing scarp face. A small radius of curvature was used to link the two straight surfaces. This was noted by Barton, Coles and Tiller (1983).

7.1.3 Pore water pressures

The calculation of the pore water pressures at the shear surface was preceded by the construction of a flow net for each cross section. An initial representation of the water balance regime within the undercliff has been presented by Barton and Thomson (1984). Figure 7-2 is a diagrammatic representation of the water balance regime.

Thomson (1987) presented two figures depicting the distribution of equipotentials of water pressure both within the landslide colluvium and the in-situ mass. One of these figures, for February 1984, is reproduced in Figure 7-3. The accuracy of its construction is discussed after the assumptions for the production of full flow nets for this thesis have been given.

The flow of water through the landslide debris contained within the D bench requires assumptions with respect to the supply of water, routes of flow and the properties of the material within the slope. Two cases have been identified which cover the supply of water to the D bench.

Case A

Water only enters the landslide debris from the Plateau Gravel source. The source is supplied by rainfall on the Plateau Gravel catchment area behind the study area and flows either directly onto the undercliff through the Plateau Gravel or percolates into the Barton Clay below and then flows into the undercliff at various levels within the slope.

Case B

Water only enters the landslide debris from direct rainfall onto the undercliff. Cases A and B are illustrated diagrammatically in Figure 7-4.

For both of these conditions the construction of a flow net to represent the direction of flow and the distribution of pore water pressures has been assumed to be governed by the following criteria:-

(i) The landslide debris is homogeneous.
(ii) The permeability of the landslide debris is isotropic.
(iii) The basal shear surface is impermeable.
(iv) The flow of water represents steady state.

These criteria do not strictly reflect the conditions within the bench as the landslide debris is a mixture of the Barton Clay, in various stages of degradation, and the Plateau Gravel. This combination is unlikely to produce either a homogeneous debris material with isotropic or definable anisotropic permeabilities. The bounding shear surface has been observed as 'glassy' smooth and is assumed to be impermeable.

Steady state flow can only be maintained where there is a

constant throughput of water in the slope. In Case A this is possible although the Plateau Gravel source is prone to variation in supply due to the available rainfall. Case B is not steady state, unless a constant intensity of rainfall occurs over a period of time, and is only illustrated to consider the other major source of water in the undercliff. Thomson (1987) calculated the water balance regime within the D bench between 26 August 1983 and 5 September 1984. This regime defined five elements to describe water movement in the undercliff as follows.

(i) Rainfall
(ii) Plateau Gravel drainage reaching the undercliff.
(iii) Water storage changes.
(iv) Actual evaporation.
(v) Outflow.

The water balance illustrated the proportion of water supplied by direct rainfall and the proportion from the Plateau Gravel source. The results show that the split was highly variable and neither supply was dominant although the Plateau Gravel source did provide the most constant supply which varied more with seasonal than daily rainfall variations.

Two flow nets constructed are illustrated in Figures 7-5 and 7-6. Figure 7-5 shows Case A where water reaches the D bench only from the Plateau Gravel source. The flow net was constructed on a section drawn from contours of the undercliff in November 1980. The outflow of water is shown to take place over a considerable area of seepage face at the downslope end of the section.

Figure 7-6 illustrates the entry of water into the D bench solely from rainfall. The flow net is constructed using the basic criteria detailed earlier and in addition that the area of section defined by the flow lines must ensure equal volumes of water travel down each flow channel. This

latter criterion can be applied simply as the intensity of rainfall is constant over the whole cross-section. Water exits the D bench through a seepage face.

The two flow nets given in Figures 7-5 and 7-6 illustrate the two basic flow conditions found within the D bench. Neither fully represents the true field condition due to the variability in material characteristics within the colluvium and the transient nature of a water supply which in both cases is supplied by rainfall. For the purpose of the back analysis and further stability analyses, calculations the flow nets shown in Figures 7-5, 7-7 and 7-8 were used to generate pore water pressure data at the shear surface bounding the D bench. All three nets were produced using water flow from the Plateau Gravel source as this represented the 'steadier' state conditions.

The above discussion details how the flow nets produced were derived from a consideration of four criteria for flow conditions within the slope and assumptions with respect to both water input and output from the slope. These conditions have produced the nets in Figures 7-5 to 7-8. Thomson (1987) produced a plot of the equipotential distribution based on field data and this is reproduced in Figure 7-3. The source of the field equipotential values is represented on the figure but in the D bench the data is seen to be limited. Comparison of the layout of equipotentials in Figures 7-3 and 7-5 is possible as the position of the section line is the same and although the sections represent different dates the cross sections are similar in topographic shape. At the rear of the D bench the equipotentials lie in similar positions in both flow nets. However further downslope the equipotentials of Thomson incline more and more towards the seaward edge of the bench until they lie at acute angles to the basal shear plane. For a flow regime to exist under the conditions imposed by the position of the equipotentials shown by Thomson water must flow across the basal bedding

plane shear surface into the fissured Barton Clay below and the shear plane is therefore not considered to be a flow line.

It must be appreciated that Thomson (1987) was depicting the general distribution of equipotentials throughout the cliff (including the cliff top area as well as the whole of the undercliff) and did not consider the seepage distribution on the detail of a single bench as considered here. Thomson (personal communication) has stressed that the complexity of the bench areas, involving rapid variations in permeability and anisotropy ratio together with their rapid meteorologically imposed changes, present difficulties for obtaining solutions and that since this was not directly relevant to his work, he made no attempt to produce a full flow net in his thesis. In the absence of other data, Thomson (1987) kept rigidly to the available piezometric data for his plot of the equipotential distribution.

In the interpretation provided here in Figure 7-5 a governing assumption has been that the translational portion of the shear surface is a flow line. In constructing the flow net it is found that the piezometric data cannot be exactly accommodated by this requirement. It is considered that the piezometers were located either in a seam of gravel through which water flowed with a relative rapidity or been located in a barely degraded block of Barton Clay which is relatively isolated from the true flow condition in the bench.

The adoption of flow nets to model flow within the D bench has been chosen as the only method to estimate potential pore water pressures for the back analysis calculations. The use of the pore pressure ratio r_u was not considered due to its gross simplification of groundwater condition. It was considered better to construct a flow net based on simple but valid boundary conditions. Ideally the slope

should have been instrumented to measure the pore water pressures at the shear surface directly. But, as discussed in detail by Thomson (1987), piezometers installed in a continuously moving mass of landslide debris do not remain operational for long and conventional piezometers may not equilibrate fast enough to allow a true representation of pore pressures. The adoption of electrical piezometers, as described by Hutchinson and Bhandari (1971), which under test conditions reached 90% equilibration in 40 minutes, could provide a solution to the destructive nature of moving debris and be a topic of further research on a degrading slope.

7.1.4 Landslide debris

The unit weight of the landslide debris was 18.83 kNm^{-3}. This value was the mean of six in-situ density tests performed in February 1983. All six values are given in Table 7-1.

7.2 The method of analysis

The slope stability method adopted to calculate both the shear strength parameters by back analysis and the factor of safety against sliding was the 'Generalised Procedure of Slices' first published by Janbu (1954). This method was chosen to enable rapid calculations of stability analysis to be carried out on non-circular surfaces. Janbu's method in its generalised form does not need solutions derived from complex computer programs which are associated with the methods described by Morgenstern and Price (1965).

In this thesis the forms of the general equation used are as follows:-

Equation [A]

$$F = \frac{f_0 \sum \left(c'b + (W - ub)\tan\varphi'\right)\left[1/\left(1 + \frac{\tan\varphi' \tan\alpha}{F}/(1 + \tan^2\alpha)\right)\right]}{\sum(W \tan\alpha)}$$

Equation [B]

$$(W \tan\varphi') = f_0 \sum (W - ub \tan\varphi') \left[\frac{1}{(1 + \tan\varphi' \tan\alpha)} (1 + \tan^2\alpha)\right]$$

F = Factor of Safety
f_o = Correction Factor
c' = Soil Cohesion (kNm^{-2})
φ' = Angle of Internal Friction
u = Pore Water Pressure (kNm^{-2})
α = Angle of Slice Base
b = Width of Slice (m)
W = Weight of Slice (kN)

The equation was used in two forms, back analysis to establish values of residual shear strength, φ'_r, on the shear plane and also stability analysis to provide a valuation of the change in the factor of safety for the slope following a change in the stress conditions within the slope. Equation [A] is the routine stability equation and in conditions of residual shear strength, c' = 0. For back analysis the factor of safety was taken equal to 1 and the equation solved for φ'_r. Values for the correction factor f_o were derived from Janbu (1973).

In the generalised form Equation [A] can be simply considered as the ratio of forces resisting failure to the forces promoting failure. The resisting forces are derived from cohesion and friction. They act along the complete shear surface.

The driving force is a product of the weight of the slice resolved to the angle of the shear surface to the

horizontal. The downslope force is only generated in slices where $\alpha > 0°$. In each of the cross sections considered only 15% to 19% of the shear plane is inclined. The remaining horizontal section acts as a restraining force. In addition to pore water pressure changes the driving forces can be altered by an increase or reduction in the weight of debris in the inclined section of the shear surface.

7.2.1 Back analysis

In the back analysis the only unknown parameter in Equation [8] is φ'_r. The results of the back analysis on sections D1, D2 and D3 were 22.4°, 21.4° and 24.7° respectively. The values produced for $\bar{\sigma}'_m$ and $\bar{r}_u$ are listed in Table 7-2. The pore pressures indicated by the flow nets give high values of the pore pressure ratio r_u, in excess of 0.5.

Published values for residual shear strengths for Barton Clay have produced a range of values between 11.5° and 15.7° (Ho, 1982). Marsland and Butler (1967), using Barton clay from Fawley, Hants., produced values of φ'_r equal to 15° for a normal effective stress range of 50 kNm^{-2} to 400 kNm^{-2}.

The variation between the back analyses values of ϕ'_r and the published results indicates an error in the assumptions used in the back analysis calculations. In any back analysis differences between laboratory and calculated values of ϕ'_r can be due to the following reasons:-

1. Inaccurate pore water pressure information.
2. Inaccurate topographical information at the time of the failure.
3. The possibility that $c'_r > 0$.

4. Inaccurate knowledge of the shape and location of the slip plane.
5. Neglect of the effects of side friction in two dimensional analysis.

Table 7-3 lists published examples of back analysis with a summary of the reasons for variation in calculated values of φ'_r and laboratory results.

The high values of φ'_r obtained by back analysis for the Highcliffe sections is believed to be due to an overestimate of the the high pore water pressures predicted by the flow nets. Possible errors in their construction were detailed in section 7.1.3. It should be noted however that the results of the analysis implying instability (assuming the laboratory φ'_r values are correct) are in accordance with the field observations of the movements of the bench slides. Future work could be carried out to determine the actual pore pressure necessary for an exact value of $F_s = 1$.

7.2.2 Spatial variations in pore water pressures

The back analysis for the three cross sections has used flow nets to generate pore water pressure condition within the sliding unit. These three nets have generated average r_u value of 0.548, 0.532 and 0.544 for cross sections D1, D2 and D3 respectively. Due to the relatively rapid degradation of the undercliff it is possible to divide the shear surface into two sections:-

1. Inclined section.
2. Bedding plane section.

Figure 7-9 illustrates how degradation of the undercliff could cause the depression of pore water pressures in the inclined section of the cliff due to the unloading of the

inclined shear surface. The removal of material directly above the shear plane has an immediate effect of reducing the pore water pressure by an amount equal to the reduction in total stress. With time these pressures revert to an equilibrium state in balance with the total and effective stresses within the soil.

Back analysis has been carried out where the slices of the analysed section on the inclined portion of the shear surface have been made equivalent to r_u values of 0.1, 0.2 and 0.3. The pore water pressures for the rest of the shear surface are the same as the flow net predictions. The values for φ'_r are listed in Table 7-4. With reduced values of r_u the values of φ'_r generated by the back analysis drop to compensate for the increase in effective stress due to reduced pore water pressures. These generated values are more equivalent to those given by Ho (1982) and Marsland and Butler (1967).

7.3 Stability analysis

The processes of degradation which occur on the undercliff alter the conditions of stability within the slope. In this section one of the degradational processes detailed in Chapter 4 is modelled to demonstrate the change in slope stability with varying load positions, shear strength and pore water pressure criteria.

The stability analysis was carried out using the form of Janbu's Generalised Procedure. It is the same equation from which the back analysis equation was derived.

The approach to the analysis of the results of the stability calculations is based on the influence line method detailed in Hutchinson (1977) and Hutchinson (1984). This method allows the representation of the change in overall stability of a slope due to the

imposition or removal of a discrete loading at varying positions along the analysed section line. Hutchinson (1977) relates these positive or negative loadings to the effect of (toe) weighting or the removal of material from the slope respectively.

The analysis of a section with the loading applied at discrete points all along the section line indicates the influence of the loading. The position along the section where the loading has no effect is called the 'neutral point'. If several sections along a slope are analysed then the location of several neutral points allow the formation of a 'neutral line'.

Along any one cross section the location of the neutral point is dependent on both the 'physical elements' e.g. shear plane geometry and pore water conditions and also the 'type of analysis', e.g. undrained or drained. When a load is applied or a cut removed from a slope and the instantaneous 'undrained' situation is considered the neutral point occurs where the shear plane is horizontal. When longer term 'drained' analysis is considered, the neutral point occurs where the valleyward inclination of the shear plane to the horizontal is equal to the mobilised effective shear strength (measured as φ' mobilised) of the material in which the shear surface is located.

These two conditions are produced by the effect of a change in load at any particular section on the balance between resisting and driving forces which together dictate the stability of the slope element. In the 'undrained' state a change in load has no effect on the forces resisting failure as the increase in total stress is instantaneously taken up by the pore water which, having no shear strength, cannot provide any resistance to shear failure. The effective stress component, which together with the shear strength of the soil provides the resisting force, remains unchanged. The driving force to

cause slope failure is only increased where the shear surface is inclined at angles greater than zero and therefore the neutral point, where the change in loading condition has no effect on the factor of safety, occurs where the angle of the shear surface to the horizontal is equal to zero. In the case of the D bench undrained analysis would produce a 'neutral zone', Hutchinson (1977), due to the large portion of the shear surface which is planar i.e. $\alpha = 0°$, and in that zone the position of the increased or decreased load has no effect on the stability of the whole section.

In the 'drained' state a change in load effects both the driving and resisting forces and Hutchinson (1977) showed that algebraic calculation, using both the conventional method of analysis (Skempton and Hutchinson, 1969) and Bishop's simplified method (Bishop, 1954), gave a common solution to the position of the neutral point. It occurs where the angle of shear surface is equal to the mobilized shear strength (measured as φ' mobilised) of the shear surface.

The undrained and drained conditions are the two extremes of the condition which can be present on a slope where a loading has been applied or removed. The precise condition will depend on the degree of equilibration of the pore water pressures caused by the change in total stress.

7.3.1 Slump progression and the influence line technique

The application of the influence line technique described by Hutchinson (1977, 1984) to the D bench allows the effect of the downslope progression of a cliff top slump to be assessed in terms of a change from the original stability state. The cliff top slump is modelled by the

addition of an extra 2m to the depth of 4 adjacent slices, individual widths of 1.25m, to produce a load 2m high and 5m long. The slump is given the same unit weight as the rest of the slope, 18.83 kNm^{-3}.

Figures 7-10 and 7-11 show plots of changes in two variables for section D1. The analyses assume drained conditions due to the generally very slow progression of a cliff top slump downslope. The fundamental physical error in this model is the assumption that the slump moves across the surface of the existing slope which retains a constant profile. In reality the slump is incorporated in the slope and its movement downslope is accompanied by the downslope progression of the whole D bench. The D bench does however maintain an approximate constant profile due to the feeding of new debris from the F bench and the deposition of debris onto the A3 bench.

Figure 7-10 illustrates a plot of calculated values for the factor of safety (F_1) against the downslope progression of a cliff top slump. Each of the plotted lines represents a residual shear strength and an assumed piezometer level, neither of these variables having been accurately fixed by the back analysis. Predictably the cases with high values of residual shear strength (φ_r') and low pore pressure values (r_u) show the greatest value for F_1. All four curves show a family characteristic of increasing value of F_1 until a distance of 12.5m when a constant value of F_1 is attained. This steady state value corresponds to the area of the slip surface where the angle to the horizontal is zero. Also marked on the curves are the 'neutral point' locations where the addition of the slump has had no effect on the overall stability of the slope. This presentation of the position of the neutral point is an alternative to that shown by Hutchinson (1977, 1984). This latter approach using the same data is shown in Figure

7-11 where the vertical axis F_1/F_0 and F_0 is the factor of safety of the slope prior to the addition of the slump.

Figure 7-11 does not however present the symmetrical plotting of F_1/F_0 against distance given in Hutchinson (1977, Figure 7b) which shows the influence line for a non-circular slip. Whilst in Figure 7-11 crossing of the $F_1/F_0 = 1$ line does give the 'neutral point', in the construction of Figure 7-10 the curves do not remain parallel and two pairs cross over. The effect is caused by the normalization procedure of dividing the pre-slump factor of safety (F_0) into the newly calculated values F_1. Where the difference is large values of F_1/F_0 vary considerably from 1. Where the change is small then the value of F_1/F_0 is close to 1.

7.3.2 Stability zones

An alternative method of displaying the data of slump progression which emphasises the circumstance where the presence of a slump is critical to the overall stability of the slope is given in Figure 7-12. This figure illustrates 'stability zones' for a given cross section. The solid line corresponds to the upper and lower pore pressure ratios which can normally apply within the slip mass. Before the addition of a slump the horizontal line equivalent to $F_s = 1$ splits the area into two zones, A and B. Zone A is the unstable zone and zone B the stable zone.

Between the two boundary limits are a family of curves for values of r_u between 0 and 0.52. For any value of φ'_r and r_u the position of the intercept whether in zone A or zone B will indicate the stability of the slope.

The addition of a slump alters the limits of the solid

boundaries of the zones due to the change in geometry of the slope being considered. The solid lines in place represent the slope with no slump addition. The vertical markers illustrate the effect of the downslope progression of the slump defined in section 7.3.1. The lowest point on the markers represent the lowest factor of safety caused by the slump progression. The highest point represents the state where the slump has its maximum stabilizing effect.

The three markers representing $r_u = 0.52$ and $\varphi'_r = 10°$, 15° and 20° respectively do not represent the actual physical situation was the stability of the unloaded slope is less than one.

From Figure 7-12 the only critical circumstance analysed is for $r_u = 0$ and $\varphi'_r = 10°$. Here the value of F_0 is initially equal to 1.05 and the slump progression gives limits of 0.94 to 1.13. The addition of the slump causes the stable slope to fail and only when the centre of the slump is 5.3m from the head of the slope is stability regained.

7.3.3 Influence lines on the D bench

Analyses of cross sections D1, D2 and D3 based on the November 1980 contours have produced values of mobilized shear strength for each section line. These results have been given in section 7.2.2. Stability analysis of these sections using the calculated value of φ'_r and including the downslope progression of an imposed slump has allowed the location of the neutral point for each section. These positions are shown on Figure 7-13.

Hutchinson (1977, 1984) has calculated that conditions equivalent to the fully drained state predict that the neutral point will occur where the slip surface is

inclined at an angle equivalent to φ' mobilised. The results illustrated in Figure 7-13 do not correspond with this prediction and in each case the neutral points are located where the angle of the inclined shear surface is less than the mobilized shear strength.

Section	φ'_r mob	Angle of shear surface at neutral point
D1	22.37°	12°
D2	21.36°	6.25°
D3	24.72°	13.5°

Hutchinson (1977, 1984) also predicted that in the undrained case the neutral point would occur where the angle of the inclined shear surface is equal to zero. The calculated results for the D bench are therefore intermediate between the drained and undrained state.

7.3.4 Conclusions

Section 7.3 has applied slope analysis of the D bench to the modelling of the downslope progression of a cliff top slump. This is considered analogous to the influence of the addition of fill detailed by Hutchinson (1977, 1984). The influence line technique is discussed and applied to slump movement. The concept of neutral points, neutral zones and influence lines are considered a good method to illustrate the effect of slump movement. However the presentation of the 'influence' by using 'normalised' safety factors, e.g. F_1/F_0 does not directly indicate those conditions where a slope could become unstable due to the addition of a slump. The technique of defining stability areas in which the variables predict the stability of the slope and also zones of influence for the addition of a slump directly indicates whether a slope

will be made unstable.

This theory would suggest that degraded slump blocks ought to come to at least a temporary rest (or a quiescent state) at, or about, the neutral line position as shown in Figure 7-13. To some extent this is true as the movement of fresh slump blocks at the rear of the bench is relatively quick (perhaps covering the intervening distance over a winter season). However, such stability is subject to disturbance by fresh movements either at the rear or front of the bench which upset the general stability conditions. Nevertheless, there is some sign to the east and west of the study area that a "neutral line position" does mark a location where degraded slump blocks are relatively slow moving.

CHAPTER 8: DISCUSSION

CHAPTER 8: DISCUSSION

8.0 Introduction

The field research has produced results concerning both surface and sub-surface movements within the degrading slope. The three issues highlighted during the preceding sections for further discussion are as follows:-

(i) The cyclic pattern of surface movement and the cause of the surges in surface movement.
(ii) The history of the cliff top slump which formed the back scarp to the amphitheatre.

Items (i) and (ii) are closely related, as the occurrence of the surge event forms a notable part of the cyclic pattern. Discussion of these two aspects will form the basis for the first part of this Chapter.

The second section will review the historical data behind the occurrence of the amphitheatre slump and attempt to highlight more precisely the date of failure and its cause.

8.1 Surface Movements

Detailed discussion of the results of the survey of surface movement markers has been given in Chapters 4 and Appendix F. In section 4.2.3 the division of the yearly pattern of surface movements into three periods was proposed. The seasonal nature of this pattern suggests that there is a link to a seasonal variable. In a coastal location the two seasonal variables which could affect the degradation of a coastal slope are:

(i) Toe erosion.
(ii) Rainfall.

8.1.1 Toe Erosion

The continual removal of landslide debris from the base of the coastal slope maintains the unstable profile which promotes slope degradation. The intensity of toe erosion is fundamentally a function of wave erosion which is seasonally related. However the profile of the coastal slope, (see Figure 2-2) demonstrates that wave erosion generally only attacks the A3 bench and only during intense storms does direct wave attack occur onto the D scarp.

Therefore as the cyclic pattern has been registered both on the F and D benches the influence of toe erosion is not considered significant.

8.1.2 Rainfall

The effect of rainfall on the stability of a slope has frequently been documented e.g. for landslides Rico, Springhall and Mendoz (1978) and Merriam (1960) and for mudslides Hutchinson (1970) and Prior, Stephen and Archer (1974).

Rainfall is usually associated with increasing groundwater levels and therefore increasing pore water pressures in a soil mass. A slope profile which is stable during a relatively dry summer when groundwater levels and pore water pressures are low can rapidly become unstable when an increase in the quantity of rain falling increases groundwater levels and pore water pressures. Detailed study of the rainfall immediately adjacent to the study area has been carried out by Dr. R.I. Thomson and is reported in Thomson (1987). Unfortunately the study did not however match the period of surface movements discussed in this thesis.

Thomson (1987) did however report that it is possible to correlate the pattern of rainfall in the study area with rainfall data from Hurn Airport. Although the Hurn data cannot be used to predict absolute values of rainfall on the study area, it does give a similar pattern to rainfall on the undercliff.

The rainfall data were taken from the meterological site at Hurn Airport, Bournemouth, which is 12km NWW of the study area, see Figure 8-1. The data used are in the form of actual rainfall although a better indication of the amount of water remaining in the undercliff is effective rainfall. However Thomson (1987) found that due to the coastal location of the study area the correlation between effective rainfall for the study area and Hurn Airport was less satisfactory than the correlation between actual rainfalls. The difference in rates of evapo-transporation between the coastal site and Hurn being caused by their different topographical location.

8.1.2 Pattern of movement

Whilst each slope degradational process has an individual pattern of movement (as detailed in both Chapter 4 and Appendix F), a common theme of summer, surge and winter movement has been identified. Figure 8-2 shows the relationship between the Fortnightly Actual Rainfall and the movement periods derived from the recorded surface movement as detailed in Appendix F. The start of the first period of winter movement (W1/1) coincides with a 2 week period of heavy rainfall (104mm) and is followed by a 4 week period of moderate rainfall (113mm). The occurrence of the first surge period (SG1) does not however coincide with a notable rainfall peak. The second period of winter (W1/2) ends with a period of negligible rainfall, 33mm in 4 weeks. Rainfall during the second summer period was

similar to the second winter period (W1/2) and these are compared in Table 8-1. The second surge period (SG2) is marked by the highest weekly average (48mm) of the two year study period. The end of the second winter period (W2) is marked by a recorded rainfall of 6mm in 2 weeks.

Figure 8-3 illustrates the pattern of average weekly rainfalls over the two year study period. The periods of surge movement are highlighted by the highest weekly averages either during or before the defined surge period. Although differences in actual rainfall between the summer and winter periods are small, the effective rainfall total for winter will be greater due to the higher evapo-transporation rates which occur during the summer months.

Figures 8-4 to 8-12 show the fortnightly actual rainfall figures superimposed onto the cumulative movement versus time graph for the three benches, mudslide A and the five debris slides. Accelerated rates of movement occur during both the surge and winter periods.

The surges (SG1 and SG2) are marked features on the D bench, mudslide A, DS1, DS2 and DS5. It has been shown in section 5.1 that the surge event occured on the D bench and due to the superposition of mudslide and debris slides onto that bench the surges influence the pattern of movement of these features.

8.1.3 Surges - their origins?

The true nature of the two surge events is unknown. Whilst it has been established that they are movements along the D preferred bedding plane shear surface the cause and characteristics of the occurrence is not fully understood. Neither period identified as a surge can be isolated to within less than 2 weeks of its occurrence. The exact

duration of the elevated movement rate compared to other rates of movement on the undercliff is not known.

Section 8.1.2 has already indicated that both surges have been preceded by periods of increased rainfall. This suggests that the increased rates of rainfall acted as a trigger to the surge event. It is however most likely that the actual surge occurs as a combination of various conditions in the slope. These conditions are listed below:-

(i) Critical pore water pressures at the shear surface of the D bench.
(ii) Build up during summer months of an unstable slope profile.
(iii) Sudden failure of a seaward portion of the D bench causing an unloading effect and allowing the bench to 'surge' forward as a result of the drop in resisting forces. However there has been no physical evidence of this on the A3 bench.
(iv) Possible saturation of the D bench due to a storm. There has been no storms reported around the time of the surges and no physical evidence.
(v) A sudden change in the shear strength properties of the bounding shear surface. However the continual movement of the D bench during the summer months indicate that the shear strength parameters would have remained at their lowest value e.g. in a state of residual shear strength.

The most likely combination of circumstances to explain the occurrence of a surge event is therefore rapid increase of pore water pressure to a critical value to cause large ground movements of a slope profile which has attained an unstable form. During the summer the unstable form has not caused substantial movements due to the depressed summer pore water pressures. The occurrence of rapidly rising pore water pressures in an unstable profile

occurs at the end of the summer period therefore produces the surge event.

The sensitivity of the bench to the distribution of pore pressures has been demonstrated by analysis of stability in section 7-2. There it was shown that the highest conceivable distribution of pore pressures was such as to make the factor of safety much less than unity. This sensitivity to pore pressure changes is considered to be the underlying cause for the surge events.

8.2 Amphitheatre failure

The amphitheatre feature forms a central landmark within the study area. It has been identified as a multi-storey landslide and also a possible cause of the formation of mudslides A and B.

Factual data is given in section 5.0.1 indicating that the date of formation is between 18 March 1977 and 6 April 1978. More accurate dating of its origin is possible from direct historical evidence although no accounts exist to separate this event from the continual cliff top retreat noted over the whole undefended area.

Figure 8-13 is a plot of the seaward movement of the slump block with time measured directly from aerial photographic coverage. It should be noted that direct measurement from aerial photographs are prone to inaccuracy due to the scale distortion across the photograph, however these photographs were the only historical information available. Figure 8-13 contains a curve which indicates that the failure could have occurred in approximately October/November 1977. This assumes a decrease in movement rate with time for the downslope progression of the slump block. This has been observed with the March 1982 slump within the study area. The time of occurrence

coincides with the surges observed in the study area and it is possible that it was triggered by a surge event.

Figures 8-14 to 8-18 are copies of the aerial photographs both before failure and the progression of the slump until July 1982. The position of the slump is highlighted.

Figure 8-19 is a plot of overall slope angle with time for the 200m study area. Between 1959 and 1977 the overall slope angle gradually increased producing a maximum value of 21.8° in March 1977. This maximum occurred through the centre of the area of the amphitheatre slump as shown on Figure 8-14. The slope angles are taken as the angle of slope from cliff top to cliff toe and the period of increasing slope angle indicates a retreat of the toe at a rate faster than the cliff top. This assumes that the elevations of the top and toe remain the same.

The reduction in mean and maximum slope angles occurs in 1977 and is a result of the amphitheatre slump having occurred. The process of an increasing slope angle followed by a sudden drop in angle is also seen between 1959 and 1960 when aerial photographic coverage also indicated a large cliff top slump failure occurred. The substantial failures along the undercliff therefore occur in response to an increasing slope angle which finally causes a large scale failure of both cliff top and the downslope profile. It should however be noted that the amphitheatre slump was isolated to an area upslope of the D scarp and did not incorporate the A3 bench directly. The A3 bench would however have been affected by the sudden displacement of large quantities of landslide debris from above.

8.3 Summary

This chapter has discussed aspects of the field research

which have arisen from the detailed study of the degradation of the undercliff. The consideration of the pattern of movement and in particular the occurrence of the surge events has highlighted the need for knowledge on the seasonal changes in pore water pressures within an actively degrading slope.

An ability to explain the cause of a sliding event requires knowledge of a series of conditions including slope profile, pore water pressures and shear surface location and properties. Research to provide such data is needed to explain the true nature of these annual surges.

The amphitheatre cliff top slump is another area where detailed field data is needed to understand its occurrence. Due to the sudden nature of the slump, and also the surge events, continuous monitoring equipment would be required to measure ground movements throughout a depth profile in addition to the pore water pressure profile.

Both the surge and the occurrence of cliff top failures indicate the need for further field measurements in slopes. However the measurement of data in a continuously degrading slope will require the development of equipment to withstand ground movement and rapidly register the data collected.

CHAPTER 9: CONCLUSIONS

CHAPTER 9: CONCLUSIONS

9.0 Methods of field study

The field investigation has used both standard and specially developed techniques during the two year study. The success and failure of these methods has been influenced by four main factors.

(1) Destruction of field instrumentation by the movement of landslide debris.

(2) Destruction of field instrumentation by vandalism.

(3) The lack of a comprehensive network of survey reference data.

(4) The difficulty of physical access.

These four problems are considered common to most areas of slope instability being researched. Any field investigation must consider methods which will overcome these obstacles.

The successful techniques used at Naish Farm were characterised by four criteria as follows.

(a) Simple manual installation.
(b) Rapid monitoring.
(c) Inconspicuous permanent site instrumentation.
(d) Inexpensive permanent site instrumentation.

Surface peg monitoring, spalling square measurements and slip indicators were all successful methods which are recommended for a similar field investigation.

The surveying of surface pegs is not an original method of landslide study. The technique developed in this study

did however overcome all the difficulties listed above. The system of peg location allowed the rapid and accurate positioning of a peg, or any feature, on any part of the undercliff. The steel survey pegs used were inexpensive, not easily found and simple to install.

The use of bars or rods, driven perpendicular into weathering surfaces, to measure the erosion of a surface was first described by Schumm (1956). The development of that original technique to include a 'spalling square' allows a large area of the erosion surface to be measured. This has prevented any very localised 'pitting' of the erosion surface from distorting the overall rate of surface weathering. In periods when no recession of the face was apparent the 'spalling square' gave repeatable measurements of rod exposure to within 2mm.

A successful technique of shear surface detection study was the installation of slip indicators. They were inexpensive, easy to install and gave a simple method of detecting an active shear surface. Installation of the slip indicator by the vibrating hammer provided a convenient and practical method of shear surface detection at depths greater than 5m. The method is therefore invaluable in areas where vehicular access is difficult.

In contrast to the success of the slip indicators, the inclinometers installed in the undercliff were not as reliable. Inclinometer installation is best carried out where powered equipment can bore to a sufficient depth to allow the permanent anchorage of the bottom of the tube into in-situ strata. The accurate monitoring available with an inclinometer allows the definition of the precise pattern of tube deformation prior to failure. In the study area the difficulty of access prevented inclinometer installation by powered equipment. The maximum depth of installation achieved by hand was 5.4m for I8. None of the inclinometers on the D bench were located in the in-situ

Barton Clay. The tube profiles had to be located by regular surveying techniques which greatly reduced the accuracy of the inclinometer profiles.

In addition to a loss in accuracy, the rates of movement in the study area were often too rapid to allow the recording of tube deformation before failure. Only very frequent monitoring, with profiles taken at least daily, would have provided a record of tube deformation. Less frequent monitoring resulted in the inclinometer tube acting as an expensive slip indicator tube. It is considered that inclinometers are best suited to areas of low rates of movement. They must be anchored at their base and monitored frequently enough to provide data on tube deformation before catastrophic failure occurs.

9.1 Methods of desk study

Whilst the majority of the desk study was based on the field data, one particular method provided useful data to complement the field investigation. An extensive collection of aerial photographic coverage has allowed the production of a series of contour maps of the Barton Clay exposure between September 1975 and July 1982. These maps have been used to quantify the following:-

(1) The decrease in the volume of material contained within a defined area of the cliff line between May 1976 and July 1982.

(2) The recession of the cliff top scarp, the F scarp, the D scarp and the A3 scarp.

(3) The maximum, minimum and mean slope angles with the study area between September 1975 and July 1982.

The production of contour maps from aerial photographs is

considered a good method of quantifying changes in topography in an area. Direct measurements from aerial photographs, without sophisticated and expensive viewing equipment, cannot produce either the quantity or the quality of data that is available from a contoured photograph. In any geomorphological study the conversion of photographs to a contoured map is highly recommended.

9.2 Pattern of movement

The field study has produced a good understanding of the patterns of movement within the undercliff. This has resulted from a detailed knowledge of both the elevation of all the active shear planes and the velocities of surface movements.

9.2.1 Shear surfaces

The subsurface investigation has resulted in 34 different active shear surfaces being detected. Eleven different surfaces were identified; three bench slides, five debris slides, two mudslides and the amphitheatre slide surface. Whilst the presence of the preferred bedding plane shear surface is thought to be due to a feature of the sedimentary history of the Barton Clay, the remaining eight surfaces have been produced by the active degradation of the slope. Any degrading landslide area, whether active or dormant, is likely to contain a similar profusion of shear surfaces.

The instrumentation records indicated the following:-

(1) The D and A3 benches have a uniform velocity profile from the preferred bedding plane shear surface to ground surface.

(2) Debris slides are a shallow slide feature with colluvial depths not greater than 2m.

(3) Mudslides, in the study area, exist in channels. The channels can be either in existing colluvium or in-situ Barton Clay.

(4) An active shear surface exists within the D bench which is located above the D shear plane. It is restricted to the amphitheatre area and it has an average elevation 3m above the D bedding plane shear surface. It is believed to be a relict F bedding plane shear surface.

(5) The single inclinometer, Ill, in the cliff top indicated no sign of movement from either stress relief or activation of the F shear surface during the study period.

9.2.2 Surface movements

The existence of eleven active shear planes has produced a pattern of colluvial movement which varies both with the time of year and the process which is observed.

All the slide processes show a seasonal variation in velocity. The difference in summer and winter velocities is greatest in the landslide forms which have the highest moisture contents. The increase in effective rainfall during the winter period causes a rise in pore water pressures within the colluvium and a reduction in the shear strength of the landslide debris.

A cyclic yearly pattern of movement identified is common and has been recorded by Rico, Springhall and Mendoz (1976), Hutchinson (1969, 1970 and 1972) and Prior and Stephens (1968). In all the cases described the greatest proportion of movement occurred in the wet or rainy season.

The variation in surface velocity between the slide processes produces areas of large seaward displacements flanked by areas of considerably slower moving debris. This was pronounced in the areas surrounding the mudslides. Mudslides are known to enlarge their channels by engulfing slides from the channel sides (Hutchinson, 1970). It was thought that with the faster winter rates of movement, slip of the bench rubble towards the mudslide might take place. This did not occur; the dominant seaward movement of the bench rubble continued even within 1m of the side of mudslide channel A.

The rates of movement measured for the various geomorphic forms are similar to other rates recorded on other cliff slopes in southern England, notably Fairy Dell, Dorset and Beltinge, Kent. However, the rates are thought not to be the fastest which will occur. Whilst no extreme surging of the mudslides or debris slides was observed it is believed that continuous monitoring, as described by Prior and Stephens (1971), would have measured significantly higher rates of seaward displacement. The failure to observe these maximum rates is not however considered detrimental to the aims of the research.

Two short periods of relatively rapid movement were noted in the D bench. These were noted by ground surveys 14 and 28 days apart in the first and second year of the study. It has not been possible to compare accurately these periods with the 'surge' described by Hutchinson et al. (1974). The surges occurred after periods of increased rainfall although the pore water pressures at the time of failure were not known.

9.2.3 Multi-layered landslides

The detection of a profusion of shear surfaces within the D bench has led to the conclusion that there are seven areas of multi-layered landslides. Recorded surface velocities in these areas are therefore the summation of two more individual shear surface movements.

This situation can lead to a confusing first stage analysis of slide activity. Multi-layered slides, as detailed in chapter 5 can be difficult to detect. It is important that a field investigation locates all the active shear surfaces.

The existence of a large number of shear surfaces parallel and sub-parallel to the ground surface is well documented in areas affected by periglacial activity (Hutchinson, Somerville and Petley, 1973). It is also a common feature of any degrading slope. The observation of an active slide process does not preclude the existence of pre-existing shear surfaces at some greater depth.

The detection of a multi-layered landslide cannot be achieved by conventional methods of shear surface detection alone. If only one surface is anticipated only the shear surface with the fastest displacement rate will be located. For an appreciation of the possibility of a multi-layered slide on a site a geomorphology study is also required.

The method of graphical representation of multi-layered slides adopted by Ter-Stepanian and Goldstein (1969) represented idealised multi-layered slides with velocity vectors. In this project displacement vectors were used to represent an actual two layered slide. However for three layered slides an algebraic representation is believed to be more appropriate.

9.3 Geomorphological processes

Seven processes of slope degradation were identified in this study: bench sliding, mudsliding, debris sliding, cliff top slumping, spalling, stream erosion and mudruns. The latter two processes were considered to be insignificant to the degradation of the undercliff.

Bench sliding is the most important degradational process at Naish Farm. It is responsible for the movement of 93% of the total volume of colluvium. All three benches in the study area are active. Bench slides cover 76% of the plan area in the undercliff.

The process of bench sliding is not thought to be restricted to this Barton Clay exposure. Sliding processes which apparently conform to the bedding have been shown on geological sections by Brunsden and Jones (1976), Hutchinson and Hughes (1968) and Bromhead (1978).

The reason for the selection of particular bedding planes as shear surfaces is not known. The tests performed so far, see Appendix D, on unsheared material at the level of the F bedding plane shear surface indicate no mineralogical or chemical difference between the material collected at the shear plane and the zones of Barton Clay both above and below. Visually field observations, Figure D-1, do however show a lenticular structure. The sedimentation of the Barton Clay at the horizons of the preferred shear surfaces could have resulted in clay platlet orientation being parallel to the bedding. This preferred orientation would reduce the shear strength of the clay parallel to the bedding plane. Clay platlet reorientation was proposed by Skempton (1964) and work by Morgenstern and Tchalenko (1967) and Tchalenko (1968) indicated that reorientation does occur at shear surfaces and reduce shear strength.

Mudslides and debris slides are relatively minor processes of debris transport. Despite their visual 'impact' they only contain 1.3% and 5.6% of the total volume of colluvium in the study area. This is in contrast to the Beltinge and The Lees, Herne Bay sections of the Kent Coast where mudslides have been reported to be the dominant process of slope degradation (Hutchinson, 1970 and 1973).

At Naish Farm both mudslides and debris slides are relatively shallow with a depth range between 0 and 2m. Both mudslides are confined to channels bounded by discrete lateral and basal shear surfaces. They bear a closer resemblance to the mudslides of Antrim than those composed of London Clay in south-east England. Debris slides are numerous in the undercliff; within the study period three formed and the structure of several dormant debris slides were identified. The identification of debris slides in this study is believed to be the first time this process has been classified.

In both of the slide processes described above it is important to emphasise the existence of a slide mechanism as opposed to a flow mechanism. At Naish Farm the transportation of debris by a flow mechanism is confined to the mudruns.

The weathering of in-situ scarp faces both for an established gravel face, 0.1m per year and an established clay scarp, 0.5m per year, are typical of the rates of scarp recession measured elsewhere. Brunsden and Jones (1976) reported a recession rate for a sandstone face of 0.15m per year. Hutchinson (1970) indicated a recession rate of 0.44m per year for London Clay.

The activity of cliff top slumps during the study period was low. Only one measurable failure occurred. This explains the relatively low rate of cliff top recession

recorded in the study area between July 1981 and July 1983. The failure of the cliff top slumps and the weathering of in-situ faces by spalling is the only method by which 'new' material is added to the undercliff. The reduction in colluvial volume in the undercliff, Chapter 6, again demonstrates the relatively low rate of slump activity.

Inspection of aerial photographs has shown that large cliff top failures, greater than 50m long, occur at intervals along the Naish Farm to Barton-on-Sea stretch of the Barton Clay cliff line. It is clear that unless the rate of cliff top recession is slowing dramatically new slump activity is likely to occur in the near future. This will reduce the overall slope angle of the undercliff, increase the volume of debris within the undercliff and increase the rate of colluvial transportation across the undercliff.

9.4 Debris budget

A detailed budget for the movement of landslide debris is given in Tables 6-6 to 6-9. These represent a series of sub-systems through which the debris has to pass before it reaches the beach. To calculate a complex budget it is important to divide the landslide into a number of budgetary stages. In this study quantities have been used to calculate an actual budget. This is believed to be a unique achievement in slope studies.

During the period July 1981 to July 1983 the study area lost 9,038m^3 of colluvium. This is 12% of the total colluvial volume in July 1981. Both the A3 and D benches suffered a net loss in volume. Only the F bench underwent a net gain. The debris supply to the F bench by spalling and a single cliff top slump did not provide enough material to maintain the D bench. Preliminary stability

analysis.

The volumetric budget presented in this thesis cannot be directly compared to any other coastal site. The only other area of degradation for which budgetary calculations have been made is Karkavagge in Northern Scandanavia&"" (Rapp, 1960).

Comparisons between the two studies is not however possible due to the wide difference between both site geology and climate and the scale of the two studies.

In other areas active geomorphological processes have been identified but not quantified: thus Fairy Dell, Dorset (Brunsden, 1973), Dee Estuary (Pitts, 1983) and Beltingle, Kent (Hutchinson, 1970).

9.5 Stability calculations

Calculations to obtain both values of residual shear strength and the influence of a cliff top slump on the stability of the D bench have been carried out. Both back and stability analyses have used the 'Generalised Procedure of Slices' Janbu (1957).

The back analysis procedure required values of pore water pressure to be obtained. Flow nets were constructed which represented a steady state of water flow through the D bench assuming homogenity within the landslide debris. The calculated values of residual shear strength were in the range 21.36° to 24.72° compared with the reported laboratory range of 11.5° to 15.7° by Marsland and Butler (1967) and Ho (1982). Clearly the values of pore water pressures were too high but nevertheless these calculations confirm the development of instability as observed with the seasonal increase of pore pressures.

The stability analysis was used to simulate the downslope progression of a cliff top slump. The change in stability of the slope can be displayed using the influence line approach presented by Hutchinson (1977 and 1984). An influence line for the D bench is presented which shows the effect of a slump on the overall stability of the D bench.

The concept of a stability zone is introduced where for a given residual shear strength and pore water pressure condition the effect of a slump on the stability of the slope can be easily derived.

9.6 The relation between the study area and the whole outcrop of Barton Clay

This study has been restricted to a small section of the 4.8km outcrop of Barton Clay. Table 2-8 has shown that the study area is typical of the geomorphology of the undefended length of the outcrop. Barton (1973) has described the geomorphology of the outcrop to the west of Chewton Bunny. In the western section the area covered by benchslides was high and can be considered comparable to the 60-68% coverage noted in Table 2-8.

The mudslides present in the study area are relatively small compared to the large mudslide forms described by

Hutchinson (1970) at Beltinge, Kent. Only two large mudslides are present in the complete 1.4km undefended outcrop. One is located to the west of the study area at N.G.R. 422075E and the second to the east at N.G.R. 422500E. Neither of these two mudslide 'dominate' the sections in which they occur. There is no feeder corrie or mudslide snout, which periodically moves onto the beach, as described by Hutchinson (1970).

Debris slides are present throughout the undefined cliff section. They primarily occur on sections of the D scarp and F scarp. In the study area three of the five debris slides are on the F scarp slope. The occurrence of cliff top slumps, documented by Barton, Coles and Tiller (1983), is widespread and relic slumps can be seen in the cliff line to the west of Chewton Bunny. Scarp slumps, including the A3, D, F and cliff top scarp, occur all along the undercliff. The slumps present at any one point are dependent on the geographical position.

The small area studied is therefore typical of the geomorphological form present in this outcrop of Barton Clay.

Other coastal outcrops of Barton Clay in Britain are restricted to Alum Bay and Whitecliff Bay, Isle of Wight and the Isle of Purbeck. Despite the large thickness of the outcrop in Alum Bay, 76m, it does not form the same prominent undercliff as found at Highcliffe. This is partly due to the bedding which is near vertical in this coastal section. In Whitecliff Bay, where the outcrop thickness is reduced to 49m, near vertical bedding is also present.

The presence of relatively closely spaced bedding plane shear surfaces has produced a 'stepped' topography. The slope processes present are not, however, unique to the Naish Farm undercliff. Mudslides and debris slide are common in other areas of degrading argillareous slopes. Landslides which use bedding planes as basal shear surfaces have also been identified elsewhere. This study has therefore documented an area which is considered to be important and advantageous for landslide studies. A special attribute of the Barton Clay cliffs however is the high rate of degradational activity produces a good exposure of the geological strata and assists the study of the relations between landsliding and geology.

9.7 Summary

1. The data collected for this thesis has allowed the identification of seven different slope degradational processes. The three sliding processes have been found to be responsible for the movement of all landslide debris across the undercliff.

Benchsliding, which is a form of compound sliding using a preferred bedding plane shear surface as the translational section of the shear surface, transports 97% of the slip debris. The mudslides monitored did not enlarge with time and were kept supplied by the benchsliding activity.

Debris slides have been identified and characterised. This process is not believed to have been specifically identified in the Barton Clay cliffs before. They have been distinguished from mudsliding and both the origin and the pattern of movement described.

The study of the above forms of movement has also allowed the identification of parts of the degrading slope with more than one shear surface. Seven locations have been identified over the two year study period. These multi-story landslides are believed to be common but can easily escape detection.

2. The two year study period has been identified as a relatively 'quiet period'. Chapter 6 has compared the study period rates with historical rates derived from rates of cliff top recession. The reason relative inactivity has been caused by the absence of large cliff top slumping to supplement the supply of debris to the undercliff from the degradation of the in-situ Plateau Gravel/Barton Clay scarps.

3. The stability calculations have shown that pore water pressures predicted by the flow nets have produced

unrealistically high values of residual shear strength for the Barton Clay. These high values are considered to be due to the inaccuracy of the flow net assumption of homogenity of the landslide debris and also the possibility that first time failure of the in-situ cliff top scarp causing rapid unloading of the rear portion of the shear surface and a subsequent depression of pore water pressures. The sensitivity of the benches to instability resulting from high pore water pressures is considered the reason for the occurrence of the 'surges' in the D bench movement rates.

University of Southampton

PROCESSES OF SLOPE DEGRADATION IN THE BARTON CLAY CLIFFS OF CHRISTCHURCH BAY

Volume 2

TABLES

Table 1-1 Major sub-divisions of slope movement
(After Varnes, 1978)

Type of Movement	Type of Material (before failure)	Rates of Movement
1. Falls 2. Topples 3. Slides - Rotational - Translational 4. Lateral Spreads 5. Flows 6. Complex	1. Bedrock 2. Debris 3. Earth	1. Extremely rapid > 3 m/s 2. Very rapid 0.3 m/min to 3 m/s 3. Rapid 1.5 m/day to 0.3 m/min 4. Moderate 1.5 m/mo to 1.5 m/day 5. Slow 1.5 m/yr to 1.5 m/mo 6. Very slow 0.06 m/yr to 1.5 m/yr 7. Extremely slow < 0.06 m/yr

Table 1-2 Studies of mass movements on slopes

Author(s)	Date	Study Area	Predominant Geology	Type of Study	Method of Study
Barton	1973	Barton-on-Sea Hants	Barton Clay	Study of cliff degradation	General field study
Brunsden	1974	Fairy Dell Dorset	Middle Lias	Study of coastal degradation	General field study
Burland Longworth Moore	1978	Whitlesey Cambs.	Oxford Clay	Study of deep excavation	Field study including precise surveying and installation of inclinometers, piezometers and extensometers
Bromhead	1978	Herne Bay Kent	London Clay	Analysis of large scale failures	Field and laboratory study
Chandler	1972	Vestspitsbergun Denmark	Tertiary siltstone	Mudflow movements on shallow slopes	Field study including piezometer installation
Chandler	1977	A606 Leics	Upper Lias	Back analysis for stabilization works	Field study including piezometer and slope indicator installation
Chandler Pachakis Mercer Wrightman	1973	Northants, Worcs, Dorset	Solifluction mantles	Four case histories of embankment failure	Field study including trial pits, boreholes and piezometer installation
Early Skempton	1972	Waltons Wood Staffs.	Glacial deposit on Upper Coal Measures	Post failure analysis	Back analysis and laboratory testing
Hutchinson		Cromer Norfolk	Pleistocene deposits	Detailed site study	Field study, piezometer installation, boreholes and laboratory testing

Author(s)	Date	Study Area	Predominant Geology	Type of Study	Method of Study
Hutchinson	1969	Folkestone Warren, Kent	Upper Cretaceous	Detailed site study	Field study including boreholes, piezometer and laboratory analysis
Hutchinson	1970	Beltinge Kent	London Clay	Coastal mudflow	Field study with inclinometer and piezometer installation
Hutchinson Bhandari	1971	Isle of Sheppey Kent	London Clay	Mechanic of mudflow movements	Field study including electro-piezometer installation
Hutchinson Somerville Petley	1973	Bury Hill Staffs.	Etruria Marl	Post failure study	Field study including piezometers, boreholes and trial pits
Hutchinson Prior Stephens	1974	Antrim Coast N. Ireland	Lower Lias	Study of mudslide surges	Field study including continuous movement monitoring piezometers and surveys
Hutchinson Bromhead Lupini	1980	Folkestone Warren, Kent	Upper Cretaceous	Additional observation of landslide complex	Morphological study and back analysis
Hutchinson Chandler Bromhead	1981	S.W. Coast Isle of Wight	Lower Cretaceous	Cliff recession and seepage erosion	Field observations
Mitchell Eden	1972	Ottawa Valley, Canada	Leda Clay	Slope movements	Field study including inclinometers
Pitts	1983	Dee Estuary England	Glacial Deposits	Geomorphological study	General field study
Prior Eve	1975	Rosnaes Denmark	Till, Eocene Clay	Coastal landslide morphology	General field study
Rapp	1960	Karkevagge N. Scandinavia	Mica-schist and Gneiss	Development in mountain slopes	Field study

Author(s)	Date	Study Area	Predominant Geology	Type of Study	Method of Study
Sauer	1983	Denholm S. Saskatchewen Canada	Upper Cretaceous clay shales	Post failure analysis	Field studies including 'testholes'
Schumm	1956	Perth Amboy New Jersey U.S.A.	Clay-sand fill	Evolution of drainage systems and slope profiles	Field studies and surveying
Sherrell	1971	Cullumpton Devon	Upper Carboniferous	Post failure study	Field study including piezometer, inclinometer and boreholes
Skempton Brown	1961	Selset Yorks.	Boulder Clay	Post failure analysis	Field study including piezometers, boreholes and laboratory testing
Hutchinson Gostelow	1976	Hadleigh Castle, Essex	London Clay	Study of an abandoned cliff	Field study including trial pits, boreholes and laboratory testing

TABLE 2-1 A comparison of the theoretical formation of crenulate bays with the formation of Poole and Christchurch Bay (After, Wright, 1981)

Idealized constraints outlined by Silvester (1974)	Conditions present in Poole and Christchurch Bay, Wright(1981)
Wave refraction would only occur on one updrift headland.	Both Poole and Christchurch Bay have two updrift headlands to cause initial and secondary refraction.
Waves should approach the shoreline from a single predominant direction.	Poole and Christchurch Bays exist in a storm wave environment where there is no single predominant direction of wave attack.
The crenulate shaped bay development and stability hypothesis is derived from bays with homogenous beach sediment.	Beach sediment sizes coarsen in the downdrift direction around the shorelines of Poole and Christchurch Bays
Bay indentation is wholly due to wave refraction.	East Dorset and the Hampshire Coast exhibit features of a drowned coastline so the degree of indentation does not wholly reflect the action of wave refraction.
Crenulate bay formation occurs along a coast of constant lithology.	In Poole and Christchurch Bay there is a variation in the lithological resistance of the headland and the adjoining bay areas to erosion.

TABLE 2-2 Published thicknesses of the Barton Beds

Author	Barton Clay (m)	Barton Sand (m)	Total Thickness (m)
Gardner et al. (1888)	31.3*	27.4	58.5*
Burton (1925)	31.3*	27.4	58.5*
Burton (1929)	32.3*	29.3	61.6*
Burton (1933)	32.3*	29.0	61.3*
Curry (1958)	29.9*	29.0	58.8*
Barton (1973)	46.4	-	-

*, 3 metres should be added to be directly comparable with Barton.

TABLE 2-3 The cycles of deposition during the Eocene and Oligocene

Stage	Cycle Number	Beds Deposited
Bartonian	5	Lower Headon Beds Barton Beds
Auversian Lutetian	4	Upper Bracklesham Beds Lower Bracklesham Beds
Crusian Ypresian	3	Lower Bagshot Beds London Clay
Sparnacian	2	Woolwich and Reading Beds
Thanetian	1	Thanet Beds

TABLE 2-4 The particle size distribution of the zones in the Barton Clay

Horizon	Sand Content %		Silt Content %		Clay Content %	
	K	Ho	K	Ho	K	Ho
F2	1	12	34	37	65	51
F1	5	5	36	38	59	57
E	7	31	59	43	34	36
D(upper)	15	36	57	46	28	18
D(Lower)	40	13	35	58	25	29
C	38	45	25	24	37	31
A3(sand)	-	77	-	20	-	3
A3(Clay)	2	15	46	55	52	30
A2	10	9	52	37	38	54
A1	1	-	58	-	41	-
AO	47	-	18	-	35	-

K = Results from Kilbourn (1971)

Ho = Results from Ho (1982)

TABLE 2-5 The clay mineral content (parts in ten) of the Barton Clay formation

Zone	Montmorrillonite		Illite		Kaolinite		Chlorite	
	Gilkes	Ho	Gilkes	Ho	Gilkes	Ho	Gilkes	Ho
A1	2		6		2		0	
A2	3.5		4.5		2		0	
A3	2		5		3		0	
B	3		5		2		0	
C	3	5	4	4.5	3	0.5	0	0
D	2.5		4.5		3		0	
E	3		4		3		0	
F	2	3.5	4	4	3	1.5	1	1

Gilkes = Results from Gilkes (1968)

Ho = Results from Ho (1982)

TABLE 2-6 The moisture content of the Highcliffe benchslides compared to other published data

Source	Site	Sampling Date	Material	Depth of sample (m)	Moisture Content %
Author	D Bench	23.2.83	Barton Clay Colluvium	0.15	33 - 43
Author	F Bench	2.3.83	"	"	26 - 38
Author	A3 Bench	"	"	"	30 - 36
Author	MSB	29.3.83	"	0.5	43 - 46
Author	MSA	21.10.80	"	0.1	38 - 42
Hutchinson, Prior and Stephens (1974)	Antrim N.Ireland	Nov. 71	Weathered Liassic Shales	-	41 - 43
Hutchinson (1970)	Beltingle, Kent	Sept. 63	London Clay mudslide	0.5	38 - 49
Hutchinson and Bhandari (1971)	Isle of Sheppey, North Kent	1969	London Clay mudslide matrix	?	50

TABLE 2-7 The position of the preferred bedding plane shear surfaces in the Barton Clay in Christchurch Bay (After Barton, 1973)

Bench and shear surface notation	Position of shear surface	Evidence
G	0.15m above the top of G	Isolate exposure
F	0.10m above the concretionary limestone in F	Prominent
D	0.46m above the base of D	Prominent
A3	Junction of A2/A3	Prominent
A2	5.04m below top of A2	Isolated exposure
Lower A2	8.40m below top of A2	Isolated exposure
A1	0.70m above base of A1	Isolated exposure

TABLE 2-8 The areas covered by the major geomorphological units in the Naish Farm undercliff

Geomorphological unit	Undefended undercliff (m^2)		Study Area (m^2)	
	September 1975	November 1980	September 1975	November 1980
F Bench	21,003	22,509	1,450	1,580
D Bench	38,063	48,229	12,540	11,650
A3 Bench	6,621	9,390	3,320	2,460
Total Bench	65,687	80,128	17,310	15,690
Scarps	38,647	31,377	2,960	2,970
Debris Slides	2,356	4,125	4,670	5,880
Scarps and debris slides	41,003	35,502	7,630	8,850
Mudslides	2,964	1,521	690	590
Ponds	450	1,151	240	390
Total Area	110,104	118,302	25,870	25,520

TABLE 2-8a The percentage areas covered by the major geomorphological units in the Naish Farm undercliff

Geomorphological unit	Undefended undercliff		Study Area	
	September 1975	November 1980	September 1975	November 1980
F Bench	19	19	6	6
D Bench	35	41	48	46
A3 Bench	6	8	13	10
Total Bench	60	68	67	62
Scarps	34	27	11	12
Debris Slides	2	3	18	23
Scarps and debris slides	36	30	29	35
Mudslides	3	1	3	2
Ponds	1	1	1	1
Total	100	100	100	100

TABLE 3-1 Field examples of surface movement monitoring

Authors	Investigation	Monitoring Method	Range of Movements	Published Accuracy
Burland, Longworth and Moore (1978)	Ground movements caused by deep excavation in Oxford Clay	Precise Theodolite survey	0 to 165mm per year	± 5mm
Prior and Stephens (1971)	Monitoring mud-flow movements	Modified Munro water-level recorder	0 to 2500mm in 7 days	Not quoted
Hutchinson, Prior and Stephens (1974)	Monitoring mud-flow movements	Modified Munro water-level recorder	0 to 4900mm in 1 minute	Sensitive to 10mm per minute
Hutchinson (1970)	Coastal mudflow	Wooden peg taping	0 to 260mm per day	± 15mm
Penman and Charles (1974)	Embankment Dam monitoring	Trilateration, levelling and triangulation	0 to 530mm in 582 days	± 5mm

TABLE 3-2 Inclinometer tube performance

Inclinometer Tube	Install-ation date	Days to Failure	Geomorpho-logical process	Total Depth of Tube (metres)	Failure Depth (mA.O.D)	Tube Material
I1	14.10.80	2	MSA	3	-	Aluminium
I2	6. 1.81	13	Amphitheatre	3.5	9.66	Plastic
I3	12. 3.81	5	A3	2.4	1.73	Aluminium
I4	12. 3.81	Vandalized	A3	2.5	-	Aluminium
I5	7. 4.81	162	Amphitheatre	3.5	12.36	Plastic
I6	2. 7.81	70	Amphitheatre	3.0	12.36	Plastic
I7	16. 7.81	118	Amphitheatre	4.5	12.71	Plastic
I8	17.12.81	5	DS3	5.4	17.18	Plastic
I9	17.12.81	3	DS1	4.7	21.69	Plastic
I10	25. 3.82	Vandalized	D Bench	4.5	-	Plastic
I11	23.10.82	-	Cliff Top	9.0	-	Plastic

TABLE 3-4 Slip Indicator performance

Slip Indicator	Installation Date	Days to Failure	Geomorphological Process	Total Depth (m)	Failure Depth (m A.O.D.)	Tube Material Material
SPI1	12. 9.81	23	Amphitheatre	4.0	11.06	Flexible tube
SPI2	12. 9.81	23	Amphitheatre	6.03	9.29	Flexible tube
SPI3	21.10.81	29	F Bench	5.20	22.20	Flexible tube
SPI4	21.10.81	29	F Bench	4.13	23.64	Flexible tube
SPI5	21.10.81	14	D Bench	9.3	8.99/12.77	Flexible tube
SPI6	22.10.81	-	MSA	3.78	-	Flexible tube
SPI7	22.10.81	144	Amphitheatre	5.72	12.19	Flexible tube
SPI8	22.12.81	8	Amphitheatre	3.8		Semi-rigid tube
SPI9	5. 1.82	1	Amphitheatre		7.62	Semi-rigid tube
SPI0	5. 1.82	9	Amphitheatre	2.52	8.49	Semi-rigid tube
SPI11	25. 3.82	-	DS3	2.81	-	Semi-rigid tube
SPI12	25. 3.82	-	DS3	4.23	-	Semi-rigid tube
SPI13	1. 4.82	6	DS3	2.63	19.15	Semi-rigid tube
SPI14	1. 4.82	6	DS3	3.24	24.09	Semi-rigid tube
SPI15	19. 4.82	-	DS3	3.38	-	Semi-rigid tube
SPI16	19. 4.82	-	DS3	2.05	-	Semi-rigid tube
SPI17	19. 4.82	-	DS3	1.9	-	Semi-rigid tube
SPI18	19. 4.82	-	DS3	3.19	-	Semi-rigid tube
SPI19	19. 4.82	-	DS3	2.35	-	Semi-rigid tube
SPI20	22. 4.82	-	A3 Bench	3.89	-	Semi-rigid tube
SPI21	22. 4.82	-	A3 Bench	3.81	-	Semi-rigid tube
SPI22	22. 4.82	-	A3 Bench	3.98	-	Semi-rigid tube

TABLE 4-1 Major methods of shear surface detection

	INSTRUMENTATION			INSPECTION		
	Inclinometer	Slip Indicator	Geophysical	Boreholes	Trial Pits	Surface Exposures
Main Uses	Dams, Tunnels, Embankments, landslides. Installed pre or post construction. Detects change in tube inclination. Produces a velocity profile. Can give failure warning.	Landslides, normally post failure Locates shear surface if active.	Cover large areas during a site investigation Detects a contrast in resistivity, seismic refraction and gravity. Can be used in any type of investigation	Site Investigations Post failure examination	Site Investigations Post failure examination	Any Site inspection
Advantages	Highly accurate permanent until failure. Installed to great depth.	Cheap to install	Cover large area	Allows a detailed inspection to a known depth.	Allows a detailed inspection. Only limited disturbance.	No soil disturbance. Can produce unequivable evidence of failure.
Disadvantages	Do not know precise depth to shear plane. Can spiral at depth. Needs mechanical drilling.	No other information produced.	Generally none of the three properties listed have enough contrast to allow location of slip plane. Needs experienced interpretation	Expensive. Causes soil disturbance. Needs experienced. interpretation.	Limited in depth. Can be dangerous.	True surface exposure of slip plane rare.

Table 4-2 Rates of mudslide movement

Author	Site	Mudslide zone	Overall movements			Peak movements		
			Total displacement (metres)	Total time (days)	Rate (mm/day)	Total displacement (metres)	Total time (days)	Rate (mm/day)
Hutchinson (1970)	Beltinge, Kent	Accumulation	70	1764	40	5.2	20	260
Prior and Stephens (1970)	Antrim, N. Ireland	Feeder	2.51	7	360	0.198	1 hour	4750
Hutchinson, Prior and Stephens (1974)	Antrim, N. Ireland	Feeder	2.95	15	195	0.65	1	650
		Accumulation	-	-	-	-	-	-
Coles (1988)	Mudslide A Christchurch Bay Hampshire	Feeder	max 22.17	734	30	2.07	13	159
			min 8.5	734	12			
Coles (1988)	Mudslide B Christchurch Bay Hampshire	Accumulation	max 5.7	25	228	1.2	5	240
			min 1.4	25	56			

TABLE 5-1 Areas of multi-layered landslides in the Naish Farm study area

Location	Layers	Level of Active Shear Surfaces (m, A.O.D.)	Size (m^2)	Method of Detection
Debris Slide 1	2	21.7m 9.5m	530	Inclinometer Peg survey
Debris Slide 2	3	 9.5m	270	Peg survey
Debris Slide 3	2	17.2m 10.3m	980	Slip Indicator Peg survey
Debris Slide 4	2	20.0m 9.6m	360	Penetration Tests Peg survey
Debris Slide 5	2	 9.6m	270	Peg survey
Amphitheatre Floor	2	12.5m 9.5m	933	Inclinometer slip indicator Peg survey
Mudslide A	2	10.5m 9.6m	240	Penetration Tests Peg survey

TABLE 5-2 The displacement components of the areas of multi-layered landslides at Naish Farm

Complex	Study Period (Days)	Total Movement (m)	Debris Slide Component (m)	Amphitheatre Floor (m)	D Bench Component (m)
DS1	734	7.49	5.06	-	2.43
DS2	482	12.27	6.2	3.87	2.2
DS3	476	3.71	1.55	-	2.16
DS4	429	7.93	6.69	-	1.24
DS5	218	8.18	7.79	-	0.39
Mudslide A	734	22.05	19.64*	-	2.41
Amphi-theatre	734	8.27	-	6.07	2.20

* Mudslide component

TABLE 5-3 The percentage contributions of the slide components for debris slide 2 and the amphitheatre floor

Number of layers in landslides	Geomorphological processes	Total study period	Surge period SG1	Surge period SG2
3	Debris slide 2	51	14	18
	Amphitheatre floor	31	40	48
	D bench slide	18	46	34
		100	100	100
2	Amphitheatre floor	64	46	58
	D bench slide	36	54	42
		100	100	100

TABLE 5-4 The movement components of debris slide 1 for the complete study period

Period	Observed DS1 (m)			Observed D bench (m)			Actual debris slide (m)		
	Xa	Ya	Za	Xb	Yb	Zb	Xc	Yc	Zc
S1	-0.01	0.05	-0.03	-0.01	0.05	-0.01	0	0	-0.02
W1/1	-0.03	0.44	-0.17	-0.01	0.22	-0.08	-0.02	0.22	-0.09
SG1	-0.16	1.29	-0.88	-0.07	0.75	-0.32	-0.09	0.54	-0.56
W1/2	-0.44	3.14	-1.59	-0.05	0.36	-0.09	-0.39	2.78	-1.5
S2	-0.02	0.30	-0.21	-0.01	0.11	-0.04	-0.01	0.19	-0.17
SG2	-0.15	1.51	-0.75	-0.08	0.85	-0.30	-0.07	0.66	-0.45
W2	-0.13	0.71	-0.14	0	0.13	-0.04	-0.13	0.58	-0.10
S3	-0.04	0.13	-0.08	-0.03	0.11	-0.08	-0.01	0.02	0

TABLE 6-1 A summary of the colluvial budget in the budgetary study area

Geomorphological Units	Geomorphological Process	Volume Transferred (m^3)	
		July 81 to July 82	July 82 to July 83
Cliff Top to F Bench	Spalled Gravel	59	37
	Slump Volume	190	-
	Total Volume from cliff top recession data	436	278
F Bench to D Bench	Bench Slide	139.6	101.4
	Debris Slide	281	-
	Total Volume	420.6	101.4
D Bench to A3 Bench and Mudslide B	Bench Slide	2964	2487
	Mudslide A	62	114
	Amphitheatre Slide	453	370
	D Scarp recession	992	481
	Total Volume	4471	3452
A3 Bench and Mudslide B to Beach	Bench slide	5187	3667
	Mudslide B	396	348
	Total Volume	5583	4015

TABLE 6-2 A summary of the volumes of landslide debris transferred in the budgetary study area

Geomorph-ological Unit	Volume Transferred (m^3)					
	July 81 to July 82			July 82 to July 83		
	Gain	Loss		Gain	Loss	
Cliff Top	-	436	-436	-	278	-278
F Bench	436	421	+25	278	101	+177
D Bench	421	4471	-4050	101	3452	-3351
A3 Bench	4471	5583	-1112	3452	4015	-563
Beach	5583	-	+5583	4015	-	+4015

TABLE 6-3 The volumes of landslide debris moved from the cliff top to the F bench

Process		July 81 to July 82	July 82 to July 83
Gravel Spalling Rates	Length of Exposed Rod	0.13m	0.08m
	Area of Gravel Scrap	352m^2	352m^2
	Bulking Factor	1.3	1.3
	Volume of Spalled Gravel	59m^3	37m^3
Large Slump Volumes	Width	2.6m	-
	Length	8.65m	-
	Height	6.5m	-
	Bulking Factor	1.3	
	Volume of Slump	190m^3	
Total Recession Rates	Area Lost	141m^2	90m^2
	Average Scarp Height	2.38m	2.38m
	Bulking Factor	1.3	1.3
	Volume lost	436m^3	278m^3

TABLE 6-4 The volumes of landslide debris moved from the F bench to the D bench

Process		July 81 to July 82	July 82 to July 83
Bench Sliding	Frontal area	36m²	48m²
	Seaward Movement	0.01m	0.03m
	Volume	3.5m³	1.4m³
	Frontal area	40m²	145m²
	Seaward Movement	2.46m	0.69m
	Volume	10m³	100m³
	Frontal area	103m²	
	Seaward Movement	1.22m	
	Volume	126m³	
Debris Slide 3	Average Depth	1.48m	
	Frontal width	36m	
	Average Seaward Movement	5.28m	
	Volume	281m³	

TABLE 6-5 The volumes of landslide debris moved from the D bench to the A3 bench

Process		July 81 to July 82	July 82 to July 83
Bench Sliding	Frontal Area	487m²	404m²
	Seaward Movement	0.98m	2.50m
	Volume	477m³	1010m³
	Frontal Area	790m²	854m²
	Seawater Movement	3m	1.6m
	Volume	2370m³	1366m³
	Frontal Area	105m²	112m²
	Seaward Movement	1.11m	0.99m
	Volume	117m³	111m³
Mudslide A	Frontal Area	7.5m²	10m²
	Seaward	8.32m	11.38m
	Volume	62m³	114m³
Amphitheatre Slide	Frontal Area	104m²	55m²
	Seaward Movement	4.36m	6.72m
	Volume	453m³	370m³
D Scarp Recession	Bulking Factor	1.3	1.3
	Area Lost	251m²	148m²
	Scarp height	3.04m	2.5m
	Volume	992m³	481m³

TABLE 6-6 The volumes of landslide debris moved from the A3 bench to the beach

Process		July 81 to July 82	July 82 to July 83
Bench Slide	Frontal Area	374m^2	334m^2
	Seaward Movement	13.87m	10.98m
	Volume	5187m^3	3667m^3
Mudslide B	Frontal Area	23m^2	24m^2
	Seaward Movement	17.2m	14.5m
	Volume	396m^3	348m^3

TABLE 6-7 A comparison of predicted, by equation A (below), and actual rates of cliff top recession

Date	Volume Lost (m^3)	Study area length (m)	Study area Height (m)	Equivalent recession (m/y)	Actual recession (m/y)
July 81	5583	200	30	0.93	0.69
July 82	4015	200	30	0.67	0.45
July 83		200	30		

A Recession (metres per year) = $\frac{\text{Total Volume lost per year}}{\text{Study Area Length x Study Area height}}$

TABLE 6-8 Predicted velocities for the D bench using historical rates of cliff top recession

Date	Average Cliff top recession (m/y)	Volume of landslide debris added to the D Bench per metre (m^3/y)	Velocity of D bench (m/y)	Average observed velocity of D Bench (m/y)
Jan 1947				
	0.36	7.38	1.07	-
Feb 1959				
	1.30	26.65	3.67	-
April 1971				
	2.29	46.95	6.82	-
May 1976				
	2.69	55.15	8.02	-
April 1978				
	1.27	26.04	3.78	-
Nov 1980				
	0.79	16.20	2.35	-
March 1982				
	0.30	6.15	0.89	0.85
July 1982				
	0.45	9.23	1.34	1.81
July 1983				

TABLE 6-9 Calculated slide velocities from a range of cliff top recession rates

Cliff top Recession (m/y)	Volume of land-slide debris added to D bench per metre (m^3/y)	Velocity of D bench (m/y)	Volume of spall-ing debris per metre width (m^3/y)	Velocity of MSB (m/y)	Velocity of A3 bench (m/y)
0.2	4.1	0.60	2.83	9.90	3.92
0.4	8.2	1.19	2.83	15.76	6.23
0.6	12.3	1.79	2.83	21.61	8.55
0.8	16.4	2.38	2.83	27.47	10.86
1.0	20.50	2.98	2.83	33.33	13.18
1.2	24.60	3.58	2.83	39.19	15.50
1.4	28.70	4.17	2.83	45.64	17.81
1.6	32.80	4.77	2.83	50.90	20.13
1.8	36.90	5.36	2.83	56.76	22.45
2.0	41.00	5.96	2.83	62.61	24.76
2.2	49.10	6.56	2.83	68.47	77.08
2.4	49.20	7.15	2.83	74.33	29.40
2.6	53.30	7.75	2.83	80.19	31.71
2.8	57.40	8.34	2.83	86.04	34.03
3.0	61.50	8.94	2.83	91.90	36.34

Footnote Features	D bench	MSB	A3 bench
Cross sectional area (m^2)	1376	23.5	354
Depth (m)	6.88	3.36	1.77
Source width (m)	200	10	200

TABLE 6-10 The actual rates of field slide velocities during the study period

Date	Recession	Slide Velocity		
	Cliff top (m/y)	D bench (m/y)	MSB (m/y)	A3 bench (m/y)
July 81	0.69	2.14	17.2	13.87
July 82	0.45	1.82	14.5	10.98
July 83				

TABLE 6-11 Predicted rates of mudslide movement at Flow II, Beltinge, N. Kent

Rate of Recession (m/y)	Volume of debris supplied to the mudslide by cliff top recession (m^3/y)	Total volume of debris supplied to the mudslide (m^3/y)	Predicted mudslide movement (m/y)	Actual mudslide movement (m/y)
0.2	341.6	488.0	7.74	
0.39 *	666.1	951.6	15.09	18.67*
0.4	683.2	976.0	15.48	
0.6	1024.8	1464.0	23.2	
0.8	1366.4	1952.0	31.0	
1.0	1708.0	2440.0	38.7	
1.2	2049.6	2928.0	46.4	
1.4	2391.2	3418.0	54.2	
1.6	2732.8	3904.0	61.9	
1.8	3074.4	4392.0	69.6	
2.0	3416.0	4880.0	77.4	
2.2	3757.6	5368.0	85.1	
2.4	4099.2	5856.0	92.9	
2.6	4440.8	6344.0	100.6	
2.8	4782.4	6832.0	108.2	
3.0	5124.0	7320.0	116.1	

* The rate of recession and actual mudslide movement were recorded September 1961 to December 1966 and February 1962 to November 1966 respectively.

TABLE 6-12 The conditions of geology, topography and climate which promote the main processes of debris movement

Process	Geology	Topography	Climate
Slides	Strata with planes of weakness, either bedding planes or joints	Steep slopes, possibly over steepened by removal of slope toe	To initiate slides large volumes of rainfall in a short time to allow the generation of high pore pressures
Flows	Materials which have low liquid limits	Flows occur where surface water can easily accumulate to saturate the soil	Prolonged rainfall to maintain saturation
Falls	Any material will be degraded by freeze-thaw, rain wash activity. Loosely compacted material or material with a high natural water content, is very susceptible	Free standing faces of in-situ material. South facing for maximum freeze-thaw effect. Facing prevailing rain bearing wind for rain wash	Extremes of temperature occuring between day and night. Heavy rain for rain wash to remove matrix
Slope wash	Loose packed material, either in-situ or on a scree slope. Broken down into small fragments to allow suspension	Steep slopes to maintain high flow velocities and therefore enable solids to be carried in suspension	High rainfall average to provide surface flow
Chemical solution	Chemically soluble material	Inclined slopes	Enough rainfall to allow ground water movement
Wind Erosion	Very loose and fine grained material	Ground shape to allow funnelling of wind	High wind speeds

TABLE 7-1 The results of in-situ unit weight tests performed on the D bench

Sample	Collection Date	Unit Weight (KNm^{-3})
A	23 Feb 1983	19.54
B	23 Feb 1983	19.11
C	23 Feb 1983	19.02
D	23 Feb 1983	17.58
E	2 March 1983	18.01
F	2 March 1983	19.68

Mean in-situ unit weight = 18.83 kNm^{-3}

Table 7-2 Values for calculated residual shear strength (φ_r'), pore water pressure ratio ($\bar{r}_u$) and normal vertical stress ($\bar{\sigma}_n'$) for back analysed sections.

Section	φ_r' (Degrees)	$\bar{r}_u$	$\bar{\sigma}_n'$ (kNm^{-2})
D1	22.37	0.548	123.3
D2	21.36	0.532	139.8
D3	24.72	0.544	110.9

Table 7-4 Values of residual shear strength (φ_r') for varying values of pore pressure ratio (r_u)

Section	r_u		
	0.1	0.2	0.3
DS1	15.37	16.36	17.45
DS2	13.96	14.78	15.69
DS3	17.18	18.42	19.20

Table 8-1 Average weekly rainfalls at Hurn during the two year study period.

Movement Total	Total Rainfall (mm)	Length of movement period (weeks)	Average weekly rainfall (mm per week)
S1	128	11	12
W1/1	181	7	26
SG1	18	2	9
W1/2	325	20	16
S2	359	24	15
SG2	191	4	48
W2	295	14	21
S3	348	22	16

FIGURES

LOCATION OF THE STUDY AREA

FIG 1-1

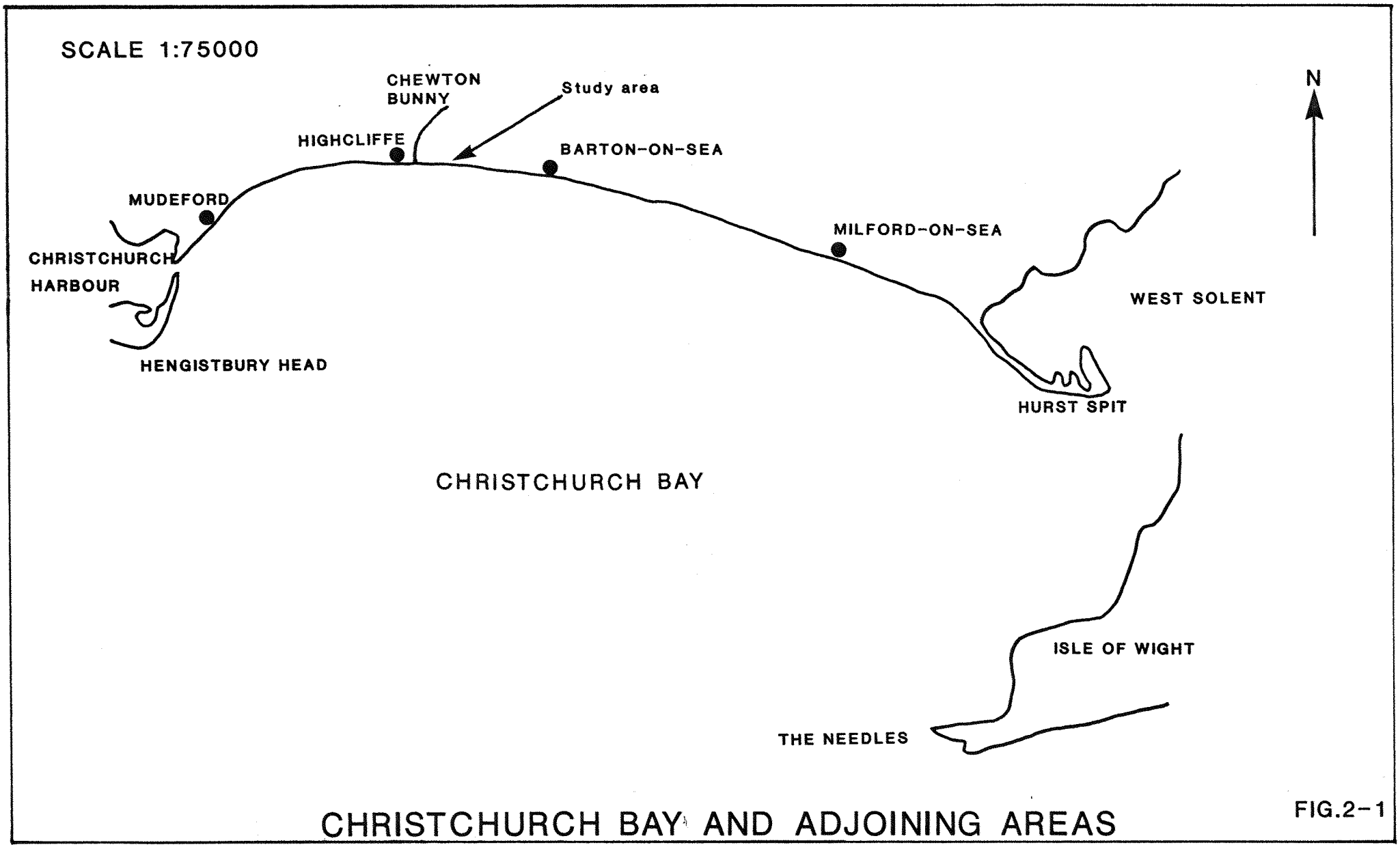

CHRISTCHURCH BAY AND ADJOINING AREAS

FIG.2-1

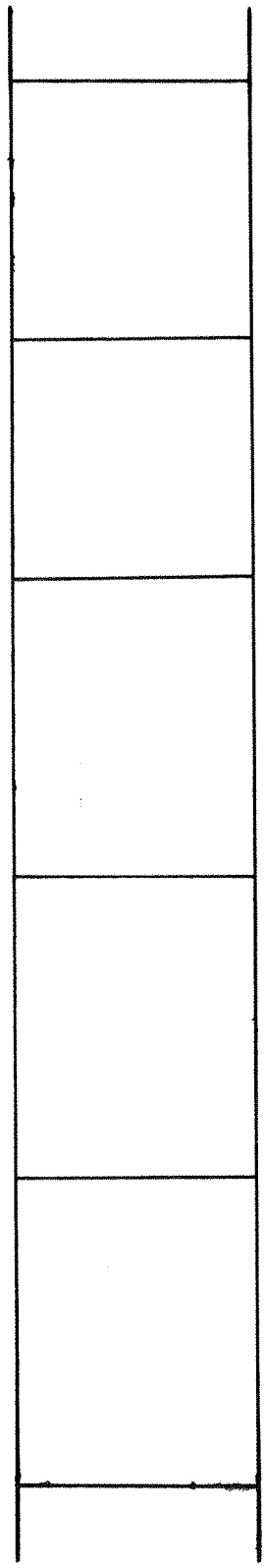

GEOLOGICAL COLUMN OF THE BARTON CLAY SEQUENCE

FIG 2-1a

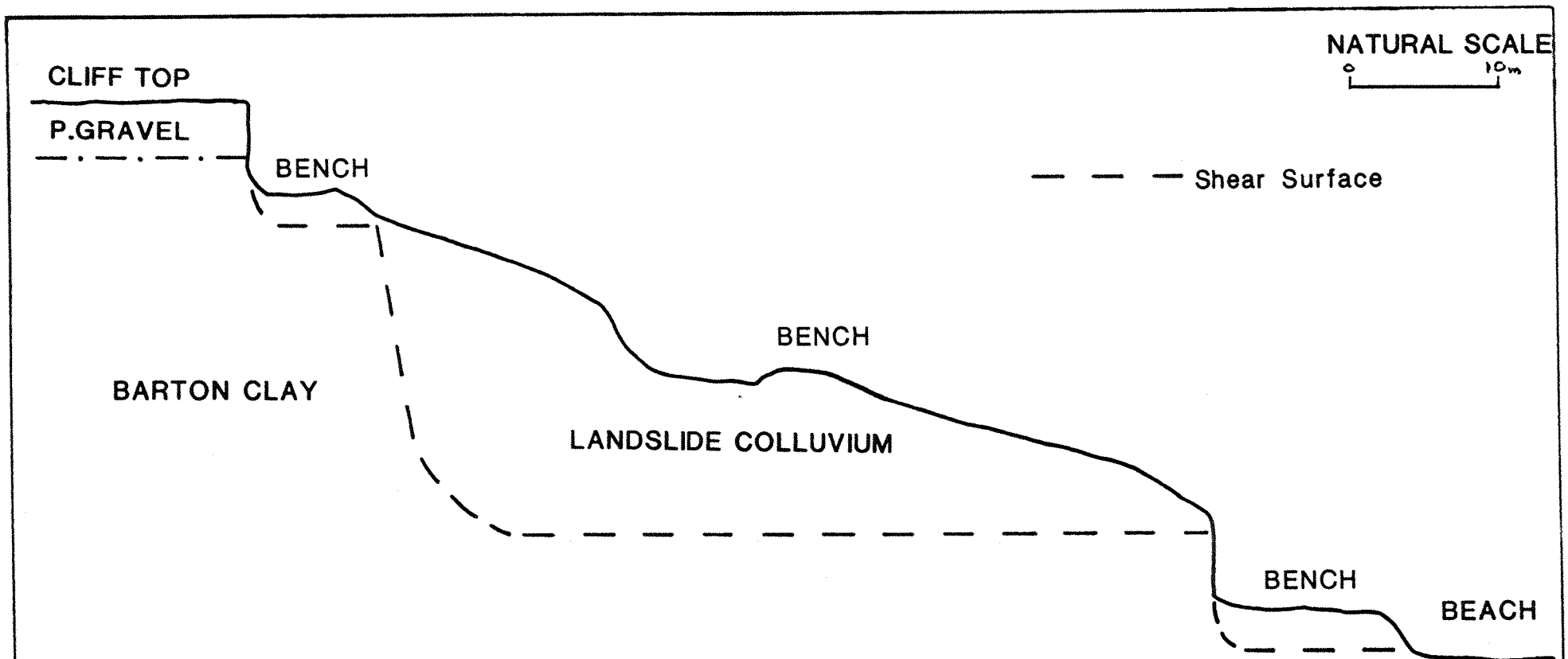

AN IDEALSED SECTION THROUGH THE ACTIVELY DEGRADING UNDERCLIFF

FIG.2-2

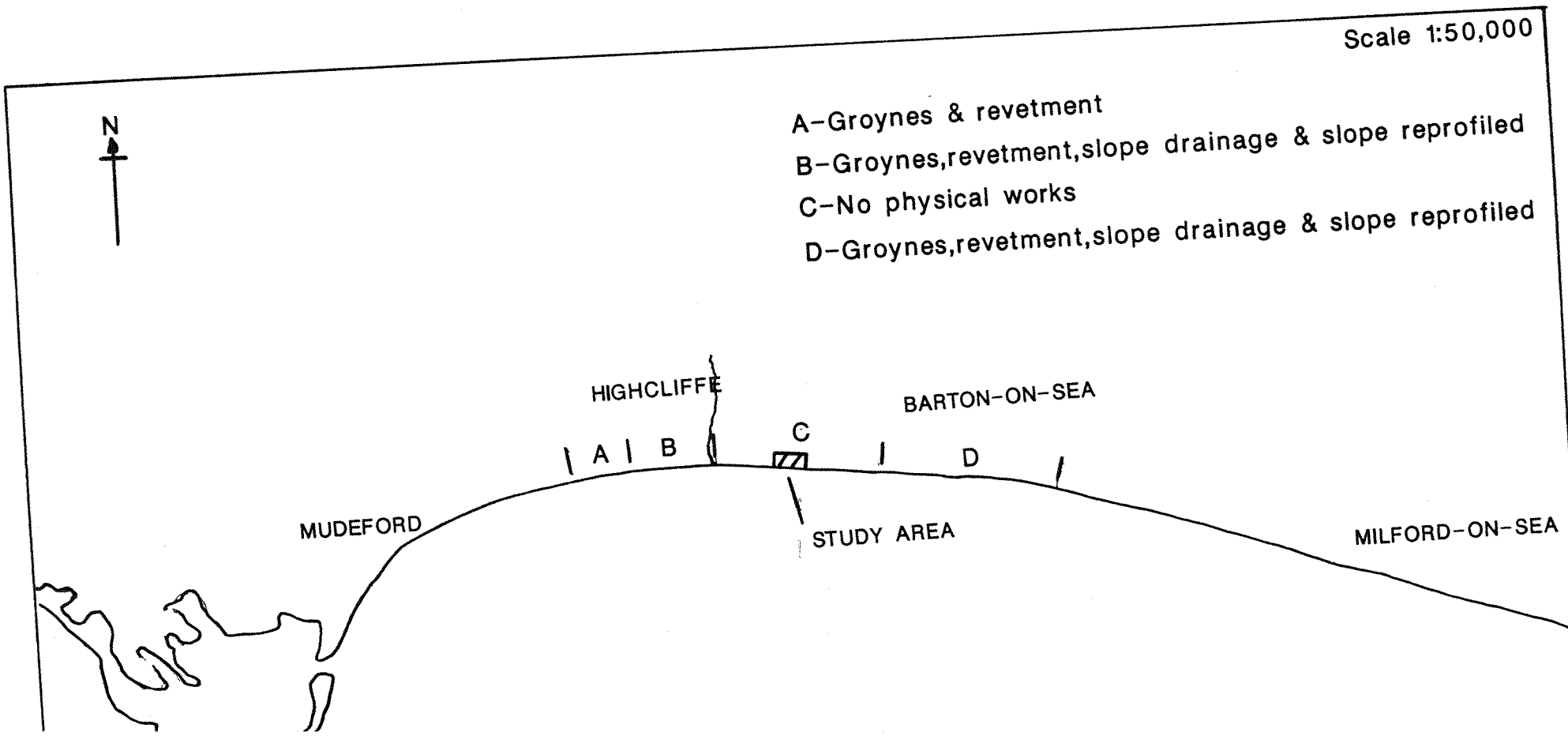
Scale 1:50,000
N
A–Groynes & revetment
B–Groynes,revetment,slope drainage & slope reprofiled
C–No physical works
D–Groynes,revetment,slope drainage & slope reprofiled
HIGHCLIFFE
BARTON-ON-SEA
A
B
C
D
MUDEFORD
STUDY AREA
MILFORD-ON-SEA

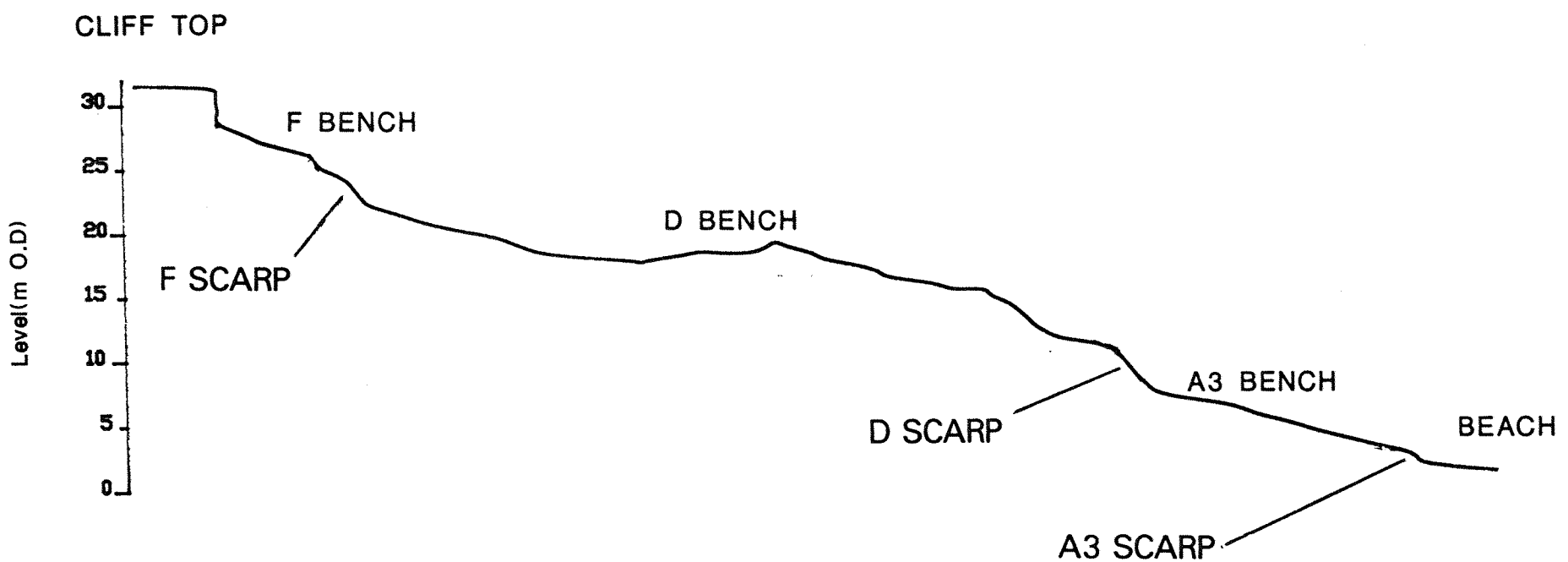

TYPICAL CROSS SECTION THROUGH THE STUDY AREA

FIG 2-2b

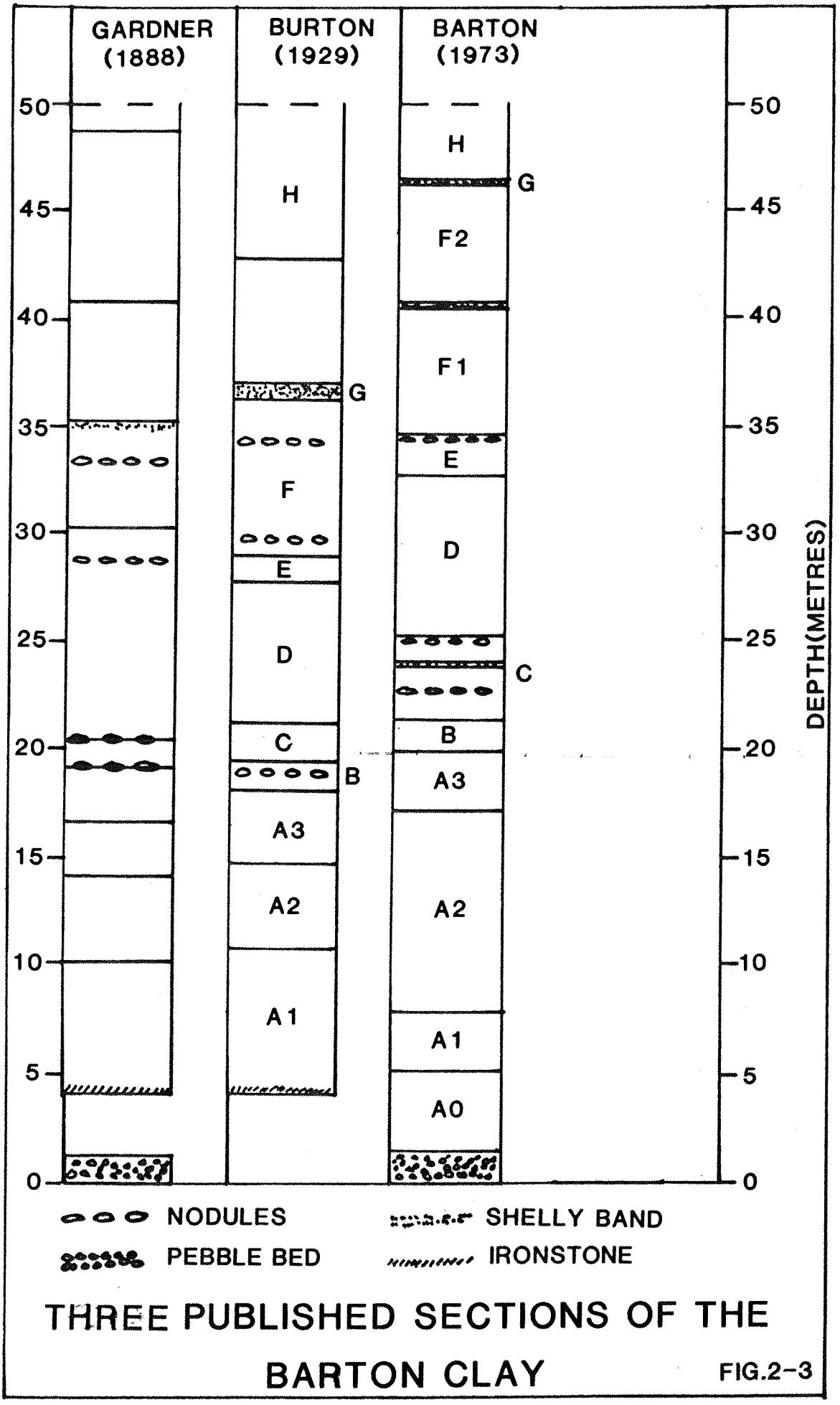

THREE PUBLISHED SECTIONS OF THE BARTON CLAY

FIG.2-3

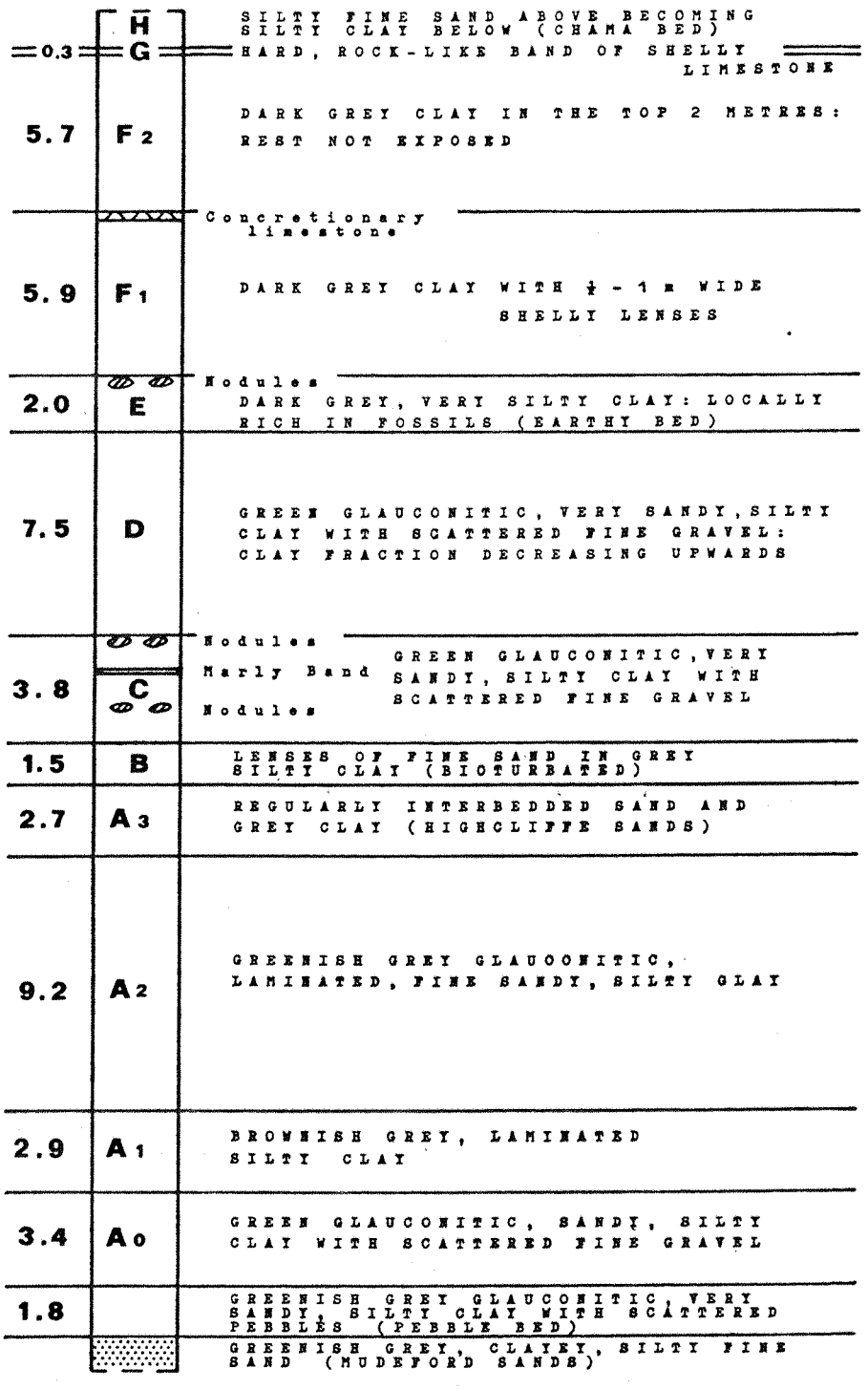

DETAILED LITHLOGICAL SECTION OF THE BARTON CLAY(After Barton,1973)

(ALL DIMENSIONS IN METRES)

FIG.2-4.

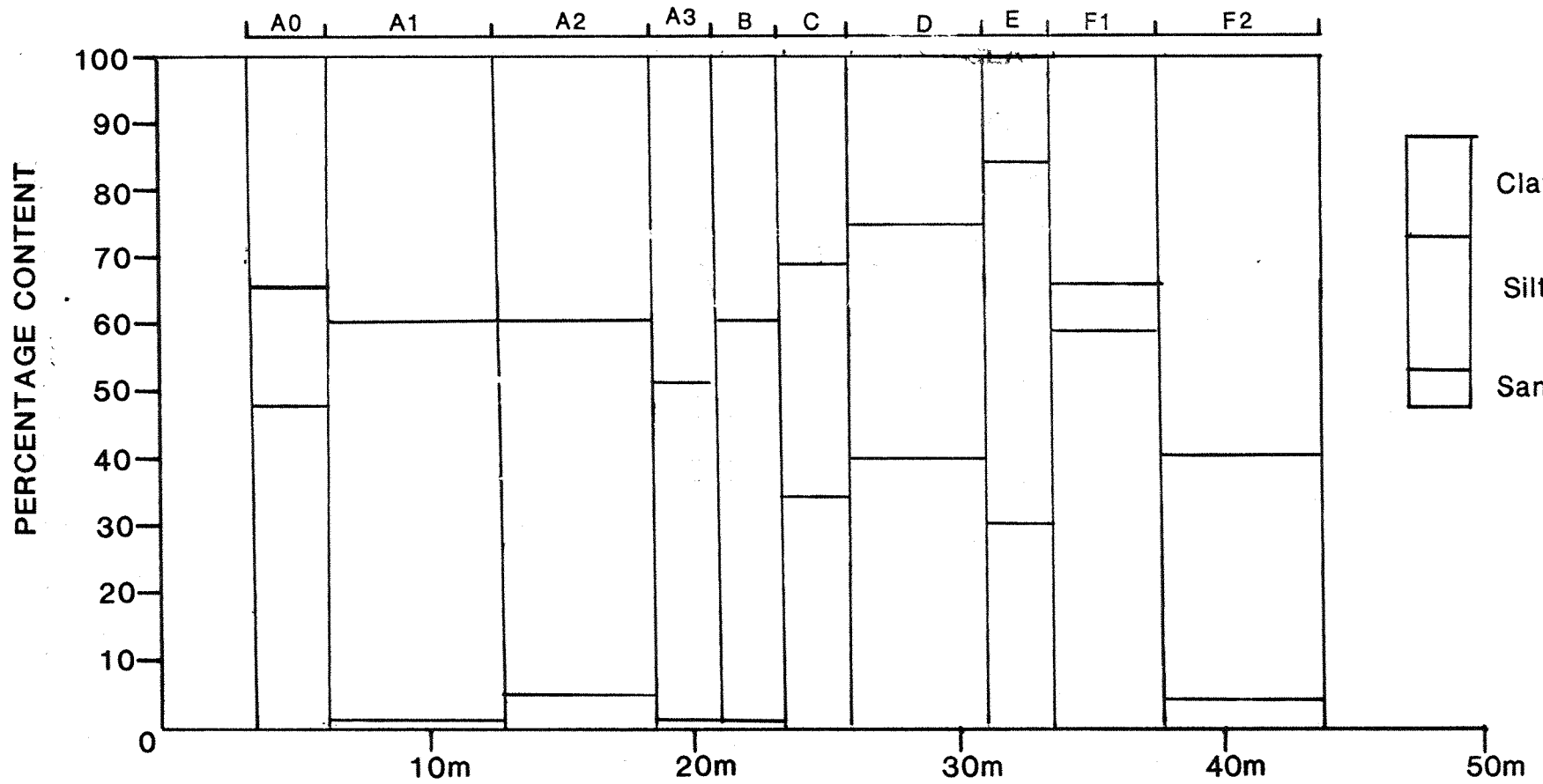

CLAY,SILT AND SAND CONTENT OF THE BARTON CLAY

FIG.2-5

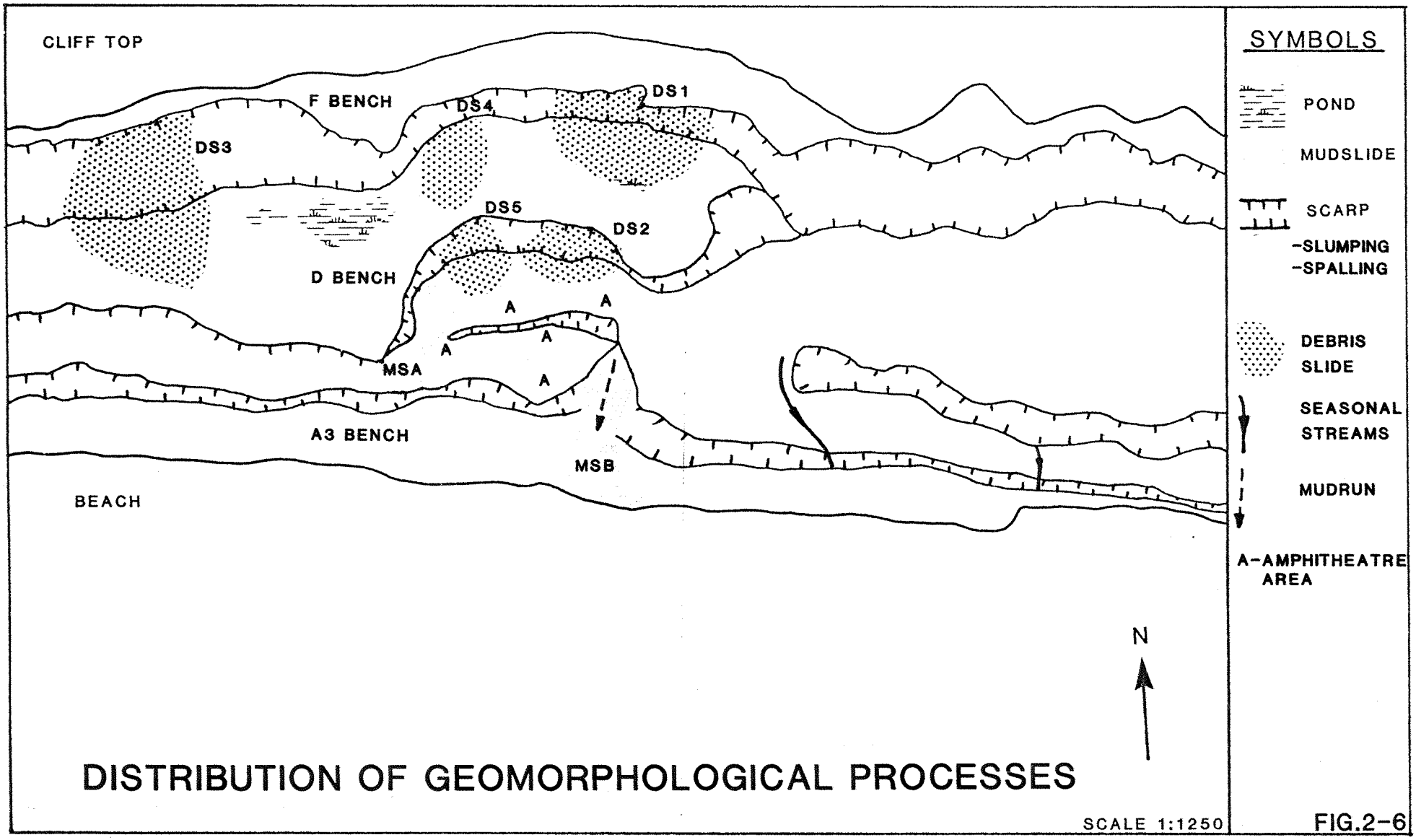

DISTRIBUTION OF GEOMORPHOLOGICAL PROCESSES

SCALE 1:1250

FIG.2-6

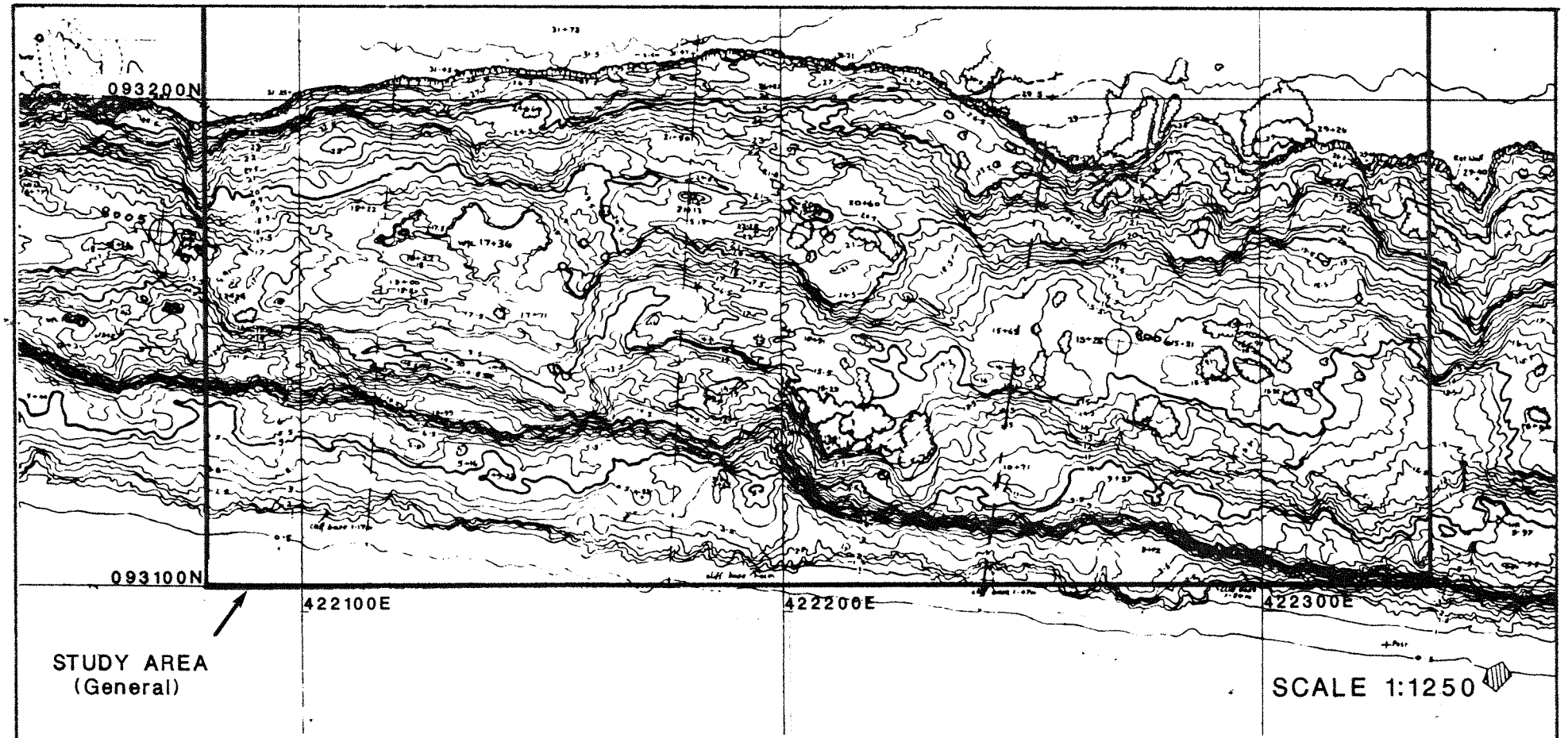

TOPOGRAPHICAL MAP
(November 1980)

FIG.2-7

A3-PREFERRED BEDDING PLANE SHEAR SURFACE

(Exposed after heavy marine erosion)

FIG.2-8

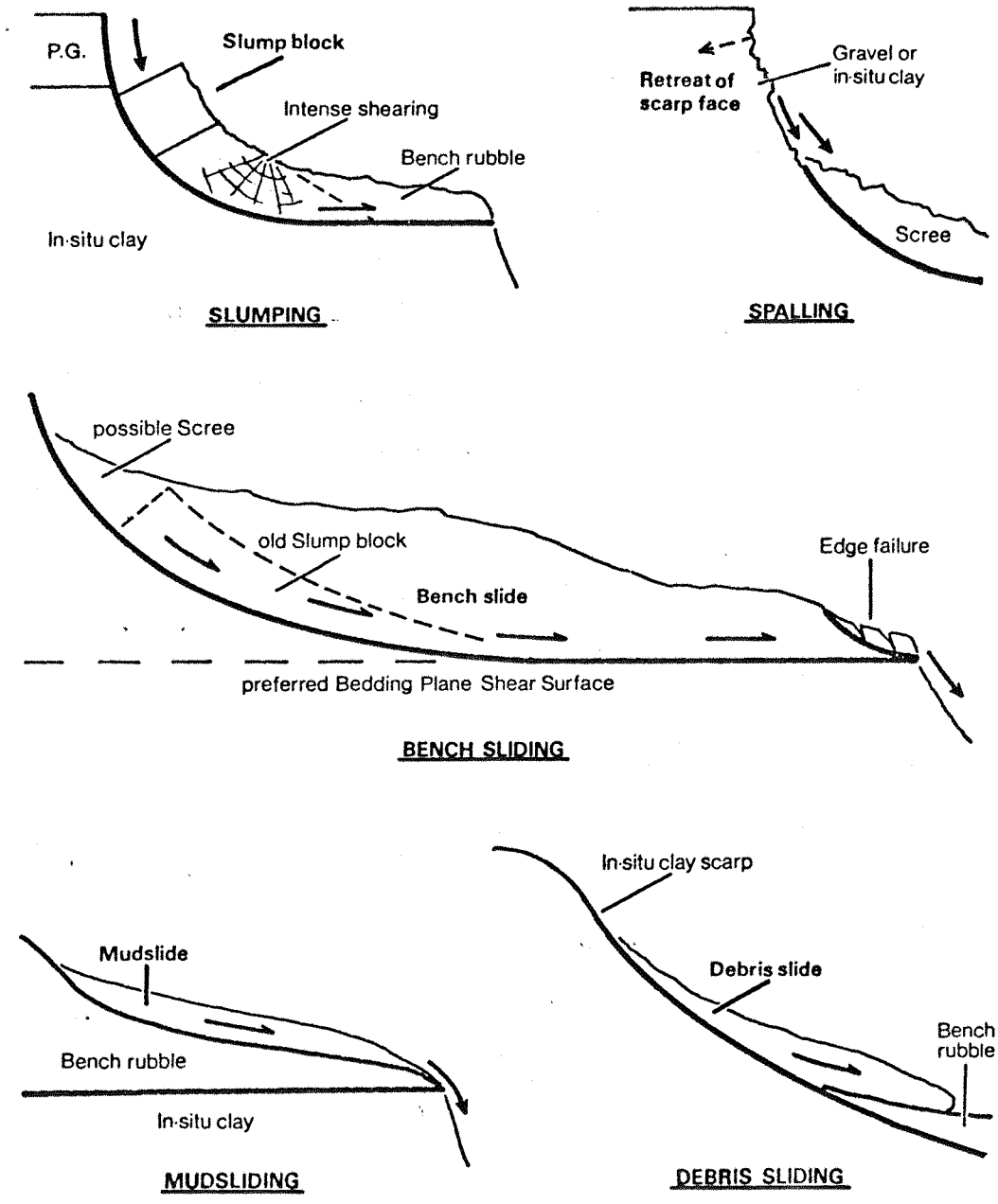

MAJOR DEGRADATIONAL PROCESSES ON THE BARTON CLAY

FIG.2-9

BENCHSLIDE

(F preferred bedding plane shear surface and F scarp)

FIG.2-10

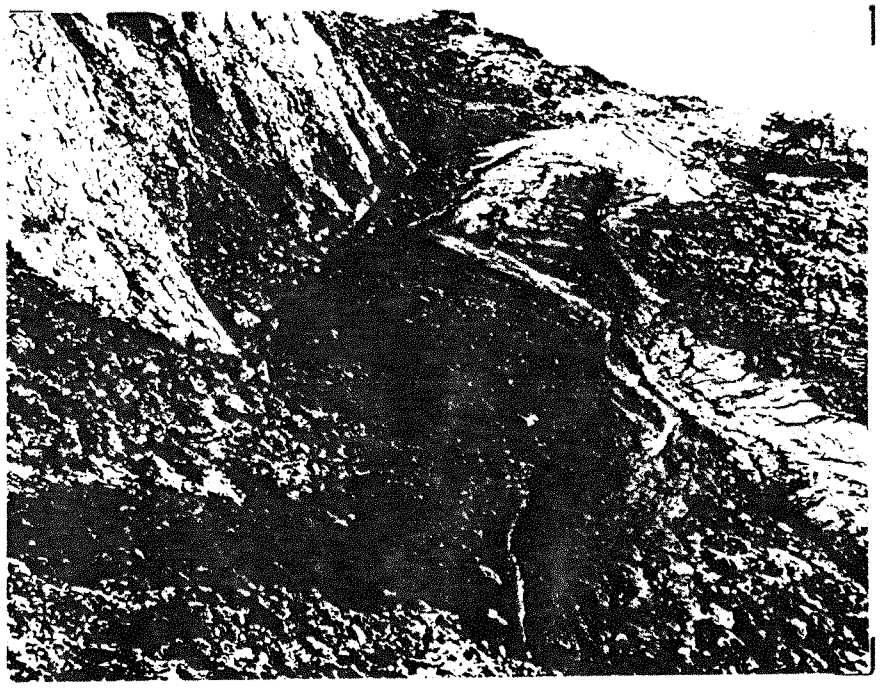

MUDSLIDE

(Mudslide B,November 1980)

FIG.2-11

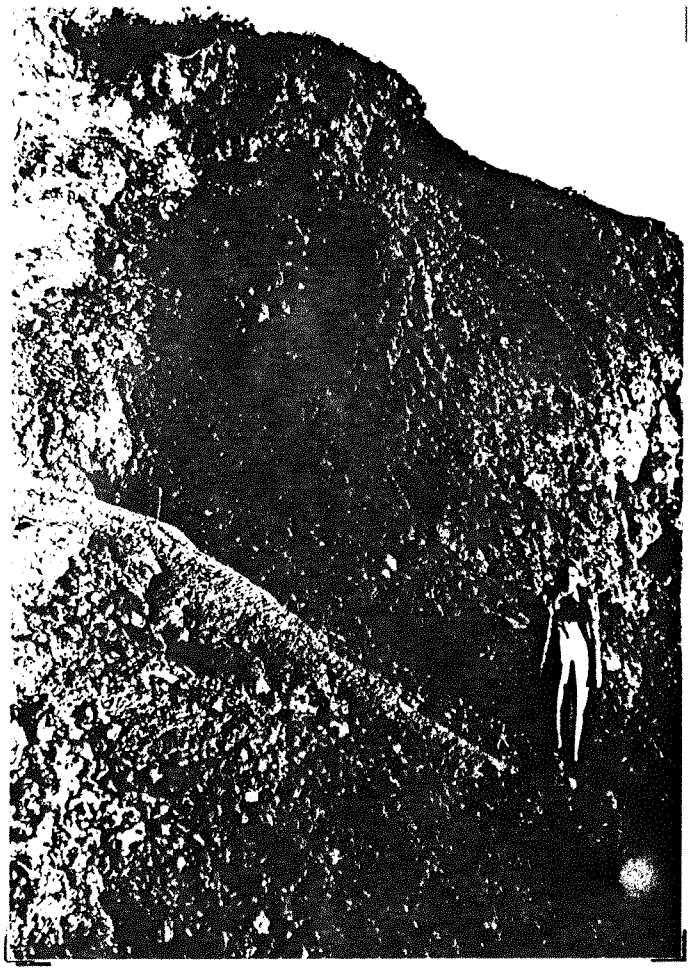

MUDRUN

(The mudrun overlies Mudslide B)

FIG.2-11a

DEBRIS SLIDE SNOUT

FIG2-12b

DEBRIS SLIDE

(Debris slide lying on D bench)

FIG.2-12

CLIFF TOP SLUMP

(Author standing on cliff top slump located on F Bench)

FIG.2-13

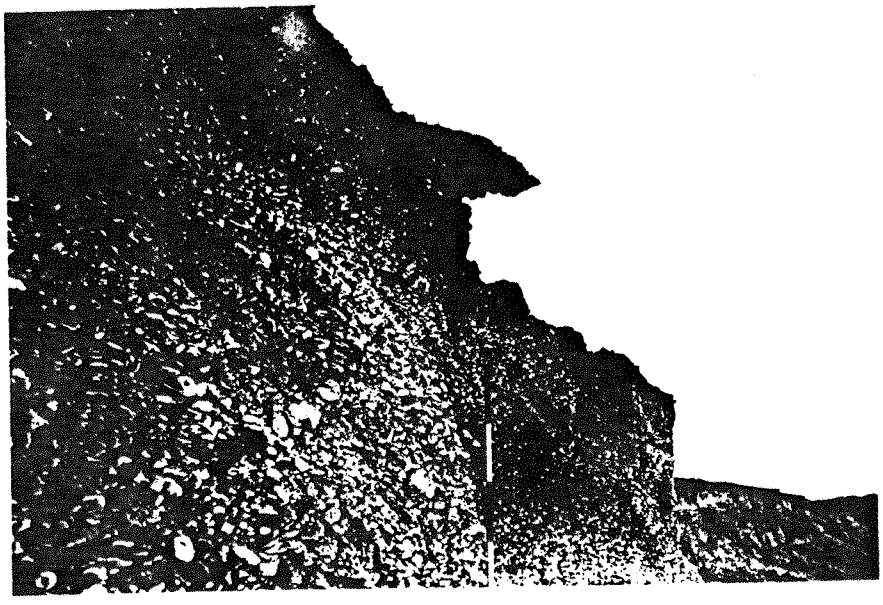

SPALLING–PLATEAU GRAVEL FACE

(Cliff top scarp,ranging rod marked in feet)

FIG.2–14

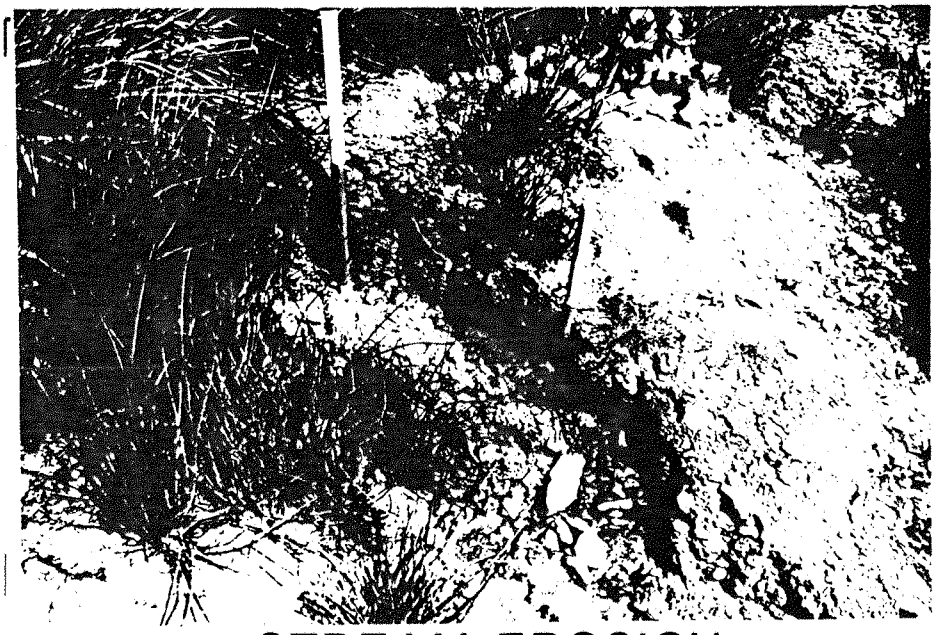

STREAM EROSION

(Stream on D bench,ranging rod marked in feet)

FIG.2–15

NOTCH IN D SCARP CUT BY MUDSLIDE B

(Mudslide debris sliding from D bench to A3 bench)

FIG. 2-16

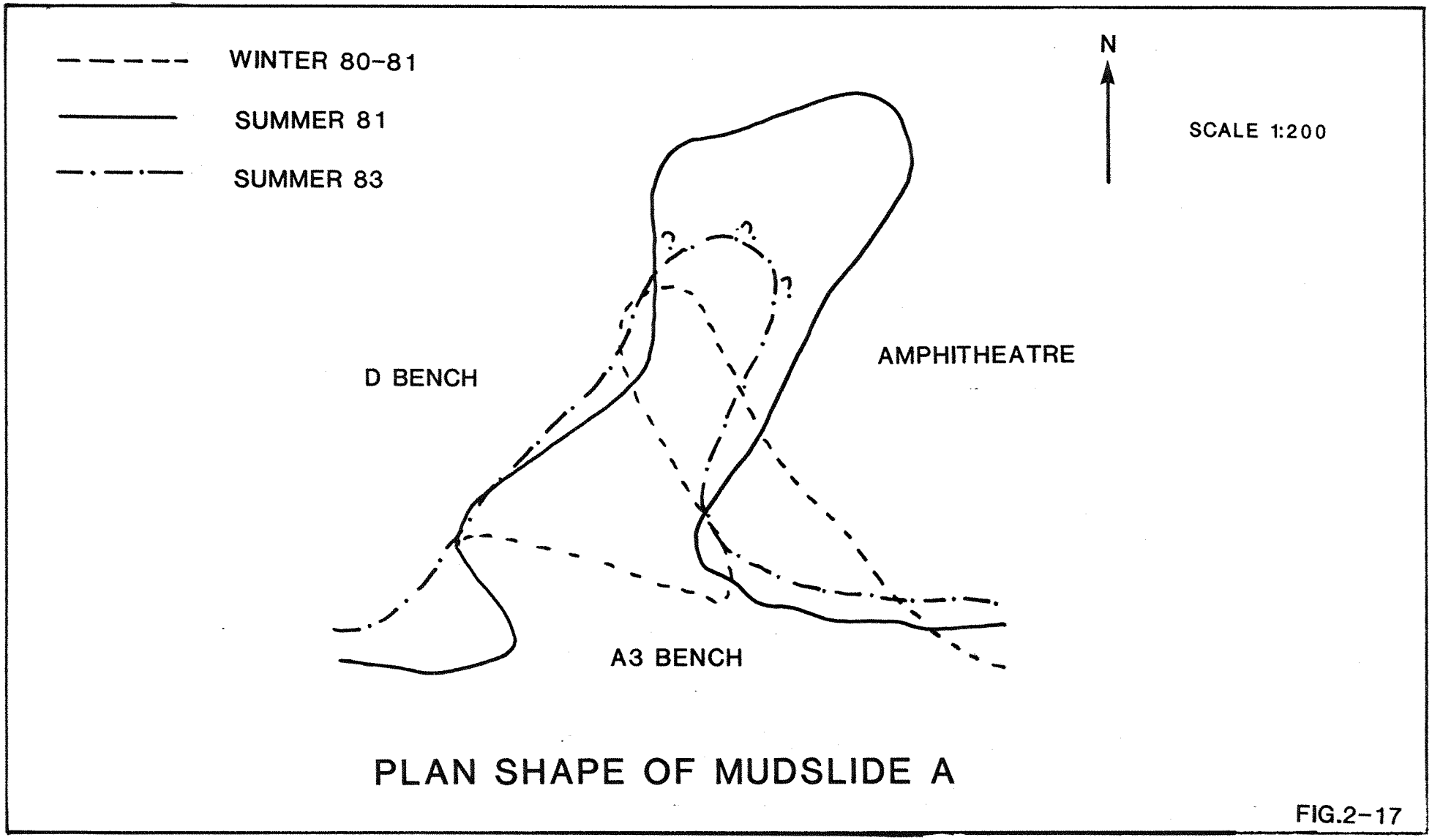

PLAN SHAPE OF MUDSLIDE A

FIG.2-17

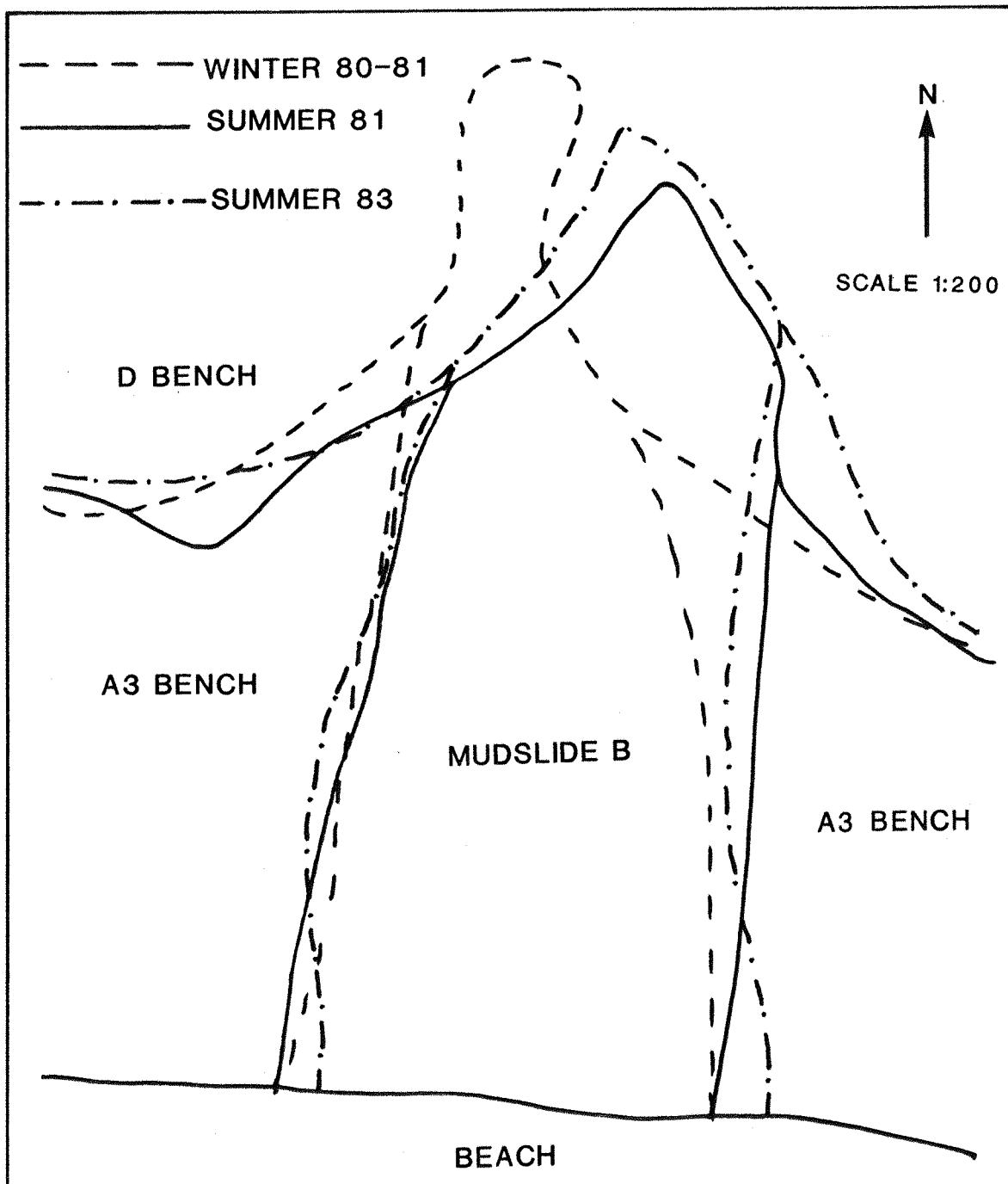

PLAN SHAPE OF MUDSLIDE B

FIG.2-18

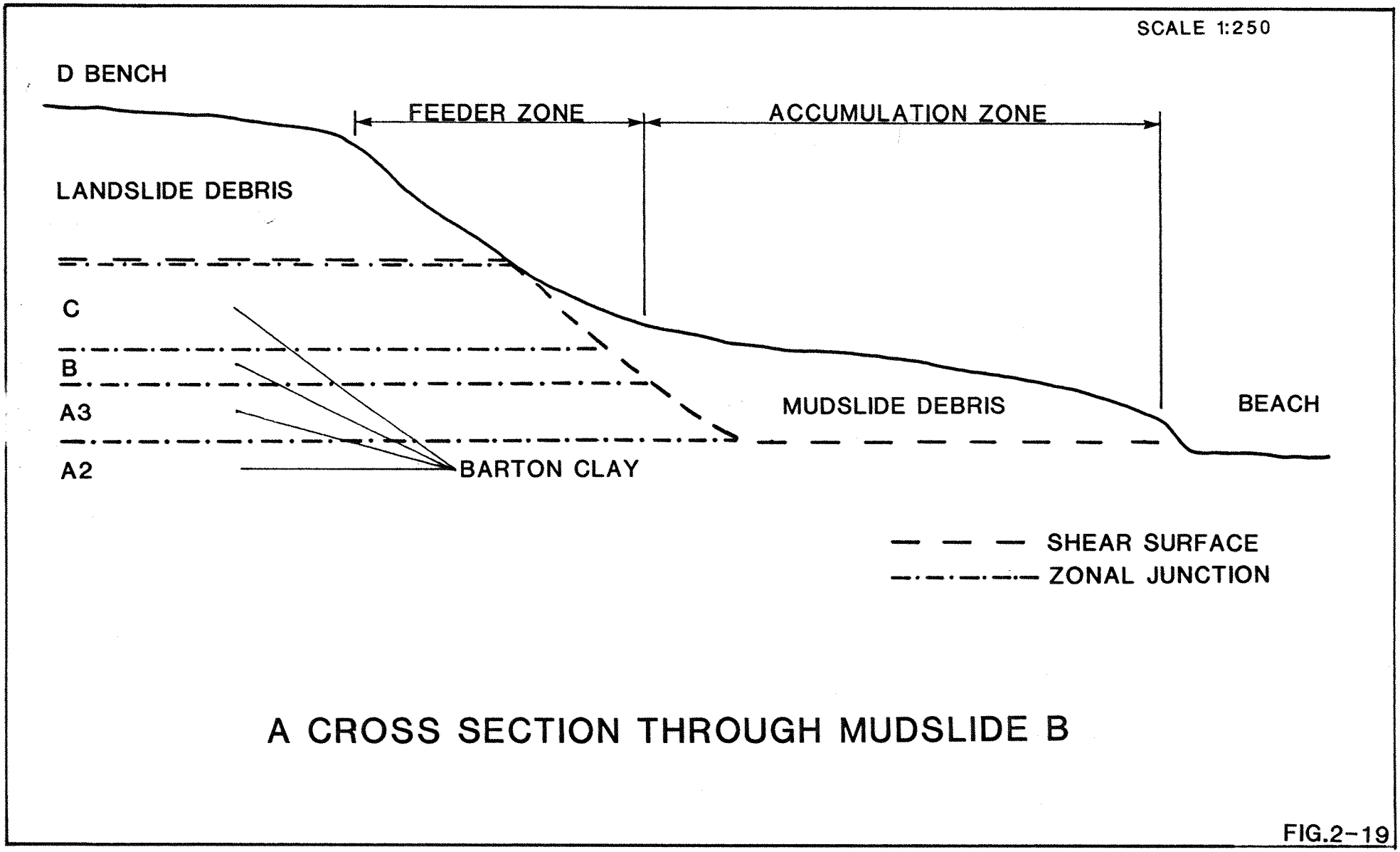

A CROSS SECTION THROUGH MUDSLIDE B

FIG.2-19

EXPOSED SHALLOW BASAL SHEAR SURFACE ON DEBRIS SLIDE 3

(Debris slide 3 lying on F Scarp,ranging rod marked in feet)

FIG.2-20

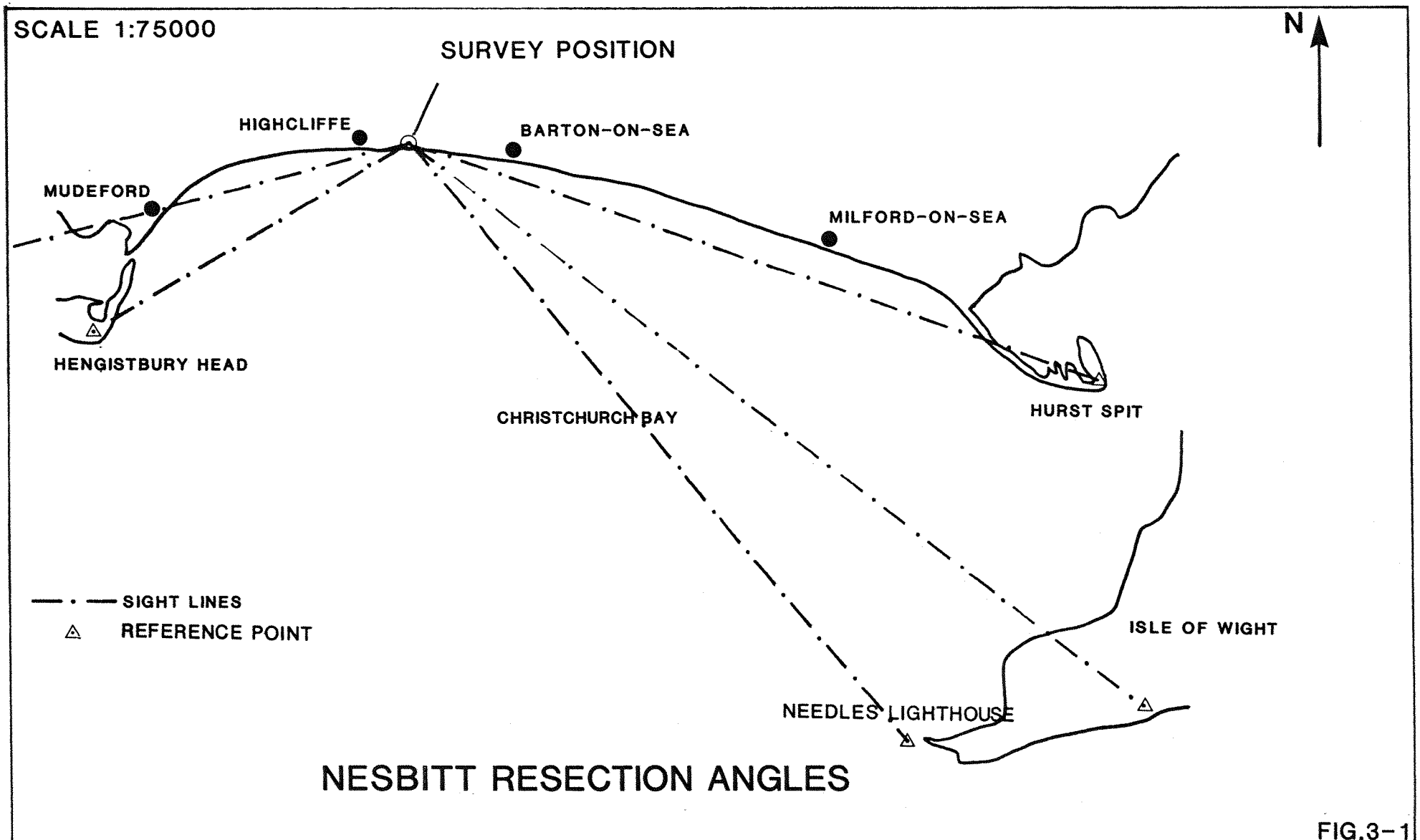

NESBITT RESECTION ANGLES

FIG.3-1

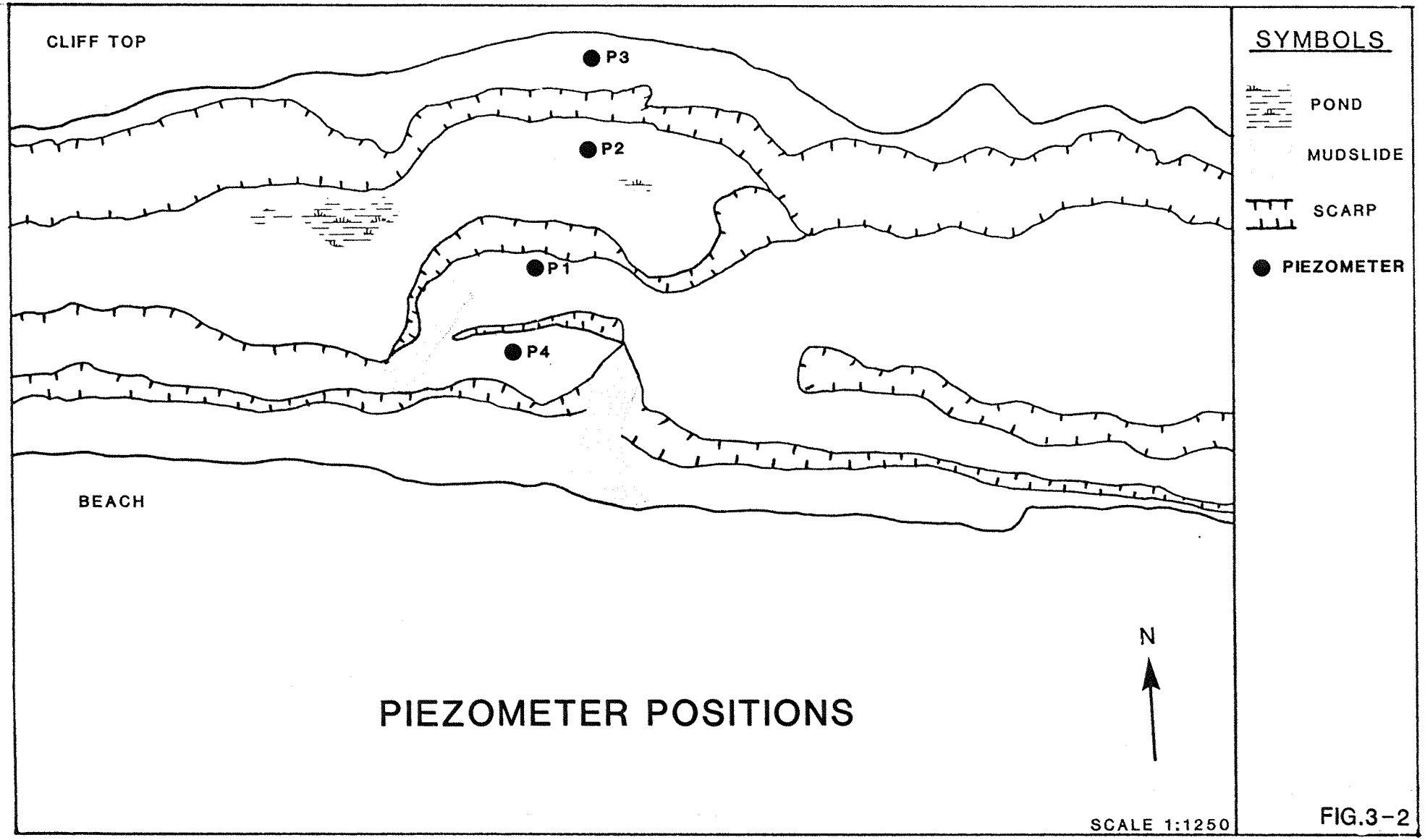
CLIFF TOP
P3
P2
P1
P4
BEACH
SYMBOLS
POND
MUDSLIDE
SCARP
PIEZOMETER
N
PIEZOMETER POSITIONS
SCALE 1:1250
FIG.3-2

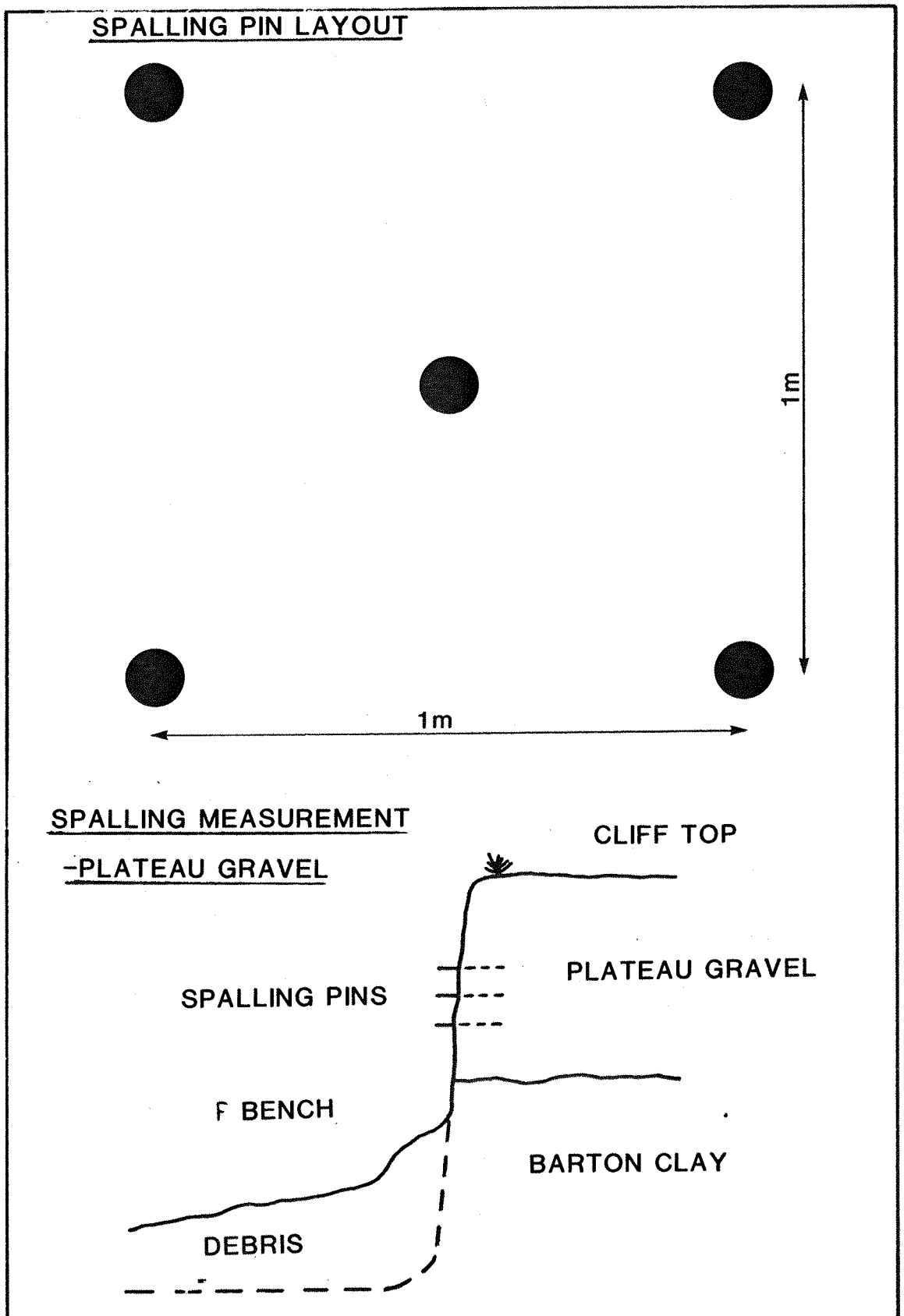

ARRANGEMENT OF SPALLING PINS

FIG.3-3

RAPID BENCH SLIDE ACTIVITY AFTER FEBRUARY 1982 CLIFF TOP SLUMP

(D bench colluvium being deposited on A3 bench, ranging rod marked in 0.5metres)

FIG.3-4

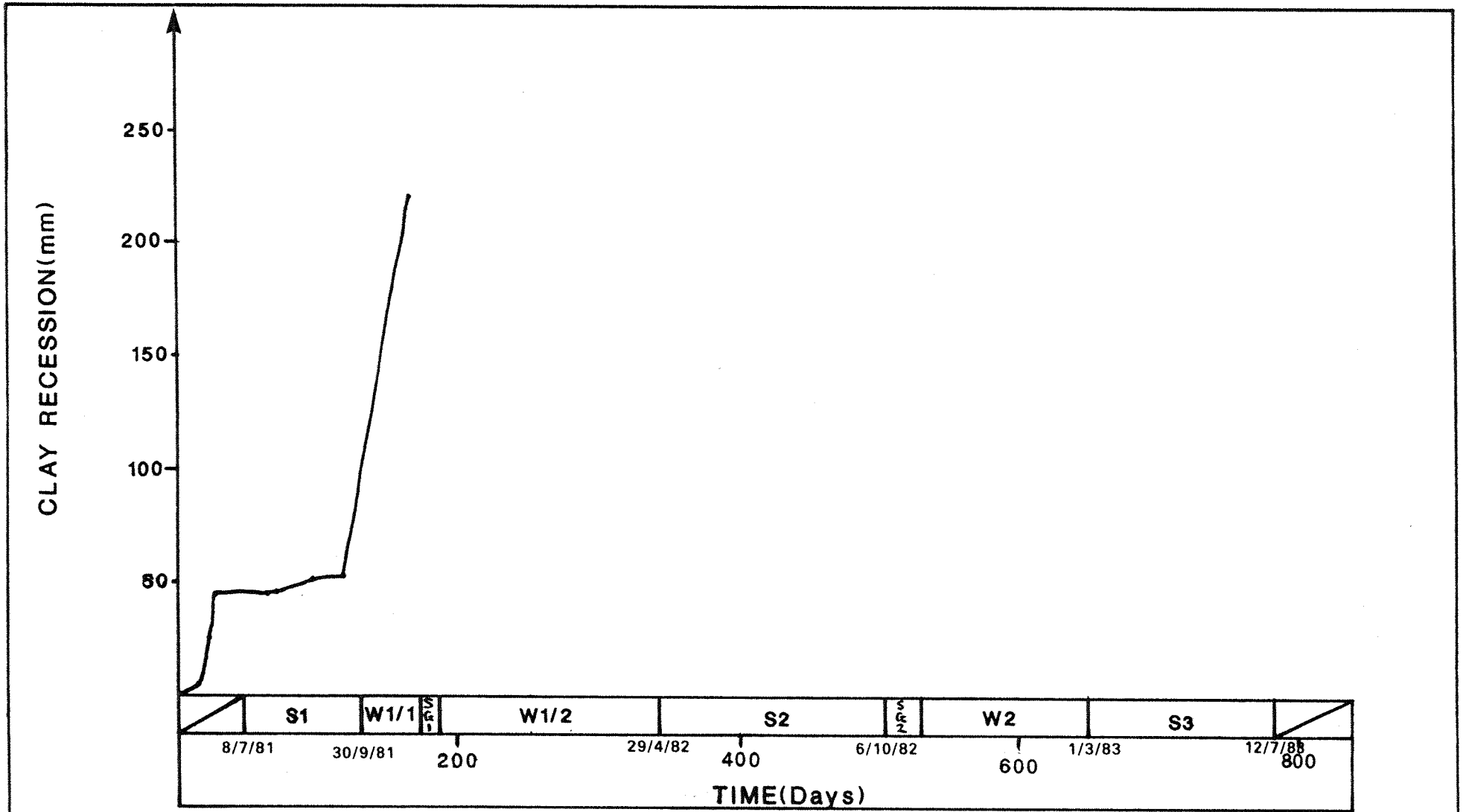

BARTON CLAY RECESSION AGAINST TIME

FIG.3-5

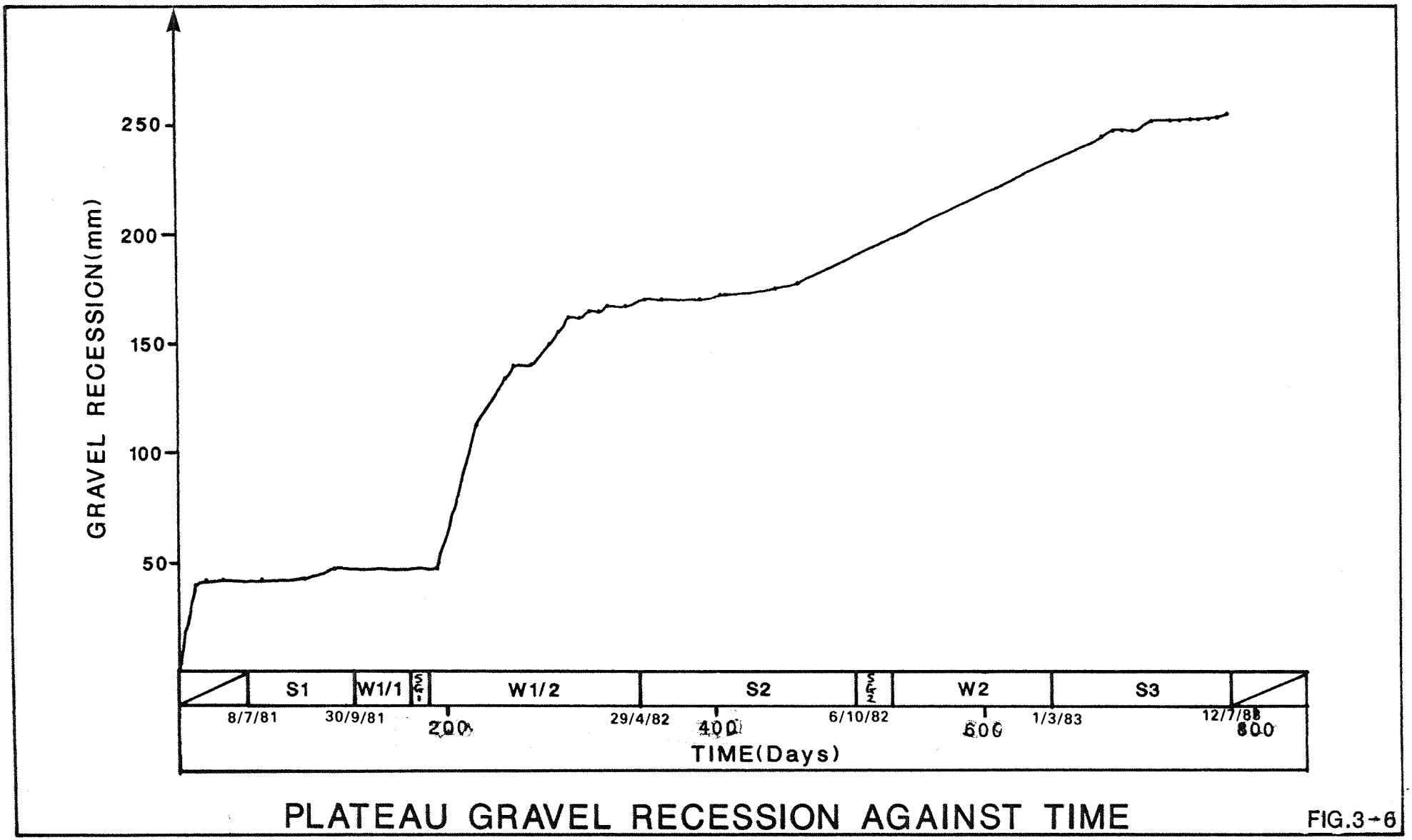

PLATEAU GRAVEL RECESSION AGAINST TIME

FIG.3-6

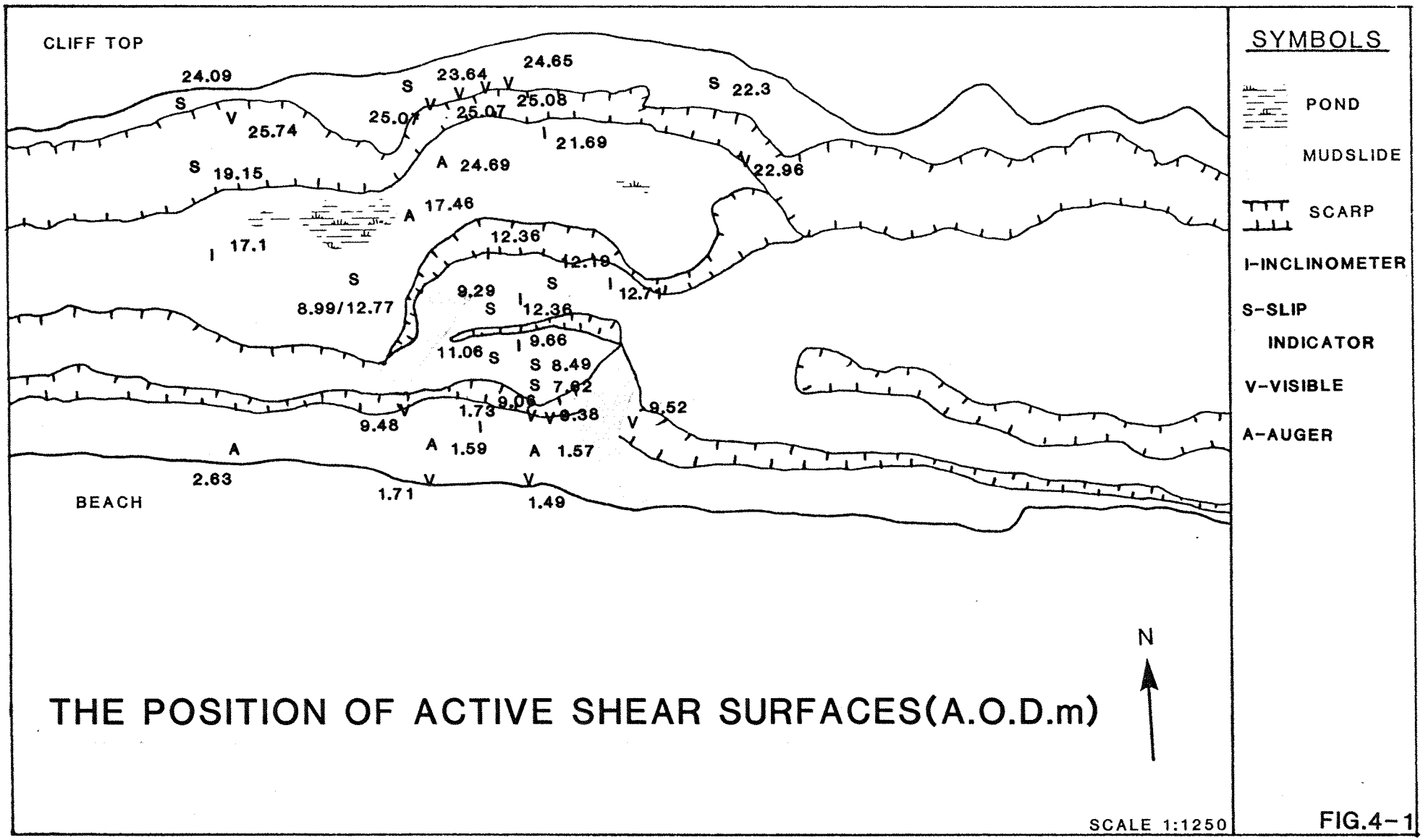
CLIFF TOP
24.09
S
V
25.74
S
19.15
I
17.1
S
8.99/12.77
A
2.63
BEACH
S
23.64
V
25.07
24.65
25.07
25.08
A
24.69
A
17.46
12.36
12.19
S
9.29
S
12.36
11.06
S
9.66
S
8.49
S
7.62
9.08
1.73
9.48
A
1.59
1.71
A
1.57
V
9.38
1.49
S
22.3
21.69
V
22.96
I
12.71
9.52
V
SYMBOLS
POND
MUDSLIDE
SCARP
I-INCLINOMETER
S-SLIP
INDICATOR
V-VISIBLE
A-AUGER
N
THE POSITION OF ACTIVE SHEAR SURFACES(A.O.D.m)
SCALE 1:1250
FIG.4-1

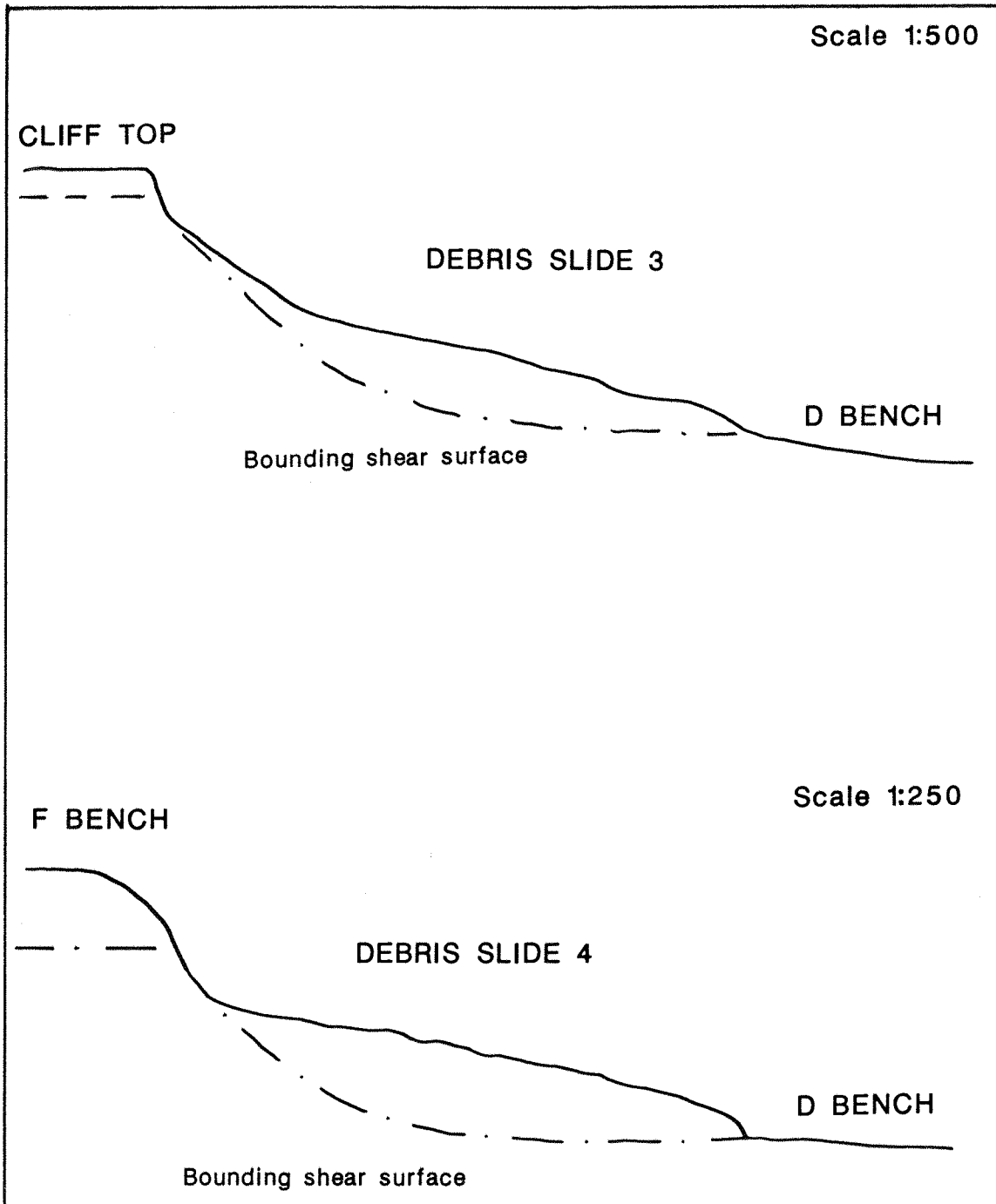

SECTIONS OF DEBRIS SLIDES 3 & 4

FIG 4-2

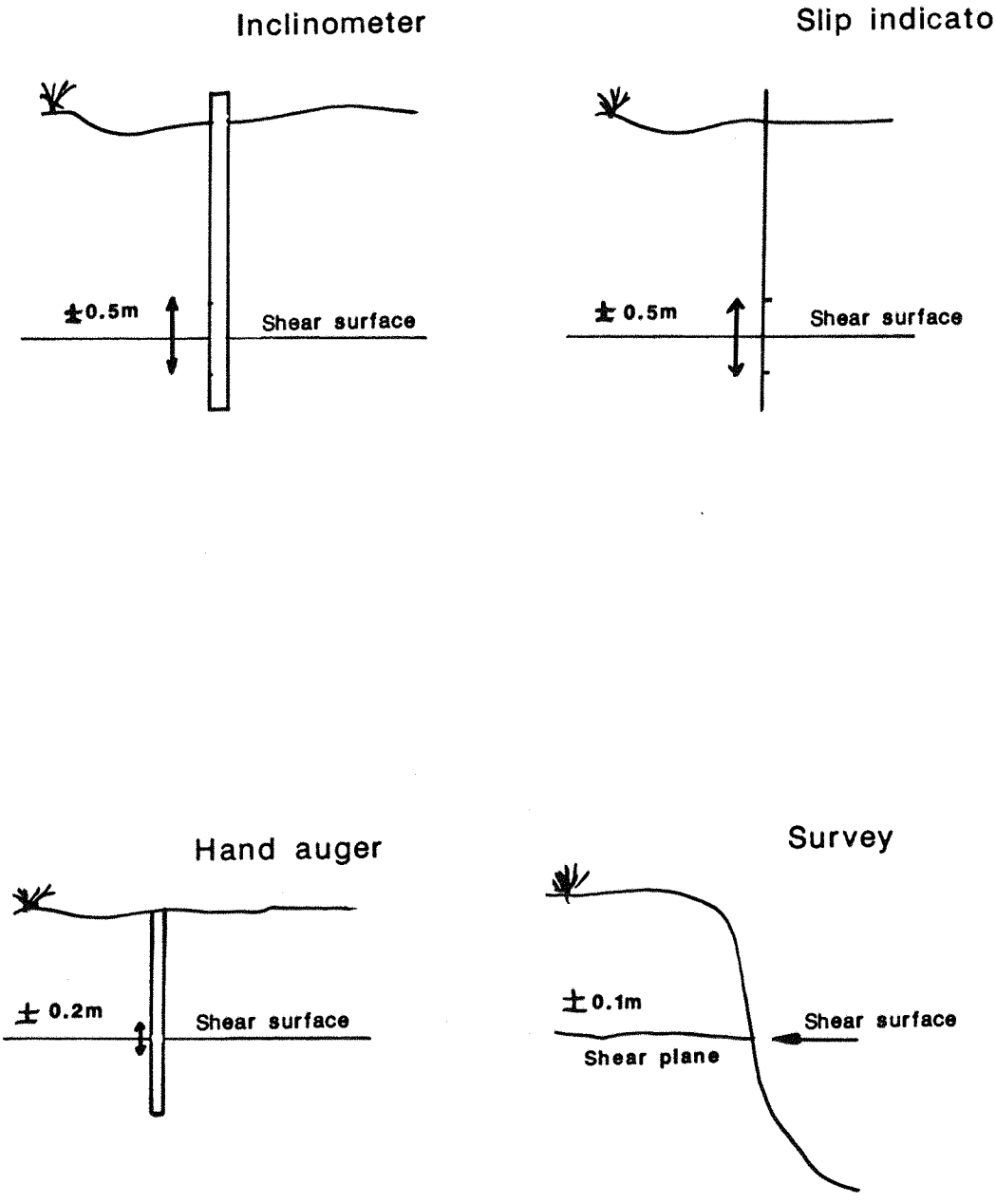

ACCURACY OF VARIOUS METHODS OF SHEAR SURFACE DETECTION

FIG 4-3

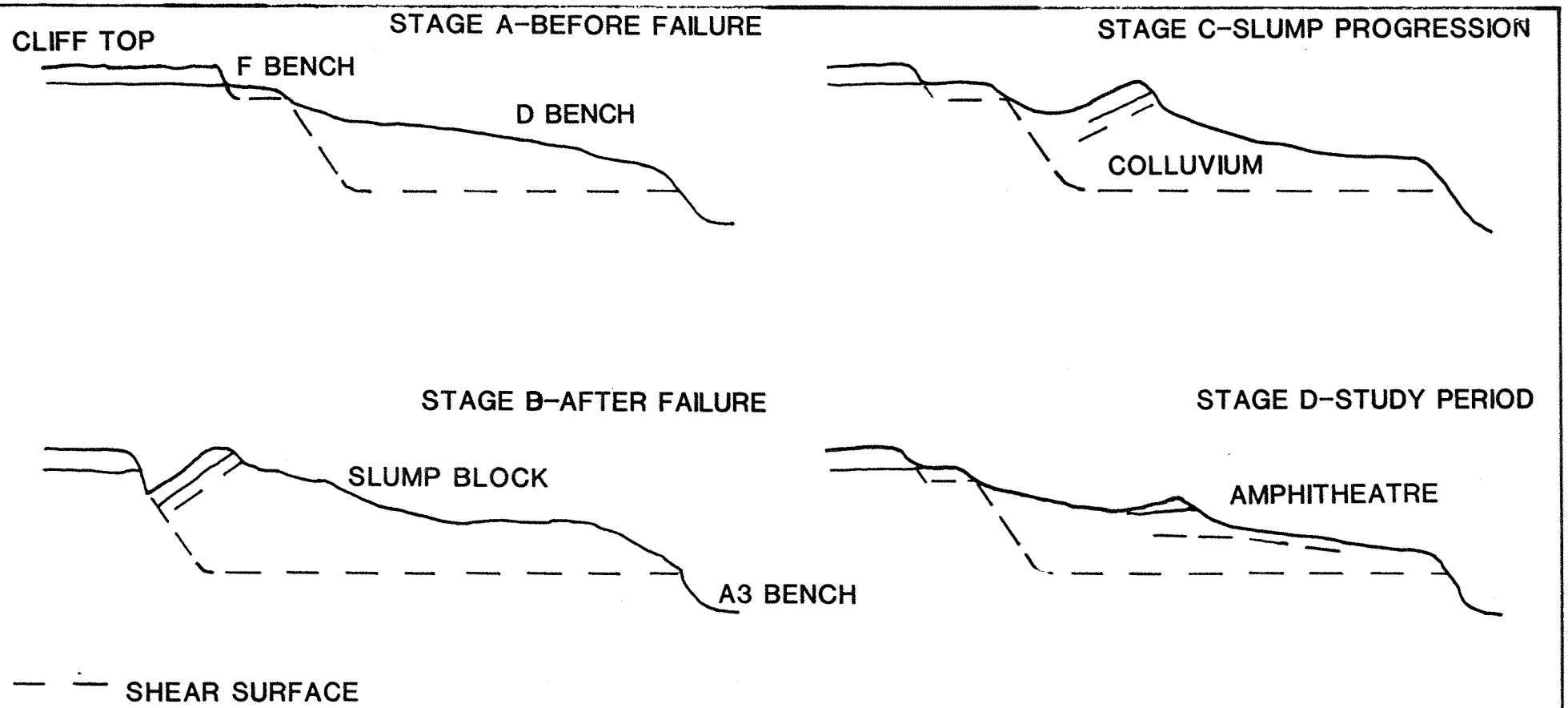

EVOLUTION OF THE AMPHITHEATRE AND THE ELEVATED SHEAR SURFACE(12.5m A.O.D)

FIG.5-1

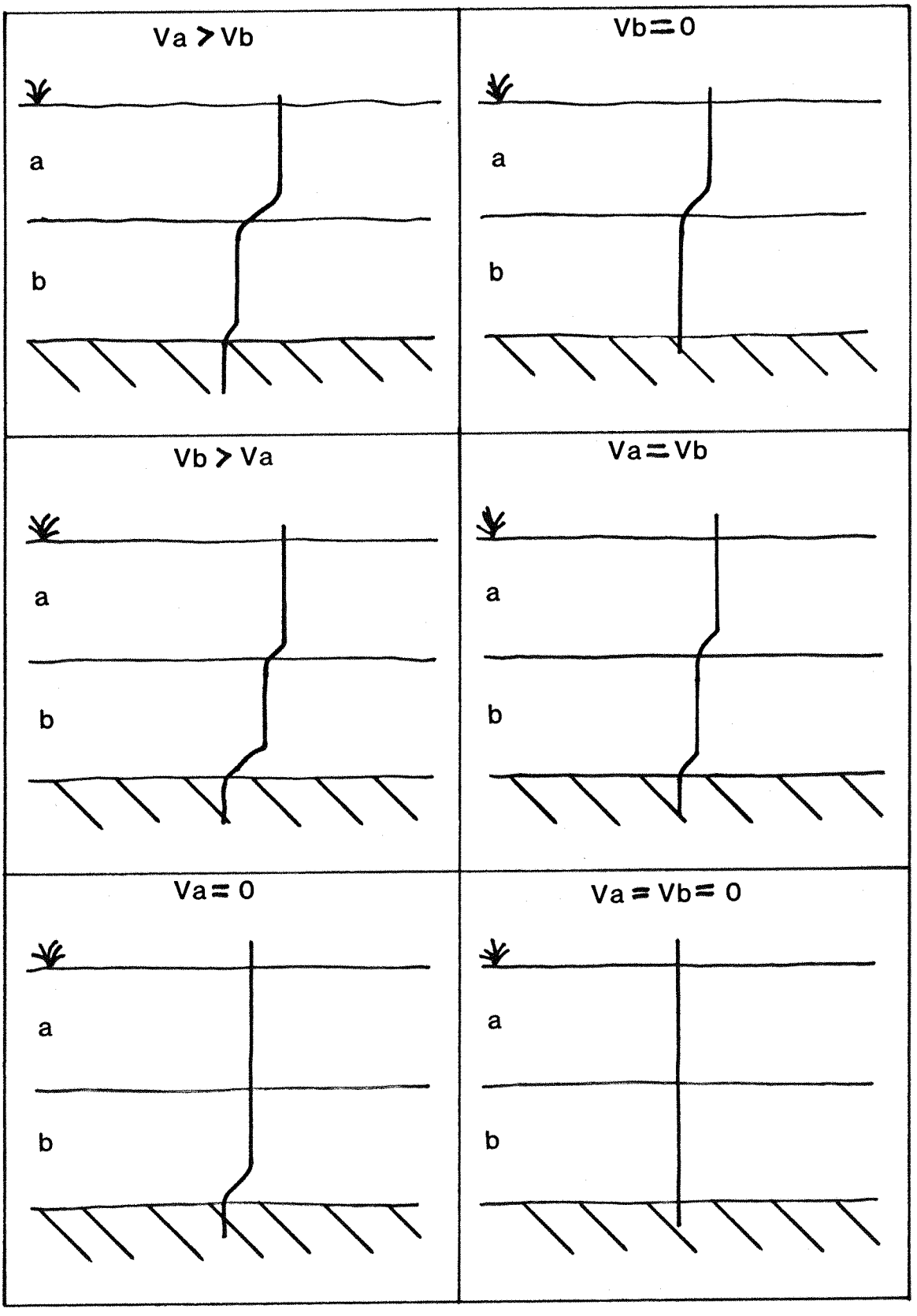

INCLINOMETER PERFORMANCE IN A MULTI-LAYERED LANDSLIDE

FIG.5-2

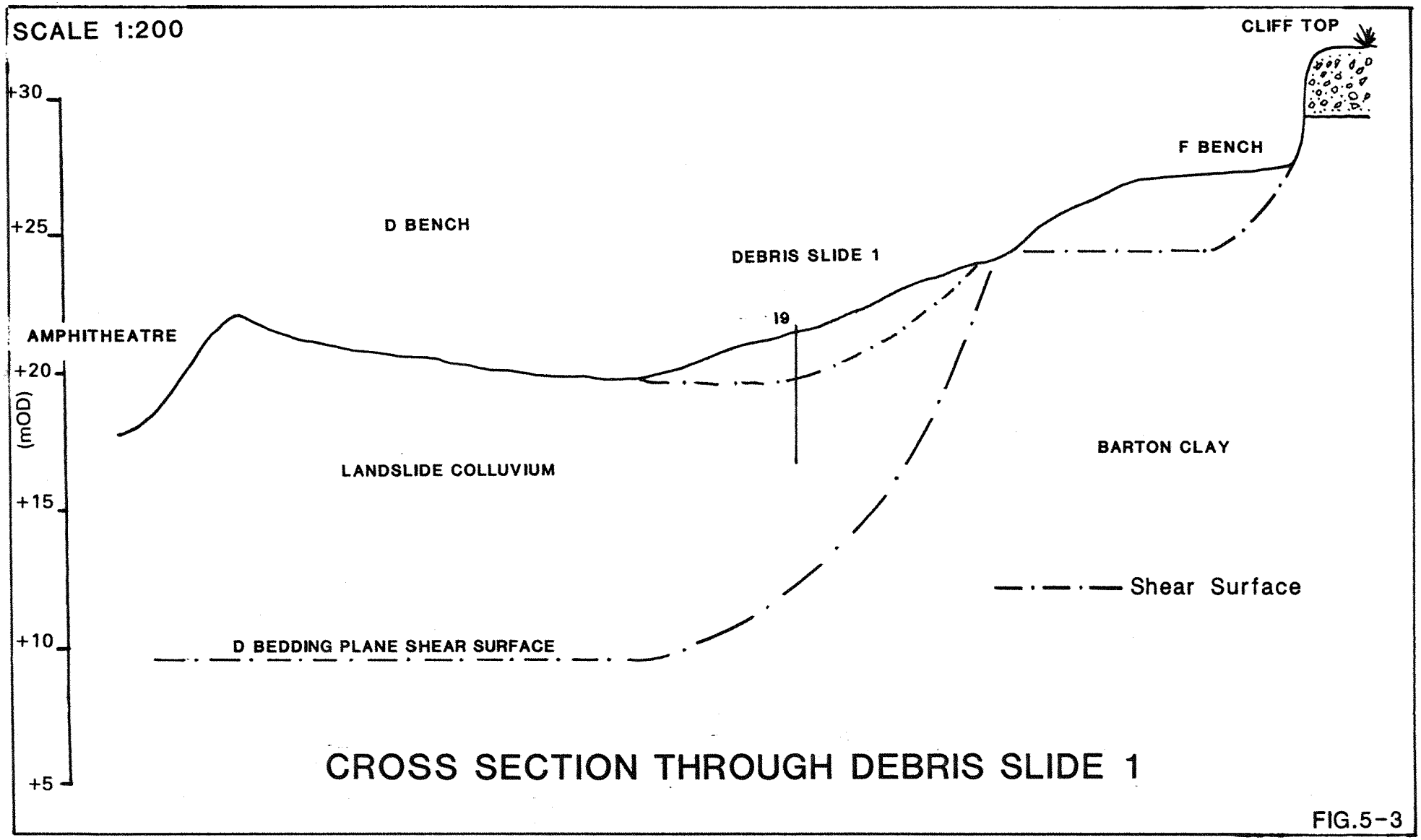

CROSS SECTION THROUGH DEBRIS SLIDE 1

FIG.5-3

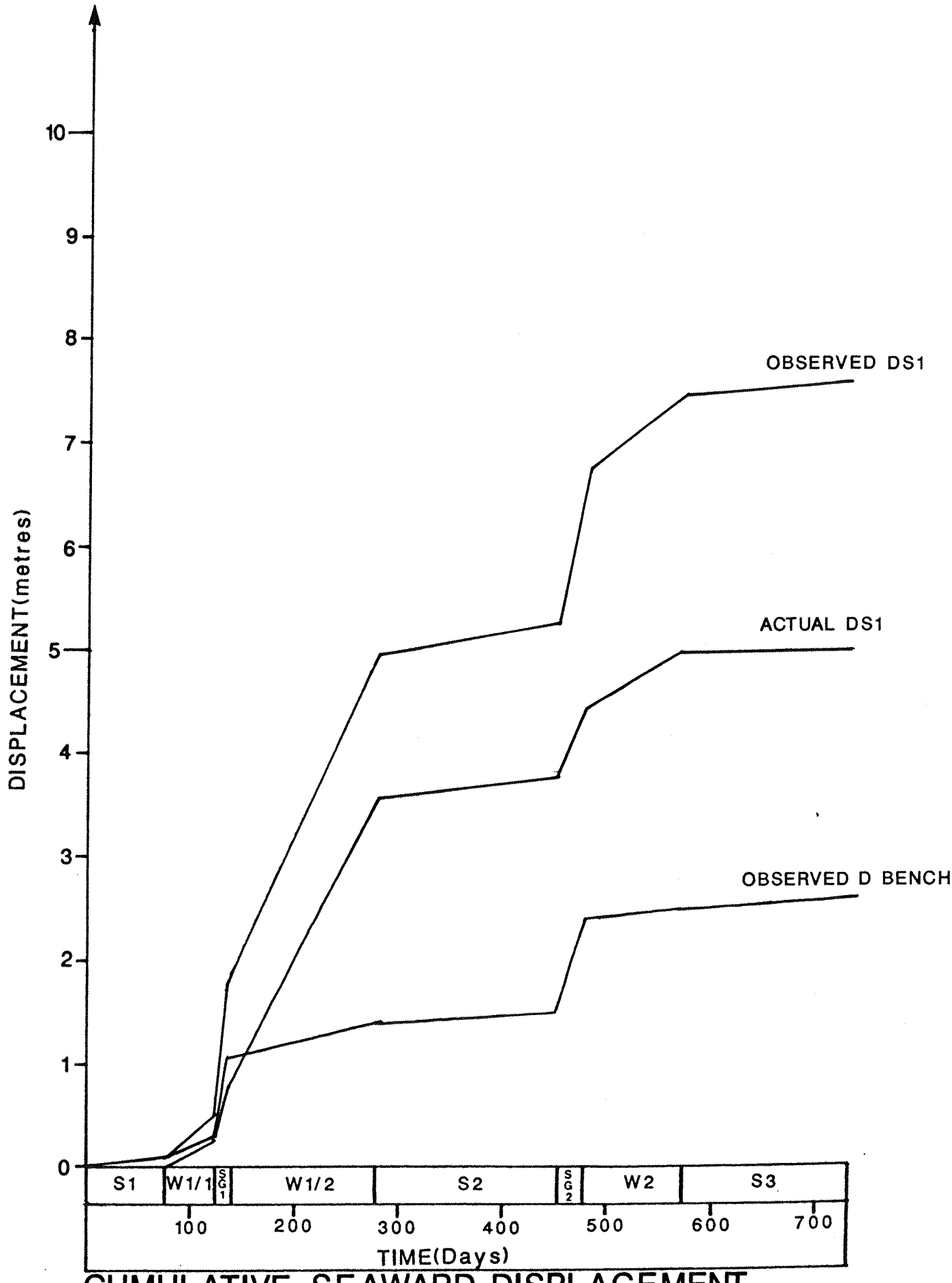

CUMULATIVE SEAWARD DISPLACEMENT COMPONENTS OF DS1 AND THE D BENCH

FIG.5-4

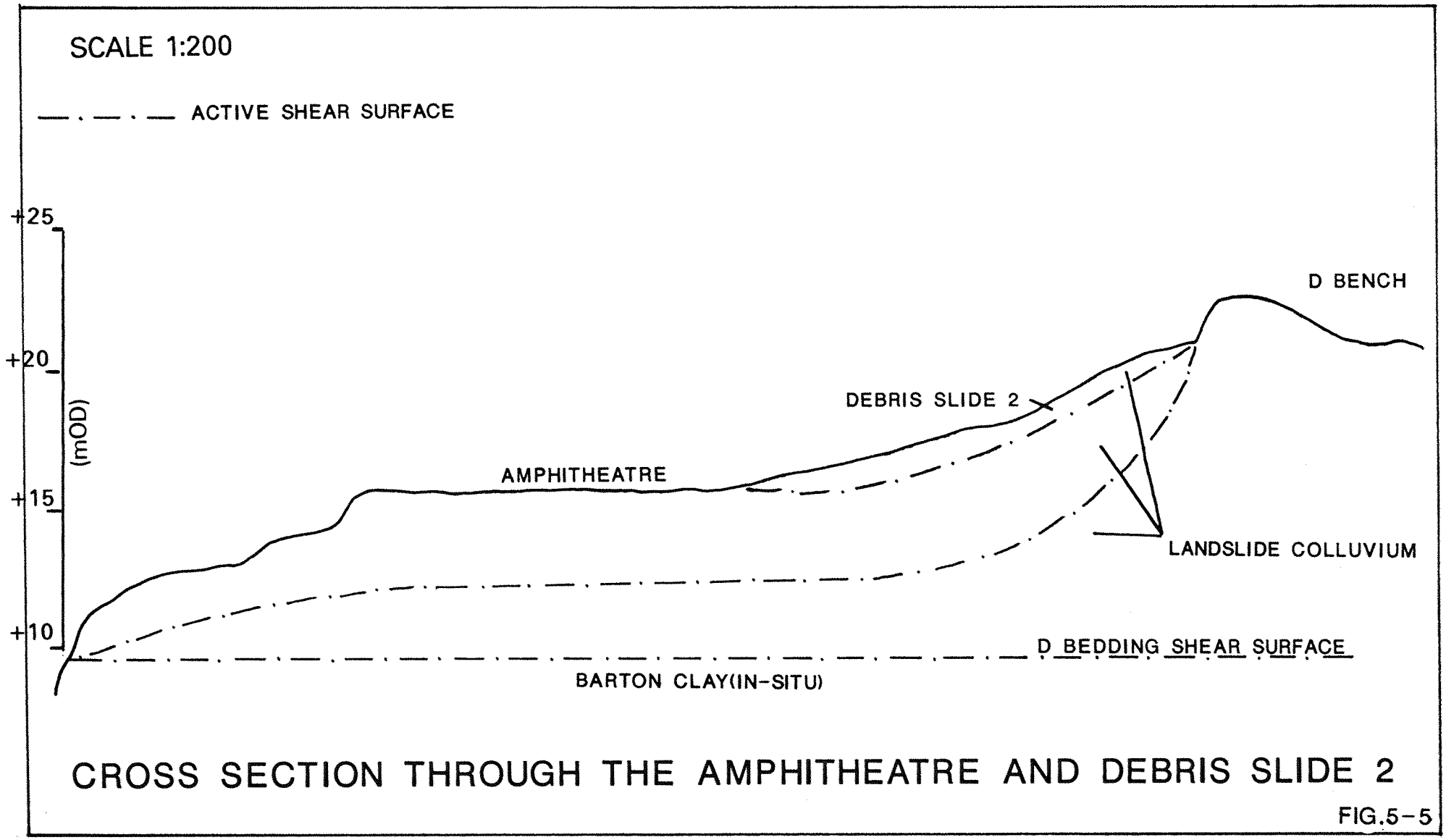

CROSS SECTION THROUGH THE AMPHITHEATRE AND DEBRIS SLIDE 2

FIG.5-5

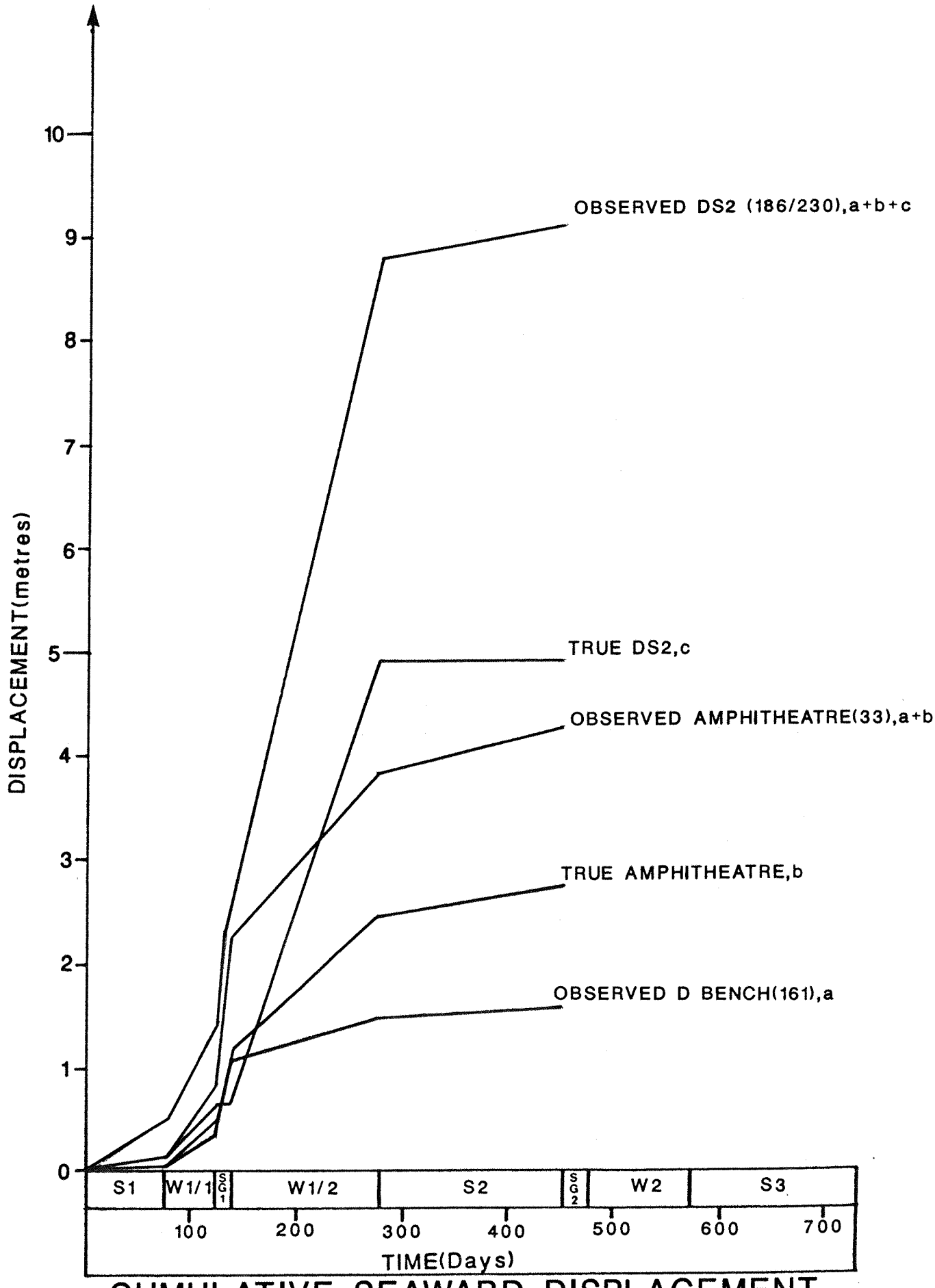

CUMULATIVE SEAWARD DISPLACEMENT COMPONENT OF THE AMPHITHEATRE AND DEBRIS SLIDE 2

FIG.5-6

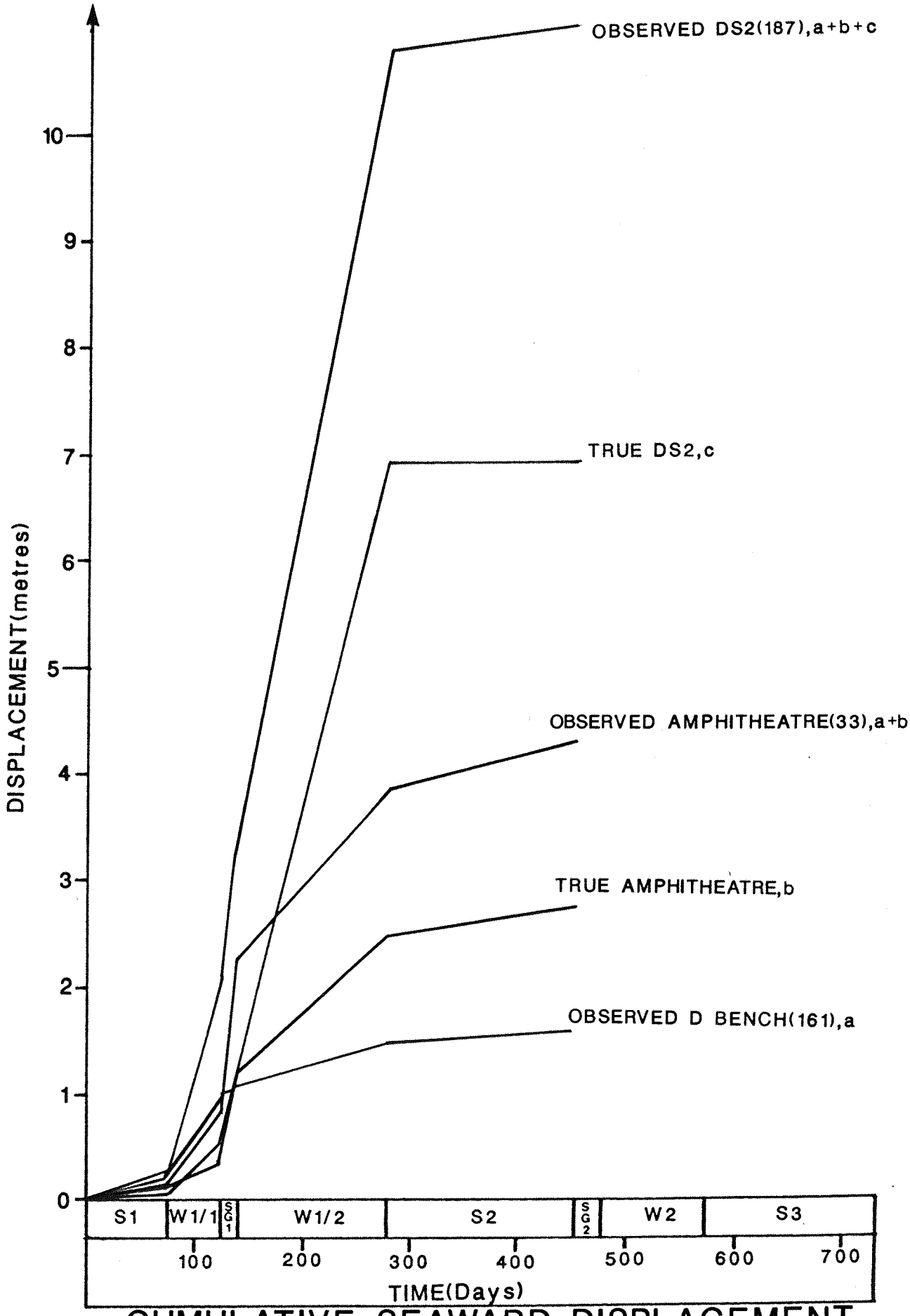

CUMULATIVE SEAWARD DISPLACEMENT COMPONENT OF THE AMPHITHEATRE AND DEBRIS SLIDE 2

FIG5-6a

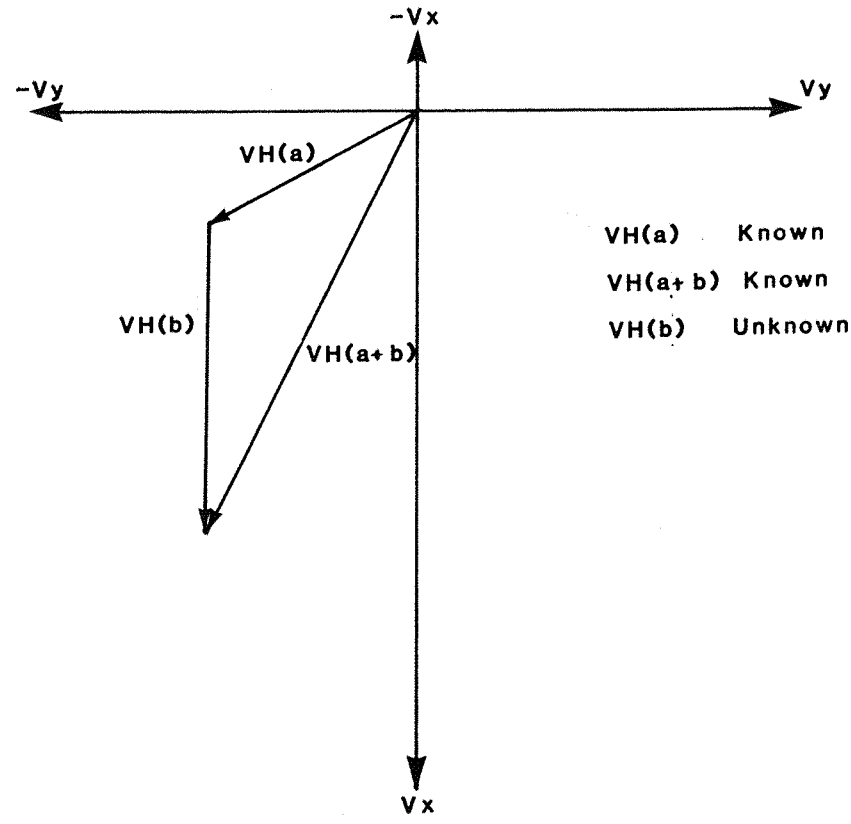

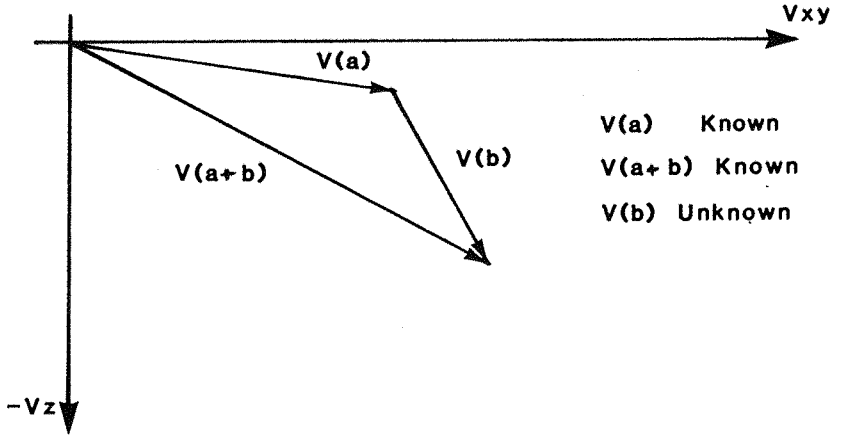

VECTOR CONSTRUCTION

(After Ter-stepanian and Goldstein, 1969)

FIG.5-7

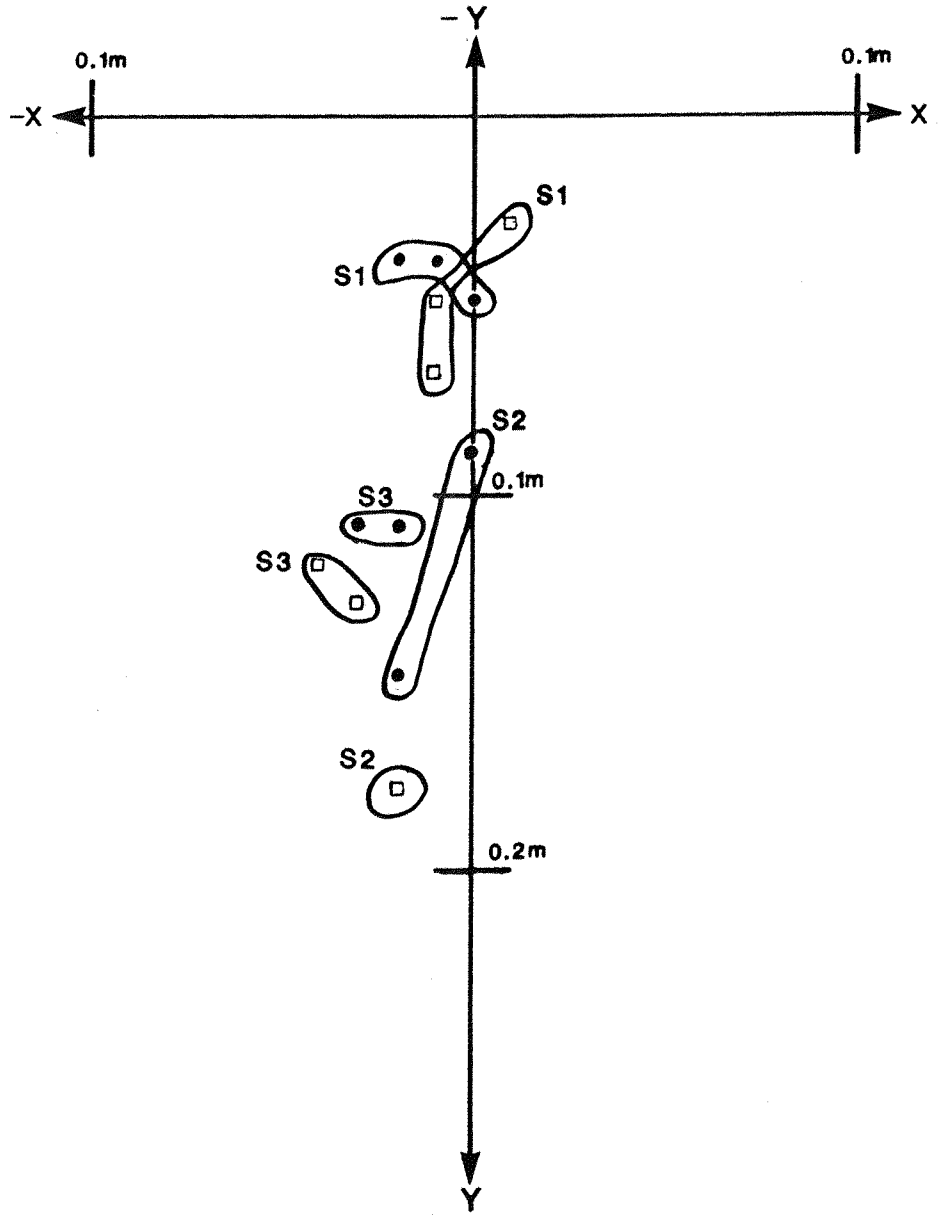

● D BENCH

□ DEBRIS SLIDE 1

HORIZONTAL DISPLACEMENTS(XY) DURING THE SUMMER PERIODS

FIG.5-8

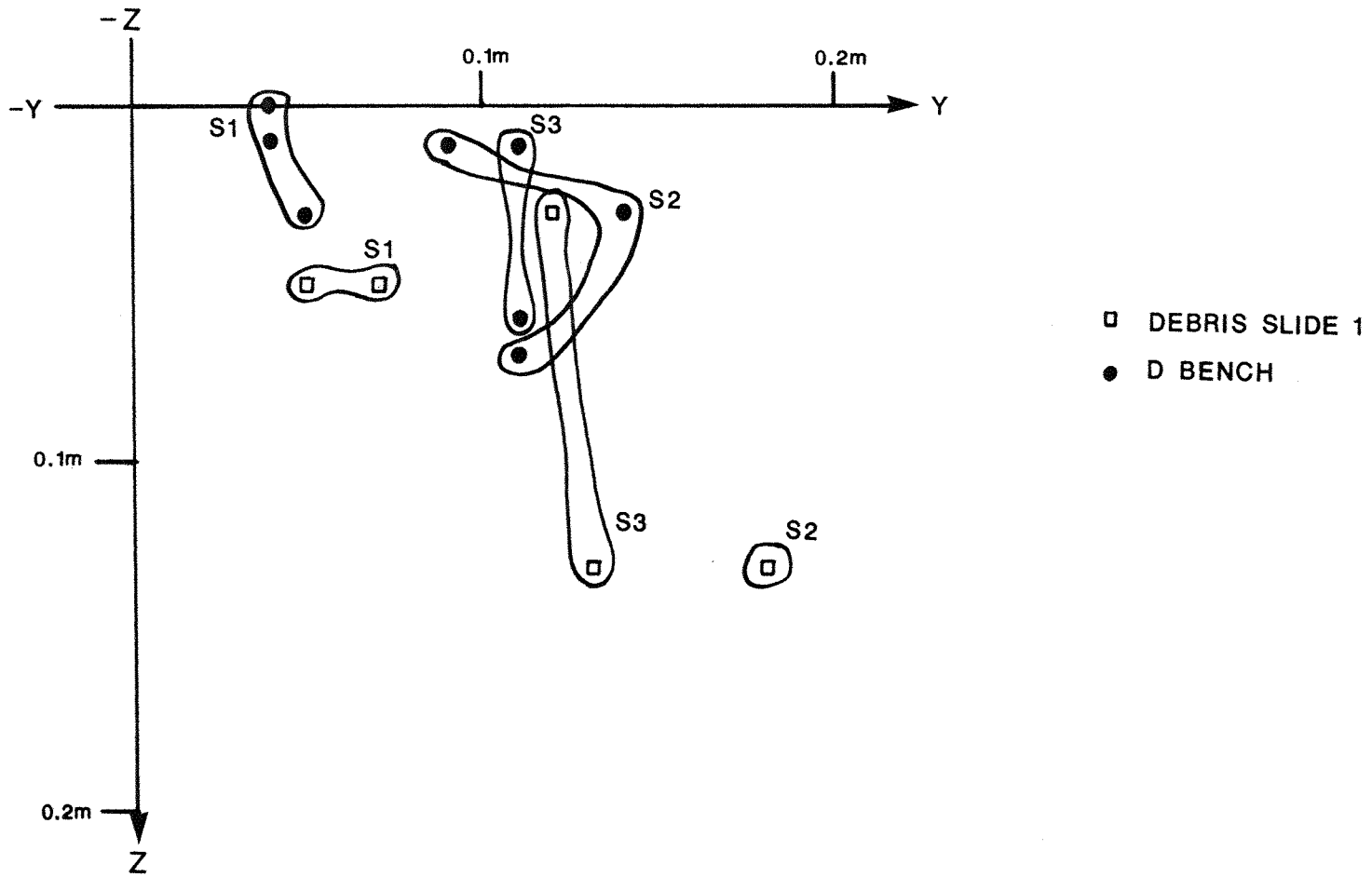

VERTICAL DISPLACEMENTS(YZ) DURING THE SUMMER PERIODS FIG.5-9

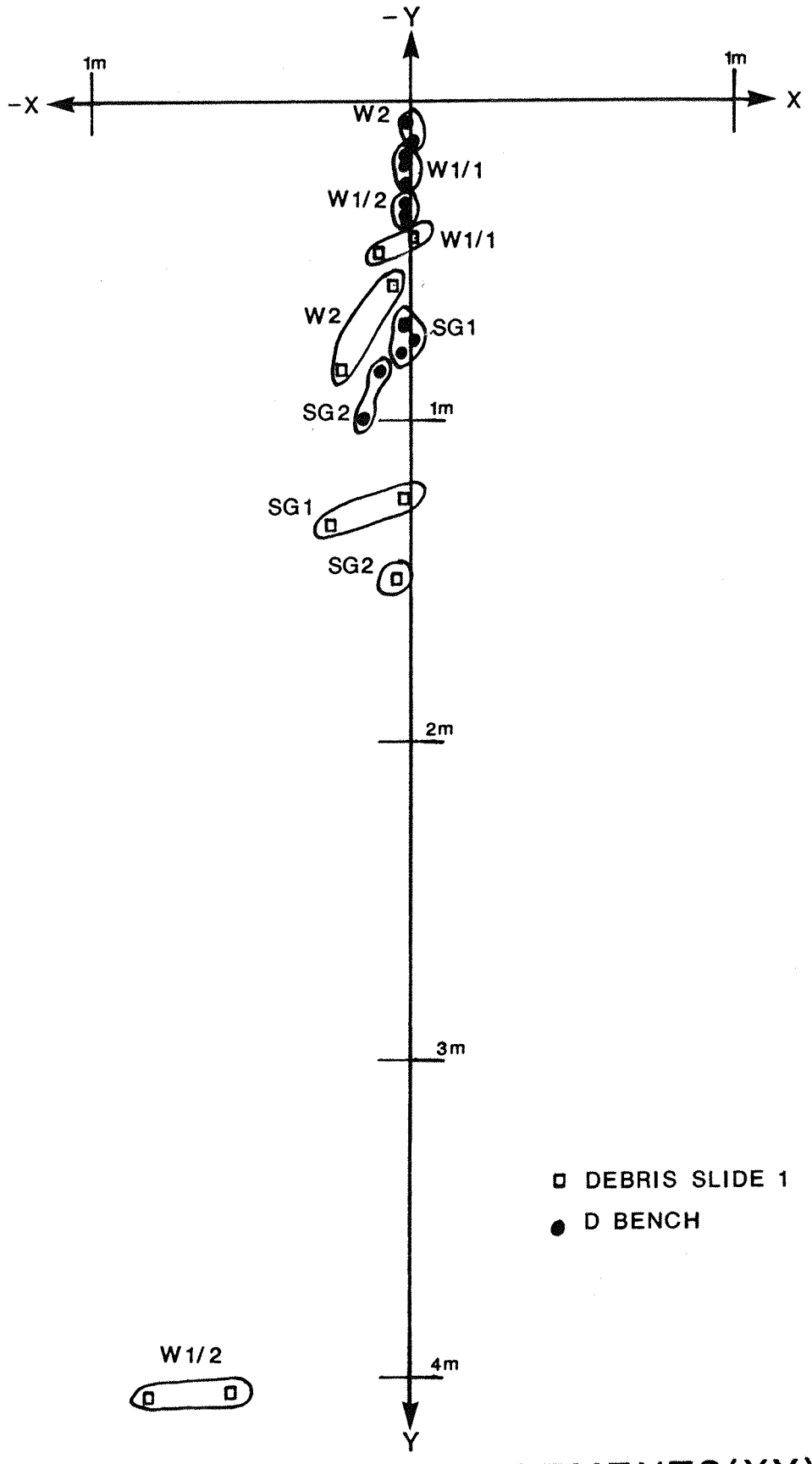

HORIZONTAL DISPLACEMENTS(XY)
DURING THE WINTER AND SURGE PERIODS

FIG.5-10

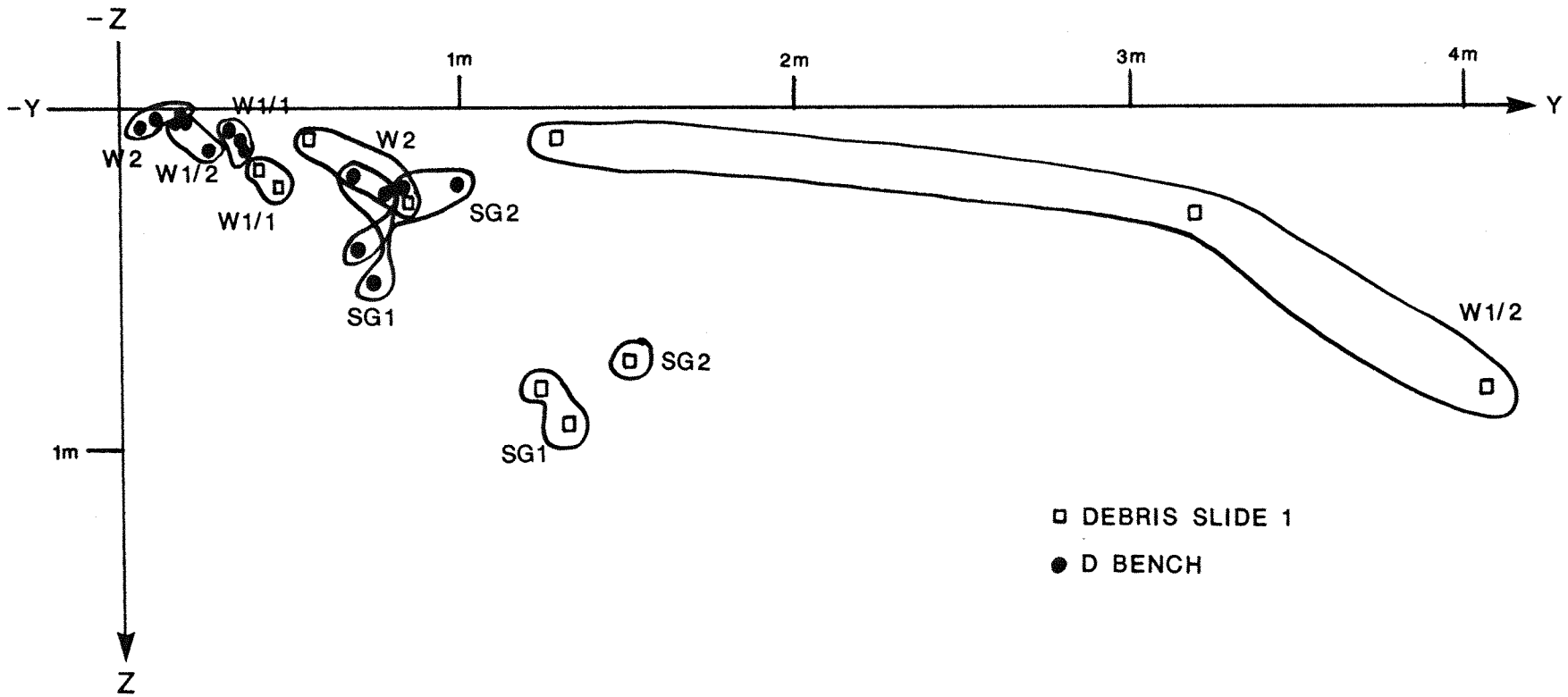

VERTICAL DISPLACEMENTS(YZ) DURING THE WINTER AND SURGE PERIODS

FIG.5-11

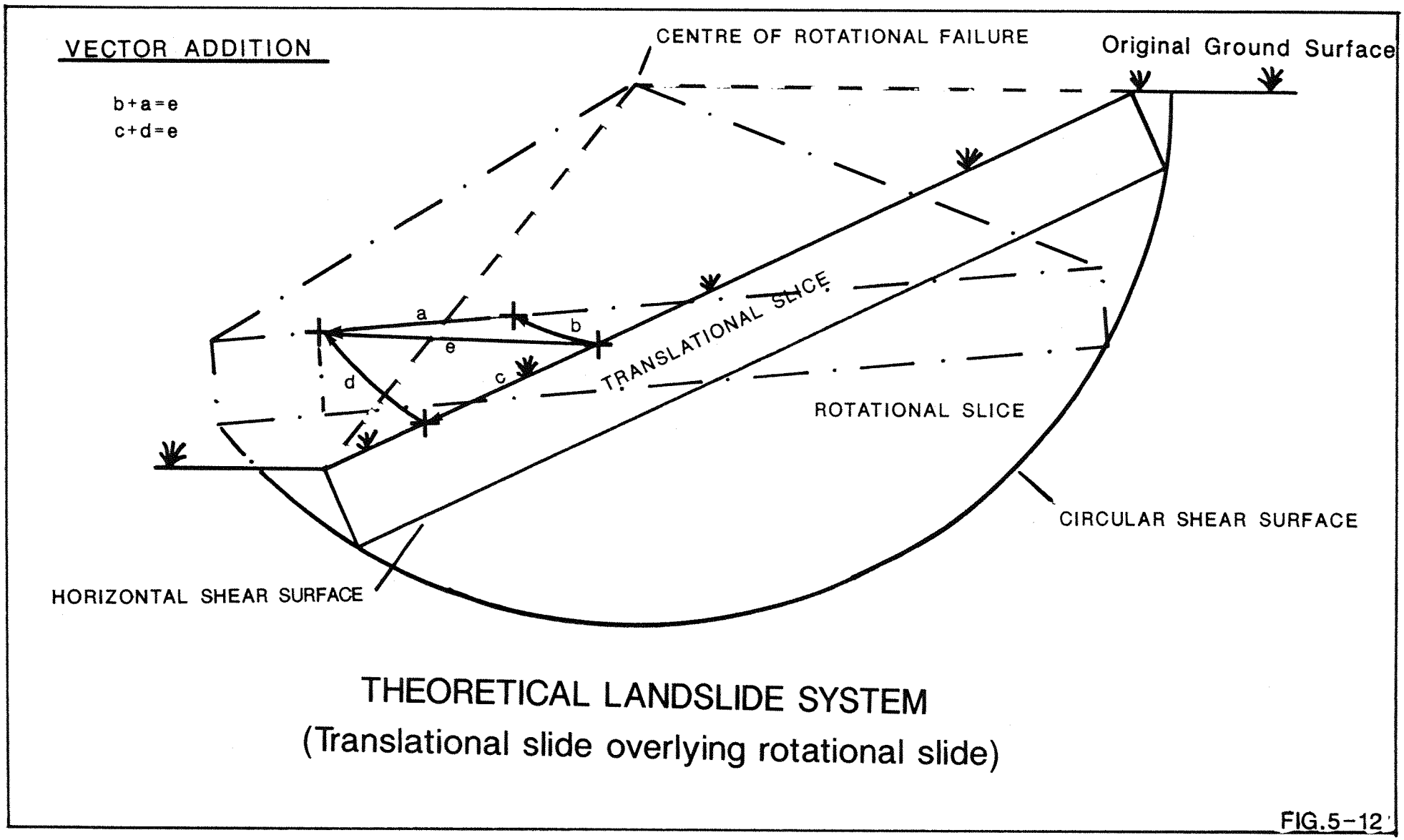

THEORETICAL LANDSLIDE SYSTEM

(Translational slide overlying rotational slide)

FIG.5-12

Symbols used in Section 5.3.2
(Also refer to Fig.5-12)

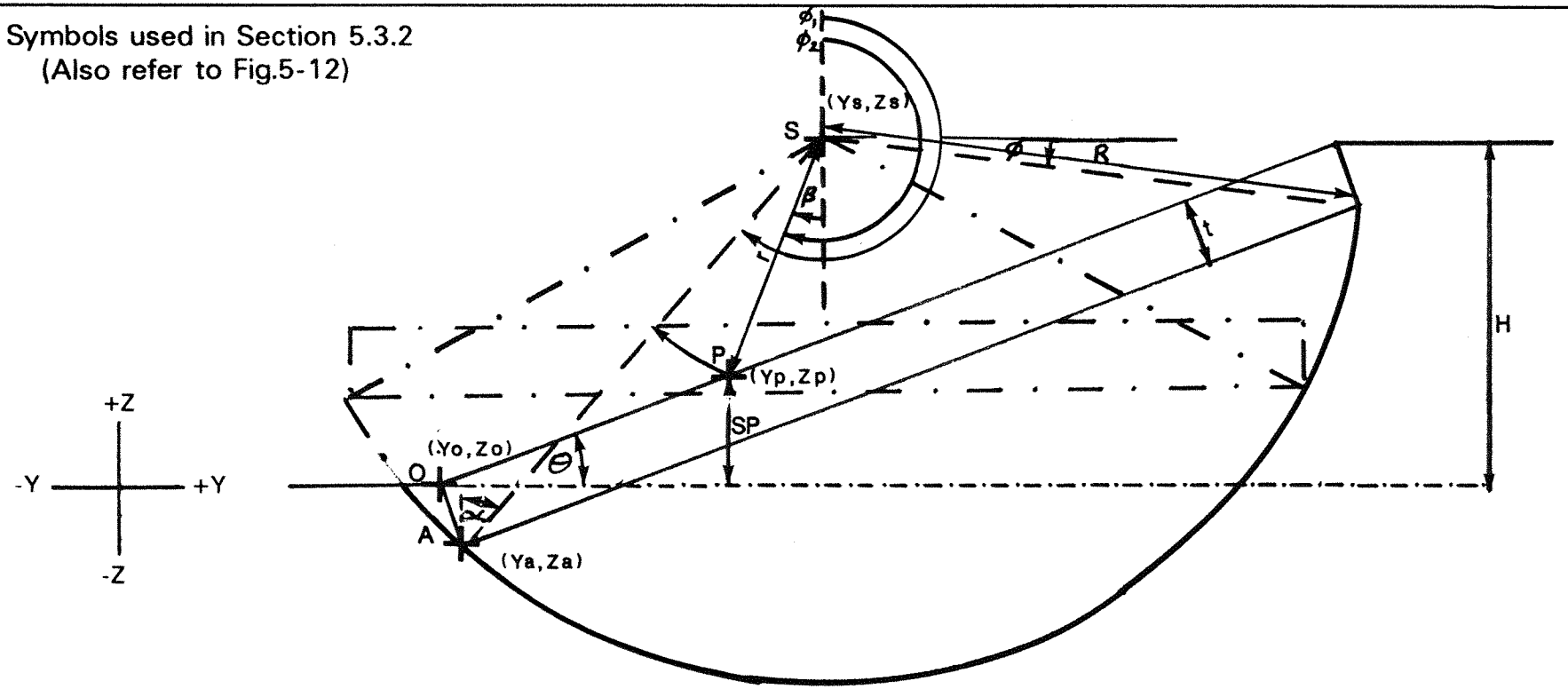

SURFACE MOVEMENTS ON A ROTATIONAL SLOPE FAILURE FIG.5-13

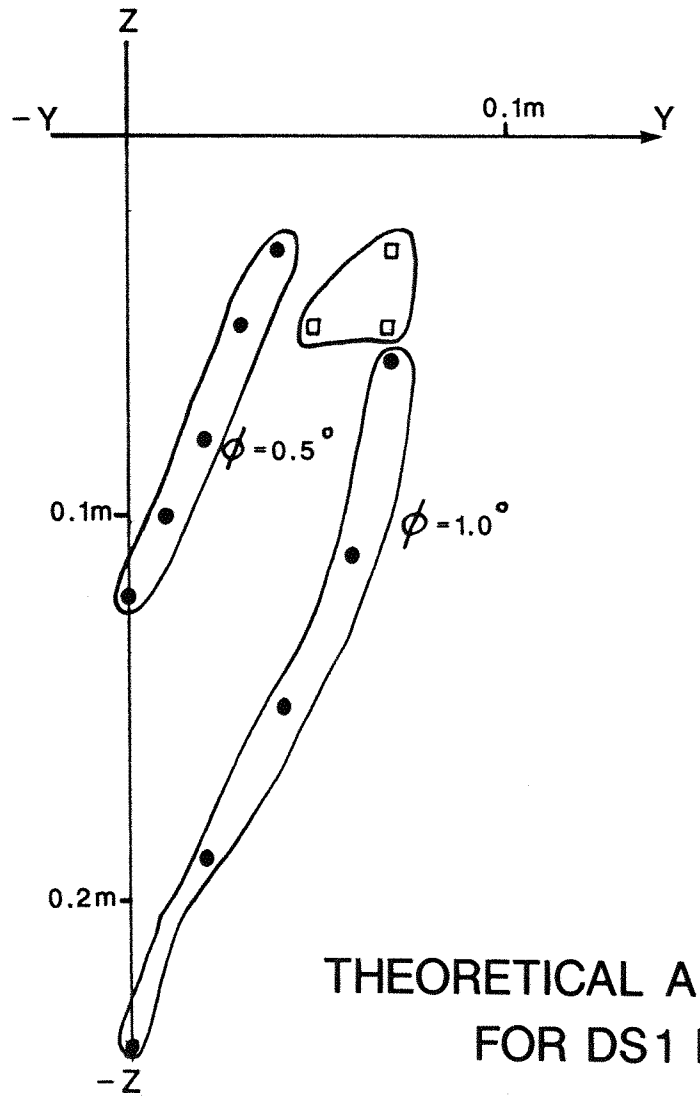

□ = DEBRIS SLIDE 1
● = THEORETICAL

THEORETICAL AND RECORDED DISPLACEMENTS
FOR DS1 DURING THE S1 PERIOD

FIG.5-14

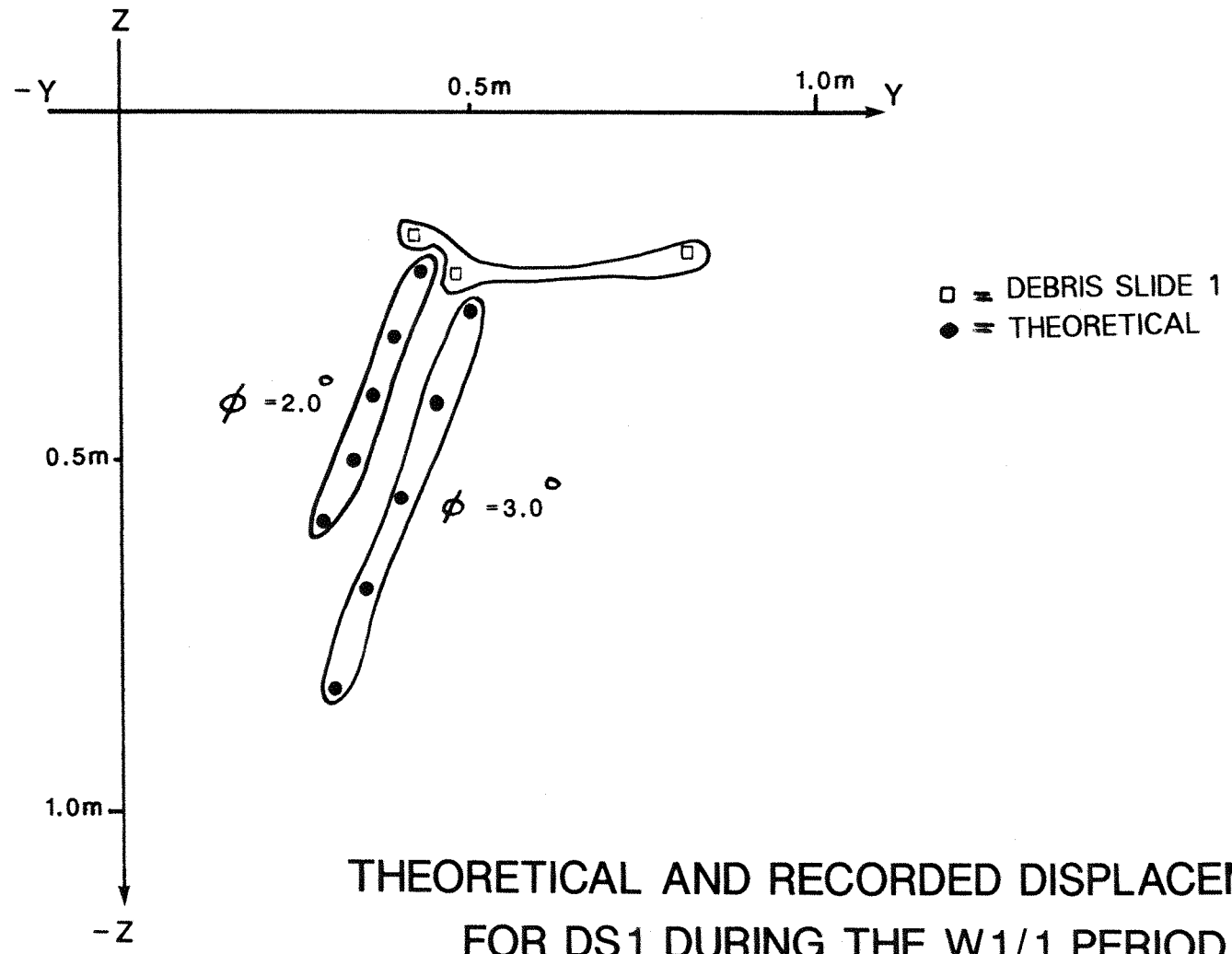

THEORETICAL AND RECORDED DISPLACEMENTS
FOR DS1 DURING THE W1/1 PERIOD

FIG.5-15

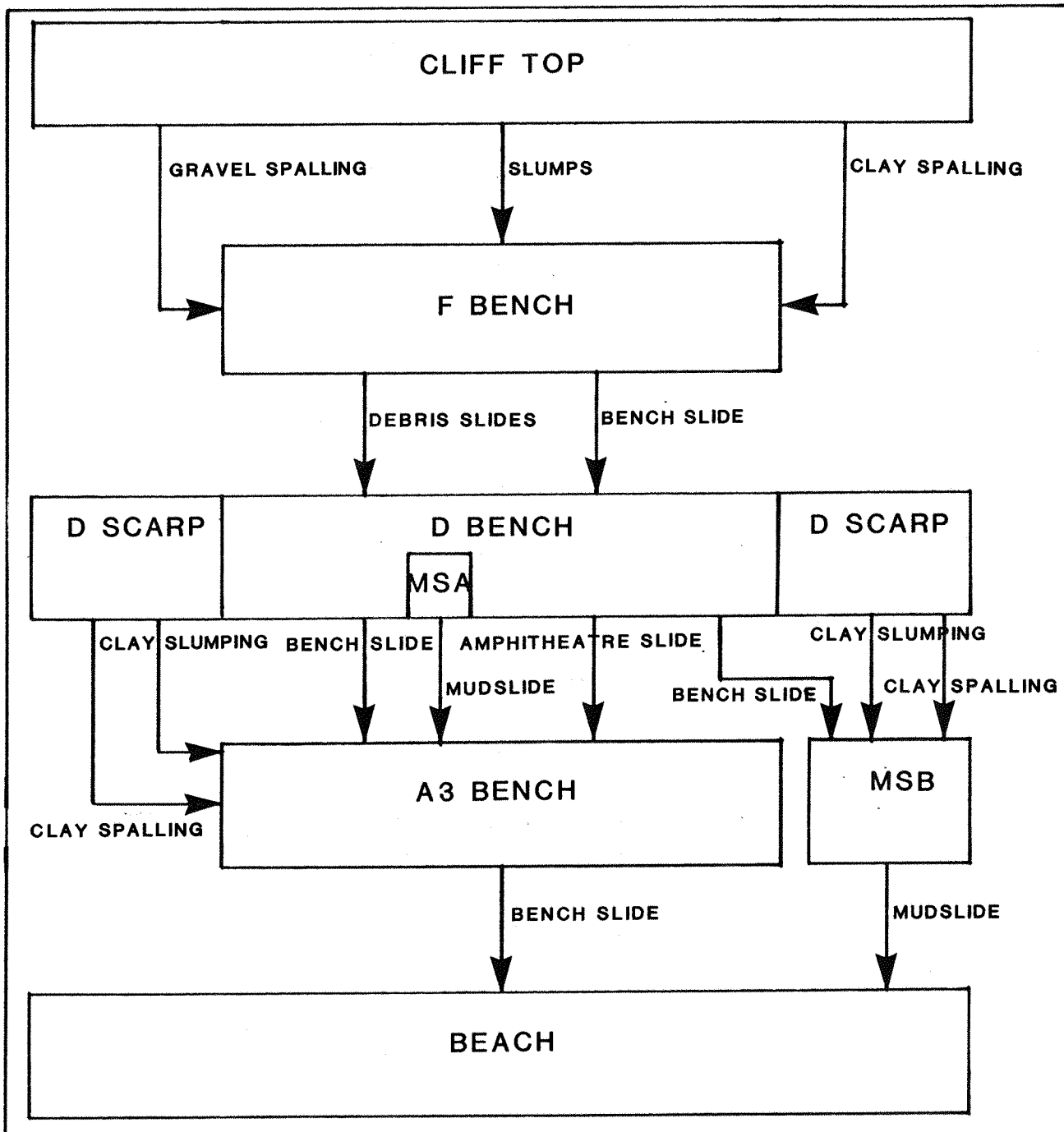

FLOW CHART OF MATERIAL MOVEMENTS IN THE UNDERCLIFF

FIG.6-1

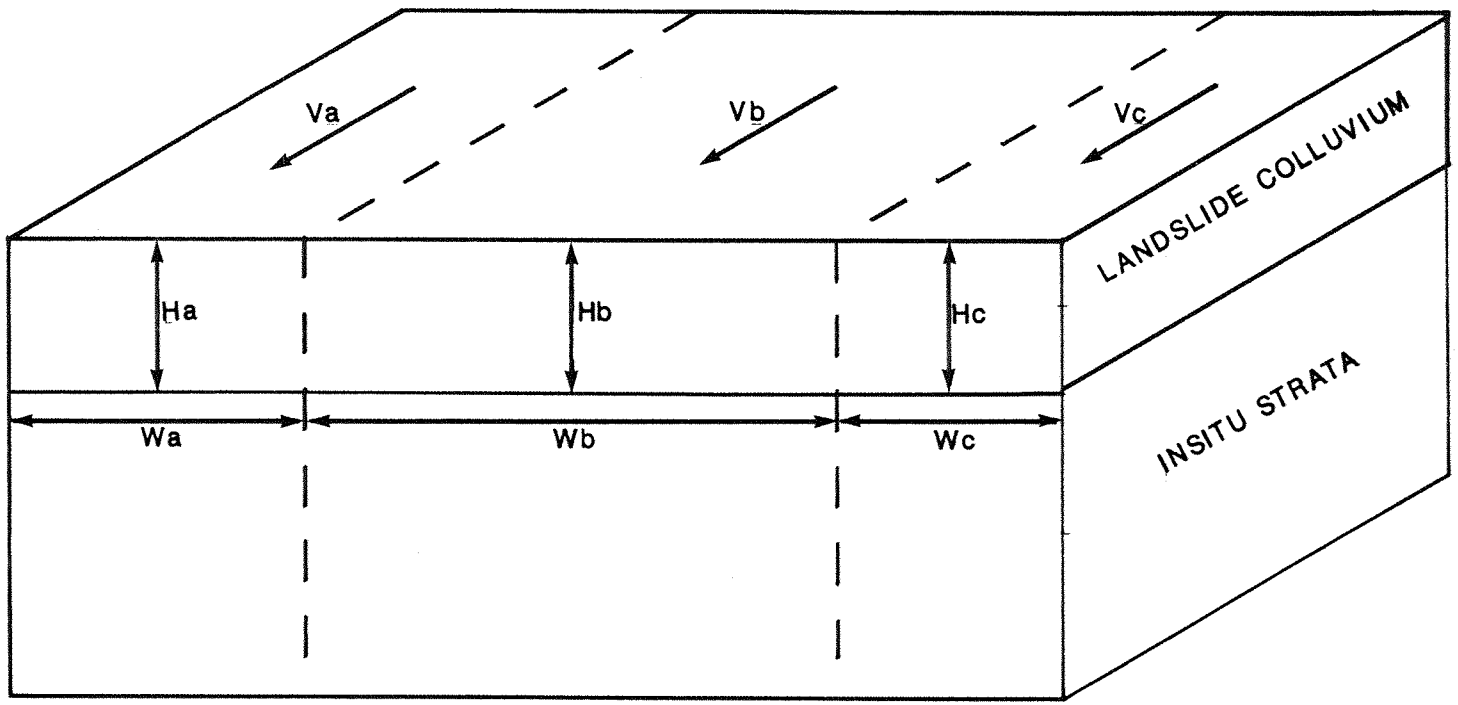

Volume per unit time = Hy*Wy*Vy per unit time

VOLUMETRIC MOVEMENT OF THE BENCHSLIDES

FIG.6-2

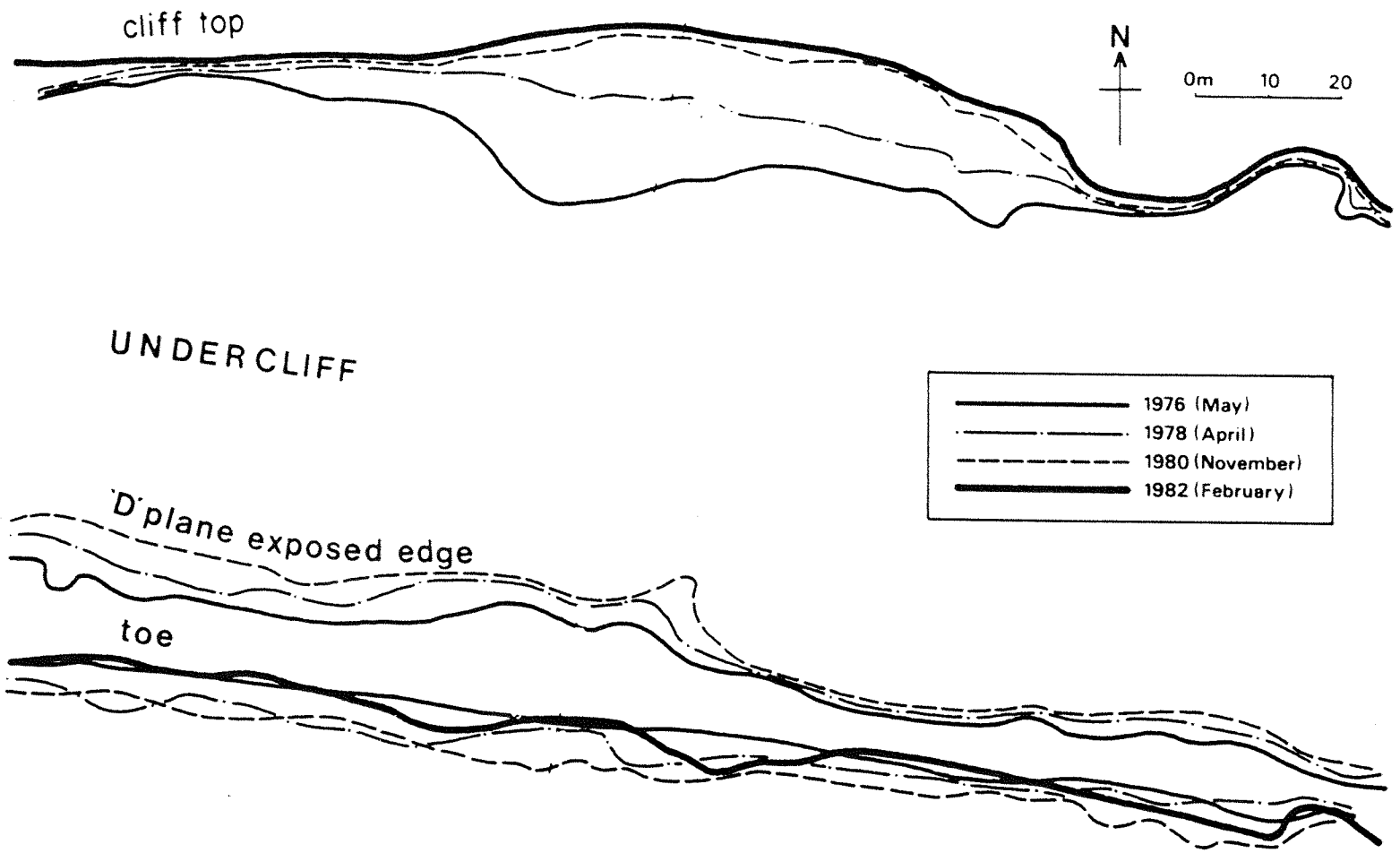

CLIFF TOP RECESSION
(After Barton and Coles, 1984)

FIG 6-3

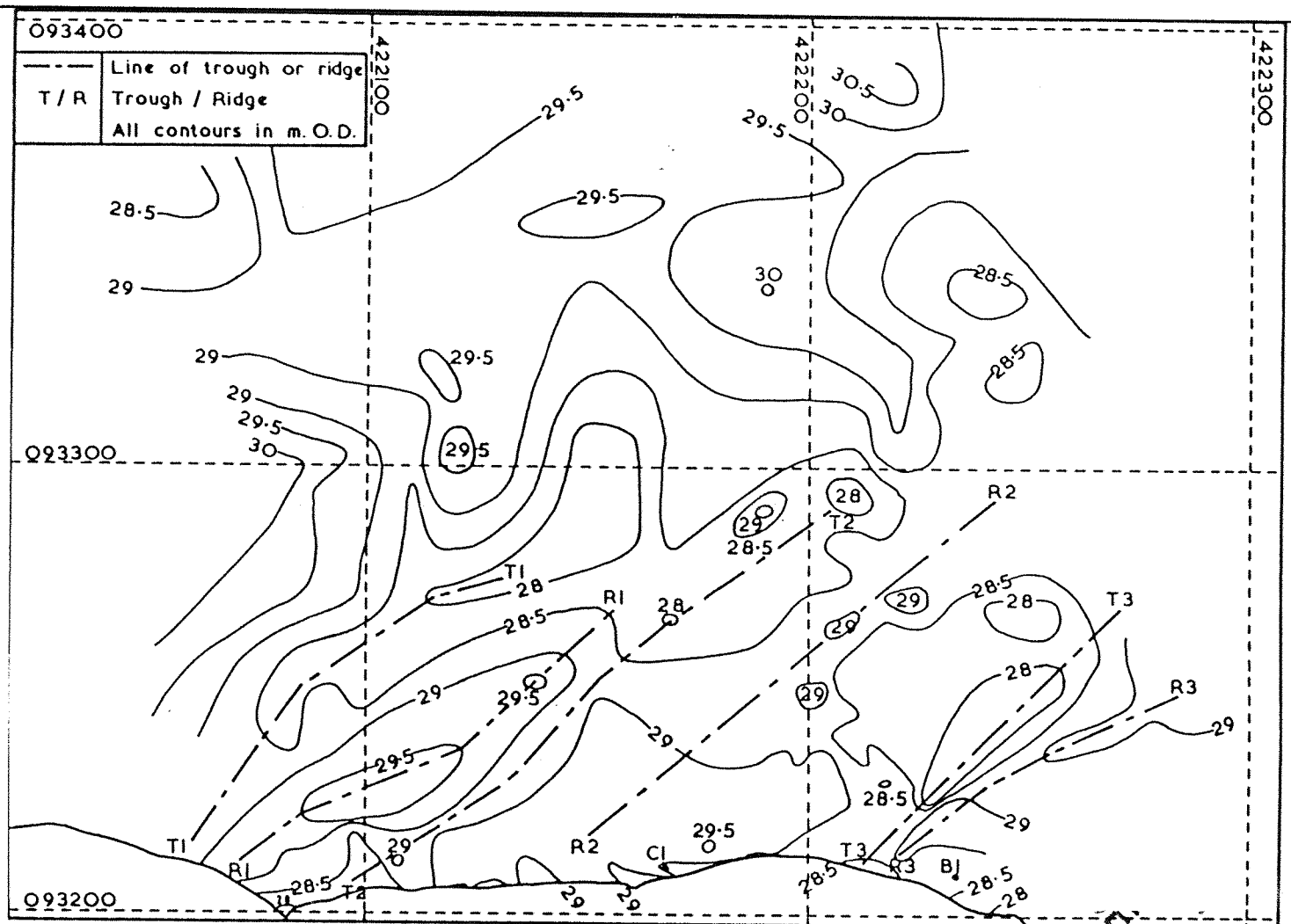

CONTOURS OF THE PLATEAU GRAVEL/BARTON CLAY INTERFACE

(After Thomson,1987)–Feb 1984

FIG 6–4

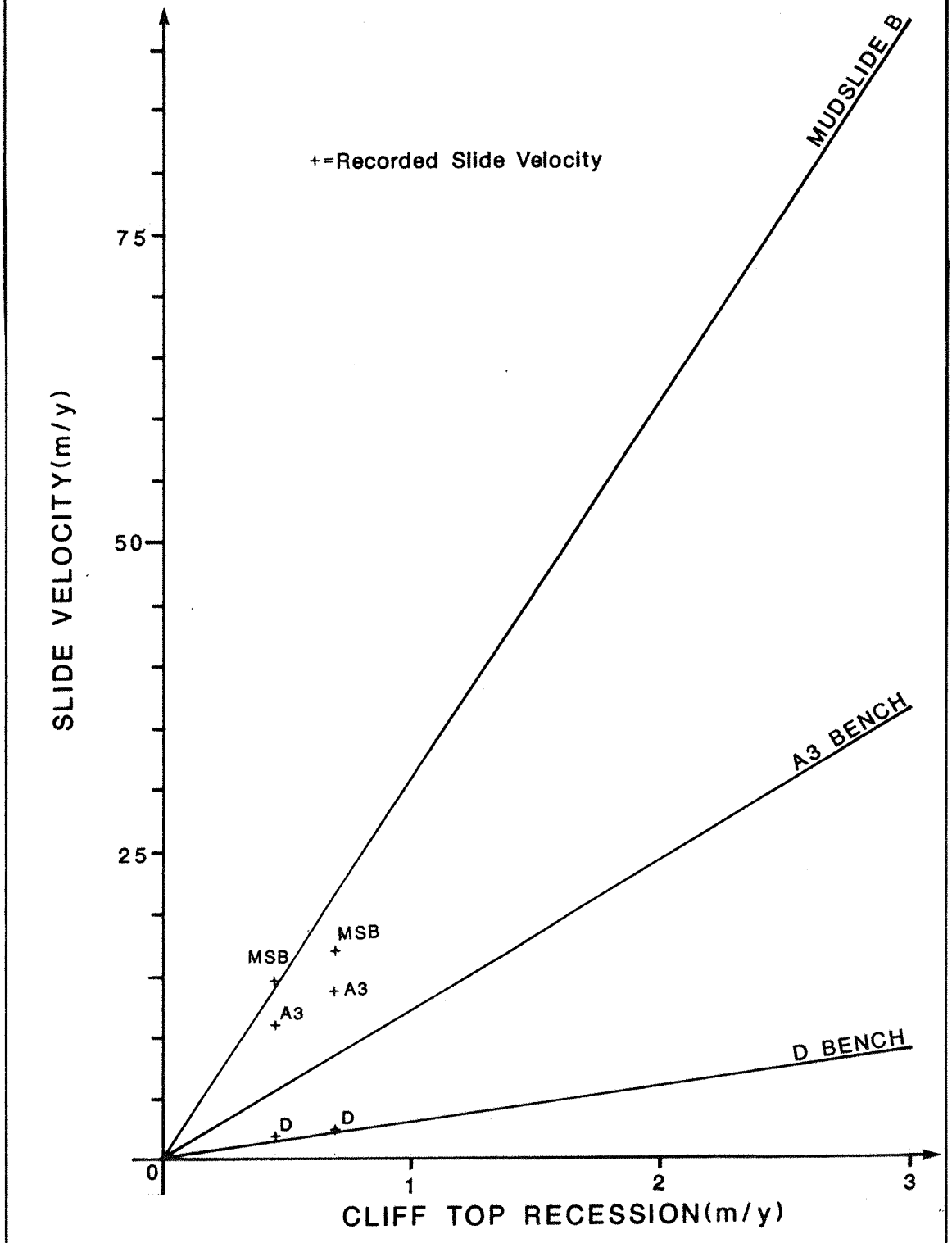

THEORETICAL SLIDE VELOCITIES AND RECORDED SLIDE VELOCITIES

FIG.6-5

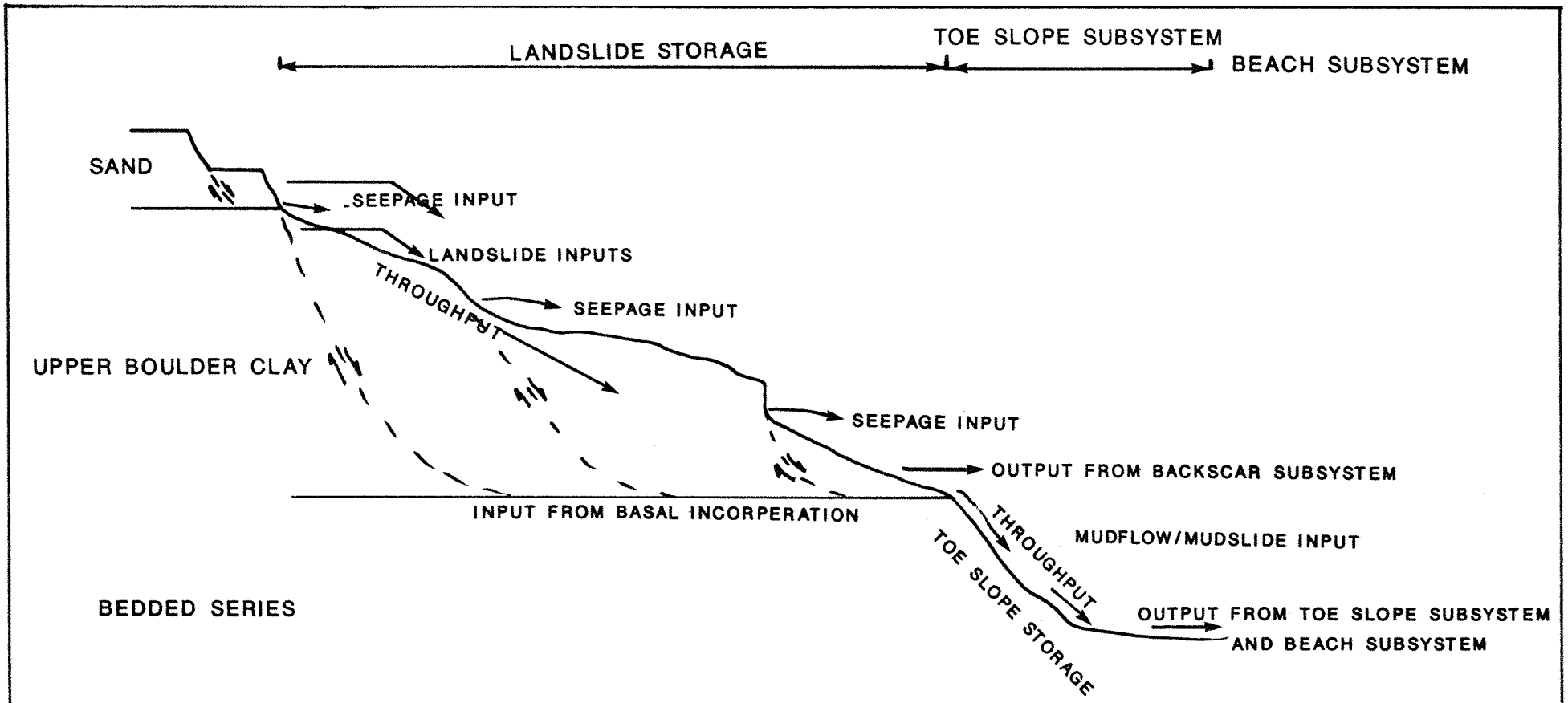

SLOPE BUDGET DIAGRAM FOR A CLADY SLOPE(After Pitts,1983)

FIG.6-6

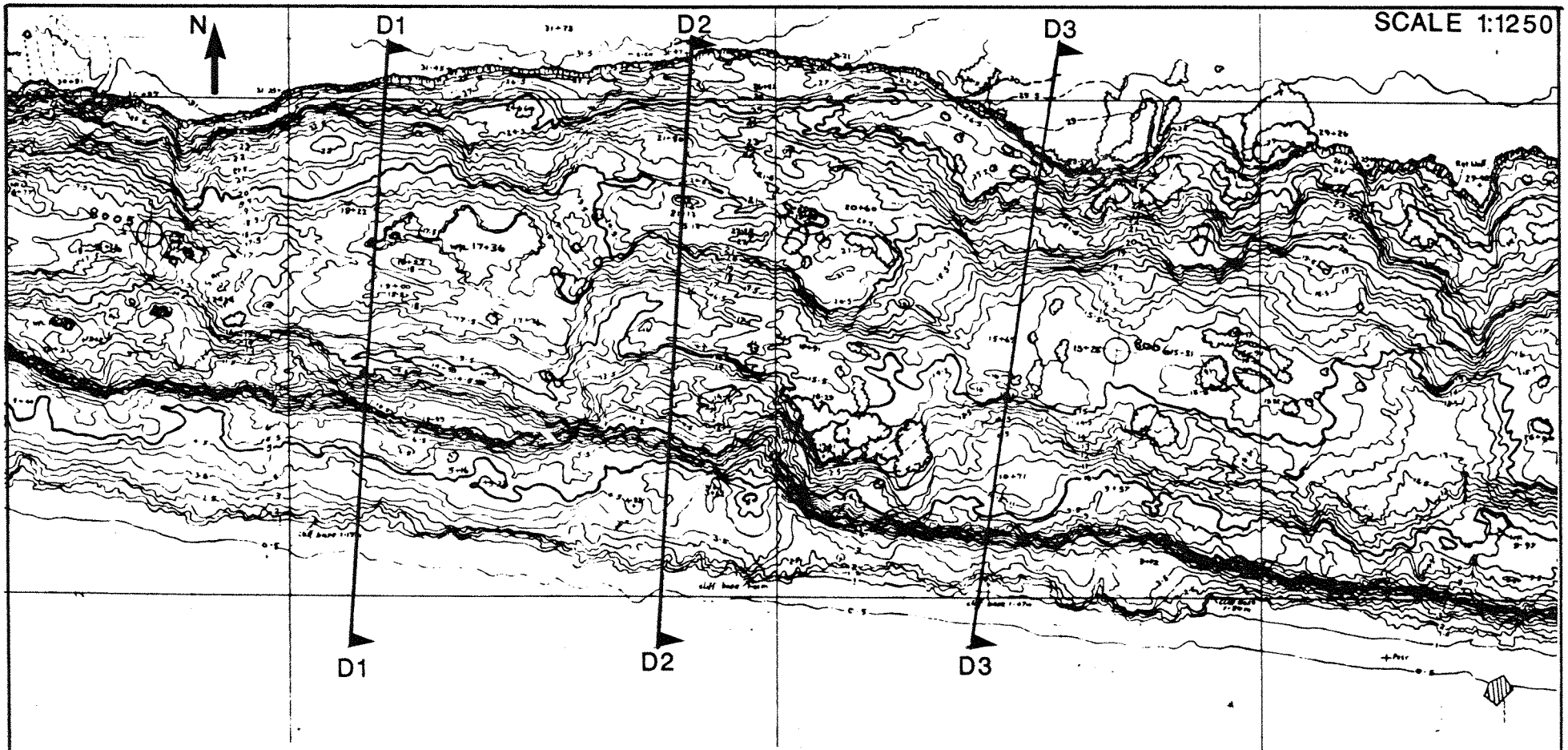

TOPOGRAPHICAL CONTOUR MAP(NOVEMBER 1980) SHOWING
THE CROSS SECTIONS USED IN THE STABILITY ANALYSIS

FIG.7-1

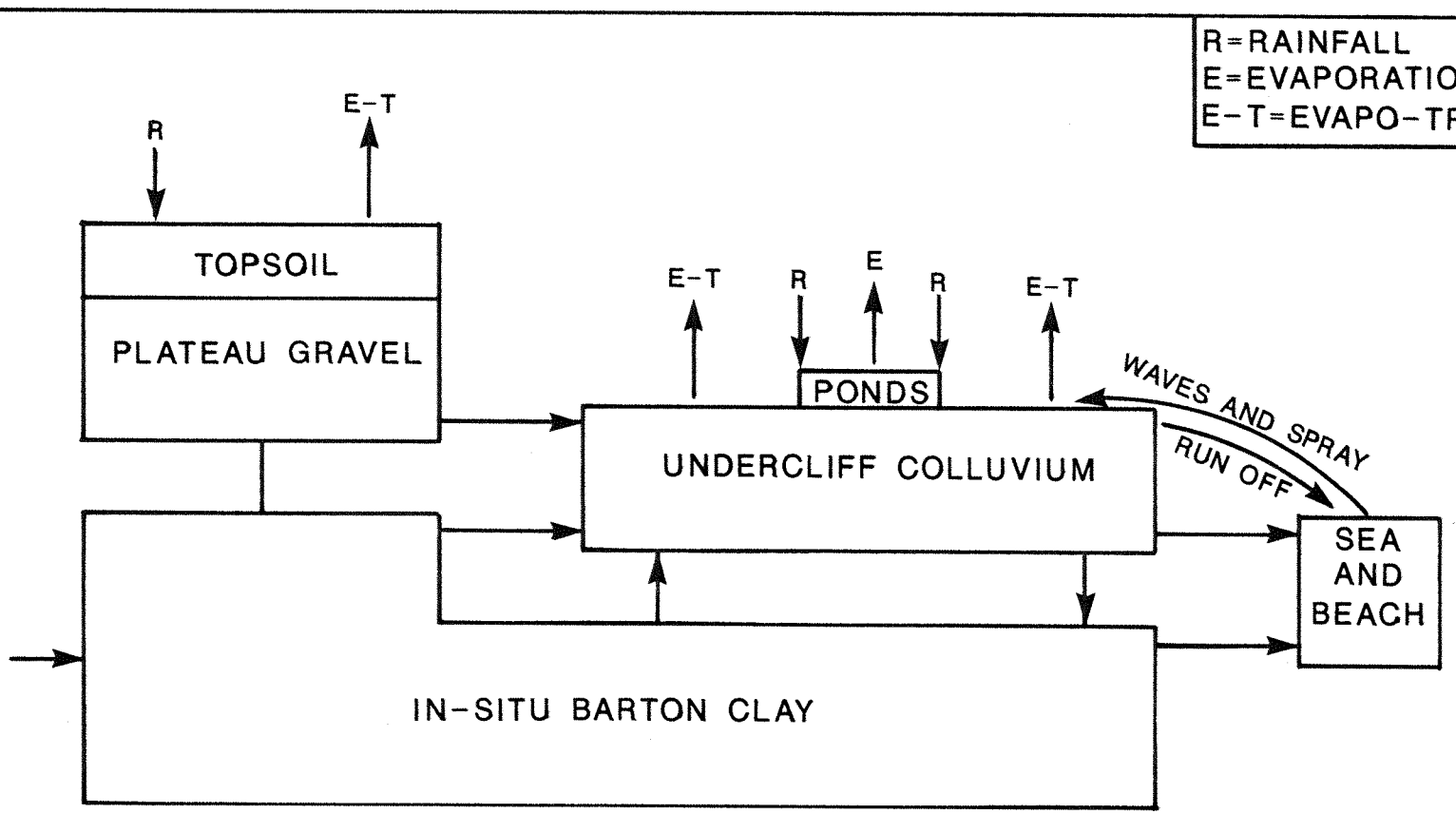

DIAGRAMMATIC REPRESENTATION OF THE WATER BALANCE REGIME(From Barton and Thomson,1984)

FIG.7-2

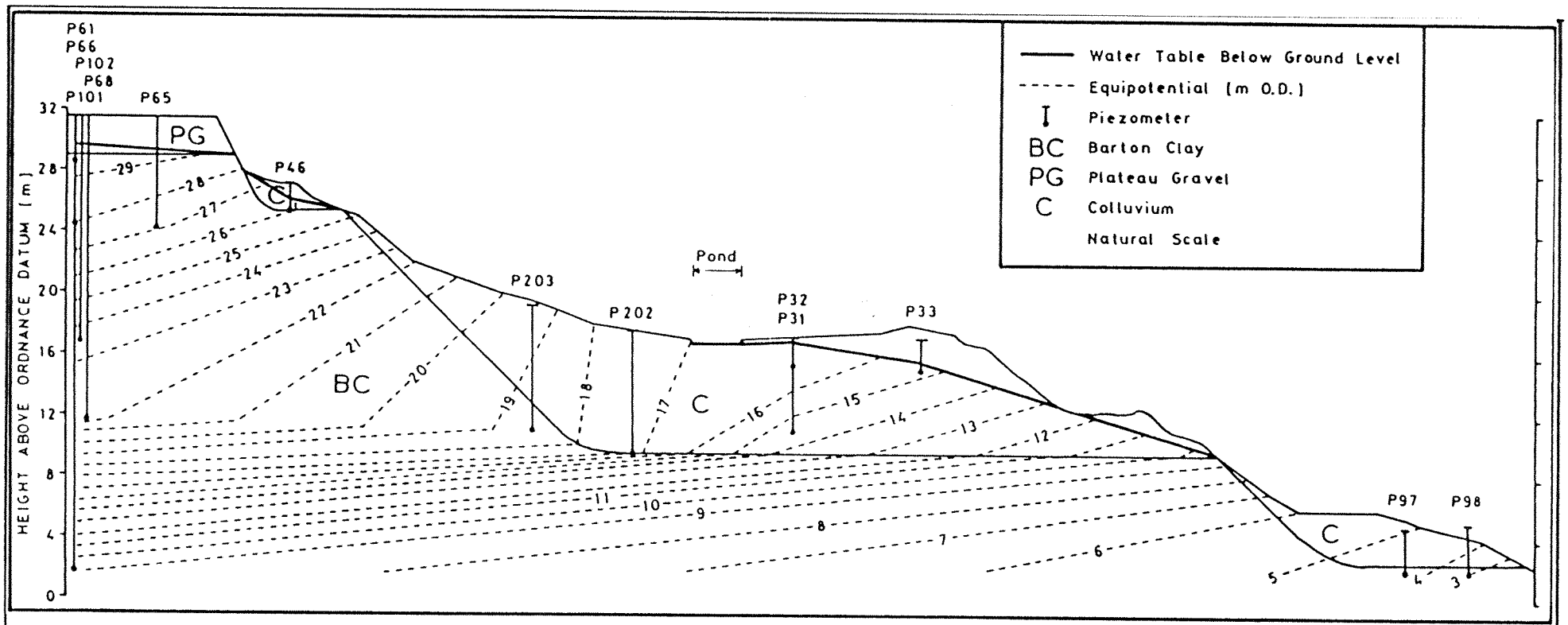

EQUIPOTENTIALS QF THE STUDY AREA(After Thomson,1987)

FIG 7-3

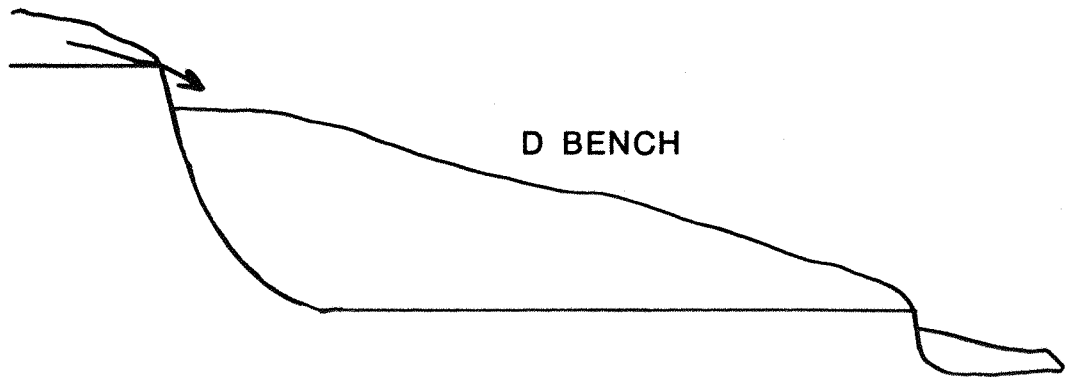

CASE A

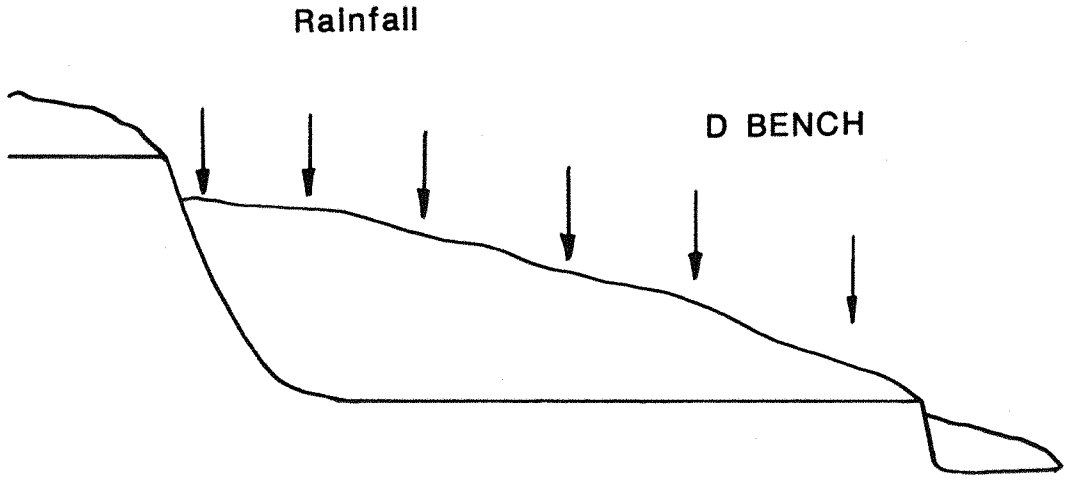

CASE B

ROUTES OF WATER INFILTRATION INTO THE D BENCH

FIG 7-4

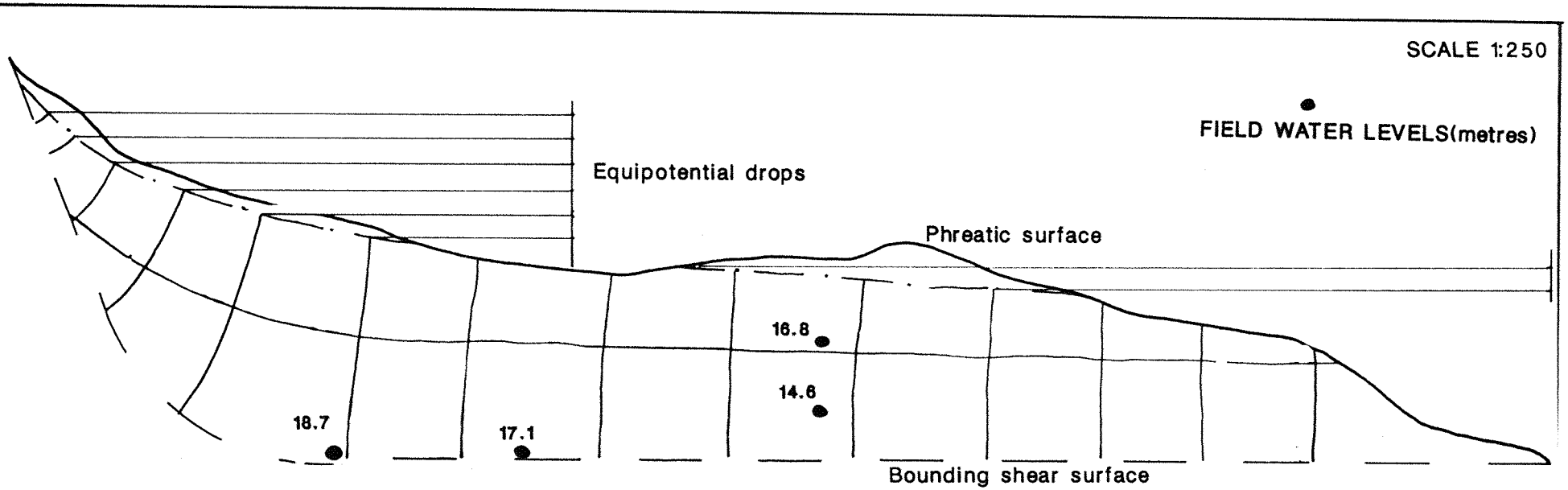

CROSS SECTION-D1 NOVEMBER 1980
FLOW NET(CASE A)

FIG 7-5

SCALE 1:250

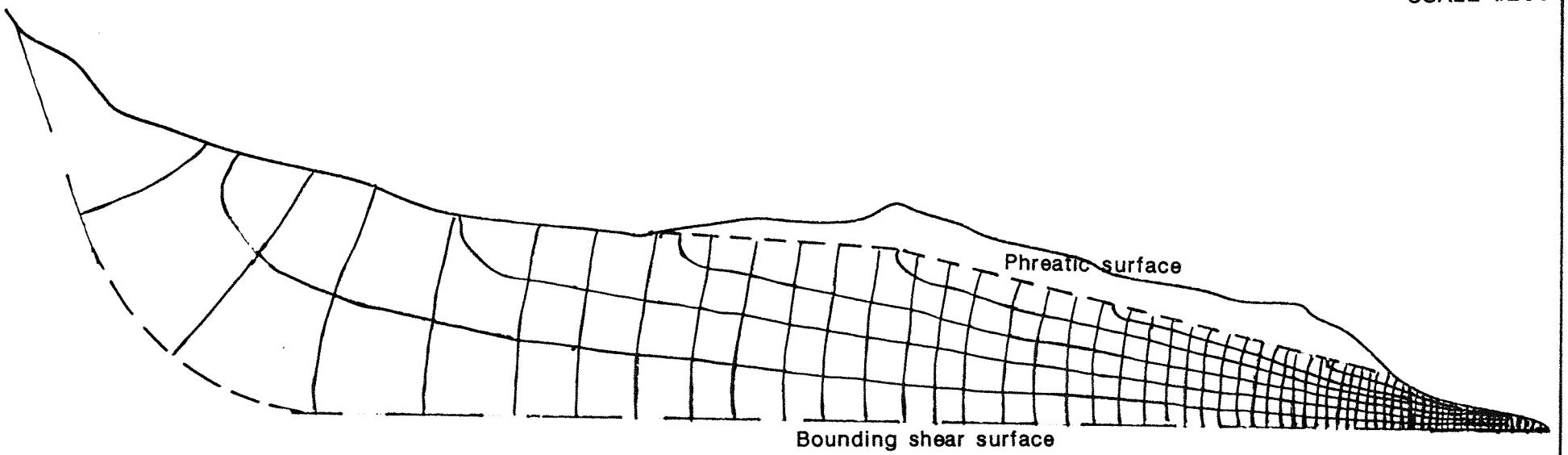

CROSS SECTION-D1 NOVEMBER 1980
FLOW NET(CASE B)

FIG 7-6

SCALE 1:250

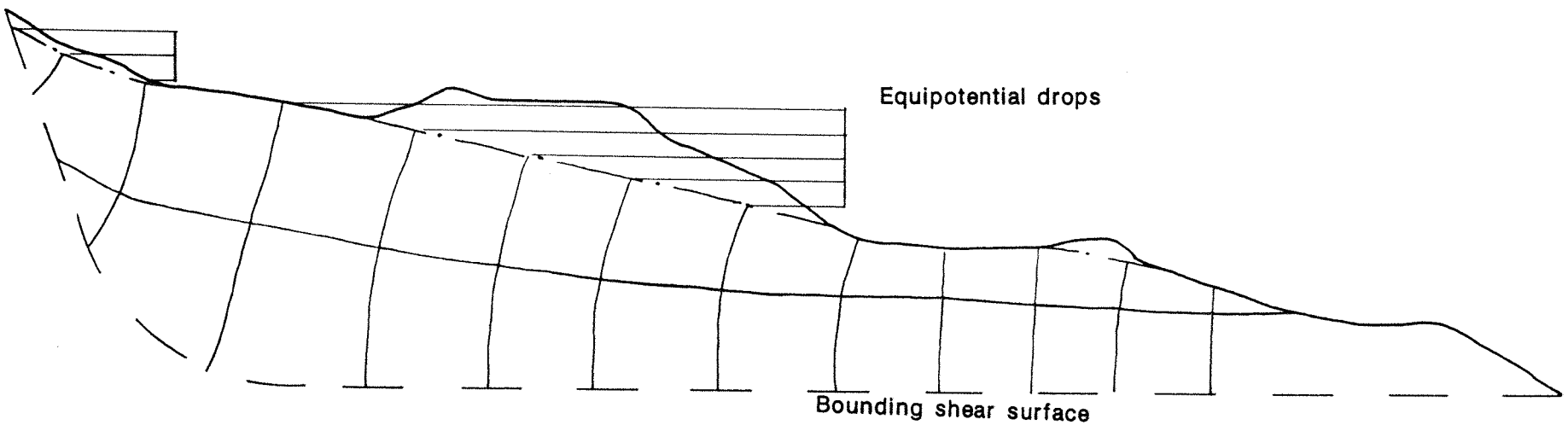

CROSS SECTION-D2 NOVEMBER 1980
FLOW NET(CASE A)

FIG 7-7

SCALE 1:250

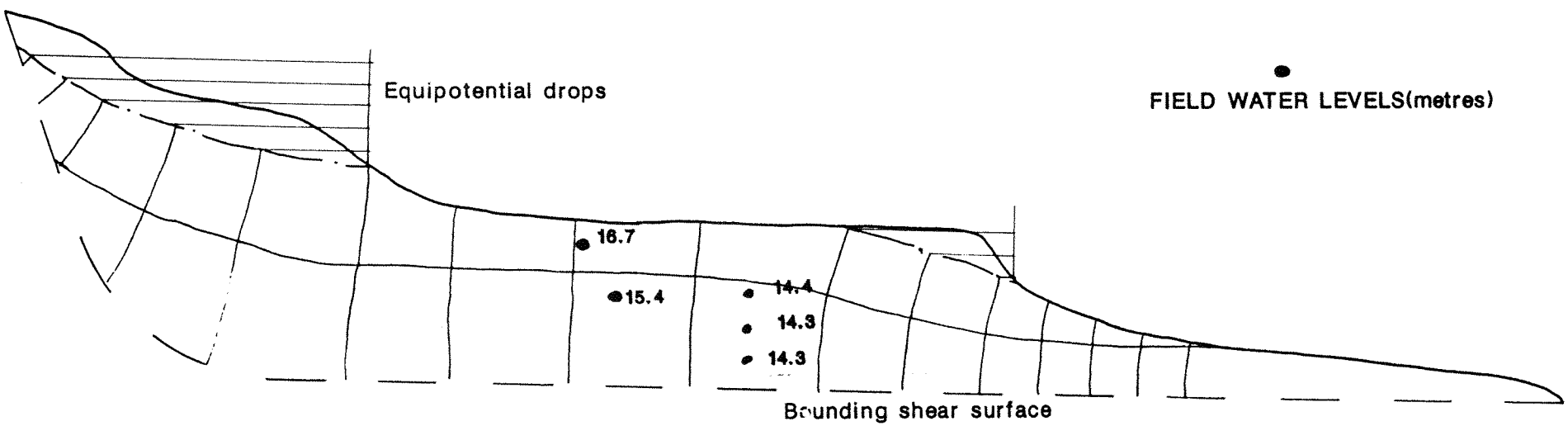

CROSS SECTION-D3 NOVEMBER 1980
FLOW NET(CASE A)

FIG 7-8

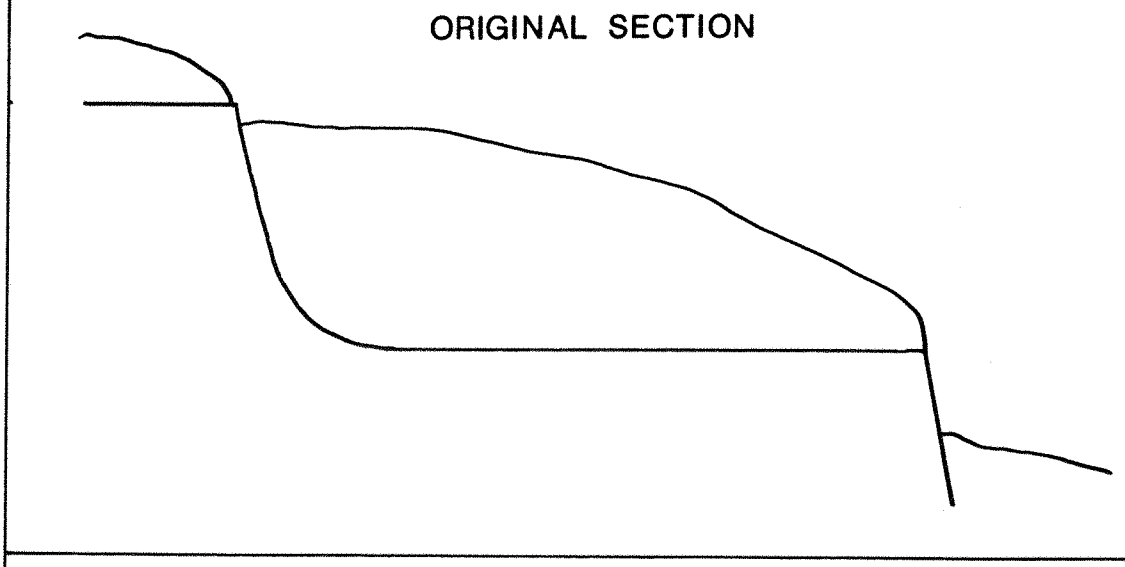

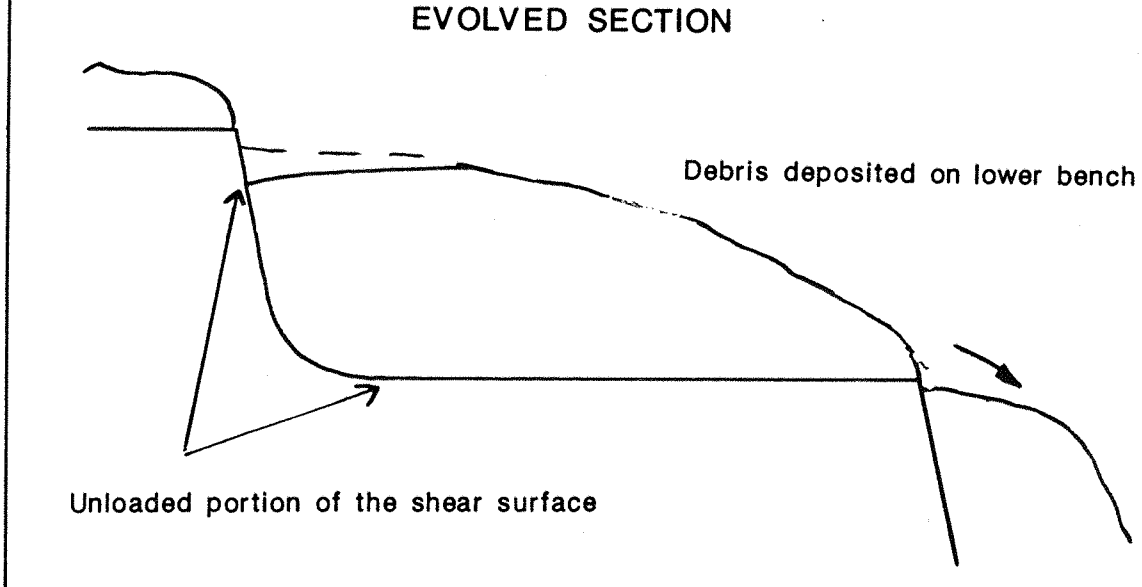

EVOLUTION OF THE BENCH SLIDE TO PRODUCE DEPRESSED PORE WATER PRESSURES

FIG 7-9

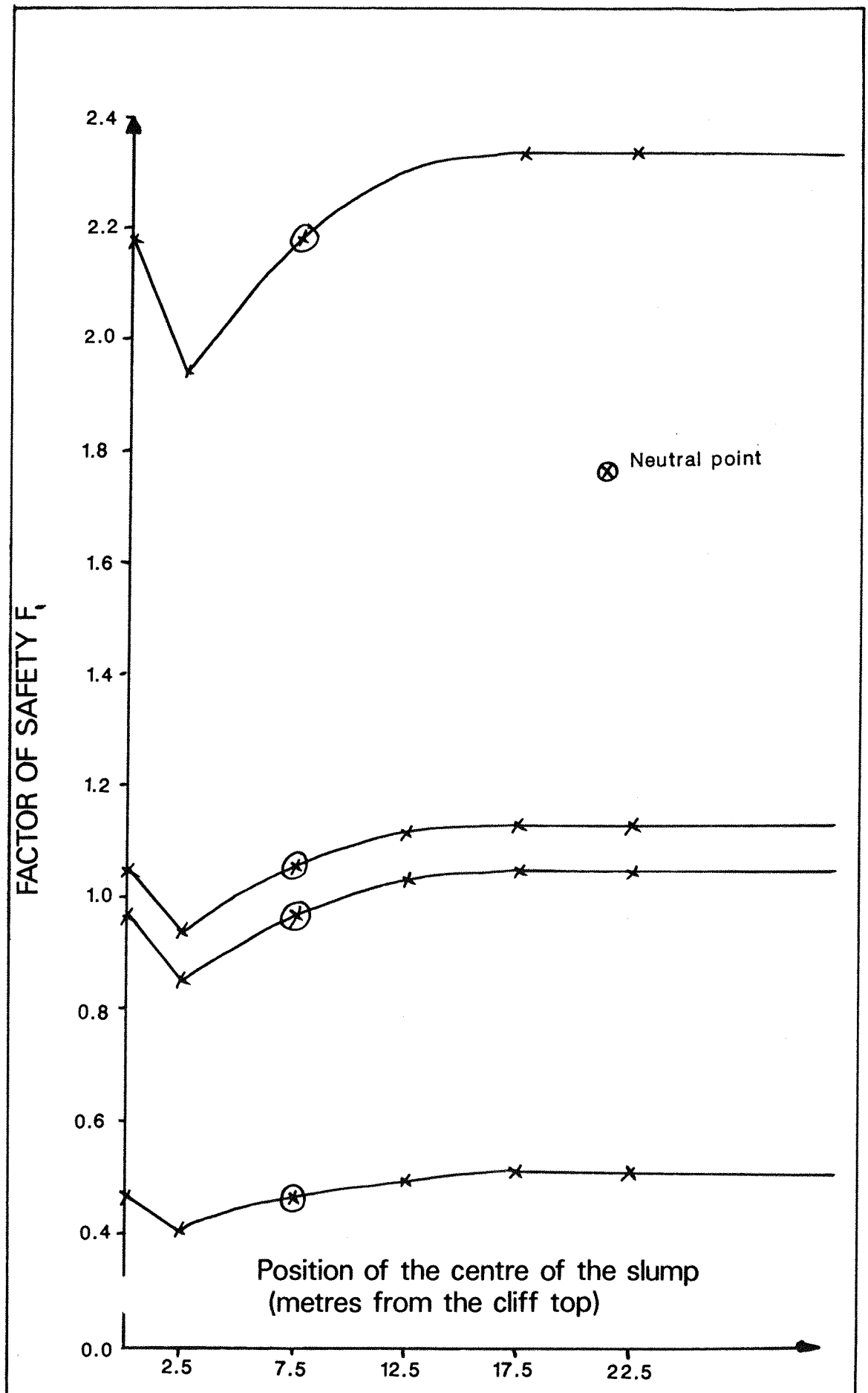

CHANGES IN THE FACTOR OF SAFETY DUE TO A MOVING CLIFF TOP SLUMP FIG 7-10

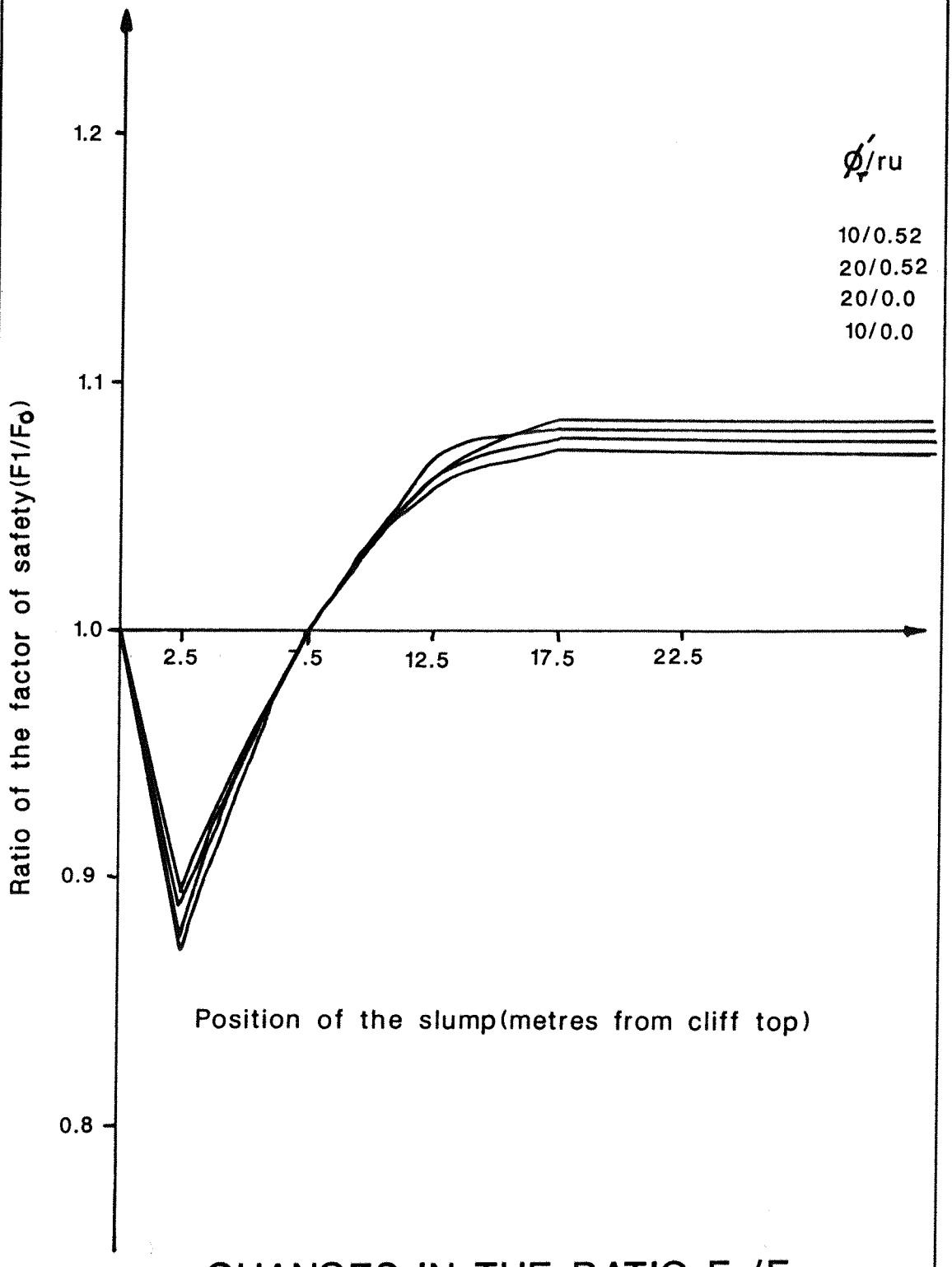

CHANGES IN THE RATIO F_1 / F_0
DUE TO A MOVING CLIFF TOP SLUMP

FIG 7-11

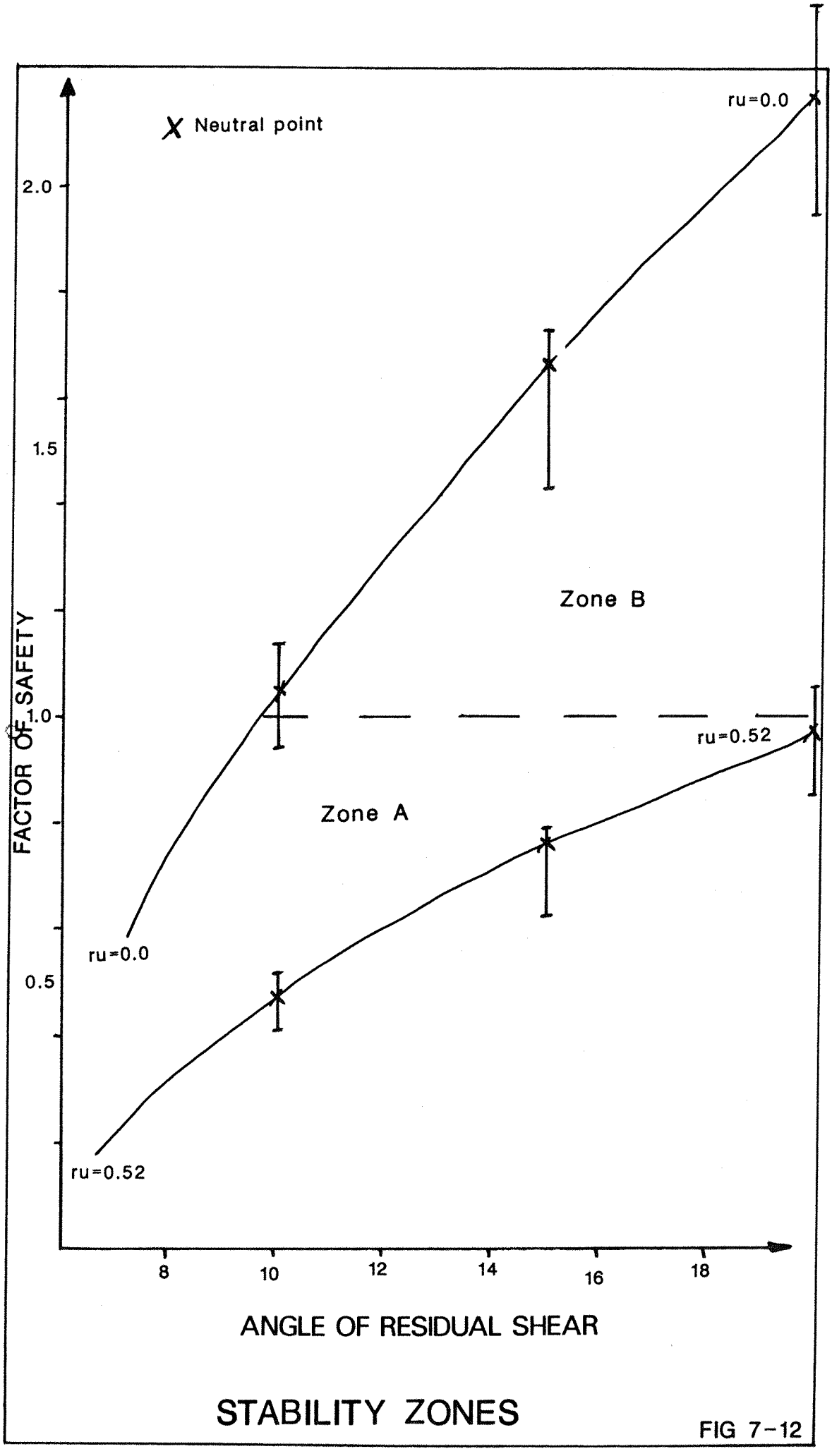

STABILITY ZONES

FIG 7-12

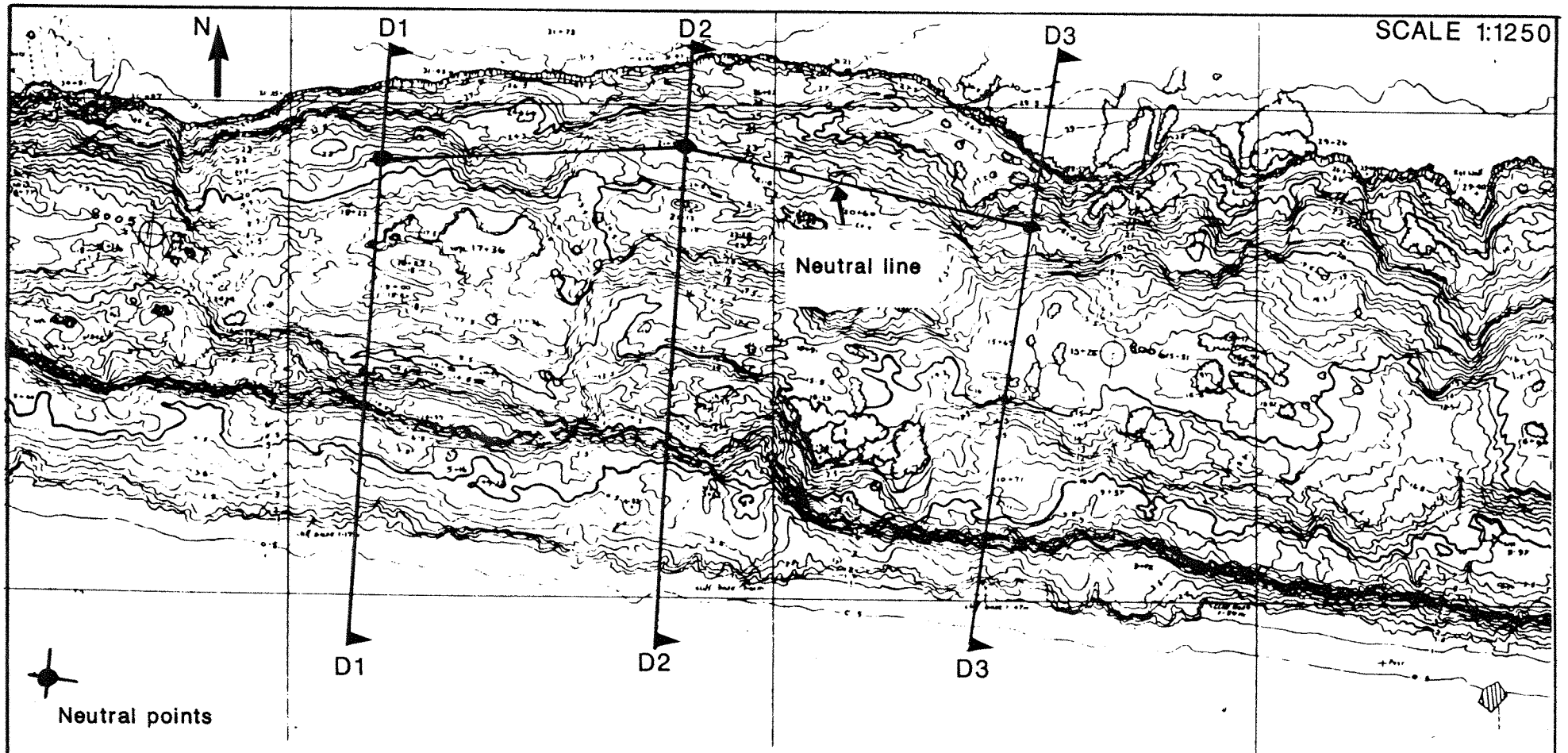

THE POSTION OF THE DRAINED NEUTRAL LINE
FOR CROSS SECTIONS D1,D2 & D3

FIG 7-13

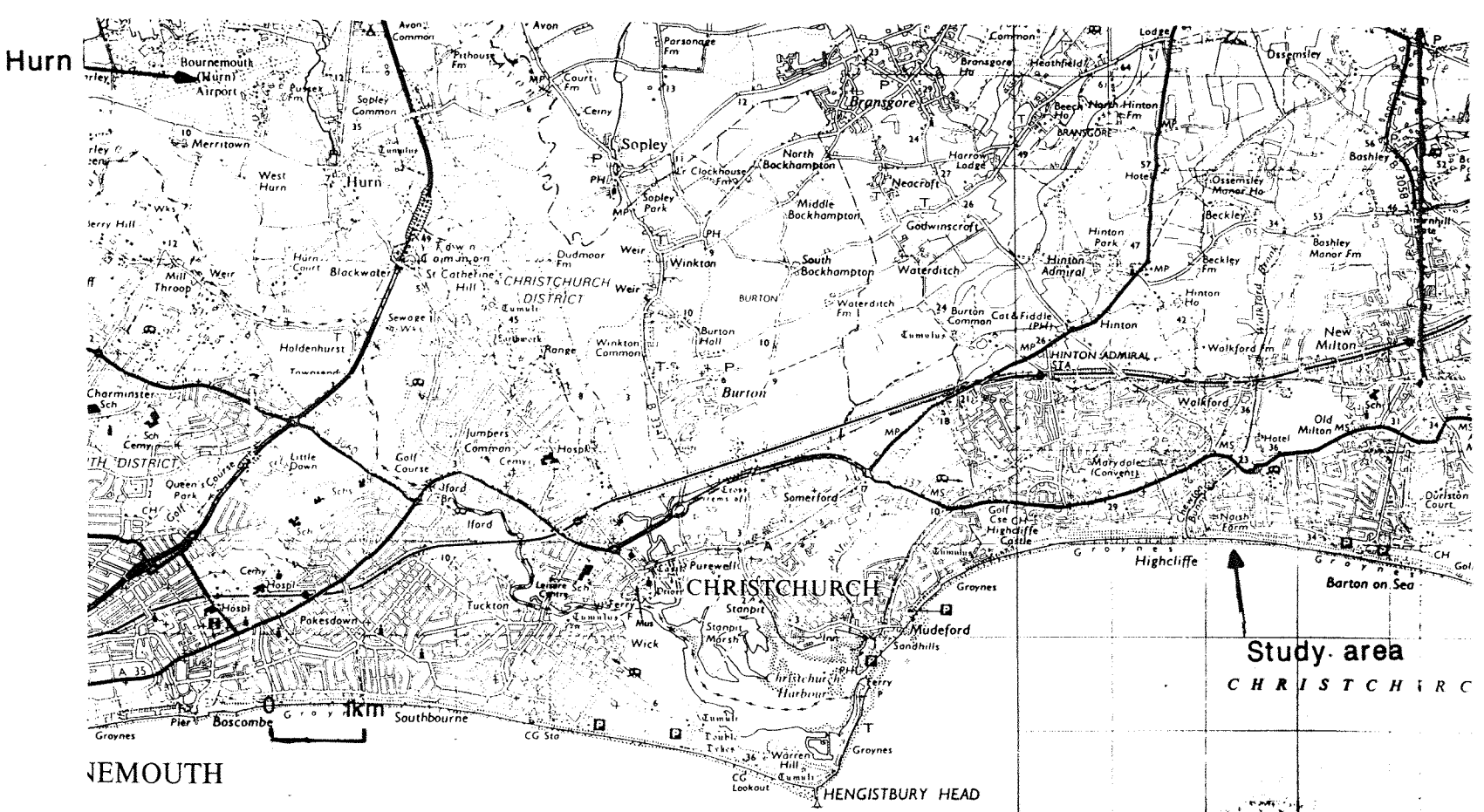

RELATIVE POSITIONS OF THE STUDY AREA AND HURN AIRPORT

FIG 8-1

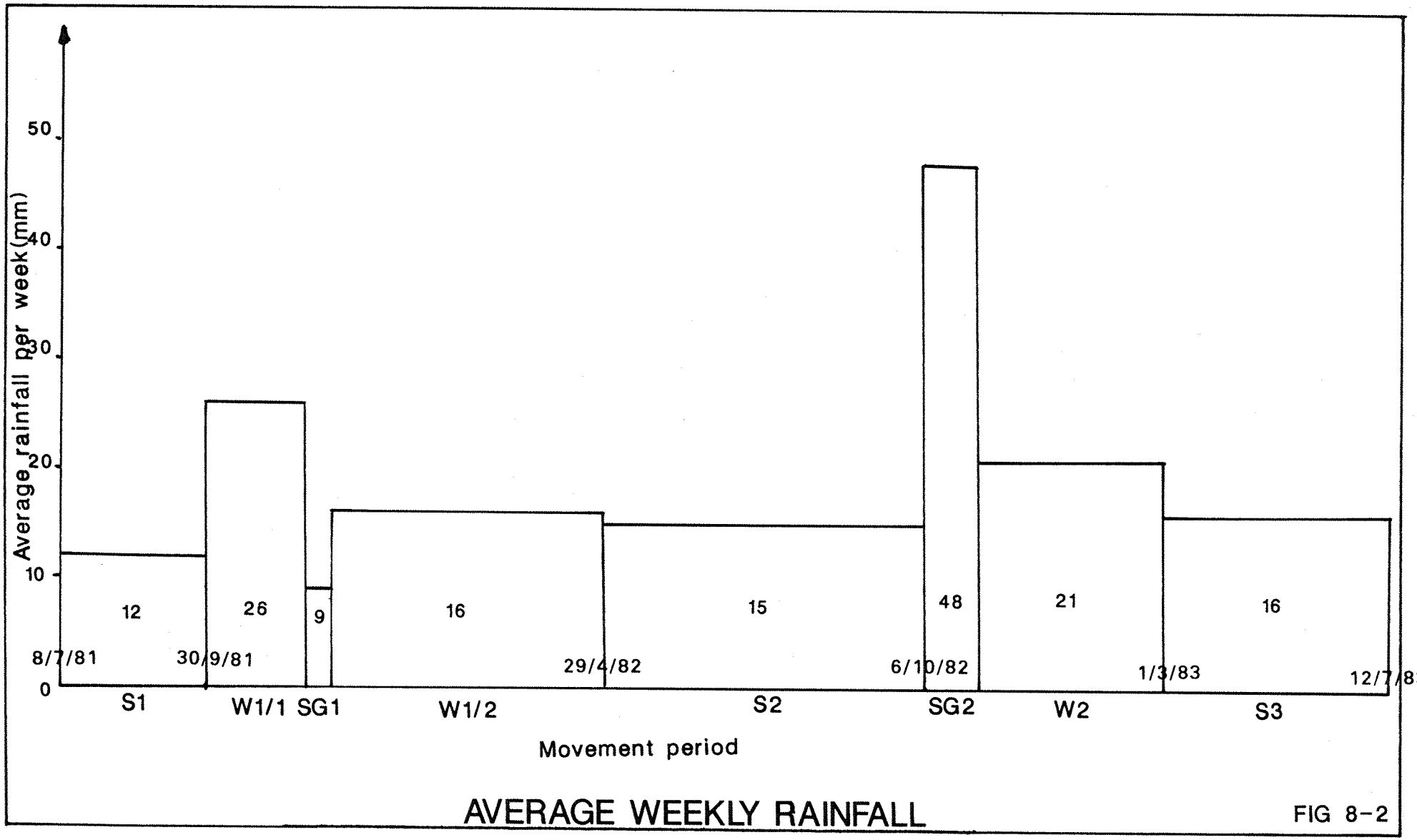

AVERAGE WEEKLY RAINFALL

FIG 8-2

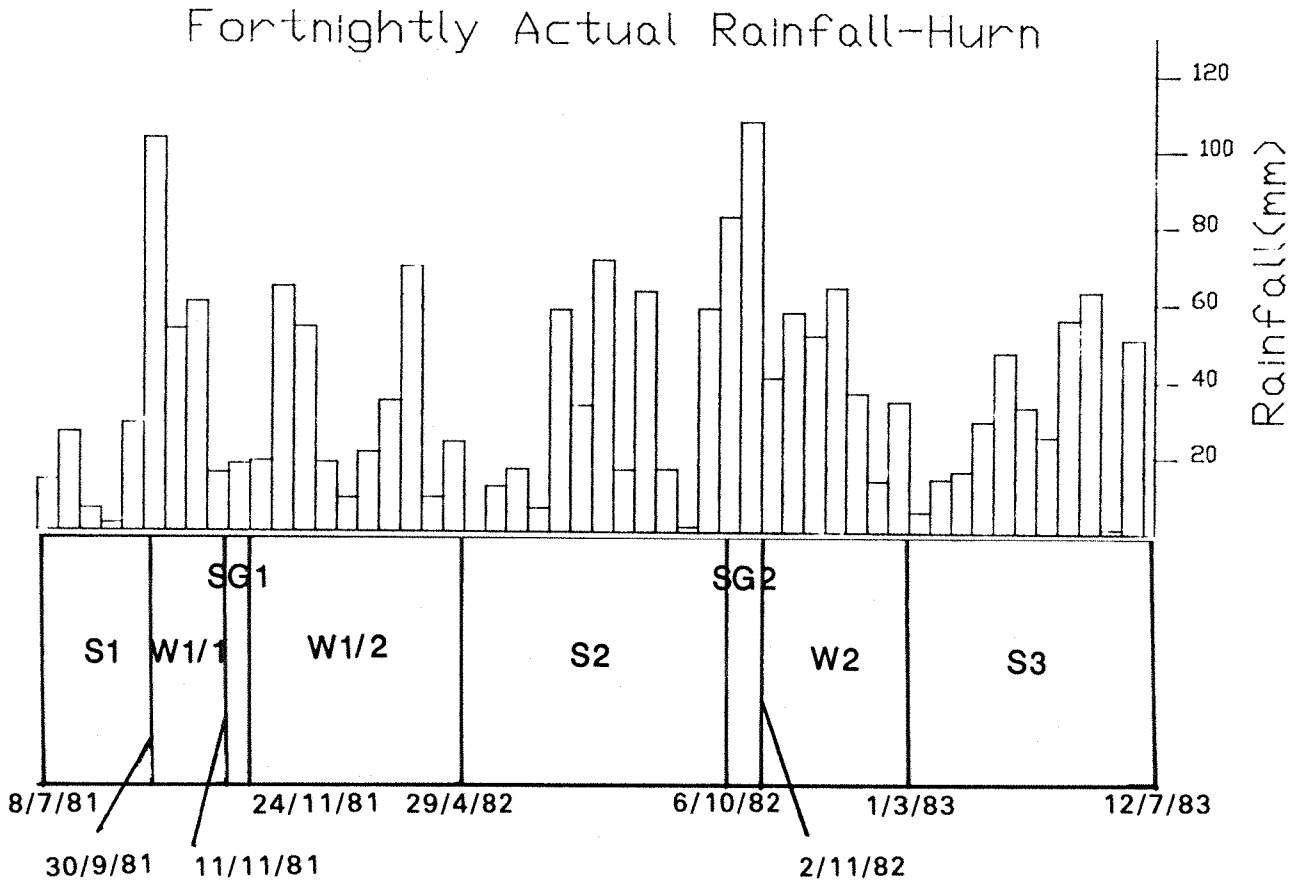

RAINFALL AND MOVEMENT PERIODS

FIG 8-3

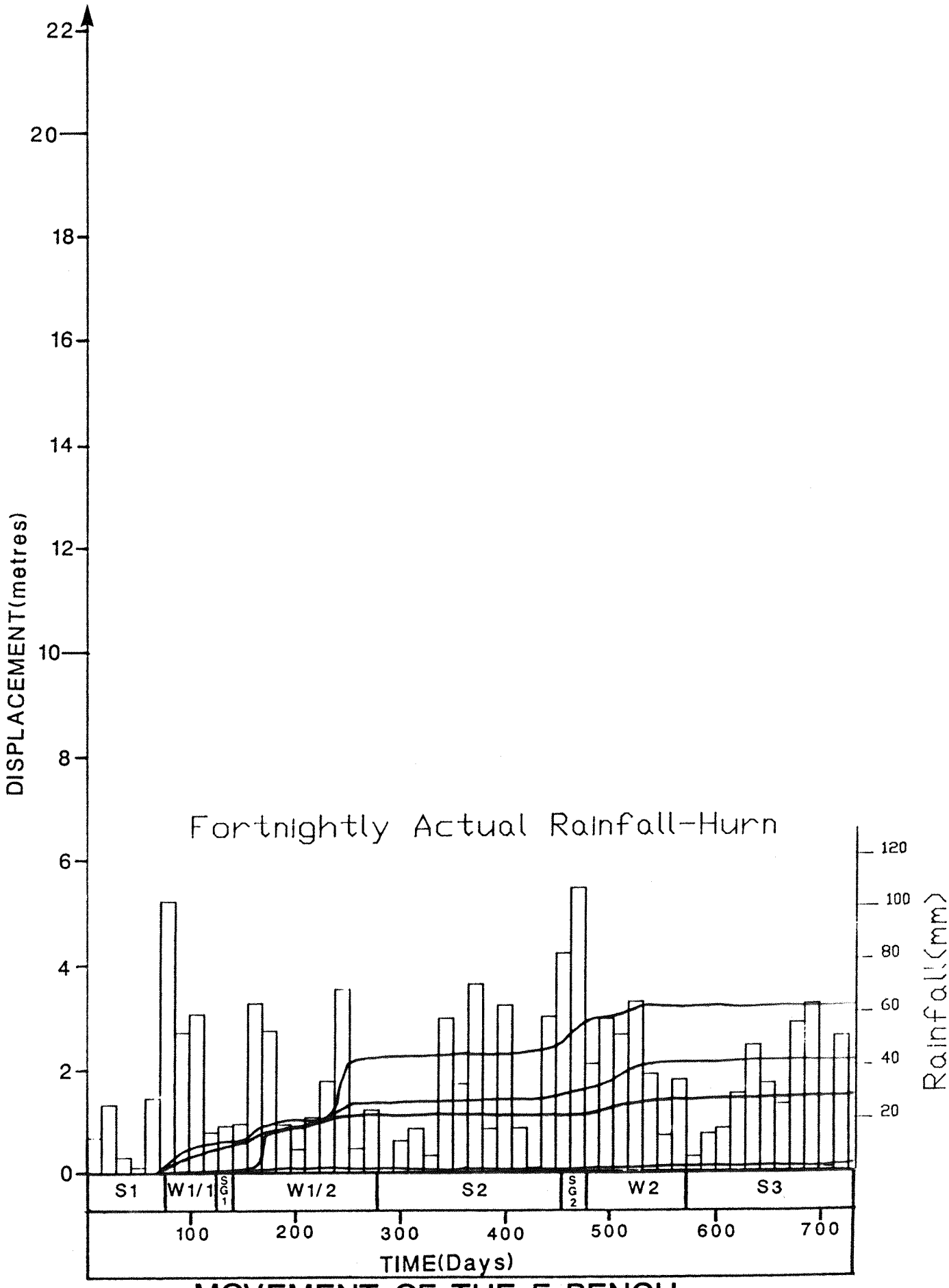

MOVEMENT OF THE F BENCH
DURING THE STUDY PERIOD

FIG 8-4

(For dates see Fig.8-3)

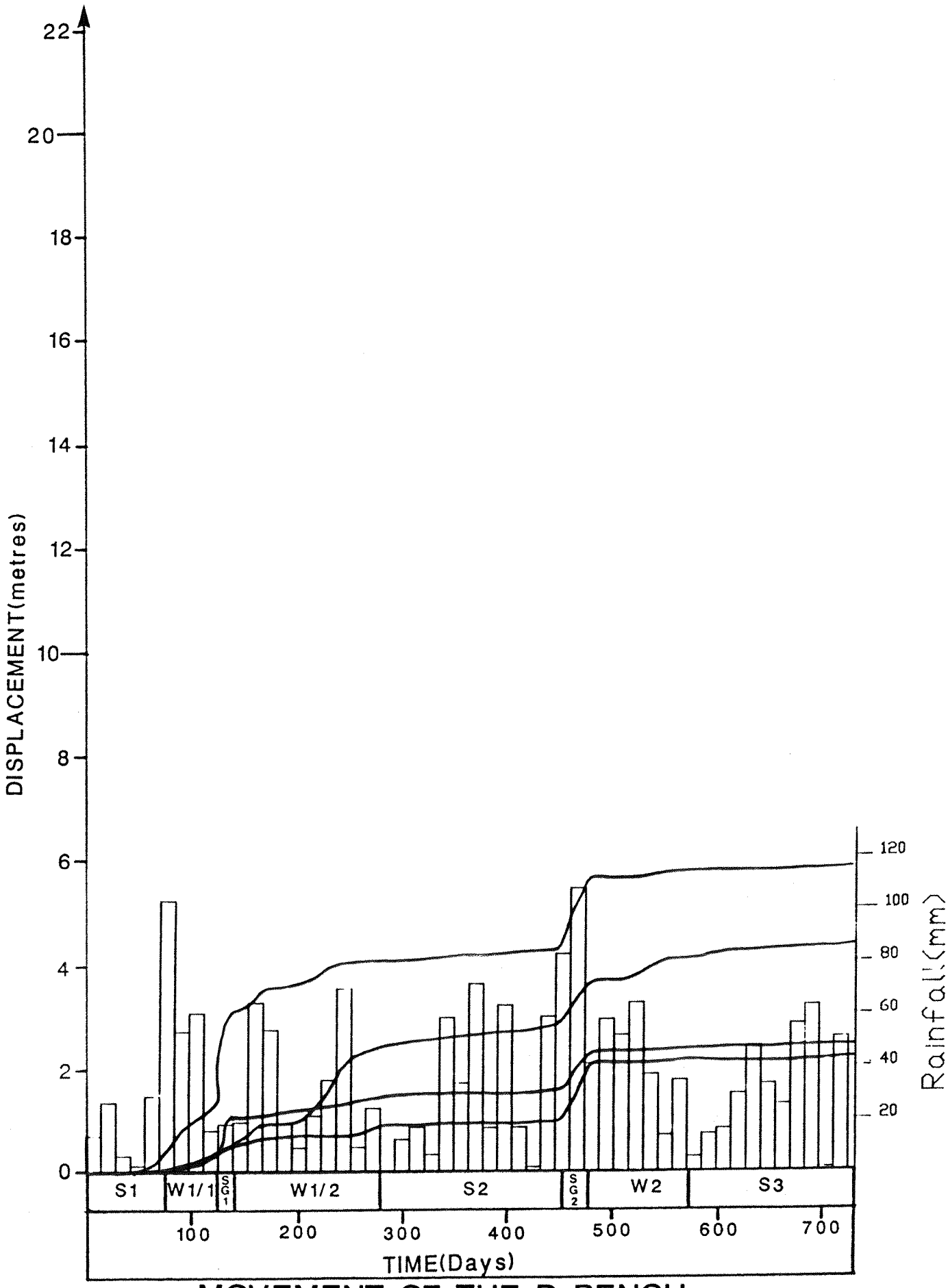

MOVEMENT OF THE D BENCH DURING THE STUDY PERIOD

FIG 8-5

(For dates see Fig.8-3)

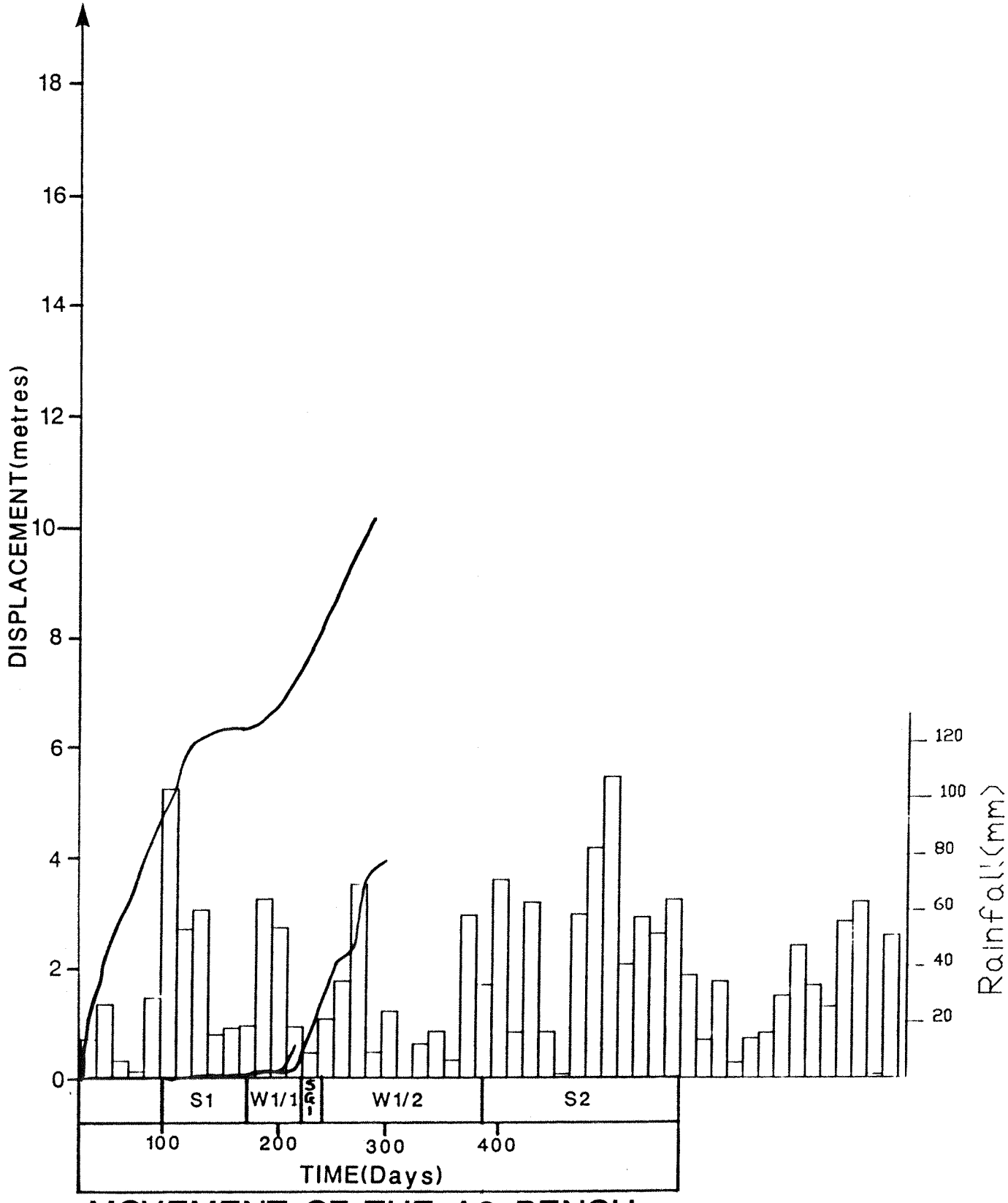

MOVEMENT OF THE A3 BENCH

FIG 8-6

(For dates see Fig.8-3)

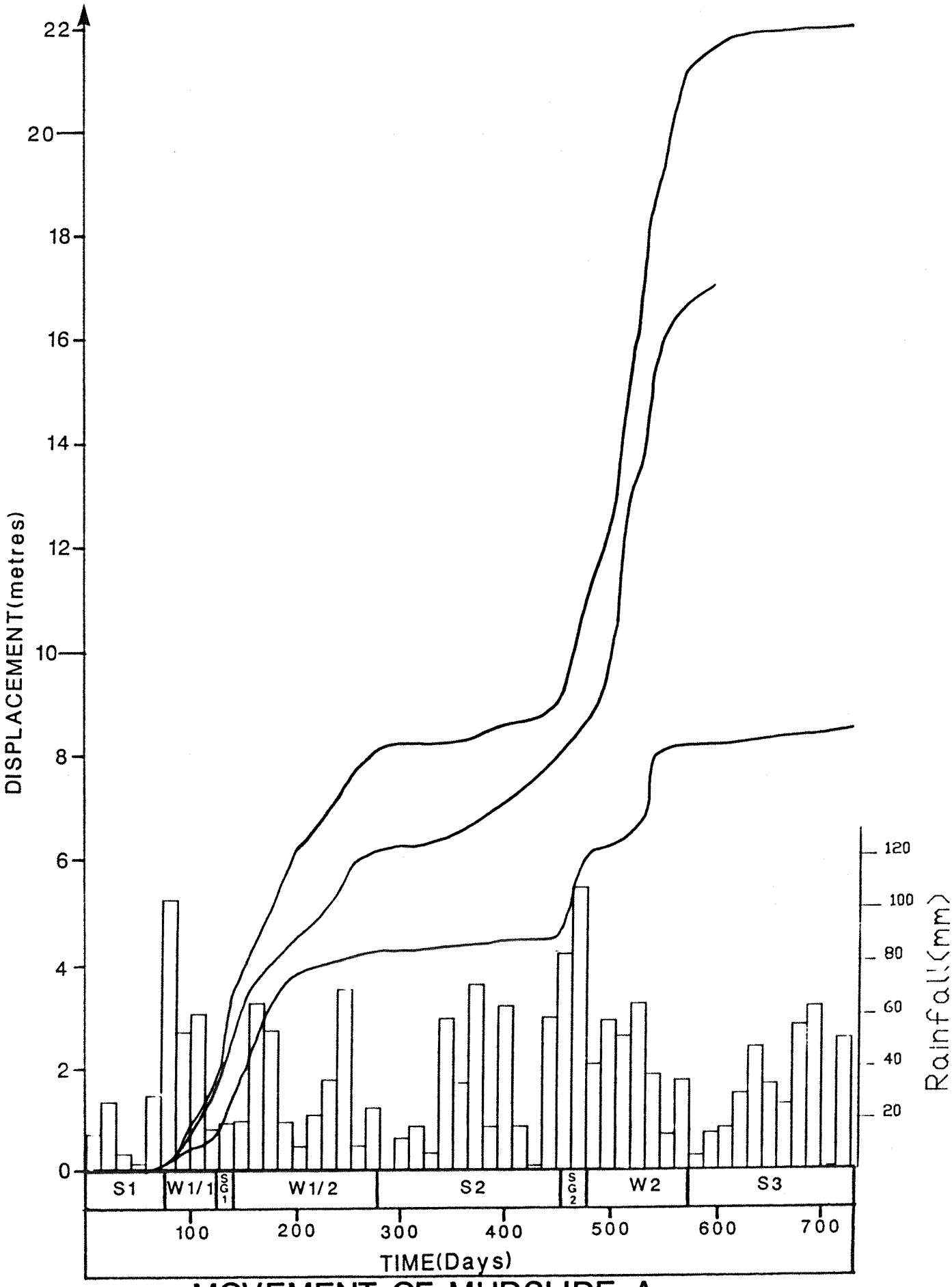

MOVEMENT OF MUDSLIDE A DURING THE STUDY PERIOD

FIG 8-7

(For dates see Fig.8-3)

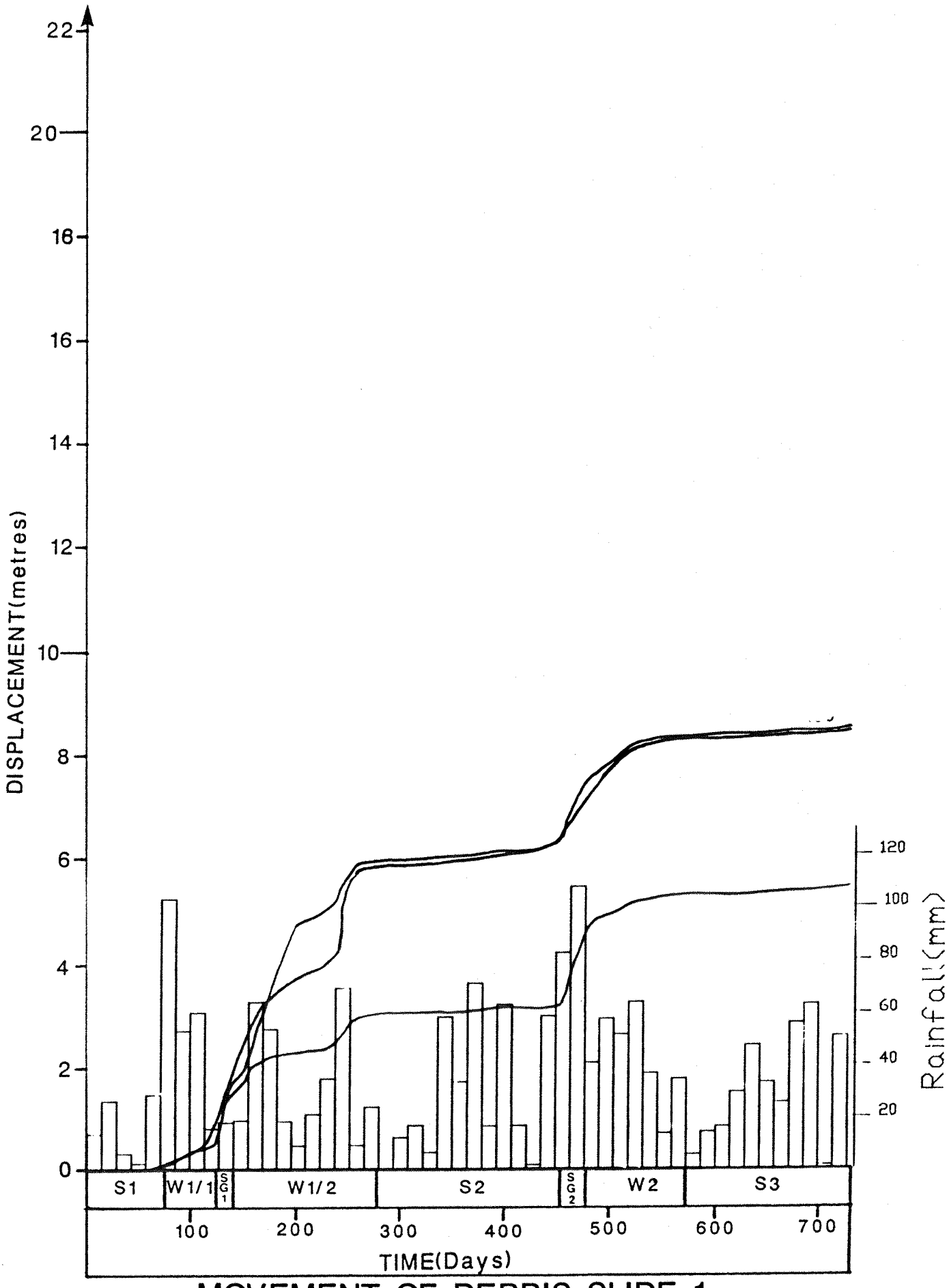

MOVEMENT OF DEBRIS SLIDE 1
DURING THE STUDY PERIOD

FIG 8-8

(For dates see Fig.8-3)

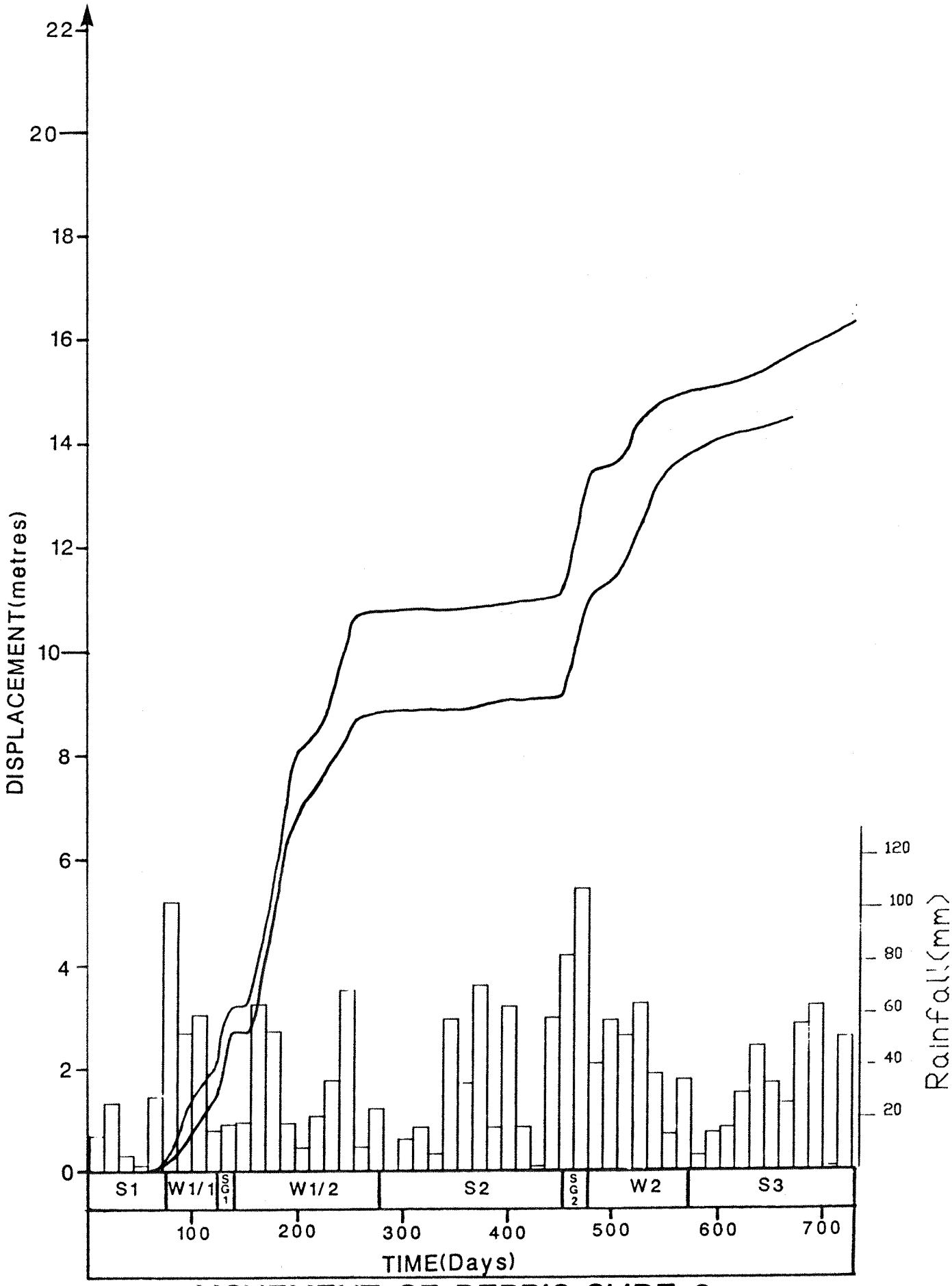

MOVEMENT OF DEBRIS SLIDE 2
DURING THE STUDY PERIOD

FIG 8-9

(For dates see Fig.8-3)

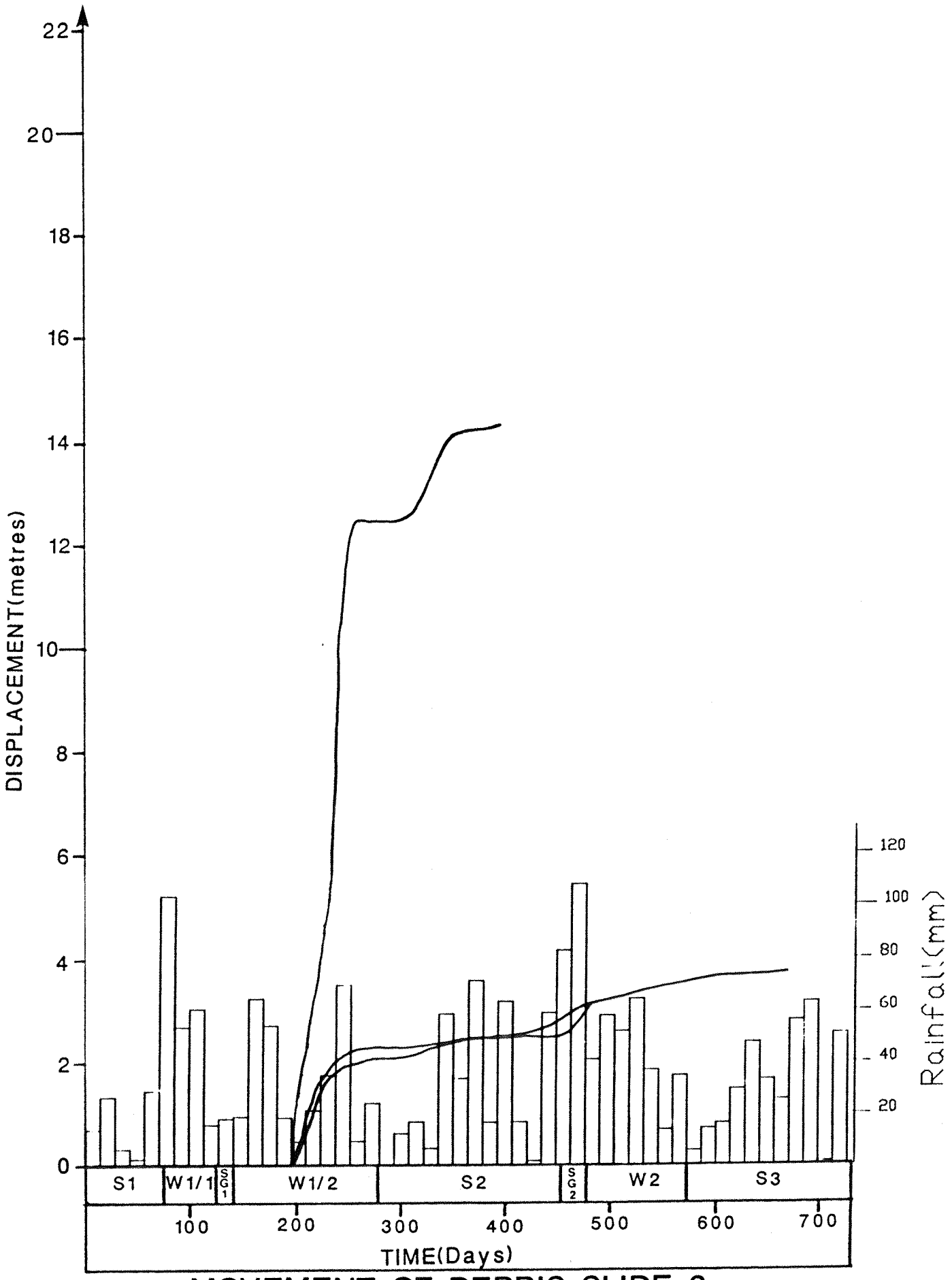

MOVEMENT OF DEBRIS SLIDE 3
DURING THE STUDY PERIOD

FIG 8-10

(For dates see Fig.8-3)

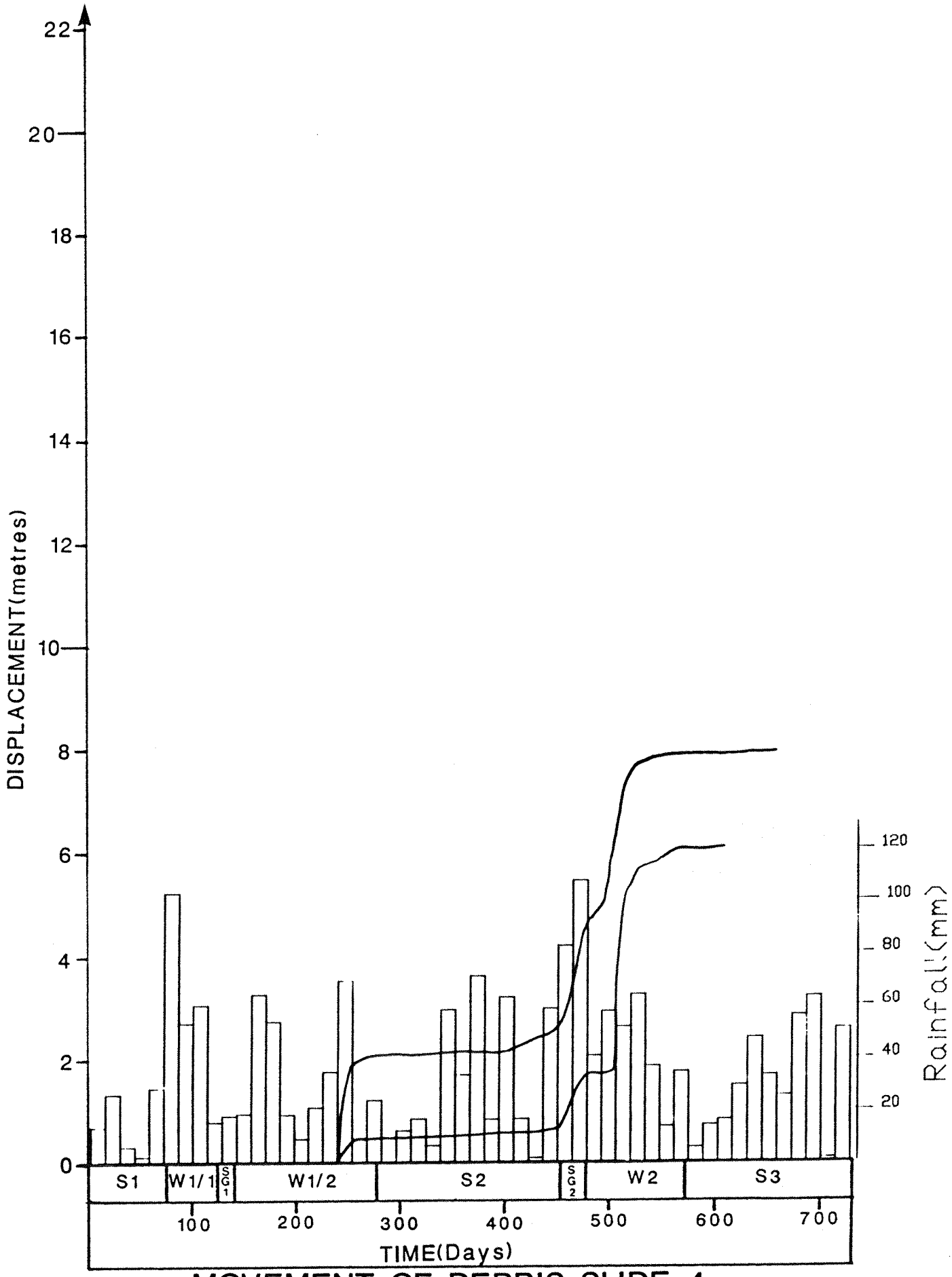

MOVEMENT OF DEBRIS SLIDE 4
DURING THE STUDY PERIOD

FIG 8-11

(For dates see Fig.8-3)

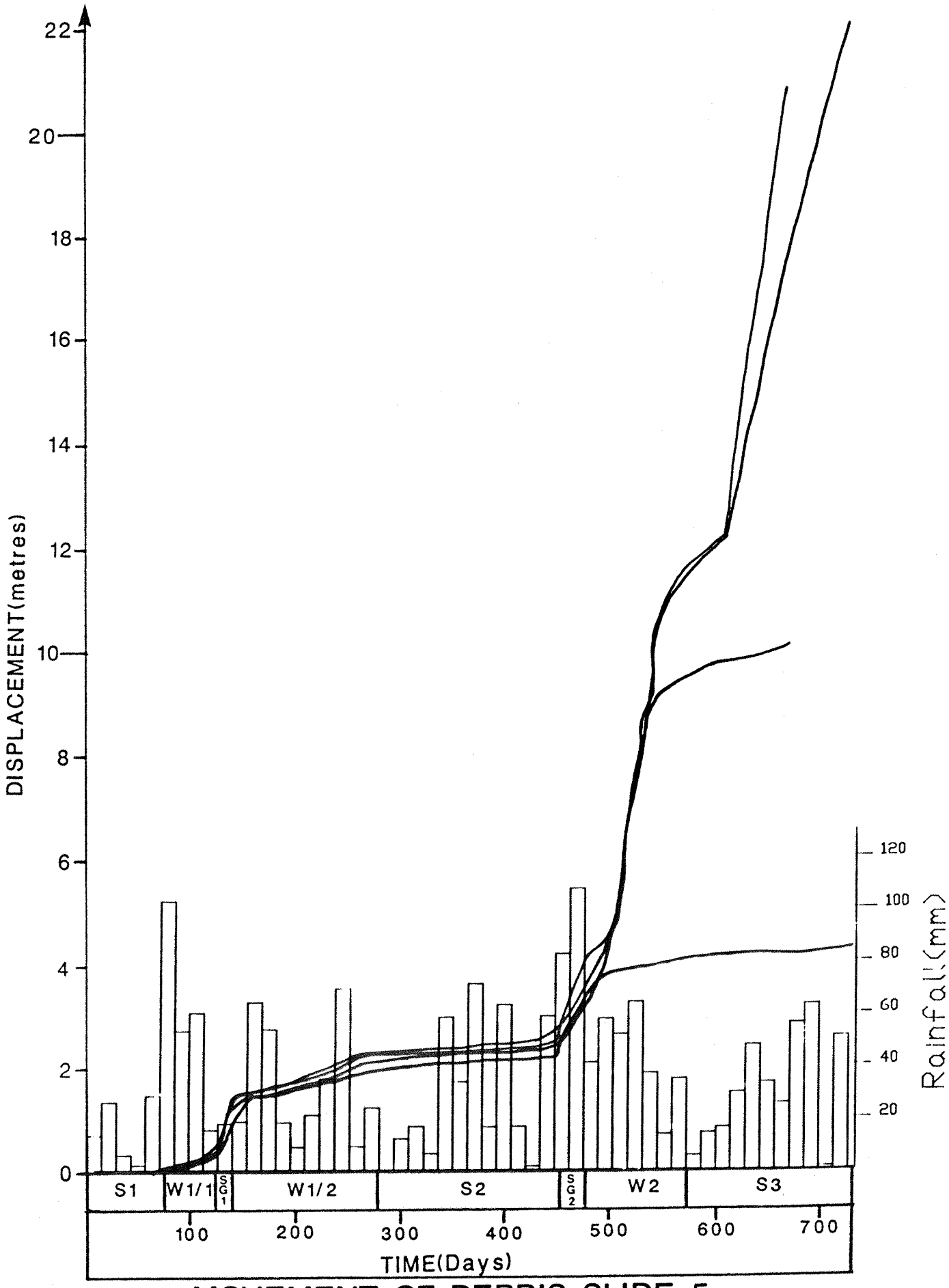

MOVEMENT OF DEBRIS SLIDE 5
DURING THE STUDY PERIOD

FIG 8-12

(For dates see Fig.8-3)

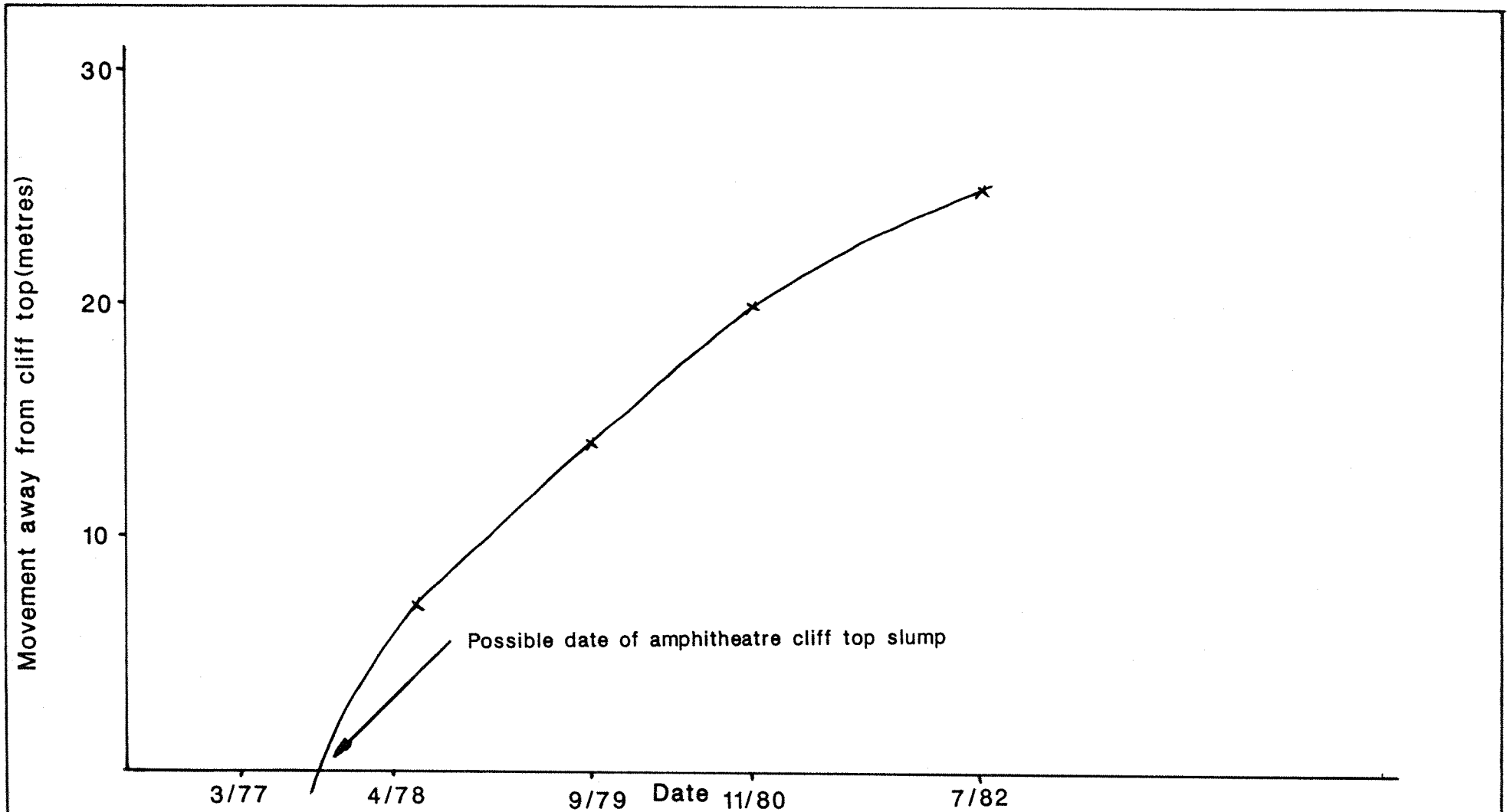

ESTIMATION OF THE DATE OF THE AMPHITHEATRE CLIFF TOP FAILURE FIG 8-13

AMPHITHEATRE SLUMP FAILURE(March 1977)

FIG 8-14

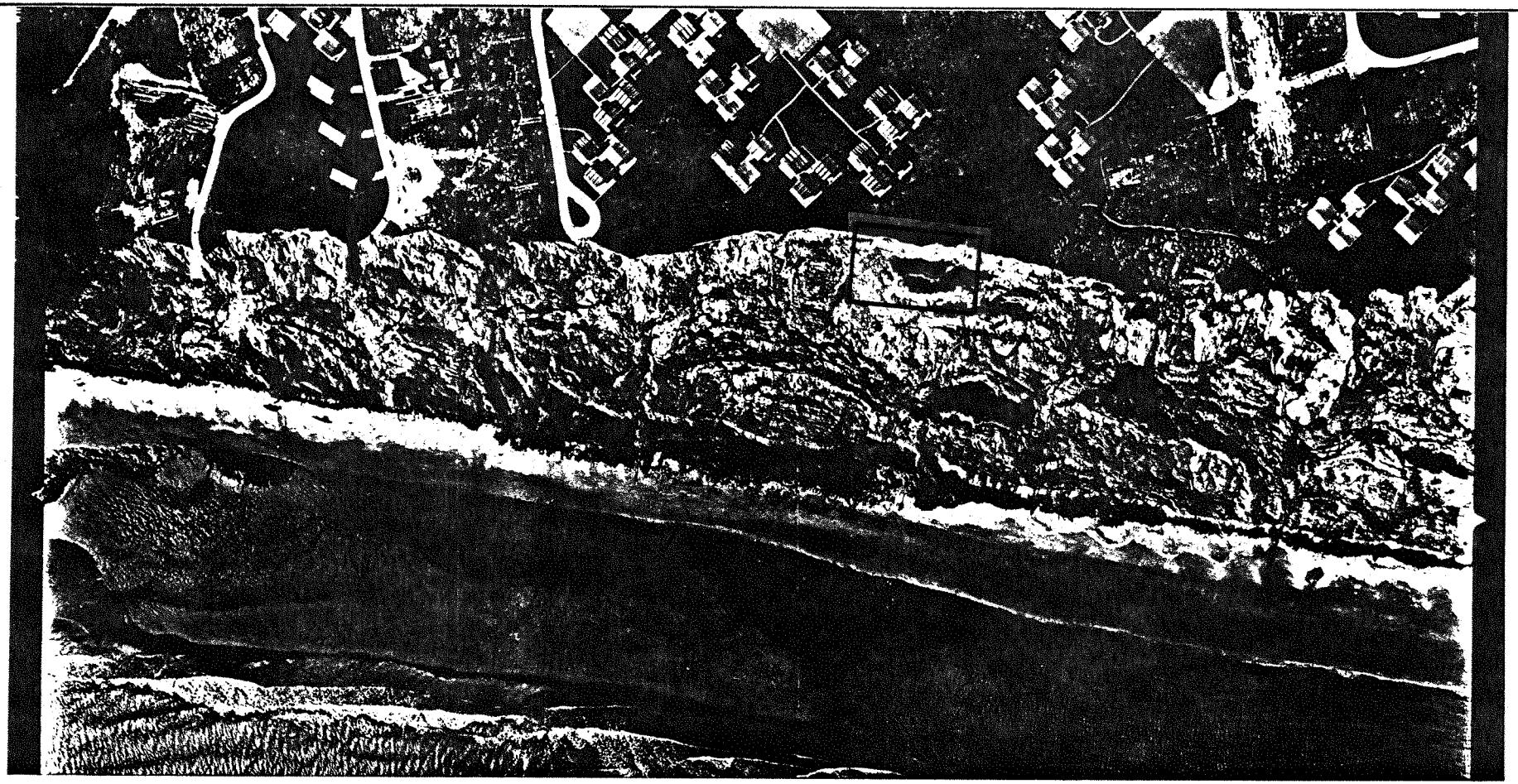

AMPHITHEATRE SLUMP FAILURE(April 1978)

FIG 8-15

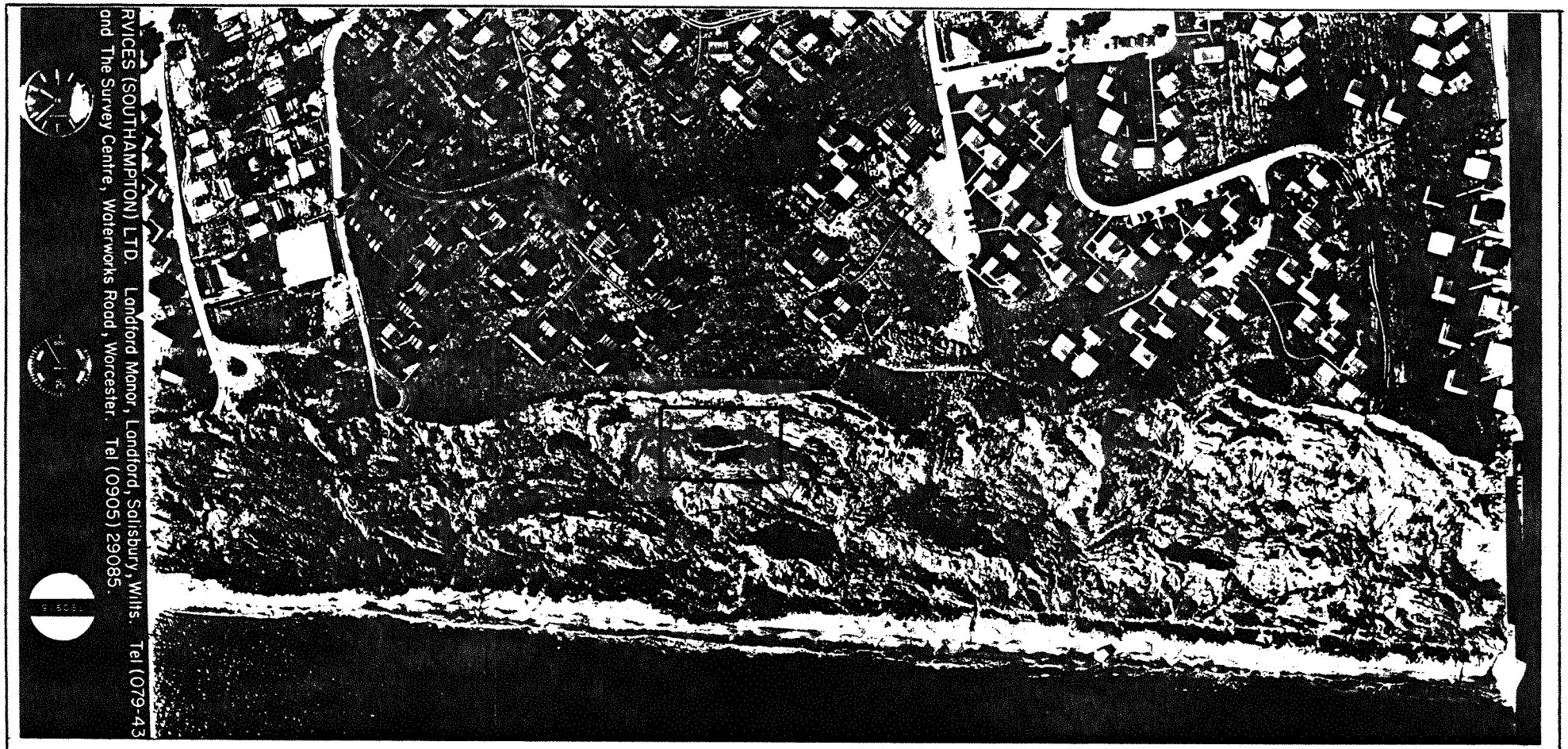

AMPHITHEATRE SLUMP FAILURE(Sept 1979)

FIG 8-16

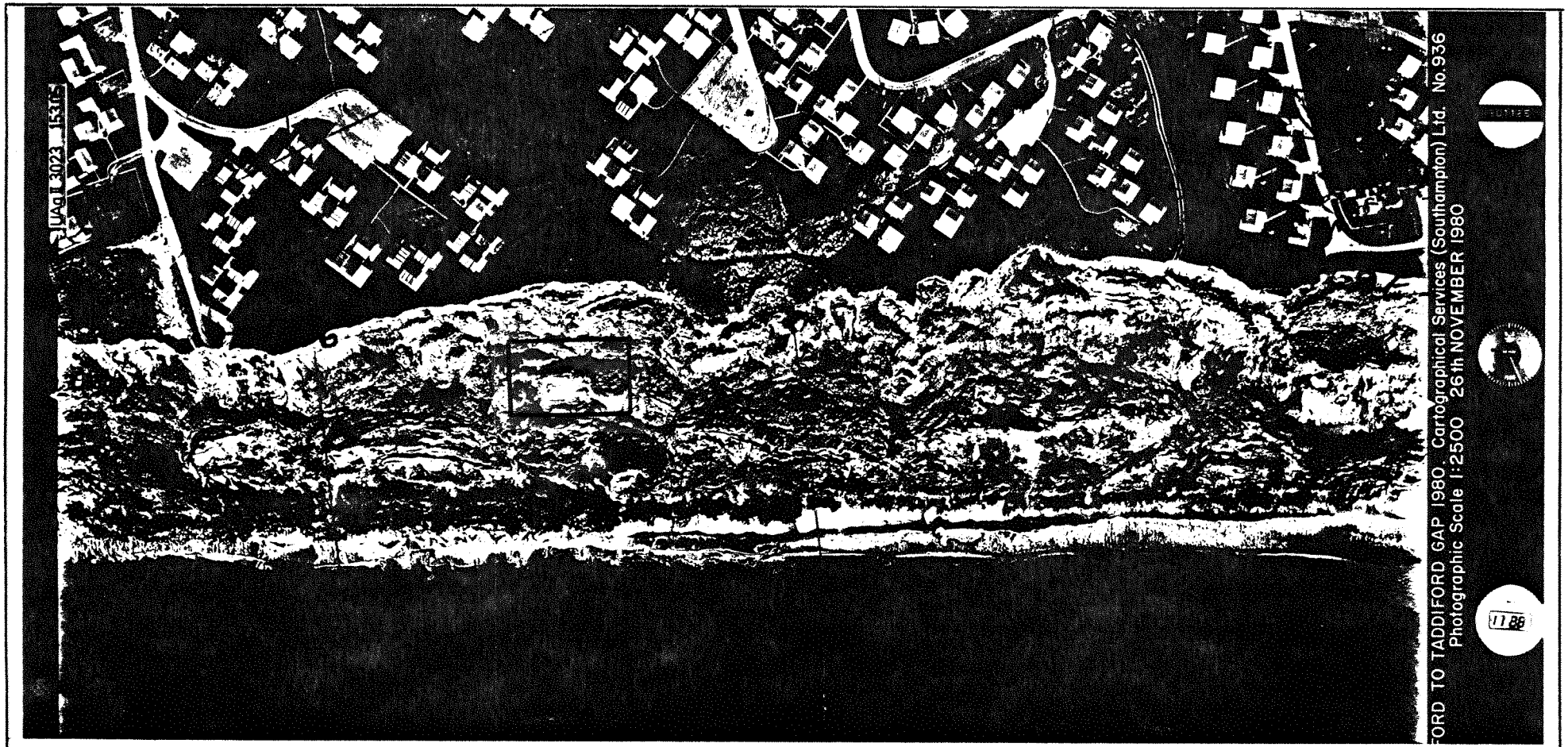

AMPHITHEATRE SLUMP FAILURE(Nov 1980)

FIG 8-17

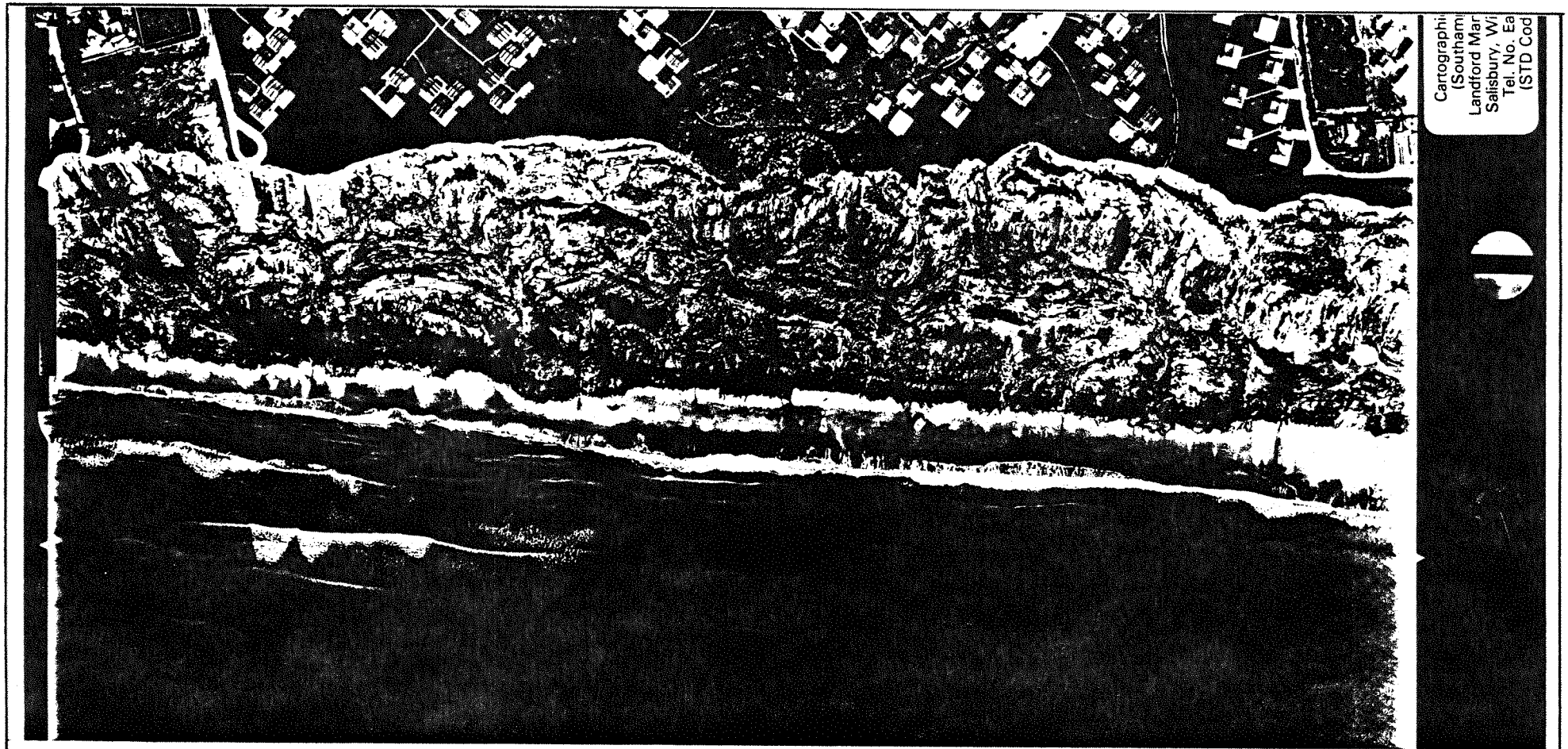

AMPHITHEATRE SLUMP FAILURE(July 1982)

FIG 8-18

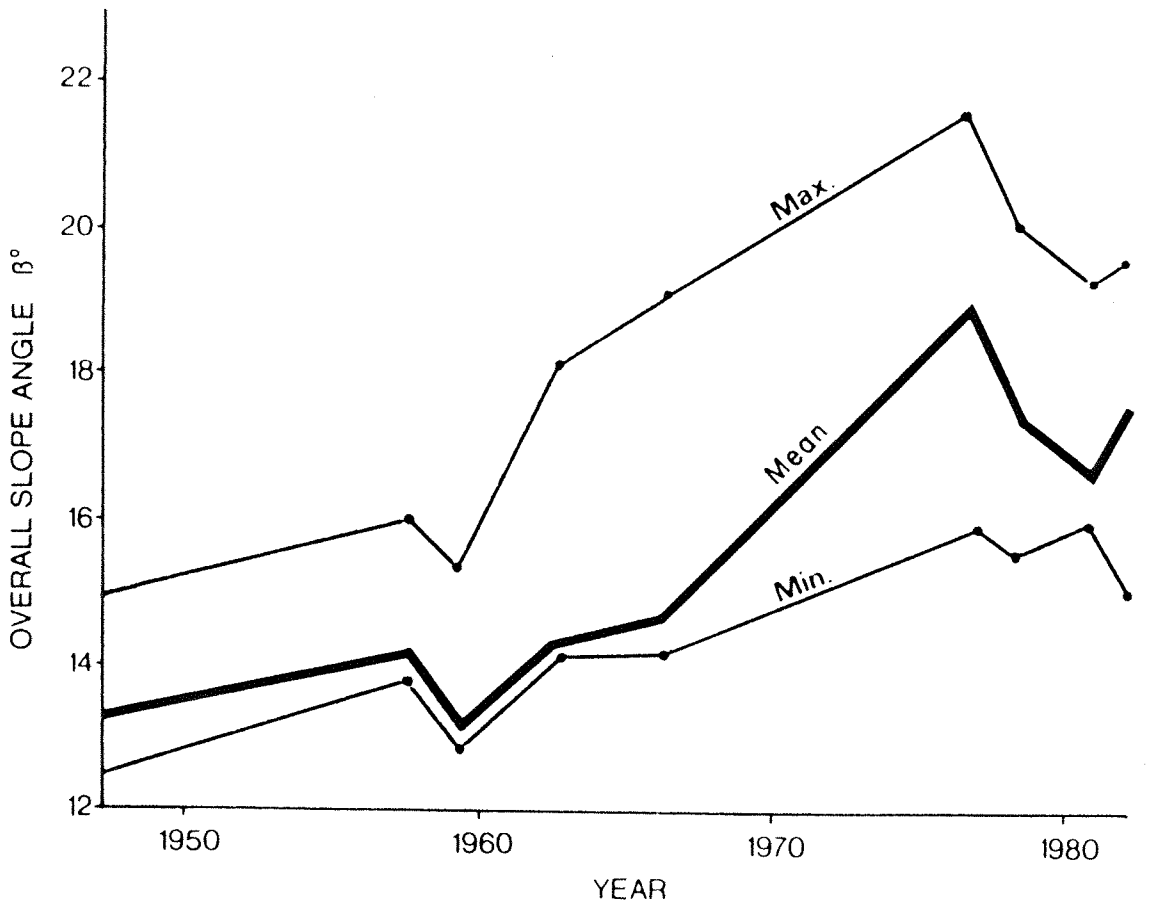

STUDY AREA SLOPE ANGLES
(After Barton and Coles,1984)

FIG 8-19

REFERENCES

ADMIRALTY, 1970. Direct methods of resection calculation, Nesbitt. In Admiralty Manual of Hydrographic Surveying, Vol 1, 360-63.

BAGNOLD, R. A. 1954. Experiments on a gravity-free dispersion of large solid spheres in a Newtonian fluid under shear. Proc. Royal. Soc. Lond, Ser. A - 225 pp 49-63.

BAGNOLD, R. A. 1954. The flow of cohesionless grains in fluids. Phil. Trans. Royal. Soc. Lond, Ser A - 249, pp 235-297.

BANNISTER, A. and RAYMOND, S. 1975. Surveying, Fourth impression, Pitman.

BARTON, M. E. Department of Civil Engineering, The University, Highfield, Southampton.

BARTON, M. E. 1973. The degradation of the Barton Clay cliffs of Hampshire. Q. J. Eng. Geol. London, 6, 423-40.

BARTON, M. E. 1984. Periglacial features exposed in the coastal cliff at Naish Farm, near Highcliffe. Proc. Hampshire Field Club and Archaeological Soc. Vol 40, 5-20, 1984.

BARTON, M. E. and COLES, B. J. 1981. The Relative Contribution of the Various Modes of Degradation to Overall Slope Retreat at Highcliffe, Hampshire. Progress Report to S.E.R.C. on GR/B.10243, January 1981.

BARTON, M. E. and COLES, B. J. 1982. The Overall Pattern and Rates of Movement in the Undercliffs at Naish Farm, Highcliffe, Hampshire. Progress Report to S.E.R.C. on GR/B/10243, October 1982.

BARTON, M. E. and COLES, B. J. 1983a. Rates of movement of soil slopes in southern England using inclinometers and surface peg surveying. Int. Sym. Field Measurements in Geomechanics. Zurich. 609-18.

BARTON, M. E. and COLES, B. J. 1983b. Application of Cliff Slope Degradation Studies to the Design of Slope Stabilisation and Coast Protection Work. Final Report to S.E.R.C. Contract GR/B/10243, December 1983.

BARTON, M. E. and COLES, B. J. 1984. The characteristics and rates of the various slope degradation processes in the Barton Clay Cliffs of Hampshire. Q.J. Eng. Geol. London, 17, 117-136.

BARTON, M. E. and THOMSON, R. I. 1984. Studies of the Water Balance in a rapidly degrading soil cliff. 4th Int. Sym. on Landslides. Toronto, Canada.

BARTON, M. E., COLES, B. J. and TILLER, G. R. 1983. A statistical study of the cliff top slumps in parts of the Christchurch Bay Coastal Cliffs. Earth. surf. processes land. 8, 409-22.

BISHOP, A. W. 1954. The use of the slip circle in the stability analysis of slopes. Geotech, 5, pp 7-17.

BISHOP, A. W., GREEN, G. E., GARGA, U. K., ANDERSON, A. and BROWN, J. D. 1971. A new ring shear apparatus and its applications to the measurement of residual strength. Geotech. 21, 273-328.

BROMHEAD, E. N. 1978. Large landslides in London Clay at Herne Bay, Kent. Q. J. Eng. Geol. London, 11, 293-304.

BROMHEAD, E. N. 1979. Factors affecting the transition between the various types of mass movement in coastal cliffs consisting largely of over consolidated clay with special reference to Southern England. Q. J. Eng. Geol. London, 12, 291-300.

BROMHEAD, E. N. 1987. The stability of slopes. Published by Surrey University Press.

BROMWELL, L. G., RYAN, C. R. and TOTH, W. E. 1971. Recording inclinometer for measuring soil movement. Proc. 4th. Pan. Am. Conf. Soil Mech. Puerto Rico. 2, 333-43.

BRONSHTEIN, I. N. and SEMENDYAYEV, K. A. 1973. A guidebook to Mathematics, Springer - Verlad.

BRUNSDEN, D. 1973. The application of system theory to the study of mass movement, Geologic. Applica E. Idrogeologica 8, 185-207.

BRUNSDEN, D. 1974. The degradation of a coastal slope, Dorset, England, Inst. Br. Geogr. Sepc. Pub 7, 79-98.

BRUNSDEN, D. and JONES, D. K. C. 1972. The morphology of a degraded landslide slope in South West Dorset. Q. J. Eng. Geol. London, 5, 205-222.

BRUNSDEN, D. and JONES, D. K. C. 1976. The evolution of landslide slopes in Dorset. Phil. Trans. Roy. Soc. London (A), 283, 605-31.

BRUNSDEN, D. and JONES, D. K. C. 1980. Relative time scales and formative events in coastal landslide systems. Zeits. Geomorphol. Supplement 34, Coasts under stress, 1-19.

BURLAND, J. B. LONGWORTH, T. I. and MOORE, J. F. A. 1978. A study of ground movement and progressive failure caused by deep excavation in Oxford Clay. Building Research Establishment, CP 33/78.

BURTON, E. ST. J. 1925. The Barton beds of Barton Cliff. Report. Brit. Assn. Advancement Sci. (Southampton). Section Transaction C, 312-14.

BURTON, E. ST. J. 1929. The Horizons of Bryozoa (Polyzoa) in the Upper Eocene Beds of Hampshire. Q. J. Geol. Soc. London, 85, 223-39.

BURTON, E. ST. J. 1931. Periodic changes in position of the run at Mudeford, near Christchurch, Hants, Proc. Geol. Assoc. 42, 157-74.

BURTON, E. ST. J. 1933. Faunal Horizons of the Barton Beds in Hampshire. Proc. Geol. Assoc. 44 , 131-67.

CHANDLER, R. J. 1972. Periglacial mudslides in Vestspitbergen and, their bearing on the origin of fossil 'solifluction' shears in low angled clay slopes. Q.J. Eng. Geol. London, 5, 223-241.

CHANDLER, R. J. 1977. Back analysis techniques for slope stabilization works: a case record. Geotech. 27, No. 4, 479-495.

CHANDLER, R. J., PACHAKIS, M., MERCER, J. and WRIGHTMAN, J. 1973. Four long-term failures of embankments founded on areas of landslip. Q. J. Eng. Geol. London, 6, 405-422.

CHATWIN, C. P. 1960. The Hampshire Basin and adjoining areas. Mem. Geol. Surv. HMSO, London.

CHOWDHURY, R. Slope Analysis. Published by Elsevier.

CHRISTIANSEN, E. A. The Denholm landslide, Saskatchewan Part 1: geology. Canada. Geotech. J. 20.

CLARK, M. J., RICKETTS, P. J. and SMALL, R. J. 1976. Barton does not rule the waves. Geog. Mag. Vol 48, 10, 580-588.

COLES, B. J. 1983. Periodic Surveying of the Undercliffs at Naish Farm, Highcliffe, Survey Data from S.E.R.C. Research Contract GR/B/1-0243, December 1983.

CORINGTON, T. 1870. The superficial deposits of the South Hampshire and the Isle of Wight. Q. J. Geol. Soc. 24, 528-51.

CURRY, D. 1958. The Barton Area. Highcliffe, Barton, Hordle Cliff and Milford-on-Sea, Hampshire.

CURRY D. 1965. The Palaeogene beds of South-east England. Proc. Geol. Assn. 76, 151-73.

DE FREITAS, M. H. and WATTERS, R. J. 1974. Some field examples of toppling failure. Geotech, 23, 495-514.

EARLY, K. R. and SKEMPTON, A. W. 1972. Investigations of the landslide at Walton's Wood, Staffordshire, Q. J. eng. Geol. London 5, 19-41.

EVERARD, C. E. 1954. The Solent river - a geomorphological study, I.B.G. Trans. and Papers No. 20, 41-58.

FISHER, G. C. 1971. Brickearth and its influence on the character of soils in the South-East, New Forest. Proc. Hants. Field Club Archaoel. Soc. 28, 99-109.

FISHER, G. C. 1975. Terraces, soil and vegetation in the New Forest, Hampshire, Area 7, 255-61.

FUKUOKO, M. 1953. Landslides in Japan. Proc. 3rd Int. Conf. Soil mech. (Zurich), 2, 234-238.

GARDNER, J., KEEPING, H. and MONCKTON, H. W. 1888. The Upper Eocene comprising the Barton and Upper Bagshot formations, Q. J. Geol. Soc. Vol 44, 578-635.

GILKES, R. J. 1968. Clay mineral provinces in the Tertiary Sediments of the Hampshire basin. Clay Minerals, 7, 351-61.

GREEN, G. E. 1973. Principles and performance of two inclinometers for measuring horizontal ground movements. Symposium on Field Instrumentation in Geotechnical Eng. (Proc. of a Conf. in 1973, Inst. of Electrical Eng.) Butterworths, pp 166-179.

GRANTHAM, R. F. 1895. Report inquiring into the Rate of Erosion of the Sea-coasts of England and Wales, and the influence of the Artificial Abstraction of Shingle or other Material in that Action. Appendix III 372-373.

SIR WILLIAM HALCROW AND PARTNERS (1971). Report on the design of the coastal defence works at Highcliffe, Hampshire.

HATRLEY, J and LOCKE, A. A. 1912. Chapter on Christchurch Hundred in Victoria County History, Hampshire Vol. 5, 84. London.

HENDERSON, G. and WEBBER, N. W. 1977. Storm surge in the UK south coast. The Dock and Harbour Authority, May, 21-22.

HENDERSON, G and WEBBER, N. W. 1979. The application of wave refraction diagrams to shoreline protection problems: with particular reference to Poole and Christchurch Bays. Q. J. Eng. Geol. London, Vol 12, 319-27.

HO, E. W. L. 1982. The residual strength of the Barton Clay. B.Sc. project. Dept of Civil Eng. University of Southampton.

HOOKER, J. J. 1975. Report of a field meeting to Barton-on-Sea, Hampshire. Tertiary Times, Vol 2, 4, 163-167.

HUTCHINSON, J. N. 1967. The free degradation of London Clay cliffs. Vol. 1 Proceedings of the Geotechnical Conference, Oslo.

HUTCHINSON, J. N. 1968a. "Mass Movement", in Encyclopedia of Geomorphoogy. Edited by Fairbridge, R.W. Reinhold, New York, pp 668-695.

HUTCHINSON, J. N. 1968b. Field meeting on the coastal landslides of Kent, 1-3 July 1086. Proc. Geol. Ass. 79, pp 227-237.

HUTCHINSON, J. N. 1969. A reconsideration of the coastal landslides at Folkstone Warren, Kent. Geotech. 19, 6-38.

HUTCHINSON, J. N. 1970. A coastal mudflow on the London Clay cliffs at Beltinge, North Kent. Geotech 20, 412-38.

HUTCHINSON, J. N. 1972. Field and laboratory studies of a fall in chalk cliffs at Jos Bay, Isle of Thanet. Stress-Strain Behaviour of Soils: Proceedings of the Roscoe Memorial Symposium; Cambridge, U.K. Foulis, Henley-on-Thames, pp 692-706.

HUTCHINSON, J. N. 1973. The response of London Clay cliffs to differing rates of toe erosion. Geol. Applicata E. Idrogeol. Bari, Italy, 8, 221-39.

HUTCHINSON, J. N. 1977. Assessment of the effectiveness of corrective measures in relation to geological conditions and types of slope movement. General Report on Theme 3 Symposium on Landslides and other Mass Movements, Prague, September 1977. Bulletin International Association of Engineering Geology, No. 16, pp 141-155. Reprinted (1978) in Norwegian Geotechnical Institute Publication, No. 124, pp 1-25.

HUTCHINSON, J. N. 1980. Various forms of cliff instability arising from coast erosion in the U.K. Fjellsprengningsteknikk - Bergmekanikk - Geoteknikk 1979: 19.1 - 19.32. Trongheim: Tapir, for Norsk Jord- og Fjellteknisk Forbund tilknyttet N.I.F.

HUTCHINSON, J. N. 1983. A pattern in the incidence of major coastal mudslides. Earth. surf. processes Land, 8, 391-7.

HUTCHINSON, J. N. 1984. An influence line approach to the stabilisation of slopes by cuts and fills. Canad. Geotech. J. 21: 363-370.

HUTCHINSON, J. N. and BHANDARI, R. K. 1971. Undrained loading, a fundamental mechanism of mudflows and other mass movements. Geotech. 21, 353-358.

HUTCHINSON, J. N. and GOSTELOW, T. P. 1976. The development of an abandoned cliff in London Clay at Hadleigh, Essex,. Phil. Trans. Roy. Soc. London (A), 283, 557-604.

HUTCHINSON, J. N. and HUGHES, M. J. 1968. The application of micropalaeontology to the location of a deep seated slip surface in the London Clay. Geotech. 18, 508-10.

HUTCHINSON, J. N., BROMHEAD, E. N. and LUPINI, J. F. 1980. Additional observations on the Folkestone Warren landslides. Q. J. Eng. Geol. London, 13, 1-31.

HUTCHINSON, J. N., CHANDLER, M. P. and BROMHEAD, E. N. 1981. Cliff recession on the Isle of Wight S. W. Coast. Proc. 10th. Int. Conf. Soil, Mech. Found. Eng. Stockholm, 1, 429-34.

HUTCHINSON, J. N., PRIOR, D. B. and STEPHENS, N. 1974. Potentially dangerous surges in an Antrim mudslide. Q. J. Eng. Geol. London, 7, 363-76.

HUTCHINSON, J. N., SOMERVILLE, S. H. and PETLEY, D. J. 1973. A landslide in periglacially disturbed Etruria Marl at Bury Hill, Staffordshire, Q. J. Eng. Geol. London, 6, 377-404.

JACKLI, H. 1957. Gegenwartsgeologie des bundnezischen Rheingebietes. Bieitr, Zur Geol - der Schweiz. geotechn. Serve: 36, Bern.

JANBU, N. 1956, Stability analyses of slopes with dimensionless parameters. Havard soil mechanics series, No. 46, pp 1-81.

JANBU, N. 1973. Slope Stability Computations. In Embankment - Dam Engineering, Casagrande Volume, 47-86.

JOHNSON, A. M. and RAHA, P. H. 1970. Mobilization of debris flows. Zeits. Geomorph. Supplement 9. New Contributions to Slope Evolution. 168-86.

JONES, D. K. C., BRUNSDEN, D. and GOODIE, A. S. 1983. A preliminary geomorphological assessment of part of the Karaiorom Highway. Q. J. Eng. Geol. London, 16, 319-330.

KEEN D. H. 1980. The environment of deposition of the South Hampshire plateau gravels. Proc. Hants Field Club Archaeol. Soc. 36, 15-24.

KELLAWAY, G. A. 1971. Glaciation and the Stones of Stonehenge - Nature, 233, 30-5.

KELLAWAY, G. A., REDDING J. H., SHEPARD-THORN, E. R., DESTOMBES, J.P. 1975. The Quaternary history of the English Channel. Phil. Trans. Royal. Soc. (A) 279, 189-218.

KILBOURN, P. C. R. 1971. Further studies of the Barton Clay coastal exposure at Highcliff, Hants, M.Sc. project. Dept. of Civil Eng. University of Southampton.

MARSLASND, A and BUTLER, M. E. 1967. Strength Measurements on stiff fissured Barton Clay from Fawley (Hants) Proc. Geoteh. Conf. Oslo. 1, 139-146.

MAUGERI, M., COSTA, C. P. and RANDAZZO, F. 1981. Reliability of the Inclinometer Measurements. Proc. 11th Int. Conf. S.M.F.E. Stockholm 2, 591-622.

McROBERTS, E. C. and MORGENSTERN, N. R. 1974. The stability of thawing slopes. Can. Geotech. Journal. 11, pp 447-469.

MELVILLE, R. V. and FRESHNEY, E. C. 1982. The Hampshire Basin and adjoining areas. Mem. Institute of Geological Sciences. HMSO.

MERRIAM, R. 1960. Portuguese Bend landslides. Palos Verdes Hills, California, Journal of Geology, 68, 140-153.

MITCHELL, R. J. and EDEN, W. J. 1972. Measured movement of clay slopes in the Ottawa area. Canadian Journal of Earth Science, 9, 1001, 8. 1001-13.

MOCKERIDGE, R. G. 1982. Highcliffe cliffs - the maintenance of coastal slopes. Proc. Conf. Shoreline Protection, Southampton, 1982, Inst. Civil Eng. 235-42.

MORGENSTERN, N. R. and PRICE, V. E. 1968. The analysis of the stability of general slip surfaces. Geotech. 15 pp 79-93.

MORGENSTERN, N. R. and TCHALENKO, J. S. 1967. Microstructural observations on shear zones from slips in natural clays. Proc. Geotech. Conf. 1, 147-52.

MUIR WOOD, A. M. 1967. Coastal Stabilisation at Barton-on-Sea, Civil Engineering and Public Works Review, December 1967, 1401-1402.

MUIR WOOD, A. M. 1971. Engineering aspects of coastal landslides. Proc. Inst. Civil. Eng. 50, 257-76.

NICHOLLS, R. Dept of Civil Eng. University of Southampton, Highfield, Southampton, SO9, 5NH.

PACK, R. T., KEATON, J. R., JEPSON, R. N. and ANDERSON, L. R. 1984. The 1983 Utah Landslide Disaster. Proc. 4th. Int. Sym. on Landslides, Toronto, Vol 1 pp 693-698.

PENMAN, A. D. M. and CHARLES, J. A. 1974. Measuring movements of embankment dams. In Field Instrumentation in Geotechnical Engineering, Wiley, New York, 359-69.

PITTS, J. 1983. Geomorphological observations as aids to the design of coast protection works on a part of the Dee estuary. Q. J. Eng. Geol. London, 16, 291-300.

PRIOR, D. B. and RENWICK, W.H. 1980. Landslides morphology and processes on some coastal slopes in Denmark and France. Zeits. Geormorph. Supplement 34. Coasts under stress, 63-86.

PRIOR, D. B and STEPHENS, N. 1971. A method of monitoring mud flow movements, Eng. Geol. 5, 239-2436.

PRIOR, D. B. and STEPHENS, N. 1972. Some movement patterns of temperate mudflows: example from North Eastern Ireland. Bull. Geol. Soc. Am. 83, 2533-44.

PRIOR, D. B., STEPHENS, N. and ARCHER, D. R. 1968. Composite mudflows on the Antrim Coast of North East Ireland. Geog. Annlr. Ser. A. 50, 65-78.

RAPP, A. 1960. Recant developments of mountain slopes in Karkevagge and surroundings, Northern Scandinavia. Geografiska Annaler, 42, 65-200.

RIB, H. T. and LIANG, T. 1978. Chapter 3: Recognition and Identification, In: SCHUSTER, R. L. and KRIZEK, R. J. (eds). Landslides Analysis and Control. Special Report 176, Transportation Research Board, U.S.A.

RICO, A., SPRINGHALL, G. and MENDOZ, A. 1976. Investigations of instability and remedial works on the Tijuana-Ensenada Highway, Mexico, Geotech, 26, 577-590.

SAITO, M. 1965. Forecasting the time of occurrence of a slope failure. Proc. 6th Int. Conf. Soil Mech. Found, Eng. Montreal 2, 537-41.

SAUER, E. K. 1983. The Denholm landslide, Saskatchewan, Part II: analysis, Canad, Geotech. J. 20, 208-220.

SCHUMM, S. A. 1956. The evolution of drainage systems and slopes in badlands at Perth Amboy, New Jersey, Geol. Soc. Am. Bull, 67, 597-646.

SHUISKY, Y. D. 1979. Some problems of coastal zone sediment budget studies (with references to the Black Sea coast of the Ukrainian SSR). Geomorphology (Moscow): U4, 89-97 (in Russian).

SIDLE, R. C. and SWANSTON, D. N. 1982. Analysis of a small debris slide in Coastal Alaskwa. Canad. Geotech. J. 19, 167-74.

SILVESTER, R. 1960. Stabilisation of sedimentary coastlines. Nature, Vol. 199. No. 4749, 467-469.

SILVERSTER, R. 1972. Growth of crenulate shaped bays to equilibrium. Proc. Am Soc. Civil. Eng. 96, pp 275-287.

SILVESTER, R. 1974. Coastal Engineering Vol 2, Elsevier Publishing Company.

SILVESTER, R. 1976. Headland defence of coasts. Proc. 15th Int. Conf. Coastal Eng. A.S.C.E. 1394-1406.

SKEMPTON, A. W. 1964. Long term stability of clay slopes. 4th Rankine Lecture. Geotech. 14, 77-102.

SKEMPTON, A. W. 1985. Residual strength of clays in landslides, folded strata and the laboratory. Special lecture to the British Geotechnical Society, Geotech, 35, 3-18.

SKEMPTON, A. W. and DELROY, F. A. 1957. Stability of natural slopes in London Clay. Proc. 4th Int. Conf. Soil Mech. Found. Eng. London, 2, 378-81.

SKEMPTON, A. W. and HUTCHINSON, J. N. 1969. Stability of natural slopes and embankment foundations. Proc. 7th Int. Conf. Soil Mech. Found. Eng. Mexico, State of the Art. 291-340.

SKEMPTON, A. W. and La ROCHELLE, P 1965. The Bradwell Slip: A short term failure in London Clay. Geotech, 15, pp 221-242.

SKEMPTON, A. W. and PETLEY D. J. 1970. Ignition loss and other properties of peats and clays form Avonmouth, King's Lynn and Cranberry Moss. Geotech. 20, 4, 343-356.

SMITH, N. 1975. "Slope Stability Studies of the Barton Clay Cliffs at Barton-on-Sea, Hampshire". B.Sc Dissertation, University of Southampton.

STEWARD, H. E. and CRIPPS, J. C. 1983. Some engineering implications of chemical weathering of pyritic shale. Q. J. Eng. Geol. London, 16, 281-289.

STOPHER, H. E. and WISE, E. B. 1966. Coast erosion problems in Christchurch Bay. Journ. Inst. Mun. Eng. 93, 328-32.

SUMMERS, L. and MADDREL, L. 1978. Development of an alternative approach to coast protection. Southampton Regional Meeting, Eng. Group. Geol. Soc.

TCHALENKO, J. S. 1968. The microstructure of London Clay. Q. J. Eng. Geol. London 1, 155-168.

TER-STEPANIAN, G. I. and GOLDSTEIN, M. N. 1969. Multi-storied landslides and strength of soft clays. Proc. 7th Int. Conf. Soil Mech. Found Eng. Mexico, 2, 693-700.

TER-STEPANIAN, G. I. and TER-STEPANIAN, H. 1971. Analysis of landslides. Proc. 4th Conf. Soil. Mech. and Foundation Eng. (Budapest) pp 449-504.

TERZAGHI, K. V. 1936. The shearing resistance of saturated soils and the angle between the planes of shear. Proceedings of 1st Int. Conf. Soil. Mech. Foundation Eng. p 54-56, Vol 1.

TERZAGHI, K. V. and PECK, R. B. 1948. Soil Mechanics in Engineering Practice. Wiley.

THOMSON, R. I. 1983. Sub-surface investigations on the cliff top at Naish Farm, Highcliffe. Progress Report to S.E.R.C. Contract GR/B/70797. June 1983.

THOMSON, R. I. 1986a. Periodic surveying of instrumentation used to gather hydrological information at Naish Farm, Highcliffe. S.E.R.C. Contact GR/B/70797. Report No. 1986/1. Dept. of Civil Eng., University of Southampton.

THOMSON, R. I. 1986b. Piezometric Measurements at Naish Farm. Highcliffe. S.E.R.C. Contact GR/B/70797. Dept. of Civil Eng., University of Southampton.

THOMSON, R. I. 1986c. Soil Moisture measurements at Naish Farm, Highcliffe. S.E.R.C. Contact GR/B/70797. Dept. of Civil Eng., University of Southampton.

THOMSON, R. I. 1987. The hydrology of the degrading soil cliffs at Naish Farm, Hampshire. Ph.D. Thesis. Dept. of Civil Eng., University of Southampton.

TOMS, A. H. and BARTLETT, D. L. 1962. Application of soil mechanics in the design of stabilizing work for embankments, cuttings and track formation. Proc. I.C.E., 21, 705-11.

U. S. ARMY 1973. U.S. Army Coastal Engineering Research Centre. Shore protection manual, Vol. 1. Department of the Army Corps of Engineers.

VALLEJO, L. E. 1980. Mechanics of mudflow mobilization in low-angled clay slopes. Eng. Geol. 16, 63-70.

VARGAS, M. and PICHLER, E. 1957. Residual soil and rock slides in Santos (Brazil). Proc. 4th Int. Conf. Soil. Mech. Found. Eng. London, 2, 394-8.

VARNE, D. J. 1958. Landslides and Engineering Practice. Highway Research Board, Special Rept. 29.

VARNES, D. J. 1978. Chapter 2: Slope movement types and processes. In: SCHUSTER, R. L. and KRIZEK, R.J. (eds) Landslides Analysis and Control, Special Report 176, Transportation Research Board, U.S.A.

WARD, W. H. 1948. A coastal landslip. Proc. 2nd Int. Conf. Soil. Mech. Rotterdam 2, 33-38.

WEST, I. M. 1964. A rapid method for thin-sectioning clays. Sedimentology, 6, 339-341.

WHITE, H. J. O. 1917. The geology of the country around Bournemouth. Mem. Geol. Surv. G.B.

WILSON, S. D. 1959. Application of the principles of soil Mechanics to open pit mining. Quart. Colorado School of Mines, Symp. on Rock Mechs; Golden, Colorado, 54 No. 3.

WRIGHT, P. 1981. Aspects of the Coastal Dynamics of Poole and Christchurch Bays. Ph.D. thesis. University of Southampton.

ZARUBA, Q. and MENCL, V. 1969. Landslides and their control. Amsterdam: Elsevier, Prague; Academia.

APPENDICES

APPENDIX A: THE SURVEY METHOD AND ERRORS

APPENDIX A THE SURVEY METHOD AND ERRORS

A.0 Introduction

The method used to locate the survey pegs within the undercliff is briefly described in Chapter 3. In this appendix the theory, calculations and errors of this technique will be discussed.

A.1 The survey method

The reference co-ordinate system for the undercliff survey was based on a network of permanent stations established on the cliff top. Their position relative to each other and to the cliff top is shown in Fig. A-1. The grid was established by assigning co-ordinates to station C1 and designating the line which passes through both stations B1 and C1 as the x-axis. The co-ordinates for the remaining stations have been calculated from survey data.

A.2 The calculation of the theodolite position

To position the survey pegs the theodolite was set up on the undercliff. The theodolite was positioned by sighting onto stations C1 and B1. The remaining stations were used to establish the accuracy of the survey.

Stations B1 and C1 were sighted at the beginning and end of each survey. The geometric relationship between B1, C1 and the theodolite is given in Fig. A-2.

A.2.1 Symbols

PP = Prism pole height (m)

D_B = Inclined distance between the theodolite and station B1 (m)

V_B = Vertical circle reading from the theodolite to station B1

H_B = Horizontal circle reading from the theodolite to station B1

D_C = Inclined distance between the theodolite and station C1 (m)

V_c = Vertical circle reading from the theodolite to station C1

H_c = Horizontal circle reading from the theodolite to station C1.

DHB = Horizontal distance between the theodolite and station B1 (m)

DHC = Horizontal distance between the theodolite and station C1 (m)

t = Horizontal distance between station B1 and station C1(m)

$\emptyset_H$ = <B1 T C1

$\emptyset_C$ = <T C1 B1

$\emptyset_B$ = < C1 B1 T

$\emptyset$ = Horizontal circle reading which is perpendicular to the x - axis

Tx, Ty, Tz = Co-ordinates of theodolite

D_{VC} = Vertical distance from the theodolite to the prism head

A.2.2 Equations

$DHB = \text{Cos } V_b \times D_b$

$DHC = \text{Cos } Vc \times Dc$

$\emptyset_h = H_b - H_c$

$$t = \sqrt{D_{Hc}^2 + D_{HB}^2 - 2D_{HC}\, D_{HB} \text{ Cos } \emptyset_H}$$

$$\emptyset c = \text{Sin } \left(\frac{\text{Sin}\emptyset h \times Dhb}{t}\right)^{-1}$$

If $\emptyset_c < 90°$

$T_x = (D_{HC} \times \text{Sin}(90-\emptyset_c)) + 500$

$T_y = (D_{HC} \times \text{Cos}(90-\emptyset_c)) + 100$

If $\emptyset_c > 90°$

$T_x = (D_{HC} \times \text{Sin}(\emptyset_c-90)) + 500$

$T_y = (D_{HC} \times \text{Cos}(\emptyset_c-90)) + 100$

$D_{VC} = \text{Tan } Vc \times D_{HC}$

$T_z = PP + 50 - D_{VC}$

$\emptyset = 90 - \emptyset_c + H_c$

Values for Tx, Ty, Tz and Ø were calculated at the beginning and end of each survey. These values were averaged to produce a theodolite position for the calculations in section A.3.

A.3 The calculation of the survey peg position

The inclined distance, vertical circle reading and horizontal circle reading were taken to each survey peg.

D_p = Inclined distance from the theodolite to the survey peg (m)

V_p = Vertical circle reading from the theodolite to the survey peg

H_p = Horizontal circle reading from the theodolite to the survey peg

X, Y, Z = Co-ordinates of the survey peg

$D_{HP} = \text{Cos } V_p \times Dp$

$Ø' = Ø + 90°$

$\propto = Ø' - Hp$

$X = Tx + (D_{HP} \text{ Cos} \propto)$

$Y = Ty + (D_{AP} \text{ Sin} \propto)$

$Z = Tz + (D_{HP} \text{ Tan } Vp)$

The calculation of the position of a survey peg was therefore a two stage calculation. Firstly, the position of the theodolite was established. Secondly, the position of the survey peg calculated.

A.4 The survey errors

The accuracy of the survey was dependent on two factors

(i) The stability of the cliff top survey stations

(ii) The errors which resulted from the survey method.

A.4.1 The cliff top stations

The survey system relied on the stability of the two stations B1 and C1. Their position was checked four times in the two year study period. The check procedure used a closed traverse. Four stations were used. The layout of the traverse is shown in Fig. A-3.

The line from A1 to A2 was used as a reference bearing. The results of the closed traverse calculations are shown in Table A-1. For this exercise the station A1 was allocated co-ordinates of 1000E, 1000N.

The accuracy of the unadjusted angles and unadjusted distances are given in Table A-2. From these traverses the stations can be assumed stationary.

An additional source of information on the stability of the cliff top was provided by the inclinometer I11. The performance of this instrument is reported in Chapter 4. No appreciable movement has occured.

A.4.2 The errors in the position of the survey pegs

The accuracy of the survey method was estimated by repeated surveying of the permanent stations G1, G3, HI, J1 and K1. These stations were surveyed at the start and finish of each peg survey. All these stations were landward and above the theodolite station.

The mean and standard deviation for each co-ordinate of each station is given in Table A-3. The average standard deviation for the fifteen ordinates was 0.01m. In the main body of the thesis the position of the survey peg is quoted to the nearest centimetre.

TABLE A-1 The results of closed traverses on the cliff top stations

	A1C1	C1B1	B1A1	Total
Date: 31 March 1982				
Length (m)	73.205	66.370	66.459	
Included Angle	56 30 00	56 37 10	66 53 30	180 00 40
Corrected Angle	56 29 50	56 36 55	66 53 15	180 00 00
Whole circle Bearing	24 28 50	261 05 45	147 59 00	
Lat +		10.273	56.350	
-	66.624			
Dep +		65.570		
-	30.335		35.234	
Northings	933.376	943.649	999.999	- 1 mm
Eastings	969.665	1035.235	1000.001	+ 1 mm
Date: 21 April 1982				
Length (m)	73.209	66.374	66.463	
Included Angle	56 29 40	56 37 00	66 53 00	179 59 40
Corrected Angle	56 29 45	56 37 05	66 53 10	180 00 00
Whole circle Bearing	24 29 00	261 06 05	147 59 15	
Lat +		10.267	56.356	
-	66.626			
Dep +		65.575		
-	30.340		35.232	
Northings	933.374	943.641	999.997	- 3 mm
Eastings	969.660	1035.235	1000.003	+ 3 mm

contd/.....

TABLE A-1 (contd)

	A1C1	C1B1	B1A1	Total
Date: 10 December 1982				
Length (m)	73.210	66.379	66.471	
Included Angle	56 29 40	56 37 05	66 53 20	180 00 05
Corrected Angle	56 29 39	56 37 03	66 53 18	180 00 00
Whole circle Bearing	24 29 00	261 06 03	147 59 21	
Lat +		10.269	56.364	
Lat -	66.627			
Dep +		65.580		
Dep -	30.340		35.235	
Northings	933.373	934.642	1000.006	+ 6 mm
Eastings	969.660	1035.240	1000.005	+ 5 mm
Date: 6 July 1983				
Length (m)	73.206	66.371	66.484	
Included Angle	56 29 30	56 37 20	66 53 40	180 00 30
Corrected Angle	56 29 20	56 37 10	66 53 30	180 00 00
Whole circle Bearing	24 29 00	261 06 10	147 59 40	
Lat +		10.265	56.361	
Lat -	66.623			
Dep +		65.572		
Dep -	30.338		35.226	
Northings	933.377	943.642	1000.003	+ 3 mm
Eastings	969.662	1035.234	1000.008	+ 8 mm

Note

All angles given in degrees, minutes and seconds

TABLE A-2 Closed traverse errors

Date	Unadjusted angle error (seconds)	Order Error (N=3)	Order*	Unadjusted distance error (mm)	Order error	Order*
31 March 1982	40	23 N	3rd	2	1:146000	1st
21 April 1982	20	11.5 N	3rd	18	1:48570	1st
10 December 1982	5	3 N	2nd	61	1:26380	1st
6 July 1983	30	17.3 N	3rd	73	1:24115	2nd

* The orders of error was suggested by Prior in "Accuracy of Highway Surveys", 11th Congress of the International Society for Photogrammetry.

TABLE A-3 The mean and standard deviation of the cliff top stations

Peg	Sample Size	x co-ordinate		y co-ordinate		z co-ordinate	
		x(m)	σ (m)	y(m)	σ (m)	z(m)	σ (m)
G1	124	431.260	0.007	106.427	0.014	49.775	0.013
G3	29	431.148	0.007	103.462	0.013	49.876	0.013
H1	109	659.410	0.009	115.377	0.017	49.558	0.012
J1	29	553.379	0.009	90.655	0.007	50.182	0.009
K1	29	465.435	0.008	99.563	0.011	50.039	0.008

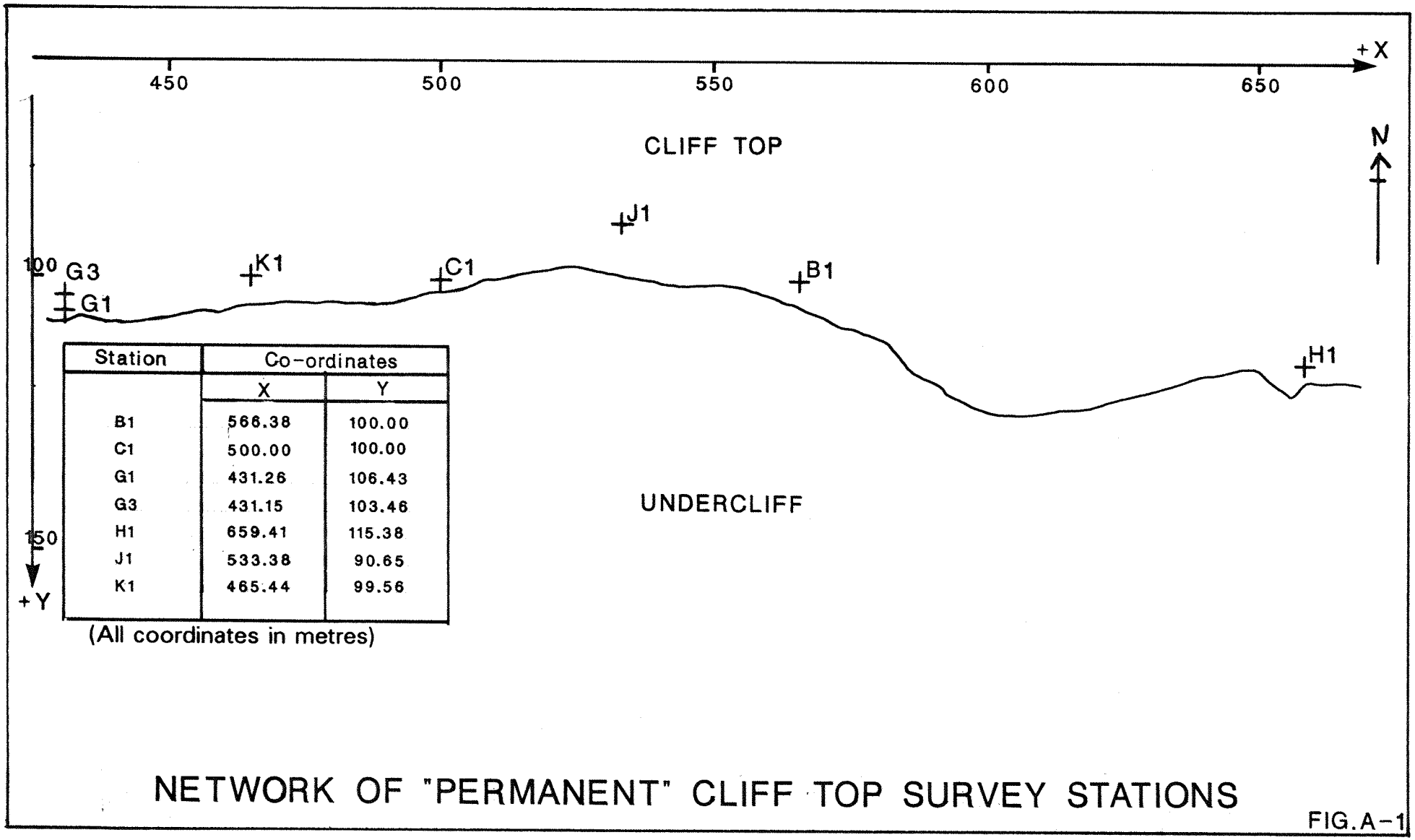

Station	Co-ordinates	
	X	Y
B1	566.38	100.00
C1	500.00	100.00
G1	431.26	106.43
G3	431.15	103.46
H1	659.41	115.38
J1	533.38	90.65
K1	465.44	99.56

(All coordinates in metres)

NETWORK OF "PERMANENT" CLIFF TOP SURVEY STATIONS

FIG.A-1

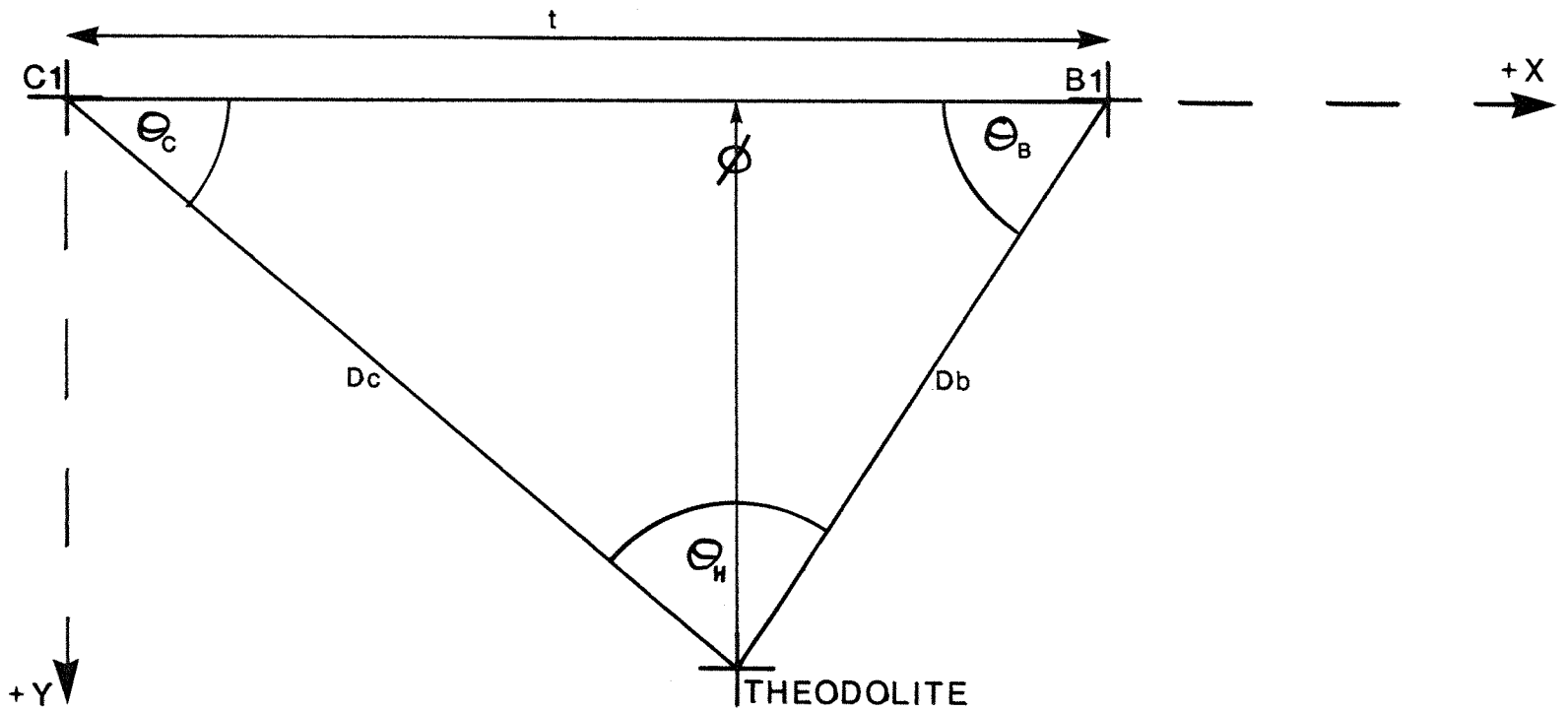

GEOMETRIC RELATIONSHIP BETWEEN CLIFF TOP STATIONS B1/C1 AND THE THEODOLITE

FIG.A-2

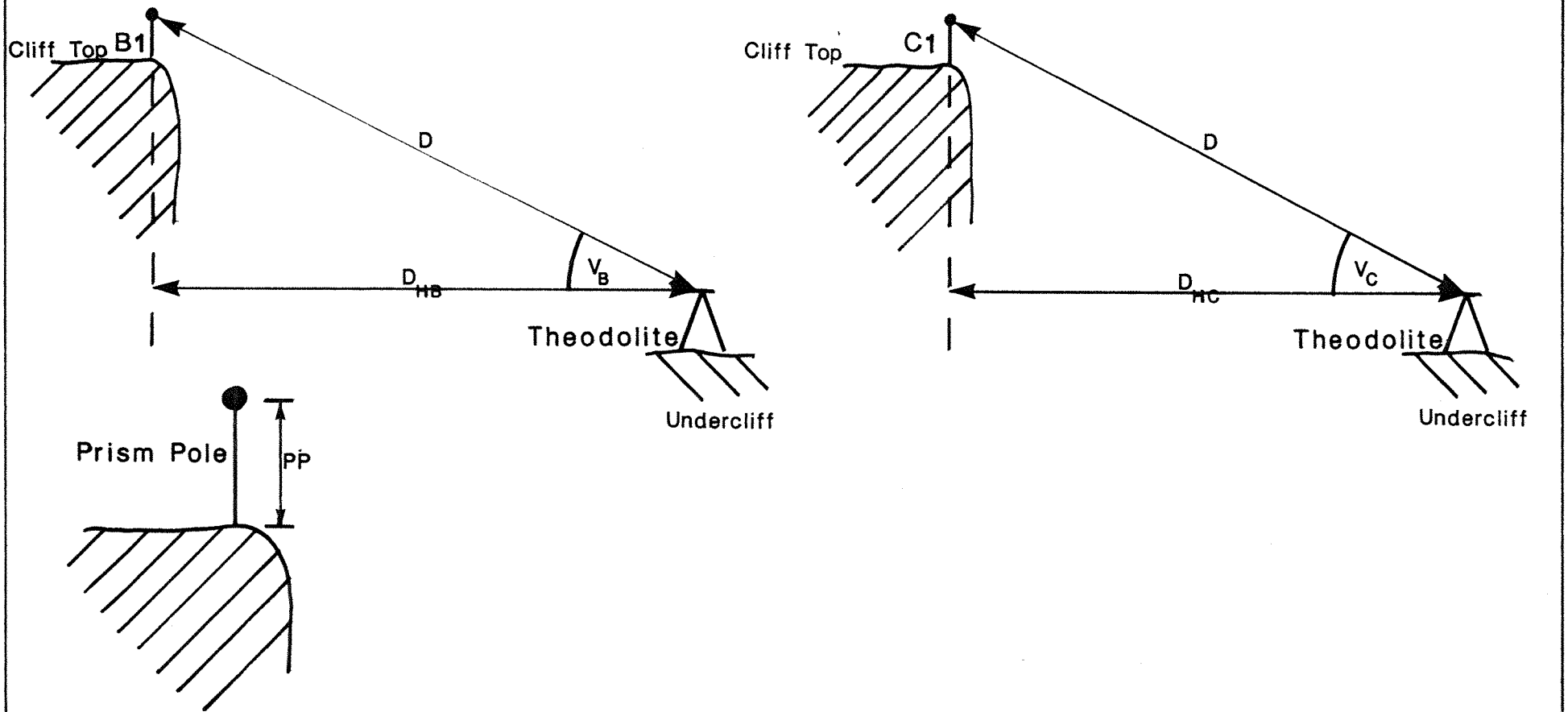

NOMENCLATURE USED TO ESTABLISH THE POSITION OF THE THEODOLITE

FIG. A-2a

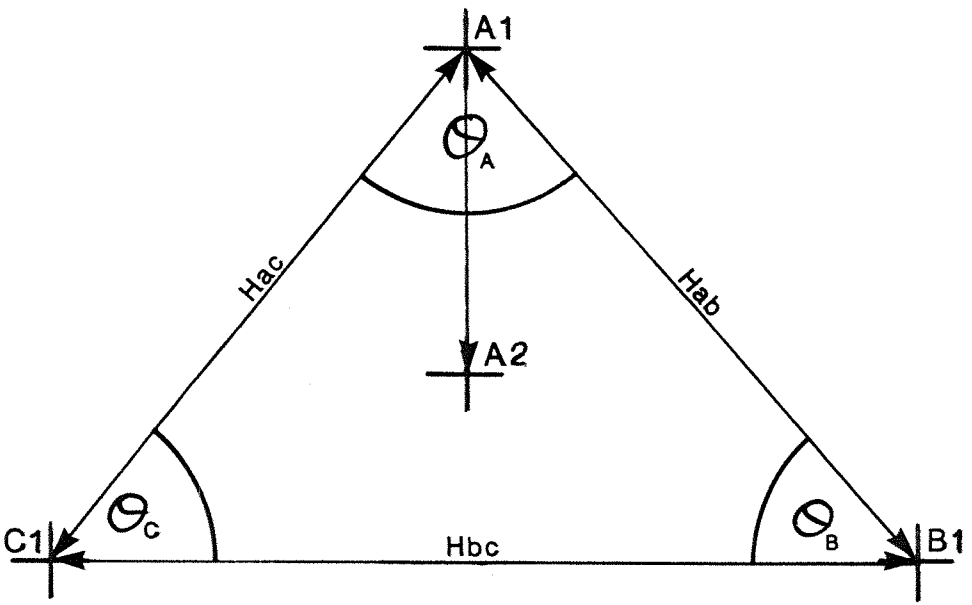

CLIFF TOP STATION TRAVERSE

FIG. A-3

APPENDIX B: THE AERIAL PHOTOGRAPHIC COVERAGE AND THE CONTOURED MAPS OF THE BARTON CLAY CLIFFS

APPENDIX B THE AERIAL PHOTOGRAPHIC COVERAGE AND THE CONTOURED MAPS OF THE BARTON CLAY CLIFFS

B.0 Aerial photographic coverage

The long term problems of coastal erosion in both Poole and Christchurch Bay has produced an extensive set of aerial photographs. Their quality and suitability for study by a researcher interested in processes of slope degradation varies considerably. Table B-1. provides a summary of the aerial photographs known to the author which cover the Barton Clay cliffs. In this table an attempt has been made to indicate the nature of the coverage.

One of the flights was financed by the research project described in this thesis. All the photographic coverage listed is suitable for study by stereoscopic techniques. The quality of the stereo image is variable.

B.1 The contour maps

Six contour maps were commisioned as part of this research study. They included five different dates and two scales. The mapping and drawing was produced by Cartographical Services (Southampton) Ltd. A list of the contour maps is shown in Table B-2.

B.1.1 Preparation of the maps

To prepare the maps a three dimensional ground control network was established. The horizontal control was provided by direct measurements from Ordnance Survey maps at 1:1250 scale. This work was carried out by Cartographical Services (Southampton) Ltd. Vertical control was carried out by the author.

To enable the contouring of three kilometres of coastline 49 vertical control points had to be established. The national grid co-ordinates and the levels of each point are listed in Table B-3.

The contours on the finalised drawings have a quoted vertical

accuracy of ± 0.2m at 1:1000 scale and ± 0.5m at 1:2500 scale.

B.1.2 Contour map information

The production of contour maps from the aerial photographs increased both the quality and the quantity of topographical information on the cliff slope. In this thesis the maps have primarily been used to fulfil 7 objectives.

i) To measure recession of the cliff top.
ii) To measure recession of the D scarp.
iii) To measure recession of the cliff toe.
iv) To measure the plan area of the undercliff.
v) To evaluate the change in material volume of the undercliff with time.
vi) To produce cross sections.
vii) To produce geomorphological maps.

TABLE B-1 The aerial photographic coverage of the Barton Clay cliffs

Date	Flight company	Client	Flying Height (feet)	Photographic Scale	Known coverage (National Grid, E)	Clarity	Stereo Imagery
12 December 1946	R.A.F.	Ministry of Housing and Local Government	16,500	1:9800	419000E to 426000E	Poor	V. Poor
17 January 1947	R.A.F.	Ministry of Housing and Local Government	28,200	1:9400	419000E to 426000E	Poor	Poor
18 September 1957	-	Ordnance Survey	-	1:6100	420000E to 426600E	Good	Good
6 May 1959	R.A.F.	Ministry of Housing and Local Government	-	1:11000	420000E to 424000E	Poor	V. Poor
31 August 1962	R.A.F.	Ministry of Housing and Local Government	30,000	1:10000	421000E to 427000E	Average	Poor

contd/.....

TABLE B-1 (contd)

17 May 1966	-	Ordnance Survey	-	1:4000	420000E to 426000E	Average	Average
8 March 1967	Aero-films Limited	-	1,250	1:2500	421000E to 424000E	Average	Good
29 March 1968	-	Ordnance Survey	-	1:10000	422000E to 431900E	Good	Average
5 July 1974	Huntings Survey Ltd	Bournemouth Borough Council	1,250	1:2500	Poole and Christchurch Bay	Good	Good
1 October 1974	Huntings Survey Ltd	Bournemouth Borough Council	1,250	1:2500	Poole and Christchurch Bay	Good	Good
25 February 1975	Huntings Survey Ltd	Bournemouth Borough Council	1,250	1:2500	Poole and Christchurch Bay	Good	Good
24 April 1975	Huntings Survey Ltd	Bournemouth Borough Council	1,250	1:2500	Poole and Christchurch Bay	Good	Good
9 September 1975	Huntings Survey Ltd	Bournemouth Borough Council	1,200	1:2400	Poole and Christchurch Bay	Good	Good

TABLE B-1 (contd)

13 May 1976	Huntings Survey Ltd	Bournemouth Borough Council	1,250	1:2500	Poole and Christchurch Bay	Good	Good
18 March 1977	Huntings Survey Ltd	Bournemouth Borough Council	1,165	1:2330	Poole and Christchurch Bay	Good	Good
6 and 23 April 1978	Huntings Survey Ltd	Bournemouth Borough Council	1,165	1:2330	Poole and Christchurch Bay	Good	Good
15 September 1979	Carto-graphical (Southam-pton) Ltd	New Forest District Council	1,250	1:2500	-	Good	Good
13 March 1980	"	"	"	"	"	"	"
26 November 1980	"	University of Southampton	"	"	419000E to 426000E	V. Good	"
July 1982	"	New Forest District Council	"	"	-	Good	"
13 September 1983	"	"	"	"	-	"	"

TABLE B-2 Details of the contour map coverage

Date	Scale	Minimum Contour Interval (m)	Coverage (National Grid, Eastings)
9 September 1975	1:2500	1.0	420400E to 423400E
13 May 1976	1:1000	0.5	422000E to 422550E
6 April 1978	1:1000	0.5	422000E to 422300E
26 November 1980	1:2500	1.0	420408E to 423340E
26 November 1980	1:1000	0.5	422000E to 422480E
July 1982	1:1000	0.5	421850E to 422640E

TABLE B-3 Details of the vertical control stations

Vertical Control Station	Level A.O.D. (metres)	National Grid (Eastings)	National Grid (Northings)
A1	8.84	420420	93050
A2	2.88	420554	93040
A3	2.88	420654	93053
A4	2.86	420818	93075
A5	2.87	421124	93080
A6	5.33	421178	93088
A7	5.74	421469	93105
A8	25.61	421625	93170
A9	27.49	421618	93278
A10	29.26	421585	93425
A11	29.55	421460	93400
A12	30.69	421350	93380
A13	30.25	421385	93278
A14	30.67	421225	93385
A15	30.43	421150	93253
A16	30.28	421025	93243
A17	28.99	420880	93270
A18	28.48	420800	93390
A19	27.85	420670	93280
A20	27.72	420710	93170
A21	23.70	420465	93250
A22	11.02	421813	93240
A23	25.55	421750	93430
A24	34.79	422623	93175
A25	35.25	422710	93345
A26	34.22	422810	93213
A27	34.23	422908	93195
A28	34.50	422975	93120
A29	34.39	42306o	93180
A30	35.06	423113	93171
A31	34.40	422953	93305
A32	34.82	422905	93323
A33	34.24	423133	93260
A34	35.08	423280	93245
A35	34.15	423260	93080
A36	34.74	423483	93213
A37	34.41	423465	93065
A38	24.62	423450	92910
A39	34.70	422565	93178
C1	31.16	422060	93215
C2	27.06	421908	93216
C3	27.56	421988	93420
C4	32.16	422113	93400
C5	32.70	422112	93355
C6	30.08	422331	93210
C7	33.72	422335	93360
C8	33.90	422280	93400
C9	33.97	422513	93180
C10	33.99	422520	93370

APPENDIX C: BACK ANALYSIS AND STABILITY ANALYSIS PROGRAMS

(Programs suitable for a BBC 'Model B' microcomputer)

```
L.
  100REM ****************************
  200REM *JANBU BACK ANALYSIS PROGRAM*
  300REM ****************************
  400REM
  500@%=&20308
  600REM
  700REM BASIC PROGRAM DATA INPUT-MANUAL
  710REM
  720REM Title of section
  730READ T$
  740PRINT"ANALYSIS ON SECTION",T$
  750REM
  800REM
  900INPUT "How many slices in the slope"N
 1000INPUT "What is the correction factor for the slope"fo
 1100REM
 1200DIM Depth(N),Alpha(N),W(N),U(N),b(N)
 1300REM
 1400ru=0
 1500INPUT "Average pore pressure ratio,if ru=0 then data needed for U" ru
 1600INPUT"Unit weight of landslide debris(Kn/m^3)"Gamma
 1700REM
 1800INPUT "PHI' estimate"PHID
 1900REM
 2000REM Increment step for PHI'
 2100 IS=1
 2200REM
 2300REM  DIRECT DATA INPUT FROM PROGRAM
 2400REM
 2500REM Slices breadths
 2600REM
 2700FOR I=1 TO N
 2800READ b(I)
 2900NEXT I
 3000REM
 3100REM Slice depths
 3200REM
 3300FOR I=1 TO N
 3400READ Depth(I)
 3500REM
 3600REM Slice weights
 3700REM
 3800W(I)=Depth(I)*b(I)*Gamma
 3900NEXT I
 4000REM
 4100REM Slices base angles
 4200REM
 4300FOR I=1 TO N
 4400READ D
 4500Alpha(I)=RAD(D)
 4600NEXT I
 4700IF ru>0 THEN 5400
 4800REM
 4900REM Water pressures at slice base
 5000REM
 5100FOR I=1 TO N
 5200READ U(I)
 5300NEXT I
 5400REM
```

```
 5500REM Calculation of WTAN@
 5600REM
 5700FOR I=1 TO N
 5800 WT=Depth(I)*b(I)*Gamma*TAN(Alpha(I))
 5900 WTT=WTT+WT
 6000NEXT I
 6100REM
 6200PHIR=RAD(PHID)
 6300REM
 6400REM Calculation of Right-side
 6500REM
 6600RST=0
 6700IF ru>0 THEN 8300
 6800REM
 6900REM   Actual pore water pressures at each slice base
 7000REM
 7100FOR I=1 TO N
 7200 A=(W(I)-U(I)*b(I))*TAN(PHIR)
 7300 B=1+((TAN(Alpha(I))^2))
 7400 C=1+((TAN(Alpha(I)))*(TAN(PHIR)))
 7500 RS=(A*B)/C
 7600 RST=RST+RS
 7700NEXT I
 7800RST=RST*fo
 7900GOTO 9000
 8000REM
 8100REM   Average pore pressure ratio
 8200REM
 8300FOR I=1 TO N
 8400 D=W(I)*(1-ru)*TAN(PHIR)
 8500 E=(COS(Alpha(I))*COS(Alpha(I))*(1+(TAN(Alpha(I))*TAN(PHIR))))
 8600 RS=D/E
 8700 RST=RST+RS
 8800NEXT I
 8900RST=RST*fo
 9000REM
 9100REM
 9200REM
 9300REM   Comparison of left and right sides of the back analysis equation
 9400REM
 9500 PDEG=DEG(PHIR)
 9600REM
 9700 TEST=WTT-RST
 9800IF ABS(TEST)<0.1 THEN 10900
 9900IF RST>WTT THEN 10200
10000 PHIR=PHIR+RAD(IS)
10100GOTO 6400
10200 PHIR=PHIR-RAD(IS)
10300 IS=IS/10
10400GOTO 6400
10500REM
10600REM     RESULTS
10700REM     *******
10800REM
10900PRINT
11000PRINT"Back analysised value for PHI' is"DEG(PHIR)
11100PRINT
11200PRINT"Slope statistics"
11300PRINT"Number of slices"N
11400PRINT"Correction factor"fo
```

```
11500PRINT"Unit weight of soil"Gamma
11600PRINT"  Slice No.      Breadth(m)        Depth(m)      Base angle(Deg)  Weigh
t(Kn/m^3)"
11700FOR I=1 TO N
11800PRINT I,"    ",b(I)," ",Depth(I),"    ",DEG(Alpha(I)),"         ",W(I)
11900NEXT I
12000END
>
```

```
L.
20000 DATA D1
20100 DATA 2.,2.,2.,2.,2.,2.,2.,2.,2.,2.,2.,2.,2.,2.,2.,2.,2.,2.,2.,2.,2.,2.,
2.,2.,2.,2.
20200 DATA 1.8,5.6,8.8,9.6,9.8,9.6,9.2,8.8,8.6,8.4,8.2,8,8,7.8,7.6,7.4,7.4,7.2,7
.2,7.1,7,6.4,5.8,4.6,3.6,2,.8
20300 DATA 65,65,55,36,14,0,0,0,0,0,0,0,0,0,0,0,0,0,0,0,0,0,0,0,0,0,0,0
20400 DATA 10.79,33.35,63.77,79.46,82.4,85.35,79.46,76.52,71.61,67.69,58.86,51.9
9,49.05,45.13,43.16,39.24,35.32,29.43,27.47,24.53,20.6,17.66,14.72,9.81,7.85,4.9
1,1.96
>
```

```
L.
20000 DATA D2
20100 DATA 2.,2.,2.,2.,2.,2.,2.,2.,2.,2.,2.,2.,2.,2.,2.,2.,2.,2.,2.,2.,2.,2.,2.,
2.,2.,2.,2.,2.,2.,2.,2.,2.,2.,2.
20200 DATA 3.4,8.4,10.6,11.8,12.6,12.6,11.4,11.,10.8,10.8,11.8,12.,11.8,11.6,11.
8,11.,10.2,9.6,8.2,6.8,5.4,4.8,4.6,4.4,4.4,4.6,5.,5.4,5.2,4.,3.4,2.8,2.4,2.
20300 DATA 65.,65.,55.,33.,18.,0.,0.,0.,0.,0.,0.,0.,0.,0.,0.,0.,0.,0.,0.,0.,0.,0
.,0.,0.,0.,0.,0.,0.,0.,0.,0.,0.,0.,0.,0.,0.,0.
20400 DATA 21.58,43.16,77.5,89.27,91.23,91.23,87.31,82.4,78.48,74.56,69.65,66.71
,62.78,58.86,52.97,48.07,44.15,41.2,38.26,35.32,33.35,30.41,28.45,26.49,24.53,22
.56,20.6,18.64,15.7,13.73,11.77,8.83,5.89,2.94
>
```

```
L.
20000 DATA D3
20100 DATA 2.,2.,2.,2.,2.,2.,2.,2.,2.,2.,2.,2.,2.,2.,2.,2.,2.,2.,2.,2.,2.,2.,2.,
2.,2.,2.,2.,2.,2.,2.,2.,2.,2.,2.
20200 DATA 1.8,5.,8.6,11.2,12.2,11.6,10.6,9.6,9.,8.4,8.,7.6,7.3,7.2,7.2,7.2,7.1,
7.1,7.,6.9,6.8,6.6,5.1,4.1,3.4,2.6,2.4,2.4,2.4,2.5,2.4,1.8,.6
20300 DATA 65.,65.,65.,46.,14.,0.,0.,0.,0.,0.,0.,0.,0.,0.,0.,0.,0.,0.,0.,0.,0.,0
.,0.,0.,0.,0.,0.,0.,0.,0.,0.,0.,0.,0.,0.,0.,0.
20400 DATA 9.81,29.43,53.96,80.44,84.37,82.4,80.44,77.5,75.54,72.59,69.65,66.71,
63.77,60.82,57.88,54.94,52.97,50.03,47.09,43.16,40.22,36.3,32.37,27.47,22.56,17.
66,13.73,11.77,9.81,6.87,4.91,3.92,1.96
>
```

RUN
ANALYSIS ON SECTION D1
How many slices in the slope27
What is the correction factor for the slope1.0365
Average pore pressure ratio,if ru=0 then data needed for U0
Unit weight of landslide debris(Kn/m^3)18.829
PHI' estimate10

Back analysised value for PHI' is 13.885

Slope statistics
Number of slices 27.000
Correction factor 1.035
Unit weight of soil 18.829

Slice No.	Breadth(m)	Depth(m)	Base angle(Deg)	Weight(Kn/m^3)
1.000	2.000	1.800	65.000	67.784
2.000	2.000	5.600	65.000	210.885
3.000	2.000	8.800	55.000	331.390
4.000	2.000	9.600	36.000	361.517
5.000	2.000	9.800	14.000	369.048
6.000	2.000	9.600	0.000	361.517
7.000	2.000	9.200	0.000	346.454
8.000	2.000	8.800	0.000	331.390
9.000	2.000	8.600	0.000	323.859
10.000	2.000	8.400	0.000	316.327
11.000	2.000	8.200	0.000	308.796
12.000	2.000	8.000	0.000	301.264
13.000	2.000	8.000	0.000	301.264
14.000	2.000	7.800	0.000	293.732
15.000	2.000	7.600	0.000	286.201
16.000	2.000	7.400	0.000	278.669
17.000	2.000	7.400	0.000	278.669
18.000	2.000	7.200	0.000	271.138
19.000	2.000	7.200	0.000	271.138
20.000	2.000	7.100	0.000	267.372
21.000	2.000	7.000	0.000	263.606
22.000	2.000	6.400	0.000	241.011
23.000	2.000	5.800	0.000	218.416
24.000	2.000	4.600	0.000	173.227
25.000	2.000	3.600	0.000	135.569
26.000	2.000	2.000	0.000	75.316
27.000	2.000	0.800	0.000	30.126

RUN
ANALYSIS ON SECTION D2
How many slices in the slope?34
What is the correction factor for the slope?1.033
Average pore pressure ratio,if ru=0 then data needed for U0
Unit weight of landslide debris(Kn/m^3)?18.829
PHI' estimate?10

Back analysised value for PHI' is 12.985

Slope statistics
Number of slices 34.000
Correction factor 1.033
Unit weight of soil 18.829

Slice No.	Breadth(m)	Depth(m)	Base angle(Deg)	Weight(Kn/m^3)
1.000	2.000	3.400	65.000	128.037
2.000	2.000	8.400	65.000	316.327
3.000	2.000	10.600	55.000	397.175
4.000	2.000	11.800	33.000	444.364
5.000	2.000	12.600	18.000	474.491
6.000	2.000	12.600	0.000	474.491
7.000	2.000	11.400	0.000	429.301
8.000	2.000	11.000	0.000	414.238
9.000	2.000	10.800	0.000	406.706
10.000	2.000	10.800	0.000	406.706
11.000	2.000	11.800	0.000	444.364
12.000	2.000	12.000	0.000	451.896
13.000	2.000	11.800	0.000	444.364
14.000	2.000	11.600	0.000	436.833
15.000	2.000	11.800	0.000	444.364
16.000	2.000	11.000	0.000	414.238
17.000	2.000	10.200	0.000	384.112
18.000	2.000	9.600	0.000	361.517
19.000	2.000	8.200	0.000	308.796
20.000	2.000	6.800	0.000	256.074
21.000	2.000	5.400	0.000	203.353
22.000	2.000	4.800	0.000	180.758
23.000	2.000	4.600	0.000	173.227
24.000	2.000	4.400	0.000	165.695
25.000	2.000	4.400	0.000	165.695
26.000	2.000	4.600	0.000	173.227
27.000	2.000	5.000	0.000	188.290
28.000	2.000	5.400	0.000	203.353
29.000	2.000	5.200	0.000	195.822
30.000	2.000	4.000	0.000	150.632
31.000	2.000	3.400	0.000	128.037
32.000	2.000	2.800	0.000	105.442
33.000	2.000	2.400	0.000	90.379
34.000	2.000	2.000	0.000	75.316

>

RUN
ANALYSIS ON SECTION D3
How many slices in the slope33
What is the correction factor for the slope1.026
Average pore pressure ratio,if ru=0 then data needed for U0
Unit weight of landslide debris(Kn/m^3)18.829
PHI' estimate10

Back analysised value for PHI' is 16.552

Slope statistics
Number of slices 33.000
Correction factor 1.026
Unit weight of soil 18.829

Slice No.	Breadth(m)	Depth(m)	Base angle(Deg)	Weight(Kn/m^3)
1.000	2.000	1.800	65.000	67.784
2.000	2.000	5.000	65.000	188.290
3.000	2.000	8.600	65.000	323.859
4.000	2.000	11.200	46.000	421.770
5.000	2.000	12.200	14.000	459.428
6.000	2.000	11.600	0.000	436.833
7.000	2.000	10.600	0.000	399.175
8.000	2.000	9.600	0.000	361.517
9.000	2.000	9.000	0.000	338.922
10.000	2.000	8.400	0.000	316.327
11.000	2.000	8.000	0.000	301.264
12.000	2.000	7.600	0.000	286.201
13.000	2.000	7.300	0.000	274.903
14.000	2.000	7.200	0.000	271.138
15.000	2.000	7.200	0.000	271.138
16.000	2.000	7.200	0.000	271.138
17.000	2.000	7.100	0.000	267.372
18.000	2.000	7.100	0.000	267.372
19.000	2.000	7.000	0.000	263.606
20.000	2.000	6.900	0.000	259.840
21.000	2.000	6.800	0.000	256.074
22.000	2.000	6.600	0.000	248.543
23.000	2.000	5.100	0.000	192.056
24.000	2.000	4.100	0.000	154.398
25.000	2.000	3.400	0.000	128.037
26.000	2.000	2.600	0.000	97.911
27.000	2.000	2.400	0.000	90.379
28.000	2.000	2.400	0.000	90.379
29.000	2.000	2.400	0.000	90.379
30.000	2.000	2.500	0.000	94.145
31.000	2.000	2.400	0.000	90.379
32.000	2.000	1.800	0.000	67.784
33.000	2.000	0.600	0.000	22.595

>

```
L.
  100REM************************************
  200REM*JANBU STABILITY ANALYSIS PROGRAM*
  300REM************************************
  400REM
  500VDU15
  600@%=&20207
  700REM
  800VDU2
  900PRINT"------------------------------------------------------------------------
-----------
"
 1000REM This program contains all the basis data for section D1,D2 and D3(inclu
ding correction factors)
 1100REM
 1200REM Unit weight of landslide debris(Kn/m^3)
 1300 Gamma=18.829
 1400REM
 1500REM Choice of section
 1600INPUT"Which section do you want to consider"S
 1700REM
 1800REM Correction factors
 1900IF S=1 THEN fo=1.035
 2000IF S=2 THEN fo=1.033
 2100IF S=3 THEN fo=1.026
 2200REM
 2300REM Back analysised Phi(r)'
 2400IF S=1 THEN PHIR=RAD(13.885)
 2500IF S=2 THEN PHIR=RAD(12.985)
 2600IF S=3 THEN PHIR=RAD(16.552)
 2700REM
 2800REM Set up array size for relevant section
 2900IF S=1 THEN DUM=0
 3000IF S=2 THEN DUM=27
 3100IF S=3 THEN DUM=61
 3200IF DUM=0 THEN 3800
 3300REM
 3400REM Read in dummy values to proceed to data required
 3500FOR I=1 TO DUM*4
 3600READ DUMMY
 3700NEXT I
 3800REM
 3900REM Set up array dimensions
 4000IF S=1 THEN N=27
 4100IF S=2 THEN N=34
 4200IF S=3 THEN N=33
 4300REM
 4400DIM Depth(N),Alpha(N),b(N),W(N),U(N),OD(N),NDF(N),SN(N),DS(N)
 4500REM
 4600REM Read in raw data from program
 4700REM
 4800REM Slices breadths
 4900FOR I=1 TO N
 5000READ b(I)
 5100NEXT I
 5200REM
 5300REM Slice depths
 5400FOR I=1 TO N
 5500READ Depth(I)
 5600 OD(I)=Depth(I)
 5700NEXT I
```

```
5800REM
5900REM Slice base angles
6000FOR I=1 TO N
6100READ Dalpha
6200 Alpha(I)=RAD(Dalpha)
6300NEXT I
6400REM
6500REM Water pressures at slice base
6600FOR I=1 TO N
6700READ U(I)
6800NEXT I
6900REM
7000REM
7100REM  Changes in slope geometry
7200REM
7300INPUT"Do you want to change anything"A$
7400IF A$="NO" THEN 14300
7500REM
7600@%=&20001
7700PRINT"You have choosen to change section D"S
7800@%=&20207
7900PRINT"Remember slice 1 is at the land ward extreme of the section"
8000REM
8100REM Here the user has a choice of changes to the slope geometry
8200REM
8300PRINT"Do you want to 1. Shorten the section"
8400PRINT"                2. Change any slice depths"
8500PRINT"                3. Impose a slump"
8600INPUT CN
8700IF CN=2 THEN 9600
8800IF CN=3 THEN 13300
8900REM
9000REM Shortening the section
9100REM
9200INPUT"How many slices do you want to remove"SR
9300N=N-SR
9400GOTO 14300
9500REM
9600REM Changes in slice depths
9700REM
9800PRINT"Do you want 1. An overall change in depth"
9900PRINT"            2. A local change in depth"
10000INPUT DN
10100IF DN=2 THEN 12200
10200PRINT"Do you want to 1.A percentage change"
10300PRINT"               2.Depth(metres) change"
10400INPUT EN
10500IF EN=2 THEN 11600
10600REM
10700REM Overall changes
10800REM
10900INPUT"Percentage change is(+/-)"PC
11000 PC=PC/100
11100FOR I=1 TO N
11200 Depth(I)=Depth(I)+(Depth(I)*PC)
11300NEXT I
11400GOTO 14300
11500REM
11600INPUT"Change(metres)"CM
11700FOR I=1 TO N
```

```
11800 Depth(I)=Depth(I)+CM
11900NEXT I
12000GOTO 14300
12100REM
12200REM Local changes
12300REM
12400INPUT"How many slices do you want to change"HS
12500FOR I=1 TO HS
12600INPUT"Slice number"SN(I)
12700INPUT"New depth(metres)"NDP(SN(I))
12800 OD(SN(I))=Depth(SN(I))
12900 Depth(SN(I))=NDP(SN(I))
13000NEXT I
13100GOTO 14300
13200REM
13300REM Slump addition
13400REM
13500INPUT"How many slices does the slump block cover"SS
13600FOR I=1 TO SS
13700INPUT"Slice number"SN(I)
13800INPUT"Depth of slump on this slice"DS(I)
13900 Depth(SN(I))=Depth(SN(I))+DS(I)
14000NEXT I
14100REM
14200REM
14300REM    Calculation of WTAN@
14400REM
14500FOR I=1 TO N
14600 W(I)=Depth(I)*b(I)*Gamma
14700NEXT I
14800REM
14900FOR I=1 TO N
15000 WT=W(I)*TAN(Alpha(I))
15100 WTT=WTT+WT
15200NEXT I
15300REM
15400REM
15500REM    Calculation of TOP-LINE
15600REM
15700REM First estimate of the factor of safety
15800 FS=2.
15900REM
16000 RST=0.
16100FOR I=1 TO N
16200 A=(W(I)-U(I)*b(I))*TAN(PHIR)
16300 B=1+((TAN(Alpha(I))^2))
16400 C=1+((TAN(Alpha(I)))*(TAN(PHIR)/FS))
16500 RS=(A*B)/C
16600 RST=RST+RS
16700NEXT I
16800RST=RST*fo
16900REM
17000REM
17100REM Test the convergence of FS
17200REM
17300 TEST=(RST/WTT)-FS
17400IF ABS(TEST)<0.001 THEN 18200
17500 FS=RST/WTT
17600REM
17700REM Repeat with newly calculated value of FS
```

```
17800REM
17900GOTO 15900
18000REM
18100REM
18200REM          RESULTS
18300REM          *******
18400REM
18500REM
18600VDU2
18700@%=&20001
18800PRINT"Cross section D"S;
18900@%=&20207
19000VDU 1,8,1,8,1,8,1,8,1,8,1,8,1,8,1,8,1,8,1,8,1,8,1,8,1,8,1,8,1,8,1,8,1,8,1,8
19100PRINT"_________________"
19200PRINT"FACTOR OF SAFETY IS "RST/WTT;
19300VDU 1,8,1,8,1,8,1,8,1,8,1,8,1,8,1,8,1,8,1,8,1,8,1,8,1,8,1,8,1,8,1,8,1,8,1,8
,1,8,1,8,1,8,1,8,1,8
19400PRINT"                          ____"
19500REM
19600REM Labels
19700REM
19800IF A$="NO" THEN 20200
19900IF CN=1 THEN 20600
20000IF CN=2 THEN 21300
20100IF CN=3 THEN 24000
20200PRINT"No change in geometry"
20300VDU3
20400END
20500REM
20600PRINT"Shortened section"
20700FOR I=1 TO SR
20800PRINT"Slice"N+I" removed"
20900NEXT I
21000VDU3
21100END
21200REM
21300PRINT"Changes in the depth of the cross-section"
21400IF DN=2 THEN 23100
21500PRINT"A change to the overall depth of the cross section"
21600IF EN=2 THEN 22300
21700IF PC>0 THEN 22000
21800PRINT ABS(PC*100),"Percent removed"
21900GOTO 22100
22000PRINT ABS(PC*100),"Percent added"
22100VDU3
22200END
22300REM
22400IF CM>0 THEN 22700
22500PRINT ABS(CM)," metres removed"
22600GOTO 22800
22700PRINT ABS(CM)," metres added"
22800VDU3
22900END
23000REM
23100PRINT"Individual slice changes"
23200FOR I=1 TO HS
23300PRINT"Slice"SN(I)
23400PRINT"Old depth"OD(SN(I))"metres"
23500PRINT"New depth"NDP(SN(I))"metres"
23600NEXT I
```

```
23700VDU3
23800END
23900REM
24000PRINT"Slump addition over"SS,"slices"
24100FOR I=1 TO SS
24200PRINT"Slice"SN(I)" depth addition"DS(I)"metres"
24300NEXT I
24400VDU3
24500END
24600REM       DATA
24700REM
24800REM DATA D1
24900 DATA 2.,2.,2.,2.,2.,2.,2.,2.,2.,2.,2.,2.,2.,2.,2.,2.,2.,2.,2.,2.,2.,2.,2.,
2.,2.,2.,2.
25000 DATA 1.8,5.6,8.8,9.6,9.8,9.6,9.2,8.8,8.6,8.4,8.2,8,8,7.8,7.6,7.4,7.4,7.2,7
.2,7.1,7,6.4,5.8,4.6,3.6,2,.8
25100 DATA 65,65,55,36,14,0,0,0,0,0,0,0,0,0,0,0,0,0,0,0,0,0,0,0,0,0,0,0,0
25200 DATA 10.79,33.35,63.77,79.46,82.4,85.35,79.46,76.52,71.61,67.69,58.86,51.9
9,49.05,45.13,43.16,39.24,35.32,29.43,27.47,24.53,20.6,17.66,14.72,9.81,7.85,4.9
1,1.96
25300REM DATA D2
25400 DATA 2.,2.,2.,2.,2.,2.,2.,2.,2.,2.,2.,2.,2.,2.,2.,2.,2.,2.,2.,2.,2.,2.,2.,
2.,2.,2.,2.,2.,2.,2.,2.,2.,2.,2.
25500 DATA 3.4,8.4,10.6,11.8,12.6,12.6,11.4,11.,10.8,10.8,11.8,12.,11.8,11.6,11.
8,11.,10.2,9.6,8.2,6.8,5.4,4.8,4.6,4.4,4.4,4.6,5.,5.4,5.2,4.,3.4,2.8,2.4,2.
25600 DATA 65.,65.,55.,33.,18.,0.,0.,0.,0.,0.,0.,0.,0.,0.,0.,0.,0.,0.,0.,0.,0.,0
.,0.,0.,0.,0.,0.,0.,0.,0.,0.,0.,0.,0.
25700 DATA 21.58,43.16,77.5,89.27,91.23,91.23,87.31,82.4,78.48,74.56,69.65,66.71
,62.78,58.86,52.97,48.07,44.15,41.2,38.26,35.32,33.35,30.41,28.45,26.49,24.53,22
.56,20.6,18.64,15.7,13.73,11.77,8.83,5.89,2.94
25800REM DATA D3
25900 DATA 2.,2.,2.,2.,2.,2.,2.,2.,2.,2,2.,2.,2.,2.,2.,2.,2.,2.,2.,2.,2.,2.,2.,2
.,2.,2.,2.,2.,2.,2.,2.,2.,2.
26000 DATA 1.8,5.,8.6,11.2,12.2,11.6,10.6,9.6,9.,8.4,8.,7.6,7.3,7.2,7.2,7.2,7.1,
7.1,7.,6.9,6.8,6.6,5.1,4.1,3.4,2.6,2.4,2.4,2.4,2.5,2.4,1.8,.6
26100 DATA 65.,65.,65.,46.,14.,0.,0.,0.,0.,0.,0.,0.,0.,0.,0.,0.,0.,0.,0.,0.,0.,0
.,0.,0.,0.,0.,0.,0.,0.,0.,0.,0.,0.
26200 DATA 9.81,29.43,53.96,80.44,84.37,82.4,80.44,77.5,75.54,72.59,69.65,66.71,
63.77,60.82,57.88,54.94,52.97,50.03,47.09,43.16,40.22,36.3,32.37,27.47,22.56,17.
66,13.73,11.77,9.81,6.87,4.91,3.92,1.96
>
```

```
Which section do you want to consider1
Do you want to change anythingNO
Cross_section_D1.
FACTOR OF SAFETY IS     1.00
No change in geometry
```

```
Which section do you want to consider1
Do you want to change anythingYES
You have choosen to change section D1.
Remember slice 1 is at the land ward extreme of the section
Do you want to 1. Shorten the section
               2. Change any slice depths
               3. Impose a slump
?1
How many slices do you want to remove3
Cross_section_D1.
FACTOR OF SAFETY IS     0.96
Shortened section
Slice  25.00 removed
Slice  26.00 removed
Slice  27.00 removed
```

```
Which section do you want to consider2
Do you want to change anythingYES
You have choosen to change section D2.
Remember slice 1 is at the land ward extreme of the section
Do you want to 1. Shorten the section
               2. Change any slice depths
               3. Impose a slump
?2
Do you want 1. An overall change in depth
            2. A local change in depth
?1
Do you want to 1.A percentage change
               2.Depth(metres) change
?1
Percentage change is(+/-)-5
Cross_section_D2.
FACTOR OF SAFETY IS     0.98
Changes in the depth of the cross-section
A change to the overall depth of the cross section
   5.00Percent removed
```

```
Which section do you want to consider2
Do you want to change anythingYES
You have choosen to change section D2.
Remember slice 1 is at the land ward extreme of the section
Do you want to 1. Shorten the section
               2. Change any slice depths
               3. Impose a slump
?2
Do you want 1. An overall change in depth
            2. A local change in depth
?1
Do you want to 1.A percentage change
               2.Depth(metres) change
?2
Change(metres).1
Cross_section_D2.
FACTOR OF SAFETY IS    1.01
Changes in the depth of the cross-section
A change to the overall depth of the cross section
   0.10 metres added
```

```
Which section do you want to consider2
Do you want to change anythingYES
You have choosen to change section D2.
Remember slice 1 is at the land ward extreme of the section
Do you want to 1. Shorten the section
               2. Change any slice depths
               3. Impose a slump
?2
Do you want 1. An overall change in depth
            2. A local change in depth
?2
How many slices do you want to change3
Slice number10
New depth(metres)11.8
Slice number11
New depth(metres)12.8
Slice number34
New depth(metres)2.6
Cross_section_D2.
FACTOR OF SAFETY IS    1.01
Changes in the depth of the cross-section
Individual slice changes
Slice  10.00
Old depth  10.80metres
New depth  11.80metres
Slice  11.00
Old depth  11.80metres
New depth  12.80metres
Slice  34.00
Old depth   2.00metres
New depth   2.60metres
```

```
Which section do you want to consider3
Do you want to change anythingYES
You have choosen to change section D3.
Remember slice 1 is at the land ward extreme of the section
Do you want to 1. Shorten the section
               2. Change any slice depths
               3. Impose a slump
?3
How many slices does the slump block cover4
Slice number1
Depth of slump on this slice.2
Slice number2
Depth of slump on this slice.4
Slice number3
Depth of slump on this slice.6
Slice number4
Depth of slump on this slice1.
Cross_section_D3.
FACTOR OF SAFETY IS     0.96
Slump addition over    4.00  slices
Slice    1.00 depth addition    0.20metres
Slice    2.00 depth addition    0.40metres
Slice    3.00 depth addition    0.60metres
Slice    4.00 depth addition    1.00metres
```

APPENDIX D: THE F BEDDING PLANE SHEAR SURFACE

APPENDIX D THE F BEDDING PLANE SHEAR SURFACE

D.0 Introduction

This appendix is a summary of preliminary tests performed on a thin layer of Barton Clay which was sampled at the same stratagraphic level as the F bedding plane shear surface.

The tests were carried out to discover a reason why the layer has a lower first time failure strength than the surrounding Barton Clay. However, laboratory tests to answer this question could not be performed in the research period.

It is important to emphasise that the physical property which is most significant to the behaviour of the Barton Clay cliffs is the first time failure strength. Once failure has occured any translation along the shear surface would cause reorientation of the clay platelets. Skempton (1985) emphasised that a drop in peak strength can occur after 0.1 mm of shear displacement. Full residual strength is, however, only realised after 100 mm to 500 mm of shear displacement.

D.1 Sampling site

Along 89% of the study area the shear plane situated approximately 0.1m above the base of the F2 zone shows signs of slide activity. Either the shear surface is exposed directly (Fig.2-10) or the geomorphology implies sliding. To understand the reason for the preferential selection of this horizon as a shear surface a section of scarp face needed to be found where shear failure had not occured.

The main trigger for a slip along any surface is the driving force provided by material above the potential shear surface. The F bedding plane shear surface was traced up dip in the direction in which the volume of overburden decreased.

An unsheared section, which consisted of the upper 0.7m of the F1 zone and the lower 0.5m of the F2 zone, was found at N.G.R. 422109E, 093200N. The level of the potential F bedding plane shear surface was 25.74m A.O.D.

D.2 Visual identification

The close proximity of the F shear surface enabled the stratagraphic level of the unsheared horizon to be traced up dip.

A thin bed, 3 to 10mm thick of lenticular shaped clay particles was identified. The particles were flattish, irregularly shaped, had shiny surfaces and an individual partical size no greater than 10mm. The layer was sandwiched between harder blocking clay. Figure D-1 illustrates the bed.

Block samples, approximately 300mm deep, were removed. The lenticular bed was at mid depth. In addition samples of the bed were carefully scooped out for laboratory tests.

D.3 Engineering properties

The following seven tests were performed on the samples collected.

i) Residual shear strength
ii) Particle size distribution
iii) Liquid limit
iv) Plastic limit
v) Plasticity Index
vi) Specific gravity
vii) Natural moisture content

The test results are listed in Table D-1.

D.4 Mineralogy

Samples of the Barton Clay above, at and below the level of potential failure were analysed by X-ray diffraction techniques. The mineralogy and the approximate percentages of each clay mineral type are given in Table D-2.

D.5 Chemistry

In addition to the inorganic content, detected by X-ray diffraction, the organic content of the lenticular bed and its

adjacent layers were obtained.

The organic content was calculated from the ignition loss caused by following the procedure detailed by Skempton and Petley (1970). Results from the tests are listed in Table D-3.

D.6 Structure

The structure of the potential shear surface was studied under very low degrees of magnification. The collection of lenticular shapes is in great contrast to the blocky clay above and below. It is however the structure of the clay platelets at the microscopic scale, $< 2\mu m$, that determines the resistance of the bed to shear failure. This assumption excludes the existence of extensive horizontal joints and fissures for which there is no evidence. The re-orientation of clay platelets due to shear displacement has been discussed by Skempton (1964).

Experimental confirmation of the proposed reorientation has been provided by the study of London Clay microstructure using a polarizing microscope, Morgenstern and Tchalenko (1967) and Tchalenko (1968). This technique requires the production of thin sections.

The preparation of thin sections of the F potential shear plane was unsuccessful. The technique used followed the method proposed by West (1964). Any attempt to modify this technique or experiment with other techniques was considered beyond the scope of the research project.

D.7 Preliminary conclusions

The test program, detailed above, has shown there is no chemical or mineralogical reason why the potential F shear surface has a low first time failure strength.

In addition, the properties listed in Tables D-1, D-2 and D-3, for the lenticular bed, are very similar to the beds immediately above and below.

These results leave one fundamental question unanswered.

What is the orientation of the clay platelets which form the potential F bedding plane shear surface?

This question has not been answered in the initial analysis of the potential failure bed.

TABLE D-1 Properties of the Barton Clay below, at and above the potential F shear surface

Property	Clay below potential F shear surface	Potential F shear surface	Clay above potential F shear surface
Residual shear strength ($\emptyset'_r$)	9.2°	9.4°	10.2°
Liquid Limit	73%	79%	74%
Plastic Limit	23%	34%	25%
Plasticity Index	51	45	48
Moisture Content	28.4%	31.6%	28.2%
Specific Gravity	2.64	2.71	2.60
Clay content	63%	64%	57%
Silt content	29%	29%	38%
Sand content	8%	7%	5%

TABLE D-2 Percentage of clay minerals in the Barton Clay below, at and above the potential F shear surface

Clay Minerals	Barton Clay Bed		
	Below	Potential Shear surface	Above
Montmorillorite	35	30	35
Illite	40	45	40
Kaolinite	15	20	15
Chlorite	10	5	10
Other Minerals present			
Quartz	✓	✓	✓
Feldspar	✓	✓	✓
Pyrite	✓	✓	✓

TABLE D-3 Organic content of the Barton Clay below, at and above the potential F shear surface

	Below	Potential Shear surface	Above
Organic Content	0.5%	0.7%	1.9%

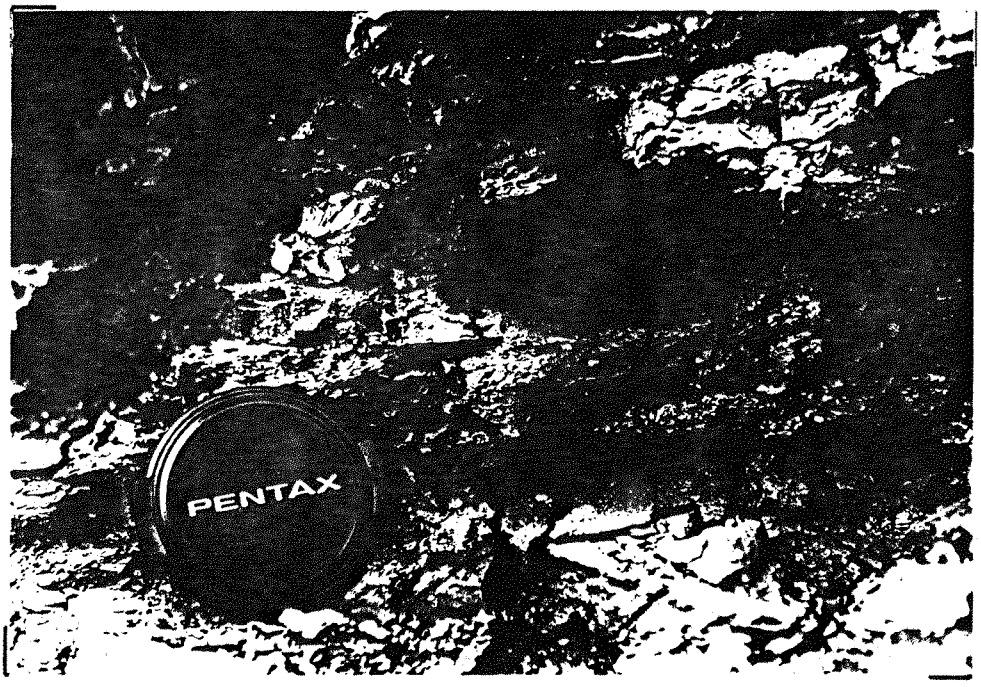

F PREFERRED BEDDING PLANE
SHEAR SURFACE(UNSHEARED)

(Preferred shear plane immediately above lens cap)

FIG.D-1

APPENDIX E: THE DETAILS OF THE CROSS SECTIONS USED IN THE BACK ANALYSIS AND STABILITY ANALYSIS (Chapter 7)

TABLE E-1 Details of section D1 in November 1980

Slice No	Base Angle (Degrees)	Mid Depth (metres)	Slice Breadth (metres)	Pore Water Pressure (kNm^{-2})	Weight (kN)
1	65	1.6	2.0	10.79	60.25
2	65	4.6	2.0	33.35	173.23
3	65	8.0	2.0	63.77	301.26
4	46	10.6	2.0	79.46	399.18
5	14	10.8	2.0	82.40	406.71
6	0	10.5	2.0	85.35	395.41
7	0	10.2	2.0	79.46	384.11
8	0	10.0	2.0	76.52	376.58
9	0	9.8	2.0	71.61	369.05
10	0	9.2	2.0	67.69	346.45
11	0	8.8	2.0	58.86	331.39
12	0	8.0	2.0	51.99	301.26
13	0	7.8	2.0	49.05	293.78
14	0	7.6	2.0	45.13	286.20
15	0	7.4	2.0	43.16	278.67
16	0	7.8	2.0	39.24	293.73
17	0	8.2	2.0	35.32	308.80
18	0	8.4	2.0	29.43	318.33
19	0	8.6	2.0	27.47	323.86
20	0	8.6	2.0	24.53	323.86
21	0	8.0	2.0	20.60	301.26
22	0	7.2	2.0	17.66	271.14
23	0	7.0	2.0	14.72	263.61
24	0	6.6	2.0	9.81	248.54
25	0	5.8	2.0	7.85	218.42
26	0	5.2	2.0	4.91	195.82
27	0	5.0	2.0	1.96	188.29
28	0	5.0	2.0	1.96	188.29
29	0	3.2	2.0	1.96	120.51
30	0	1.5	2.0	1.96	56.49
31	0	0.4	1.6	1.96	12.05

TABLE E-2 Details of section D1 in July 1982

(All slice breadths = 2m)

Slice No	Base Angle (Degrees)	Mid Depth (metres)	Pressure Head (metres)	Pore Water Pressure (kNm^{-2})	Weight (kN)
1	65	1.8	1.1	10.79	67.78
2	65	5.6	3.4	33.35	210.89
3	65	8.8	6.5	63.77	331.39
4	46	9.6	8.1	79.46	361.52
5	14	9.8	8.4	82.40	369.05
6	0	9.6	8.7	85.35	361.52
7	0	9.2	8.1	79.46	346.45
8	0	8.8	7.8	76.52	331.39
9	0	8.6	7.3	71.61	323.86
10	0	8.4	6.9	67.69	318.33
11	0	8.2	6	58.86	308.80
12	0	8	5.3	51.99	301.26
13	0	8	5	49.05	301.26
14	0	7.8	4.6	45.13	293.73
15	0	7.6	4.4	43.16	286.20
16	0	7.4	4	39.24	278.67
17	0	7.4	3.6	35.32	278.67
18	0	7.2	3	29.43	271.14
19	0	7.2	2.8	27.47	271.14
20	0	7.1	2.5	24.53	267.37
21	0	7	2.1	20.60	263.61
22	0	6.4	1.8	17.66	241.01
23	0	5.8	1.5	14.72	218.42
24	0	4.6	1.0	9.81	173.23
25	0	3.6	0.8	7.85	135.57
26	0	2	0.5	4.91	75.32
27	0	0.8	0.2	1.96	30.13

TABLE E-3 Details of section D2 in November 1980

Slice No	Base Angle (degrees)	Mid Depth (metres)	Slice Breadth (metres)	Pore Water Pressure (kNm^{-2})	Weight (kN)
1	65	0.8	1.0	21.58	15.06
2	65	2.8	2.0	43.16	105.44
3	65	8.2	2.0	77.50	233.48
4	46	10.0	2.0	98.27	376.58
5	14	11.6	2.0	91.23	436.83
6	0	12.2	2.0	91.23	459.43
7	0	12.0	2.0	87.31	451.90
8	0	11.8	2.0	82.40	444.36
9	0	11.0	2.0	78.48	414.24
10	0	11.8	2.0	74.56	444.36
11	0	12.2	2.0	69.65	459.43
12	0	11.8	2.0	66.71	444.36
13	0	11.8	2.0	62.78	444.36
14	0	12.0	2.0	58.86	451.90
15	0	10.8	2.0	52.97	406.71
16	0	10.0	2.0	48.07	376.58
17	0	9.0	2.0	44.15	338.92
18	0	8.0	2.0	41.20	301.26
19	0	6.4	2.0	38.26	241.01
20	0	6.0	2.0	35.32	225.95
21	0	6.0	1.0	33.35	225.95
22	0	6.0	2.0	30.41	225.95
23	0	6.0	2.0	28.45	225.95
24	0	6.2	2.0	26.49	233.48
25	0	6.0	2.0	24.53	225.95
26	0	5.0	2.0	22.56	188.29
27	0	4.4	2.0	20.60	165.70
28	0	3.8	2.0	18.64	143.10
29	0	3.4	2.0	15.70	128.04
30	0	2.4	2.0	13.73	90.38
31	0	2.4	2.0	11.77	90.38
32	0	3.0	2.0	8.83	112.97
33	0	1.6	2.0	5.89	60.25
34	0	0.8	2.0	2.94	30.13

TABLE E-4 Details of section D2 in July 1982

(All slice breadth = 2m)

Slice No	Base Angle (Degrees)	Mid Depth (metres)	Pressure Head (metres)	Pore Water Pressure (kNm^{-2})	Weight (kN)
1	65	3.4	2.2	21.58	128.04
2	65	8.4	4.4	43.16	316.33
3	65	10.6	7.9	77.50	399.18
4	46	11.8	9.1	89.27	444.36
5	14	12.6	9.3	91.23	474.49
6	0	12.6	9.3	91.23	474.49
7	0	11.4	8.9	87.31	429.30
8	0	11	8.4	82.40	414.24
9	0	10.8	8.0	78.48	406.71
10	0	10.8	7.6	74.56	406.71
11	0	11.8	7.1	69.65	444.36
12	0	12	6.8	66.71	451.90
13	0	11.8	6.4	62.78	444.36
14	0	11.6	6.0	58.86	436.83
15	0	11.8	5.4	52.97	444.36
16	0	11	4.9	48.07	414.24
17	0	10.2	4.5	44.15	384.11
18	0	9.6	4.2	41.20	361.52
19	0	8.2	3.9	38.26	308.80
20	0	6.8	3.6	35.32	256.07
21	0	5.4	3.4	33.35	203.35
22	0	4.8	3.1	30.41	180.76
23	0	4.6	2.9	28.45	173.23
24	0	4.4	2.7	26.49	165.70
25	0	4.4	2.5	24.53	165.70
26	0	4.6	2.3	22.56	173.23
27	0	5	2.1	20.60	188.29
28	0	5.4	1.9	18.64	203.35
29	0	5.2	1.6	15.70	195.82
30	0	4	1.4	13.73	150.63
31	0	3.4	1.2	11.77	128.04
32	0	2.8	0.9	8.83	105.44
33	0	2.4	0.6	5.89	90.38
34	0	2	0.3	2.94	75.32

TABLE E-5 Details of section D3 in November 1980

Slice No	Base Angle (Degrees)	Mid Depth (metres)	Slice Breadth (metres)	Pore Water Pressure (kNm^{-2})	Weight (kN.)
1	65	1.8	2.0	9.81	67.84
2	65	4.8	2.0	29.43	180.76
3	65	8.4	2.0	53.96	316.33
4	46	11.2	2.0	80.44	421.77
5	14	12.0	2.0	84.37	451.90
6	0	12.0	2.0	82.40	451.90
7	0	10.4	2.0	80.44	391.64
8	0	9.1	2.0	77.50	342.69
9	0	8.2	2.0	75.54	308.80
10	0	7.8	2.0	72.59	293.73
11	0	7.5	2.0	56.70	2824.35
12	0	7.0	2.0	40.22	263.61
13	0	5.2	2.0	36.30	195.82
14	0	4.3	2.0	32.37	161.93
15	0	3.4	2.0	27.47	128.04
16	0	3.0	2.0	22.56	112.97
17	0	3.0	2.0	17.66	112.97
18	0	2.8	2.0	13.73	109.44
19	0	2.5	2.0	11.77	94.15
20	0	2.3	2.0	9.81	86.61
21	0	2.3	2.0	6.87	86.61
22	0	2.0	2.0	4.91	75.32
23	0	1.9	2.0	3.92	71.55
24	0	1.6	2.0	1.96	60.25
25	0	0.9	2.0	1.96	33.89
26	0	0.5	0.4	1.96	3.77

TABLE E-6 Details of section D3 in July 1982

(All slice breadths = 2m)

Slice No	Base Angle (degrees)	Mid Depth (metres)	Pressure Head (metres)	Pore Water Pressure (kNm^{-2})	Weight (kN)
1	65	1.8	1.0	9.81	67.78
2	65	5	3.0	29.43	188.29
3	65	8.6	5.5	53.96	323.86
4	46	11.2	8.2	80.44	421.77
5	14	12.2	8.6	84.44	421.77
6	0	11.6	8.4	82.40	436.83
7	0	10.6	8.2	80.44	399.18
8	0	9.6	7.9	77.50	361.52
9	0	9	7.7	75.54	338.92
10	0	8.4	7.4	72.59	316.33
11	0	8	7.1	69.65	301.26
12	0	7.6	6.8	66.71	286.20
13	0	7.3	6.5	63.77	274.90
14	0	7.2	6.2	60.82	271.14
15	0	7.2	5.9	57.88	271.14
16	0	7.2	5.6	54.94	271.14
17	0	7.1	5.4	52.97	267.37
18	0	7.1	5.1	50.03	267.37
19	0	7	4.8	47.09	263.61
20	0	6.9	4.4	43.16	259.84
21	0	6.8	4.1	40.22	256.07
22	0	6.6	3.7	36.30	248.54
23	0	5.1	3.3	32.37	192.06
24	0	4.1	2.8	27.47	154.40
25	0	3.4	2.3	22.56	128.04
26	0	2.6	1.8	17.66	97.91
27	0	2.4	1.4	13.73	90.38
28	0	2.4	1.2	11.77	90.38
29	0	2.3	1.0	9.81	90.38
30	0	2.5	0.7	6.87	94.15
31	0	2.4	0.5	4.91	90.38
32	0	1.8	0.4	3.92	67.78
33	0	0.6	0.2	1.96	22.60

APPENDIX F: THE FIELD INVESTIGATION

APPENDIX F: THE FIELD INVESTIGATION

F.0 Introduction

In this appendix the results of the surface movement monitoring and the position of the active shear surfaces are given. These data contribute to the understanding of the pattern and characteristics of surface movements recorded between July 1981 and July 1983.

F.1 Subsurface results

This section details the results of five different methods used to detect the position of shear surfaces within the study area.

Each technique has produced results which when combined form a map of the depths to active shear surfaces within the study area, Fig. 4-1.

The installation technique for the inclinometer and slip indicator equipment is described in Chapter 3.

F.2 Inclinometer results

Table 3-2 lists the performance of the eleven inclinometers installed during the study period. The profiles of inclinometers I2, I3, I5, I6, I7, I8, I9 and I10 are displayed in Figs. F-1 to F-8. These profiles were calculated by summating displacements from the top of the tube. Tables F-1 to F-8 list the XY co-ordinates of the inclinometer tops at the time the tube was profiled. Only I11 was anchored at its base and remained in operation until the end of the field study. No continuous record of the position of the top of the tube was required. Displacements were summated from the tube

base at 8.5m below ground level. The profiled shape of Il1 is illustrated in Fig. F-9.

F.2.1 Individual tube performance

F.2.1.1 Il

Inclinometer Il was pushed by hand through the soft matrix of mudslide A and then hammered into the base of the mudslide channel. One profile was taken immediately after installation. The next day the rate of mudslide movement had caused the tube to be bent over to 45° before a second profile could be taken. The tube was completely immersed in the mudslide after 3 days.

Rod penetration tests on mudslide A established a maximum mudslide depth of 1.7m. The average depth of the soft mudslide matrix was 1.2 metres. Further installation of inclinometer tubes to this shallow depth was not considered worthwhile.

During the winter of 1980/81 the rate of surface movement of mudslide A was six times greater than the Beltinge inclinometers, averaging 84mm per day over a sixty three day period. This rate of mudslide movement, the shallow depth of the mudslide and the general inaccessibility of the lower portion of mudslide A prevented further investigation into the velocity profile.

However, the clearly defined channel pictured in Fig. F-10 left no doubt that mudslide A was governed by the same geomorphological process described by Hutchinson for the Beltinge mudslides. The soft matrix of the mudslide slid seawards along a channel with clearly defined basal and lateral shear surfaces.

F.2.1.2 I2

Inclinometer I2 was installed approximately 10 metres from the seaward edge of the amphitheatre. The tube was profiled for a total of 84 days although failure occurred within 13 days of installation. The first two site visits, on the 8 and 15 January 1981, resulted in a 3.5m profile. The second of these profiles indicated a change in tube curvature over the bottom one half metre of the inclinometer. The next profile on the 21 January 1981 could only be performed to a maximum depth of 3 metres.

The tube failed 3.25m below the ground surface; a failure depth of 9.66m A.O.D. The level coincides with the elevation surveyed for the D bedding plane shear surface on the D scarp.

After the initial failure I2 was profiled for another 71 days. The top of the tube moved seaward 2.21m Y. The inclination of the tube remained near vertical during this movement although the last three profiles did indicate an increase in velocity with increasing depth. Between the 21 January 1981 and 2 April 1981 the total inclination of the tube from the vertical increased from 0.84° to 7.56°. The sliding movements recorded up to the 5 March 1981 implied translational sliding across the D bedding plane shear surface. After 5 March 1981 the inclinometer tube was incorporated in an edge failure.

F.2.1.3 I3

Inclinometer I3 was installed in the A3 bench. The aluminium tube was pushed by hand into the soft colluvium of the A3 bench and then hammered in for the last half metre. The installation site was approximately 5 metres from the D scarp and 10 metres from the seaward edge of the A3 bench. Due to the large movements already observed

on the A3 bench the tube was positioned and profiled immediately after installation.

The initial profile was to a depth of 2.5m from the top of the tube. Five days later the inclinometer had moved 1.03m Y seawards and the instrumentation torpedo could only be lowered to a maximum depth of 2m below ground level. The tube had failed 5 days after installation. The failure depth was between 1.23m and 1.73m A.O.D. Ground survey levels of 1.71m, 1.73m and 1.49m A.O.D. were taken on the A3 bedding plane shear surface, Fig. 2-8.

After 17 March 1981 the inclinometer was profiled until 25 August 1981, the tube was then made inoperative due to vandalism. During this 161 day period 18 profiles were recorded. They indicated that the movement of colluvium across the A3 bench took place due to translational sliding. The inclinometer tube remained within four degrees of vertical over its whole depth during the 5.41m Y of seaward movement. This is illustrated in Fig. F-2.

Ninety eight days after the final profile the inclinometer tube was deposited on the beach. It had been displaced seawards a total distance of 10.08m Y since installation. The recovered tube, pictured in Fig. F-11 and Fig. F-12, illustrates the deformed profile.

The deformed tube was in two parts; an upper 2.45m section and a shorter length 0.59m long which included the penetration tip. The major section which had remained virtually upright during the complete period of instrumentation, was kinked 1.4m from the top. The kink was positioned at the level of tube exposure when the inclinometer was found on the beach.

Recovery of the shorter lower section occurred nine days after the removal of the main tube from the beach. Inspection of the two sections indicate that the initial

tube failure occurred along a distinct plane: the zone of tube deformation was narrow, Fig. F-11. However, despite the severity of the kink in the tube the two sections could not have been separated. If they had the lower section would have remained embedded in the A2 in-situ clay beneath the A3 bench. The lower section must have been pulled clear from its shallow penetration of the A2 clay and dragged seawards by the translation of the main tube. Physical separation occurred when the main tube was pulled clear of the beach.

F.2.1.4 I4

Inclinometer I4 was sited in the A3 bench on the western extreme of the study area. It was installed by simply pushing the tube into the colluvium and then hammering the tube for the last half metre. The initial profile and ground position were taken immediately after installation. The inclination was recorded to a depth of 2.5m below the top of the tube approximately 1.9m below ground level.

No further observations were made as the tube was vandalised four days after installation.

F.2.1.5 I5

Inclinometer I5 was sited in the amphitheatre. The top of the tube was 16.07m A.O.D. and the tube was installed to a depth of 3.8m. It was sited in the rear of the amphitheatre, 10m seaward of DS2. Unlike I1, I2 and I3 this inclinometer tube did not fail within a few days of installation. It did not penetrate the D bedding plane shear surface.

The first nineteen profiles took place over 162 days: the top of the tube moved 690mm seawards. Figure F-3

illustrates the seaward progression of the tube. The initial profile had an overall inclination of 3.2°, this increased to 5.4° by the 16 September 1981. Movement of the tube over this 162 day period was due to a translational slide over a near horizontal shear surface at a level lower than 12.27m A.O.D.

The twentieth profile on 5 October 1981 was only taken over a 3m depth. The inclinometer torpedo could not drop below 3.4m from the ground surface. This indicated a failure plane between 12.27m and 12.67m A.O.D. The failure coincided with the onset of increased movement. The top of the tube accelerated from a daily rate of 6mm Y between 7 April 1981 and 16 September 1981 to 13mm Y per day between 16 September 1981 and 4 November 1981.

F.2.1.6 I6

Inclinometer I6 was sited in the rear section of the amphitheatre. It was situated 3m seaward of the colluvium which formed the rear scarp and eight metres to the east of the head of mudslide A. The site was overriden by DS5 in the winter 1982-83.

The tube was installed to a depth of 3m and three profiles were taken during July 1981. The tube was translated 20mm Y in this eight day period. No significant deformation of the tube took place. The next profile, 49 days later on 3 September 1981, was limited to 2.5m. The tube had failed between 12.24m and 12.74m A.O.D. Over the 49 days between the two profiles the top of the tube had moved seawards 50mm Y.

Two subsequent profiles were taken 13 and 32 days after 3 September 1981. They could only be taken to two metres below ground level. The tube had again deformed to prevent passage of the torpedo.

F.2.1.7 I7

Inclinometer I7 was installed in the rear of the amphitheatre 24m to the east of I6. It was sited 4.5m seaward of DS2 and to a depth of 4.5m. Twelve profiles were taken over 118 days: failure occurred between 3m and 3.5m below ground level.

The first six profiles took place over 54 days. Ground surveys registered 40mm Y of seaward movement for the top of the tube. The overall inclination of the tube changed by 0.06°: no significant deformation of the tube occurred. During the next 57 days ground movements increased and the inclinometer top moved 670mm Y. Again the tube did not deform although the overall inclination did alter by 0.77° over the 4.5m total depth. The colluvium into which the inclinometer had been installed was sliding on a shear surface at least 4.5m below the ground surface, at a level lower than 11.2m A.O.D.

Between 12 and 19 November 1981 the inclinometer top moved 670mm Y. This moderate rate of movement caused failure of the inclinometer tube at a level between 12.21m and 12.71m A.O.D. A shear surface within the colluvium had become active; this was in addition to that responsible for the translation of the whole 4.5m of inclinometer tube. The level of this upper shear surface coincided with that detected in I5 and I6, both of these tubes were also located within the amphitheatre. A final tube profile was taken to a depth of 3m.

Despite recording three profiles in the 14 days before failure no tube deformation for I7 was registered. The failure of I7 emphasises the difficulty in using inclinometers in areas of rapidly changing movement rates.

F.2.1.8 I8

Inclinometer I8 was located in the lower eastern portion of DS3. The tube was installed to a total depth of 5.4m from the ground surface. Three profiles were taken and one ground survey position. The tube failed four days after installation: 2 metres below the ground surface.

Interpolation from an adjacent survey peg, number 167, indicated an overall surface movement of 100mm Y in four days prior to the failure. The relatively shallow failure depth occurred at the basal shear plane of the debris slide.

Tube deformation between 1.5m and 2.5m below the ground surface was noted before failure.

F.2.1.9 I9

Inclinometer I9 was sited in the central portion of DS1. Two profiles were taken and one ground survey position. The tube was installed to a depth 5m below ground level. Failure occurred five days after installation at 0.88m below the surface.

Interpolated surface movement from peg 223 indicated a seaward displacement of 480mm Y in the five days prior to failure. Failure occurred on the basal shear surface of debris slide 1. The two profiles taken indicated some tube distortion in the upper two metres of the inclinometer tube before failure.

F.2.1.10 I10

Inclinometer I10 was located 40m to the east of the amphitheatre on the eastern portion of the D bench. It

was installed to a depth of 4.5m and remained operative for 83 days before being vandalised. Eight profiles were recorded.

The tube translated seawards 220mm Y in 83 days and changed in overall inclination by 0.2°. No failure of the inclinometer occurred before it became inoperative. The seaward movement implied sliding over a shear surface below 10.91m A.O.D.

F.2.1.11 Ill

Inclinometer Ill was installed in the cliff top on 23 October 1982. It was still operative in December 1984. The tube is situated 4.5m from the cliff edge, directly behind the centre line through the amphitheatre. The auger hole into which Ill was placed indicated a plateau gravel thickness of 2.4m overlying the Barton Clay.

From exposures of the F preferred bedding plane shear surface, within the study area, the F shear surface was estimated to be seven metres below ground level at this drilling site. The inclinometer was installed to a depth of 9 metres below ground level.

The tube profiles for Ill were recorded on a weekly basis. Unlike the undercliff inclinometers the profiles were summated from the bottom of the tube: movement was anticipated along the F preferred bedding plane shear surface.

Since installation the tube has not deformed more than 2mm over its whole length.

F.3 Slip indicator results

The installation of slip indicators in the study area

located nine active shear surfaces. One failure occurred on the F bench, five inside the amphitheatre, one in the western portion of the D bench and two in DS3. The details of installation and the slip indicator performance are summarised in Table 3-3.

F.3.1 Failure depths

F.3.1.1 F Bench

The two slip indicators on the F bench were installed 67m apart. They marked the approximate eastern and western extremes of the amphitheatre rim. SPI3 produced a definite failure depth of 22.2m A.O.D. Field observations show that at the section the F bedding plane shear surface should have been at 24.6m A.O.D. Failure at this lower depth prompted inspection of the surrounding area, this indicated that to the east and behind the amphitheatre was an intact cliff top failure block. An exposed shear surface, visually identical to the F shear surface was levelled at 22.96m A.O.D. If the level of slip indicator failure and the exposed surface are linked, the shear surface and therefore the failure block was back tilted 2°. This inclination agrees with the mode of backtilting cliff top slump failure outlined in Barton, Coles and Tiller (1983). The presence of the failure block also explains the topographical discontinuity in this area.

SPI4 did not indicate a positive failure depth before it was vandalised.

F.3.1.2 D Bench

SPI5 was located 12m to the west of the amphitheatre. The tube was installed to 9m below the ground surface. Failure occurred at 9m to 9.5m A.O.D. at the level of the

D bedding plane shear surface.

F.3.1.3 Amphitheatre

The five failures in the amphitheatre were divided between the D preferred bedding plane shear surface and the elevated shear surface detected by I5, I6 and I7. SPI2, SPI9 and SPI10 failed along the basal shear surface of the D bench. SPI2, situated 29m from the D scarp, detected the shear surface at 9.29m A.O.D. SPI9 and SPI10, 6 and 8 metres from the scarp edge respectively, failed at 7.62m and 8.49m A.O.D. These failure levels are below the predicted level of the D shear surface. Their proximity to the scarp edge resulted in the indicators being incorporated in an edge failure.

The elevated shear surface was located by SPI1 and SPI7. SPI7 installed 31m from the D scarp edge failed at 12.19m A.O.D. and corresponds to the inclinometer failure depths. SPI1 only 15m from the scarp edge failed at the greater depth of 11.06m A.O.D. This lower elevation could be linked to the plane detected by SPI7: the shear surface would have a seaward inclination of 4.7°, from the horizontal.

F.3.1.4 Debris slide 3

The two failed slip indicators, SPI13 and SPI14, were part of a network of nine indicators installed in DS3 to establish the shape of the shear surface. The two failures occurred at 2.12m and 0.49m below ground level and within 6 days of installation. The other indicators were all covered in the rapid downslope movement of colluvium which occurred at the time of installation.

F.4 Auger detection of shear surfaces

F.4.1 Piezometer installation

During the installation of seven piezometers (by Dr. R.I. Thomson) a distinct change was noted in the character of the colluvium. The physical effort required to achieve any further penetration beyond a certain level and inspection of the auger turnings indicated penetration into the in-situ clay.

Figure 4-1 illustrates the positions of the auger holes and the depths of the in-situ Barton Clay. Two holes pierced the F shear surface. One installation reached the D shear surface at the head of mudslide B and four piezometer holes penetrated the A2 zone of the Barton Clay.

The seven levels all correspond with major exposures of the preferred bedding plane shear surfaces.

F.4.2 Debris slide 4

The detection, by augering, of shear surfaces within the colluvium was used to define the basal shear surface of DS4. The slide formed in Spring 1982 and the augering was carried out on 17 and 20 December 1982. Ten holes were drilled. The depth of slide debris ranged between 1.08m and 3.04m.

Whilst the detection of a shear surface between two ages of debris was not as distinct as the change from colluvium to in-situ clay it was possible to map the newly formed slide. The fresh colluvium had overriden fresh vegetation (mainly grass) on its lower slopes and a gravel strewn surface on the upper levels. Careful operation of the auger and inspection of the auger turnings enabled the

change from fresh to old colluvium to be noted.

Figure F-13 illustrates the outline of DS4 and locates the depth of overlying colluvium. The slide is shallow was the head and near the edge of the downslope snout. Maximum depths are found in the central zone where material from the steeper rear section had accumulated. The range of depths seems comparable with the failure surfaces detected by I8 and I9 on DS3 and DS1 respectively and SPI13 and SPI14 on DS3.

F.4.3 Mudslide A

The shape of the channel which contained mudslide A was profiled by the penetration of the mudslide matrix by steel rods. Five cross sections were taken. They identified a shallow channel with an average depth of 1.2m and a maximum depth of 1.7m. The lateral and basal shear surface of mudslide were clearly defined.

The shape and location of the profiles are illustrated in Fig. 13a.

F.5 Surveyed shear planes

A characteristic of the combination of structural geology and geomorphology in this outcrop of the Barton Clay is to expose the active preferred bedding plane shear surfaces along scarp faces. The three surfaces active within the study area have all been observed, Figure F-14 illustrates the levels taken during the field study.

The F bedding plane shear surface was not exposed at the start of the study period. Only movements prior to the formation of debris slide 4 exposed an identifiable length. Four levels were taken on this fresh exposure.

In addition an inspection of the rear slope of debris slide 3 resulted in the identification of a short length of F bedding plane shear surface, 60m to the west of the first site. The west to east dip between the two sites is approximately 0.7° compared to 0.5° Barton (1973).

The D scarp is exposed over the whole length of the study area. However, access is severely limited and only four levels were obtained. Whilst the levels were within a range from 9.06m to 9.52m A.O.D. they did not descend with the direction of dip. The exposures, especially those in the central section of the amphitheatre may have been displaced in an edge failure and produced misleading exposure levels.

The A3 scarp is rarely exposed and the three levels measured followed a period of force 5 to 7 south to south westerly winds between 18 November 1981 and 27 November 1981. The highest elevation was levelled at 1.79m A.O.D.

F.6 The application of the ground survey to surface movements

The primary purpose of the ground survey network described in Chapter 3 was to measure surface movements within the undercliff. The data collected is used in this thesis to study four aspects of slope degradation.

(i) The overall pattern of surface movement.

(ii) The movement characteristics of the slope degradation processes.

(iii) Multi-layered landslides.

(iv) The volume of material moved and the colluvial budget.

Items (i) and (ii) are discussed in Chapter 4. Items (iii) and (iv) are discussed in Chapters 5 and 6 respectively.

F.6.1 The data collection

Between 8 July 1981 and 12 July 1983 forty two surveys were carried out. In the summer periods a survey took place every four weeks. In winter the frequency was increased to a survey every two weeks. The 734 day total study period included thirteen surveys in 1981, twenty two in 1982 and seven in 1983. One hundred and fifty three different peg positions were used and twenty four pegs were monitored over the complete study period.

The first survey monitored the position of seventy seven pegs. Subsequent movements over the two year period caused the loss of fifty two of these original pegs. As pegs were lost they were replaced to maintain the necessary coverage: 76 replacement pegs were used.

F.6.2 The data calculations

Each survey was processed to produce a set of three dimensional co-ordinates for each peg (see Appendix A). The full set of survey movement results are included in Coles (1983). It contains 24 records lasting 734 days and 129 records which extend between 15 days and 615 days.

F.6.3 Division of the movement cycle

F.6.3.1 Overall pattern of degradation

Over the two year study period the majority of the undercliff has had a common pattern of movement. The

pattern is seasonal and is most easily identified in the movements of the D bench. Three survey pegs which completed the study period illustrate this cycle, see Fig. F-15. They covered 170m of the study area from east to west. Their cycle of movement has been divided into eight sections. Each section has an approximate constant rate of movement. The name, length and date of each section is given in Table F-9.

To supplement the survey data the surface movement readings obtained for the water balance study conducted by Dr. R.I. Thomson. The survey dates differ from the periods already defined in Table F-9 but the extra coverage does compliment the peg data. The four periods of piezometer surface movement are summarised in Table F-10.

F.6.3.2 The movement characteristics of the geomorphological processes

To establish the movement characteristics of individual processes it is necessary to combine the 24 complete peg records with the less extensive survey data to provide a 734 day coverage.

Of the seven geomorphological processes listed in section 2.3, bench slides, mudslides, debris slides, spalling and slumping were monitored over the total study period. Mudruns and stream erosion were considered insignificant to the movement of colluvium within the undercliff. the data collected by the surveying of pegs is suited to the characterization of bench sliding, mudsliding and debris sliding.

F.6.4 Movement data notation

The description of peg movements in sections F.7.1 to

F.7.8 and F.8.1.1 to F.8.3.6 is summarised in Table F-11. The movements quoted are either the total movement recorded during one of the twelve subdivisions of the two year study period outlined in Tables F-9 and Table 5-10 or a daily rate of displacement. The three dimensional survey grid is used to indicate the plane of movement. Displacements are classified as being in the horizontal plane (XY), the vertical plane (Z) or the seawards direction (Y).

F.7 The overall pattern of surface movement

In this section a brief description is given of the surface movements which occurred during each period. The description is supplemented by maps of the study area depicting both the magnitude and the direction of surface movement.

The rates of movement are described using the scale presented by Varnes (1978, Fig. 2-1a). This system divides movement velocities into seven categories illustrated in Fig. F-16. The range of movement varies from 60mm per year to 3m per second.

At Highcliffe movement rates range from no displacement in three months to over 290mm per day. The range of movements for each geomorphological process is illustrated against the expanded section of the full scale in Fig. F-16.

F.7.1 First summer (S1) (8/7/81 to 30/9/81) Table F-12, Fig. F-17

Throughout the whole undercliff the rate of movement was very slow. Only DS2, the A3 bench and the edge of the amphitheatre moved with rates in the slow category. The F bench was essentially stationary over the 110m covered by

survey pegs. Although two pegs, 151 and 152 which both bordered DSl. registered 30mm Y. The whole of the D bench moved within the limited range 20mm Y to 110mm Y. The higher rates occurred on the eastern flank; the central region behind the amphitheatre had an average rate of 40mm Y. To the west movements were registered between 10mm Y and 20mm Y. Higher velocities were detected near the seaward edge of the bench. A peak rate for peg 171 (270mm Y, - 120mm Z) was recorded adjacent to an internal failure scarp to the east of the amphitheatre.

The A3 bench was monitored by two survey pegs. Peg 216 was located in the accumulation zone of mudslide B and registered ten times the movement rate of the other A3 bench survey peg. Peg 217 placed within the A3 bench moved 60mm Y: - 60mm Z. The movement rate of the A3 bench was very similar to the bulk of the D bench.

Debris slide 1 indicated velocities above the adjacent D bench. The average was 60mm Y, - 40mm Z compared to 40mm Y, - 10mm Z. Debris slide 2 contained movements similar to the amphitheatre floor. Only peg 191 (110mm Y, - 90mm Z) registered a larger displacement.

Mudslide A moved with the same speed as the amphitheatre floor, the range varied between 70mm Y and 100mm Y. Mudslide B was not monitored due to vandalism. The rear portion of the amphitheatre, called the floor, moved with the same velocity as the D bench. During this period the floor included mudslide A. Seaward of the floor area pegs adjacent to the internal amphitheatre scarp indicated the largest movement rates in the entire study area. Pegs 199, 202 and 203 moved 1640mm Y, 1540mm Y and 3760mm Y respectively. The latter movement bordered on the moderate category of movement rates. The large displacements occurred in zones of intense disruption where internal scarps mark the rear boundaries of compound edge failures.

F.7.2 **First winter, part one (W1/1)** (30/9/81 to 11/11/81) Table F-13, Fig. F-18

All areas in the undercliff except the F bench showed a marked increase in surface velocity between 22 September 1981 and 11 November 1981. The movement of the four pegs on the F bench ranged from 10mm Y, 30mm Z to 10mm Y, -20mm Z. These are very similar displacements to those recorded for the first summer.

The D bench generally increased rates of movement five fold. To the west peg coverage showed a range of seaward movement between 70mm Y and 320mm Y within 30 metres. Peg 166, the faster mover, was located on the site of several old debris slides. Possible debris slide reactivation would account for this displacement well over the local background figure.

The central D bench had a uniform range of horizontal movements between 180mm Y and 270mm Y. Only peg 164 registered an appreciably lower rate, 120mm Y.

Pegs near the D scarp and those incorporated in an edge failure gave the fastest movement rates. Peg 167 (1190mm Y, - 640mm Z) and peg 171 (870mm - 360mm) illustrate the rapidity of the edge failure mode.

The A3 bench accelerated from a daily rate during the first summer of 0.8mm Yd to 16mm Yd. Debris slide 1 increased in velocity over an area 40m wide; it incorporated pegs 151 and 152 and had a peak movement of 820mm Y, - 210mm Z. Debris slide 2 was more active. The eastern rim of the amphitheatre back scarp registered a local maximum movement of 2000mm Y; - 620mm Z.

Mudslide A exhibited rates of movement higher than the surrounding bench. Movement in the upper sections averaged 1440m Y compared to the amphitheatre floor: 800mm

Y. The lower section moved with moderate velocity. Peg 213 monitored for the first eight days of the first winter period (W1/1) moved 550mm Y, - 610mm Z equivalent to 70mm Yd compared to the adjacent amphitheatre figure of 40mm Yd. Mudslide B registered movements of 70mm Yd over a fifty day period. Pegs adjacent to the feeder channel were incorporated and had daily rates of 90mm Yd to 160mm Yd.

In the amphitheatre floor four pegs moved between 760mm Y and 980mm Y. The range was lower than the mudslides but higher than the D bench values. The amphitheatre edge moved 2200mm Y. Rapid depletion of the forward area of the amphitheatre promoted internal failure of the amphitheatre floor.

F.7.3 First surge (SGI) (11/11/81 to 24/11/81) Table F-14, Fig. F-19

During this period a substantial part of the study area moved seawards with velocities in the moderate category. The D bench registered a peak rate of 40mm Yd. This contrasts with 2mm Yd for the same peg during the first winter period. The surge increased the rate of movement of all the processes active on the D bench. Only the F bench did not show an appreciable increase in velocity.

The pegs on the F bench registered a maximum seaward movement of 30mm Y. No change in elevation occurred. Within the D bench pegs moved over a range of 470mm Y, - 610mm Z in the west, 720mm Y, - 280mm Z over the centre and to a local maximum of 1160mm Y, - 440mm Z in the east.

Debris slides 1 and 2 increased in velocity due to the surge effect. DS1 averaged 1380mm Y, - 850mm Z over a width of 44 metres and DS2 1160mm Y, - 70mm Z. The amphitheatre and mudslide A had an average velocity of 1420mm Y, - 130mm Z and 1730mm Y, - 240mm Z respectively.

The survey data indicates that the surge movements were the result of a relatively large translation along the D preferred bedding plane shear surface.

F.7.4 First winter, part two (W1/2) 24/11/81 to 29/4/82)

Table F-15, Fig. F-20

After the surge period the velocity throughout the study area returned to rates similar to those recorded during W1/1. A cliff top slump occurred between 9 and 18 March 1982. This disrupted the central F bench; pegs 223, 224, 225 and 226 registered seaward movement of 130mm Y, 270mm Y, 950mm Y and 300mm Y respectively in a nine day period. The eastern extreme of the F bench remained virtually dormant.

The western and central regions of the D bench registered daily velocities half those recorded for W1/1. In the west peg 165 moved 300mm Y, - 240mm Z; this fell within the range of movement for the central pegs of 240mm Y to 380mm Y and - 70mm Z to - 120mm Z. To the east higher velocities were recorded. Peg 175 on a relic debris slide registered a local maximum of 2150mm Y, - 860mm Z. The average for the eastern area was 1630mm Y compared to 330mm Y for the western and central regions.

The change in ground conditions during the winter periods made the A3 bench impassable. Winter movement rates were confined to the monitoring of inclinometer I3. Between 25 August 1981 and 1 December 1981 this moved 3630mm Y, a daily rate of 40mm Y.

Debris slide 1, affected on its western flank by the cliff top slump, increased its average displacement from 10mm Yd, - 40mm Zd to 20mm Yd, - 3mm Zd between the two winter periods. Debris slide 2 also became more active. The central portion registered a maximum peak rate for the

total study area of 7590mm Y, - 2770mm Z.

Mudslide A was impossible to monitor over the whole of the first winter period. Peg 219, lost after 23 February 1982, moved 4240mm Y, - 1070mm Z a daily rate of 50mm Yd. This was faster than the amphitheatre floor which averaged 2120mm Y, - 470mm Z a daily average of 20mm Y. The seaward edge of the amphitheatre was very active and pegs within this area were subject to large drops in elevation. Peg 200 moved 4790mm Y, - 1360mm Z during the full 141 day period.

F.7.5 Second summer (S2 and SP2) (29/4/82 to 6/10/82)

Tables F-16, F-17
Fig. F-21

The second summer period was the longest study period. Two new debris slides were monitored; one to the west, debris slide 3 (DS3), and the second behind the western rim of the amphitheatre, DS4. These features are discussed in sections F.8.3.3 and F.8.3.4.

The F bench was monitored by 7 pegs; activity either side of the central zone was minimal. In the central region the effects of the cliff top slump, the formation of DS4 and the activity of DS1 caused some movement. Peg 225 positioned directly in front of the slump moved 200mm Y, - 60mm Z.

All the D bench pegs in the western and central areas were confined to a movement range of 160mm Y, - 100mm Z to 90mm Y, 10mm Z. To the east the average movement was appreciably higher at 290mm Y, - 250mm Z.

Three of the four debris slides moved in the very slow category. Only DS3 was in the slow range. The bulk of DS1 moved at an average seawards rate just above the central D bench, 180mm Y compared to 100mm Y. The extreme

upslope area moved faster; peg 223 (500mm Y, - 350mm Z). DS2 did not distinguish itself from the amphitheatre back scarp, the whole 60m east-west area had a movement range between 250mm Y, - 100mm Z and 290mm Y, - 130mm Z. DS3 was divided into two areas the upper region and the snout. Peg 253, in the steep rear section, moved 780mm Y, - 460mm Z. This contrasts with 490mm Y, - 420mm Z for peg 246 further downslope. DS4 moved across the western section of the central D bench. Peg 252 moved 530mm Y, - 170mm Z compared to 70mm Y, - 50mm Z for peg 164 positioned on the D bench 8 metres downslope of the debris slide snout.

Mudslide A merged into the movement pattern of the amphitheatre floor. Peg 30, which had been incorporated into the mudslide during March 1982, moved 360mm Y, - 300mm Z compared to peg 33, 15 metres to the east in the central amphitheatre which registered 360mm Y, - 600mm Z. The amphitheatre edge was the most active area. Pegs 196 and 200 moved 650mm Y, - 450mm Z and 640mm Y, - 90mm Z respectively.

F.7.6 Second surge (SG2 and SGP2) (6/10/82 to 2/11/82)

Table F-18, F-19, Fig. F-22

The second surge was marked by an abrupt change in movement rates from slow to moderate velocities, in excess of 50mm Yd. No previous acceleration of the benches had been noted, unlike the first surge period (SG1).

The second surge displayed similar characteristics to the first surge period.

(1) There was no comparable increase in velocity on the F bench compared to the D bench.

(2) The surge movement was recorded across the entire D bench.

(3) The surge movement was a translational displacement along the D bench preferred bedding plane shear surface.

The F bench at the eastern and western extremes of peg coverage moved 20mm Y, - 10mm Z. The central pegs 224, 225 and 226 moved with an average seaward rate of 320mm Y. The higher activity in the central region, 36m wide, was caused by the progressive downslope movement of the March 1982 slump block.

The western section of the D bench moved substantially faster than either the central or eastern areas. Respective average velocities for the three areas were 1550mm Y, - 880mm Z, 840mm Y, 30mm Z and 670mm Y - 250mm Z. Inside the amphitheatre the floor displayed a uniformity of movement. Over a 37 metre width the range of displacements were within a range 1790mm Y to 1910mm Y and - 2000mm Z to - 3200mm Z.

Direct comparison of daily rates of movement between the two surge periods is difficult. The length of time between the surveys which defined the surge periods are different: 13 days for SG1 and 27 days for SG2. Any comparison of daily rate is distorted by the days either side of the surge event. The duration of the surge is not known. Piezometer movement data has confined the second surge to eight days between 20 October 1982 and 28 October 1982. Field experience of cliff top failures suggests that the failure could occur in less than 24 hours. Three cliff top slumps numbered 1, 2 and 6, in Table 1, Barton, Coles and Tiller (1983) occurred between site visits on successive days.

F.7.7 Second winter (W2 and WP2) (2/11/82 to 1/3/83)

Table F-20, F-21, Fig. F-23

After the second surge the D bench returned to velocities

similar to those recorded after the first surge. During the second winter a fifth debris slide (DS5) formed in the western side of the amphitheatre backscarp.

The F bench followed the same pattern of movement registered in the second summer and the second surge. The active central section was flanked by a dormant western limb and a mildly active eastern zone. Average movements for west, central and eastern areas were 10mm Y: 0mm Z, 330mm Y: - 80mm Z and 250mm Y: - 20mm Z respectively.

The western and central regions of the D bench over a 130 metre width registered a small range of seaward movement between 50mm Y and 190mm Y. To the east movement increased to a maximum of 1060mm Y. The higher movements measured in this region were influenced by both edge failure and debris slides.

Debris slide activity was varied. DSl was active in the snout area where peg 276 moved 930mm Y: - 10mm Z but less so further upslope: peg 224 moved 450mm Y: - 30mm Z. DS2 was active on the upslope section due to the collapse of parts of the amphitheatre rim. Peg 286 moved 2360mm Y: - 1010mm Z. No pegs on DS3 were monitored over the complete second winter period. DS4 had an average movement of 3500mm Y: - 30mm Z; the upper slopes registered higher velocities at 5260mm Y: - 800mm Z. Pegs on the snout of DS4 experienced uplift averaging + 370mm Z. Debris slide 5 produced large displacements both in the slide itself and downslope in the amphitheatre floor. On the debris slide peg 184 and access tube 10 moved 7,380mm Y: - 3,210mm Z and 8,550mm Y: - 3,590mm Z respectively. Directly below DS5 on the amphitheatre floor peg 30 increased daily velocity from 90mm Yd during SG2 to 110mm Yd in the second winter.

Across the amphitheatre floor velocities decreased west to east away from the advancing snout of DS5. In the centre

the average was 4,470mm Y: - 790mm Z. The edge failure area could not sustain a survey peg for the full 91 day second winter period. Peg 261 monitored between 2 November 1982 and 30 November 1982 moved a total of 2760mm Y: - 440mm Z; a daily rate of 100mm Yd.

F.7.8 Third summer (S3 and SP3) (1/3/83 to 12/7/83)

Tables F-22, F-23, Fig. F-24

The last monitoring period contained a range of movements from the extremely slow velocities in the F bench to the moderate rates recorded on and surrounding DS5.

The F bench was dormant over a 60m width between pegs 154 and 225. To the east 271 and 150 averaged 70mm Y: - 50mm Z. The western region of the D bench moved on average 30mm Y; this increased behind the amphitheatre to an average of 110mm Y: - 60mm Z. The eastern section was displaced by similar rates; two pegs 173 and 266 averaged 70mm Y: - 10mm Z. Other pegs within the area were well above the bench background due to debris slide and edge failure activity: pegs 174 and 175 were displaced seawards 200mm Y and 220mm Y respectively.

Debris slide 1 moved at a rate barely above the adjacent D bench; 150mm Y compared to 110mm Y. Debris slide 2 was active at the snout; 1400mm Y: - 250mm Z. Debris slide 3 moved 50mm Y - 10mm Z over 72 days, a rate faster than the surrounding D bench. Debris slide 4 moved with similar rates to DS1: 150mm Y compared to 160mm Y for DS1 and 110mm Y for the D bench.

Debris slide 5 retained daily movement rates similar to those recorded in the second winter. Peg 281 registered 60mm Yd compared to 80mm Yd for peg 184 during W2. These moderate rates of movement were present over the debris slide and downslope on the amphitheatre floor. Peg 193,

at the snout, moved 10,540mm Y: - 3,120mm Z. To the east velocities dropped to 3,960mm Y: - 20mm Z.

F.8 The movement characteristics of the geomorphological processes

This section describes the pattern of surface movement for each geomorphological process either over the complete study period or from the start of its formation.

For each process a plot of absolute cumulative movement against time has been drawn. Where complete records are not available the movement records are supplemented by short term information from adjacent sites.

From the description of each process conclusions are compiled of the general characteristics of each process.

F.8.1 Benches

F.8.1.1 F Bench (Fig. F-25)

Although the F bench is a single geomorphological unit the 130m length recognisable in the study area can be divided into three sections.

To the west, between N.G.R. 422110E and 422160E, the bench moved between 20mm Y and 90mm Y in 734 days (an extremely slow movement rate). This rate neared the limit of surveying accuracy and the subsequent movement pattern is affected by the survey errors. However, the change in displacement rates appears to be gradual with no sudden steps and can be classified as a creep rate.

A central section of the F bench between 422160E and 422240E was monitored by 8 pegs. Figure 5-11 illustrates

the pattern of movement for two sites approximately 25m apart. Initially pegs 151 and 152 were surveyed; these were both lost after 11 November 1981 and replaced on 24 November 1981 with pegs 224 and 225 respectively. The two sites followed a similar pattern of movement although the 152/225 summation was significantly larger than the 151/224 total: 3140mm Y compared to 2100mm Y for a 673 day period. Peg 225 was directly seaward of the March 1982 slump.

The central F bench section moved with a pattern of very slow rates over the summer months, slow rates over the winter months and four distinct surges. The surges were registered between consecutive surveys 14 days apart and the movement rates were in the high end of the slow range and the moderate range. The peak rate was 110mm Yd for 225 between 9 March 1982 and 18 March 1982. This step corresponded with the March 1982 slump. The remaining slow to moderate movements occurred during the transition from summer to winter movement rates. The overall movement for 151/224 and 152/225 for the total study period was 2mm Yd and 4mm Yd respectively.

East of 422240E the F bench is disrupted and to the east of 422290E becomes indistinct: only after another 130m does the F bench reappear to remain a permanent feature.

Peg 150 monitored this short section. It moved very slowly until December 1981 when a 34 day period of slow category movement resulted in a seaward advance of 770mm Y.

Subsequently the movement followed a slow winter rate and a very slow summer rate. Over the total study period the average movement was 2mm Yd.

The central and eastern areas registered a distinct winter/summer, slow/very slow movement pattern. The

western section did not vary with seasonal changes in the undercliff.

F.8.1.2 D Bench (see Fig. F-26)

The central zone of the D bench is occupied by the amphitheatre. It splits the D bench into three areas. Fig. 5-12 illustrates the common pattern of movement present over the whole bench. It is the basis of the selection of the eight divisions of the movement cycle described in section 5.0.3.

The western section between 422080E and 422160E was sparsely monitored. The 165/241 summation contains the 3 summer periods, two surge-periods and two winter periods. The 167/250 summation came from an area close to the D scarp. The total seaward displacement for 165/241 and 167/250 was 2190mm Y and 5830mm Y respectively. The pattern of movement for the two sites showed early movement of peg 167 which had moved 1190mm Y between 22 September 1981 and 11 November 1981 compared to 70mm Y for peg 165. Subsequent patterns were similar.

The central section of the bench between 422160E and 422240E was the area directly behind the amphitheatre. Figure 5-12 illustrates the uniform pattern of movement found in this area. These records show a similarity in both magnitude and pattern of movement over a 70m width. The bench exhibited a very slow movement rate over all three summer periods: the maximum daily rate was 1mm Yd. The three winter periods produced a slow rate with a maximum value of 5mm Yd during W1/1 and an average value of 2mm Yd. The two winters were linked to the preceding summers by two surge periods. These raised the rates of movement a magnitude higher than the average winter rate: 56mm Yd and 31mm Yd for SG1 and SG2 respectively.

The eastern section, 422240E to 422350E moved significantly faster than either the central or western sections. The eight divisions of the movement cycle were less distinct although both surges were registered. Typical of the bench was peg 174, it registered average daily summer rates for S1, S2 and S3 as 1mm Yd, 2mm Yd and 1mm Yd respectively: a very slow movement. However, the first winter produced an overall daily rate of 12mm Yd compared to 7mm Yd for peg 161 in the central zone and 5mm Yd for peg 165/241 in the west. This pattern continued with higher average daily rates for both summer and winter periods than the central or western areas. Only during SG2 did the average daily rate become similar across the total D bench 30mm Yd in the east and 31mm Yd in the centre.

F.8.1.3 A3 Bench (Figure F-27)

The movements recorded for the A3 bench were concentrated in the initial study period. The longest movement record (264 days) was based on the inclinometer I3. The bench registered a maximum daily rate of 206mm Yd and an average daily rate of 38mm Yd. Two pegs, 216 and 217, were installed during the summer of 1981 and survived for 84 and 154 days respectively.

The movement rate for the A3 bench between March 1981 and mid-June 1981 was 51mm Yd. A short summer period followed until September 1981 during which peg 217 dropped to a daily average of 1mm Yd. The subsequent increase in rates in winter 1981 raised the daily average rate to 37mm Yd and 43mm Yd for I3 and peg 217 respectively.

Whilst the survey record for the A3 bench was only a total of 272 days the pattern and magnitude of movements is seen to be distinctly different than the D or F benches. The periods of 'faster' winter movement were longer and

retained a more constant rate of displacement. 'Summers' were shorter and not terminated by an initial, distinctly abrupt short-lived surge.

F.8.2 Mudslides

Of the two mudslides identified the majority of the survey data is concentrated on mudslide A.

F.8.2.1 Mudslide A

Unlike the benches mudslide A did not remain an unaltered feature during the observation period. Early observations were taken between 6 November 1980 and 8 January 1981 (63 days). The mudslide at this time was confined to a distinct channel cut into the bench debris, Fig. F-10. The mudslide markers were monitored by taping.

The resulting measurements show an increasing rate of movement as the marker moved seawards. The surface slope of the mudslide increased from 11° to 30° over 18 metres towards the D scarp. Daily movement rates ranged from 85mm Yd to 430mm Yd. The pattern of mudslide movement during this brief winter observation did indicate a constant overall rate of movement with no sign of major acceleration or deceleration.

Between July 1981 and July 1983 the channel containing mudslide A moved towards the edge of the D scarp with the rest of the D bench. The eastern boundary coalesced with the bench rubble and the exact position of the lateral shear surface was lost. The western boundary, whilst retaining a clear existence, progressed further west by side inclusion. The head region did not advance upslope and therefore the whole feature shortened in length as the mudslide slid over the D scarp.

The coverage of movement patterns during a substantial part of the study period, 601 days, gave a summated total displacement of 21,150mm Y for pegs 30/214 and 17,100mm Y for pegs 220/267. These figures actually exceed the total length of the mudslide and are only a representation of the activity of the mudslide during the 2 year period.

Figure F-28 illustrates the two summated tracks. The pattern of movement is split into four sections; two summer and two winter. Initial movement of the mudslide between 8 July 1981 and 22 September 1981 averaged 1mm Yd. The winter acceleration which included the surge SG1 increased the average daily rate to 3mm Yd. After 14 April 1982 the movement slowed to 1mm Yd. The acceleration into the second winter was marked by SG2 and the elevated winter rate continued until 1 February 1983 after which peg 214 was lost. The average daily rate for the second winter was 11mm Yd.

F.8.2.2 Mudslide B

The monitoring of movements within mudslide B was severely limited by the treacherous nature of the mudslide and its surrounds in winter and vandalism in summer. No continuous record of displacement was made during the study period.

Isolated observations indicate rates of movement generally in excess of mudslide A. Records for pegs 206 and 207 during the onset of W1, produced daily seaward movements over a 28 day and a 7 day period of 130mm Yd and 160mm Yd.

A study of mudslide B occurred in Spring 1983, during a period of high mudslide activity. Figure F-29 illustrates the rate of movement with time recorded over a 26 day period. The marker, MSB3, registered peak movements of 288mm Yd during the fourteen days between 29 March 1983

and 12 April 1983. This period contained a range of movement between 20mm Yd and 288mm Yd.

Whilst the overall coverage was too short to provide a pattern of movement the following points are worth noting:-

(i) Maximum velocities were recorded in the steepest and narrowest section of the mudslide.
(ii) The velocity of points across the mudslide, perpendicular to the direction of movement, were uniform.
(iii) The velocity of a survey peg varied greatly over a short period of time. Marker MSB6 decreased in daily rate from 89mm Yd to 21mm Yd in 26 days.

F.8.3 Debris slides

Whilst debris slides are easily recognizable their locality, slope angle, size, source of debris and ground water conditions results in a diversity of both the pattern and the magnitude of movement recorded.

F.8.3.1 Debris slide 1

Debris slide 1 was a permanent feature throughout the study period. Peg records, Fig. F-30, demonstrate a pattern of movement very similar to those illustrated in Fig. F-26 for the central D bench. The total magnitude of movement between the two geomorphological units was considerably different: debris slide 1 averaged 7000mm Y compared to 2350mm Y for the central D bench.

Two complete and one summated record are shown in Fig. 5-16. They indicate a uniformity in the pattern of movement and a small variation in the total magnitude of

movement over the whole slide.

The first summer period produced similar rates of movement for the debris slide and the D bench; an average daily rate of 0.5mm Yd and 1mm Yd respectively. The acceleration in movement rates during the first part of the first winter was more pronounced on the debris slide than the D bench. At the end of the first part of the first winter the debris slide had moved an average of 440mm Y compared to 190mm Y for the D bench. The elevated movement rate during the first surge raised the daily seaward displacement to 99mm Yd. The second part of the first winter reduced the daily rate of movement to 30mm Yd.

The second summer was characterised by average rates of movement between 0 and 1mm Yd: the same as the first summer. The second surge raised daily seaward rates to 56mm Yd; this was below the rate calculated for the first surge. During the second winter the debris slide and the D bench moved 8mm Yd and 2mm Yd respectively. This difference decreased in the third summer to a total displacement of 140mm Y for the debris slide and 120mm Y for the bench.

The continual comparison of the bench and debris slide characteristics shows that the debris slide during the winter is a factor of two to four times more active than the bench. In summer the velocities are very similar; the debris slide appears to 'rest' on top of the bench and exhibits the movement characteristics of the bench.

F.8.3.2 Debris slide 2

Debris slide 2 was more active than debris slide 1. Colluvium from the back scarp of the amphitheatre slid seawards down a shear surface which varied in depth from

being exposed at the ground surface to a maximum depth of two metres. Peg 187 moved a total of 16,360mm Y in the complete 734 day study period including a vertical displacement of - 5,750mm Z.

The pattern of movement, Fig. F-31, bore a similarity to both mudslide A and the bench movements. All eight periods identified in 5.0.3.1 are recognisable although the rates during the first surge are matched by movements during the second part of the first winter by pegs 186 and 187. In the three summer periods the daily rates were 2mm Yd, 2mm Yd and 11mm Yd. These were higher than the background bench movements. The S3 rate was influenced by the disruption caused by the development of DS5. The two long winter periods, W1/2 and W2, produced movements of 54mm Yd and 17mm Yd: the former rate fell within the moderate category of velocities.

F.8.3.3 Debris slide 3

Debris slide 3 formed during November and December 1981.

Extensive movement monitoring followed in January 1982. Unlike DS1 and DS2, DS3 was formed from the debris of fresh cliff top failures. The cliff top directly behind DS3 receded a maximum of six metres between November 1980 and July 1981 compared to an average recession rate over 200 metres of cliff top between N.G.R. 422100E and 422300E of 1.15m during the same period.

The initial recorded velocities were large. Peg 244 registered a peak daily velocity of 425mm Yd over a fourteen day period and moved a total of 11,910mm Y in 61 days, 204mm Y per day. Figure F-32 illustrates the displacement distribution over the active 61 day period between 21 January 1982 and 23 March 1982. The longer records are isolated to survey pegs installed on the

debris slide fringes where velocities were smaller. Pegs 242 and 246 showed an initial peak in debris slide activity from 21 January 1982 to 23 March 1982. Subsequently the seaward movement was small only 1,460mm Y in the following 418 days until 12 May 1983. This compares well with the average movement of 1,770mm Y for the adjacent western D bench for the same period.

Debris slide 3 transported a substantial volume of colluvium (1,617m^3) downslope in early 1982. After initially moving down an 18° rear slope the colluvium came to rest on the gentler 12° slope of the main D bench. With the cessation of the localised cliff top recession the debris source was exhausted and a substantial part of the slide material coalesced with the D bench and adopted the same rates and pattern of movement as the D bench slide.

F.8.3.4 Debris slide 4

Debris slide 4 formed four months after DS3. Localised failure of the cliff top scarp and subsequent accelerated movement of the F bench, over a 20 metre width, caused colluvium to collect on the rear slopes of the D bench behind the western rim of the amphitheatre. Movement of the colluvium on the rear of the D bench formed DS4. It exposed the F scarp and the F bedding plane shear surface, Figure 2-10. The snout of the slide moved downslope and covered a vegetated area of the bench.

The continuous record, from 9 March 1982, peg 252, is illustrated in Figure F-33. As with DS3 the rates of movement were largest during formation. Peg 252 moved 1,810mm Y in 14 days, equivalent to 129mm Yd.

After 14 April 1982 the movement moderated until the surge, SG2. The summer velocity for peg 252 was 2mm Yd

compared to 1mm Yd for the adjacent D bench. However, after 2 November 1982 the daily rate accelerated to 36mm Yd compared to 2mm Yd for the D bench. The combined record 251/273 indicates a very similar pattern to peg 252 although the total movements over 371 days were 6,060mm and 7,800mm respectively.

Unlike Debris slide 3 this slide remained active after the initial formation. The supply of colluvium continued as the movement records for the central F bench confirm.

F.8.3.5 Debris slide 5

Debris slide 5 formed on the western side of the back scarp to the amphitheatre. It remained separate from DS2 although the adjoining boundaries are not distinct. The cause of the formation of DS5 was not clear although collapse of the rear scarp of the amphitheatre provided a fresh supply of colluvium which formed the slide.

Survey pegs 183, 184 and 193 were positioned on the area of amphitheatre back scarp which formed the debris slide. Their continuous record, figure F-34, illustrated an acceleration after the second surge and subsequent to the debris slide formation. Peak rates of movement occurred between 30 November 1982 and 14 December 1982 when daily movement for 183 and 193 were 165mm Yd and 166mm Yd respectively. The moderate velocities continued until 4 January 1983 when the daily seaward rate dropped to 4mm Yd for peg 184. After 15 March 1983 the rate of movement increased to give an average daily velocity of 14mm Yd between 15 March 1983 and 12 May 1983.

Debris slide 5 registered the maximum seaward movement of the five debris slides despite its short existence. Pegs 184 and 193 moved 16,460mm Y and 17,700mm Y respectively over 175 days and 236 days. Since formation on 2 November

1982 the slide maintained an overall rate of movement in the moderate category. No appreciable decrease in velocity occurred during spring or early summer 1983. The D bench registered a reduced movement rate after 1 February 1983.

F.9 General conclusions

This appendix contains very detailed information on surface movements within the study area. It has concentrated on the three slide activities which transport landslide debris across the undercliff.

The movements are seasonal. This is a predictable conclusion but the detailed survey work performed has shown the exact percentage of movement which has occurred in each seas. In addition the start of each winter period is preceded by a 'surge' movement in the D bench. This short lived movement can be responsible for over 75% of the yearly movements recorded in particular areas.

The seasonal relationship between the movements of different slide processes also shows the active and then dormant nature of some shear planes. During periods of low activity debris slides can exhibit the same movement characteristics as the bench they lie on. Displacement rates increase when the shallow basal shear surface becomes active and the debris slides increase in velocity above the rates of their adjacent benches.

This behaviour is highlighted when the movement characteristics of benches, debris slides and mudslides are considered individually. The benches are generally active throughout the year and have a small range of velocities. Both mudslides and debris slides show a much larger range. The true rates of movement are however masked due to the multi-layered natures of the slide

behaviour (see Chapter 5).

The detailed nature of the surface movements are important in enabling the volume of debris moved within the undercliff to be evaluated. Simple averaging of velocities for a few isolated survey points can be misleading. The extensive programme of surface monitoring allows gaps both in time and space to be accurately bridged.

TABLE F-1 Surface co-ordinates of inclinometer I2

Date	Depth (m)	Profile	x (m)	y (m)
8 January 81	3.5	a	515.92	168.56
15 January 81	3.5	b	515.86	168.60
21 January 81	3.0	c	515.80	168.63
27 January 81	3.0	d	515.83	168.69
17 February 81	3.0	e	515.88	168.85
24 February 81	3.0	f	515.87	168.87
5 March 81	3.0	g	515.87	169.72
17 March 81	3.0	h	515 87	170.26
26 March 81	3.0	i	515.73	170.66
2 April 81	3.0	j	515.88	170.84

TABLE F-2 Surface co-ordinates of inclinometer I3

Date	Depth (m)	Profile	x (m)	y (m)
12 March 81	2.5	a	514.68	189.43
17 March 81	2.0	b	515.37	190.46
26 March 81	2.0	c	515.75	191.04
2 April 81	2.0	d	515.76	191.53
9 April 81	2.0	e	515.77	192.03
28 April 81	2.0	f	515.95	192.95
14 May 81	2.0	g	516.10	193.73
21 May 81	2.0	h	516.17	194.07
28 May 81	2.0	i	516.24	194.42
4 June 81	2.0	j	516.30	194.76
17 June 81	2.0	k	516.42	195.36
25 June 81	2.0	l	516.42	195.48
2 July 81	2.0	m	516.42	195.59
8 July 81	2.0	n	516.42	195.69
15 July 81	2.0	o	516.41	195.70
24 July 81	2.0	p	516.41	195.73
31 July 81	2.0	q	516.42	195.75
6 August 81	2.0	r	516.42	195.76
25 August 81	2.0	s	516.43	195.87
1 December 81	-	-	516.42	199.51

TABLE F-3 Surface co-ordinates of inclinometer I5

Date	Depth (m)	Profile	x (m)	y (m)
7 April 81	3.5	a	520.66	156.53
9 April 81	3.5	b	521.21	156.41
14 April 81	3.5	c	521.66	156.26
28 April 81	3.5	d	521.52	156.45
14 May 81	3.5	e	521.46	156.66
21 May 81	3.5	f	521.29	156.75
28 May 81	3.5	g	521.22	156.85
4 June 81	3.5	h	521.15	156.94
17 June 81	3.5	i	521.03	157.10
25 June 81	3.5	j	521.02	157.12
2 July 81	3.5	k	521.01	157.14
8 July 81	3.5	l	521.00	157.15
15 July 81	3.5	m	521.01	157.17
24 July 81	3.5	n	521.01	157.18
31 July 81	3.5	o	521.02	157.19
6 August 81	3.5	p	521.02	157.19
25 August 81	3.5	q	521.02	157.21
3 September 81	3.5	r	521.02	157.21
10 September 81	3.5	s	521.02	157.22
5 October 81	3.0	t	520.97	157.48
15 October 81	3.0	u	520.93	157.67

TABLE F-4 Surface co-ordinates of inclinometer I6

Date	Depth (m)	Profile	x (m)	y (m)
8 July 81	3.0	a	513.36	148.80
15 July 81	3.0	b	513.36	148.82
16 July 81	3.0	c	513.36	148.82
3 September 81	2.5	d	513.36	148.87
16 September 81	2.0	e	513.36	148.88
5 October 81	2.0	f	513.31	149.05

TABLE F-5 Surface co-ordinates of inclinometer I7

Note:- The failure of tube I7 occurred on the same dates as the large surface movement, recorded by surface pegs, in the D bench

Date	Depth (m)	Profile	x (m)	y (m)
24 July 81	4.5	a	536.66	154.21
31 July 81	4.5	b	536.66	154.22
6 August 81	4.5	c	536.66	154.22
25 August 81	4.5	d	536.66	154.24
3 September 81	4.5	e	536.65	154.25
16 September 81	4.5	f	536.65	154.25
5 October 81	4.5	g	536.62	154.41
15 October 81	4.5	h	536.57	154.56
28 October 81	4.5	i	536.53	154.70
4 November 81	4.5	j	536.52	154.77
12 November 81	4.5	k	536.49	154.92
19 November 81	3.0	l	536.45	155.59

TABLE F-6 Surface co-ordinates of inclinometer I8

Date	Depth (m)	Profile	x (m)	y (m)
17 December 81	5.4	a	-	-
18 December 81	5.4	b	-	-
21 December 81	2.0	c		
22 December 81	-	-	448.66	130.66

TABLE F-7 Surface co-ordinates of inclinometer I9

Date	Depth (m)	Profile	x (m)	y (m)
17 December 81	5.0	a	-	-
21 December 81	5.0	b	-	-
22 December 81	-	-	522.82	119.22

TABLE F-8 Surface co-ordinates of inclinometer I10

Date	Depth (m)	Profile	x (m)	y (m)
25 March 82	4.0	a	584.65	156.60
1 April 82	4.5	b	584.66	156.62
7 April 82	4.5	c	584.66	156.64
14 April 82	4.5	d	584.67	156.65
22 April 82	4.5	e	584.68	156.69
5 May 82	4.5	f	584.68	156.71
19 May 82	4.5	g	584.69	156.75
16 June 82	4.5	h	584.72	156.82

TABLE F-9 The sub-divisions of surface movement data from survey pegs

Period	Label	Start Date	Finish Date	Duration in days	Number of pegs
Summer	S1	8. 7.81	30. 9.81	84	75
Winter	W1/1	30. 9.81	11.11.81	42	66
Surge	SG1	11.11.81	24.11.81	13	49
Winter	W1/2	24.11.81	29. 4.82	156	52
Summer	S2	29. 4.82	6.10.82	160	52
Surge	SG2	6.10.82	2.11.82	27	51
Winter	W2	2.11.82	1. 3.83	119	53
Summer	S3	1. 3.83	12. 7.83	133	47

TABLE F-10 The sub-division of surface movement data from piezometer and access tube data

Period	Label	Start Date	Finish Date	Duration in days	Number of pegs
Summer	SP2	5. 5.82	6.10.82	154	13
Surge	SPG2	6.10.82	9.11.82	34	10
Winter	WP2	9.11.82	1. 3.83	112	21
Summer	SP3	1. 3.83	18. 7.83	139	25

TABLE F-11 An explanation of the movement notation

Example	Explanation
270mm XY	The survey peg has moved 270mm in the horizontal plane during a study period.
270mm Y	The survey peg has moved 270mm in a seaward direction in a study period.
-270mm Z	The survey peg has moved 270mm in the vertical plane. The negative sign indicates a fall in elevation. This has occured during a study period.
80mm XYd	The survey peg has moved an average of 80mm in the horizontal plane during one day of the sample period.
80mm Yd	The survey peg has moved an average of 80mm in a seaward direction during one day of the sample period.
-80mm Zd	The survey peg has moved 80mm in a vertical direction during one day of the sample period. The negative sign indicates a fall in elevation

TABLE F-12 The surface movements between 8 July 1981 and 30 September 1981 — S1

Peg No	xy (metres)	z (metres)	Daily xy (mm/day)	Daily z (mm/day)	Direction (Degrees)	Seaward (metres)
150	0.0	0	0	0	-	0.0
151	0.03	0	0	0	180	0.03
152	0.03	0	0	0	162	0.03
153	0.0	0	0	0	-	0.0
154	0	0	0	0	0	0
155	0	-0.04	0	-1	0	0
156	0.06	-0.04	1	-1	180	0.06
157	0.05	-0.05	1	-1	191	0.05
158	0.07	-0.05	1	-1	180	0.07
159	0.07	-0.03	1	0	188	0.07
160	0.04	-0.03	0	0	146	0.03
161	0.05	-0.03	1	0	180	0.05
162	0.04	0	1	0	194	0.04
163	0.04	-0.01	1	0	207	0.04
164	0.02	0	0	0	207	0.02
165	0.03	-0.01	0	0	252	0.01
166	0.02	-0.01	0	0	180	0.02
167	0.11	-0.07	1	-1	185	0.11
168	0.07	-0.04	1	-1	196	0.07
169	0.10	-0.03	1	0	174	0.10
170	0.07	-0.01	1	0	180	0.07
171	0.27	-0.12	4	-2	188	0.27
172	0.11	-0.04	1	-1	180	0.11
173	0.06	-0.03	1	0	180	0.06
174	0.08	-0.09	1	-1	180	0.08
175	0.09	-0.05	1	-1	180	0.09
176	0.01	-0.05	0	-1	225	0.01
177	0.03	-0.01	0	0	198	0.03
178	0.11	-0.01	1	0	135	0.08
179	0.07	0	1	0	172	0.07
180	0.04	-0.01	1	0	207	0.04
181	0.06	-0.03	1	0	180	0.06
182	0.03	-0.01	0	0	198	0.03
183	0.04	-0.01	1	0	194	0.04
184	0.04	0	1	0	207	0.04
185	0.05	0	1	0	191	0.05
186	0.08	0.01	1	0	194	0.08
187	0.13	0	2	0	119	0.06
188	0.10	0.01	1	0	246	0.04
189	0.06	-0.01	1	0	180	0.06
190	0.09	-0.02	1	0	167	0.09
191	0.44	-0.09	6	-1	256	0.11
192	0.06	0.01	1	0	162	0.06
193	0.07	0	1	0	172	0.07
194	0.06	0	1	0	189	0.06
195	0.08	-0.04	1	-1	173	0.08
196	0.09	-0.01	1	0	180	0.09
197	0.04	-0.01	1	0	166	0.04
198	0.40	0.28	5	4	184	0.40

contd/.....

TABLE F-12 (contd)

Peg No	xy (metres)	z (metres)	Daily xy (mm/day)	Daily z (mm/day)	Direction (Degrees)	Seaward (metres)
199	2.87	-0.36	38	-5	125	1.64
200	0.08	0.02	1	0	173	0.08
201	0.08	0	1	0	180	0.08
202	1.70	0	22	0	155	1.54
203	3.79	-1.05	50	-14	173	3.76
204	0.12	0.01	2	0	180	0.12
205	0.09	0	1	0	174	0.09
206	0.10	0	1	0	186	0.10
207	0.12	0	2	0	189	0.12
208	0.07	-0.01	1	0	188	0.07
209	0.09	0	1	0	180	0.09
210	0.09	0.01	1	0	174	0.09
211	0.10	0.01	1	0	180	0.10
212	0.11	-0.01	1	0	175	0.11
213	0.10	-0.01	1	0	174	0.10
214	0.08	-0.05	1	-1	180	0.08
215	0.09	-0.02	1	0	180	0.09
216	0.60	0.31	8	4	190	0.59
217	0.06	-0.06	1	-1	180	0.06
218	0.10	-0.03	1	0	174	0.10
219	0.09	-0.06	1	-1	186	0.09
28	0.07	-0.01	1	0	172	0.07
30	0.07	-0.01	1	0	188	0.07
32						
33	0.07	-0.01	1	0	188	0.07
34	0.07	0	1	0	172	0.07

TABLE F-13 The surface movements between 30 September 1981 and 11 November 1981 - W1/1

Peg No	xy (metres)	z (metres)	Daily xy (mm/day)	Daily z (mm/day)	Direction (Degrees)	Seaward (metres)
150	0.03	0	1	0	162	0.03
151	0.54	-0.22	11	-4	177	0.54
152	0.43	-0.10	9	-2	180	0.43
153	0.01	-0.02	0	0	135	0.01
154	0.02	-0.01	0	0	153	0.02
155	0.02	0.01	0	0	180	0.02
156	0.29	-0.19	6	-4	178	0.29
157	0.42	-0.18	8	-4	177	0.42
158	0.82	-0.21	16	-4	181	0.82
159	0.49	-0.24	10	-5	192	0.48
160	0.20	-0.13	4	-3	169	0.20
161	0.27	-0.13	5	-3	182	0.27
162	0.18	-0.05	4	-1	183	0.18
163	0.20	-0.05	4	-1	186	0.20
164	0.13	-0.07	3	-1	198	0.12
165	0.07	-0.07	1	-1	172	0.07
166	0.34	-0.13	7	-3	199	0.32
167	1.23	-0.64	25	-13	194	1.19
168	0.56	-0.16	11	-3	192	0.55
169	0.31	0.02	6	0	205	0.28
170	0.48	-0.09	10	-2	163	0.46
171	0.89	-0.36	18	-7	192	0.87
172	0.23	-0.05	5	-1	173	0.23
173	0.12	-0.05	2	-1	189	0.12
174	0.14	-0.11	3	-2	176	0.14
175	0.28	-0.10	6	-2	172	0.28
176	0.13	-0.09	3	-2	167	0.13
177	0.22	-0.04	4	-1	167	0.21
178	0.29	-0.02	6	0	200	0.27
179	0.26	-0.02	5	0	180	0.26
180	0.23	-0.04	5	-1	187	0.23
181	0.24	-0.03	5	-1	189	0.24
182	0.21	-0.02	4	0	180	0.21
183	0.28	-0.04	6	-1	180	0.28
184	0.29	-0.05	6	-1	184	0.29
185	0.71	-0.01	14	0	191	0.70
186	1.39	-0.67	28	-13	186	1.38
187	2.00	-0.62	40	-12	182	2.00
188	1.53	-0.99	31	-20	197	1.47
189	1.88	-0.65	38	-13	189	1.86
193	0.29	-0.03	6	-1	182	0.29
194	0.23	-0.01	5	0	175	0.23
195	1.05	-0.30	21	-6	105	1.01
196	0.85	-0.19	17	-4	184	0.85
197	0.37	-0.10	7	-2	196	0.36
198	4.40	-1.70	88	-34	216	3.56
199	2.42	-1.06	48	-21	176	2.41
200	1.25	-0.05	25	-1	182	1.25
201	1.91	-0.84	38	-17	175	1.90
202	2.03	-0.16	41	-3	172	2.01

contd/.....

TABLE F-13 (contd)

204	2.19	-0.22	44	-4	178	2.19
205	2.35	-0.29	47	-6	178	2.35
208	2.94	0.21	59	4	240	1.46
209	2.94	-0.48	59	-10	181	7.94
212	1.93	-0.17	39	-3	178	1.93
214	1.41	-1.00	28	-20	170	1.39
215	1.64	-0.74	33	-15	183	1.64
217	2.30	-0.15	46	-3	180	2.30
218	1.64	-0.57	33	-11	188	1.63
219	1.56	-0.32	31	-6	185	1.54
28	1.48	-0.51	30	-10	170	1.46
30	1.10	-0.24	22	-5	189	1.09
31	0.99	-0.25	20	-5	189	0.98
32	0.88	-0.19	18	-4	190	0.87
33	0.78	-0.27	16	-5	194	0.76
34	0.44	-0.11	9	-2	227	0.30

TABLE F-14 The surface movements between 11 November 1981 and 24 November 1981 - SG1

Peg No	xy (metres)	z (metres)	Daily xy (mm/day)	Daily z (mm/day)	Direction (Degrees)
150	0.03	0		0	162
153	0.01	0.01	1	1	45
154	0.03	0	2	0	18
155					
156	1.13	-0.84	87	-65	184
157	1.25	-0.83	96	-64	183
158	1.81	-0.78	140	-60	184
159	1.35	-0.93	104	-72	190
160	0.68	-0.05	52	-4	172
161	0.75	-0.51	58	-39	178
162	0.70	-0.20	54	-15	187
163	0.80	-0.25	62	-19	191
164	0.72	-0.39	55	-30	200
165	0.47	-0.61	36	-47	187
167	1.79	-0.39	138	-30	187
169	1.14	-0.04	88	-3	177
170	1.06	-0.07	81	-5	173
171	1.08	-0.23	83	-18	186
172	0.62	-0.11	48	-8	174
173	0.29	-0.14	22	-11	182
174	0.42	-0.33	32	-25	180
175	1.16	-0.44	89	-34	177
176	0.40	-0.40	31	-31	171
177	0.70	-0.20	54	-15	162
178	1.06	-0.07	82	-5	181
179	0.99	-0.14	76	-11	181
180	0.95	-0.19	73	-15	187
181	1.04	-0.19	80	-15	189
182	1.04	-0.09	80	-7	185
183	1.10	-0.11	84	-8	186
184	1.10	-0.09	84	-7	186
185	1.11	-0.03	86	-2	185
186	1.25	-0.01	96	-1	184
187	1.14	-0.03	88	-2	183
188	1.08	-0.01	83	-1	182
189	1.24	-0.26	96	-20	184
193	1.10	-0.06	84	-5	186
194	1.09	-0.03	84	-2	184
195	1.45	-0.12	112	-9	178
196	1.45	-0.12	112	-9	182
197	1.15	-0.10	89	-8	182
199	2.11	-0.24	162	-18	180
200	1.62	0.02	125	2	182
212	2.07	-0.12	159	-9	180
214	1.81	-0.35	140	-27	176
215	1.80	-0.36	139	-28	183
217	1.32	-0.07	102	-5	180
218	1.78	-0.31	137	-24	185
219	1.79	-0.10	138	-8	184

contd/.....

TABLE F-14 (contd)

219	1.79	-0.10	138	-8	184
220	1.52	-0.15	117	-12	174
28	1.70	-0.22	131	-17	179
30	1.57	-0.13	120	-10	185
31	1.51	-0.10	116	-8	184
32	1.00	-0.10	77	-8	198
33	1.39	-0.11	107	-8	185
34	1.99	-0.42	153	-32	212

TABLE F-15 The surface movements between 24 November 1981 and 29 April 1982 - W1/2

Peg No	xy (metres)	z (metres)	Daily xy (mm/day)	Daily z (mm/day)	Direction (Degrees)	Seaward (metres)
150	1.05	-0.26	7	-2	179	1.05
153	1.23	-0.37	9	-3	177	1.23
154	0.07	0.02	1	0	164	0.07
155	0.01	0.01	0	0	225	0.01
157	1.31	-0.08	9	-1	180	1.31
158	3.23	-0132	23	-2	187	3.20
159	4.15	-0.83	29	-6	191	4.07
161	0.38	-0.12	3	-1	186	0.38
162	0.33	-0.07	2	0	187	0.33
163	0.36	-0.09	3	-1	189	0.36
164	0.27	-0.10	2	-1	208	0.24
169	0.59	-0.05	4	0	186	0.59
170	2.01	-0.45	14	-3	166	1.95
172	2.17	-0.57	15	-4	172	2.15
173	0.97	-0.39	7	-3	177	0.97
174	1.82	-0.47	13	-3	165	1.76
175	2.27	-0.86	16	-6	161	2.15
177	0.36	-2.05	3	-15	166	0.35
178	0.83	-0.31	6	-2	188	0.82
179	3.19	-2.25	23	-16	203	2.94
180	0.57	-0.22	4	-2	194	0.55
181	0.65	-0.25	5	-2	188	0.84
182	0.51	-0.14	4	-1	184	0.51
183	0.77	-0.19	5	-1	179	0.77
184	0.84	-0.22	6	-2	183	0.84
185	0.96	-0.13	7	-1	190	0.94
186	6.41	-3.57	45	-25	197	6.12
187	7.68	-2.77	54	-20	189	7.59
193	0.85	-0.23	6	-2	176	0.85
194	0.71	-0.19	5	-1	149	0.61
196	4.83	-1.98	34	-14	184	4.82
197	1.83	-0.69	13	-5	196	1.76
200	4.80	-1.36	34	-10	184	4.75
218	3.76	-1.66	27	-12	194	3.65
220	3.66	-1.41	26	-10	167	3.57
223	4.08	-3.86	29	-27	187	4.05
224	0.84	-0.29	6	-2	208	0.74
225	1.72	-0.14	12	-1	182	1.72
226	0.83	0	6	0	175	0.83
227	0.02	0.02	0	0	243	0.01
231	3.01	-1.20	21	-9	193	2.93
233	0.69	-0.47	5	-3	198	0.66
239	2.67	-0.62	19	-4	192	2.61
28	3.95	-1.78	28	-13	182	3.95
30	2.70	-0.57	19	-4	190	2.66
31	1.89	-0.32	13	-2	193	1.84

contd/.....

TABLE F-15 (contd)

32	2.31	-0.52	16	-4	186	2.30
33	1.75	-0.48	12	-3	196	1.69
165	0.31	-0.24	2	-2	193	0.30

TABLE F-16 The surface movements between 29 April 1982 and 6 October 1982 - S2

Peg No	xy (metres)	z (metres)	Daily xy (mm/day)	Daily z (mm/day)	Direction (Degrees)	Seaward (metres)
150	0.05	0.o	0	0	180	0.05
154	0	-0.o2	0	0		0
155	0.00	-0.07	0	0		0
157	0.18	-0.13	1	-1	186	0.18
161	0.11	-0.07	1	0	180	0.11
162	0.09	-0.01	1	0	180	0.09
163	0.14	-0.05	1	0	188	0.14
164	0.09	-0.05	0	0	216	0.07
168	0.19	0	1	0	186	0.19
169	0.19	-0.03	1	0	186	0.19
172	0.40	-0.10	2	-1	174	0.19
173	0.16	-0.06	1	0	176	0.16
174	0.37	-0.26	2	-1	169	0.36
175	0.27	-0.21	2	-1	153	0.24
177	0.11	0.03	1	0	170	0.11
178	0.21	-0.07	1	0	188	0.21
180	0.20	-0.09	1	-1	191	0.20
181	0.25	-0.10	1	-1	185	0.25
182	0.15	-0.08	1	0	191	0.15
183	0.29	-0.23	2	-1	215	0.24
184	0.25	-0.08	1	0	182	0.25
186	0.29	-0.13	2	-1	184	0.25
187	0.27	-0.14	2	-1	188	0.27
193	0.25	-0.06	1	0	182	0.25
194	0.18	-0.05	1	0	186	0.18
196	0.65	-0.45	4	-3	185	0.65
197	0.23	0.06	1	0	175	0.23
198	0.42	-0.14	2	-1	191	0.41
200	0.64	-0.09	4	-1	184	0.64
203	0.41	-0.28	2	-2	181	0.41
224	0.07	-0.02	0	0	207	0.06
225	0.20	-0.06	1	0	186	0.20
226	0.06	-0.01	0	0	180	0.06
227	0.0	-0.02	0	0	-	0
239	0.26	-0.03	2	0	189	0.26
246	0.57	-0.42	3	-2	211	0.49
250	0.16	-0.10	1	-1	194	0.16
251	0.15	-0.31	1	-2	180	0.15
252	0.53	-0.17	3	-1	177	0.53
253	0.85	-0.46	5	-3	156	0.78
30	0.36	-0.03	2	0	186	0.36
31	0.32	-0.02	2	0	184	0.32
32	0.30	-0.03	2	0	188	0.30
33	0.36	-0.06	2	0	180	0.36
179	0.24	-0.01	2	0	182	0.24

TABLE F-17 The surface movements between 5 May 1982 and 6 October 1982 - SP2

Peg No	xy (metres)	z (metres)	Daily xy (mm/day)	Daily z (mm/day)	Direction (Degrees)
P7	0.35	-0.08	2	-1	180
P8	0.04	0	0	0	194
P9	0.19	-0.05	1	0	177
P10	0.26	-0.06	2	0	180
P11	0.11	-0.13	1	-1	175
P13	0.03	-0.01	0	0	162
P14	0.10	-0.14	1	-1	174
P15	0.20	-0.03	1	0	177
P16	0.44	-0.10	3	-1	191
P18	0.11	-0.02	1	0	190
P19	0.27	-0.02	2	0	186
P24	0.15	-0.04	1	0	164
P25	1.60	0	10	0	182

TABLE F-18 The surface movements between 6 October 1982 and 2 November 1982 - SG2

Peg No	xy (metres)	z (metres)	Daily xy (mm/day)	Daily z (mm/day)	Direction (Degrees)
150	0.01	-0.03	1	-1	315
154	0.04	0.01	2	0	194
155	0.01	0	0	0	180
157	1.52	-0.75	56	-28	186
161	0.71	-0.42	26	-16	181
162	0.84	-0.24	31	-9	186
163	1.01	-0.23	37	-9	188
164	0.87	-0.35	32	-13	202
168	1.71	0.02	63	1	181
169	1.39	-0.12	52	-4	184
171	2.95	-0.49	109	-18	190
172	1.52	-0.26	56	-10	175
173	0.78	-0.22	29	-8	175
174	0.89	-0.36	33	-13	168
175	0.74	-0.57	28	-21	160
177	0.72	-0.19	27	-7	161
178	1.46	-0.35	54	-13	184
180	1.34	-0.35	50	-13	190
181	1.59	-0.37	59	-14	189
182	1.46	-0.41	54	-15	184
183	1.65	0.25	61	9	178
184	1.66	-0.32	61	-12	185
186	1.96	-0.70	73	-26	189
187	2.50	1.27	93	47	196
197	1.80	-0.32	67	-12	185
224	0.23	-0.02	8	-1	203
225	0.49	-0.09	18	-3	188
226	0.24	0	9	0	178
227	0.02	0.01	1	0	180
228	2.55	-0.56	95	-21	188
246	1.06	-1.34	39	-50	203
250	1.33	-1.02	49	-38	185
251	1.08	-1.02	40	-38	186
252	2.00	-1.15	74	-43	182
253	3.46	-0.38	128	-14	161
258	1.79	-0.73	66	-27	189
259	1.21	-0.98	45	-36	209
260	3.58	-0.53	132	-20	186
261	4.30	-0.44	155	-16	180
263	1.92	-0.31	71	-11	187
264	1.81	-0.02	67	-1	183
265	1.49	-0.07	55	-3	187
266	0.36	-0.18	13	-7	166
30	2.43	-0.23	90	-9	187
31	1.32	-0.07	49	-3	197
32	1.91	-0.14	71	-5	185
33	1.82	-0.07	67	-3	186

TABLE F-19 The surface measurements between 6 October 1982 and 9 November 1982 - SPG2

Peg No	xy (metres)	z (metres)	Daily xy (mm/day)	Daily z (mm/day)	Direction (Degrees)
P7	0.91	-0.63	27	-19	180
P8	0.11	-0.03	3	-1	207
P9	1.52	-0.39	45	-11	180
P13	0.01	-0.39	0	-11	225
P15	1.51	-0.20	44	-6	181
P16	1.40	-0.32	41	-9	184
P18	1.37	-0.09	40	-3	186
P19	2.09	-0.11	61	-3	187
P24	1.17	-0.15	34	-4	170
P25	1.44	-0.07	42	-2	182

TABLE F-20 The surface movements between 2 November 1982 and 1 March 1983 - W2

Peg No	xy (metres)	z (metres)	Daily xy (mm/day)	Daily z (mm/day)	Direction (Degrees)	Seaward (metres)
150	0.25	-0.02	3	0	189	0.25
154	0.01	0	0	0	135	0.01
155	0.01	-0.01	0	0	180	0.01
157	0.57	0.09	6	1	185	0.57
161	0.07	-0.05	1	-1	180	0.07
162	0.12	-0.06	1	-1	175	0.12
163	0.19	-0.03	2	0	186	0.19
164	0.17	-0.04	2	0	205	0.15
168	3.71	-1.31	41	-14	177	3.71
169	2.29	-0.30	25	-3	186	2.28
172	2.25	-0.42	25	-5	174	2.24
173	1.06	-0.33	12	-4	172	1.05
174	1.44	-0.46	16	-5	166	1.40
175	0.49	-0.32	5	-3	154	0.44
177	0.10	-0.02	1	0	163	0.10
178	1.67	-1.17	18	-13	204	1.53
181	0.38	-0.16	4	-2	180	0.38
182	0.27	-0.15	3	-2	180	0.27
184	7.41	-2.51	81	-28	175	3.38
187	1.55	-3.21	17	-35	196	1.49
197	1.95	-0.38	21	-4	195	1.89
224	0.49	-0.03	5	0	194	0.48
225	0.29	-0.06	3	-1	190	0.29
227	0.0	0	0	0	-	0
250	0.13	0.54	1	6	180	0.13
252	3.28	0.38	36	4	182	3.28
258	0.98	0.50	11	5	185	0.98
259	0.37	0.51	4	6	207	0.33
263	3,21	-0.51	35	-6	191	3.14
264	5.62	-0.81	62	-9	192	5.51
266	0.05	-0.02	1	0	180	0.05
267	7.92	-2.48	87	-27	190	7.80
268	0.25	-0.15	3	-2	207	0.22
269	0.87	-0.37	10	-4	193	0.85
271	2.14	0.36	24	4	204	1.95
272	5.27	-0.64	58	-7	177	5.26
274	1.42	-0.12	16	-1	186	1.41
276	0.94	-0.01	10	0	187	0.93
278	0.24	-0.04	3	0	168	0.23
280	0.13	-0.06	1	-1	189	0.13
281	2.07	-1.85	23	-20	170	2.04
282	0.37	0.48	4	5	182	0.37
283	0.64	-0.14	7	-2	186	0.64
284	1.34	-0.06	15	-1	171	1.32
285	1.77	-0.23	19	-3	197	1.69
286	2.45	-1.01	27	-11	195	2.36
292	0.1e	-0.01	1	0	193	0.13

contd/...

TABLE F-20 (contd)

293	0.08	-0.07	1	-1	180	0.08
294	0.42	-0.80	5	-9	181	0.40
30	10.07	-3.10	111	-34	194	9.75
31	6.74	-0.70	74	-8	188	6.67
32	5.00	-1.65	55	-18	186	4.98
33	4.33	-0.19	48	-2	191	4.26

TABLE F-21 The surface movements between 9 November 1981 and 1 March 1983 - WP2

Peg No	xy (metres)	z (metres)	Daily xy (mm/day)	Daily z (mm/day)	Direction (Degrees)
P7	0.13	-0.07	1	-1	189
P8	0.31	0.04	3	0	191
P9	1.68	-1.14	15	-10	191
P15	0.98	-0.13	9	-1	182
P16	0.23	-0.06	2	-1	198
P18	0.44	-0.03	4	0	238
P19	5.39	0	48	0	184
P24	0.67	-0.11	6	-1	163
AT1	0.13	-0.05	1	0	193
AT2	1.41	-1.25	13	-11	193
AT3	1.09	-0.06	10	-1	196
AT4	5.49	-0.07	49	-1	184
AT6	0.18	-0.07	2	-1	202
AT7	0.18	-0.04	2	0	223
AT8	0.04	0	0	0	304
AT10	8.55	-3.59	76	-32	178
4/2	0.11	0.01	1	0	195
4/1	0.04	0.01	1	0	201
3/3	0.12	-0.02	1	0	200
1/6	0.08	-0.10	1	-1	220
1/7	0.05	-0.10	0	-1	233

TABLE F-22 The surface movements between 1 March 1983 and 12 July 1983 - S3

Peg No	xy (metres)	z (metres)	Daily xy (mm/day)	Daily z (mm/day)	Direction (Degrees)	Seaward (metres)
150	0.03	-0.03	0	0	225	0.02
154	0.0	0.01	0	0	-	0
155	0.0	0.01	0	0	-	0
157	0.13	-0.13	1	-1	193	0.13
159						
161	0.11	-0.10	1	-1	195	0.11
162	0.11	-0.06	1	0	190	0.11
164	0.12	-0.04	1	0	200	0.11
168	0.26	-0.05	2	0	180	0.26
169	0.77	-0.18	5	-1	187	0.76
172	0.57	-0.21	4	-1	168	0.56
173	0.09	0.01	1	0	162	0.09
174	0.21	-0.03	1	0	166	0.20
175	0.23	-0.13	1	-1	162	0.22
177	0.11	-0.05	1	0	142	0.09
178	1.15	-0.97	7	-6	208	1.02
181	0.19	-0.05	1	0	196	0.18
182	0.22	-0.09	1	-1	193	0.21
184	9.30	-2.41	58	-15	181	9.30
187	1.71	-0.25	11	-2	215	1.40
193	10.60	-3.12	66	-19	186	10.54
194	0.23	-0.05	1	0	190	0.23
197	8.08	-0.40	54	-2	135	6.11
225	0.0	-0.05	0	0	-	0
227	0	0	0	0	-	-
250	0.08	-0.05	0	0	180	0.08
258	0.74	-0.45	5	-3	186	0.74
259	0.01	-0.07	D	0	225	0.01
263	2.57	-0.66	16	-4	184	2.56
266	0.06	-0.02	0	0	149	0.05
268	0.04	-0.02	0	0	194	0.04
269	0.12	-0.03	1	0	198	0.12
271	0.12	-0.09	1	-1	200	0.11
272	0.17	-0.16	1	-1	190	0.17
274	0.18	-0.15	1	-1	186	0.18
276	0.15	-0.15	1	-1	188	0.15
277	0.19	-0.11	1	-1	196	0.18
278	0.10	-0.15	1	-1	186	0.10
280	0.11	-0.03	1	0	180	0.11
281	10.29	-7.99	64	-19	172	10.20
282	0.02	-0.08	0	0	207	0.02
283	0.19	-0.08	1	0	198	0.18
293	0.02	-0.05	0	0	207	0.02
294	0.90	-0.34	6	-2	176	0.90
34	3.97	0.02	25	0	183	3.96

TABLE F-23 The surface movements between 1 March 1983 and 18 July 1983 - SP3

Peg No	xy (metres)	z (metres)	Daily xy (mm/day)	Daily z (mm/day)	Direction (Degrees)
P7	0.12	-0.08	1	-1	185
P8	0.04	0	0	0	180
P9	1.00	-1.09	7	-8	209
P10	0.83	-1.17	6	-8	184
P11	0.03	-0.01	0	0	162
P14	0.13	-0.01	1	0	157
P15	0.62	-0.44	4	-3	176
P16	0.05	0.02	0	0	169
P24	0.48	-0.06	3	0	158
AT2	1.03	-0.77	7	-6	208
AT3	0.89	-0.08	6	-1	196
AT6	0.04	0	0	0	153
AT7	0.10	-0.03	1	0	197
AT8	0.01	0.01	0	0	270
AT13	0.12	0.29	1	2	180
AT14	0.45	-0.02	3	0	183
AT15	0.16	-0.12	1	-1	173
AT16	0.02	0.01	0	0	243
AT17	0.03	0.01	0	0	135
4/2	0.11	-0.04	1	0	185
4/1	0.10	-0.04	1	0	174
1/7	0.02	0	0	0	117
5/1	0.06	-0.02	0	0	149
1/8	0.03	0.01	0	0	135

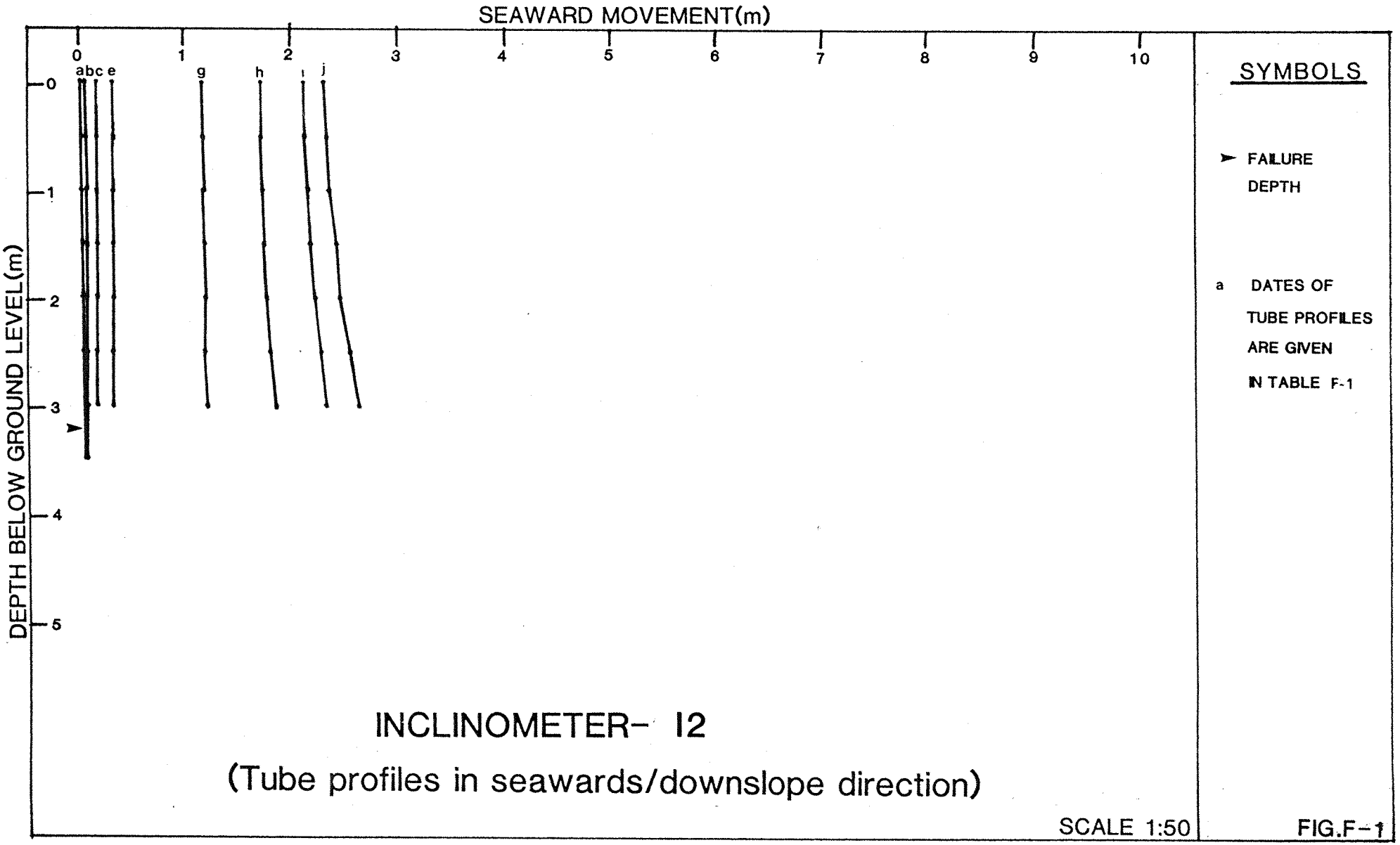

INCLINOMETER- I2

(Tube profiles in seawards/downslope direction)

SCALE 1:50

FIG.F-1

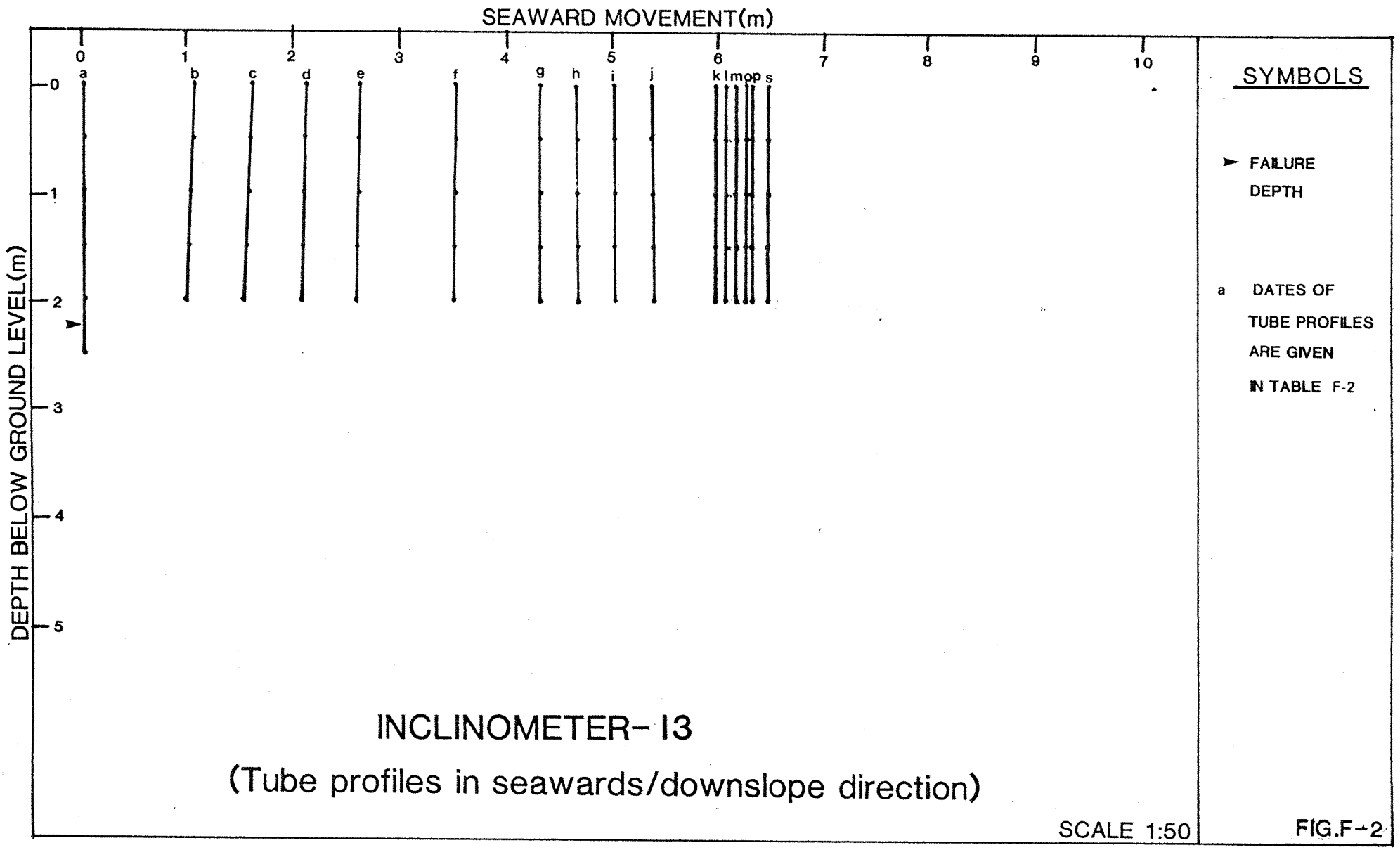

INCLINOMETER- I3

(Tube profiles in seawards/downslope direction)

SCALE 1:50

FIG.F-2

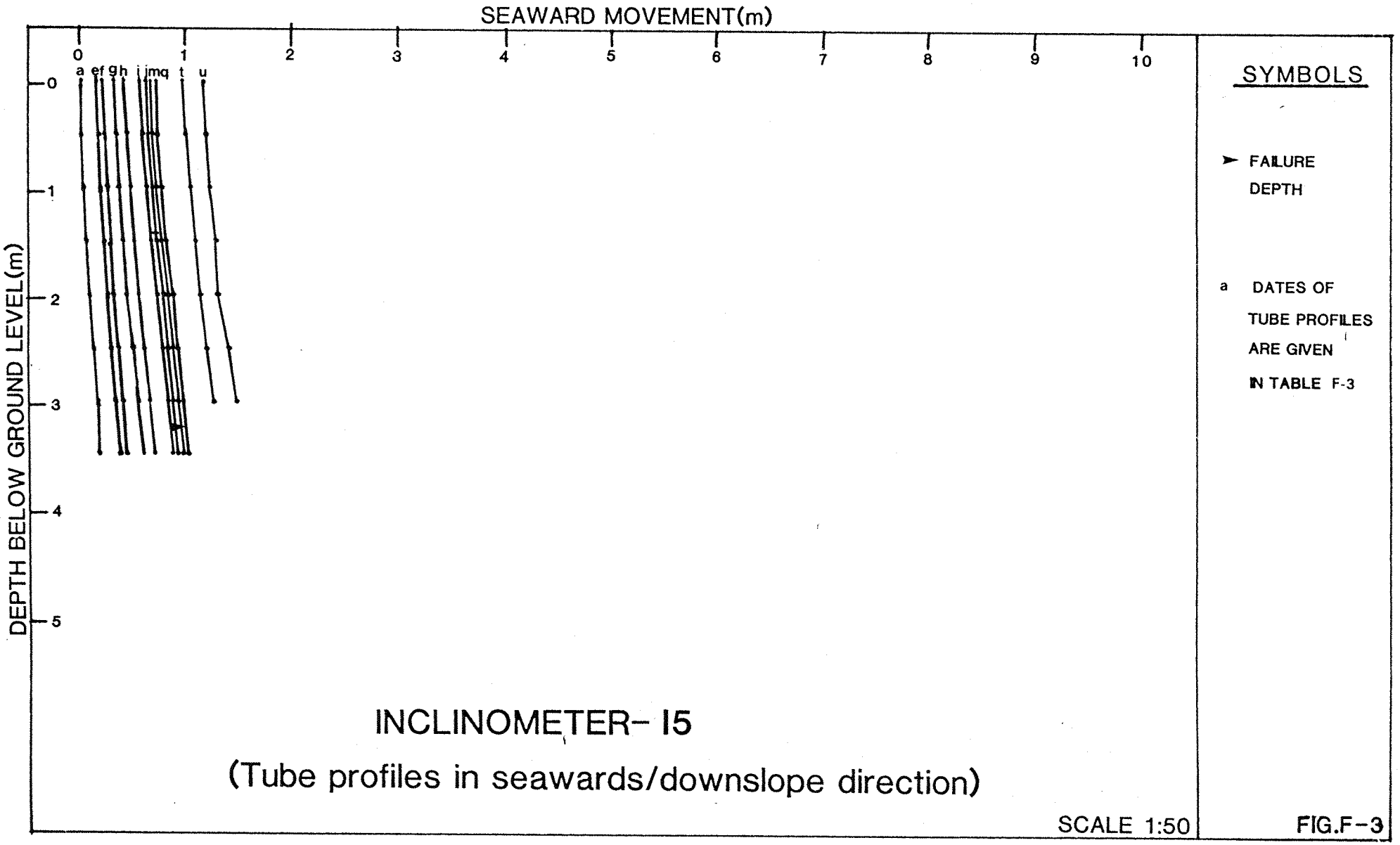

INCLINOMETER- I5

(Tube profiles in seawards/downslope direction)

SCALE 1:50

FIG.F-3

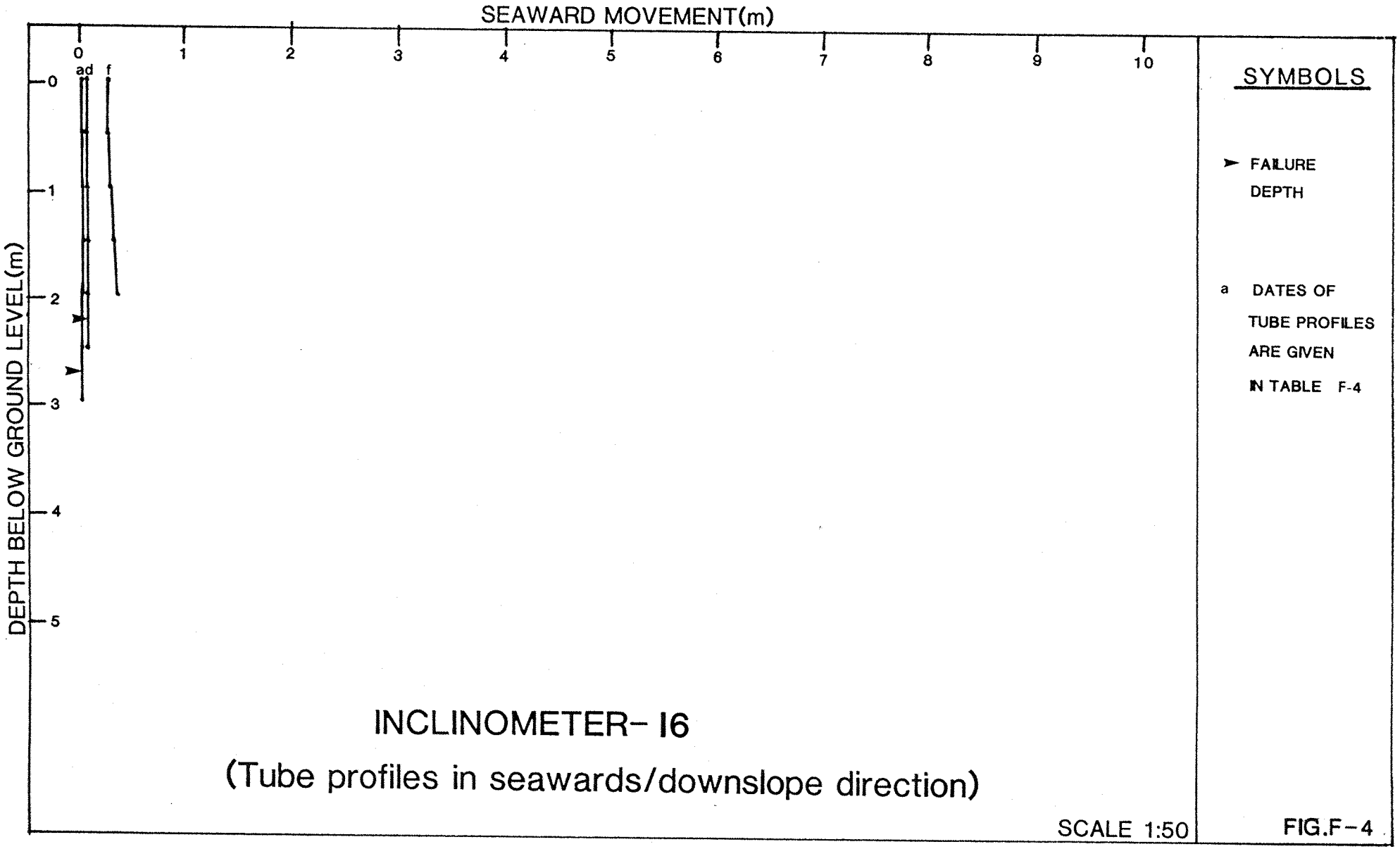

INCLINOMETER- I6

(Tube profiles in seawards/downslope direction)

SCALE 1:50

FIG.F-4

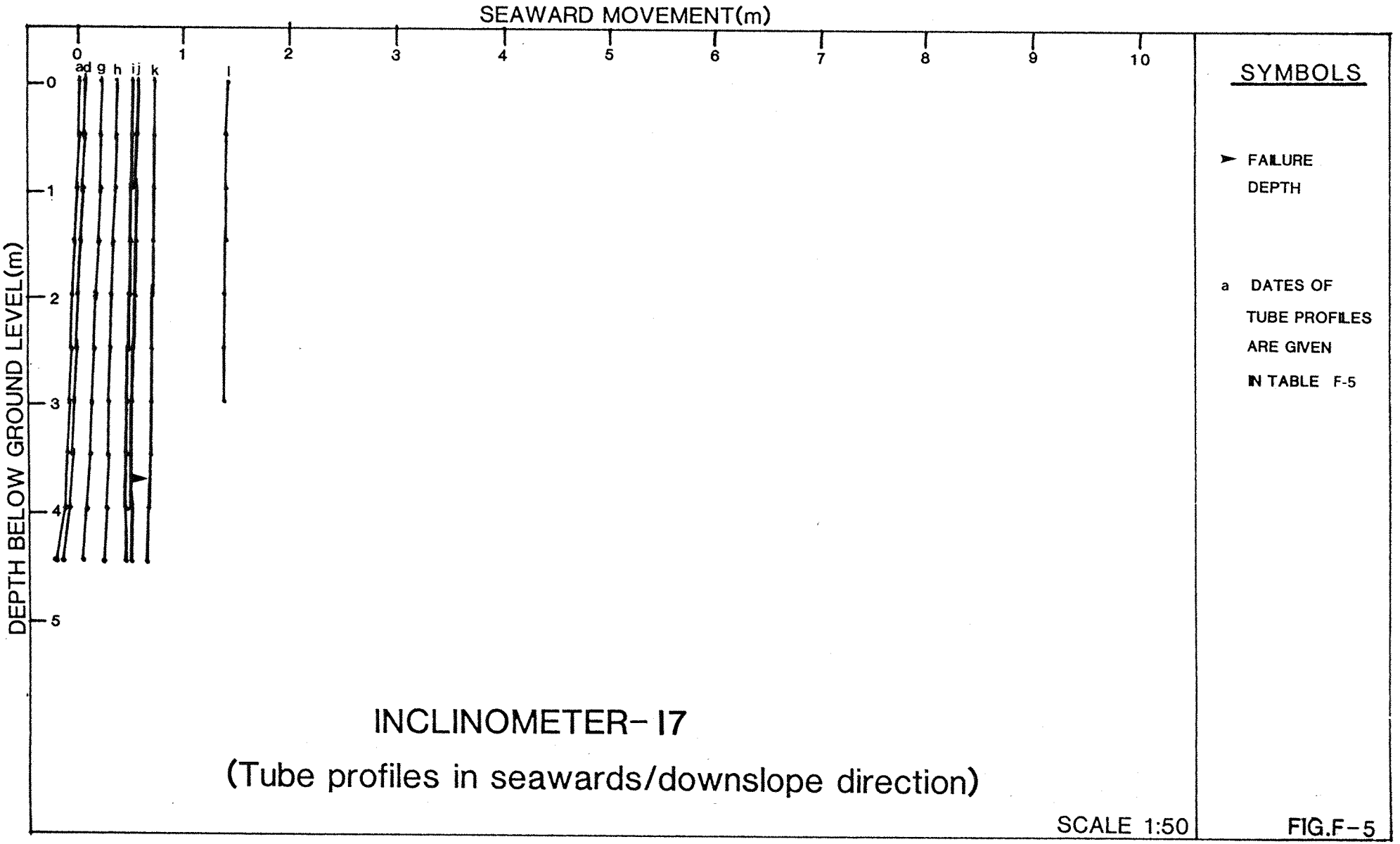

INCLINOMETER-17

(Tube profiles in seawards/downslope direction)

SCALE 1:50

FIG.F-5

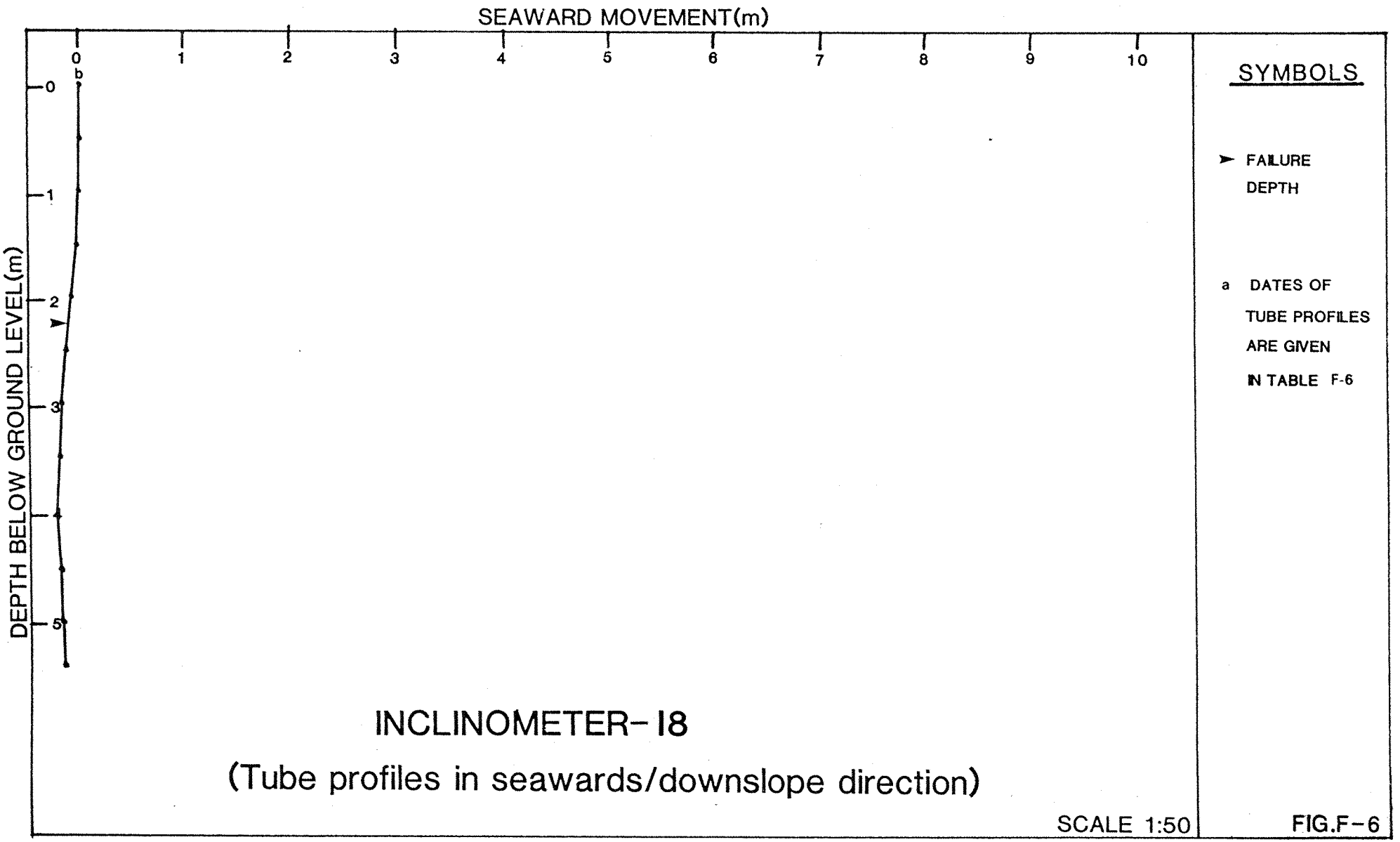

INCLINOMETER-18

(Tube profiles in seawards/downslope direction)

SCALE 1:50

FIG.F-6

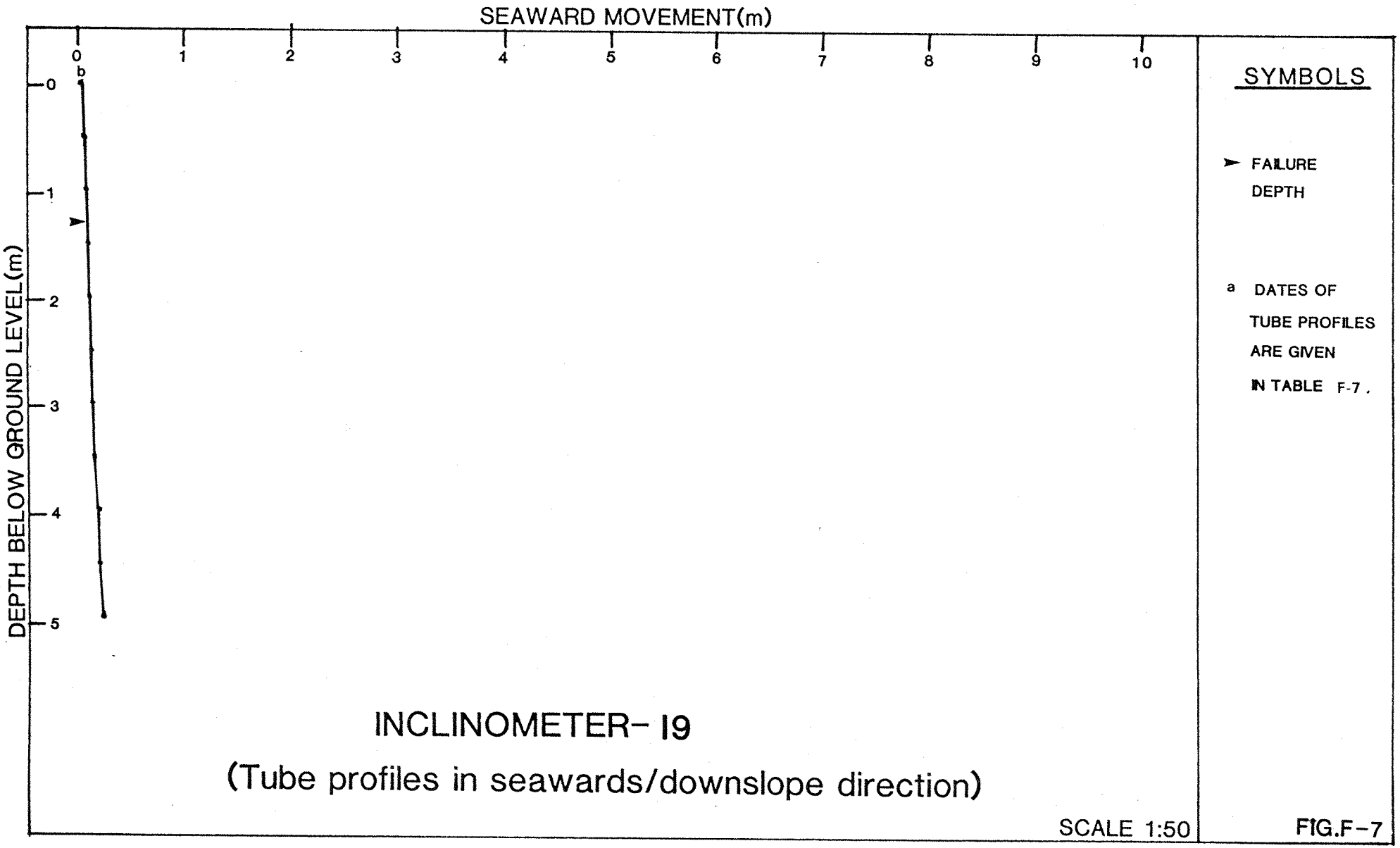

INCLINOMETER- 19

(Tube profiles in seawards/downslope direction)

SCALE 1:50

FIG.F-7

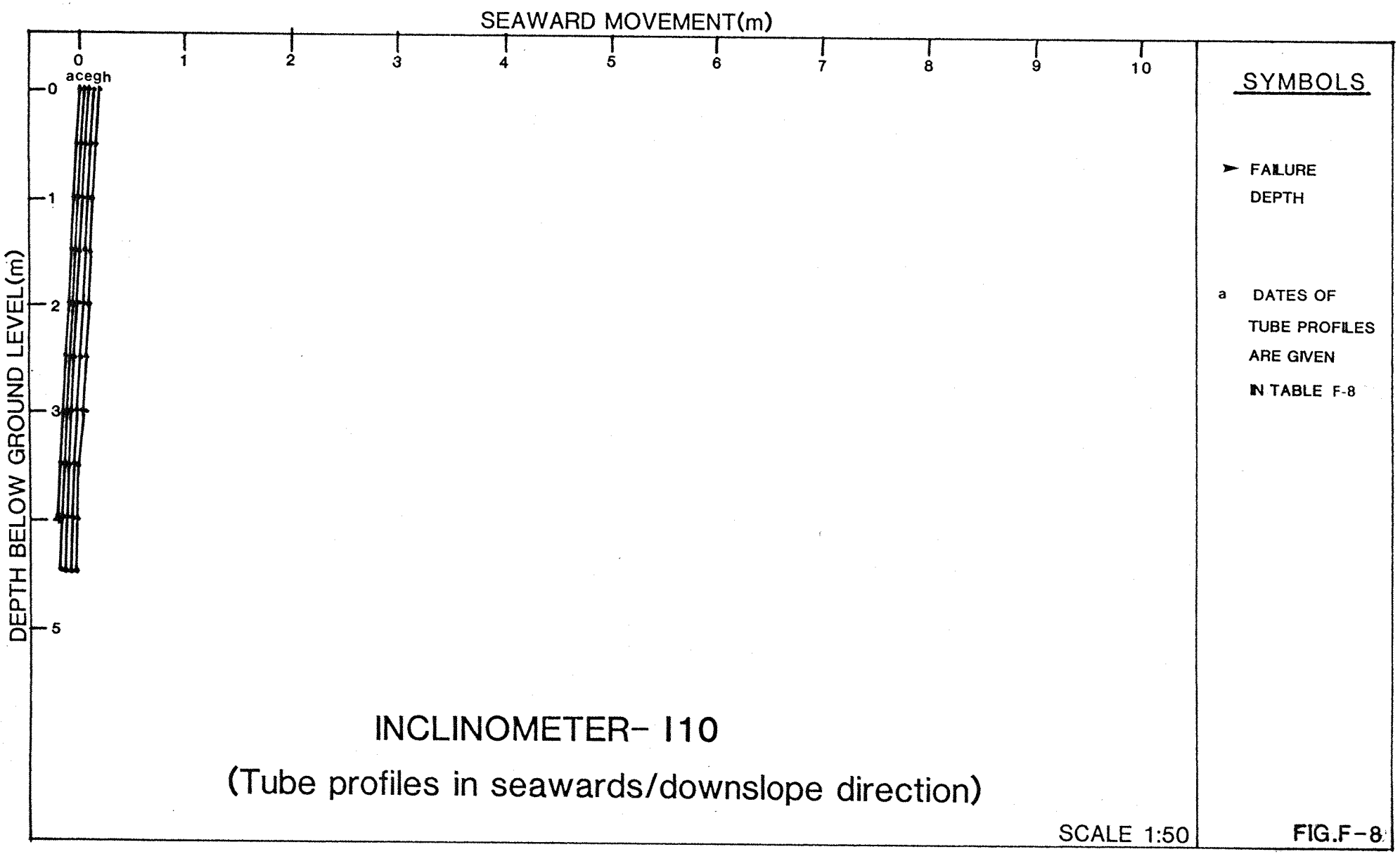

INCLINOMETER- I10

(Tube profiles in seawards/downslope direction)

SCALE 1:50

FIG.F-8

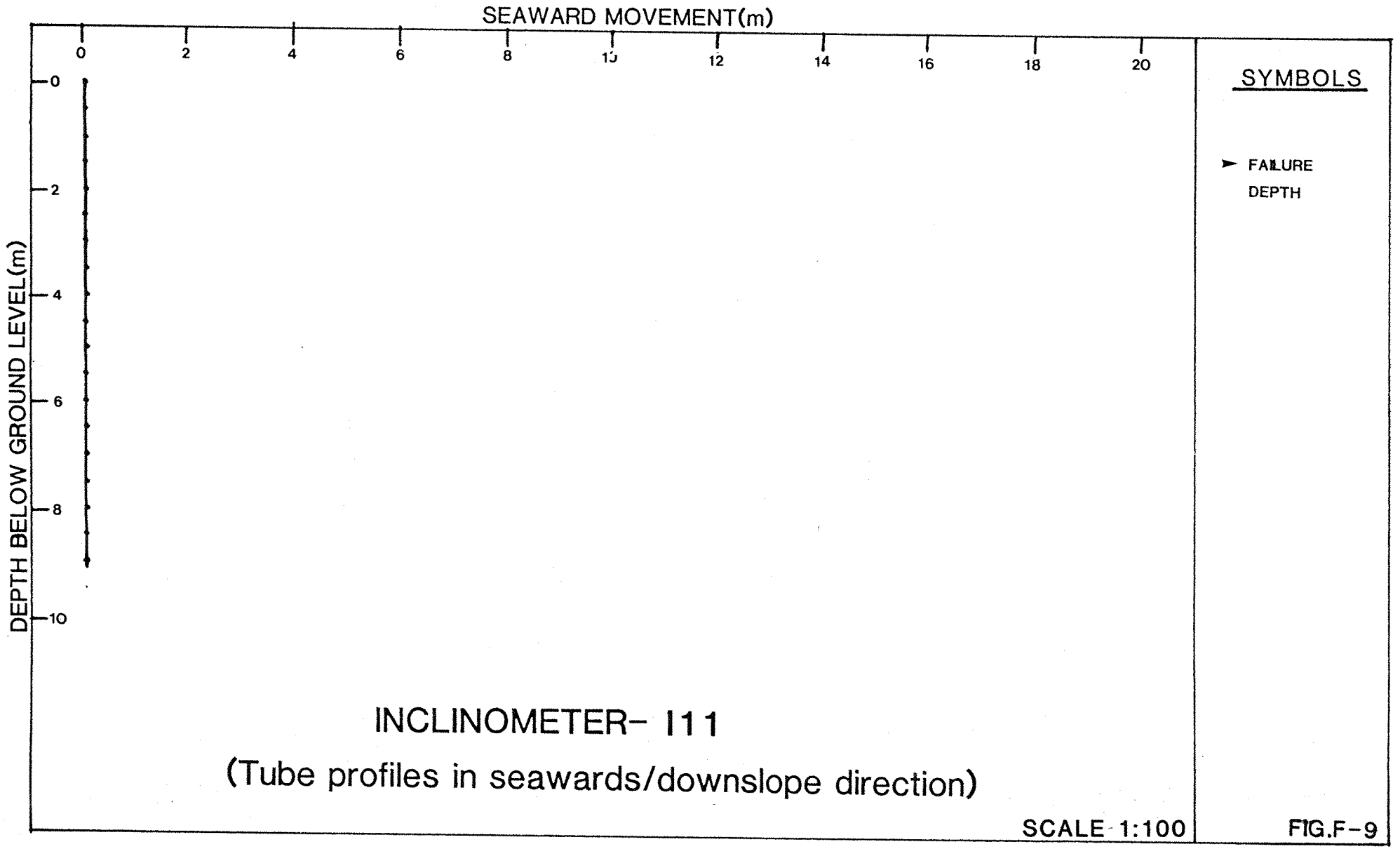

INCLINOMETER- I11

(Tube profiles in seawards/downslope direction)

SCALE 1:100

FIG.F-9

MUDSLIDE CHANNEL

(Mudslide A,November 1980)

FIG.F-10

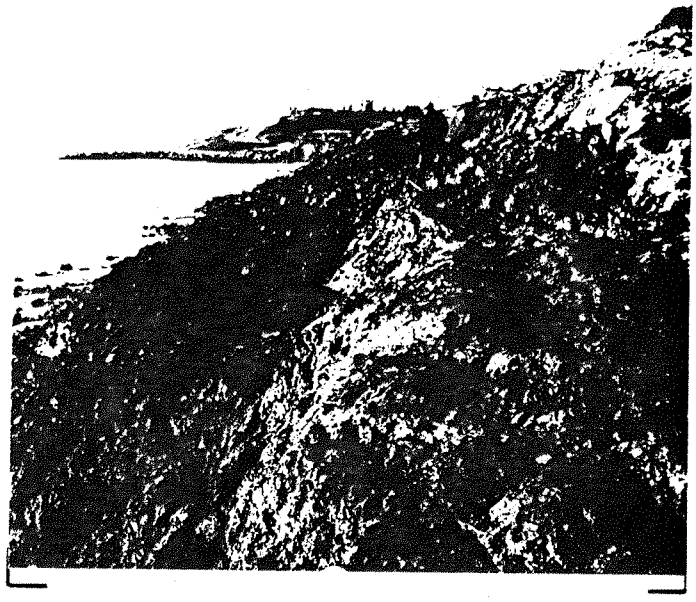

EGDE FAILURE OF A3 BENCH

(View looking west towards Chewton Bunny, Mr.A.Brookes standing on A3 bench)

INCLINOMETER I3-RECOVERED FROM BEACH

(Scarp kink at pinched section is the position of A3 shear surface,ranging rod marked in 0.5metres)

FIG.F-11

SCALE 1:20

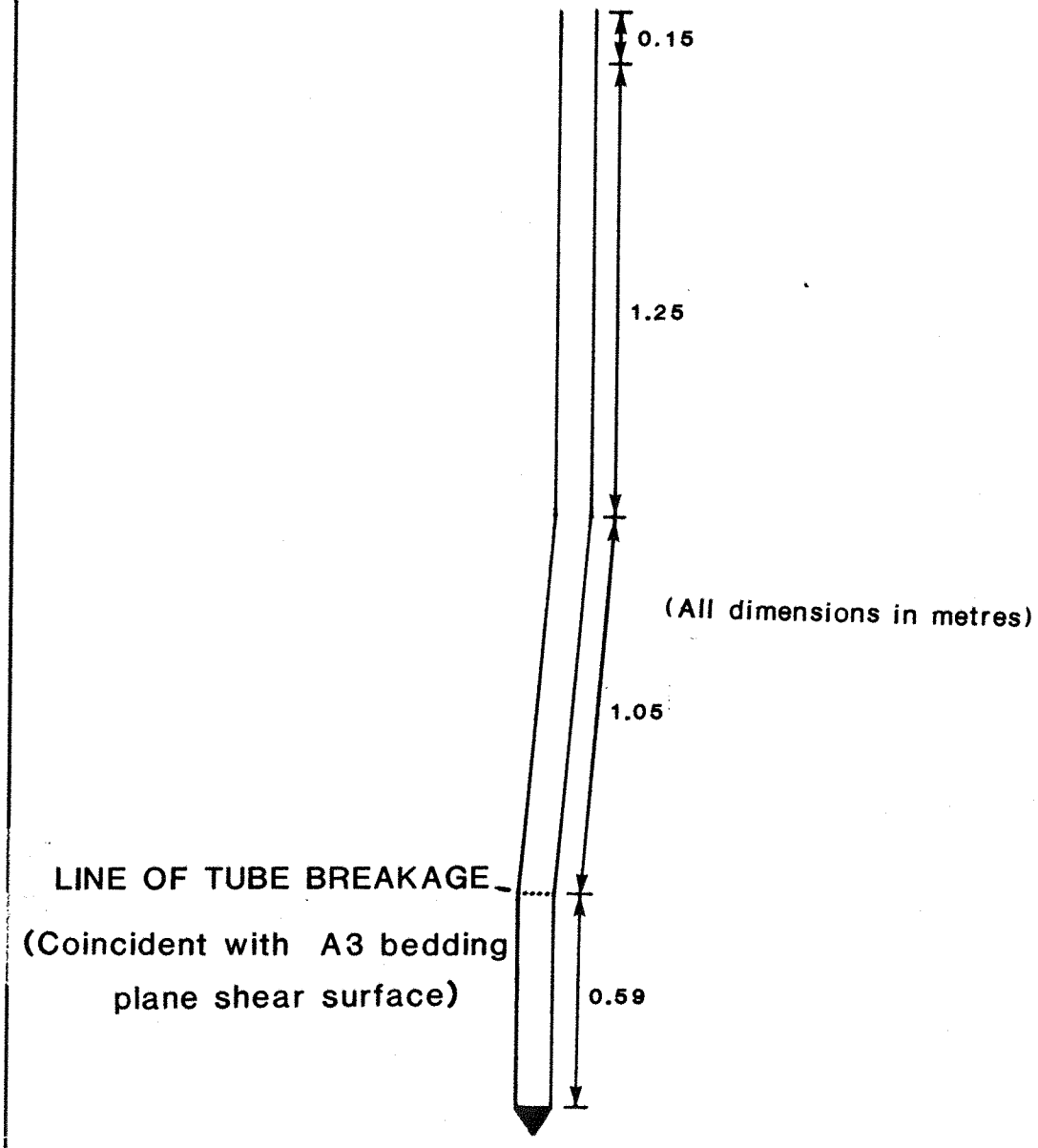

DEFORMED SHAPE OF INCLINOMETER I3
(Recovered 1-12-1981)

FIG.F-12

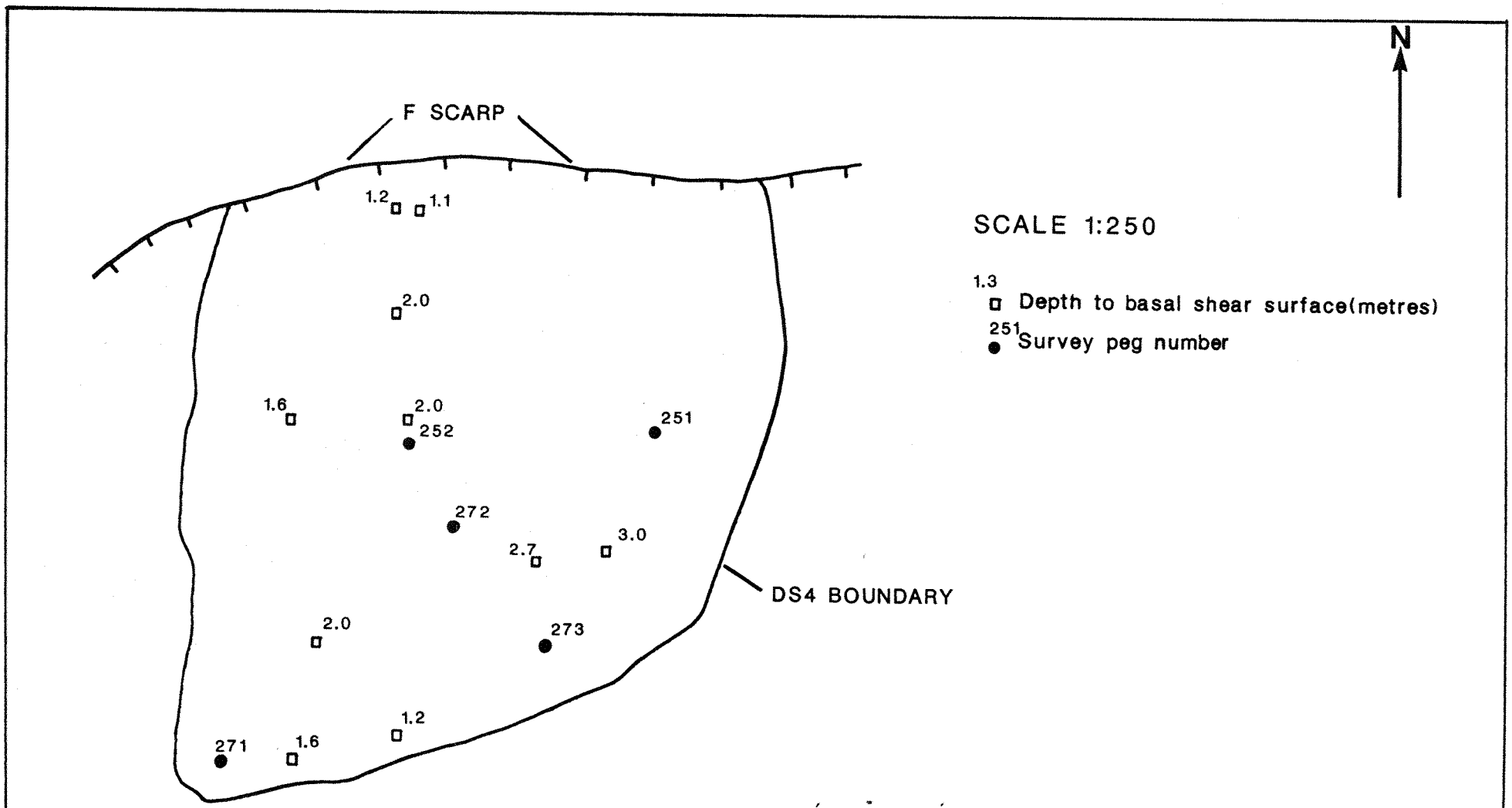

OUTLINE OF DS4 AND THE DEPTHS TO THE BASAL SHEAR SURFACE

FIG.F-13

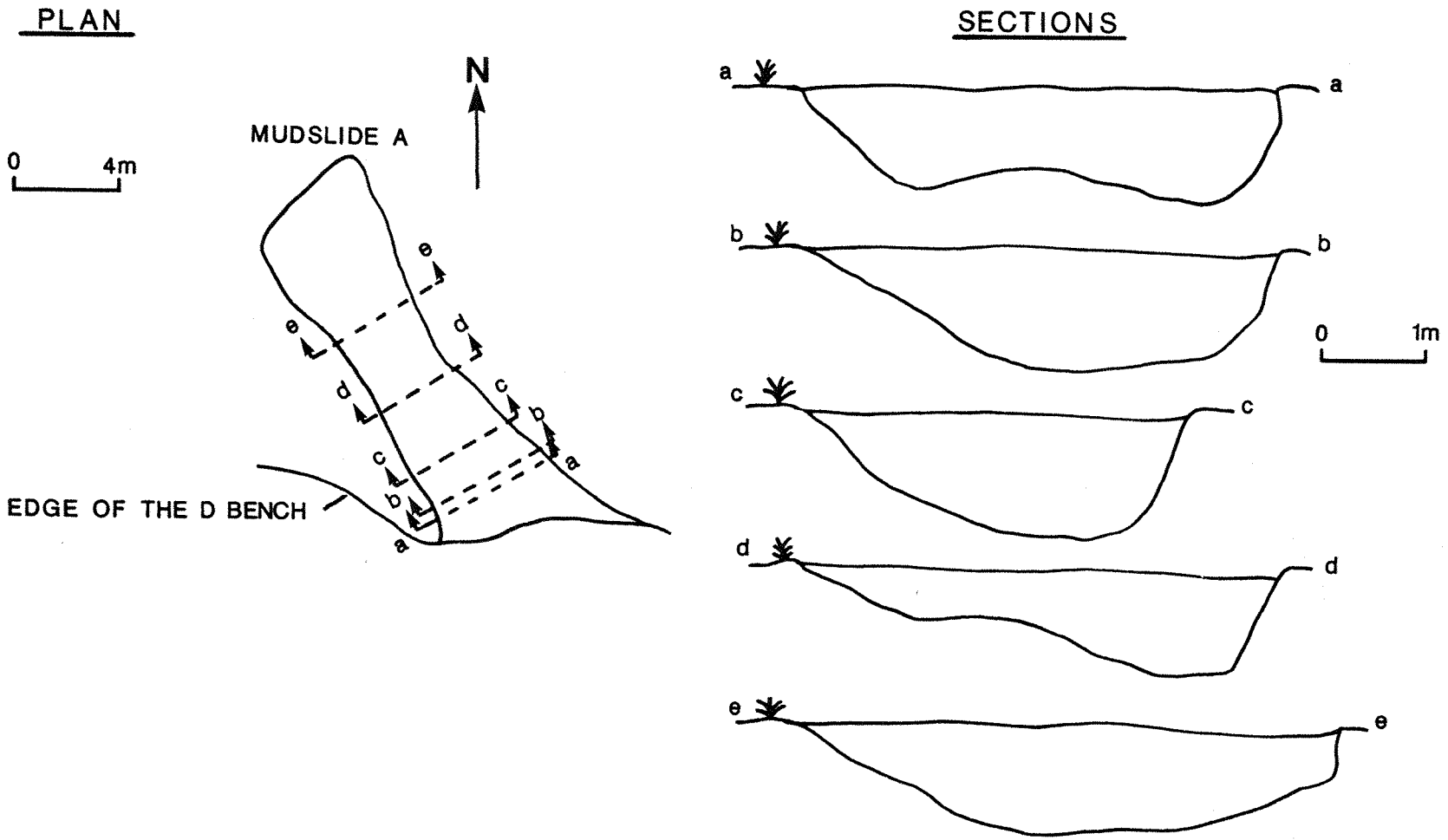

PLAN AND CROSS SECTION OF MUDSLIDE A DURING NOVEMBER 1980

FIG.F-13a

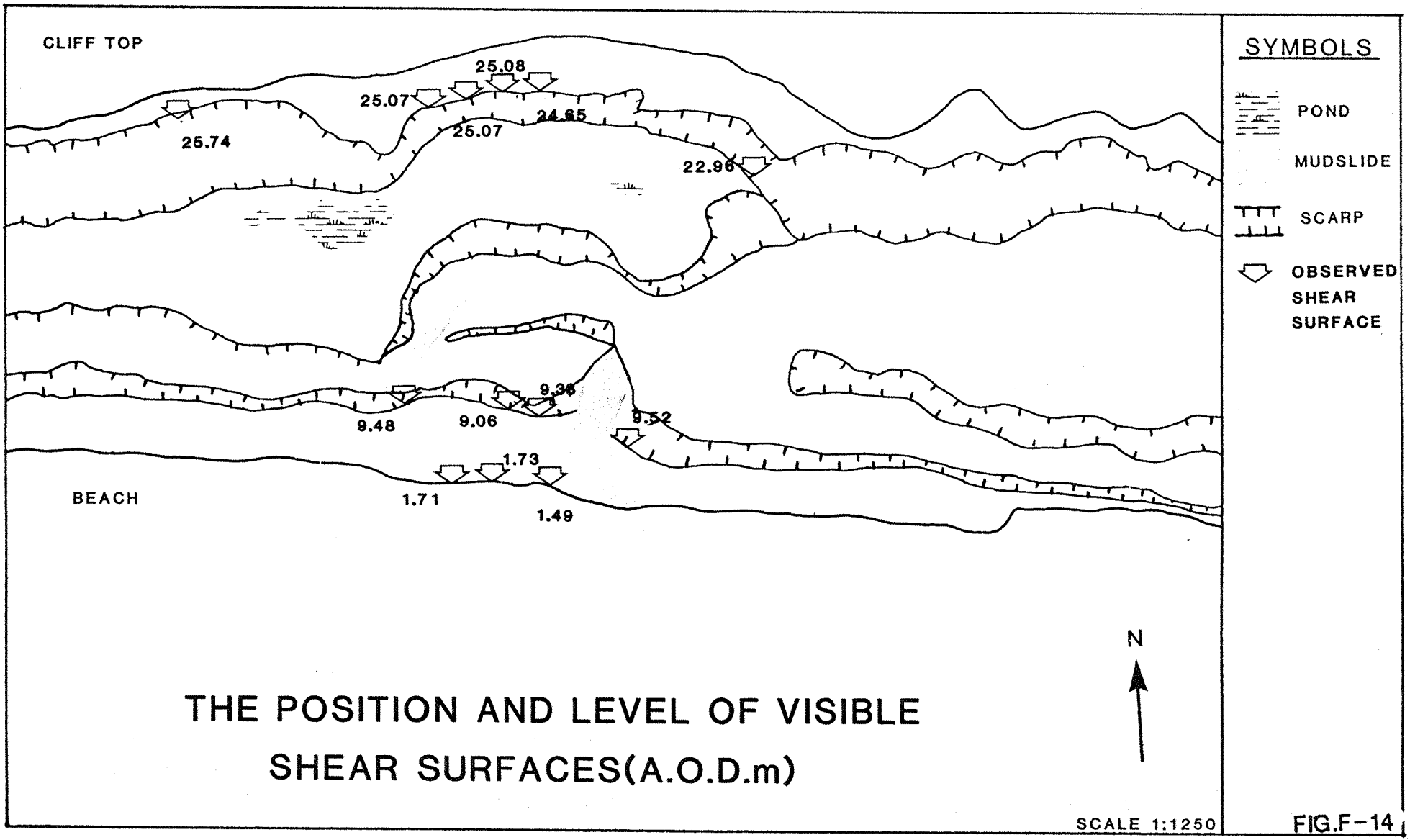

THE POSITION AND LEVEL OF VISIBLE SHEAR SURFACES(A.O.D.m)

FIG.F-14

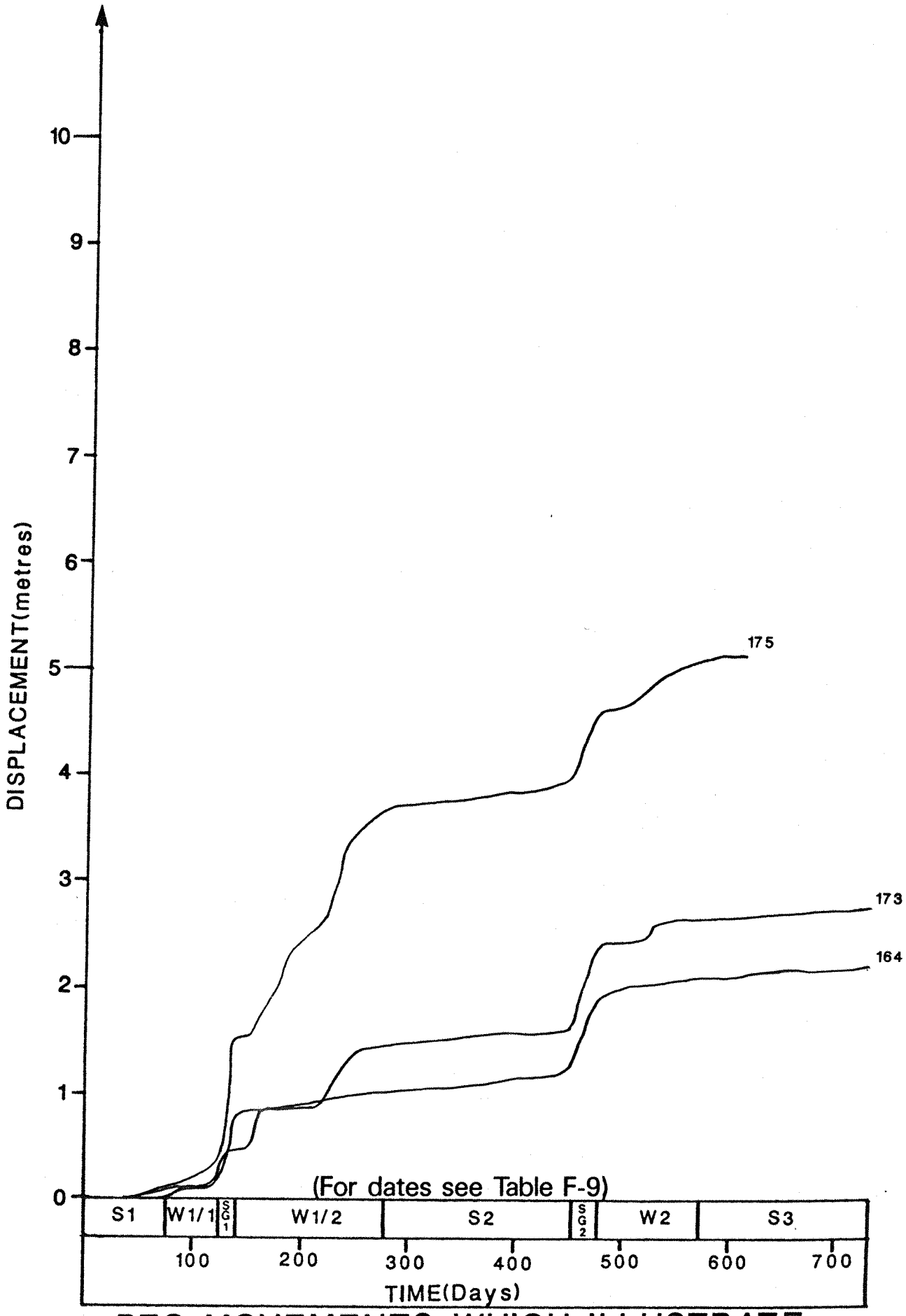

PEG MOVEMENTS WHICH ILLUSTRATE THE CYCLIC PATTERN OF MOVEMENT

FIG.F-15

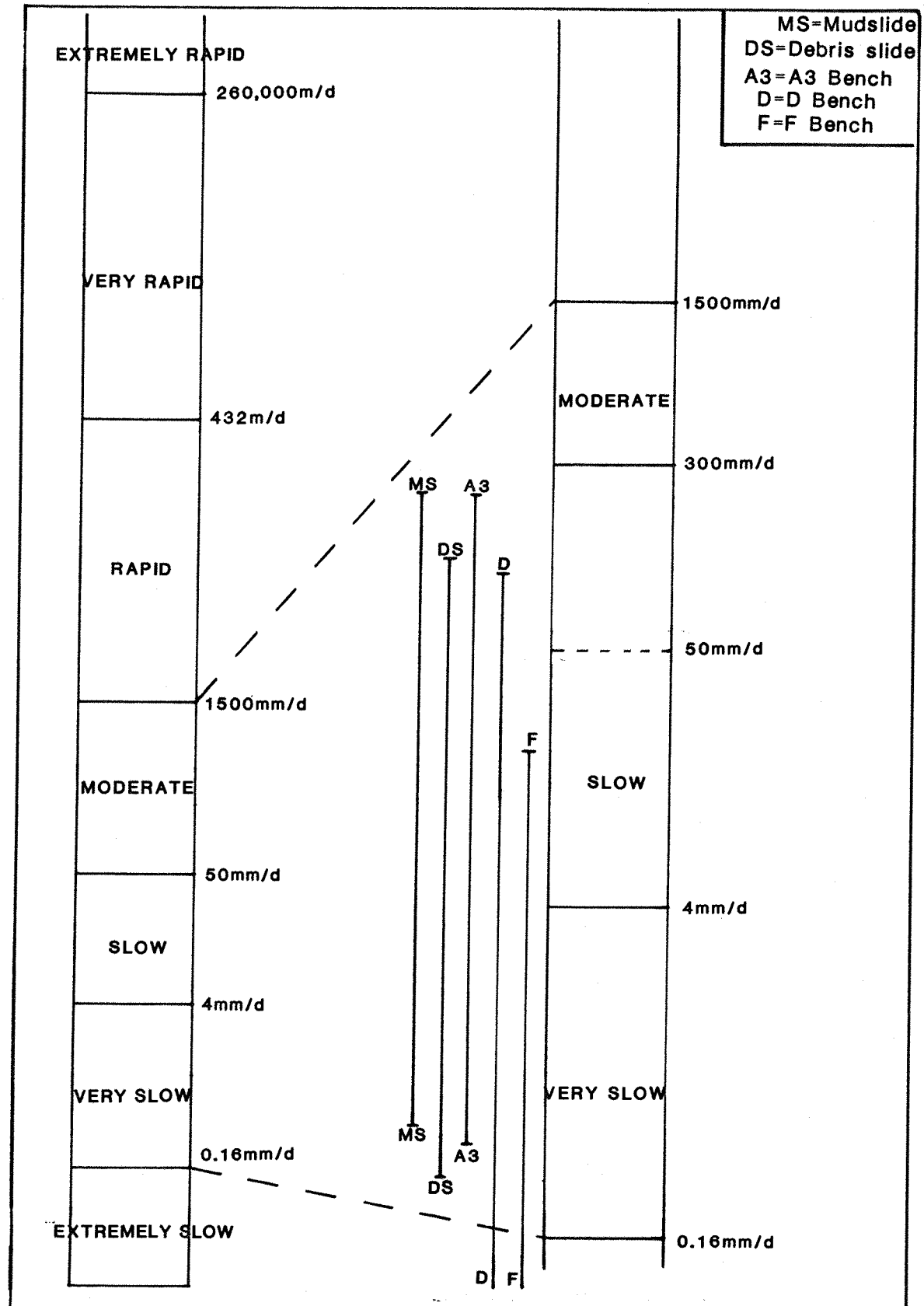

RATE OF MOVEMENT SCALE

FIG.F-16

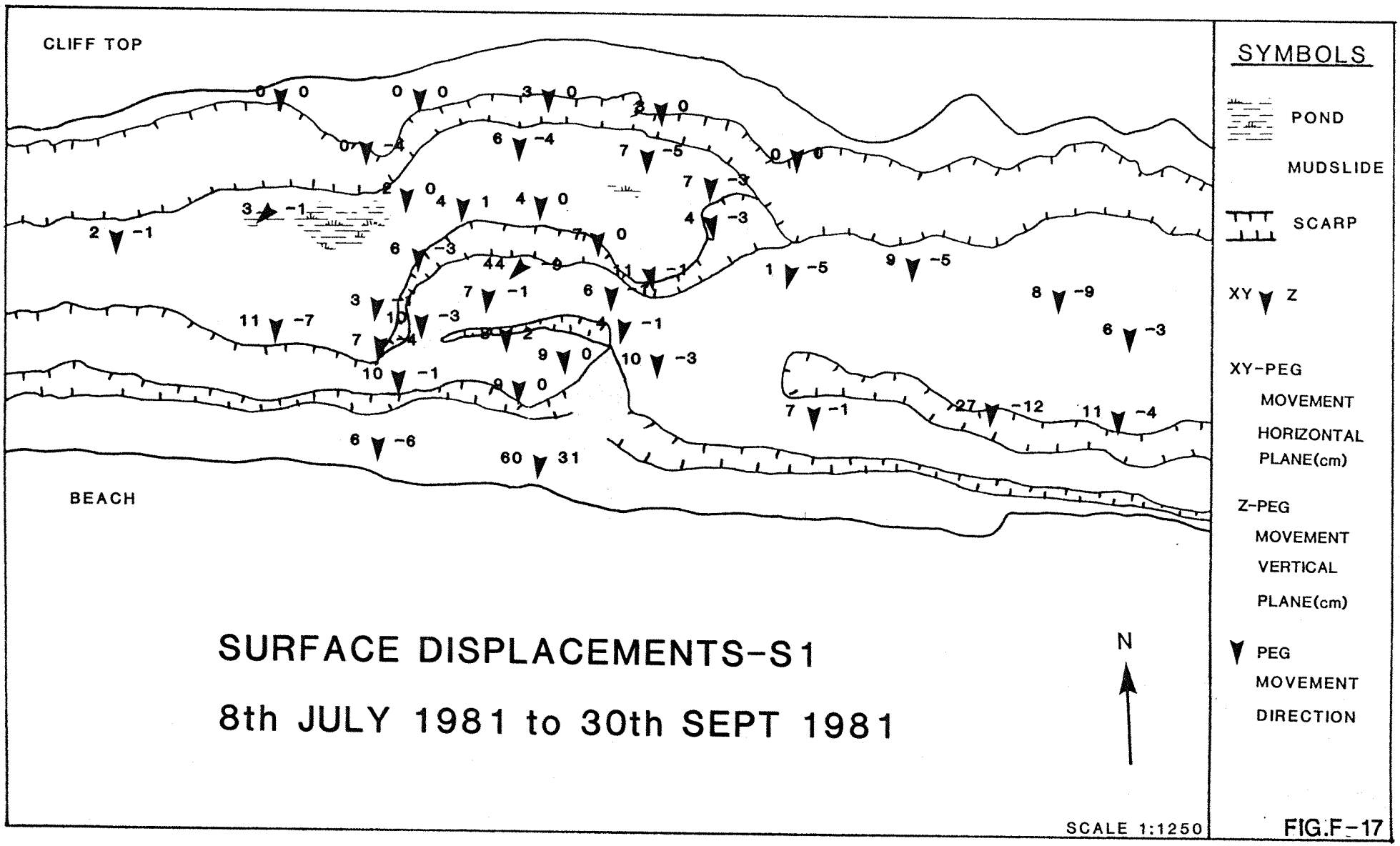
CLIFF TOP
BEACH
SYMBOLS
POND
MUDSLIDE
SCARP
XY Z
XY-PEG MOVEMENT HORIZONTAL PLANE(cm)
Z-PEG MOVEMENT VERTICAL PLANE(cm)
PEG MOVEMENT DIRECTION
N
SURFACE DISPLACEMENTS-S1
8th JULY 1981 to 30th SEPT 1981
SCALE 1:1250
FIG.F-17

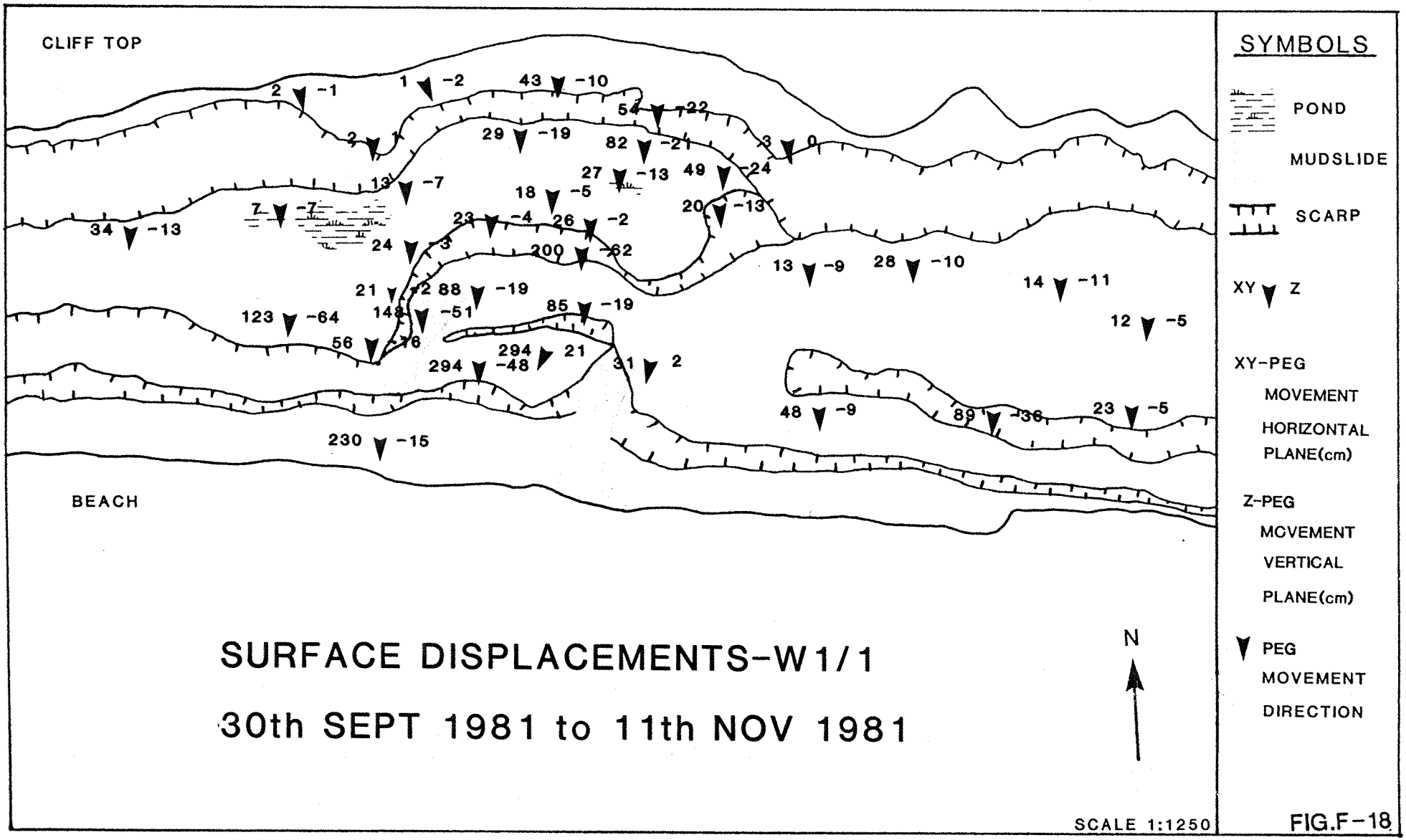
CLIFF TOP
2 -1
1 -2
43 -10
54 -22
29 -19
82 -21
3 0
27 -13
49 -24
13 -7
18 -5
20 -13
7 -7
34 -13
23 -4
26 -2
24 3
200 -62
13 -9
28 -10
14 -11
21 2
88 -19
123 -64
148 -51
85 -19
12 -5
56 -76
294 21
294 -48
31 2
48 -9
89 -36
23 -5
230 -15
BEACH
SYMBOLS
POND
MUDSLIDE
SCARP
XY Z
XY-PEG MOVEMENT HORIZONTAL PLANE(cm)
Z-PEG MOVEMENT VERTICAL PLANE(cm)
PEG MOVEMENT DIRECTION
N
SURFACE DISPLACEMENTS-W1/1
30th SEPT 1981 to 11th NOV 1981
SCALE 1:1250
FIG.F-18

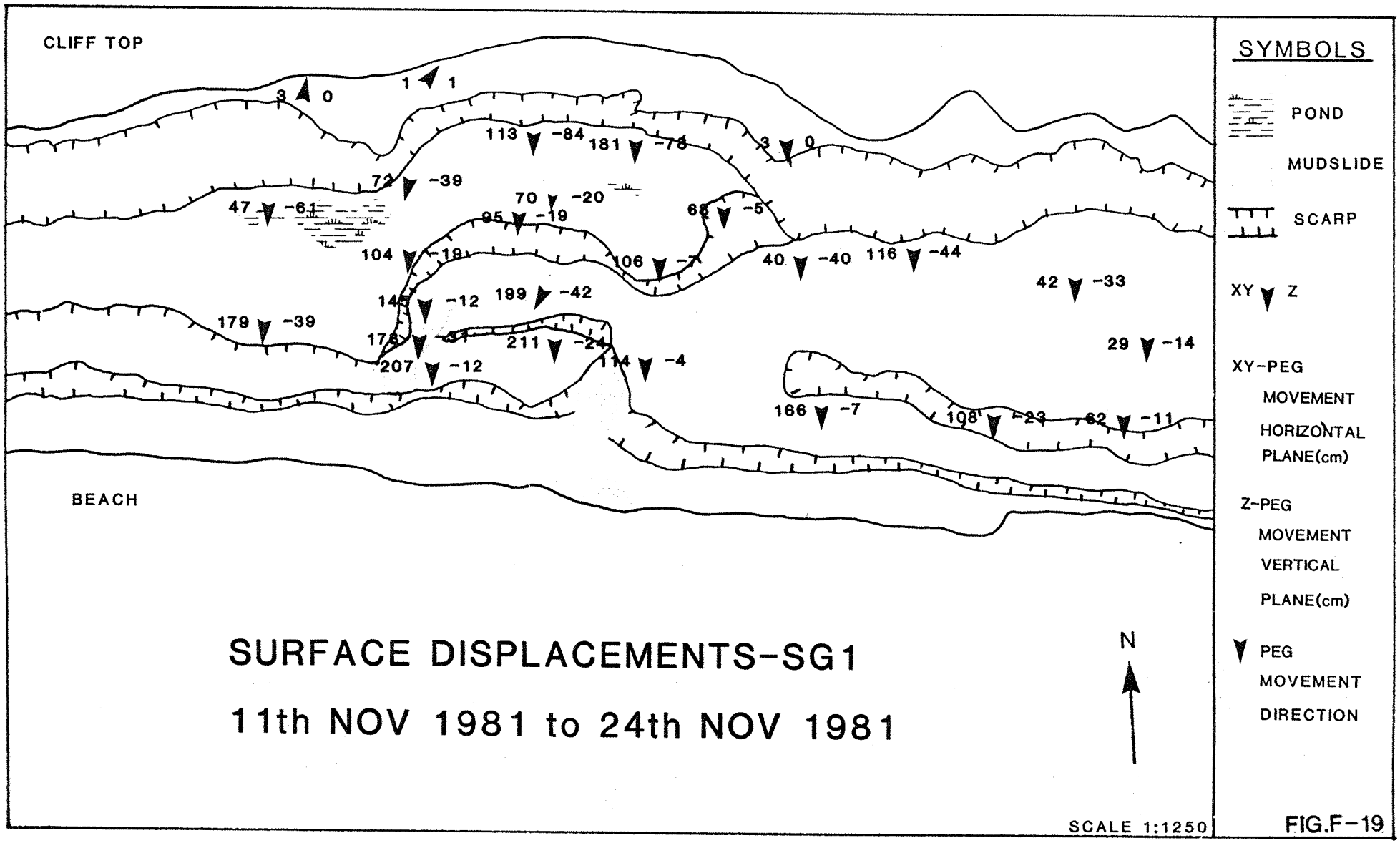
CLIFF TOP
BEACH
3 0
1 1
113 -84
181 -78
3 0
72 -39
47 -61
70 -20
95 -19
68 -5
104 -19
106 -7
40 -40
116 -44
42 -33
145 -12
199 -42
179 -39
175 -31
211 -24
29 -14
207 -12
114 -4
166 -7
108 -23
62 -11
SYMBOLS
POND
MUDSLIDE
SCARP
XY Z
XY-PEG MOVEMENT HORIZONTAL PLANE(cm)
Z-PEG MOVEMENT VERTICAL PLANE(cm)
PEG MOVEMENT DIRECTION
N
SURFACE DISPLACEMENTS-SG1
11th NOV 1981 to 24th NOV 1981
SCALE 1:1250
FIG.F-19

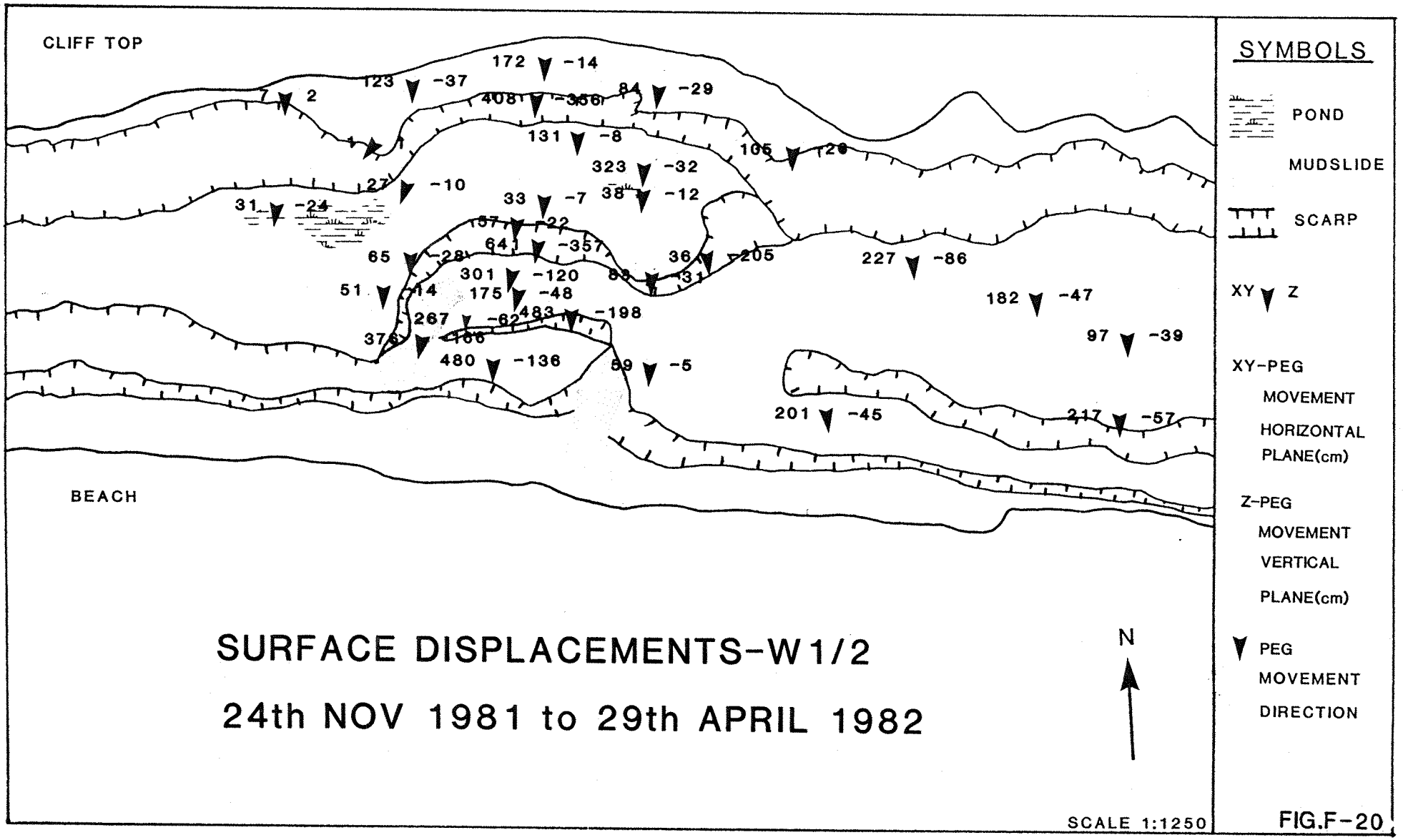
CLIFF TOP
BEACH
172 -14
123 -37
2
408 -356
84 -29
131 -8
323 -32
105 -28
27 -10
31 -24
33 -7
38 -12
57 -22
641 -357
65 -28
36 -205
227 -86
301 -120
51 -14
175 -48
182 -47
267 -62
483 -198
97 -39
480 -136
59 -5
201 -45
217 -57
SURFACE DISPLACEMENTS-W1/2
24th NOV 1981 to 29th APRIL 1982
N
SCALE 1:1250
SYMBOLS
POND
MUDSLIDE
SCARP
XY Z
XY-PEG MOVEMENT HORIZONTAL PLANE(cm)
Z-PEG MOVEMENT VERTICAL PLANE(cm)
PEG MOVEMENT DIRECTION

FIG.F-20

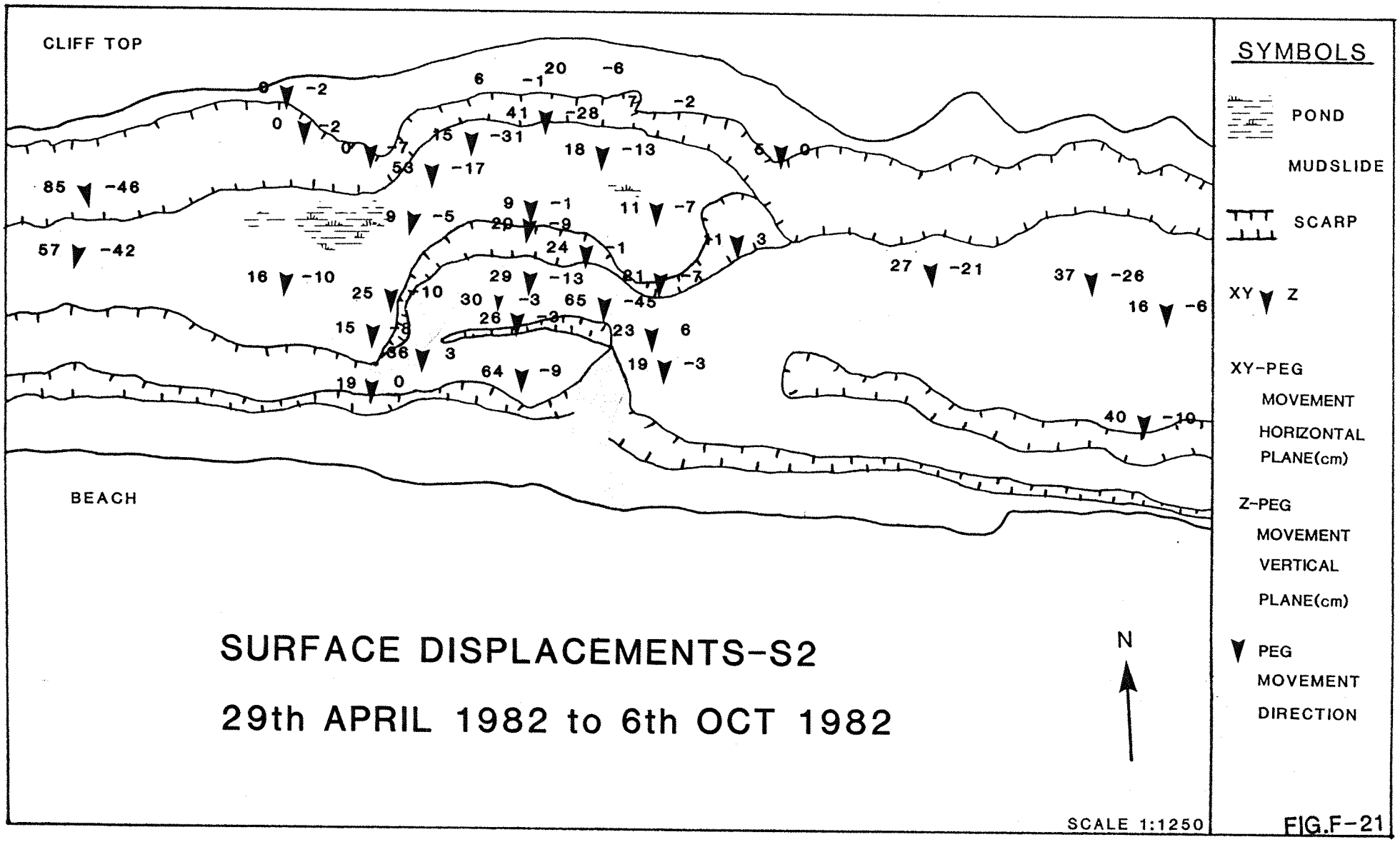
CLIFF TOP
BEACH
SYMBOLS
POND
MUDSLIDE
SCARP
XY Z
XY-PEG MOVEMENT HORIZONTAL PLANE(cm)
Z-PEG MOVEMENT VERTICAL PLANE(cm)
PEG MOVEMENT DIRECTION
N
SURFACE DISPLACEMENTS-S2
29th APRIL 1982 to 6th OCT 1982
SCALE 1:1250
FIG.F-21

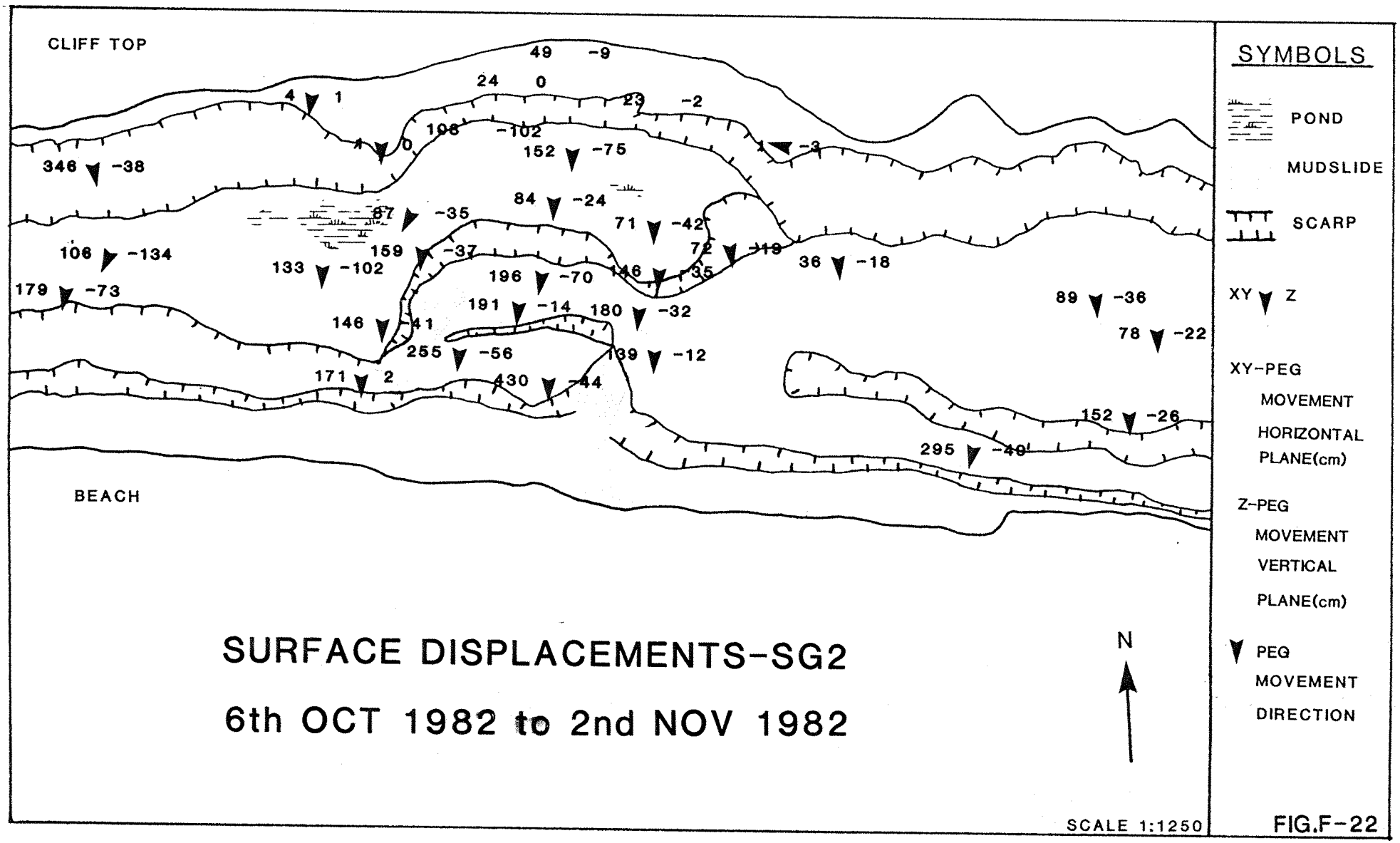
CLIFF TOP
49 -9
24 0
4 1
23 -2
108 -102
0
152 -75
346 -38
-3
84 -24
87 -35
71 -42
106 -134
159 -37
72 -19
133 -102
36 -18
196 -70
46 35
179 -73
89 -36
191 -14
180 -32
146 41
78 -22
255 -56
139 -12
171 2
430 -44
152 -26
295 -49
BEACH
SYMBOLS
POND
MUDSLIDE
SCARP
XY Z
XY-PEG MOVEMENT HORIZONTAL PLANE(cm)
Z-PEG MOVEMENT VERTICAL PLANE(cm)
PEG MOVEMENT DIRECTION
N
SURFACE DISPLACEMENTS-SG2
6th OCT 1982 to 2nd NOV 1982
SCALE 1:1250
FIG.F-22

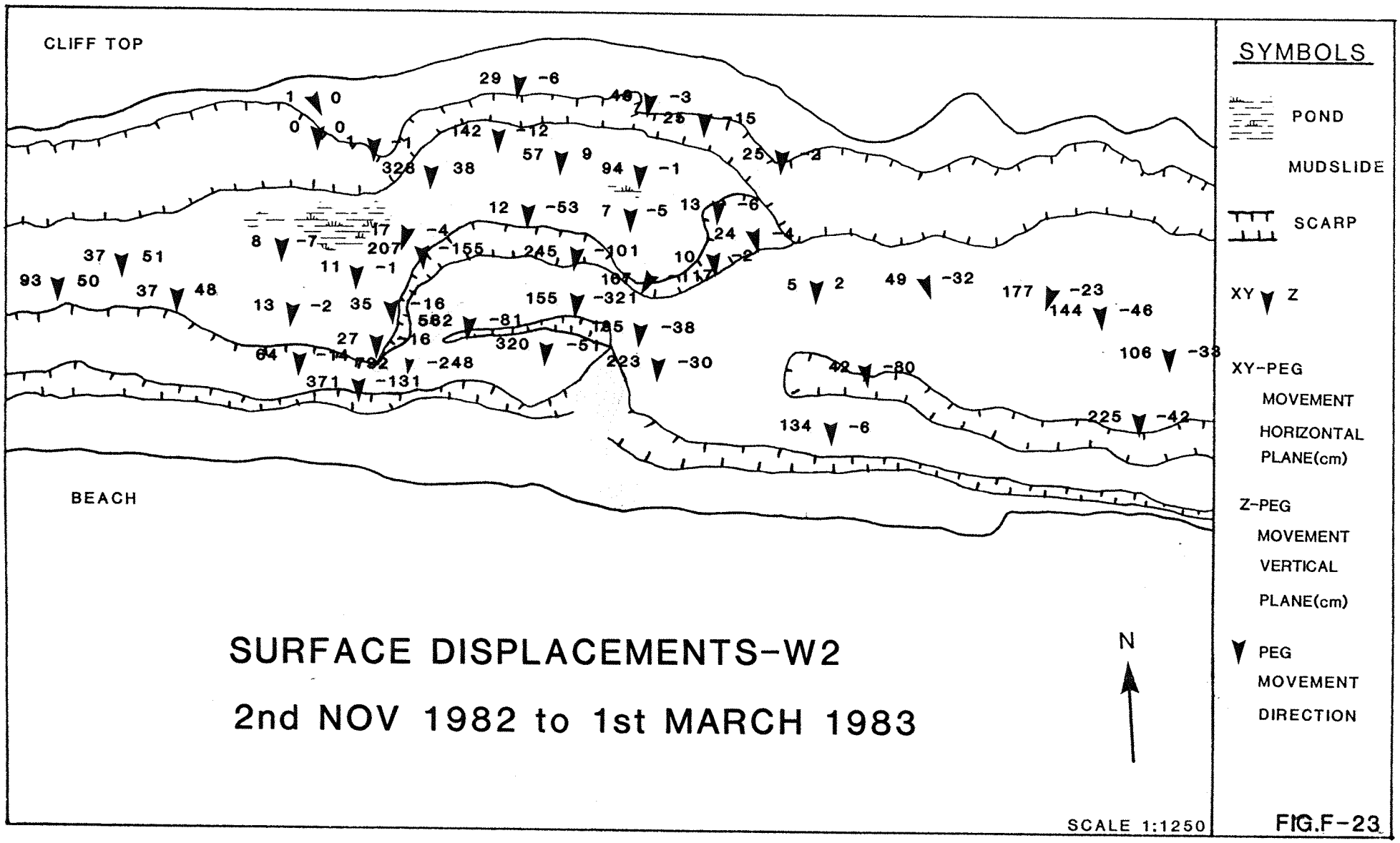
CLIFF TOP
BEACH
1 0
0 0
0 -1
29 -6
46 -3
25 15
142 -12
328 38
57 9
94 -1
25 -2
12 -53
7 -5
13 -6
17 -4
8 -7
207 -155
245 -101
24 -4
10 -2
37 51
93 50
37 48
11 -1
13 -2
35 -16
155 -321
582 -81
27 16
320 -51
185 -38
64 -14
192 -248
371 -131
223 -30
5 2
49 -32
177 -23
144 -46
106 -33
42 -80
225 -42
134 -6
SYMBOLS
POND
MUDSLIDE
SCARP
XY Z
XY-PEG MOVEMENT HORIZONTAL PLANE(cm)
Z-PEG MOVEMENT VERTICAL PLANE(cm)
PEG MOVEMENT DIRECTION
N
SURFACE DISPLACEMENTS-W2
2nd NOV 1982 to 1st MARCH 1983
SCALE 1:1250
FIG.F-23

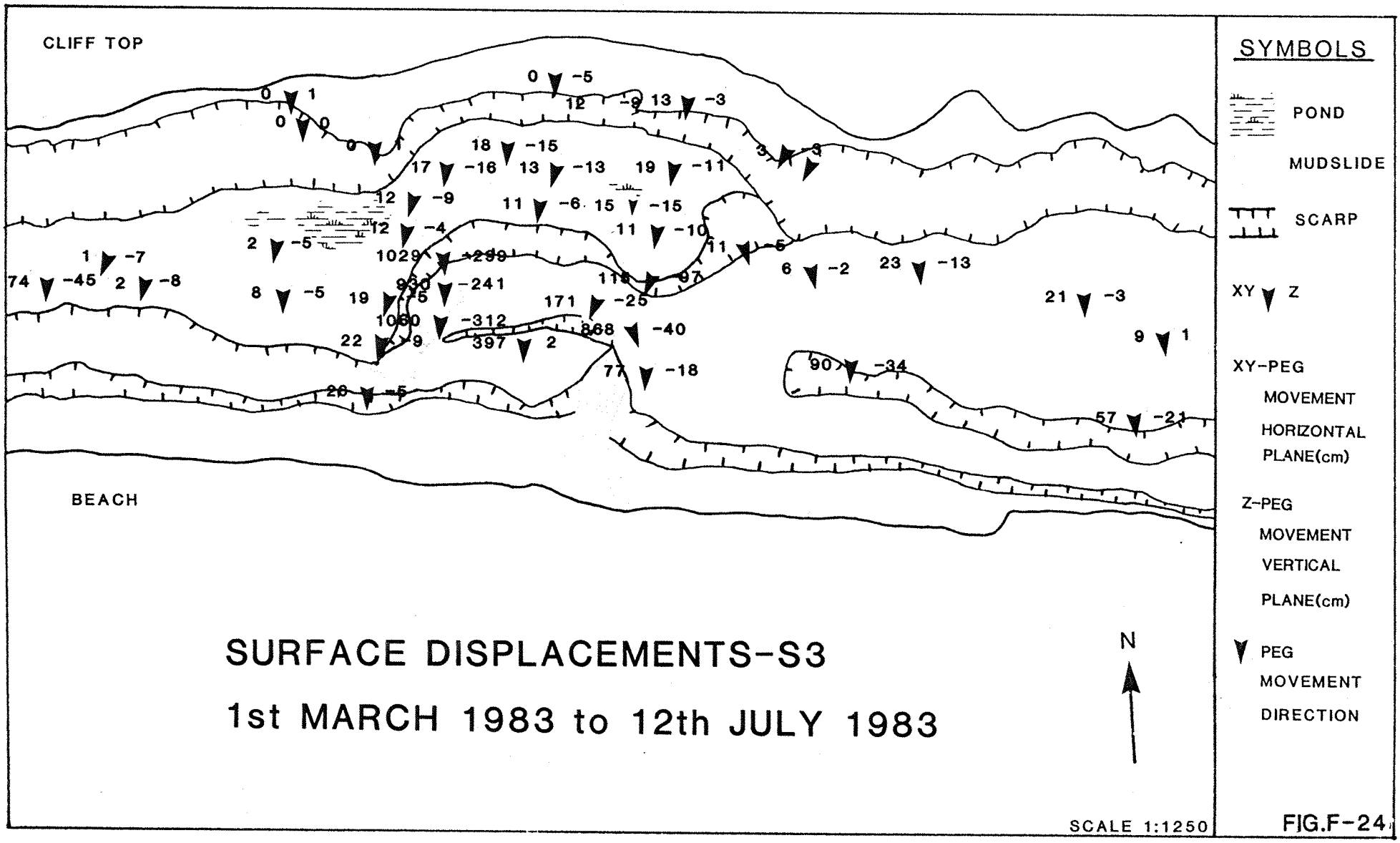
CLIFF TOP
BEACH
SYMBOLS
POND
MUDSLIDE
SCARP
XY Z
XY-PEG MOVEMENT HORIZONTAL PLANE(cm)
Z-PEG MOVEMENT VERTICAL PLANE(cm)
PEG MOVEMENT DIRECTION
N
SURFACE DISPLACEMENTS-S3
1st MARCH 1983 to 12th JULY 1983
SCALE 1:1250
FIG.F-24

Period	Label	Start Date	Finish Date	Duration in days	Number of pegs
Summer	S1	8. 7.81	30. 9.81	84	75
Winter	W1/1	30. 9.81	11.11.81	42	66
Surge	SG1	11.11.81	24.11.81	13	49
Winter	W1/2	24.11.81	29. 4.82	156	52
Summer	S2	29. 4.82	6.10.82	160	52
Surge	SG2	6.10.82	2.11.82	27	51
Winter	W2	2.11.82	1. 3.83	119	53
Summer	S3	1. 3.83	12. 7.83	133	47

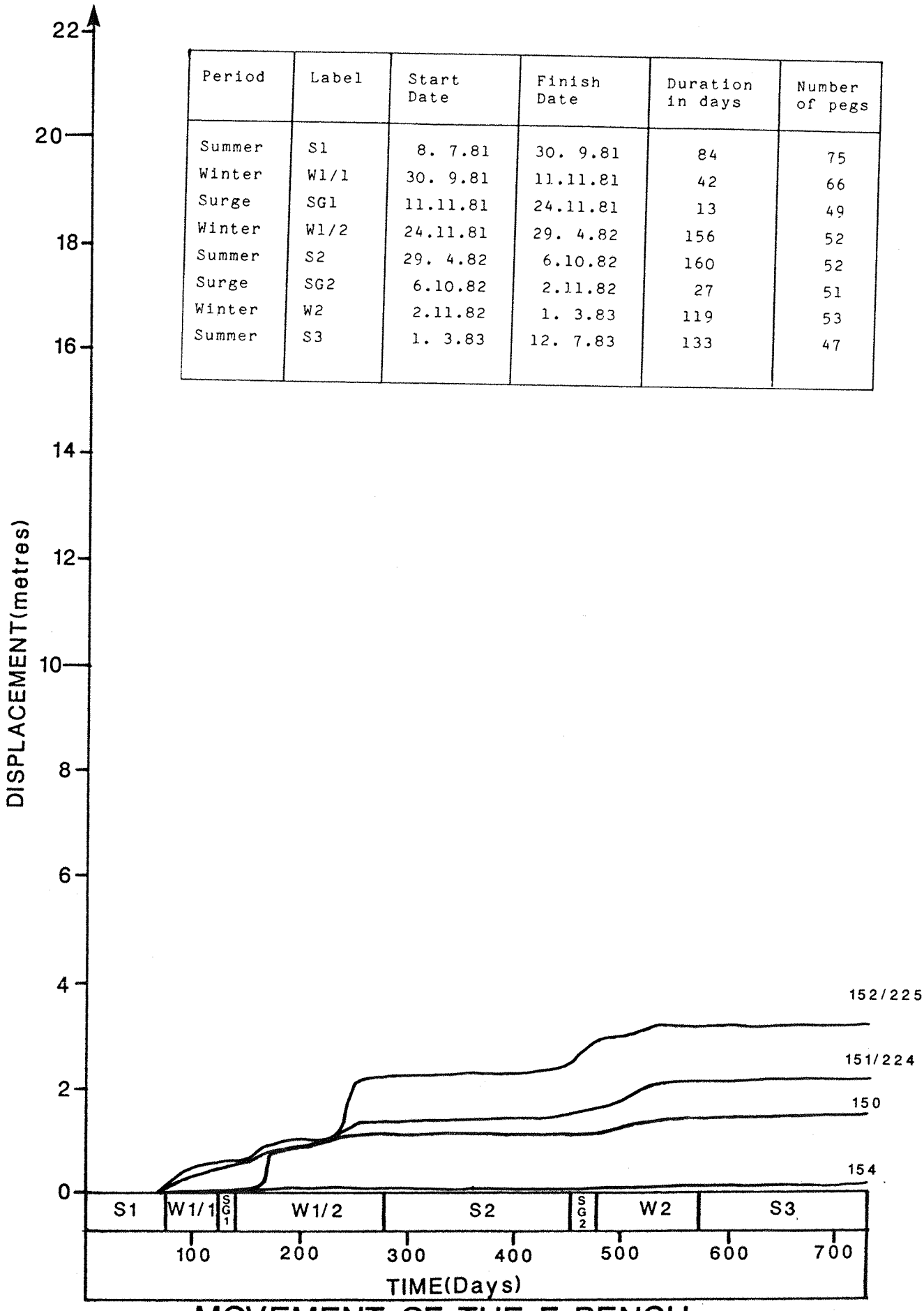

MOVEMENT OF THE F BENCH DURING THE STUDY PERIOD

FIG.F-25

Period	Label	Start Date	Finish Date	Duration in days	Number of pegs
Summer	S1	8. 7.81	30. 9.81	84	75
Winter	W1/1	30. 9.81	11.11.81	42	66
Surge	SG1	11.11.81	24.11.81	13	49
Winter	W1/2	24.11.81	29. 4.82	156	52
Summer	S2	29. 4.82	6.10.82	160	52
Surge	SG2	6.10.82	2.11.82	27	51
Winter	W2	2.11.82	1. 3.83	119	53
Summer	S3	1. 3.83	12. 7.83	133	47

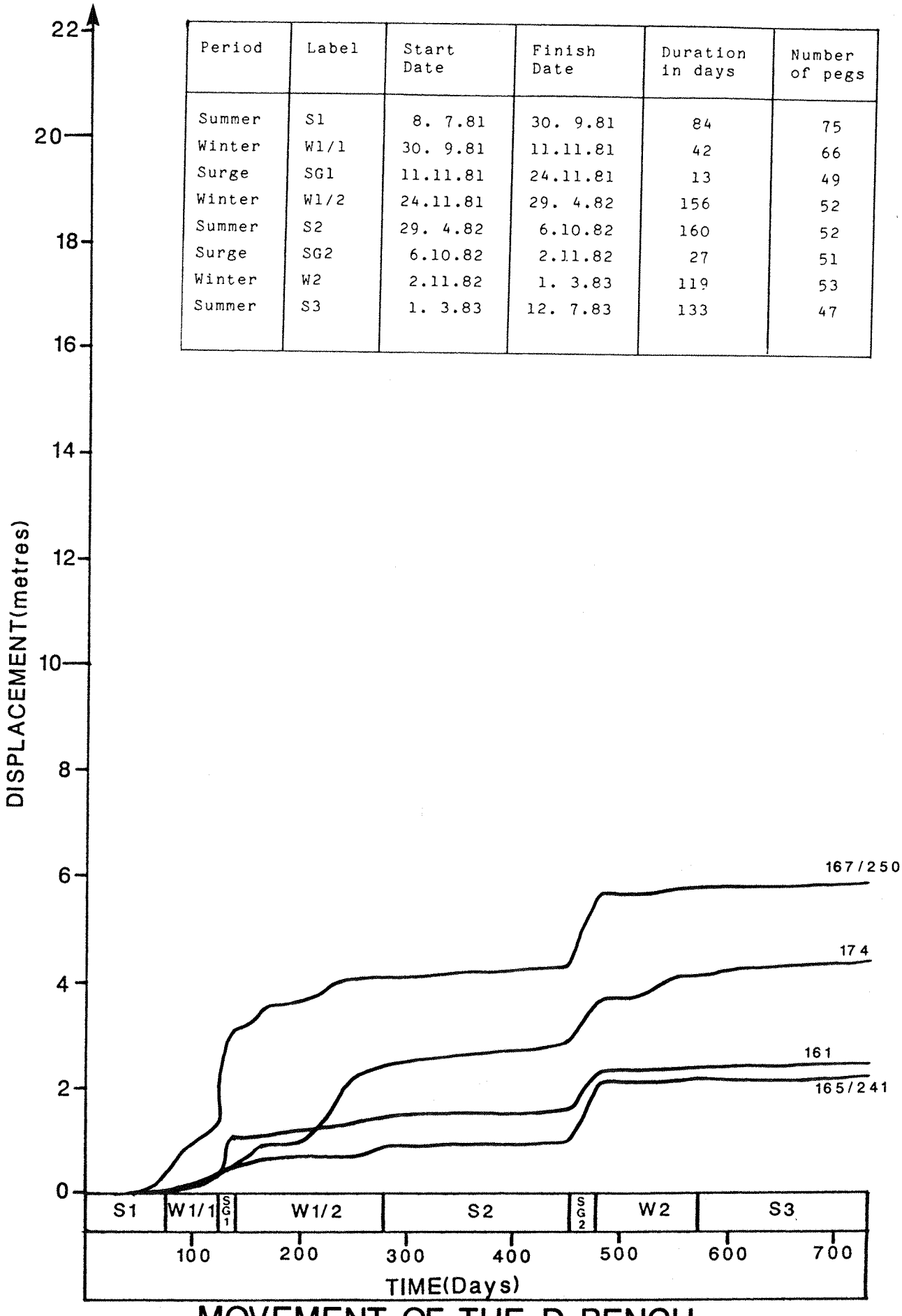

MOVEMENT OF THE D BENCH DURING THE STUDY PERIOD

FIG.F-26

Period	Label	Start Date	Finish Date	Duration in days	Number of pegs
Summer	S1	8. 7.81	30. 9.81	84	75
Winter	W1/1	30. 9.81	11.11.81	42	66
Surge	SG1	11.11.81	24.11.81	13	49
Winter	W1/2	24.11.81	29. 4.82	156	52
Summer	S2	29. 4.82	6.10.82	160	52
Surge	SG2	6.10.82	2.11.82	27	51
Winter	W2	2.11.82	1. 3.83	119	53
Summer	S3	1. 3.83	12. 7.83	133	47

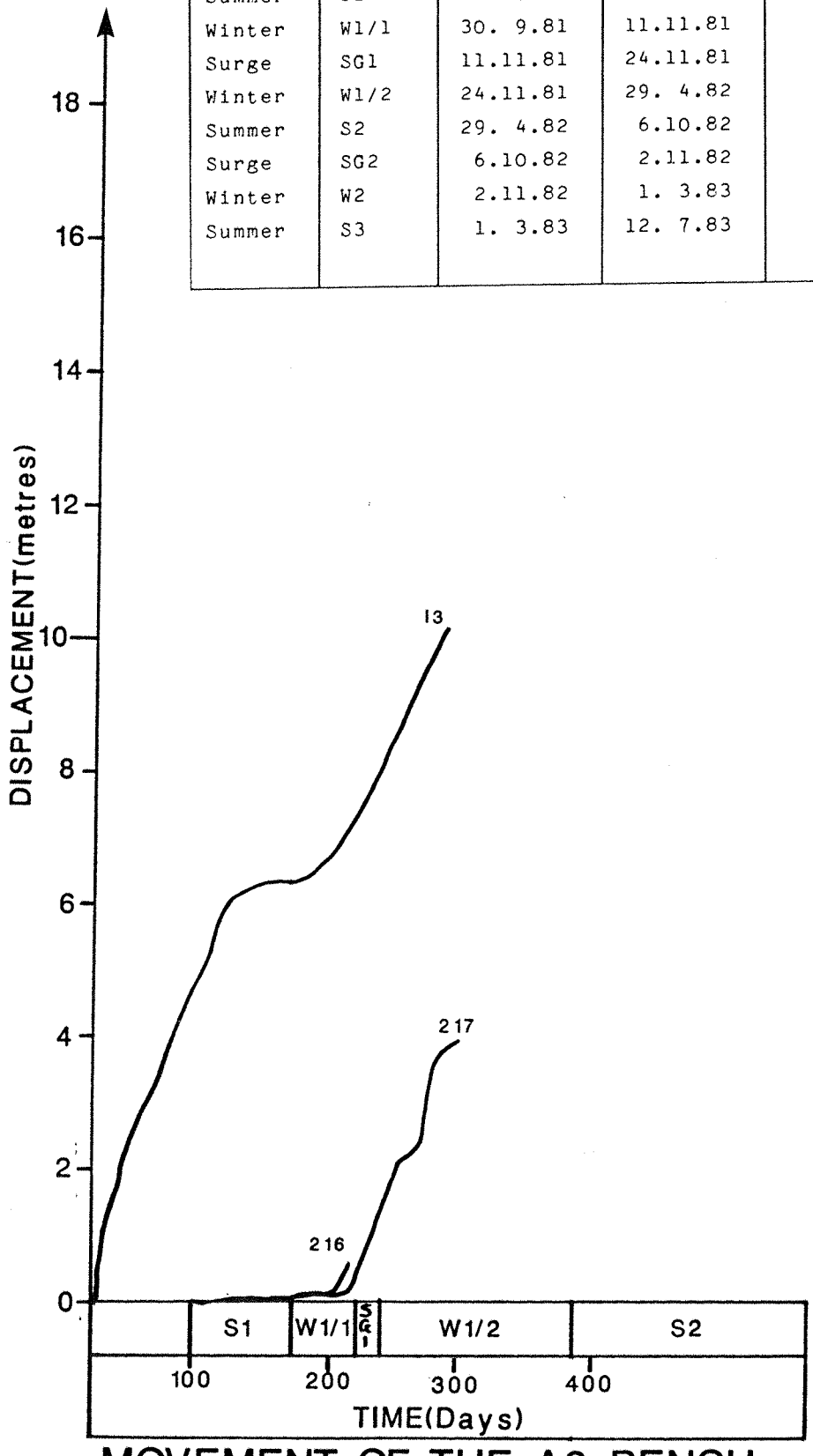

MOVEMENT OF THE A3 BENCH

FIG.F-27

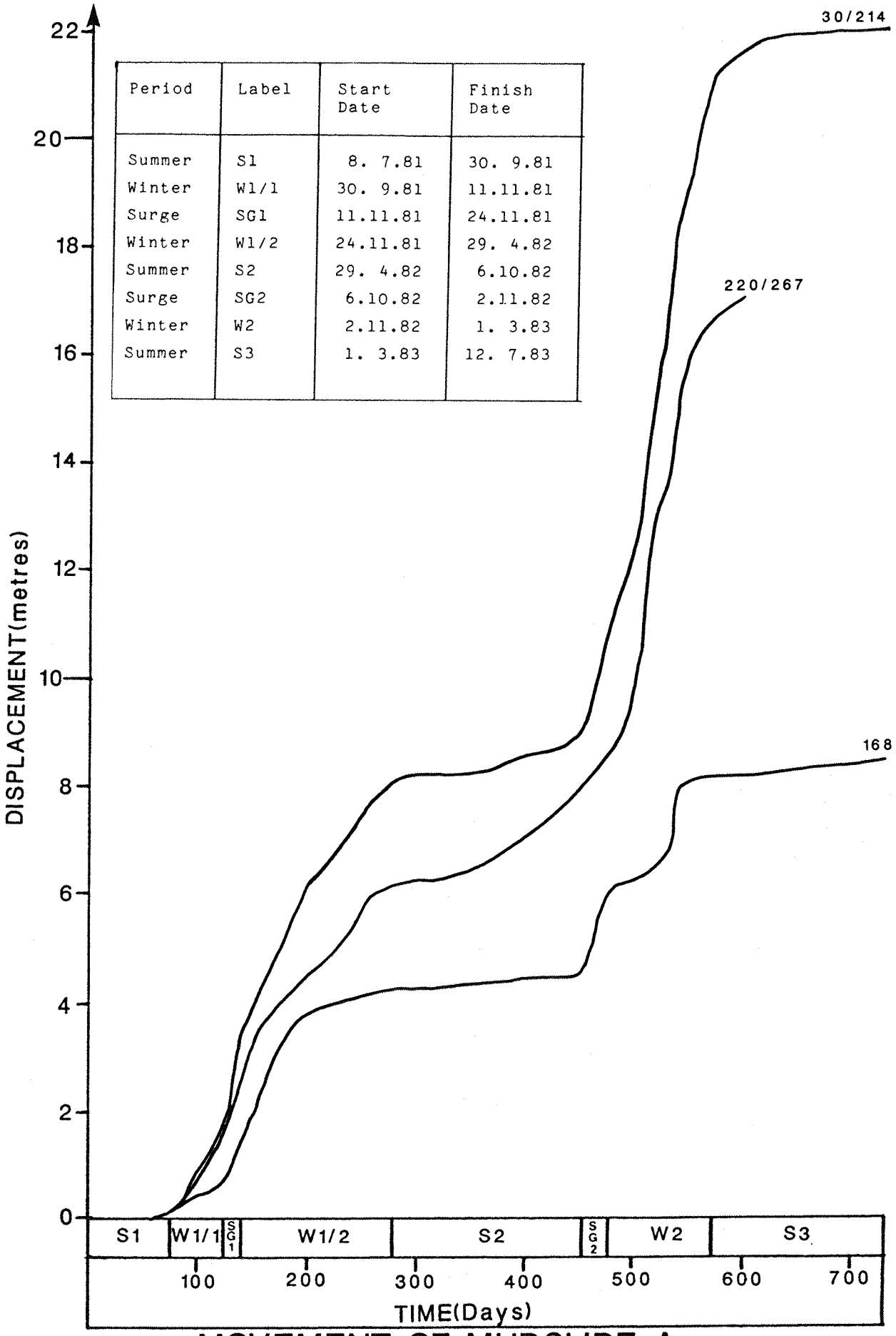

Period	Label	Start Date	Finish Date
Summer	S1	8. 7.81	30. 9.81
Winter	W1/1	30. 9.81	11.11.81
Surge	SG1	11.11.81	24.11.81
Winter	W1/2	24.11.81	29. 4.82
Summer	S2	29. 4.82	6.10.82
Surge	SG2	6.10.82	2.11.82
Winter	W2	2.11.82	1. 3.83
Summer	S3	1. 3.83	12. 7.83

MOVEMENT OF MUDSLIDE A DURING THE STUDY PERIOD

FIG.F-28

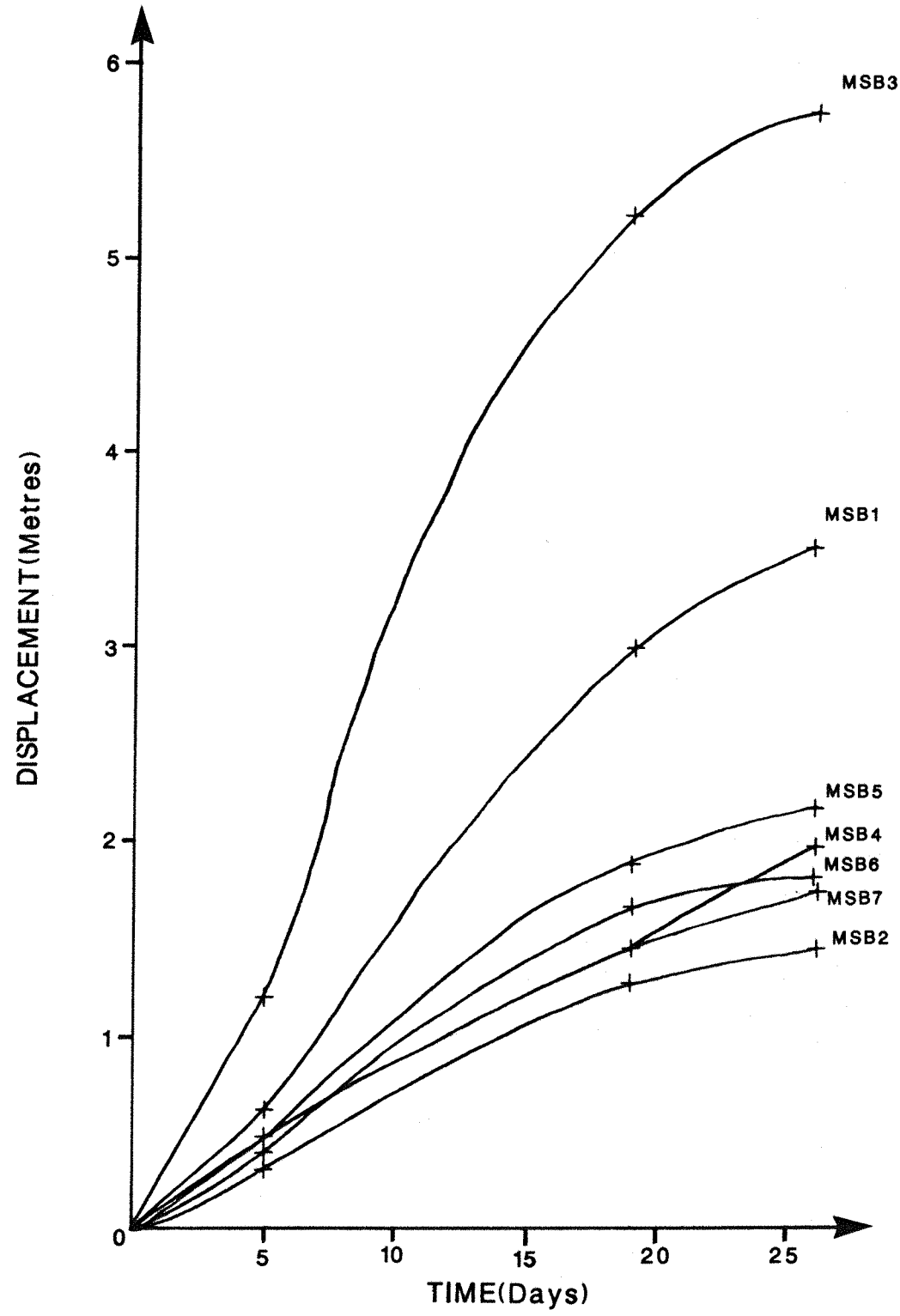

MOVEMENT OF MUDSLIDE B DURING SPRING 1983

FIG.F-29

Period	Label	Start Date	Finish Date	Duration in days	Number of pegs
Summer	S1	8. 7.81	30. 9.81	84	75
Winter	W1/1	30. 9.81	11.11.81	42	66
Surge	SG1	11.11.81	24.11.81	13	49
Winter	W1/2	24.11.81	29. 4.82	156	52
Summer	S2	29. 4.82	6.10.82	160	52
Surge	SG2	6.10.82	2.11.82	27	51
Winter	W2	2.11.82	1. 3.83	119	53
Summer	S3	1. 3.83	12. 7.83	133	47

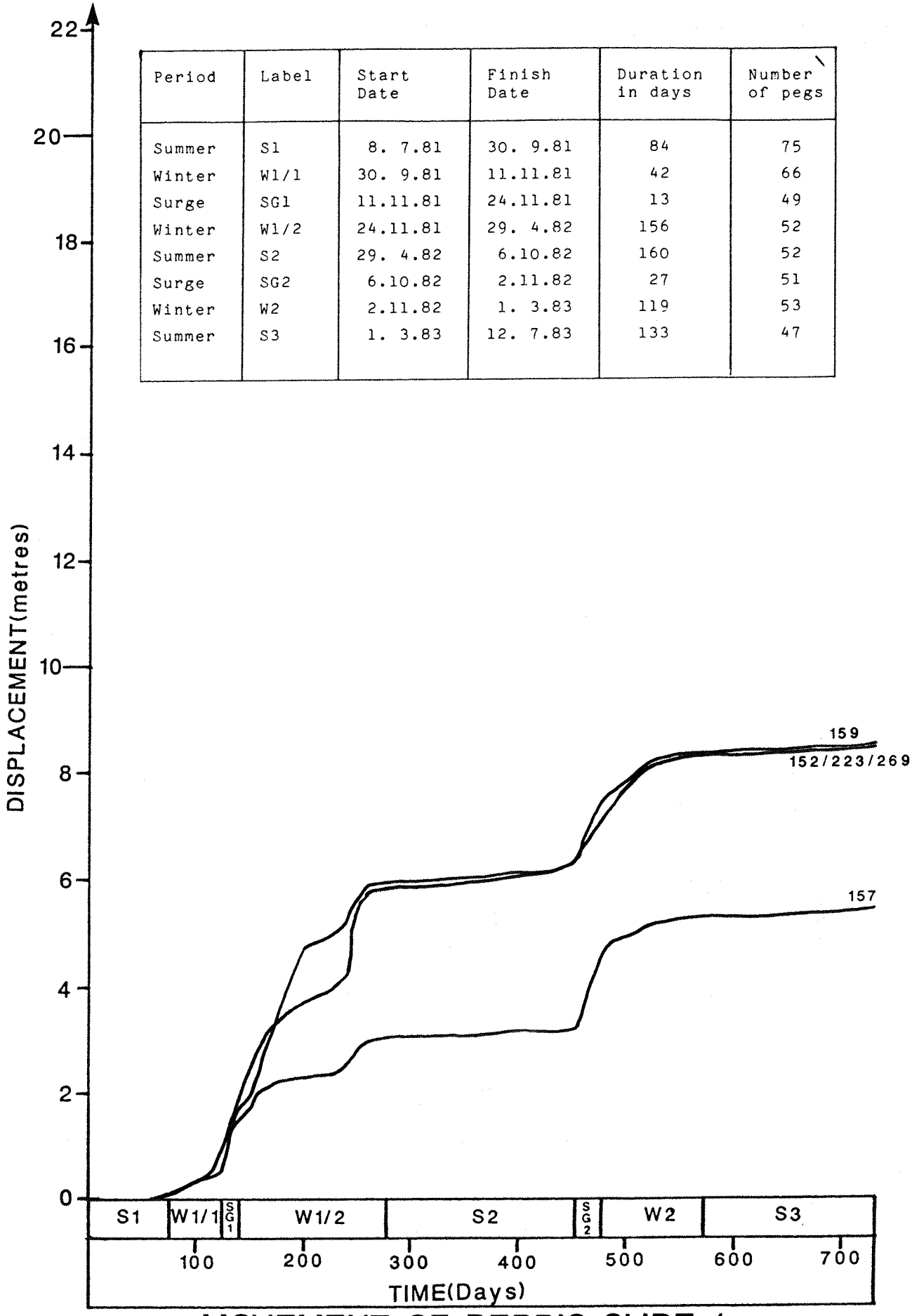

MOVEMENT OF DEBRIS SLIDE 1 DURING THE STUDY PERIOD

FIG.F-30

Period	Label	Start Date	Finish Date	Duration in days	Number of pegs
Summer	S1	8. 7.81	30. 9.81	84	75
Winter	W1/1	30. 9.81	11.11.81	42	66
Surge	SG1	11.11.81	24.11.81	13	49
Winter	W1/2	24.11.81	29. 4.82	156	52
Summer	S2	29. 4.82	6.10.82	160	52
Surge	SG2	6.10.82	2.11.82	27	51
Winter	W2	2.11.82	1. 3.83	119	53
Summer	S3	1. 3.83	12. 7.83	133	47

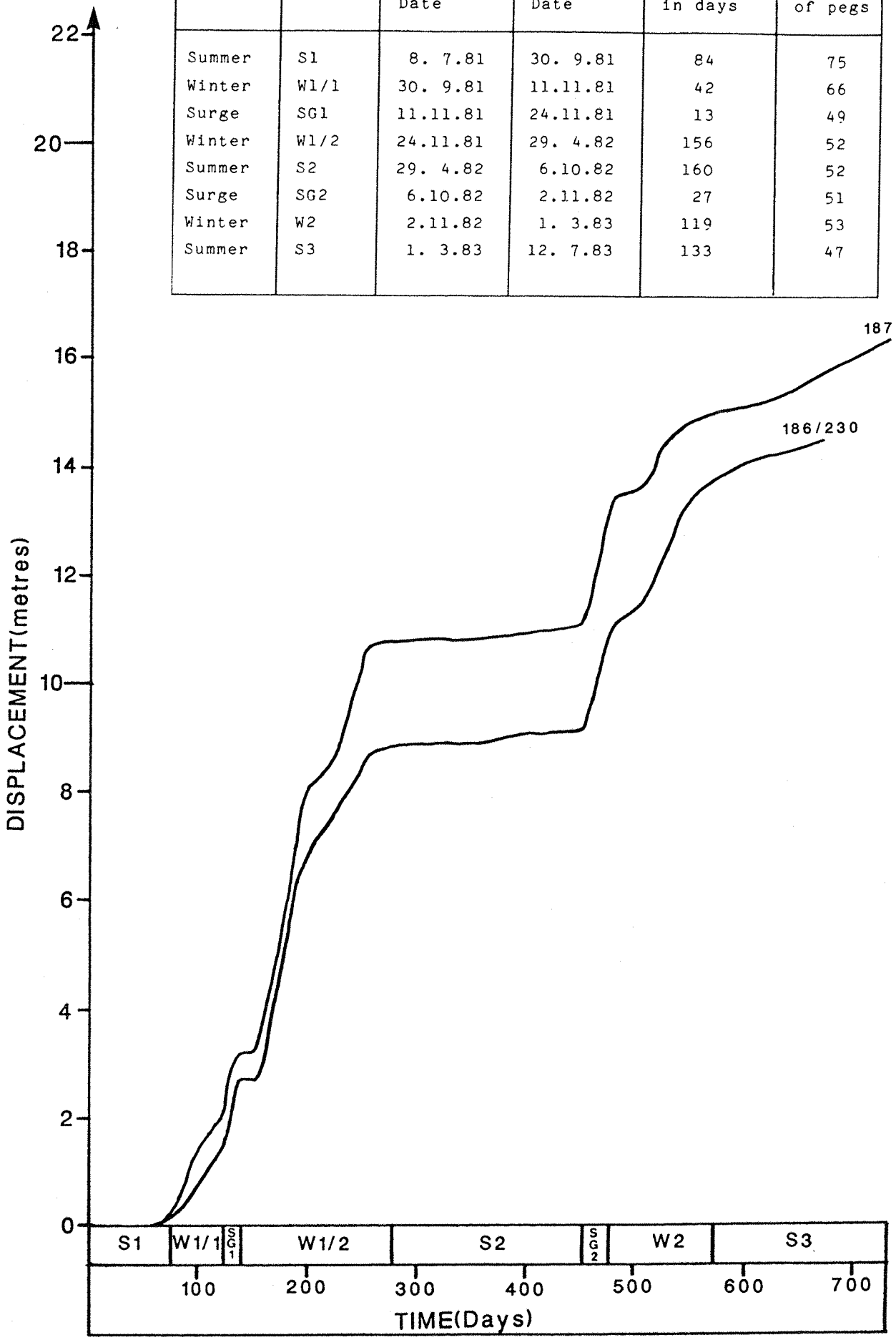

MOVEMENT OF DEBRIS SLIDE 2 DURING THE STUDY PERIOD

FIG.F-31

Period	Label	Start Date	Finish Date	Duration in days	Number of pegs
Summer	S1	8. 7.81	30. 9.81	84	75
Winter	W1/1	30. 9.81	11.11.81	42	66
Surge	SG1	11.11.81	24.11.81	13	49
Winter	W1/2	24.11.81	29. 4.82	156	52
Summer	S2	29. 4.82	6.10.82	160	52
Surge	SG2	6.10.82	2.11.82	27	51
Winter	W2	2.11.82	1. 3.83	119	53
Summer	S3	1. 3.83	12. 7.83	133	47

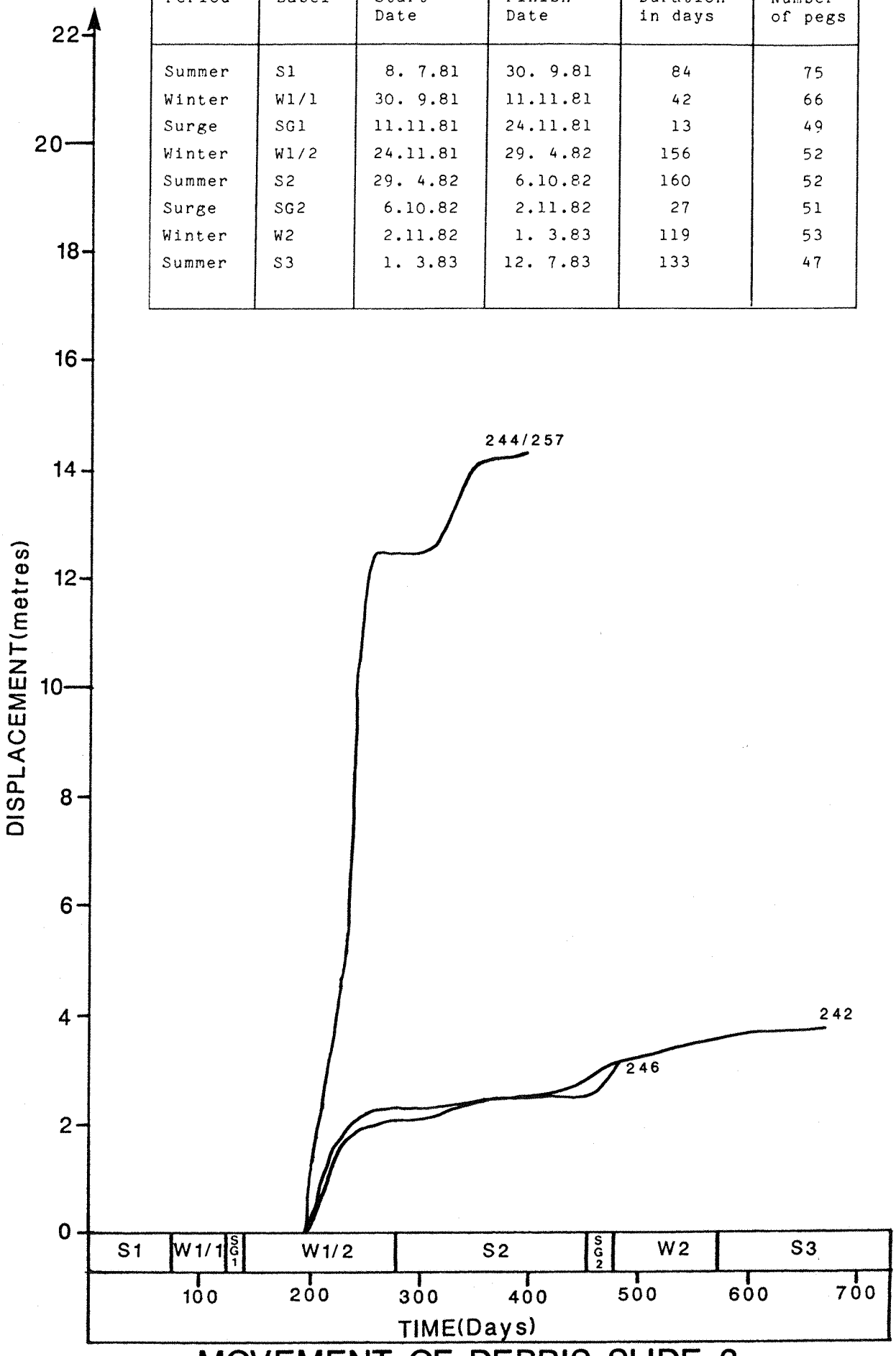

MOVEMENT OF DEBRIS SLIDE 3
DURING THE STUDY PERIOD

FIG.F-32

Period	Label	Start Date	Finish Date	Duration in days	Number of pegs
Summer	S1	8. 7.81	30. 9.81	84	75
Winter	W1/1	30. 9.81	11.11.81	42	66
Surge	SG1	11.11.81	24.11.81	13	49
Winter	W1/2	24.11.81	29. 4.82	156	52
Summer	S2	29. 4.82	6.10.82	160	52
Surge	SG2	6.10.82	2.11.82	27	51
Winter	W2	2.11.82	1. 3.83	119	53
Summer	S3	1. 3.83	12. 7.83	133	47

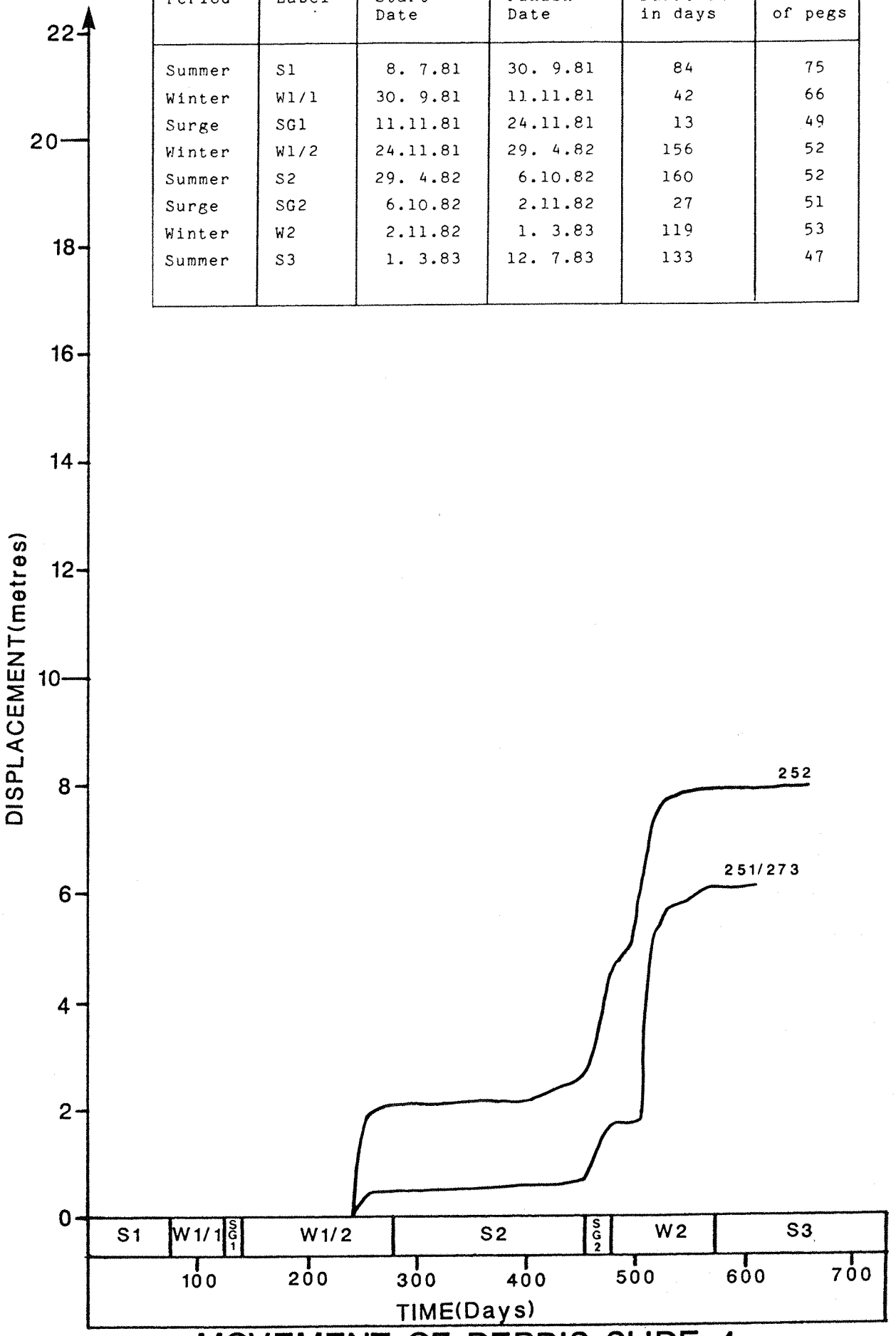

MOVEMENT OF DEBRIS SLIDE 4 DURING THE STUDY PERIOD

FIG.F-33

Period	Label	Start Date	Finish Date
Summer	S1	8. 7.81	30. 9.81
Winter	W1/1	30. 9.81	11.11.81
Surge	SG1	11.11.81	24.11.81
Winter	W1/2	24.11.81	29. 4.82
Summer	S2	29. 4.82	6.10.82
Surge	SG2	6.10.82	2.11.82
Winter	W2	2.11.82	1. 3.83
Summer	S3	1. 3.83	12. 7.83

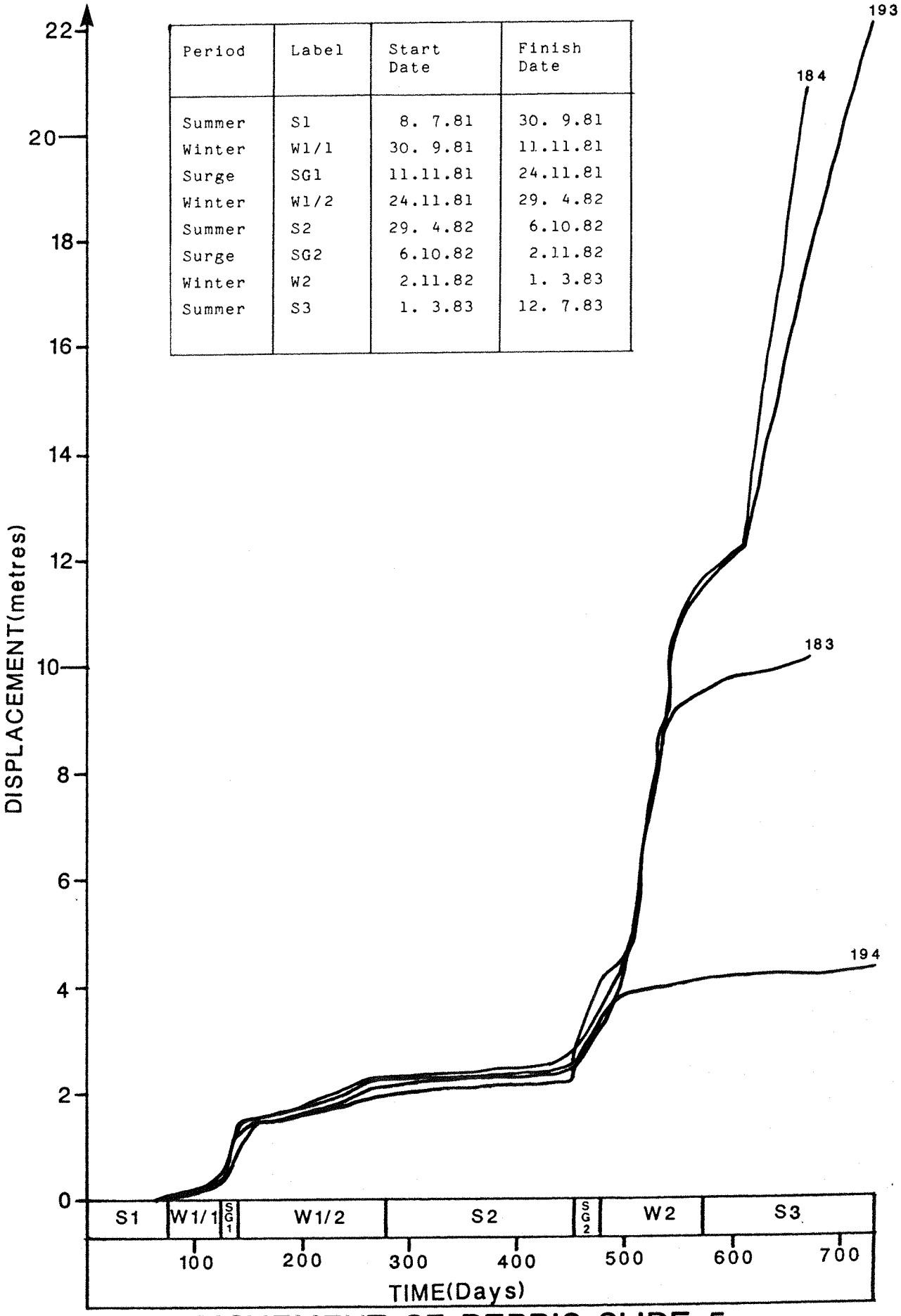

MOVEMENT OF DEBRIS SLIDE 5
DURING THE STUDY PERIOD

FIG.F-34